

ISCHP 2019

7th - International Scientific Conference on Hardwood Processing

PROCEEDINGS



27 - 30 August, 2019
Biobased Structures and Materials
Delft University of Technology
Delft, The Netherlands

Edited by:
Jan-Willem van de Kuilen
Wolfgang Gard

PREFACE

The 7th International Scientific Conference on Hardwood Processing (ISCHP) is hosted by Delft University of Technology in the Netherlands. After Canada (2007 and 2015), France (2009), USA (2011), Italy (2013) and Finland (2017). The scientific collaborators in the ISCHP family take in turn the responsibility of the conference organization, increasing the visibility of the conference by extending the family with new members every time.

The 12-year old history of ISCHP shows that interest in hardwoods and related natural resources is growing rapidly around the world. Topics covered by ISCHP conferences deal with species properties and quality, primary and secondary processing of hardwoods as well as hardwood applications. ISCHP 2019 will host representatives from countries from Europe, Africa, North- and South-America and Asia.

The Biobased Structures and Materials group of the TU Delft took the opportunity to invite the ISCHP family to Delft for the 2019 Conference. Building with wood has a long tradition in the Netherlands, whether traditional windmills, houses, boat building, bridges or hydraulic works. The centuries old Dutch international trade history of wood, has made the country a particular case for a variety of wood applications. Moreover, just as we are inspired by the many cultures and countries involved in wood trade and use, we hope that this conference will stimulate and inspire the participants from around the world to explore the potentials for hardwoods even more. The conference deals also with bamboo, a material that resembles wood behavior in many aspects.

More than 40 scientific contributions, including four keynote and two company R&D presentations are presented at the conference. The company presentations will give an industrial point of view on research and development as well as academic cooperation that lead up to the successful introduction of products on the 'wood' market.

Papers written on the presentations have undergone a scientific peer-review process. They are available for readers in an electronic format in the Conference Proceedings. A selected number of papers will be published in a special issue of the European Journal of Wood and Wood Products, a SpringerNature publication.

We would like to express our sincere thanks to all ISCHP 2019 participants, as a conference thrives by their willingness to present their scientific work and actively participate in this conference, giving merit to previous ISCHP conferences while paving the way for the future.

The members of the scientific committee are gratefully acknowledged for their support, feedback and review activities. We truly appreciate all the time and effort of the TU Delft staff members who contributed to ISCHP 2019, both with respect to the organization, the proceedings and the excursion. Without them, ISCHP 2019 would not have been possible.

Jan-Willem van de Kuilen & Wolfgang Gard
Conference chairs

SCIENTIFIC COLLABORATION



FINANCIAL SUPPORT



ISCHP 2019 COMMITTEES

Conference Chairs:

Wolfgang Gard
Jan-Willem van de Kuilen

Local organizing committee:

Abhijith Kamath
Xiuli Wang
Michele Mirra
Claire de Bruin
Geert Ravenshorst
Wolfgang Gard
Jan-Willem van de Kuilen

Scientific committee:

Jean-Francois Bouffard, FPInnovations Canada
Pierre Blanchet, Université Laval, Canada
Torsten Lihra, Université Laval, Canada
Urs Buehlmann, Virginia Tech, USA
Stefano Berti, CNR Ivalsa, Italy
Frederic Rouger, FCBA, France
Erkki Verkasalo, LUKE, Finland
Alfredo Dias, University of Coimbra, Portugal
Jan-Willem van de Kuilen, TU Munich, Germany / TU Delft, the Netherlands
Wolfgang Gard, TU Delft, the Netherlands

Keynote Presentations

Eric de Munck

Hardwoods: Trade, Regulation and Promotion

Netherlands Timber Trade Federation, Almere, the Netherlands

Peter Zanen

Structures with tropical hardwoods

Wijma Kampen BV, Kampen, the Netherlands

Alfredo Dias

Hardwood research and development in Portugal

University of Coimbra, Portugal

Li Haitao

Research and application on bamboo building materials

Nanjing Forestry University, Nanjing, China

Company R&D presentations:

Arjan van der Vegte

MOSO Bamboo, Zwaag, the Netherlands

Pieter Rozema

Brookhuis Applied Data Intelligence BV, Enschede, the Netherlands

Table of Contents

Session I

Effect of Thermo-Mechanical Modification on Mechanical Properties and Water Resistance of Plantation-Grown Vietnamese Acacia and Rubberwood	1
Variability in content of hydrophilic extractives and individual phenolic compounds in black locust STEM	11
Thermally modified birch wood interaction with liquids	18
Performance of thermally modified beech and ash wood in outdoor applications	27
Effect of Thermal Modification on Physical and Mechanical Properties of <i>Brachystegia spiciformis</i> and <i>Julbernardia globiflora</i> from Mozambique	35
Marketing of Urban and Reclaimed Wood Products	43
The potential of wood acetylation	49
Life cycle inventory for currently harvested birch roundwood	60

Session II

Laminated veneer lumber hollow cross-sections for temporary soil nailing	71
Testing and modelling of hardwood joints using beech and azobé	85
Use of northern hardwoods in glued-laminated timber: a study of bondline shear strength and resistance to moisture	93
Blue gum: Assessment of its potential for load bearing structures	104
Experimental and numerical evaluation of the structural performance of Uruguayan <i>Eucalyptus grandis</i> finger-joint	112
Mangium (<i>Acacia mangium</i>) and Sengon (<i>Falcataria moluccana</i>) Smoked Woods Resistance to Subterranean Termite Attack	124
French beech – a new opportunity in wood housing	129
Monitoring of Birch Veneer Moisture Content During the Drying Process by Single-Sided NMR technique	138

Session III

Wood coloring by reactive stains	144
Study on the wettability of Pannónia poplar (<i>P.x euramericana</i> Pannónia) from two Hungarian plantations: Győr and Soltvadkert	152
Lathe Checks Formation, Measurement and Effect on Plywood Quality - European Hardwoods	156
High-value composite products from fast growing <i>Eucalyptus</i> trees	161

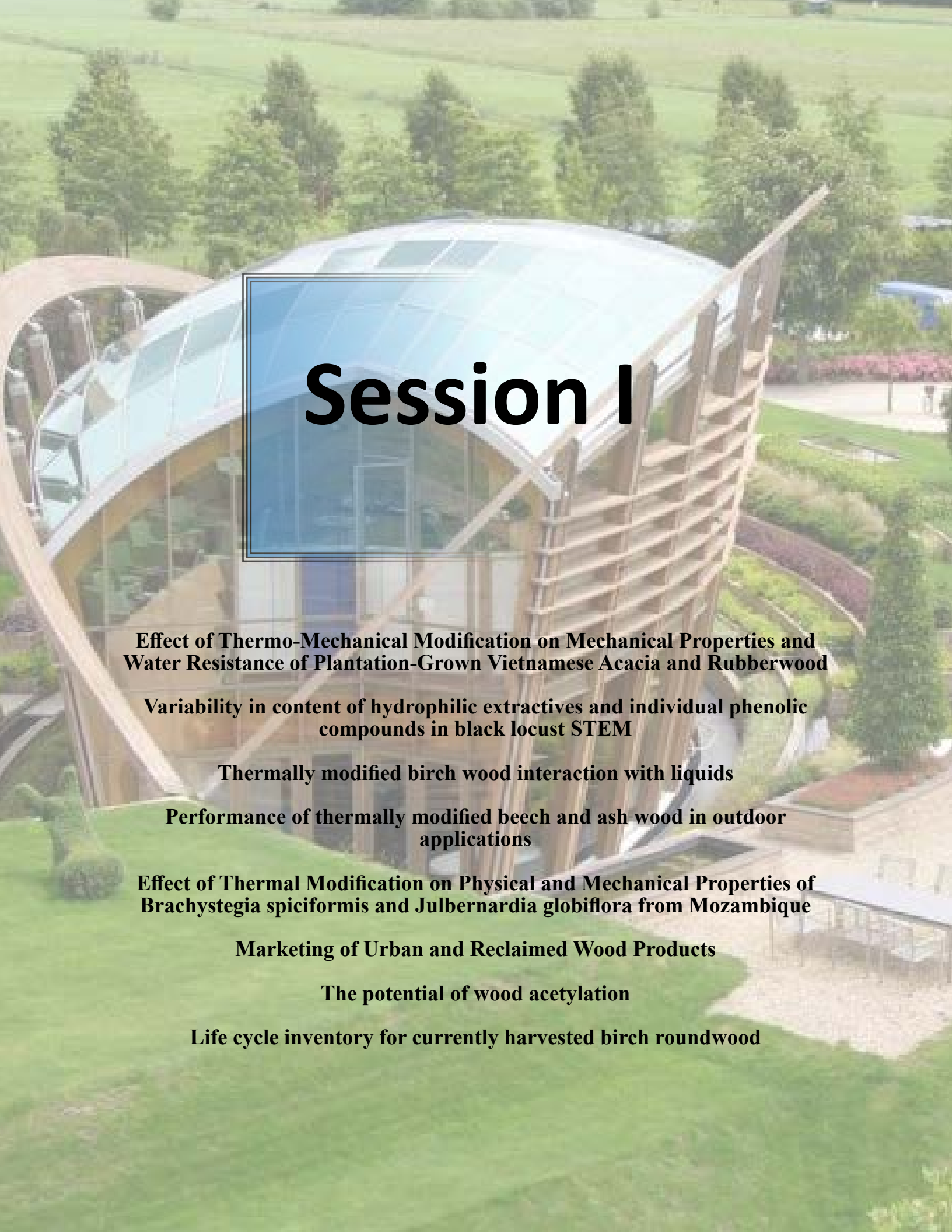
Influence of slope of grain on the mechanical properties of hardwoods and the consequences for grading	169
Mechanical performance of wood-based products fabricated with Portuguese Poplar	176
Vertical Forest Engineering: Applications of Vertical Forests with Self-Growing Connections in High-Rise Buildings	184
Biodynamic timber sheet pile – vegetation retaining structure	198

Session IV

Machine strength and stiffness prediction with focus on different acoustic measurement methods	211
Strength grading of hardwoods using transversal ultrasound	220
Glued structural products made of beech wood: quality of the raw material and gluing issues	230
Tension strength capacity of finger joined beech lamellas	244
European beech (<i>Fagus sylvatica</i> L.) glued laminated timber: Lamination strength grading, production and mechanical properties	252
Yield optimization and surface image-based strength prediction of beech	268
A timber guard rail for highways made of hardwoods	278
Portuguese hardwoods: an overview of its potential for construction purposes	286

Poster Presentations

Evaluation of Drying and Anatomical Characteristic of Mongolian Oak Lumber by Kiln Drying due to storage time after sawing	296
Wood Properties and Drying Characteristics of Korean Sawtooth Oak (<i>Quercus acutissima</i> Carruth.) Wood	302
Vertical Forest Engineering: Applications of Vertical Forests with Self-Growing Connections in High-Rise Buildings	309
Ageing phenomena of oak wood-animal glue bonded assemblies for preservation of cultural heritage	310
US Hardwoods and Market Opportunities in Easter Europe	311
Deep Learning for Lumber Identification	312



Session I

Effect of Thermo-Mechanical Modification on Mechanical Properties and Water Resistance of Plantation-Grown Vietnamese Acacia and Rubberwood

Variability in content of hydrophilic extractives and individual phenolic compounds in black locust STEM

Thermally modified birch wood interaction with liquids

Performance of thermally modified beech and ash wood in outdoor applications

Effect of Thermal Modification on Physical and Mechanical Properties of *Brachystegia spiciformis* and *Julbernardia globiflora* from Mozambique

Marketing of Urban and Reclaimed Wood Products

The potential of wood acetylation

Life cycle inventory for currently harvested birch roundwood

Effect of Thermo-Mechanical Modification on Mechanical Properties and Water Resistance of Plantation-Grown Vietnamese Acacia and Rubberwood

Rulong Cao¹, Juhani Marttila¹, Veikko Möttönen^{2*}, Henrik Heräjärvi², Pekka Ritvanen³, and Erkki Verkasalo²

¹School of Forest Sciences,
University of Eastern Finland
(UEF), 80100 Joensuu, Finland

² Production Systems, Natural
Resources Institute Finland (Luke),
80100 Joensuu, Finland

³KWS Timber Tech Ltd, 70100
Kuopio, Finland

*Corresponding author: E-mail veikko.mottonen@luke.fi, phone +358295325053

ABSTRACT

*Low density and poor mechanical performance often limit utilization of sawn wood from fast-growing plantation forests. Thermo-mechanical modification of timber (TMTM®) is one innovation for improving the utilization rate of light-weight wood species. The objective of this study was to determine the effects of thermo-mechanical modification and subsequent thermal modification on dry density, modulus of elasticity (MOE), compression strength, Brinell hardness and swelling behavior in immersion test on two fast-grown Vietnamese species, acacia (*Acacia mangium*) and rubberwood (*Hevea brasiliensis*). Test boards were modified in an industrial kiln where tangential thickness compression of 14% and 12% were aimed to acacia and rubberwood, either with or without subsequent thermal modification at 190 °C. Dry density, MOE, Brinell hardness, compression strength, and dimensional changes in water immersion of specimens were measured from the modified and reference materials, the latter ones being kiln dried at 50 °C. The results showed that changes in the mechanical properties were more evident for rubberwood than for acacia. In rubberwood, the MOE and compression strength of wood thermo-mechanically modified with or without thermal modification were higher than those of kiln-dried reference specimens throughout the thickness profile. In acacia similar differences between the modified and reference specimens were observed only in the surface layer. Density and Brinell hardness of thermo-mechanically modified rubberwood were higher than those of reference specimens, but after thermal modification they did not differ from (acacia) or were lower (rubberwood) than those of thermo-mechanically modified materials. Subsequent thermal modification increased the water resistance of thermo-mechanically modified specimens.*

Keywords: acacia, drying, rubberwood, thermo-mechanical modification, thermal modification

BRIEF ORIGINAL

Vietnamese acacia (*Acacia mangium*) and rubberwood (*Hevea brasiliensis*) boards were modified using tangential thickness compression either with or without subsequent thermal modification at 190 °C. Changes in density, modulus of elasticity, compression strength, Brinell hardness and swelling behavior between untreated and modified wood were studied. The results showed that changes in the physical and mechanical properties were more evident for rubberwood than for acacia. The unfavourable effects of any single modification method can be partly compensated by applying combinations of modifications and by the use of appropriate process parameters.

1. INTRODUCTION

In general, mechanical properties of wood are highly dependent on wood density (Pelit et al. 2018). Fast-growing acacia (*Acacia mangium*) and rubberwood (*Hevea brasiliensis*) plantations have been successfully commercialized in Southeast Asia thanks to their adaptability to various conditions and short rotation period (e.g., Nguyen 2013; Hai et al. 2015). However, their applications in wood product industries are limited by their relatively low density and poor dimensional stability (Mohammed Raphy et al. 2011; Teoh et al. 2011; Nambiar et al. 2014; Shukla and Sharma 2018).

Densification or compression in transverse direction is considered as an effective and environmentally friendly method to increase the density of wood. Densification reduces the void volume of lumens and reshapes the

morphology of cells without loss of lignin, resulting in improvement of mechanical properties such as modulus of elasticity, compression strength, tensile strength, hardness, and abrasion resistance of low-density wood species (Anshari et al. 2011; Sandberg et al. 2013). However, once the atmospheric humidity and heat in compression process terminate, elastic energy stored in microfibrils of compressed wood will be released, resulting in the thickness along compression springing back towards its original shape, which is defined as “shape memory” or “set recovery” (Navi and Sandberg 2012). This phenomenon is concerned as the biggest problem regardless of the mechanical property elevation of compressed wood (e.g., Möttönen et al. 2015).

It is important to improve the dimensional stability of densified wood in the direction of compression, because changed thickness indicates changes in properties, thereby implying the success of densification. Although the shape memory cannot be totally eliminated, it can be restricted by adjusting the heat, compressive force, and pressing time during the densification process (e.g., Navi and Girardet 2000; Kúdela et al. 2018). Depending on the combination of relative humidity and temperature used during the process, densification can be categorized into two types, thermo-hydro-mechanical modification (THM) and thermo-mechanical modification (TM). In THM process, atmospheric temperature and humidity are well-controlled and the compressive forces are subjected against the radial or tangential direction of wood (Dogu et al. 2010; Sandberg and Kutnar 2016). In TM, the compression process takes place in an open system without detailed control of relative humidity, being also widely applied in the industries (Kúdela et al. 2018). If the conditions are well-controlled in THM, higher values in density and stronger surface layers would thereby be achieved resulting in surfaces well applicable in flooring, furniture, and decorative uses (Gao et al. 2016).

Post-compression thermal treatment is known as another effective way to improve the dimensional stability of compressed wood, thereby offsetting the shape memory of THM (e.g., Gong et al. 2010; Möttönen et al. 2013; Yan and Morrell 2014; Möttönen et al. 2015; Sandberg and Kutnar 2016; Marttila et al. 2017; Sandberg et al. 2017). During the thermal modification process, wood is exposed to high temperature ($\geq 160^{\circ}\text{C}$) conditions (e.g., Millet and Gerhards 1972; Hillis 1975; Kocaefe et al. 2015). In this process, the structure of wood chemical components will be altered to different extent, thereby affecting other properties of wood (e.g., hygroscopicity, equilibrium moisture content, dimensional stability, fungal and insect resistance, mechanical properties, colour, and odour) (e.g., Sandberg et al. 2017). Optimized parameters during the modification processes need to be designed for specific species, considering their different characteristics (Sandberg et al. 2013).

Fast-growing plantations of acacia (*Acacia mangium*) and rubberwood (*Hevea brasiliensis*) have been successfully commercialized in Southeast Asia thanks to their adaptability to various conditions and short rotation period (Nguyen 2013; Hai et al. 2015). However, their applications in wood product industries are limited because of their low density and poor dimensional stability of wood (Mohammed Raphy et al. 2011; Teoh et al. 2011; Nambiar et al. 2014; Shukla and Sharma 2018). The timber is mostly used by kraft pulping industries.

The objective of this article is to investigate the effect of THM and combined THM and subsequent thermal modification on selected mechanical properties, i.e., modulus of elasticity, compression strength, and Brinell hardness, as well as extreme-condition swelling behavior of acacia and rubberwood.

2. MATERIALS AND METHODS

Logs of two different tree species from Vietnam, acacia (*Acacia mangium*) and rubberwood (*Hevea brasiliensis*) were transported by sea freight in green condition to Juankoski, Finland and then sawn to boards and thermo-mechanically modified. The pilot modification kiln patented by KWS Timber Tech Ltd allows wood drying, mechanical compression, and subsequent thermal modification in one single kiln unit. Different combinations of processes can be achieved by adjusting parameters such as temperature, hydraulic pressure, relative humidity, and treatment time. The boards were divided into six groups: four groups of sawn timber treated through different ways and two reference groups dried at 50°C in the oven but without any modification (Table 1).

Before modification, the boards were placed between perforated aluminum plates where the moisture content of boards could be indirectly controlled by the air circulation rate between these plates in the kiln (Fig. 1). Drying and hydraulic compression proceeded simultaneously. The drying temperature was steadily increased up to 130°C for acacia and 120°C for rubberwood, and the nominal degrees of mechanical compression (thickness change / original thickness) for acacia and rubberwood were set to 14 and 12 per cent, respectively. After drying and mechanical compression, a three-hour thermal modification at 210°C was instantly applied to the two groups of boards. During this process, certain amount of steam was applied in the kiln to protect the boards from darkening. After the thermal modification process, the system was cooled down, and pressure was released.

The moisture content (MC, %) and dry density (ρ_b , kg/m³) of the specimens from all boards were determined by the gravimetric method. The size of specimens which were taken from the other end of boards was 50 × 80 × 50 mm and 60 × 80 × 50 mm (thickness × width × length) for modified and unmodified boards, respectively. Modulus of elasticity (MOE) was determined by static three-point bending test according to the standard ISO13061-4, where the applied forces caused the deflection in the mid-span of each board. Materest model FMT-MEC 100kN material testing device was used to carry out MOE test and record the MOE value of each board. Prior to MOE test, the boards of groups of A and K were dried in an oven with a temperature of 50°C for roughly 2 weeks, while those of AC, ACT, KC, KCT were conditioned indoors for two weeks in order to achieve the adequate moisture level (12±5%) required by the tests.

Compression strength parallel to the grain of each test specimen was determined according to ISO 13061-12:2017. All samples were stored in the conditioning chamber at 20 °C, 65% relative humidity until their mass was stable. The ultimate stress (σ , MPa) was determined using gradually increasing load in parallel to the grain direction:

$$\sigma = F_{max}/(a*b) \quad (1)$$

where F_{max} is the maximum load force (N), a and b are the cross-sectional dimensions of the test specimen (mm).

The moisture contents of the mechanical test specimens from groups A and K were computationally adjusted to 12% by using the following formulae, which are valid for moisture contents of 12±5%:

$$E_{12} = E_w/(1-\alpha*(W-12)) \quad (2)$$

$$\sigma_{12} = \sigma*(1+ \alpha*(W-12)) \quad (3)$$

where E_{12} is the calibrated MOE value at the moisture content of 12%, σ_{12} is the calibrated compression strength at the moisture content of 12%, α is the correction factor (0.02) for the moisture content, W is the moisture content of wood during the test, determined according to ISO 13061-1.

Before immersion test, all test specimens were stabilized in the normal climate chamber at 20 °C, 65% relative humidity until their equilibrium moisture content (EMC) was reached, i.e., the mass did not change anymore. After that, the initial length, width and thickness of specimens were measured by caliper. Next, the specimens were soaked in buckets filled with water and stored in room temperature for 14 days. The dimensions were measured from the same positions once again after the 14 days of soaking. The dimensional changes were determined according to the formula:

$$\alpha = ((L_1-L_0)/L_0) *100\% \quad (4)$$

Where α is the swelling rate in length, width, and thickness (%), L_0 is the initial dimension (length, width, and thickness) (mm), L_1 is the dimension (length, width, and thickness) after the 14-day immersion (mm).

Brinell hardness (HB) (kg/mm²) of the test specimens was determined according to the standard EN 1534 (2010):

$$HB = 2F/(g*\pi*D*(D-(D_2-d_2)1/2)) \quad (5)$$

where F is the maximum load applied (1,000 N), g is the acceleration of gravity (9.81 m/s²), π is the “pi” factor (3.14), D is the diameters of the indenter (10 mm), d is the average value of the diameter of the two residual indentations [(d_1+d_2)/2 mm] on specimen surface, d_1 and d_2 being the diameters of the residual indentation along the grain and across the grain, measured by caliper.

3. RESULTS AND DISCUSSION

3.1. DRY DENSITY

Mean values and standard deviations (STD) of moisture content (MC), dry density, modulus of elasticity (MOE), Brinell hardness (HB), compression strength from core part (CS-C), compression strength from surface part (CS-S) of acacia (A), thermo-mechanically modified acacia (AC), thermo-mechanically modified acacia with subsequent thermal modification (ACT), rubberwood (K), thermo-mechanically modified rubberwood (KC), and thermo-mechanically modified rubberwood with subsequent thermal modification (KCT) are shown in Table 2. Mean values, STDs, and significance levels (* the mean difference is significant at 0.05 level) of dimensional stability in different directions (T=thickness, L=length, W=width; thickness is along the direction of compression, length is along the longitudinal direction) of experimental groups of A, AC, ACT, K, KC, and KCT are given in Table 3. ANOVA

results of dry density, MOE, HB, CS-C, CS-S, and swelling T (thickness direction) of experimental groups of A, AC, ACT, K, KC, and KCT are listed in Table 4.

Statistically significant difference was detected between K&KC, KC&KCT, suggesting that thermo-mechanical modification had a positive effect on dry density of rubberwood (increase by 7.3%) while subsequent thermal modification decreased the dry density from KC to KCT by 7.5%. This might indicate that the thermo-mechanical modification changed the structure of rubberwood tissue to contain less void space and more fibres per unit volume, thereby increasing the dry density (Kutnar et al. 2008; Fang et al. 2012). After the subsequent thermal modification, degradation of holocellulose, evaporation of certain extractives or volatile organic compounds (VOCs) could lead to the mass loss of cell walls (Sandberg and Kutnar 2016; Severo et al. 2016; Shukla and Sharma 2014).

On the other hand, no difference was found between the experimental groups of acacia. High initial moisture content or inappropriate compression temperature, pressure, or time might lead to the failure of compression where the whole thickness profile of acacia samples was not totally penetrated by the compressive pressure (Kúdela et al. 2018). Another reason could be that the strong spring-back effect in AC specimens counterbalanced the positive effect of compression on the density of acacia (Pelit et al. 2018). The long lasting sea fright of logs at green state may also have had adverse effects on physical and mechanical properties of wood.

3.2. MODULUS OF ELASTICITY (MOE)

Regarding MOE values, thermo-mechanical modification and thermo-mechanical modification with subsequent thermal modification lead to an improvement of 39.5% and 35.9% in rubberwood, whereas there was no increase observed in acacia.

Several studies show that densification is an effective way to improve the mechanical properties of wood (e.g., Kutnar et al. 2008; Anshari et al. 2011; Fang et al. 2012; Möttönen et al. 2015; Gao et al. 2016). Generally, the bending stiffness of wood improves proportionally to density increase as a result of compression (Kutnar 2012). Increasing temperature up to 150 °C during compression also has a positive effect on MOE value of wood as it reduces the spring-back effect of compressed wood, although the increase of MOE caused by high temperature is not as obvious as that caused by high compression ratio (Tabarsa and Chui 1997; Lamason and Gong 2007).

The effect of thermal modification is dependent on the wood species, temperature, initial moisture content, surrounding atmosphere, and reaction time (Mitchell 1988). Therefore, the effects of thermal modification on MOE can be either positive (Fang et al. 2012; Shi et al. 2007) or negative (Gong et al. 2010; Johansson and Morén 2006), depending on the parameters applied during the process. High temperature and long processing time may decrease the MOE due to the deterioration of wood components, hemicellulose in the first hand (Yan and Morrell 2014; Korkut and Aytin 2015). In addition, since the proportion of amorphous cellulose decreases with increasing temperature (e.g., Sivonen et al. 2002; Yıldız and Gümüşkaya 2007), an increase in crystallinity of cellulose may cause an increase of the MOE. However, elevation in the MOE is associated with the reduced moisture content in the modified wood (Xie et al. 2013). Usually moisture content is negatively correlated with MOE below the FSP (Kretschmann 2010).

3.3. COMPRESSION STRENGTH

Both thermo-mechanical modification and thermo-mechanical modification with subsequent thermal modification increased the compression strength of surface specimens of acacia by 23%, while the change in compression strength of core specimens was not significant. In case of rubberwood, the increments in compression strength of surface and core specimens were 19.9% and 25.0%, respectively.

There are several explanations for increment of compression strength achieved by thermal treatment. Firstly, crystallization and degradation of cellulose in amorphous region increases the proportion of crystalline cellulose, which increases the stiffness of wood in its longitudinal direction (Anderson et al. 2005; Yıldız et al. 2006); secondly, increased cross-linking of lignin polymer network can better connect and stiffen cellulose fibrils and prevent them from bending or crashing when they are subjected to compressive forces, thereby increasing the longitudinal compression strength of wood (Boonstra et al. 2007). It could also be explained by the fact that the lower moisture content detected in all modified specimens, i.e., decreased amount of bound water, resulted in increased compression strength of wood.

3.4. SWELLING BEHAVIOR IN IMMERSION TEST

The results show that compared to untreated specimens, both modification treatments and both species swell more in the direction of compression, i.e., 385%, 218%, 172%, and 114% higher dimensional changes in AC, ACT, KC, and

KCT, respectively, compared to their references. It seems that the irreversible set recovery phenomenon explained the swelling in the modified samples, in addition to the reversible hygroscopicity of wood itself (Fang et al. 2012).

As much as 21% less thickness swelling was detected in KCT specimens compared with KC specimens, which indicates that the set-recovery of rubberwood was partially eliminated. This might be explained by the following mechanisms: Firstly, thermal modification above 200°C can increase the cross-linking network in lignin, which increases the hydrophobicity of wood and reduces its swelling (Santos 2000). Secondly, the stored elastic stresses are released because of the degradation of hemicellulose in high temperature (Navi and Sandberg 2012). Elimination of some hygroscopic hydroxyl groups due to the depolymerization of carbohydrates explains the improved hydrophobicity in thermally modified wood (Xie et al. 2013). In addition, in cellulose components, amorphous regions in cellulose is degraded due to acid catalysis in high temperature, which increases the crystallinity and thereby decrease the accessibility of water molecules in hydroxyl groups (e.g., Cai et al. 2018; Kúdela et al. 2018).

3.5. BRINELL HARDNESS

Elevation of Brinell hardness of 58% was detected in KC samples, whereas no difference was found between A and AC. Flattening of fibre lumens and vessels in thermo-mechanical modification may increase the Brinell hardness of wood (Fang et al. 2012). However, slight loss of Brinell hardness takes place due to increased temperature during the thermo-mechanical modification (Fang et al. 2012). Typically, higher degree of compression leads to higher Brinell hardness value, although Rautkari et al. (2013) argued that Brinell hardness is mainly influenced by the density and hardness of the surface layer. In addition to varying densities among wood species, other factors such as modification temperature, final density, moisture content, techniques of measurement, and measuring conditions (e.g., load level, loading time) also have influence on the results (Holmberg 2000; Gašparík et al. 2016).

On the other hand, compared to AC and KC, subsequent thermal modification caused the reduction of Brinell hardness in ACT and KCT by 33% and 41%, respectively, which was probably due to the deterioration of cell wall structures (Pelit et al. 2015). High temperature and long processing time typically result in greater reduction in Brinell hardness because of the degradation of hemicellulose and lignin in high temperatures (Fang et al. 2012; Salca and Hiziroglu 2014). In addition to that, reduction of hardness due to the heat treatment was found to be highest for wood species with high density (Kesik et al. 2014; Salca and Hiziroglu 2014).

3.6. ECONOMIC ASSESSMENT OF THE PROCESS

A comprehensive assessment of the economy of thermo-hydro-mechanical modification would require an analysis of the entire value chain, from raw materials to end products (c.f., Sandberg et al. 2017). Compared to conventional processes the advantages gained by the THM modification include shorter production lead time, lower raw material and energy costs per cubic meter and improved properties and quality of end products. High temperature drying and modification of THM modification reduces the process time to minimum of 2 days compared to 10-20 days with conventional methods. As a result of reduced process time, labour, energy and product related capital costs are also lower. Low-priced domestic small diameter timber can be utilised in THM process enabling the replacement of more expensive and imported large diameter timber. The lower quality of small diameter timber can be compensated by densification which, to some extent, increases the hardness and strength of wood. The smaller production capacity of the THM modification kiln compared to conventional kiln of comparable size or price range is the main disadvantage from the economic point of view.

4. CONCLUSIONS

Thermo-mechanical modification is a potential technique to improve some properties of rubberwood (e.g., density, MOE, compression strength, Brinell hardness) and acacia (surface compression strength), but modified wood swells more than non-modified under extreme conditions. Post-compression thermal modification improves the dimensional stability under such conditions, but reduces the hardness of the surface.

The unfavourable effects of any single modification method can be partly compensated by applying combinations of modifications and by the use of appropriate process parameters. Therefore, further experiments are needed to investigate the influence of treatment time, compressive force, and modification temperature on acacia and rubberwood properties.

ACKNOWLEDGEMENTS

The study materials and funding were provided by KWS Timber Tech Oy, Kuopio, and the experiment was carried out at Natural Resources Institute Finland (LUKE), Joensuu, and the University of Eastern Finland (UEF), Joensuu. The authors express their gratitude to these institutions, and their individuals who provided support to this study.

REFERENCES

- Anshari B, Guan Z, Kitamori, A, Jung K, Hassel I, Komatsu K (2011) Mechanical and moisture-dependent swelling properties of compressed Japanese cedar. *Construction and Building Materials* 25(4):1718–1725.
- Boonstra M, Van Acker J, Tjeerdma B, Kegel E (2007) Strength properties of thermally modified softwoods and its relation to polymeric structural wood constituents. *Annals of Forest Science* 64(7):679–690.
- Cai C, Antikainen J, Luostarinen K, Mononen K, Heräjärvi H (2018) Wetting-induced changes in thermally modified Scots pine and Norway spruce wood surface. *Wood Science and Technology* 52(5): 1181–1193.
- Dogu D, Tirak K, Candan Z, Unsal O (2010) Anatomical investigation of thermally compressed wood panels. *BioResources* 5(4):2640–2663.
- Fang CH, Mariotti N, Cloutier A, Koubaa A, Blancet P (2012) Densification of wood veneers by compression combined with heat and steam. *European Journal of Wood and Wood Products* 70(1):155–163.
- Gao Z, Huang R, Lu J, Chen Z, Guo F, Zhan T (2016) Sandwich compression of wood: Control of creating density gradient on lumber thickness and properties of compressed wood. *Wood Science and Technology* 50(4):833–844.
- Gašparik M, Gaff M, Šafaříková L, Vallejo CR, Svoboda T (2016) Impact Bending Strength and Brinell Hardness of Densified Hardwoods. *BioResources* 11(4):8638–8652.
- Gong M, Lamason C, Li L (2010) Interactive effect of surface densification and post-heat-treatment on aspen wood. *Journal of Materials Processing Tech.* 210(2):293–296.
- Hai PH, Duong LA, Toan NQ, Ha TTT (2015) Genetic variation in growth, stem straightness, pilodyn and dynamic modulus of elasticity in second-generation progeny tests of *Acacia mangium* at three sites in Vietnam. *New Forests* 46(4):577–591.
- Hillis WE (1975) The role of wood characteristics in high temperature drying. *J. Institute Wood Sci.* 7:60–67.
- Holmberg H (2000) Influence of grain angle on Brinell hardness of Scots pine (*Pinus sylvestris* L.). *Holz als Roh- und Werkstoff* 58(1):91–95.
- Johansson D, Morén T (2006) The potential of colour measurement for strength prediction of thermally treated wood. *Holz als Roh- und Werkstoff* 64(2): 104–110.
- Kesik HI, Korkut S, Hiziroglu S, Sevik H (2014) An evaluation of properties of four heat treated wood species. *Industrial Crops & Products* 60:60–65.
- Kocaepe D, Huang X, Kocaepe Y (2015) Dimensional Stabilization of Wood. *Current Forestry Reports* 1(3):151–161.
- Korkut S, Aytin A (2015) Evaluation of physical and mechanical properties of wild cherry wood heat-treated using the thermowood process. *Maderas: Ciencia y tecnología* 17(1):171–178.
- Kretschmann DE (2010) Mechanical properties of wood. Madison, U.S. Department of Agriculture, Forest Service, Forest Products Laboratory: General technical report FPL-GTR-190
- Kutnar A, Kamke FA, Sernek M (2008) The mechanical properties of densified VTC wood relevant for structural composites. *Holz als Roh- und Werkstoff* 66(6):439–446.
- Kúdela J, Rousek R, Rademacher P, Rešetka M, Dejmal A (2018) Influence of pressing parameters on dimensional stability and density of compressed beech wood. *European Journal of Wood and Wood Products* 76(4): 1241–1252.
- Kutnar A (2012) Compression of wood under saturated steam, superheated steam, and transient conditions at 150°C, 160°C, and 170°C. *Wood Science and Technology* 46(1):73–88.
- Lamason C, Gong M (2007) Optimization of pressing parameters for mechanically surface-densified aspen. *Forest Products Journal* 57(10):64–68.
- Marttila J, Owusu Sarpong B, Möttönen V, Heräjärvi H (2017) Case hardening and equilibrium moisture content of European aspen and silver birch after industrial scale thermo-mechanical timber modification. *ISCHP 2017: 6th International Conference on Hardwood Processing*. Lahti, Finland, pp. 156–165.
- Millet MA, Gerhards CC (1972) Accelerated ageing: residual weight and flexural properties of wood heated in air at 115°C to 175°C. *Wood Sci.* 4:193–201.
- Mitchell P (1988) Irreversible property changes of small loblolly pine specimens heated in air, nitrogen, or oxygen. *Wood and fiber science: journal of the Society of Wood Science and Technology* 3:320–335.

Effect of Thermo-Mechanical Modification on Mechanical Properties and Water Resistance of Plantation-Grown
 Vietnamese Acacia and Rubberwood

- Mohammed Raphy KM, Anoop EV, Aruna P, Sheena VV, Ajayghosh V (2011) Provenance variation in wood chemical properties of *Acacia mangium willd.* and *Acacia auriculiformis cunn.*, grown in a wet humid site in Thrissur district of Kerala, South India. *Journal of the Indian Academy of Wood Science* 8(2):120–123.
- Möttönen V, Bütün Y, Heräjärvi H, Marttila J, Kaksonen H, (2015) Effect of combined compression and thermal modification on mechanical performance of aspen and birch wood. *Pro Ligno* 11(4):310–317.
- Möttönen V, Reinikkala M, Heräjärvi H, Luostarinen K (2013) Effect of compression and thermal modification on selected technical properties of European aspen and silver birch. In: Berti, S., Achim, A., Fioravanti, M., Lihra, T., Loewe Munoz, V., Marchal, R., Wiedenbeck, J. & Zanuttini, R. (eds.). *4th International Scientific Conference on Hardwood Processing 2013, 7th - 9th October 2013. Florence, Italy. Proceedings.* pp. 165-171.
- Nambiar EKS, Harwood CE, Kien ND (2014) *Acacia* plantations in Vietnam: Research and knowledge application to secure a sustainable future. *Southern Forests: a Journal of Forest Science* 77(1):1–10.
- Navi P, Girardet F (2000) Effects of Thermo-Hydro-Mechanical Treatment on the Structure and Properties of Wood. *Holzforschung* 54(3):287–293.
- Navi P, Sandberg D (2012) *Thermo-hydro-mechanical wood processing.* CRC, Boca Raton
- Nguyen BT (2013) Large-scale altitudinal gradient of natural rubber production in Vietnam. *Industrial Crops & Products* 41(1):31–40.
- Pelit H, Sönmez A, Budakçı M (2015) Effects of Thermomechanical Densification and Heat Treatment on Density and Brinell Hardness of Scots Pine (*Pinus sylvestris* L.) and Eastern Beech (*Fagus orientalis* L.). *BioResources* 10(2):3097–3111.
- Pelit H, Budakçı M, Sönmez A (2018) Density and some mechanical properties of densified and heat post-treated Uludağ fir, linden and black poplar woods. *European Journal of Wood and Wood Products* 76(1):79–87.
- Rautkari L, Laine K, Kutnar A, Medved S, Hughes M (2013) Hardness and density profile of surface densified and thermally modified Scots pine in relation to degree of densification. *Journal of Materials Science* 48(6):2370–2375.
- Salca E, Hiziroglu S (2014) Evaluation of hardness and surface quality of different wood species as function of heat treatment. *Materials and Design* 62:416–423.
- Sandberg D, Haller P, Navi P (2013) Thermo-hydro and thermo-hydro-mechanical wood processing: An opportunity for future environmentally friendly wood products. *Wood Material Science & Engineering* 8(1):64–88.
- Sandberg D, Kutnar A (2016) Thermally modified timber: Recent developments in Europe and North America. *Wood and Fiber Science* 48:28–39.
- Sandberg D, Kutnar A, Mantanis G (2017) Wood modification technologies - a review. *iForest* 10:895–908. - doi: 10.3832/ifor2380-010
- Santos JA (2000) Mechanical behaviour of Eucalyptus wood modified by heat. *Wood Sci. Technol.* 34:39–43.
- Severo ETD, Calonego FW, Sansígolo CA, Bond B (2016) Changes in the Chemical Composition and Decay Resistance of Thermally-Modified *Hevea brasiliensis* Wood. *PLoS ONE* 11(3): e0151353. <https://doi.org/10.1371/journal.pone.0151353>
- Shi JL, Kocaepe D, Zhang J (2007) Mechanical behaviour of Québec wood species heat-treated using ThermoWood process. *Holz als Roh- und Werkstoff*, 65(4):255–259.
- Shukla S, Sharma S (2014) Effect of high temperature processing under different environments on physical and surface properties of rubberwood (*Hevea brasiliensis*). *Journal of the Indian Academy of Wood Science*, 11(2):182–189.
- Shukla S, Sharma S (2018) Effect of high temperature treatment of *Hevea brasiliensis* on density, strength properties and resistance to fungal decay. *J Indian Acad Wood Sci* 15(1):87–95.
- Sivonen H, Maunu SL, Sundholm F, Jämsä S, Viitaniemi P (2002) Magnetic Resonance Studies of Thermally Modified Wood. *Holzforschung*, 56(6):648–654.
- Tabarsa T, Chui YH (1997) Effects of hot-pressing on properties of white spruce. *Forest Products Journal* 47(5):71-76.
- Teoh Y, Don MM, Ujang S (2011) Assessment of the properties, utilization, and preservation of rubberwood (*Hevea brasiliensis*): A case study in Malaysia. *Journal of Wood Science* 57(4):255–266.
- Xie Y, Fu Q, Wang Q, Xiao Z, Militz H (2013) Effects of chemical modification on the mechanical properties of wood. *European Journal of Wood and Wood Products* 71(4):401–416.
- Yan L, Morrell JJ (2014) Effects of Thermal Modification on Physical and Mechanical Properties of Douglas-Fir Heartwood. *BioResources*, 9(4):7152–7161.
- Yildiz S, Gezer ED, Yildiz UC (2006) Mechanical and chemical behavior of spruce wood modified by heat. *Building and Environment* 41(12):1762–1766.
- Yildiz S, Gümüşkaya E (2007) The effects of thermal modification on crystalline structure of cellulose in soft and hardwood. *Building and Environment*, 42(1):62–67.

Effect of Thermo-Mechanical Modification on Mechanical Properties and Water Resistance of Plantation-Grown Vietnamese Acacia and Rubberwood

Table 1. Treatments and number of boards in the six treatment groups.

Code	Group	Treatment	Number of boards	Compression degree	Time and temperature in thermal treatment
A	Unmodified acacia	Reference, 50°C oven-drying	14	-	-
AC	Thermo-mechanically modified acacia	Compression, kiln drying	10	14%	-
ACT	Thermo-mechanically modified acacia with subsequent thermal modification	Compression & thermal treatment	9	14%	210 °C, 3h
K	Unmodified rubberwood	Reference, 50°C oven-drying	12	-	-
KC	Thermo-mechanically modified rubberwood	Compression, kiln drying	11	12%	-
KCT	Thermo-mechanically modified rubberwood with subsequent thermal modification	Compression & thermal treatment	10	12%	210 °C, 3h

 Table 2. Mean value (\bar{x}) and standard deviation (s) of physical and mechanical properties

Treatment	MC (%)		Dry density (kg/m ³)		MOE (MPa)		HB (kg/mm ²)		CS-C (MPa)		CS-S (MPa)	
	\bar{x}	s	\bar{x}	s	\bar{x}	s	\bar{x}	s	\bar{x}	s	\bar{x}	s
	Untreated (A)	65.8	27.3	571	65	10.6	2.3	2.6	0.9	49.6	2.0	49.6
Compression (AC)	7.1	2.2	590	79	9.8	1.2	2.8	1.1	56.5	2.8	61.2	1.9
Compression & thermal (ACT)	3.1	0.4	553	70	10.6	1.0	1.9	0.6	58.8	1.9	61.0	3.1
Untreated (K)	47.9	7.2	620	40	8.1	0.8	2.5	0.5	49.7	1.4	49.7	1.4
Compression (KC)	6.0	0.3	665	40	11.3	1.4	3.9	0.9	59.4	1.9	59.8	2.4
Compression & thermal (KCT)	4.2	0.2	615	38	11.1	0.8	2.3	0.4	60.8	1.7	63.5	1.2

 Table 3. Mean value (\bar{x}), standard deviation (s), and significance level (p) of dimensional stability in tangential (T), longitudinal (L) and radial (W) directions

Treatment	Swelling T	Swelling L	Swelling W	
A	\bar{x}	1.1%	0.2%	0.7%
	s	0.7%	0.1%	0.5%
	p	0.001*	0.666	0.202

Effect of Thermo-Mechanical Modification on Mechanical Properties and Water Resistance of Plantation-Grown Vietnamese Acacia and Rubberwood

AC	\bar{x}	5.4%	0.1%	0.9%
	<i>s</i>	1.5%	0.3%	0.6%
	<i>p</i>	0.000*	0.978	0.616
ACT	\bar{x}	3.5%	0.1%	1.3%
	<i>s</i>	2.9%	0.1%	0.7%
	<i>p</i>	0.045*	0.996	0.022*
K	\bar{x}	2.7%	0.1%	2.3%
	<i>s</i>	0.8%	0.3%	1.1%
	<i>p</i>	0.000*	0.958	0.001*
KC	\bar{x}	7.4%	-0.1%	1.3%
	<i>s</i>	1.1%	0.1%	0.4%
	<i>p</i>	0.000*	0.987	0.231
KCT	\bar{x}	5.8%	-0.0%	1.8%
	<i>s</i>	0.9%	0.1%	0.4%
	<i>p</i>	0.000*	1.000	0.001*

Table 4. Significance level of the difference in dry density, MOE, Brinell hardness (HB), compression strength in the core (CS-C) and surface layer (CS-S), and swelling (T) between different treatments (significant at $p \leq 0.05$, marked with*)

Factor	Dry density	MOE	HB	CS-C	CS-S	Swelling T
A-AC	0.786	0.478	0.538	0.176	0.004*	0.000*
A-ACT	0.826	0.998	0.008*	0.124	0.021*	0.012*
AC-ACT	0.493	0.584	0.001*	0.974	1.000	0.085
K-KC	0.027*	0.000*	0.000*	0.007*	0.005*	0.000*
K-KCT	0.959	0.000*	0.578	0.002*	0.000*	0.000*
KC-KCT	0.019*	0.806	0.000*	0.981	0.597	0.002*



Fig. 1. A set of acacia boards (60×80×1200 mm) after the compression and thermal modification process.

Variability in content of hydrophilic extractives and individual phenolic compounds in black locust stem

Viljem Vek¹, Ida Poljanšek¹ and Primož Oven¹

¹ Department of Wood Science and Technology
University of Ljubljana, Biotechnical Faculty
Jamnikarjeva 101, 1000, Ljubljana, Slovenia

ABSTRACT

*The main goal of this study was to investigate the amounts of hydrophilic extractives in bark and wood samples of black locust stem (*Robinia pseudoacacia* L.). The concentrations of extractives were highest in the outermost samples of heartwood. Knotwood of black locust contained less DHR than heartwood. Significantly less hydrophilic compounds were extracted from bark and sapwood samples. This study shows that heartwood of black locust can be considered a source of value-adding compounds. The investigation showed significant variability in the content of extractives in a radial direction and less pronounced axial variability within the black locust stems.*

1. INTRODUCTION

Black locust (*Robinia pseudoacacia* L.) heartwood is characterized by high resistance against fungi and insects and high natural durability, even when in water (Sachsse 1984; Scheffer and Morrell 1998). Black locust wood is therefore used in various external applications, such as shipbuilding, masts, mining timber and vineyards (Bostyn et al. 2018; Torelli 2003; Vítková et al. 2017). Despite the spread of this wood species in Europe (Vítková et al. 2017) and relatively broad applicability of its wood (Sachsse 1984; Torelli 2003), understanding of the content and distribution of extractives within a black locust tree remains surprisingly fragmentary.

A literature review revealed that either only axial or only radial variability in the content of extractives within a black locust tree has received attention. There has been no integral study showing not only the content of groups of extractives but data on the content of individual compounds within the tree. The distribution of characteristic phenolic compounds in the radial direction of the stem at different times in a season was provided by Magel et al. (1994; 1991) when studying heartwood formation in black locust. It was demonstrated that the extractive fraction soluble in a methanol/water solvent was higher in mature heartwood than in juvenile heartwood, but data on the content of individual compounds are not given (Dünisch et al. 2010; Latorraca et al. 2011). Axial variation of extractives within trees has been demonstrated with data on the fraction extracted with dichloromethane and the fraction obtained after extracting wood with hot water, but variation in the content of individual compounds was not shown. The content of hot-water extractives increased in heartwood but decreased in sapwood from the bottom to the top of the stems, while the reverse occurred for the dichloromethane extractive content of sapwood (Adamopoulos et al. 2005).

The aim of the investigation was qualitative and quantitative analysis of hydrophilic extractives in bark and wood samples of black locust (*Robinia pseudoacacia* L.). The radial and axial variability of hydrophilic extractives and individual compounds was also investigated within the trees. In addition to intact stem samples that included sapwood, heartwood and knots, a sample of wounded stem was included in the research in order to evaluate the contribution of traumatic structure to the variability of extractives and to examine the content of extractives in compartmentalization tissues that are formed after wounding.

* Corresponding author; e-mail: viljem.vek@bf.uni-lj.si

2. MATERIALS AND METHODS

2.1. SAMPLING OF BLACK LOCUST TREES

Bark and wood samples of six adult black locust (*Robinia pseudoacacia* L.) trees felled at the end of January 2016 in a suburban forest (44°56'46.8"N 13°40'05.1"E) were included in the present investigation. The sample trees were on average 22 m high, with a diameter of 26 cm at breast height (Vek et al. 2019). Four stem disks were sawn from each felled tree at 0.20 m, 3.30 m, 6.40 m, and 9.50 m. Discs containing knotwood (KW) were sampled in the crowns of the harvested trees.

After the sample discs had been air dried for a month, a radial profile of stem wood was obtained by taking an oriented series of samples in a direction from the periphery towards the pith (Fig. 1). One sample of bark (B), one sample of sapwood (SW) and several samples of heartwood (HW) were taken from each of the sampled stem discs. Heartwood was sampled according to the age of samples (number of annual rings). The youngest outermost heartwood sample was marked HW1 and the oldest sample near the pith HW5 (Fig. 1). Because some of the stems had been injured, wound-associated wood was also sampled. The reaction zone (RZ), wound-wood (WW) and discoloured and/or decayed wood (DW) were sampled as already described (Vek et al. 2014).

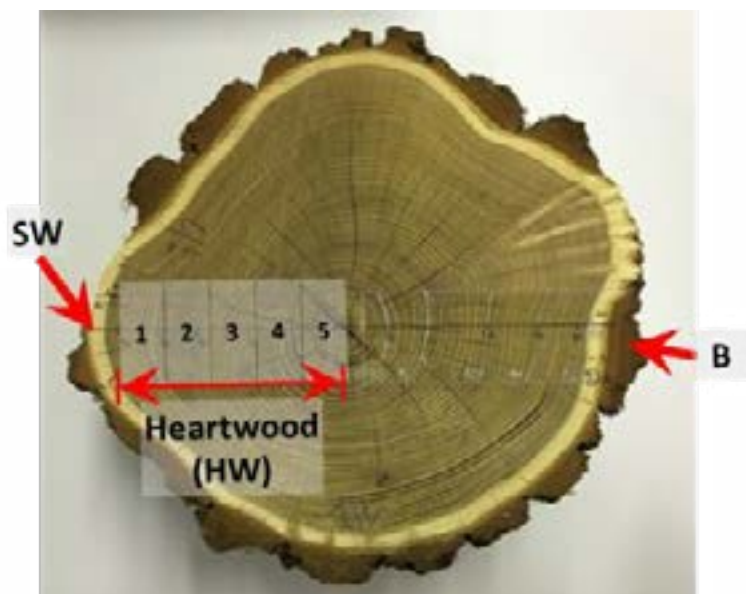


Figure 1: Stem disc of black locust (*Robinia pseudoacacia* L.).

All sample discs were visually inspected and the position of sampling was defined (Fig. 1). The age of samples was estimated by counting the annual growth rings. More than 170 samples of black locust were prepared for the purposes of the study. Following overnight oven drying at 50 °C, wood blocks were disintegrated with a Retsch SM 2000 cutting mill using a 1 mm bottom sieve. The wood meal was placed in sealed bottles and stored in a dark and cold place until further analysis.

2.2. EXTRACTION OF BARK AND WOOD SAMPLES

Before extraction, the bark and wood samples of black locust were freeze-dried in a Telstar LyoQuest lyophilizer at 0.040 mbar and - 82 °C, to a constant mass. Extraction of the dried material was done in a Soxhlet apparatus with 90% acetone (aq, v/v) for 6 hours at 110 °C, according to the protocol described in Vek et al. (2019). All the extracts were transferred into amber-coloured bottles and stored in a freezer at -25 °C.

2.3. CHEMICAL ANALYSIS OF BLACK LOCUST EXTRACTIVES

The content of hydrophilic extractives was measured gravimetrically by drying 10 ml of wood extract to a constant mass (mg/g dw).

Total phenols were measured according to a protocol similar to those already described (Scalbert et al. 1989; Singleton and Rossi 1965; Vek et al. 2013; Vek et al. 2014). However, diluted 2N Folin-Ciocalteu's phenol reagent (aq) and an aqueous solution of sodium carbonate (75 g/l) were added to each wood extract. The reaction was performed in a 4.5 ml disposable macro cell closed with a 10 × 10 mm polyethylene lid. After incubation of the reaction mixtures, the absorbance was measured at 765 nm by Perkin-Elmer Lambda UV-Vis. Gallic acid was used as a reference for semi-quantitative and relative evaluation of total phenols. The results were determined by the standard curve of gallic acid (concentration range between 0 mg/l and 500 mg/l) and expressed in milligrams of gallic acid equivalents per gram of dried wood sample (mg GAE/g).

Detailed information on chemical identities and quantities of compounds was obtained by high performance liquid chromatography (HPLC). Chromatographic analysis was performed on the Thermo Scientific Accela HPLC system. The HPLC had a quarter 600 pump and a photodiode array detector (PDA). Separation of samples was done on a Thermo Accucore C18 column (4.6 ID × 150 mm, 2.6 μm). Water (A) and methanol (B), both containing 0.1% of formic acid, served as a mobile phase. The flow rate of the mobile phase was set at 1000 μl/min. The gradient used was 5 - 95% of solvent (B). Both the auto-sampler containing sample trays and the column oven were thermostated, at 5 °C and 30 °C, respectively. Three microliters of wood extract were injected into the column for each HPLC run. Absorbance was measured at 280 nm and UV spectra were recorded from 200 nm to 400 nm. Robinetin (Rob) was also qualitatively checked at 363 nm, which gave a maximum absorption for Rob. Peak identities were investigated by comparison of retention times and UV spectra of separated compounds with those of analytical standards. Dihydrorobinetin (DHR), Rob and piceatannol (PT) were identified and quantified. The samples were measured in triplicate. The contents were expressed in milligrams of dihydrorobinetin (DHR) and robinetin (Rob) per gram of dry wood (mg/g dw). The chromatographic method was linear in the selected concentration range ($R^2 \geq 0.99$).

2.4. STATISTICS

Basic statistical analysis was performed with Statgraphics software. The data were first checked for normal distribution, and analysis of variance (ANOVA) and Fisher's least significant difference (LSD) procedure at a 95.0% confidence level were performed. Structural formulas of compounds were prepared with Perkin Elmer's ChemDraw software.

3. RESULTS AND DISCUSSION

3.1. QUALI- AND QUANTITATIVE COMPOSITION OF BARK AND WOOD EXTRACTS OF BLACK LOCUST

Extraction of bark and wood samples gave comparable amounts of hydrophilic extractives (HE) (ANOVA, $p = 0.076$). Extraction of more than one hundred samples showed HW of black locust to contain an average of 6.05 % (w/w dw) of hydrophilic extractives (HE). In contrast to Sablik et al. (2016), the HW of trees investigated in our study contained larger amounts of HE than bark (B) samples. Knotwood (KW) and heartwood (HW) samples contained higher contents of HE than did bark (B) and sapwood (SW) (Fig. 2) (LSD test). The relatively large amount of HE in SW samples can be explained by the presence of non-structural storage carbohydrates in sapwood (Höll 1972; Magel et al. 1994).

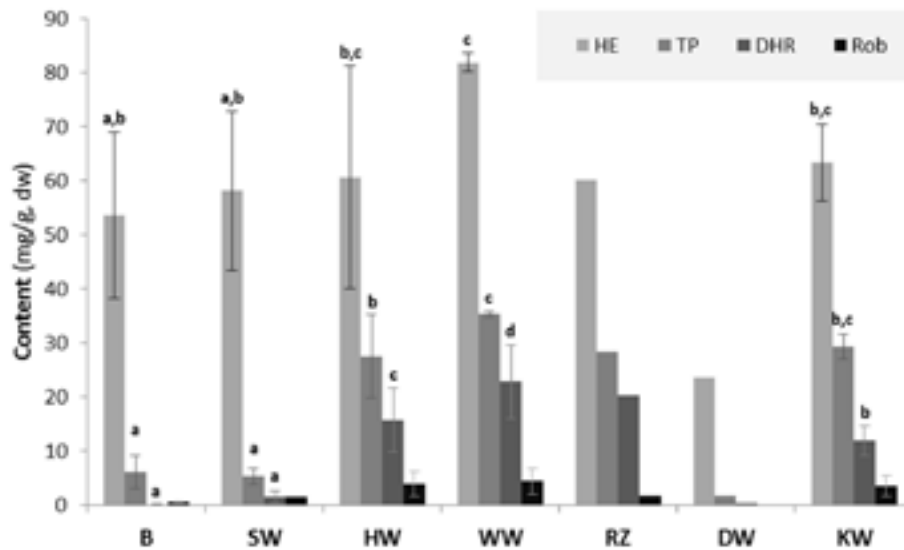


Figure 2: Content of hydrophilic extractives (HE), total phenols (TP), dihydrorobinetin (DHR) and robinetin (Rob) in bark and wood samples of black locust (*Robinia pseudoacacia* L.). B = bark; SW = sapwood; HW = heartwood; WW = wound-wood; RZ = reaction zone; DW = decayed wood; KW = knotwood. ^{a-d}, different letters on the error bars of the same series of columns indicate statistically significant differences at a 95% confidence level (LSD test).

Spectrophotometric analysis revealed significant differences in total phenols (TP) among the studied samples of black locust (ANOVA, $p_{TP} < 0.001$, $p_{DHR} < 0.001$) (Fig. 2), while HPLC analysis confirmed DHR to be the dominant and characteristic compound of wood extracts of black locust (Fig. 2), accompanied by the presence of low amounts of Rob and PT. Chromatographic analysis revealed significant differences in the content of DHR among the studied samples of black locust (ANOVA, $p_{TP} < 0.001$, $p_{DHR} < 0.001$) (Fig. 2). The largest contents of Rob were measured in HW (3.9 ± 2.30 mg/g) and KW ($3.4 \text{ mg} \pm 1.88$) extracts. However, the content of Rob was excluded from statistical analysis since the measured values were not normally distributed. The data were positively skewed, meaning that low Rob contents occurred more often than would be expected with a normal distribution. A skewed distribution of the concentrations of phenolic extractives in heartwood samples of Scots pine (*Pinus sylvestris* L.) was also reported by Harju and Venäläinen (2006).

Among the samples of intact stems (B, SW, HW, KW), the highest amounts of phenolic extractives (TP) and DHR were characteristic of HW and KW samples (LSD test) (Fig. 2). Significantly lower amounts were measured in B and SW (Fig. 2). Analysis of SW revealed the presence of DHR only. Only B extracts contained piceatannol (PT) in addition to DHR and small amounts of Rob. On average, 60.5 ± 20.6 mg/g of HE, 27.5 ± 7.62 mg/g of TP, 15.7 ± 5.87 mg/g of DHR, and 3.9 ± 2.30 mg/g of Rob were measured in the HW samples. Compared to SW samples, the amounts of DHR and Rob in HW extracts were 10.5- and 2.7-times larger. These results confirm the findings of other research groups that have reported the chemical composition of extractives in wood of black locust (Bostyn et al. 2018; Magel et al. 1994; Reinprecht et al. 2010; Sablik et al. 2016). Slightly higher amounts of DHR and Rob were mentioned in the reports of Sanz et al. (2011; 2012b).

HW samples contained significantly larger amounts of DHR than did KW samples (LSD test) (Fig. 2). On the other hand, KW contained significantly larger amounts of phenolic compounds than B, SW and HW (LSD test) (Fig. 2). Compared to the stemwood samples of black locust, the relative contents of extractives in KW were not as high as has been reported for coniferous knotwood, in which knots contained more than hundreds of times more phenolic extractives than heartwood of the same tree (Willför et al. 2003a; Willför et al. 2003b; Willför et al. 2004).

The presence of DHR in bark samples of black locust has already been reported by other research groups (Magel et al. 1994), whereas the presence of PT in bark extract is reported here for the first time. It was reported that larger amounts of B extractives than obtained in our study can be gained by extracting bark of black locust with a mixture of methanol and water (Sablik et al. 2016). PT and resveratrol were identified at a significant concentration in mature heartwood of black locus by Sergent et al. (2014), but this was not confirmed by our chromatographic analysis. In addition to flavonoids, bark of trees can contain polyphenols of higher molecular mass, i.e., condensed tannins (Holmbom 2011; Smith et al. 1989). Oligomers of condensed tannins containing robinetinidol, i.e., prorobinetinidins,

have also already been reported for seasoned HW of black locust (Sanz et al. 2012a; Sanz et al. 2011). These compounds were not recovered from the samples with the extraction procedure applied in our study.

3.2. VARIABILITY OF EXTRACTIVES WITHIN TREES

Table 1 shows the distribution of extractives along the black locust stems in HW only. Our investigation showed an absence of significant vertical variation in the average amounts of HE, TP and DHR along the stems of the investigated trees (ANOVA; p HE > 0.050, p TP > 0.050, p DHR > 0.050) (Table 1). In spite of the ANOVA results, a clear decrease of the DHR content with increasing height of the HW sampling can be read from Table 1. Our investigation showed that the HW disc samples taken at 0.2 m had significantly larger DHR contents than samples taken at 9.5 m (Table 1) (LSD test). Similar findings for HE were reported for B by Adamopoulos et al. (2005), but the authors extracted larger amounts of HE from the HW samples from a tree top (Adamopoulos et al. 2005).

Table 1: Contents of hydrophilic extractives, total phenols and dihydrorobinetin in heartwood (HW) samples of black locust (*Robinia pseudoacacia* L.). Discs containing heartwood samples were taken at 0.2 m, 3.3 m, 6.4 m and 9.5 m above the ground.

Sampling height	Hydrophilic extractives (mg/g dw)		Total phenols (mg GAE/g dw)		Dihydrorobinetin (mg/g dw)	
	avg	SD	avg	SD	avg	SD
	0.2	62.1 ^a	25.14	28.9 ^a	8.14	18.4 ^b
3.3	57.0 ^a	19.89	26.4 ^{a,b}	8.23	15.6 ^{a,b}	5.50
6.4	64.9 ^a	19.91	28.1 ^{a,b}	8.25	15.7 ^{a,b}	5.13
9.5	57.6 ^a	16.25	27.5 ^{a,b}	5.26	14.1 ^a	5.03

^{a-b}; Different letters within the same column indicate statistically significant differences at a 95.0% confidence level (Fisher's least significant difference (LSD) procedure).

The content of hydrophilic extractives was highest in the younger part of the heartwood. The extracts of older parts of heartwood (HW4 and HW5) had comparable HE concentrations as B and SW samples (LSD test). In comparison to the oldest HW5 samples, significantly more HE was extracted from B and SW. Significant differences in the content of HE, total phenols and DHR were found for the HW samples of the radial series (ANOVA, p HE < 0.001, p TP < 0.001, p DHR < 0.001). The LSD test showed that the youngest heartwood (HW1) contained significantly higher amounts of hydrophilic extractives, total phenols and DHR than older parts (HW2, HW3, HW4, and HW5). This is in contrast to Magel et al. (1994), who found that DHR augmented within the heartwood up to a more or less constant level irrespective of the sampling season. On the other hand, maximum values of Rob have been shown to be characteristic of older parts of HW (Magel et al. 1994). The relatively regular distribution of phenolic compounds in HW observed in our study could hardly be explained solely by variation in the content of non-structural carbohydrates at the sapwood-heartwood boundary, which are considered to be a major source of heartwood compounds in black locust (Magel et al. 1994; 1991). We assume that the smaller content of phenolic extractives from the HW samples in the inner parts of a black locust stem can be explained by the phenolics being chemically bonded to the cell wall and being therefore not extractable with the extraction conditions used in this study. This is in accordance with UV microspectrophotometry results showing a higher content of flavonoids deposited in the walls of cells in mature (inner) HW than in juvenile (outer) HW (Dünisch et al. 2010).

3.3. EXTRACTIVES IN TRAUMATIC WOOD STRUCTURES

The phytochemical profile of wound associated wood tissues differed from that of intact stemwood. The highest amounts of HE were found in wound-wood (WW), which is formed because of stem injury (LSD test). Chemical analysis revealed that WW contained 81.8 ± 1.72 mg of HE, 35.3 ± 0.55 mg/g of total phenols, 22.8 ± 6.75 mg/g of DHR and 4.5 ± 2.36 mg/g of Rob (Fig. 2). It is assumed that the higher content of HE and TP in WW than in intact SW and HW can be explained by the two-stage process, which involves WW formation and therefore transformation of WW to HW. This observation indicates that DHR may be classified as phytoalexin (Hart and Shrimpton 1979; Pearce 1990; Sergent et al. 2014), although further studies are needed to confirm this speculation.

The lowest concentrations of HE were measured in decayed wood (DW) (LSD test) (Fig. 2). Lower amounts of extractives and the absence of DHR and Rob in DW can be explained by fungal degradation of flavonoids. The reaction

zone (RZ) was a narrow and darkly coloured morphological barrier that separated heartwood from decayed parts in a stem, contained significantly larger amounts of quantified hydrophilic extractives than DW and higher amount of DHR than unaffected HW. These results support the finding (Vek et al. 2014) that traumatic tissues formed in wood contribute to the variability of extractive content within a tree.

4. CONCLUSION

The results of the study indicate a significant radial and less pronounced axial variability in the amounts of extractives in intact stem tissues of black locust (*Robinia pseudoacacia* L.). The highest contents of hydrophilic extractives, total phenols, dihydrorobinetin and robinetin were characteristic of heartwood. Lowest amounts of hydrophilic extractives were extracted from sapwood and bark. Examination of extractives content along the trees revealed that the content of DHR decreases acropetally.

ACKNOWLEDGEMENTS

The authors would like to thank Urban Innovative Actions (project Applause, UIA02-228) and the Slovenian Research Agency for financial support of program P4-0015. Many thanks also to Mrs. Helena Zorn and Mr. Miloš Mervič, both from the Slovenia Forest Service (Tolmin Regional Unit), for providing professional assistance with collecting the material, and to Mr. Martin Cregeen for language editing. The guideline and template has been kindly provided for use by the International Scientific Conference on Hardwood Processing - ISCHP2019.

REFERENCES

- Adamopoulos S, Voulgaridis E, Passialis C (2005) Variation of certain chemical properties within the stemwood of black locust (*Robinia pseudoacacia* L.) *Holz Roh- Werkst* 63:327-333.
- Bostyn S, Destandau E, Charpentier J-P, Serrano V, Seigneur J-M, Breton C (2018) Optimization and kinetic modelling of robinetin and dihydrorobinetin extraction from *Robinia pseudoacacia* wood *Ind Crops Prod* 126:22-30.
- Dünisch O, Richter HG, Koch G (2010) Wood properties of juvenile and mature heartwood in *Robinia pseudoacacia* L *Wood Sci Technol* 44:301-313.
- Harju AM, Venäläinen M (2006) Measuring the decay resistance of Scots pine heartwood indirectly by the Folin-Ciocalteu assay *Can J For Res* 36:1797-1804
- Hart JH, Shrimpton DM (1979) Role of stilbenes in resistance of wood to decay *Phytopathology* 69:1138-1143.
- Höll W (1972) Starke und Starkeenzyme im Holz van *Robinia pseudoacacia* L. *Holzforschung* 26:41-45.
- Holmbom B (2011) Extraction and utilisation of non-structural wood and bark components. In: Alén R (ed) *Biorefining of forest resources. vol book 20. Paper Engineers' Association/Paperi ja Puu Oy, Helsinki*, pp 178-224.
- Latorraca JVF, Dunisch O, Koch G (2011) Chemical composition and natural durability of juvenile and mature heartwood of *Robinia pseudoacacia* L. *Anais Da Academia Brasileira De Ciencias* 83:1059-1068.
- Magel E, Jayallemand C, Ziegler H (1994) Formation of heartwood substances in the stemwood of *Robinia pseudoacacia* L. II. Distribution of nonstructural carbohydrates and wood extractives across the trunk *Trees-Struct Funct* 8:165-171.
- Magel EA, Drouet A, Claudot AC, Ziegler H (1991) Formation of heartwood substances in the stem of *Robinia pseudoacacia* L. I. Distribution of phenylalanine ammonium lyase and chalcone synthase across the trunk *Trees-Struct Funct* 5:203-207.
- Pearce RB (1990) Occurrence of decay-associated xylem suberization in a range of woody species *Eur J Plant Pathol* 20:275-289
- Reinprecht L, Zubkova G, Marchal R (2010) Decay resistance of laminated veneer lumbers from black locust wood *Wood research* 55:39-52.
- Sablík P, Giagli K, Paril P, Baar J, Rademacher P (2016) Impact of extractive chemical compounds from durable wood species on fungal decay after impregnation of nondurable wood species *Eur J Wood Wood Prod* 74:231-236.
- Sachsse H (1984) *Einheimische nutzhölzer und ihre bestimmung nach makroskopischen merkmalen*. Verlag Pul Parey, Hamburg, Berlin
- Sanz M, de Simon BF, Cadahia E, Esteruelas E, Munoz AM, Hernandez MT, Estrella I (2012a) Polyphenolic profile as a useful tool to identify the wood used in wine aging *Analytica Chimica Acta* 732:33-45.
- Sanz M et al. (2011) Effect of toasting intensity at cooperage on phenolic compounds in acacia (*Robinia pseudoacacia*) heartwood *J Agric Food Chem* 59:3135-3145.

- Sanz M *et al.* (2012b) Polyphenols in red wine aged in acacia (*Robinia pseudoacacia*) and oak (*Quercus petraea*) wood barrels *Analytica Chimica Acta* 732:83-90.
- Scalbert A, Monties B, Janin G (1989) Tannins in wood: Comparison of different estimation methods *J Agric Food Chem* 37:1324-1329.
- Scheffer TC, Morrell JJ (1998) *Natural durability of wood: A worldwide checklist of species*. Oregon State University. Research Contribution 22
- Sergent T, Kohnen S, Jourez B, Beauve C, Schneider YJ, Vincke C (2014) Characterization of black locust (*Robinia pseudoacacia* L.) heartwood extractives: identification of resveratrol and piceatannol *Wood Sci Technol* 48:1005-1017.
- Singleton VL, Rossi JA, Jr. (1965) Colorimetry of total phenolics with phosphomolybdic-phosphotungstic acid reagents *Am J Enol Vitic* 16:144-158.
- Smith AL, Campbell CL, Walker DB, Hanover JW (1989) Extracts from black locust as wood preservatives: Extraction of decay resistance from black locust heartwood *Holzforschung* 43:293-296.
- Torelli N (2003) Robinija (*Robinia pseudoacacia* L.) in njen les *Les* 54:6-10.
- Vek V, Oven P, Poljansek I (2013) Content of Total Phenols in Red Heart and Wound-Associated Wood in Beech (*Fagus sylvatica* L.) *Drvna Ind* 64:25-32.
- Vek V, Oven P, Ters T, Poljansek I, Hinterstoisser B (2014) Extractives of mechanically wounded wood and knots in beech *Holzforschung* 68:529-539.
- Vek V, Poljanšek I, Oven P (2019) Efficiency of three conventional methods for extraction of dihydrorobinetin and robinetin from wood of black locust *Eur J Wood Wood Prod* 77: 891-901 doi:10.1007/s00107-019-01430-x
- Vítková M, Müllerová J, Sádlo J, Pergl J, Pyšek P (2017) Black locust (*Robinia pseudoacacia*) beloved and despised: A story of an invasive tree in Central Europe *For Ecol Manage* 384:287-302.
- Willför S, Hemming J, Reunanen M, Eckerman C, Holmbom B (2003a) Lignans and lipophilic extractives in Norway spruce knots and stemwood *Holzforschung* 57:27-36.
- Willför S, Hemming J, Reunanen M, Holmbom B (2003b) Phenolic and lipophilic extractives in Scots pine knots and stemwood *Holzforschung* 57:359-372.
- Willför S, Nisula L, Hemming J, Reunanen M, Holmbom B (2004) Bioactive phenolic substances in industrially important tree species. Part 1: Knots and stemwood of different spruce species *Holzforschung* 58:335-344.

Thermally modified birch wood interaction with liquids

Dace Cirule^{1*}, Anrijs Verovkins¹, Ingeborga Andersone¹, Edgars Kuka^{1,2}, and Bruno Andersons¹

¹Laboratory of Wood Biodegradation and Protection
Latvian State Institute of Wood Chemistry
Riga, LV-1006, Latvia

²Faculty of Material Science and Applied Chemistry
Riga Technical University
Riga, LV-1048, Latvia

ABSTRACT

*Large research work is currently being performed concerning different elaborated new wood protection methods. However, combining industrially well-approbated processes is also considered potentially quite promising and such approach is being actively studied. This study is part of a project that is aimed at improving wood service properties by combining thermal modification (TM) and impregnation with Cu-organic preservatives. The objective of the present study was to investigate peculiarities of interaction between liquids and TM birch wood (*Betula* spp.). This knowledge is essential for proper TM wood post-treatments involving its impregnation as well as for evaluation of potential wood moisture dynamics in outdoor applications.*

Changes caused by TM (150-170°C) in a closed system under elevated pressure in wood wettability, permeability, liquid absorption capacity, and drying characteristics were evaluated. The results concerning absorption capacity, which is mainly related to wood anatomical features and is density dependent, indicated to reduced absorption capacity of TM wood compared with unmodified birch of similar density. Permeability, which characterises the ease with which liquid is transported through wood porous system, was evaluated by capillary absorption tests through the specimens' tangential and radial surfaces. TM made birch wood less permeable through both surfaces as well as less anisotropic regarding transverse absorption rates. Moreover, TM caused also decrease in drying rates for wood impregnated with both water as well as biocide solution. Reduction in permeability influences impregnation process of boards and not full saturation was detected for TM boards when impregnation schedule providing complete saturation for unmodified boards was applied. On the other hand, less water was absorbed by TM boards exposed to rain on outdoor weathering racks.

1. INTRODUCTION

Thermal modification (TM) is a commercial wood treatment method aimed at enhancement of wood dimensional stability and biological durability without using any chemicals. Several industrial-scale TM processes differing in the treatment parameters such as environment, temperature, time are developed and industrially implemented (Hill 2011). Despite process differences, all TM causes complex reactions including certain destruction of low-molecular substances and hemicelluloses, reorganisation of lignin and cellulose and evaporation of volatile compounds resulting in wood weight losses and alteration of its properties (Militz and Altgen 2014).

It is well recognized that regardless of the applied TM process and treatment parameters, reduction of certain degree in wood hygroscopicity, which characterizes the interaction between wood and water vapour, takes place. Changes in wood sorptive behaviour in various humidity ranges have been intensively studied and numerous results concerning different aspects of wood equilibrium moisture content (EMC) alteration due to TM are available. It is found that the reduction of EMC considerably varies depending on the used TM method, temperature, time as well as on the treated wood species and characteristics of the individual specimen (Chirkova et al. 2007, Militz and Altgen 2014, Willems et al. 2015).

Much less focus has been on studying peculiarities of interaction between TM wood with liquids. Moreover, the reported results are quite fragmentary and, contrary to the observed similar trend of reduced EMC due to the TM, no common trend has been found and both increase and decrease in wood liquid water uptake are reported for TM wood (Metsä-Korttilainen et al. 2006, Johansson et al. 2006, Pfriem 2011). In addition, majority of this research is done on softwoods. Another wood characteristic influencing its interaction with liquids is surface wettability which is evaluated by measuring contact angle. However, results regarding TM caused alteration of wood surface wettability also are inconsistent. Alongside with usually observed increase in contact angle due to the TM also decrease in contact angle for TM wood treated at lower temperatures are reported (Hakkou et al. 2005, Kocaefe et al. 2008, Metsä-Korttilainen and Viitanen 2012). Nevertheless, when used in exterior applications wood quite often is exposed to

* Corresponding author: E-mail: dace.cirule@edi.lv

occasional contact with liquid water in a form of rain or dew. Consequently water absorption of certain extent can take place which will inevitably influence wood moisture content. Alteration of wood moisture content causes dimensional changes that can result in surface check and crack formation. Moreover, elevated wood moisture content negatively affects its mechanical strength. In addition, moisture content is crucial for the germination and growth of decay fungi. Therefore, the time of wood wetness above certain critical level is of great importance. This time depends on both water absorption and desorption velocities implying the importance of drying rate when long wood service life expectations in outdoor use are considered. Impregnation with biocide or fire-retardant water solutions is another area for which knowledge about wood interaction with liquid water is of greater significance (Rapp et al. 200, Van Acker et al. 2015).

Nevertheless TM imparts improved bio-resistance to wood, adequate wood protection against biodegradation is ensured only by wood treatment at temperatures that cause significant reduction of wood mechanical strength (Kamdem et al. 2002, Metsä-Kortelainen and Viitanen 2010, Candelier et al. 2017). Consequently, the application area of TM wood with high bio-durability is greatly restricted due to its declined strength properties. On the other hand, the most efficient biocide compositions containing chromium and arsenic, that were traditionally most widely used for wood impregnation to upgrade its bio-resistance, have been banned because of concerns about their environmental effects. As a result impregnation with copper-based formulations has become the main preservation method in use (Freeman and McIntyre 2008). However, the service properties of wood materials impregnated with these formulations are often unsatisfactory unless high biocide dose is introduced into wood. Furthermore, despite numerous investigations, no other simple wood protection method has been found yet for fully satisfactory result regarding wood potential performance in its end-use.

Therefore different complex treatment processes, including pre- or post-treatment of TM wood, aimed at prolonging the service life of wood materials are now intensively investigated and the results reported (Ahmed et al. 2013, Wang et al. 2013, Baysal et al. 2014, Salman et al. 2016, Turkoglu et al. 2016).

The objective of the present study was to evaluate TM caused changes in birch (*Betula* spp.) wood interaction with liquid water and copper-based preservative solutions. This study is a part of the research project evaluating the possibility to improve wood bio-durability combining wood thermal treatment at mild conditions and impregnation with a commercial biocide. In the project two the most commercially important wood species of Latvia are used: the dominant softwood pine (*Pinus sylvestris* L.) and the dominant hardwood birch.

2. MATERIALS AND METHODS

2.1. MATERIALS

Kiln-dried boards of birch (*Betula* spp.) wood measuring $700 \times 100 \times 25$ mm were used for the thermal modification (TM). The modification was carried out in a multifunctional wood modification device of the WTT (Denmark) production. The boards were thermally treated in a closed system in a water-vapor medium under elevated pressure (0.6 – 0.8 MPa depending on the TM temperature) for 1 h at the peak temperature. Three peak temperatures were used: 150, 160 and 170 °C. The designations used in the present paper for wood treated at these temperatures are as follows: TM150, TM160, TM170. The TM boards were conditioned (RH 65 ± 5 %; 20 ± 2 °C) for at least two weeks before preparing the specimens for tests as well as subjecting them to impregnation.

2.2. IMPREGNATION

Impregnation was performed with boards ($700 \times 100 \times 25$ mm) as well as specimens of two sizes, namely, $20 \times 20 \times 5$ mm and $20 \times 20 \times 100$ mm ($R_{ad} \times T_g \times L$) which were conditioned before impregnation. Impregnation was performed with the vacuum-pressure method in a laboratory autoclave (vacuum 1 kPa for 30 min, pressure 0.8 MPa for 1 h). For impregnation water as well as copper-azole type biocide solutions of three concentration (0.5%, 0.85%, 1.2%) were used.

2.3. CONTACT ANGLE

Contact angle was measured with a goniometer Dataphysics OCA20 (Germany) by applying sessile-drop method and using water droplet with volume of 10 μ l. For each specimen contact angles were recorded for 10 droplets on the wood tangential surface during 30 s at a fixed interval of 1 s and the average contact angle values were calculated. Contact angles were measured for ten pre-conditioned (RH 65 ± 5 %; 20 ± 2 °C) specimens of each wood type.

2.4. LIQUIDS ABSORPTION

Capillary water absorption through radial (Rad) and tangential (Tg) surfaces was evaluated by using ten cubic specimens (20 x 20 x 20 mm) per surface with annual ring and grain orientations strictly parallel to the edges. Four contiguous walls of that one intended for water absorption were sealed with waterproof coating. After conditioning (RH 65 ± 5 %; 20 ± 2 °C) the specimens were installed into a frame that restricted water evaporation from the container and fixed in a position in which the contact surface was 2 ± 0.2 mm under the water. The weight of the specimens was regularly recorded during six days period. The test was carried out in controlled environment (RH 65 ± 5 %; 20 ± 2 °C).

Liquid absorption capacity of wood was evaluated by impregnation of small specimens (20 × 20 × 5 mm), which ensured liquid penetration into the entire specimen volume. The amount of absorbed liquid was determined gravimetrically by recording mass of specimen before and after impregnation.

For evaluation of liquid penetration into the middle part of boards, 10 cm long section from board middle was cut out immediately after board impregnation. The section was divided in 12 similar pieces and moisture content was gravimetrically measured for each piece. Average moisture content for edge pieces and central pieces was calculated.

For outdoor exposure boards measuring 700 × 100 × 25 with sealed end grains were installed on a weathering rack inclined at an angle of 45° to the horizontal and facing south. Collection of run-off rain water from each board was accomplished by fastening plastic edgings to prevent water miss and accumulating all water in a sealed bottle through a funnel fixed at the board end.

2.5. DRYING

Drying tests were performed on impregnated specimens of three size, namely, 20 × 20 × 5 mm, 20 × 20 × 100 mm, and 25 × 100 × 700 mm (boards). The specimens were impregnated according to the above described impregnation process and then exposed to drying at RH 65 ± 5 % and 20 ± 2 °C with regular mass control. The moisture content was calculated as the ratio to dry mass of the specimen.

3. RESULTS

3.1. CONTACT ANGLE

Wood surface wettability is influenced by many factors including its anatomical structure, density, and chemical composition. Certain alteration in these wood characteristics is typical for the wood subjected to the TM. Results of contact angle measurements for unmodified and TM birch wood are presented in Figure 1.

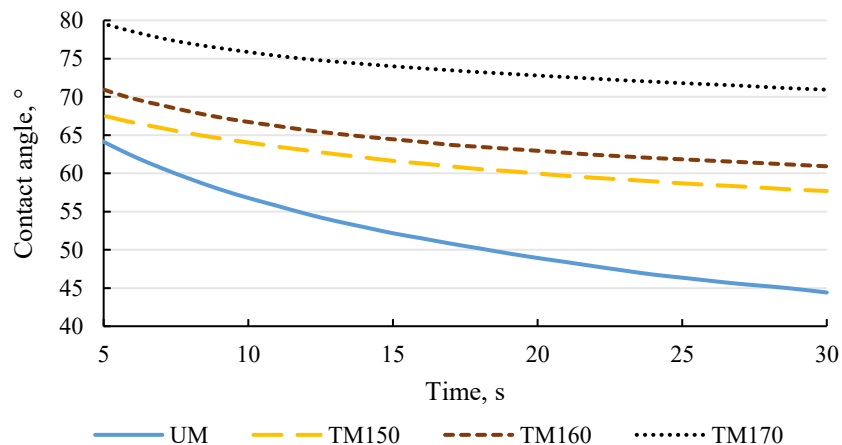


Figure 1: Contact angle of unmodified (UM) and thermally (TM) modified birch wood

As can be seen, the contact angles of the TM wood regardless of the treatment temperature are greater comparing with unmodified wood. This indicates to reduction in wettability of birch wood due to TM. Moreover, the higher the TM temperature the greater contact angle increase with more pronounced differences for TM wood treated at 170°C (TM170). This somewhat contradicts with the results reported by Kocaefe et al. (2008) who observed insignificant influence of the TM treatment temperature on the wood contact angle.

3.2. LIQUID WATER ABSORPTION

When wood is exposed to liquid water, water absorption into wood occurs through water vapour diffusion and liquid water capillary flow with the latter being the governing process in wood impregnation. Capillary absorption without applying any additional force characterizes the ease of the liquid penetration into wood. Capillary absorption depends on such wood characteristics as species, density, location of its origin in the trunk (sapwood, heartwood, juvenile wood), pretreatment history, as well as the penetrating liquid (Thomas 1976, Siau 1984, Johansson 2006). However, wood anisotropic anatomical structure causes significant differences of liquid flow in wood principal directions regardless of its characteristics. Common feature of all woods is that the flow rate in the longitudinal direction is much greater than in the lateral directions (Siau 1984). However, transverse movement of fluid is pivotal for wood impregnation treatment, as normally the ratio of the board transverse sections area is rather small and the liquid penetration through it is of secondary importance. Moreover, in wood outdoor applications predominately its lateral surfaces are exposed to potential contact with liquid water. Therefore, in the present study capillary absorption tests through wood radial and tangential surfaces were performed for evaluation of TM effect on wood liquid uptake characteristics.

Table 1: Capillary water absorption (g/m^2) of unmodified (UM) and thermally modified (TM) birch wood through radial (Rad) and tangential (Tg) surfaces

Wood type	Surface	Time, h				
		6	24	48	72	144
UM	Rad	356 (46)	649 (73)	869 (88)	1011 (96)	1431 (114)
	Tg	480 (66)	949 (130)	1320 (183)	1585 (226)	2293 (342)
TM150	Rad	172 (13)	327 (19)	462 (22)	562 (28)	859 (37)
	Tg	161 (11)	339 (21)	498 (30)	619 (37)	971 (56)
TM160	Rad	174 (19)	342 (35)	487 (47)	596 (56)	914 (83)
	Tg	177 (20)	351 (31)	506 (40)	622 (48)	935 (71)
TM170	Rad	91 (6)	201 (18)	301 (28)	370 (35)	556 (50)
	Tg	93 (8)	199 (17)	296 (25)	367 (29)	558 (44)

Standard deviations in parentheses

As it was expected, more water in equal time period was absorbed through the tangential surface (into radial direction) into unmodified birch wood (Table 1). This result agrees well with the findings that wood rays, which themselves enable liquid flow from the cambium towards the pith in living trees, are the dominant pathways for liquid water lateral ingress into wood. The predominant route for liquid transport through the radial surface (in tangential direction) goes through pits located in the radial walls of wood cells. However, hardwood fibres possess scanty pit structure which is the crucial obstacle influencing the tangential flow (Murmanis 1979, Siau 1984).

The results show that TM significantly retards liquid water uptake into birch wood through the both studied lateral surfaces. Johansson et al. (2006) detected reduction in water absorption rate also in longitudinal direction of TM birch wood. However, dissimilar extent of TM caused reduction in absorption rate was observed for water movement through the radial and tangential surfaces. Regardless of the applied TM temperature, greater decrease was recorded for capillary absorption through the tangential surface resulting in almost equal water uptake in both directions for the TM wood. These results demonstrate that TM makes birch wood more isotropic regarding lateral water absorption rate. Moreover, quite similar capillary absorption rate was detected for TM birch specimens treated at the two lower temperatures (TM150 and TM160). The highest used TM temperature (TM170) caused somewhat greater reduction through both surfaces but with the same trend of more reduction through the tangential surfaces resulting in similar water uptake regardless of the surface.

The laboratory results stating reduced liquid water absorption tendency of TM birch wood were confirmed also by a test in which unmodified and TM boards were exposed outdoors on weathering racks. Water absorption behaviour of the boards was measured indirectly by collecting the run-off water. The results are presented in Figure 2. Because of big variation in the water volumes collected after individual rain episodes, average amounts were calculated for each treatment and the results expressed as relative volumes to the run-off water collected from the unmodified boards.

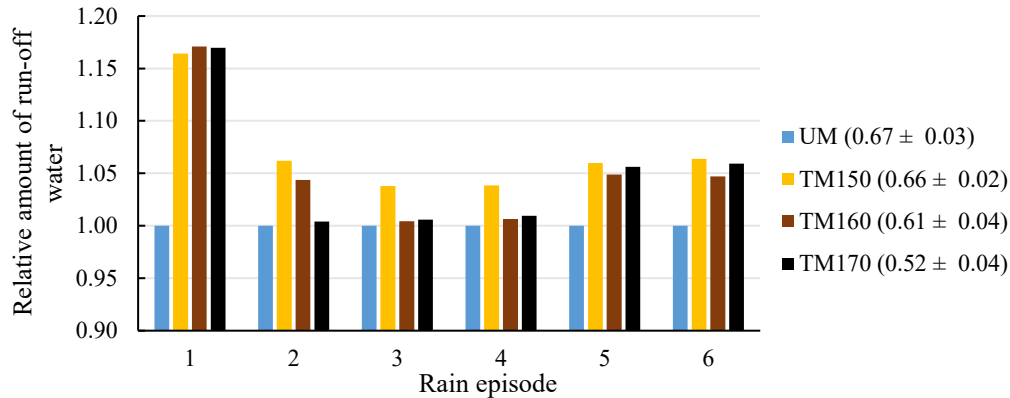
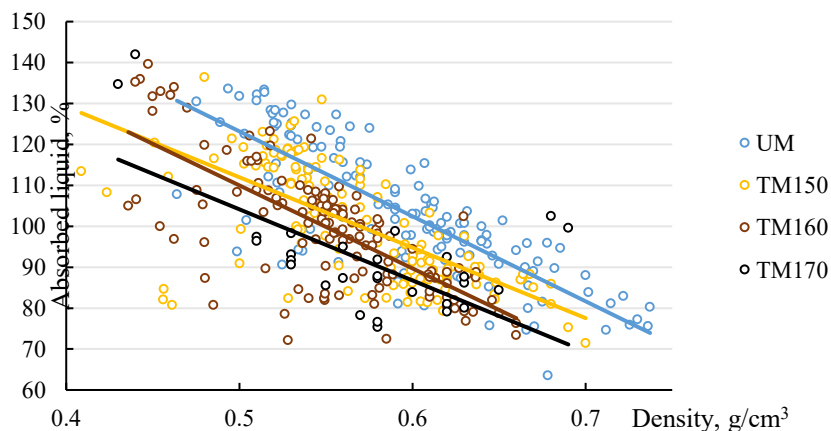


Figure 2: Relative amount of run-off water collected from unmodified (UM) and thermally modified (TM) boards exposed outdoors

In general more water was collected from the TM boards indicating that less water was absorbed by them. However, for certain rain episodes no difference was observed among TM boards treated at different temperatures as it could be expected from both the contact angle measurement and the capillary absorption test results. Moreover, just TM boards treated at the lowest temperature (TM150) absorbed less water which could be explained with wood structural and density peculiarities of individual boards. Another factor influencing absorption is the level of board re-drying before the next rain episode.

Liquid absorption capacity is another important wood characteristic when its impregnation is considered. It depends mainly on both the total wood porosity as well as interconnectivity of pores. To ensure complete liquid penetration, small specimens with high surface area to volume ratio (specific surface) and high ratio of the transverse surfaces were used for evaluation of wood liquid absorption capacity. No substantial difference of the absorbed amount was detected for the studied liquids, namely water and biocide solutions. Therefore in Figure 3 are presented joint results for absorbed amount of liquid depending on wood density without separating results of individual liquids.

Figure 3. Absorbed liquid of unmodified (UM) and thermally modified (TM) birch wood depending on wood density



As it was expected, the general trend for both unmodified and TM wood was that the absorbed liquid amount per mass of wood correlates with wood density and less liquid is absorbed by wood of higher density. Comparing unmodified and TM wood of similar densities, less liquid was absorbed by the TM wood. Moreover, the higher the TM temperature the more reduction was recorded in the absorbed liquid by wood of similar density. Zauer et al. (2013) have reported about decrease in wood cell wall density due to TM. On the other hand, reduction of bulk wood density

after TM also is reported (Widmann et al. 2012). Both these changes can have antipodal influence on the wood void volume which limits the potential amount of a liquid that can be introduced into wood. Another reason for reduction in absorption capacity could be formation of some closed cavities due to wood structural transformations caused by TM (Boonstra et al. 2006).

Penetration of the impregnation liquid into the whole volume is substantial prerequisite for high impregnation liquid retention and even distribution which are important indicators of treatment efficiency. Impregnation result depends mainly on wood permeability characteristics, impregnation solution chemical composition and the used treatment process (c-36). As it was demonstrated by the capillary absorption test, TM imparts reduced permeability to birch wood. However, during impregnation, the applied pressure not only aid liquid penetration into the wood through its capillary system but can also facilitate the liquid movement by creating extra pathways through entailing collapses in weaker wood anatomical structures. To evaluate the possible changes caused by the TM, boards were impregnated by applying treatment parameters found in preliminary experiments to ensure even liquid distribution throughout the whole board volume of unmodified birch wood. Similarly with the absorption capacity test, difference in introduced liquid amount depending on the used impregnation solution was not observed. In the Figure 4, average moisture content in centre and edges of board cross-section, calculated for all used impregnation solutions, are presented.

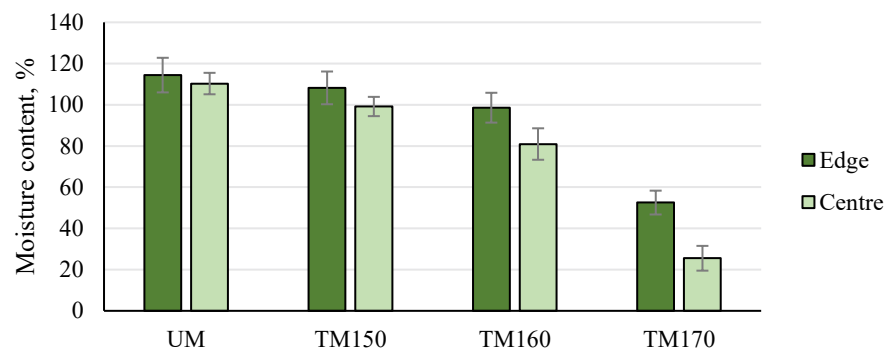
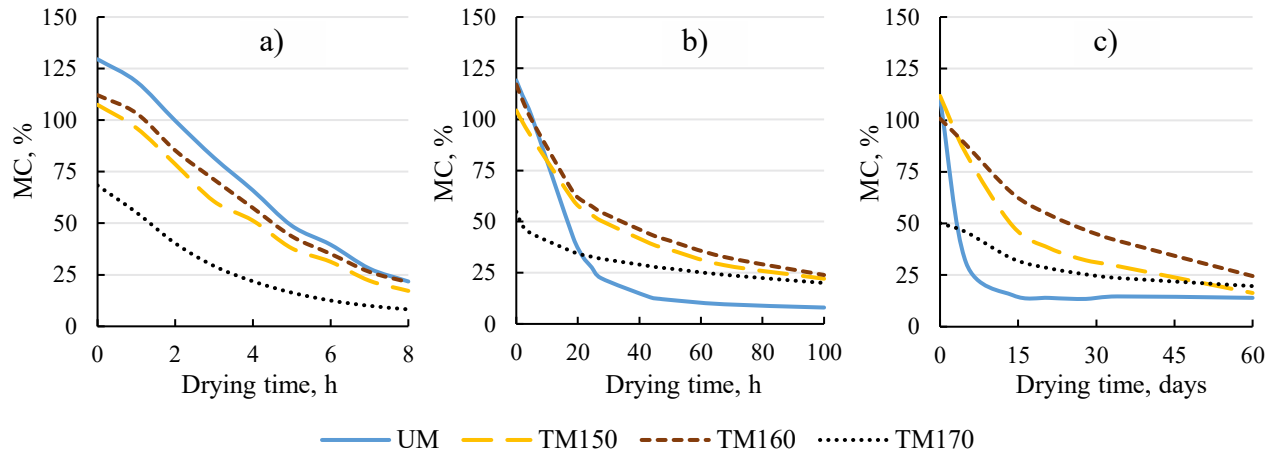


Figure 4: Moisture content in centre and edges of unmodified (UM) and thermally modified (TM) birch wood boards after impregnation

The lower moisture content of TM boards agrees with the finding of reduced absorption capacity comparing with unmodified wood. As it was expected, similar water content was detected in unmodified wood board central part and next to edges implying even distribution of the liquid through the board cross-section. The lowest treatment temperature (TM150) used in the present study did not cause substantial penetration unevenness in the impregnated boards. However, TM at higher temperatures impart wood characteristics that hinder penetration of liquid into wood not only in a case of capillary absorption but also when pressure is applied. Substantially lower moisture content detected in the board central part for TM wood treated at 160 °C and especially at 170 °C suggest necessity of longer impregnation time for satisfactory TM wood impregnation results. However, prolonged process time decreases production capacity and increases its costs.

3.2. WOOD DRYING

Wood drying is a complex process including free water transport caused by capillary forces and diffusion controlled evaporation (Siau, 1984). Proper drying rate is a favourable characteristic for wood materials that can come in contact with liquid water during their service life because extended desorption phase has a decisive influence upon the time with elevated moisture content (Rapp et al. 2000, Van Acker et al. 2015). Proper drying rate is a favourable characteristic for wood materials that can come in contact with liquid water during their service life. On the other hand, it was found that prolonged time of wood wetness after impregnation is advisable for copper fixation (Humar and Lesar 2009). In the present study, the focus was on the moisture exclusion from impregnated specimens up to wood moisture content (MC) of 25% which was suggested to be the limit of wood MC beyond which wood is subjected



to high degradation hazard (Rapp et al. 2000). The results of the drying tests are shown in Figure 5.

Figure 5: Moisture content (MC) changes during drying at RH 65% and 20°C of impregnated unmodified (UM) and thermally modified (TM) birch wood specimens of different size: a) 20×20×5 mm, b) 20×20×100 mm, c) 25×100×700 (boards)

Quite similar release of water was recorded for both unmodified and TM wood small specimens which were characterised by large specific surface (6.0 cm^{-1}) as well as high transverse surfaces proportion (67%) implying larger contribution of longitudinal water transport during drying (Figure 5a). Nevertheless slightly faster drying was observed for unmodified wood, TM wood treated at 170 °C reached MC of 25% most quickly because of the substantially less absorbed water during impregnation. The larger specimens were characterised by almost three times smaller surface area to volume ratio (2.2 cm^{-1}) and the transverse surfaces proportion of only 9%. For them not only reduction of drying rate in general but also substantial difference in drying rate between unmodified and TM specimens was observed (Figure 5b). In this experiment, it took 24 hours for the unmodified wood specimens to reach the 25% MC limit comparing with six hours in the experiment with the smaller specimens even though the initial MC of the smaller specimens was for 10% higher. However, the most pronounced effect of the different size and ratio of specimens was observed for the TM wood for which drying was considerably impeded. For the TM wood regardless of treatment temperature almost three times longer drying time was needed to reach the 25% MC limit comparing with unmodified wood. Extremely slow drying was detected for the TM wood treated at 170 °C.

Similar trend regarding significant differences of water release for unmodified and TM wood was observed also drying boards (Figure 5c). The unmodified boards reached the state of MC below 25% in less than one week while for TM boards it took four and more weeks depending on TM temperature. At 170 °C treated boards, likewise the specimens (20 × 20 × 100 mm) of the same treatment, released water most slowly. However, because of substantially lower initial MC, these boards reached the limit of 25% MC in shorter drying time compared with TM boards treated at lower temperatures. The results of drying experiments carried out on specimens of different size suggest that TM causes retardation of water exclusion from deeper layers. We hypothesize that the slowdown of water release from impregnated TM specimens of larger size could be caused by surface clogging with TM degradation products dissolved in water and transported towards the water evaporation zone. However this hypothesis must be proved in further experiments.

4. CONCLUSIONS

The results show that in the present study applied thermal modification in a closed system under elevated pressure caused substantial alteration in birch wood interaction with liquids. Similar results were observed when both water

and copper-azole type biocide solutions of different concentration were used for evaluations. The results demonstrate that wood wettability which was assessed by contact angle measurements and permeability which was evaluated by capillary water absorption in transverse directions (through tangential and radial surfaces) were reduced due to thermal modification. These changes make satisfactory impregnation of thermally modified birch wood more difficult comparing with unmodified wood. On the other hand decreased absorption of rain water was observed for thermally modified wood during its outdoor exposure. The results of the drying tests show that thermally modified birch wood dry much slower comparing with unmodified birch wood except specimens with very high surface-to-volume ratio. The hindered drying could be quite a challenge when impregnation is considered.

ACKNOWLEDGMENTS

The authors gratefully acknowledge the financial support by the European Regional Development Fund project No. 1.1.1.1/16/A/133.

REFERENCES

- Ahmed, S.A., L. Hansson, and T. Morén. 2013. Distribution of preservatives in thermally modified Scots pine and Norway spruce sapwood. *Wood Sci. Technol.* 47(3):499-513.
- Baysal, E., S. Degirmentepe, H. Toker, and T. Turkoglu. 2014. Some mechanical and physical properties of AD-KD 5 impregnated and thermally modified Scots pine wood. *Wood Research* 59(2):283-296.
- Boonstra, M.J., J.F. Rijdsdijk, C. Sander, E. Kegel, B. Tjeerdsma, H. Militz, J. Van Acker, and M. Stevens. 2006. Microstructural and physical aspects of heat treated wood. Part 2. *Hardwoods. Maderas. Ciencia y tecnologia* 8(3):209-217.
- Candelier, K., S. Hannouz, M.F. Thévenon, D. Guibal, P. Gérardin, M. Pétrissans, and R. Collet. 2017. Resistance of thermally modified ash (*Fraxinus excelsior* L.) wood under steam pressure against rot fungi, soil-inhabiting micro-organisms and termites. *Eur. J. Wood Prod.* 75(2):249-262.
- Chirkova, J., B. Andersons, I. Andersone. 2007. Study of the structure of wood-related biopolymers by sorption methods. *Bioresources* 4(3):1044-1057.
- Freeman, M. and C.R. McIntyre. 2008. A comprehensive review of copper-based wood preservatives. *Forest Prod. J.* 58(11):6-27.
- Hakkou, M., M. Pétrissans, A. Zoualiam and P. Gérardin. 2005. Investigations of wood wettability changes during heat treatment on the basis of chemical analysis. *Polymer Degradation and Stability.* 89:1-5.
- Hill, C.A.S. Wood modification: an update. *Bioresources* 6(2): 918-919.
- Humar, M. and B. Lesar. 2009. Influence of dipping time on uptake of preservative solution, adsorption, penetration and fixation of copper-ethanolamine based wood preservatives. *Eur. J. Wood Prod.* 67:265-270.
- Johansson, D., M. Sehlstedt-Persson and T. Morén. 2006. Effect of heat treatment on capillary water absorption of heat-treated pine, spruce and birch. In: *Wood Structure and Properties '06* Ed. by S.Kurjatko, J.Kúdela, and R.Lagaña, pp.251-255.
- Kamdem, D. P., A. Pizzi, and A. Jermannaud. 2002. Durability of heat-treated wood. *Holz als Roh- und Werkstoff* 60:1-6.
- Kocaeffe, D., S. Poncsak, G. Doré G., and R. 2008. Younsi. Effect of heat treatment on the wettability of white ash and soft maple by water. *Holz als Roh- und Werkstoff* 66:355-361.
- Metsä-Kortelainen, S., T. Antikainen, and H. Viitaniemi. 2006. The water absorption of sapwood and heartwood of Scots pine and Norway spruce heat-treated at 170°C, 190°C, 210°C and 230°C. *Holz als Roh- und Werkstoff* 64:192-197.
- Metsä-Kortelainen, S. and H. Viitanen. Wettability of sapwood and heartwood of thermally modified Norway spruce and Scots pine. *Eur. J. Wood Prod.* 70:135-139.
- Metsä-Kortelainen, S. and H. Viitanen. 2010. Effect of fungal exposure on the strength of thermally modified Norway spruce and Scots pine. *Wood Mater. Sc. Eng.* 1:13-23.
- Militz, H. and M. Altgen. 2014. Processes and properties of thermally modified wood manufactured in Europe. In: *Deterioration and Protection of Sustainable Biomaterials. ACS Symposium Series, vol. 1158:269-285.*
- Murmanis, L. and M. Chudnoff. 1979. Lateral flow in beech and birch as revealed by the electron micro-scope. *Wood Sci. Technol.* 13:79-87.
- Pfriem, A. 2011. Alteration of water absorption coefficient of spruce (*Picea abies* (L.) Karst.) due to thermal modification. *Drvna Industrija*, 62(4):311-313.
- Rapp, A.O., R.D. Peek, and M. Sailer. 2000. Modelling the moisture induced risk of decay for treated and untreated wood above ground. *Holzforschung* 54:111-118.
- Salman, S., A. Pétrissans, M.F. Thévenon, S. Dumarçay, and P. Gérardin. 2016. Decay and termite resistance of pine blocks impregnated with different additives and subjected to heat treatment. *Eur. J. Wood Prod.* 74(1):37-42.

-
- Siau J.F. 1984. *Transport Processes in Wood*. Spriner Verlag, Berlin, Heidelberg. 248 pp.
- Thomas, R.J. 1976. *Anatomical features affecting liquid penetrability in three hardwood species*. *Wood and Fiber* 7(4):256-263.
- Turkoglu, T., E. Baysal, M. Yuksel, H. Peker, C. Sacli, I. Kureli, and H. Toker. 2016. *Mechanical properties of impregnated and heat treated oriental beech wood*. *Bioresources* 11(4):8285-8296.
- Van Acke, J., J. Van den Bulcke, I. De Windt, S. Colpaert, and W. Li. 2015. *Moisture Dynamics of modified wood and the relevance towards decay resistance*. In: *Proceedings of the Eight European Conference on Wood Modification, October 26-27, 2015, Helsinki, Finland*. pp. 44-55.
- Wang, W., Y. Zhu, and J. Cao. 2013. *Evaluation of copper leaching in thermally modified southern yellow pine wood impregnated with ACQ-D*. *Bioresources* 8(3):4687-4701.
- Widmann, R., J.L. Fernandez-Cabo, and R. Steiger 2012. *Mechanical properties of thermally modified beech timber for structural purposes*. *Eur. J. Wood Prod.* 70(6):775-784.
- Willems, W., M. Altgen, and H. Militz. 2015. *Comparison of EMC and durability of heat treated wood from high versus low water vapour pressure reactor systems*. *Int. Wood Prod. J.* 6(1): 21-26.
- Zauer, M., A. Pfriem, and A. Wagenführ. 2013. *Toward improved understanding of the cell-wall density and porosity of wood determined by gas pycnometry*. *Wood Sci. Technol.* 47(6):1197-1211.

Performance of thermally modified beech and ash wood in outdoor applications

Miha Humar*, Boštjan Lesar, and Davor Kržišnik

Department for wood science and technology
University of Ljubljana, Biotechnical Faculty
Jamnikarjeva 101, SI1000, Ljubljana, Slovenia
miha.humar@bf.uni-lj.si

ABSTRACT

The majority of the European wood species are classified as non-durable according to EN 350 standard. Even important wood species like English oak are not classified as durable anymore. Regardless of that, there is a growing demand for durable wood used in exposed applications. In order to improve durability of non-durable wood species, there were various approaches developed. However, some of them, like biocidal protection, are not always accepted by customers. Therefore alternative methods for improvement of durability were developed, thermal wood modification being the most commercially successful. Although this method was developed quite some time ago, in service test of thermally modified hardwoods are rare. In order to assess performance of modified hardwoods (beech, ash) in service, model house was constructed in 2013 in Ljubljana. In the respective test facility, decking and façade elements are made of various modified (beech, ash) and non-modified hardwoods (beech, ash, English oak, sweet chestnut). Wood exposed in respective location is regularly monitored (moisture content, decay ...). Results of the model corresponds to the actual service life rather well. Development of decay depends of the exposure scenario. Beech wood exposed on decking is completely degraded. In addition, thermal modification seems to work fine on hardwood specimens, as there is no decay determined on none of the exposed samples after 5 years of exposure.

1. INTRODUCTION

Wood is one of the most important building materials. It is frequently used outdoors where it is exposed to weathering and degradation. In Europe, wood-degrading fungi are the predominant reason for failures of wood used in outdoor applications (Schmidt, 2006). In order to prevent fungal decay and to achieve desired service lives, there are various solutions used, namely use of biocides, wood modification, proper design, and use of domestic or imported durable wood species (Reinprecht, 2016). More recently, consumers are avoiding tropical wood species, therefore the importance of domestic wood species is increasing. Unfortunately, the majority of European wood species does not provide sufficiently high durability (CEN, 2016). Therefore, special emphasis is given to the utilization of domestic wood species (FTP, 2018).

Service life prediction of wooden objects is challenging, because the time during which a particular wooden structure will fulfil its function depends on a variety of factors such as wood material used, protection applied, and different climate-related parameters (Isaksson et al., 2013 and 2014). In addition to the material-inherent durability, the moisture and temperature conditions inside the wood, i.e., the material climate, are the most important factors influencing the ability of fungi to decompose wood (Schmidt, 2006; Brischke et al., 2008). These two factors are influenced by the design of the construction, the exposure conditions, and local climatic conditions (microclimate).

More recently, a new concept to characterize the durability of wood-based materials and to predict the service life of wood was proposed by Meyer-Veltrup et al. (2017; 2018) taking into account the material-inherent protective properties, the moisture performance and the climate and design induced exposure dose of wooden structures. This approach was successfully applied to untreated wood (De Angelis et al., 2018; Brischke et al., 2018). In this study, this modelling approach will be expanded to differently modified and wood treated with hydrophobic system.

2. MATERIAL AND METHODS

2.1. MATERIALS

This study investigated the performance of eight different wood species and wood-based materials used in a decking application (Table 1). The group of selected materials consisted of eight untreated wood species namely European beech (*Fagus sylvatica*), European ash (*Fraxinus excelsior*), Sweet chestnut (*Castanea sativa*) and English oak heartwood (*Quercus sp.*). Norway spruce (*Picea abies*) served as a reference.

Thermal modification (TM) was performed according to the commercial process Silvapro® (Silvaproduct, Slovenia) with initial vacuum in the first step of the treatment (Rep et al., 2004). The modification was performed for 3 h at the target temperature 210 °C. Impregnation was performed with a 5 % commercially available natural wax dispersion with solid content up to 50 % by weight (Montax 50, Romonta, Germany) (Humar et al., 2017). Impregnation was performed according to the full cell process in a laboratory impregnation setup. It consisted of 30 min vacuum (80 kPa), 180 min pressure (1 MPa), and 20 min vacuum (80 kPa).

Table 1: Eight different investigated wood species and wood-based materials

	Wood species					Treatment	
	Norway spruce (<i>Picea abies</i>)	European ash (<i>Fraxinus excelsior</i>)	European beech (<i>Fagus sylvatica</i>)	Sweet chestnut (<i>Castanea sativa</i>)	English oak (<i>Quercus sp.</i>)	thermal modification	impregnation with natural wax
Abbreviation	PA	FE	FS	CS	Q	TM	NW
PA	×						
FE		×					
FE-TM		×				×	
FS			×				
FS-TM			×			×	
FS-TM-NW			×			×	×
CS				×			
Q					×		

2.2. OUTDOOR EXPOSURE

Outdoor exposure was performed at wooden model house unit at the Department of Wood Science and Technology in Ljubljana, Slovenia (46°02'55.7"N 14°28'47.3"E, altitude 293 m), where the in-service performance of façade and decking elements were tested. The test specimens with a cross section of 2.5 × 5.0 cm² were exposed horizontally on the walls of the model house facing to all four cardinal directions. At least seven samples of the same material were exposed on the decking. The in-service testing started in October 2013 and the prime objective was to monitor the occurrence and development of decay (functional service life) and the moisture performance. Decay was visually evaluated annually and rated (0 – no attack; 1 – slight attack; 2 – moderate attack; 3 severe attack; 4 – failure) as prescribed by EN 252 (CEN, 2015). Mark 4 means that mechanical properties has decreased for 90% or more at least at one part of the specimen. Within this study, only the decking specimens were considered.

For moisture content (MC) measurements, resistance sensors were applied at nine positions and linked to a signal amplifier (Gigamodule, Scantronik, Germany) that enabled wood MC measurements between 6 % and 60 %. Pairs of stainless-steel screws with a diameter of 3.9 mm and length of 25 mm served as resistance sensors, fastened in the middle of the tangential surface with a distance of 32 mm between each other. The screws were insulated with a universal heat-shrinking tube except for the tip, which served as the point of measurement. Sensors were located at least 20 cm from axial planes. The electrical resistance of the wood was measured every twelve hours and these data were used for calculating the wood MC. Resistance characteristics for each material were determined as reported by Kržišnik et al. (in press) using the methodology described by Brischke and Lampen (2014).

2.3. DURABILITY TEST AGAINST WOOD-DESTROYING BASIDIOMYCETES

A decay test was performed according to a modified CEN/TS 15083-1 (CEN 2005) procedure. Specimens ($1.5 \times 2.5 \times 5.0 \text{ cm}^3$) conditioned at normal climate were steam-sterilized in an autoclave before incubation with decay fungi; 350 mL experimental glass jars with aluminium covers and cotton wool with 50 mL of potato dextrose agar (DIFCO, Fisher Scientific, USA) were prepared and inoculated with white rot fungi *Trametes versicolor* (L.) Lloyd (ZIM L057) and two brown rot fungi (*Gloeophyllum trabeum* (Pers.) Murrill (ZIM L018) and *Fibroporia vaillantii* (DC.) Parmasto (ZIM L037). The fungal isolates originated from the fungal collection of the Biotechnical Faculty, University of Ljubljana. One week after inoculation, two specimens per jar were positioned on a plastic HDPE mesh, which was used to avoid direct contact between the samples and the medium. The assembled test glasses were then incubated at $25 \text{ }^\circ\text{C}$ and 80 % relative humidity (RH). After incubation, specimens were cleaned from adhering fungal mycelium, weighed to the nearest 0.0001 g, oven-dried at $103 \pm 2 \text{ }^\circ\text{C}$, and weighed again to the nearest 0.0001 g to determine mass loss through wood-destroying basidiomycetes. Five replicate specimens per material/wood species were used in this test.

2.4. SHORT-TERM CAPILLARY WATER UPTAKE TEST

Measurements on five replicate specimens ($1.5 \times 2.5 \times 5.0 \text{ cm}^3$) were carried out at $20 \text{ }^\circ\text{C}$ and $50 \pm 5 \text{ } \%$ RH, on a Tensiometer K100MK2 device (Krüss, Hamburg, Germany), according to a modified EN 1609 (CEN, 1997) standard, after conditioning at $20 \text{ }^\circ\text{C}$ and 65 % RH until constant mass. The axial surfaces of the specimens were positioned to be in contact with the test liquid (distilled water) and their masses were subsequently measured continuously every 2 s for up to 200 s. Depending on the final weight of the immersed sample and the square surface of the axial surface of specimens, the uptake of water was calculated in g/cm^2 .

2.5. LONG-TERM WATER UPTAKE TEST WITH DRYING PROCESS ABOVE FRESHLY ACTIVATED SILICA GEL

Long-term water uptake was based on the leaching procedure. Before the test, specimens ($1.5 \times 2.5 \times 5.0 \text{ cm}^3$) were oven-dried at $60 \pm 2 \text{ }^\circ\text{C}$ until constant mass and weighed to determine the oven-dry mass. The dry wood blocks were placed in a glass jar and weighted down to prevent them from floating; 100 g of distilled water was then added per specimen. The mass of the specimens was determined after 24 h, and the MC of five replicate specimens was calculated.

2.6. WATER VAPOUR UPTAKE IN A WATER-SATURATED ATMOSPHERE WITH DRYING PROCESS ABOVE FRESHLY ACTIVATED SILICA GEL

Specimens ($1.5 \times 2.5 \times 5.0 \text{ cm}^3$) were oven-dried at $103 \pm 2 \text{ }^\circ\text{C}$ until constant mass and weighed to determine their oven-dry mass. The specimens were stacked in a glass climate chamber with a ventilator above distilled water. Specimens were positioned on mesh above the water using thin spacers (Meyer-Veltrup et al., 2017). After 24 h of exposure, they were weighed again, and MC was calculated. Specimens were then left in the same chamber for an additional three weeks until constant mass was achieved. In addition to wetting, outdoor performance is also influenced by drying. In general, wood that dries out quicker performs better. After three weeks of conditioning, wet specimens were positioned above freshly activated silica gel for 24 h in a closed container, and the MC of the specimens was calculated according to the procedure described by Meyer-Veltrup et al. (2017). Five replicate specimens were used for this analysis.

2.7 FACTOR APPROACH FOR QUANTIFYING THE RESISTANCE DOSE DRD

A modelling approach was applied according to Meyer-Veltrup et al. (2017) and Isaksson et al. (2014) in order to predict the field performance of the examined materials. The model describes climatic exposure on the one hand, and the resistance of the material on the other hand. The acceptance of the chosen design and material is expressed as follows,

$$\text{Exposure} \leq \text{Resistance} \quad (1)$$

The exposure can be expressed as an exposure dose (D_{Ed}) determined by daily averages of temperature and MC. The material property is expressed as the resistance dose (D_{Rd}) in days [d] with optimum moisture and temperature conditions for fungal decay (Isaksson et al., 2013).

$$D_{\text{Ed}} \leq D_{\text{Rd}} \quad (2)$$

where D_{Ed} is the exposure dose [d] and D_{Rd} is the resistance dose [d]. The exposure dose D_{Ed} depends on the annual dose at a specific geographical location and several factors describing the effect of driving rain, local climate, sheltering, distance from the ground, and detail design. Isaksson et al. (2014) give a detailed description of the development of the corresponding exposure model. The present study focused on the counterpart of the exposure dose, which is the resistance, expressed as resistance dose D_{Rd} . This is considered to be the product of the critical dose D_{crit} and two factors taking into account the wetting ability of wood (k_{wa}) and its inherent durability (k_{inh}). The approach is given by the following Eq. 3 according to Isaksson et al. (2014),

$$D_{Rd} = D_{crit} \times k_{wa} \times k_{inh} \quad (3)$$

where D is the critical dose corresponding to decay rating 1 (slight decay) according to EN 252 (CEN, 2015) [d], k_{wa} is a factor accounting for the wetting ability of the tested materials [-], relative to the reference Norway spruce, and k_{inh} is a factor accounting for the inherent protective properties of the tested materials against decay [-], relative to the reference Norway spruce. Based on the results of the various moisture tests presented in this paper, the wetting ability factor k_{wa} was evaluated. The methodology for the calculation of k_{wa} followed the Meyer-Veltrup procedure (2017), except that the size of the specimens differed. The original model prescribes specimens ($0.5 \times 1.0 \times 10.0 \text{ cm}^3$) that are of a different shape from that used in the present study ($1.5 \times 2.5 \times 5.0 \text{ cm}^3$). Since the methodology is based on relative values, the sample size has a minor influence on the outcome. Results from durability tests were used to evaluate the inherent resistance factor k_{inh} , and both factors were used to determine the resistance dose D_{Rd} of the respective wood materials examined in this study. Only basidiomycetes were applied to determine k_{inh} in this research. Terrestrial microcosm tests and in-ground durability tests were not performed, as prescribed by the original Meyer-Veltrup approach (2017).

3. RESULTS AND DISCUSSION

3.1. RESISTANCE DOSE

The resistance of different wood species and treated or modified wood products in above ground applications is primarily dependent on the degree of inherent material resistance against fungal decay (k_{inh}), but also on the wetting ability (k_{wa}) of the respective material. The material resistance dose D_{Rd} is a product of both factors and the respective critical dose D_{crit} as summarized for all materials in Table 2. Since k_{inh} and k_{wa} are normalized to Norway spruce, the relative material resistance dose (rel. D_{Rd}) of Norway spruce is 1.0. The rel. D_{Rd} of Beech (FS) is 0.88, while the rel. D_{Rd} of Ash (FE; 1.22). The highest relative D_{Rd} among the non-treated wood species was determined for Oak (Q; 5.92) and Sweet chestnut (CS; 6.40) (Table 2). Rel. D_{Rd} of Oak (Q; 5.92) was similar to those reported by Meyer-Veltrup et al. (2017) (Q; 5.10). This confirms the robustness and reliability of the approach. However, the main objective of the study reported by Meyer-Veltrup et al. (2017) was to determine the rel. D_{Rd} of non-treated wood. In contrast, this study is focussing on wood treated with water repellents (wax) and (thermally) modified wood.

Table 2: Material resistance dose D_{Rd} , data for k_{inh} and k_{wa} calculated based on the Meyer-Veltrup et al. (2018) methodology

Material	k_{inh}	k_{wa}	D_{Rd}	rel. D_{Rd}
PA	1.0	1.0	325	1.00
FE	1.2	1.0	396	1.22
FE-TM	2.9	1.9	1771	5.45
FS	0.9	1.0	284	0.88
FS-TM	2.6	2.1	1773	5.46
FS-TM-NW	3.3	2.6	2815	8.66
CS	5.0	1.3	2080	6.40
Q	3.9	1.5	1923	5.92

Thermal modification improved both, the inherent protective properties against fungal decay and the wetting ability. This is in line with findings from previous studies (e.g. Esteves and Pereira, 2009). Rather comparable effect of thermal modification was determined at ash and beech wood. Thermal modification combined with a wax treatment resulted in the highest rel. D_{Rd} , e.g. for wax treated and thermally modified Beech (FS-TM-NW, 8.66). Seemingly, wax treatment and thermal modification act synergistically. Thermal modification improves durability and sorption properties of wood, while wax treatment improves its resistance against liquid water uptake (Humar et al., 2017).

3.2. MOISTURE PERFORMANCE OF DECKING

Moisture dynamics are an essential parameter for the overall outdoor performance of wood beside its inherent durability. Aggregated wood MC data are presented in Table 3. In addition to average and extreme data, the percentage of wet days, i.e., days when wood MC exceeded a particular threshold, are reported. All measurements were performed at least 20 mm below the wood surface. Therefore, surface wood MC might have been even higher. Different thresholds could be taken into account. In general, the 25 % MC threshold is considered to be the minimum MC required for fungal decay of untreated wood, since it represents a conservative FSP value, however, lower values are possible if fungi can transport water from an adjacent moisture source to the wood (Höpken, 2015; Meyer and Brischke, 2015). Fibre saturation is rather a range than a fixed threshold (Popper and Niemz, 2009) and varies between 22 % and 36 %, depending on the wood species.

Table 3: Measurements of moisture content (MC) of wood decking at the wooden model house unit. Calculated median and average values of all measurements, and the number and percentages of the measurements with MC equal to or higher than 25 % are shown. Measurements were performed in the period between 11.4.2014 and 26.11.2018 (n = 3381)

Material	Average MC (%)	Median MC (%)	No of meas. MC > 25 %	% of meas. MC > 25 %
PA	27.9	21.7	1.075	31.8 %
FE	14.6	14.0	94	2.8 %
FE-TM	17.5	16.8	779	23.0 %
FS	27.3	25.7	1.747	51.7 %
FS-TM	18.9	19.5	811	24.0 %
FS-TM-NW	17.7	14.0	771	22.8 %
CS	17.3	15.6	608	18.0 %
Q	16.6	15.8	370	10.9 %

Median values are more indicative than average values, as the resistance-based measurements are rather inaccurate at higher MC. Therefore, we will focus on median values in the following. The highest median value among hardwoods was reported for Beech wood. The median MC was 25.7 %, where 51.7 % of the measurements were above the threshold of 25 %. Low moisture performance of beech wood was expected, and has been reported for instance by Žlahtič-Zupanc et al., (2018). This coincides with its good permeability (CEN, 2016). Surprisingly, thermally modified wood did not exhibit high moisture performance. However, the moisture performance of freshly modified wood was rather good (Table 2). The excellent moisture performance of freshly thermally modified wood has been often reported (e.g. Esteves and Pereira, 2009). However, as can be seen from data presented in Table 3, exposure under Use Class 3.2 conditions led apparently to increased water uptake (Humar et al., 2015; Van Acker et al., 2015; Žlahtič-Zupanc et al., 2018). This can be ascribed to the formation of micro-cracks, bacterial degradation of pit membranes and blue staining may have caused the drop of moisture performance (Schwarze et al., 2006). The combination of thermal modification and wax treatment considerably improved the moisture performance of decking elements (Table 3, Figure 1). Wax formed a hydrophobic layer on the surface that limited penetration of liquid water into the wood (Humar et al., 2017). Thus, wax treated thermally modified beech wood exhibited the lowest median MC of 14.0 %. Due to anatomical features, heartwoods (Q, and CS) revealed rather good moisture performance as well (Table 3).

High moisture performance of wax treated thermally modified wood (FS-TM-NW) becomes evident from Figure 1. At almost any time the MC of the thermally modified and wax treated wood was significantly below the MC of the untreated reference. This is another proof for the synergistic effect of wax and thermal modification. However, from Figure 1 it can be resolved, that the moisture performance of beech wood decreased after a certain period of exposure. We presume, that the decreased moisture performance can be associated with fungal decay. Fungi open new voids in the cell matrix, which results in better permeability (Žlahtič and Humar, 2017). This phenomenon could be utilised as bio-incising prior to impregnation (Schwarze et al., 2006). The increased moisture content of decayed wood cannot be ascribed to the changed relation between electrical resistance and moisture content, as confirmed by Brischke and co-workers (2018).

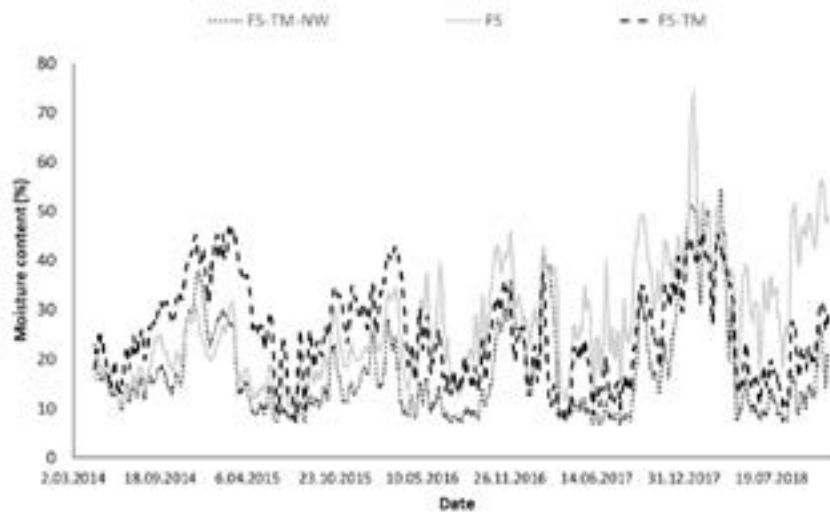


Figure 1: MC of beech (FS), thermally modified beech (FS-TM) and wax treated thermally modified beech (FS-TM-NW) decking of model house in Ljubljana in the period between 11.4.2014 and 26.11.2018. Plots displayed are moving averages of 20 measurements.

3.3. DECAY RATE DEVELOPMENT IN THE DECKING OF THE MODEL HOUSE

Decay on the decking of model house was developing progressively. During the first year of exposure, there was no decay determined on the decking of the model house in Ljubljana. In the second year first signs of decay developed on Beech (FS). This is in line with findings from previous studies (Meyer-Veltrup et al., 2017). In the third year, decay proceeded. In addition, decay developed on Ash (FE). In the fourth year, the first signs of decay appeared on Oak (Q) as well. After four years of exposure only Sweet chestnut (CS) and thermally modified wood remained without visible signs of decay (Table 4). After five years of exposure, Norway spruce wood was completely degraded, followed by Beech. The wood is useless. Mechanical properties are decreased up to 90%. However, the first stages of decay usually can not be resolved from the bending or compression strength. Decay is not uniform, therefore mechanical properties are challenging to determine. In addition, mechanical properties in service are challenging to determine. Brown rot fungi caused the majority of decay on softwood species, e.g. fruiting bodies of *Gloeophyllum sp.* were found. On hardwoods, white rot was more dominant. Fruiting bodies of *Trametes versicolor* were found frequently.

Table 4: Decay rating of the decking elements determined according to EN 252 (CEN, 2015)

Material	Average decay rating of the decking elements				
	2014	2015	2016	2017	2018
PA	0.0	1.0	2.4	3.7	4.0
FE	0.0	0.0	1.0	1.4	2.1
FE-TM	0.0	0.0	0.0	0.0	0.0
FS	0.0	1.0	2.2	3.1	3.7
FS-TM	0.0	0.0	0.0	0.0	0.0
FS-TM-NW	0.0	0.0	0.0	0.0	0.0
CS	0.0	0.0	0.0	0.0	0.0
Q	0.0	0.0	0.0	0.5	0.9

3.4. MODELLING DECAY RATES OF TREATED AND MODIFIED WOOD

More recently, a new concept to characterize the durability of wood-based materials and to predict the service lives of wood was proposed by Meyer-Veltrup et al. (2017; 2018) taking into account the material-inherent protective properties, the moisture performance and the climate and design induced exposure dose of wooden structures. This approach was successfully applied to untreated wood (De Angelis et al., 2018; Brischke et al., 2018).

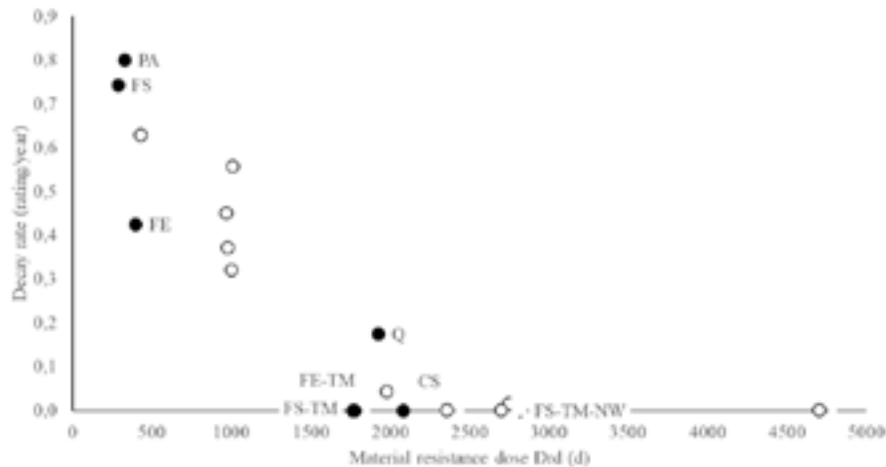


Figure 2: Mean decay rate of the decking at model house in Ljubljana versus the material resistance dose D_{Rd} . Black markers indicates tested materials, while white ones indicate softwoods that were assed in parallel, but are not part of the respective study.

The main objective of this study was to validate the model approach by Meyer-Veltrup et al. (2017), which has been developed and validated for untreated wood of numerous different species. The material resistance dose D_{Rd} was well correlated with the decay rates of the decking as shown in Figure 2. From this graph it can be clearly seen linear relationship between Decay rate and material resistance dose in the first years of exposure. It is expected, that this relationship would be similar for more durable materials, with higher D_{Rd} , we just have to prolong the exposure and wait the decay to develop. By implementing also the effect of inherent protective properties, the material resistance is represented in a more comprehensive manner compared to solely using temperature and MC data for establishing an exposure dose. Furthermore, the positive effect of thermal modification and water repellent treatments on the outdoor performance of the examined materials is considered and most likely synergistic effects between moisture performance and inherent durability as well. Although, in particular, the preservative treated decking showed no decay yet, the model fit well the decay rates in general. However, to distinguish better between different highly durable materials it might be necessary to implement further long-term data (i.e. field test data exposed for several decades) of the latter.

4. CONCLUSIONS

The results clearly indicate that the dose D_{Rd} was well correlated with the decay rates of the decking of the model house. The model approach, taking into account the material-inherent protective properties, the moisture performance, and the climate and design induced exposure dose of wooden structures, proved to be accurate on modified and preservative treated wood as well. Furthermore, the positive effect of thermal modification and water repellent treatments on the outdoor performance of the examined materials became evident as well as synergistic effects between moisture performance and inherent durability. Since the number of long-term field tests for which corresponding lab decay and moisture dynamic tests had been performed is rather scarce, it might be meaningful to sample from longer running tests for further subsequent validation of the model approach. This might work also for structures in-service with a known service life that show first signs of decay.

ACKNOWLEDGEMENTS

The authors acknowledge the support of the Slovenian Research Agency within the framework of project L4-7547, program P4-0015 and the infrastructural center (IC LES PST 0481-09). Part of the research was also supported by the project: TIGR4smart (C3330-16-529003) and Wood and wood products over a lifetime (WOOLF).

REFERENCES

Brischke, C. and S. Lampen. 2014. Resistance based moisture content measurements on native, modified and preservative treated

- wood. *European Journal of Wood and Wood Products*. 72:289–292.
- Brischke, C., Stricker, S., Meyer-Veltrup, L. and L. Emmerich. 2018. Changes in sorption and electrical properties of wood caused by fungal decay. *Holzforschung*. Online first.
- Brischke, C., Hesse, C., Meyer-Veltrup, L. and M. Humar. 2018. Studies on the material resistance and moisture dynamics of Common juniper, English yew, Black cherry, and Rowan. *Wood Material Science & Engineering*. 13(4):222-230.
- CEN. 1997. EN 1609 Thermal insulating products for building applications - Determination of short term water absorption by partial immersion. European Committee for Standardization, Brussels, Belgium.
- CEN. 2015. EN 252 Field test method for determining the relative protective effectiveness of a wood preservative in ground contact. European Committee for Standardization, Brussels, Belgium.
- CEN. 2016. EN 350 - Durability of wood and wood-based products - Testing and classification of the durability to biological agents of wood and wood-based materials. European Committee for Standardization, Brussels, Belgium.
- CEN/TS 15083-1. 2005. Durability of wood and wood-based products - Determination of the natural durability of solid wood against wood-destroying fungi, test methods - Part 1. European Committee for Standardization, Brussels, Belgium.
- De Angelis, M., Romagnoli, M., Vek, V., Poljanšek, I., Oven, P., Thaler, N., Lesar, B., Kržišnik, D. and M. Humar. 2018. Chemical composition and resistance of Italian stone pine (*Pinus pinea* L: wood against fungal decay and wetting. *Industrial crops and products*. 117:187-196.
- Esteves, B. M. and H.M. Pereira. 2009. Wood modification by heat treatment: A review. *Bioresources*. 4(1):370-404.
- FTP. The Forest-based Sector Technology Platform (2018). Vision 2040 of the European forest-based sector. Brussels. <http://www.forestplatform.org> (accessed 20.2.2019)
- Höpken, M. 2015. Investigations on the growth and moisture transport of indoor wood decay fungi in piled wood specimens (In German.. Master thesis. University Hamburg, Department Biology, Germany
- Humar, M., Kržišnik, D. and B. Lesar. 2017. Thermal modification of wax-impregnated wood to enhance its physical, mechanical, and biological properties. *Holzforschung*. 71:57–64.
- Humar, M., Kržišnik, D., Lesar, B., Ugovšek, A., Rep, G., Šubic, B., Thaler, N., and M. Žlahtič. 2015. Monitoring of window, door, decking and façade elements made of thermally modified spruce wood in use. In: 8th European Conference on Wood Modification (ECWM8). Helsinki, Finland: Aalto University:419-428.
- Isaksson, T., Brischke, C. and S. Thelandersson. 2013. Development of decay performance models for outdoor timber structures. *Materials and Structures*. 46:1209-1225.
- Isaksson, T., Thelandersson, S., Jermer, J. and C. Brischke. 2014. Beständighet för utomhusträ ovan mark. Guide för utformning och materialval (Rapport TVBK-3066). Lund University, Division of Structural Engineering, Lund, Sweden.
- Kržišnik, D., Lesar, B., Thaler, N., Planinšič, J. and M. Humar. in press. A study of moisture performance of wood determined in laboratory and field trials.
- Meyer, L. and C. Brischke. 2015. Fungal decay at different moisture levels of selected European-grown wood species. *International Biodeterioration & Biodegradation*. 103:23-29.
- Meyer-Veltrup, L., Brischke, C., Alfredeisen, G., Humar, M., Fløte, P.-O., Isaksson, T., Larsson-Brelid, P., Westin, M. and J. Jermer. 2017. The combined effect of wetting ability and durability on outdoor performance of wood – Development and verification of a new prediction approach. *Wood Sci. Technol*. 51(3):615-637.
- Meyer-Veltrup, L., Brischke, C., Niklewski, J. and E. Frühwald Hansson. 2018. Design and performance prediction of timber bridges based on a factorization approach. *Wood Material Science & Engineering*. 13(3):167-173.
- Popper, R. and P. Niemz. 2009. Wasserdampfsorptionsverhalten ausgewählter heimischer und überseeischer Holzarten. *Bauphysik*. 31(2):117-121.
- Reinprecht, L. 2016. *Wood Deterioration, Protection and Maintenance*. John Wiley & Sons, Oxford, 366.
- Rep, G., Pohleven, F. and B. Bučar. 2004. Characteristics of thermally modified wood in vacuum. Proceedings of the 34th scientific conference of the International Research Group on Wood Protection, Stockholm.
- Schmidt, O. 2006. *Wood and Tree Fungi. Biology, Damage, Protection and Use*. Springer, Berlin.
- Schwarze, F. W. M. R., Landmesser, H., Zraggen, B. and M. Heeb. 2006. Permeability changes in heartwood of *Picea abies* and *Abies alba* induced by incubation with *Physisporinus vitreus*. *Holzforschung*. 60:450-454.
- Van Acker, J., Van den Bulcke, J., De Windt, I., Colpaert, S. and W. Li. 2015. Moisture dynamics of modified Wood and the Relevance Towards Decay Resistance. In: 8th European Conference on Wood Modification (ECWM8). Helsinki, Finland: Aalto University:44-55.
- Žlahtič, M. and M. Humar. 2017. Influence of artificial and natural weathering on the moisture dynamic of wood. *BioResources*. 12:117-142.
- Žlahtič Zupanc, M., Lesar, B. and M. Humar. 2018. Changes in moisture performance of wood after weathering. *Construction & building materials*. 193:529-538.

Effect of Thermal Modification on Physical and Mechanical Properties of *Brachystegia spiciformis* and *Julbernardia globiflora* from Mozambique

Feliz Nhacila Jr¹, Eunice Siteo¹, Ernesto Uetimane Jr¹, Alberto Manhica², Andrade Egas¹, and Veikko Möttönen^{3*}

¹Eduardo Mondlane University
Faculty of Agronomy and Forest
Engineering, Maputo, 257,

Mozambique
²Agrarian National Research
Institute Ministry of Agriculture
Maputo, 3658, Mozambique

³Natural Resources Institute Finland,
Production systems, 80100 Joensuu,
Finland

*Corresponding author: E-mail veikko.mottonen@luke.fi, phone +358295325053

ABSTRACT

Msasa (Brachystegia spiciformis Benth.) and red msasa (Julbernardia globiflora Benth. Troupin) are the most abundant tree species in the Miombo forests in Mozambique. However, they are hardly used for any high value added wood products due to the lack of knowledge about the properties of their wood. Furthermore, the timber of both species (especially the light coloured sapwood section) is characterised by very low resistance against fungal and insect attack. In this study, three different intensities of thermal modification were used to treat the sawn timber of both species and afterwards assess wood properties responses, namely mass loss, equilibrium moisture content, oven-dry density, colour change and selected mechanical properties. Both thermally modified and untreated specimens were prepared according to ISO standards.

The results shows that the untreated light coloured sapwood of both wood species darkened gradually as the thermal treatment intensity increased. The contrasting colour between sapwood and heartwood sections nearly disappeared and levelled for samples exposed to the highest treatment intensity. On average all tested wood properties changed significantly after the most intense treatment level was applied. Despite degradation of mechanical properties in both species, an optimal combination of temperature and treatment time was possible to achieve. The study concluded that the overall recorded changes of the tested wood properties in both species increase the range of applications including the new appealing colour resembling the most appreciated and sought after tropical hardwoods.

Keywords: Brachystegia spiciformis, Julbernardia globiflora, Thermal modification, colour changes, physico-mechanical properties,

BRIEF ORIGINAL

Mozambican msasa (*Brachystegia spiciformis*) and red msasa (*Julbernardia globiflora*) boards were heat treated using three different thermal modification temperature: 215, 230, and 245 °C. Changes in density, modulus of elasticity, modulus of rupture, Brinell hardness and compression strength between untreated and thermally modified wood were studied.

1. INTRODUCTION

The world's fast growing population and associated wood consumption is outpacing the natural forests' capacity to meet the demand, particularly in the tropics where in spite of high diversity of wood species, very few are selectively harvested in unprecedented alarming rates (Uetimane et al. 2018). A large number of tropical hardwood species is

overlooked due to the poor knowledge on their timber properties including the local lack of cost effective technologies to process into competitive end products. This is particularly true for the group of light coloured and perishable timbers where toxic chemicals must be impregnated to ensure prolonged service life.

Therefore, environmental concerns on toxic chemicals impregnated in wood to enhance its properties have triggered research on alternative and environmental friendly wood processing methods such as thermal modification. This approach consists basically on exposing pre-kilned wood to high temperature ranges (180 - 250 °C) for relatively short periods resulting in changes to its natural structure. Typically, during thermal modification the wood is exposed to permanent changes in its colour, physico-mechanical properties and chemical structure. In general after thermal treatments, light coloured wood species tend to acquire darker tones resembling some natural dark coloured endangered and precious tropical hardwoods. Another typical acquired feature is improved resistance to biodegradation somewhat associated to acquired hydrophobicity compared to untreated solid wood (Hill 2006; Dubey 2010; Srinivas and Pandey 2012; Militz and Altgen 2014).

In Mozambique, wood thermal modification could be a suitable technology for processing non-durable lesser known/lesser used species such as *Brachystegia spiciformis* and *Julbernardia globiflora*. If successfully applied, this technology could potentially open new market opportunities as well as saving overexploited wood species (Sosef et al. 1998; Peres 2010).

Despite enjoying a large share of the Mozambique forest growing stocks (Marzolli 2007) both *Brachystegia spiciformis* (msasa) and *Julbernardia globiflora* (red msasa) timbers are interchangeably mainly used for railway sleepers after pressure impregnation in creosote treatment plants. This decay resistive but toxic processing option restricts a wider range of uses. Therefore, this study is aimed at assessing wood properties responses induced by different thermal treatment levels of both *B. spiciformis* and *J. globiflora*. It is expected that a friendly environmental processing technology such as the thermal modification will ensure improved properties of a group of lesser used species which could enable their use for both indoor and outdoor applications and relieve pressure on the most sought after timbers across the country.

2. Materials and methods

2.1 Material and samples origin

The samples of *Brachystegia spiciformis* and *Julbernardia globiflora* were obtained from 10 mature undated dominant trees (five of each species) growing in humid miombo natural forests of Cheringoma district, Sofala province, Mozambique (S 18°45'21,9" E 034°55'27,1"). The identities of tree species were confirmed at the Eduardo Mondlane University Xylarium through vouchered reference specimens. A batch containing 121 planks of *Brachystegia spiciformis* and 64 planks of *Julbernardia globiflora* was transported to Luxhammar Ltd. (Mikkeli, Finland) where the thermal modification treatments were carried out. For the experiment, pre-kiln dried sapwood planks – nominal size (600 × 50 × 25mm³) (Long × Radial × Tang) of both species (average of 12% moisture content) – were exposed to three thermal treatment levels and distributed in the following sub-sets as shown on table 1. All sample lengths were shortened to length of 500mm to fit the thermal modification chamber.

2.2 METHODS

2.2.1 BRIEF DESCRIPTION OF THE THERMAL MODIFICATION METHOD

The wood specimens of both tree species were heat treated by the Luxhammar thermal modification process method developed by Luxhammar corporation (Luxhammar 2019). The entire thermal modification process consists of five different stages: Initial heating (temperature raised to 100°C), preconditioning and drying, actual thermal modification with high temperature up to 250°C, conditioning (restoration of moisture), and cooling. The processes in this study were carried out in an air tight stainless steel kiln chamber (research sized) using three temperature range intensities, 215°C (T1), 230°C (T2) and 245°C (T3), for 2 hours at saturated steam environment. Due to the shortage of wood material of *Julbernardia globiflora*, it was not included in the T3 treatment. However T3 treatment was used for *Brachystegia spiciformis* to enable also the further studies on the effects of different treatment processes on resistance to decay and termites of miombo wood species. The reference (untreated) specimens were separated after the pre-drying in convention drying kiln to the target moisture content of 10–12%.

2.2.2 ASSESSMENT OF WOOD PROPERTIES RESPONSES TO THERMAL MODIFICATION

Effect of Thermal Modification on Physical and Mechanical Properties of *Brachystegia spiciformis* and
Julbernardia globiflora from Mozambique

For all subset of specimens the following wood properties listed in table 2 were tested before and after each thermal treatment level using untreated samples as reference control. Statistical differences between untreated samples and each treatment level within each wood species were calculated by mean of Tukey's multiply range test at $p < 0.005$. The mechanical tests were performed using the universal material testing machine Zwick Z050 (Germany) according to specific standards listed in the Table 2.

The mass loss (ML) of all specimens was calculated by weighing before and after each thermal treatment level and expressed in %. Specimens from each treatment were oven-dried to absolute dry weight and compared to monitor changes of the oven-dry density. Likewise, after each treatment the specimens were left in standard room climate (20, 65% relative humidity) until equilibrium moisture content (EMC) was achieved. Reflectance spectra of different treatments were measured using Konica Minolta CM-2600d portable spectrophotometer. Spectral data between 360 and 740 nm visible wavelength range was converted to CIEL*a*b* color coordinates using 2° standard observer and D65 light source. Lastly, the color difference (ΔE^*_{ab}) between the modified and unmodified specimens was calculated using CIE76 standard (Commission International de l'Eclairage, CIE), which corresponds to the distance between two points in the three-dimensional color coordinate system, and is calculated by the equation:

$$\Delta E^*_{ab} = ((\Delta L^*)^2 + (\Delta a^*)^2 + (\Delta b^*)^2)^{1/2} \quad [-] \quad (1)$$

where ΔL^* , Δa^* and Δb^* reflect the changes of lightness (L^*) and chromatic parameters redness (a^*) and yellowness (b^*) between the measurements on the treated samples.

Brinell hardness (HB) of wood was measured and calculated according to EN 1534 as follows:

$$HB = 2F / (\pi * D * (D - (D^2 - d^2)^{1/2})) \quad [\text{MPa}] \quad (2)$$

where F is the nominal force, D is the diameter of the steel ball, and d is the diameter of the residual indentation. As a difference from EN 1534, the estimated value for the diameter of the residual indentation (d) was calculated from the depth of the residual indentation (h, mm) measured by the material testing machine as follows:

$$d = 2 * (10h - h^2)^{1/2} \quad [\text{mm}] \quad (3)$$

The tests for MOE (E_w) and MOR ($\sigma_{b,W}$) were carried out according to standards ISO 13061-4 (2014) and ISO 13061-3 (2014), respectively, using 20×20×340mm, clearwood specimens as follows:

$$E_w = Pl^3 / 4bh^3f \quad [\text{MPa}] \quad (4)$$

where P is the load equal to the difference between the upper and lower limits of loading (N), l is the span (mm), b is the width of the test specimen (mm), h is the height of the test specimen (mm), f is the deflection at the upper and lower limits of loading (mm), and

$$\sigma_{b,W} = 3P_{\max}l / 2bh^2 \quad [\text{MPa}] \quad (5)$$

where P is the maximum load (N), l is the span (mm), b is the width of the test specimen (mm), h is the height of the test specimen (mm).

The figures describing the tested mechanical properties of MOE and MOR (before and after thermal treatments) were adjusted to 12% moisture content to address moisture variation amongst the subset of specimens modified in different thermal intensities, by using the following formulae, which are valid for moisture contents of 12±5%:

$$E_{12} = E_w / (1 - \alpha * (W - 12)) \quad [\text{MPa}] \quad (6)$$

$$\sigma_{b,12} = \sigma_{b,W} [1 + \alpha * (W - 12)] \quad [\text{MPa}] \quad (7)$$

where α is the correction factor for the moisture content, equal to 0,04, and W is the moisture content of wood.

3. RESULTS AND DISCUSSION

3.1 PHYSICAL PROPERTIES

3.1.1 COLOUR CHANGE

Thermally modified wood is widely known for inducing permanent structural changes on treated samples. Colour change in different shades of darkness is probably the most striking and recognized feature of thermally modified wood. Predictably, in this study, all thermal treatment levels produced visible change in colour as shown by the overall colour change parameter (ΔE^*ab) (Table 3). In fact, ΔE^*ab larger than 2 is visually perceived by naked human eye (Witzel et al. 1973; Hon and Minemura 2001).

Additionally, remarkable uniformity in colour was achieved as inferred by the negligible variations in all treatment levels for the two species. The acquired colours could potentially add value to both wood species due to similarities to expensive, rare, endangered precious tropical hardwoods. For consumers, the decorative look often prevails, and colour is in fact, a determining factor for the selection of a specific wood (Esteves and Pereira 2009; Dos Santos et al. 2014).

3.1.2 MASS LOSS, OVEN-DRY DENSITY AND EQUILIBRIUM MOISTURE CONTENT

The mass loss (ML) increased and the EMC and oven-dry density decreased as the thermal treatment level was increased (Table 4). One of the key structural changes in heat treated wood is improved hydrophobicity and lower oven-dry density due to progressive evaporation of extractives and thermal degradation of the main chemical components such as wood components, hemicelluloses, cellulose and lignin (Pockrandt et al. 2018).

The reduced EMC of thermally modified wood can be explained by several factors including degradation of the amorphous regions of cellulose triggering cross-linking reactions that potentially hinder moisture intake (Jermer et al. 2003; Mitani and Barboutis 2014; Adeyemi et al. 2017). Hydrophobicity and reduced density are improved wood features with potential for new applications where decay resistance and dimensional stability are critical. The ML of the thermally treated wood samples is indicative of degradation of wood polymers mainly by the hemicelluloses in this range of temperature, which are the most thermally-sensitive wood components (Mohebbi and Sanaei 2005; Poncsak et al. 2006; Kocaefe et al. 2007).

3.2 Mechanical properties

3.2.1 BENDING STRENGTH

Thermal modification is known to induce permanent changes in the wood structure. The wood responses of *B. spiciformis* and *J. globiflora* to thermal modification are shown below (Fig.1). There is a clear trend of decline in bending strength (MOE and MOR) for both species as the treatment intensity was increased. Similar trends were reported elsewhere for hardwoods (Korkut et al. 2008; Korkut 2012).

The MOR of both wood species decreased over 50 % of reference value, while the MOE dropped by 6% in *B. spiciformis* and beyond 6% in *J. globiflora* with the highest treatment intensity. According to Tukey multiple range test (at $p < 0.05$) all induced changes are significantly different from the reference untreated samples since heat-treated samples turned brittle. According to Jämsä and Viitaniemi (2001), due to deterioration in mechanical properties, the use of thermal modified wood as load-bearing structural material should be restricted. However, a balance is needed to establish optimal treatment to allow a wide range of applications for the end product. For example, T2 treatment level seems suitable as no considerable gain is obtained by the very intense T3 applied to *B. spiciformis* timber.

3.2.2 BRINELL HARDNESS AND COMPRESSION STRENGTH PARALLEL TO GRAIN

Like in static bending (MOE and MOR), both compression strength and Brinell hardness suffered statistically significant decline as the thermal treatment intensity was increased (Fig. 2). All treatment levels caused decrease on Brinell hardness for *B. spiciformis*. Exceptionally, a slight increase was recorded for *J. globiflora* sample subjected to T1 treatment level, but a decrease for sample subjected to T2 level. Brinell hardness is a very important quality parameter for parquet and flooring materials as it measures the resistance against indentation. The resulting values of Brinell hardness after the T1 treatment for *B. spiciformis* (26.0 MPa) and T2 treatment for *J. globiflora* (32.4 MPa) are within range of most wood floorings. However, the Brinell hardness of *B. Spiciformis* samples subjected to T3 treatment level (20.2 MPa) was not comparable to Brinell hardness of untreated birch (23.4 MPa) or oak (30.5 MPa) wood (Heräjärvi 2004; Swaczyna et al. 2011), which typically are used for flooring materials in Europe.

For both species, thermal treatments led to 20% decrease of compression strength parallel to grain. Similar results were claimed by Korkut (2012), who studied wood responses of three thermally treated tropical hardwood species. As mentioned earlier mild thermal intensity treatment should be deployed if the decrease in strength properties is to be kept within critical limits.

4. SUMMARY

This study was aimed at testing wood properties responses by mean of thermal treatment of two low-value and abundant, but relatively lesser known/used native hardwoods from Mozambique. Based on measured parameters, it can be concluded that nearly all measured wood properties experienced statistically significant changes after all treatment levels. More specifically, from control reference samples to the highest treatment level, the results show that *B. spiciformis*'s timber experienced a maximum ML of 27%, while the oven-dry density reduced from 0.65 g/cm³ to 0.56 g/cm³, the EMC dropped from 7% to 3%. With regard to *J. globiflora*, the ML induced by the highest treatment level was 23%, oven-dry density decreased from 0.81 g/cm³ to 0.74 g/cm³ and the EMC reduced from 8% to 3%. Changes in mechanical properties were also significant from reference samples to the highest treatment. For *B. spiciformis*, MOE reduced from 9150.48 to 8212.57 MPa, MOR from 43.88 to 21.60 MPa, compression strength parallel to grain decreased from 25129 to 17794 MPa and the Brinell hardness from 2.64 to 2.02 MPa. The samples from *J. globiflora* followed the same trend as its MOE reduced from 11037.46 to 10277.40 MPa, MOR from 50.02 to 23.39 MPa, compression strength parallel to grain from 29365.75 to 22935.08 MPa.

The study concluded that thermally modified wood of both species could potentially be used for flooring due to new appealing dark colour and low EMC associated with hydrophobicity. The overall assessment of the results suggest that thermal modification is potentially an effective method for processing low-value, but abundant wood species to relieve the current pool of overexploited tropical hardwoods.

5. ACKNOWLEDGEMENTS

The study was carried out in the framework of a project (FORECAS II project) financed by the Ministry for Foreign Affairs of Finland to which financial support is gratefully acknowledged. The authors also gratefully acknowledge LevasFlor Ltd. (Beira, Mozambique) for providing the sawn wood material for the tests and Luxhammar Ltd. (Mikkeli, Finland) for carrying out the thermal modification treatments.

REFERENCES

- Adeyemi IE, Babatola O, Mayowa OJ, Adeola FJ (2017) Impact of Heat Treatment on Physico-Mechanical Properties of Thermally Modified *Anthocleista djalensis* Wood. *Journal of Materials Sciences and Applications* 3(2):28–34. Retrieved from <http://www.aascit.org/journal/jmsa>.
- Dos Santos DVB, de Moura LF, Brito JO (2014) Effect of Heat Treatment on Color, Weight Loss, Specific Gravity and Equilibrium Moisture Content of Two Low Market Valued Tropical Woods. *Wood Research* 59(2):253–264.
- Dubey MK (2010) Improvements in Stability, Durability and Mechanical Properties of Radiata Pine Wood after Heat-Treatment in a Vegetable Oil. PhD Thesis. University of Canterbury, New Zealand. 211 pp.
- Esteves BM, Pereira HM (2009) Wood modification by heat treatment: A review. *BioResources* 4(1):370–404.
- Heräjärvi H (2004) Variation of basic density and Brinell hardness within mature Finnish *Betula pendula* and *B. pubescens* stems. *Wood and Fiber Sci.* 36:216–227.
- Hill CAS (2006) *Wood Modification: Thermal and Other Process*. John Wiley & Sons. 249 pp.
- Hon DNS, Minemura N (2001) Color and discoloration. In: Hon, D.N.S., Shiraishi, N. (Eds.) *Wood and Cellulosic Chemistry*. Marcel Dekker, New York. pp. 385–442.
- ISO/CIE 11664-6 (2014) *Colorimetry - Part 6-CIEDE 2000-Colour difference formula*. International Standards Organisation, Geneva.
- ISO 13061-2 (2014) *Wood-Determination of density for physical and mechanical tests*. International Standards Organisation, Geneva.
- ISO 13061-5 (1975) *Wood-Test methods – Determination of ultimate stress in compression parallel to grain*. International Standards Organisation, Geneva.

Effect of Thermal Modification on Physical and Mechanical Properties of *Brachystegia spiciformis* and *Julbernardia globiflora* from Mozambique

- ISO 13061-3 (2014) *Wood – Determination of modulus of elasticity in static bending*. International Standards Organisation, Geneva.
- ISO 13061-4 (2014) *Wood – Determination of ultimate strength in static bending*. International Standards Organisation, Geneva.
- Jämsä S, Viitaniemi P (2001) *Heat treatment of wood- Better durability without chemicals*. In: *Proceedings of special seminar held in Antibes, France, city*, 68 p.
- Jermer J, Bengtsson C, Brem F, Clang A, Ek-Olausson B, Edlund M (2003) *Heat-treated wood – durability and technical properties Swedish Wood Association project 2001-025*.
- Kocaepe D, Chaudhry B, Poncsak S, Bouazara M, Pichette A (2007) *Thermogravimetric study of high temperature treatment of aspen: Effect of treatment parameters on weight loss and mechanical properties*, *Journal of Materials Science* 42(3):355–361.
- Korkut S (2012) *Performance of three thermally treated tropical wood species commonly used in Turkey*. *Industrial Crops and Products* 36(1):355–362.
- Korkut S, Akgül M, DüNDAR T (2008) *The effects of heat treatment on some technological properties of Scots pine (Pinus sylvestris L.) wood*. *Bioresource Technology* 99 (6): 1861–1868.
- Luxhammar 2019. *Luxhammar thermal modification technology*. Available at: <http://www.luxhammar.com/index.php>.
- Marzoli A (2007) *Inventário Florestal Nacional: Avaliação integrada das florestas de Moçambique*. Direção Nacional de Terra e Florestas, Ministério da Agricultura. Maputo. 92 pp.
- Militz H, Altgen M (2014) *Processes and Properties of Thermally Modified Wood Manufactured in Europe*.
- Mitani A, Barboutis I (2014) *Changes Caused by Heat Treatment in Color and Dimensional Stability of Beech (Fagus sylvatica L.) Wood*. *Drvna Industrija*, 65(3), 225–232.
- Mohebbi B, Sanaei I (2005) *Influences of the hydro-thermal treatment on physical properties of beech Wood (Fagus orientalis)*. In: *Annual Meeting Bangalore (36)*, New Delhi. *Proceedings: Tarbiat Modarress University*.
- Peres CA (2010) *Conservation Biology for All: Ovexploitation*. Oxford 24 pp.
- Pockrandt M, Jebrane M, Cuccui I, Allegretti O, Uetimane Jr E, Terziev N (2018) *Industrial Thermowood® and Termovuoto thermal modification of two hardwoods from Mozambique*. *Holzforchung* 72(8): pp. 701–709.
- Poncsak S, Kocaepe D, Bouazara M, Pichette A (2006) *Effect of high temperature treatment on the mechanical properties of birch (Betula papyrifera)*. *Wood Science and Technology* 40 (8): pp. 647–663.
- Sosef MSM, Hong LT, Prawirohatmodjo S (1998) *Plant Resources of South-East Asia No 5(3) Timber Trees: Lesser- Known timbers*. Backhuys Publishers. 859 pp.
- Srinivas K, Pandey KK (2012) *Effect of Heat Treatment on Color Changes, Dimensional Stability, and Mechanical Properties of Wood*. *Journal of Wood Chemistry and Technology* 32:304–316.
- Swaczyna I, Kędzierski A, Tomusiak A, Cichy A, Różańska A (2011) *Hardness and wear resistance tests of the wood species most frequently used in flooring panels*. *Ann. WULS-SGGW, Forestry and Wood Technology* 76: 82–87.
- Uetimane Jr E, Jebrane M, Terziev N, Daniel G (2018) *Comparative wood anatomy and chemical composition of Millettia mossambicensis and Millettia stuhlmannii from Mozambique*. *Bioresouces* 13(2):3335-3345.
- Witzel RF, Burnham RW, Onley JW (1973) *Threshold and supra threshold perceptual color differences*. *J. Optical Society of America* 63(5):615–625.

Effect of Thermal Modification on Physical and Mechanical Properties of *Brachystegia spiciformis* and *Julbernardia globiflora* from Mozambique

Table 1. Number of wood samples for each tested thermal modification

Treatment	Temperature, °C	Time, h	<i>Brachystegia spiciformis</i>	<i>Julbernardia globiflora</i>
Untreated	-	-	9	7
T1	215	2	43	27
T2	230	2	40	29
T3	245	2	29	-

Table 2. Tested wood properties and specific standards

Tested wood properties	Standard
Equilibrium moisture content, mass loss and oven-dry density	ISO 13061-2:2014
Colour/spectral reflectance	ISO/CIE 11664-6:2014(E)
Bending strength: MOE & MOR*	ISO 13061-3:2014 & ISO 13061-4:2014
Brinell hardness	ISO 13061-12:2017
Compression strength	ISO/DIS 13061-5 & ISO 3132:1975

*MOE-Modulus of Elasticity; MOR-Modulus of Rupture; ISO-International Standards Organization

Table 3. Colour changes by treatment level and wood species

Wood species	Treatment	Colour coordinate			Overall colour change ΔE^*_{ab}
		L^*	a^*	b^*	
<i>B. spiciformis</i>	Untreated	77.09 (3.73)	6.20 (1.90)	23.32 (2.11)	-
	T1	44.54 (2.11)	8.98 (0.55)	19.75 (1.58)	33.33 (5.43)
	T2	36.11 (1.49)	7.26 (0.56)	13.19 (1.58)	42.37 (4.17)
	T3	33.26 (1.37)	6.22 (0.58)	10.90 (1.26)	45.19 (7.00)
<i>J. globiflora</i>	Untreated	75.35 (6.88)	6.59 (2.34)	23.41 (1.97)	-
	T1	42.12 (2.19)	10.40 (0.81)	18.13 (1.76)	34.49 (3.72)
	T2	34.00 (0.87)	7.44 (0.56)	11.28 (1.09)	42.87 (5.50)

Standard deviations in parenthesis

Table 4. Mass loss, EMC and oven-dry density changes after thermal modifications

Wood species	Thermal treatment levels	ML (%)	EMC (%)	Oven-dry density (g/cm ³)
<i>B. spiciformis</i>	Reference	-	7 (0.01)	0.65 (0.03)
	T1	15 (0.01)	4 (0.00)	0.61 (0.07)
	T2	24 (0.05)	3 (0.00)	0.58 (0.04)
	T3	27 (0.01)	3 (0.01)	0.55 (0.03)
	<i>J. globiflora</i>	Reference	-	8 (0.02)
	T1	21 (0.02)	5 (0.02)	0.74 (0.07)
	T2	24 (0.01)	3 (0.00)	0.74 (0.04)

Standard deviation in parenthesis; ML-mass loss; EMC-Equilibrium moisture content

Effect of Thermal Modification on Physical and Mechanical Properties of *Brachystegia spiciformis* and *Julbernardia globiflora* from Mozambique

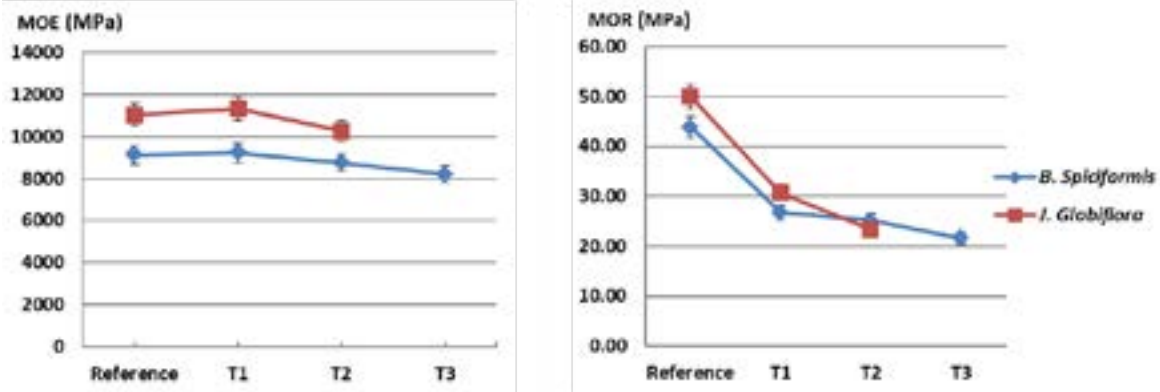


Fig. 1. Bending stiffness and strength changes in timbers of *B. spiciformis* and *J. globiflora* after different thermal treatment

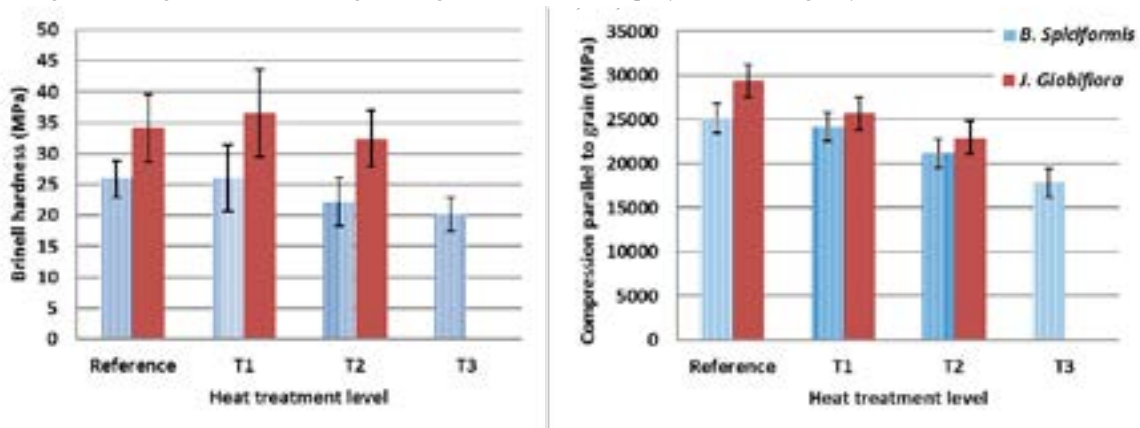


Fig. 2. Changes in Brinell hardness and compression strength of *B. spiciformis* and *J. globiflora* after thermal modification

Marketing of Urban and Reclaimed Wood Products

Dr. Omar Espinoza*, Anna Pitti

Department of Bioproducts and Biosystems Engineering
University of Minnesota
St. Paul, Minnesota, 55114, United States

ABSTRACT

In the United States, trees felled in urban areas and wood generated through construction and demolition are primarily disposed of as low-value resources, such as biomass for energy, landscaping mulch, composting, or landfill. An emerging industry makes use of these underutilized resources to produce high-value added products, with associated benefits for the environment, the local economy, and consumers. Research was carried out to increase the understanding of the marketing practices of urban and reclaimed wood industries. This paper presents the results from a nationwide survey of these companies. The results indicate that a majority of companies in this industry are small firms, operating for less than 10 years, produce mostly to order, and sell their products at comparatively higher prices than similar products made from traditional sources. Promotional messages included quality, aesthetics, and customization, conveyed through company webpages, word of mouth, and social media. Distribution channels used include direct sales, online sales, and retail sales. Partnerships are critical for effective raw material procurement. Respondents indicated optimistic growth expectations, despite barriers associated with urban and reclaimed wood materials and production

1. INTRODUCTION

Traditionally, logs from trees originating in urban areas of the US and wood elements generated through construction and demolition (C&D) projects have been disposed of as low value resources, typically through chipping, burning, or landfilling. There are approximately 74 billion trees in urban areas of the US, and when trimming or removal is necessary, they are considered “wood waste” (Sherrill 2017). It was estimated that, of the 34.2 million tons of wood-based municipal solid waste (MSW) generated in 2010, 18.4 million tons of woody yard trimmings, like urban logs and limbs, were disposed of, with 4.0 million tons available for recovery (Bratkovich, Howe et al. 2014). Reclaimed wood includes all previously utilized wood products brought back into circulation, largely originating from structures like old barns and buildings. In 2010, approximately 36.4 million tons of C&D wood waste were generated in the US, with approximately 17.3 million tons available for recovery (Howe, Bratkovich et al. 2013, Bratkovich, Howe et al. 2014).

In recent years, industries have emerged to capitalize on timber from urban trees and reclaimed wood by offering unique aesthetics, historical significance, sustainability, and sentimentality derived from inimitable wood supplies. The urban and reclaimed wood industries operate using a circular economy business model, working to upcycle raw materials traditionally regarded as waste or of low value. By closing industrial loops, a circular economy operates beyond the traditionally linear *take, make, waste* production to address resource scarcity, environmental impact, and economic benefits, effectively providing social, natural, and economic capital (Lieder and Rashid 2016, Ellen MacArthur Foundation 2019). Specifically, the urban and reclaimed wood industries provide economic opportunities in their communities through high value-added production, and by salvaging raw materials from landfills, firms offer both environmental and social benefits associated with opportunities for waste reduction and forest regeneration, respectively. Additional environmental benefits brought forth as a result of urban and reclaimed wood production include increased carbon sequestration potential, decreased energy consumption, and decreased global warming potential (Gu and Bergman 2018, Sherrill and Bratkovich 2018).

Due to the newly established nature of the urban and reclaimed wood industries, minimal literature specific to marketing practices exists. A variety of sources were consulted to gather an understanding of each industry and how attributes are relayed to consumers, including company and network webpages, reports, online articles, and a number of other sources. The urban wood industry largely comes together through industry network collaboration to provide their members with a number of resources, including information for efficient production and targeted marketing

* Corresponding author: Dr. Omar Espinoza; E-mail: oaespi@umn.edu

materials, as depicted through the nationally operating Urban Wood Network (Urban Wood Network 2019) and Urban, Salvaged, and Reclaimed Woods (Urban 2019) network operating in California. Reclaimed wood products can generate demand from consumers through environmental certifications, specifically Forest Stewardship Council (FSC) reclaimed wood certification potential. The Forest Stewardship Council, an organization that maintains certification standards for sustainably managed forests and supply chains, has expanded their certification to include post-consumer reclaimed material, including a majority of value-added reclaimed wood products (Forest Stewardship Council 2011). Additionally, reclaimed wood materials can receive Leadership in Energy and Environmental Design (LEED) accreditation, a rating system that provides credits for applicable life cycle impact reductions, as well as FSC Certification, material reuse, and regional sourcing (U.S. Green Building Council 2019). Both urban wood network collaboration and reclaimed wood recognition reinforce raw material reliability to consumers, in turn helping firms in marketing their products. This publication presents the results of a research project that used a nation-wide survey to develop an industry profile of firms operating in the urban and reclaimed wood industries, with emphasis on marketing practices.

2. RESEARCH OBJECTIVE

The main objective of this study was to identify current marketing practices in the urban and reclaimed wood industries. To accomplish this goal, the following specific objectives were proposed: (1) develop a profile of value-added urban and reclaimed wood manufacturers, (2) identify current marketing practices, and (3) identify industry opportunities and barriers.

3. METHODS

A nationwide survey was conducted to outline current marketing practices and major characteristics of firms in the target population, namely value-added production firms using urban logs or reclaimed wood components as raw materials. Because these industries are relatively new and lack specific Census classification designation, a list of 386 firms was compiled through Internet searches, social media, state and regional databases, personal contacts, and other means. The final distribution list contained what authors categorized as 151 *urban wood* companies and 238 *reclaimed wood* enterprises, but survey results later indicated that many firms utilize both urban and reclaimed wood raw materials, which will be referred to as raw materials from *mixed-sources*.

The questionnaire was developed in Qualtrics, an online survey software system and was distributed via email to companies in the industry list (Qualtrics 2005). Questions included company characteristics, customer characteristics, products, wood species, distribution channels, promotional messaging and platforms, opportunities, and barriers.

4. RESULTS AND DISCUSSION

After closing the survey, 132 usable responses were obtained, and an adjusted response rate of 37.2% was calculated (Dillman, Smyth et al. 2009). This response rate is considerably above the median and average response rates for surveys to North American forest products industries, of 26.0% and 31.6%, respectively (Bumgardner, Montague et al. 2017).

4.1. COMPANY CHARACTERISTICS

Respondents consisted of 36 *urban wood* firms, 41 *reclaimed wood* firms, and 55 *mixed-source* firms. For most questions, responses by mixed-source firms resembled those by urban wood firms to a higher degree than those of reclaimed wood firms. Overall, a majority of firms have been in operation less than 10 years (43.2%), and 36.4% were operating more than 15 years. Companies were asked the US regions where their products were sold (Midwest, Northeast, Southwest, and Northwest), or if they exported. Multiple responses were possible, and a majority of participating firms reported sales in the *Midwest* and *Northeast* (approximately 50.0% of respondents for each region). Approximately 18.9% of firms reported having export operations, and twice as many reclaimed wood firms indicated exporting than either mixed-source or urban wood firms (29.3%, 14.5%, and 13.9% of firms, respectively).

Number of employees and monthly raw material consumption in board feet were used to estimate general firm size and production capacity. In general, urban wood and mixed-source firms were smaller than reclaimed wood operations, with 86.1%, 67.3% and 46.3% of respondents, respectively, having fewer than 10 employees. Reclaimed wood firms also consumed the highest volume of raw material per month (an average 26.7 thousand board feet, or

MBF), followed by mixed-source (16.4 MBF) and urban wood firms (6.1 MBF). It should be noted, however, that the reported raw material consumption varied widely, ranging from 100 to 200,000 bf per month.

Firms were also asked to report their reasons for entering the industry. Responses were largely reflective of raw material characteristics as a source of differentiation, including desire for unique raw materials, a supply of wood otherwise being underutilized or wasted, and sustainable and local products, with 90.9%, 89.4%, and 77.3% of respondents, respectively, ranking these reasons as “Important” or “Extremely Important.”

4.2. CUSTOMER CHARACTERISTICS

By understanding who their customers are, firms can tailor their marketing strategies, target specific segments, and develop successful products. Survey results indicate that the consumer is as a 35-54-year-old with upper middle-income status, where gender was noted as irrelevant to purchasing.

4.3. MARKETING MIX

This study sought to outline marketing strategies implemented by the urban and reclaimed wood industries. For this, the “marketing mix” was used as a framework, specifically analyzing product, price, promotion, and placement. Product analysis consisted of species used and product categories, pricing was studied in relation to the competition, promotional analysis included messaging and platforms, and placement considered distribution channels.

Products manufactured and species used by participating firms varied widely, particularly between raw material group. Urban wood firm product offerings most frequently included slabs, furniture, mantels, lumber, beams, tableware, and accessories; while reclaimed wood firms identified mantels, beams, furniture, flooring, millwork, stair parts, lumber, and doors as their most common products. Mixed source firm responses primarily aligned with urban wood firm responses, including furniture, slabs, mantels, lumber, beams, millwork, and flooring. The five most common wood species used in production of urban wood products were all hardwoods (walnut, white oak, cherry, ash, and hard maple), while reclaimed wood firms produce with both hardwoods and softwoods (Douglas-fir, pine, southern yellow pine, white oak, and red oak). Mixed source firm responses were closely aligned with those reported by urban wood companies, including walnut, white oak, red oak, ash, and hard maple. Overall, participating firms reported primarily made-to-order (MTO) production over made-to-stock (MTS) (61.0% and 39.0% of sales, respectively). Reclaimed wood firms allocated a higher percentage to MTO production than either urban wood or mixed source firms (71.9%, 53.9%, and 58.1% of sales, respectively).

Participating firms also indicated that urban and reclaimed wood prices were often higher than the competition’s, with 36.3% reporting prices “Slightly higher” or “Much higher” compared to 29.5% indicating prices “Slightly lower” or “Much lower.” From analysis of survey responses for product and price, it can be stated that urban and reclaimed wood firms, in general, adopt a differentiation strategy, making high-end products and producing largely against firm orders. Primary promotional messages were identified to highlight attributes such as *quality*, *aesthetics*, and *customization* (Table 1), often relayed to consumers via *word of mouth*, *company webpage*, and *social media* (Table 2), with 93.2%, 81.1%, and 65.9% of firms rating these three promotional platforms as “Important” or “Extremely important.” Lastly, the most common distribution channels utilized by participating firms include *direct sales* (88.6% of firms), *online sales* (53.0%), and *retail sales utilizing a company-owned store or showroom* (47.7%). *Export sales* were less prevalent but reported by 13.6% of firms. Responses on promotional platforms and distribution channels highlight the customer-centric nature of the urban and reclaimed wood industries.

Table 1: Marketing messages as identified by participating firms

Messaging theme	Not at all important	Slightly important	Moderately important	Important	Extremely important
Sustainability	2 (1.5%)	6 (4.5%)	18 (13.6%)	37 (28%)	65 (49.2%)
Aesthetics	0 (0%)	2 (1.5%)	4 (3%)	32 (24.2%)	90 (68.2%)
Quality	1 (0.8%)	1 (0.8%)	3 (2.3%)	22 (16.7%)	101 (76.5%)
Customization	4 (3%)	2 (1.5%)	18 (13.6%)	33 (25%)	70 (53%)
Emotional value	3 (2.3%)	7 (5.3%)	35 (26.5%)	41 (31.1%)	42 (31.8%)
Historical significance	4 (3%)	12 (9.1%)	23 (17.4%)	49 (37.1%)	40 (30.3%)
Local and domestic sourcing	3 (2.3%)	8 (6.1%)	22 (16.7%)	45 (34.1%)	50 (37.9%)

* Rows do not add up to 100% because companies did not answer this question.

Pearson's chi-squared test: *Local and domestic sourcing* displayed significant association between promotional messaging and raw material group: $\chi^2 = 17.39$; **p-value = 0.026** ($p < 0.05$).

Table 2: Marketing platforms as identified by participating firms

Promotional platform	Not at all important	Slightly important	Moderately important	Important	Extremely important
Company webpage	1 (0.8%)	9 (6.8%)	12 (9.1%)	26 (19.7%)	81 (61.4%)
Word of mouth	0 (0%)	1 (0.8%)	5 (3.8%)	27 (20.5%)	96 (72.7%)
Public relations	9 (6.8%)	24 (18.2%)	33 (25%)	22 (16.7%)	36 (27.3%)
Social media	3 (2.3%)	11 (8.3%)	26 (19.7%)	39 (29.5%)	48 (36.4%)
Newspapers or magazines	28 (21.2%)	45 (34.1%)	32 (24.2%)	13 (9.8%)	7 (5.3%)
Events	30 (22.7%)	38 (28.8%)	22 (16.7%)	23 (17.4%)	13 (9.8%)

* Rows do not add up to 100% because companies did not answer this question.

Pearson's chi-squared test: "word of mouth" and "events" display significant association between promotional platform and raw material group: $\chi^2 = 16.41$; **p-value = 0.012** ($p < 0.05$) and $\chi^2 = 19.446$; **p-value = 0.013** ($p < 0.05$), respectively.

Other promotional platforms: Architects and designers, craft shows, paid advertising, partnerships with third party sellers, radio, reviews (Yelp, Google), seeing products within the community, slab wagon on the street, tours, TV commercial, YouTube presence

4.4. SUPPLY CHAIN PARTNERSHIPS

Partnerships are critical to urban and reclaimed wood production due to their role in raw material procurement. The survey asked firms to identify sourcing collaborations by selecting from a list. Urban wood partners included *tree removal firms* (83.3% of firms), *arborists* (77.8%), *homeowners* (75.0%), *city governments* (69.4%), and *urban foresters* (58.3%). Primary reclaimed wood partners included *deconstruction firms* (78.0%), *demolition firms* (75.6%), *building owners* (70.7%), and *construction and remodeling firms* (51.2%). The most frequently cited partnerships by mixed-source firms aligned closely with those of urban wood companies, ranked as follows: *homeowners* (72.7%), *tree removal firms* (63.6%), *arborists* (58.2%), *building owners* (56.4%), *deconstruction firms* (52.7%), *urban foresters* (49.1%), *city governments* (49.1%), and *construction and remodeling firms* (45.5%).

4.5. GROWTH

When asked about prospects for growth, firms reported largely optimistic expectations, with 85.6% anticipating modest to significant growth in the next five years. Such expectations reinforce confidence within these industries that urban and reclaimed wood demand is not merely a fad, but firms have established plans for the foreseeable future. To facilitate growth, firms will need to overcome barriers, the most important of which were identified as *lack of financial resources* (rated as "Large" or "Extreme" barrier by 31.8% of respondents), *lack of storage space* (25.0%), and *underperforming or insufficient marketing efforts* (22.0%).

Table 2: Barriers to industry growth

Barrier	Not a barrier	Slight barrier	Moderate barrier	Large barrier	Extreme barrier
Poor relationships with suppliers	73 (55.3%)	28 (21.2%)	18 (13.6%)	7 (5.3%)	0 (0.0%)
Lack of market research / poorly identified markets	55 (41.7%)	31 (23.5%)	4 (3%)	14 (10.6%)	1 (0.8%)
Lack of storage space for raw materials	54 (40.9%)	18 (13.6%)	3 (2.3%)	23 (17.4%)	10 (7.6%)
Difficulty working non-traditional raw materials	52 (39.4%)	33 (25.0%)	18 (13.6%)	8 (6.1%)	3 (2.3%)
Quantity and/or quality of raw materials	48 (36.4%)	29 (22.0%)	35 (26.5%)	16 (12.1%)	1 (0.8%)
Lack of financial resources	35 (26.5%)	26 (19.7%)	23 (17.4%)	29 (22.0%)	13 (9.8%)
Under-performing or insufficient marketing effort	32 (24.2%)	42 (31.8%)	22 (16.7%)	20 (15.2%)	9 (6.8%)
Lack of consumer awareness	23 (17.4%)	32 (24.2%)	46 (34.8%)	20 (15.2%)	6 (4.5%)

* Rows do not add up to 100% because companies did not answer this question.

Pearson's chi-squared test: *Local and domestic sourcing* displayed significant association between promotional messaging and raw material group: $\chi^2 = 17.39$; **p-value = 0.026** ($p < 0.05$).

5. SUMMARY

The objective of this research was to identify current marketing practices in the urban and reclaimed wood industries via an industry survey, with focus on developing a manufacturer profile, identifying current marketing practices, and outlining opportunities and barriers. Results indicate that a majority of participating firms have operated for less than 10 years or more than 15 years, and reclaimed wood firms tend to operate at higher capacities than urban wood firms. Major reasons for entering each industry are associated with raw material characteristics as a source of differentiation. Typical consumers are 35-54 years of age with upper middle-income status, where gender was noted as irrelevant to purchasing. Almost all firms maintained at least one supply chain partnership, but an average of four partners was reported.

Products and species were variable between raw material groups, and firms primarily produce to-order over stock product. Pricing was, in general, higher than the competition. Messages of quality, aesthetics, and customization were emphasized using word of mouth, company webpages, and social media. Primary distribution channels consisted of direct sales, online sales, and retail sales. Firms almost unanimously anticipate growth going forward, but they will need to overcome barriers like lack of financial resources, lack of storage space, and inadequate marketing efforts.

ACKNOWLEDGEMENTS

The authors would like to thank all the companies that participated in this study who contributed their time and thoughts to better understand the urban and reclaimed wood industries.

REFERENCES

- Bratkovich, S., Howe, J., Bowyer, J., Pepke, E., Frank, M. and Fernholz, K. 2014. *Municipal Solid Waste (MSW) and Construction and Demolition (C&D) Wood Waste Generation Recovery in the United States*, Dovetail Partners Inc.: 16.
- Bumgardner, M., Montague, I. and Wiedenbeck, J. 2017. *Survey Response Rates in the Forest Products Literature from 2000 to 2015*. *Wood and Fiber Science* 491: 84-92.
- Dillman, D., Smyth, J. and Christian, L. 2009. *Internet, Mail, and Mixed-Mode Surveys: The Tailored Design Method*, John Wiley & Sons, Inc.
- Ellen MacArthur Foundation. 2019. "What is the Circular Economy?". 2019, from <https://www.ellenmacarthurfoundation.org/circular-economy/what-is-the-circular-economy>.
- Forest Stewardship Council. 2011. *FSC Standard: Sourcing reclaimed material for use in FSC Product Groups or FSC Certified Projects*: 11.
- Gu, H. and R. Bergman. 2018. *Life cycle assessment and environmental building declaration for the Design*

- Building at the University of Massachusetts. Madison, WI, U.S. Department of Agriculture, Forest Service, Forest Products Labor: 71.*
- Howe, J., Bratkovich, S., Bowyer, J., Frank, M. and Fernholz, K. 2013. *The Current State of Wood Reuse and Recycling in North America and Recommendations for Improvements. Dovetail Partners Inc.: 167.*
- Lieder, M. and A. Rashid. 2016. "Towards Circular Economy Implementation: A Comprehensive Review in Context of Manufacturing Industry." *Journal of Cleaner Production 115: 36-51.*
- Qualtrics. 2005. Provo, Utah.
- Sherrill, S. 2017. *Harvesting Urban Timber: The Complete Guide, Echo Point Books & Media.*
- Sherrill, S. and S. Bratkovich. 2018. *Estimates of Carbon Dioxide Withheld from the Atmosphere by Urban Hardwood Products, Dovetail Partners, Inc.: 39.*
- U.S. Green Building Council. 2019. *LEED v4 for Building Design and Construction.*
- Urban, Salvaged, and Reclaimed Woods. 2019. from <https://urbansalvagedwoods.com/>.
- Urban Wood Network. 2019. "Urban Wood Network." from <http://urbanwoodnetwork.org/>.

The potential of wood acetylation

Ferry Bongers¹ and Stephen J. Uphill²¹Accsys Group, Westervoortsedijk 73, NL-6827 AV,
Arnhem, the Netherlands²Accsys Group, Brettenham House, 19 Lancaster Pl,
London WC2E 7EN, UK

ABSTRACT

*Wood, having the lowest embodied energy of any mainstream building material, is carbon neutral. As such, wood, our only naturally renewable construction resource, helps combat global warming by absorbing carbon from the atmosphere and storing it away for the life of the wood product. Not only is wood renewable, but it is also biodegradable and sustainable. Nature is programmed to recycle wood back into its basic building blocks of carbon dioxide and water through biological, thermal, aqueous, photochemical, chemical, and mechanical degradations. Once broken down, these elements contribute to the circle of life by providing nutrients or biomass energy for the growth of new plant life which will grow and, in turn, absorb atmospheric carbon. The rate of recycling depends on the natural durability of the wood species. Many tropical hardwoods are known for their durability characteristics. However, a large number of higher yield sustainable softwood and hard wood species do not possess inherent durability, dimensional stability and other valued characteristics. By altering the wood cell wall polymers at the molecular level, the properties of wood species with low durability could be enhanced. Acetylation is well known to increase the resistance of wood against wood decaying fungi and destructive insects as well as improving the dimensional stability in moist circumstances. Acetylation of wood creates opportunities to improve the utilization of low value soft and hardwood species and to extend the balance of carbon sequestration capabilities of otherwise non-durable species. For the first commercial production of acetylated wood, Accsys Group has utilised the acetylation technology on radiata pine (*Pinus radiata* D. Don). For world-wide production of acetylated wood using a wider range of species and use in new application areas with varying material property requirements, other wood species will be considered. This paper gives an overview of research done on acetylation of soft and hardwood species and their performance in a series of applications.*

1. INTRODUCTION

Since the early-days mankind has utilized trees for its timber for building material, paper, fuel, art and other craftwork, and has been important for development of the human society. Wood is a renewable and biodegradable. Nature is programmed to recycle it, in a timely way, back into its basic building blocks of carbon dioxide and water through biological, thermal, aqueous, photochemical, chemical, and mechanical degradation processes. Most problems with timber in service are associated with wood destroying fungi under high humidity conditions and dimensional changes in changing climates. Furthermore, wood exposed outdoors undergoes photochemical degradation caused by ultraviolet radiation, and is subjected to discoloration due to mould and blue stain fungi.

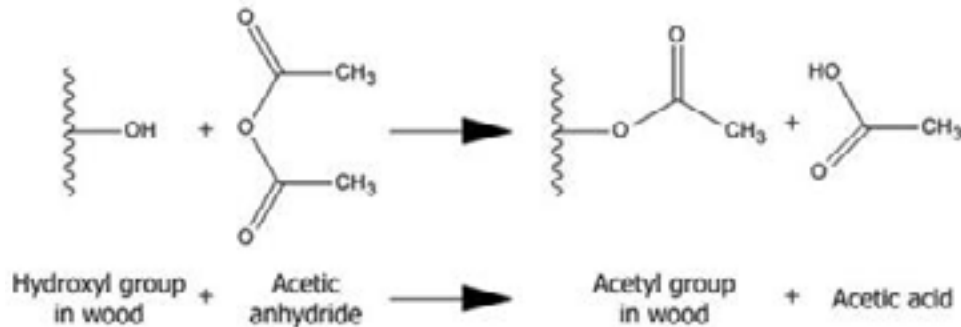
The rate of recycling depends on the natural durability of the wood species. Many tropical hardwoods are known for their durability characteristics. However, a vast majority of the world's wood species do not possess inherent durability, dimensional stability and other valued characteristics such as highly attractive surfaces (aesthetics), defect free qualities and easiness of processing. The world's supply of durable wood suitable for long term performance in outdoor applications is becoming more and more scarce. Furthermore, environmental regulations on the use of toxins to enhance the durability of wood species are increasing. An environmentally friendly alternative is the chemical modification of wood which results in improved wood performance. By altering the wood matrix on a molecular level, the properties of wood species with low durability can be enhanced. Acetylation is well known to increase the resistance of wood against wood decaying fungi and destructive insects as well as improving the dimensional stability in humid circumstances (Rowell and Dickerson 2014).

2. ACETYLATION OF WOOD

2.1. ACETYLATION PROCESS

Acetylation of wood has been studied extensively and has shown to be one of the most suitable methods for improvement of technical properties of low durable wood species (Hill 2006, Rowell and Dickerson 2014). In the last

decade most work has been done with uncatalyzed acetic anhydride and without solvent as described by Rowell *et al.* (1986). The reaction of acetic anhydride with wood results in esterification of the accessible hydroxyl groups in the cell wall to acetyl groups with the formation of by-product acetic acid (Figure 1). It is a single-addition process and all weight gain is accounted by the acetyl groups added. The wood also swells during the acetylation process. When the wood is acetylated to high extent (20 weight percent gain and more) the volume is almost similar to that of



'green'(undried untreated) wood (Rowell and Dickerson 2014).

Figure 1: Schematic reaction of acetic anhydride with wood.

2.2. SUITABLE WOOD SPECIES

Solid wood

Over the last century, acetylation of different wood species has been tried, both on laboratory as well as (semi)commercial scale. When a sufficient degree of acetylation is achieved the resistance against fungal decay and the dimensional stability in changing climates can be improved considerably. Generally all wood species which are easily dried, have a good liquid impregnatable and have a low to intermediate density (300 to 700 kg/m³) have high potential for the acetylation process. Also important is the dimension of the boards for the feasibility of acetylation. In general, the higher surface area to volume ratio, the easier acetylation becomes. Other factors for commercial production are purchasing characteristics (available volume, dimensions, quality, price and properties), acetylation economics and potential markets (Bongers *et al.* 2008).

With refractory wood species of large dimensions, such as spruce and Douglas fir, non-uniform acetylation results in wood quality issues such as distortions and cracking, and low performance. The presence of different qualities within a board of good permeable wood species (sapwood, heartwood, reaction wood, knots, resins) can also lead to uneven acetylation and associated wood quality issues. To improve permeability of wood species different methods have been tried over the years. Common methods for preservative treatments are pre-steaming and incising, but do not result in full penetration of the cross section. Other methods to improve acetylation with refractory wood species such as fungal pre-treatment (Messner *et al.* 2003), super-critical CO₂ impregnation, and microwave acetylation are not exploited commercially.

Currently Accsys Group is commercially acetylating Radiata pine (*Pinus radiata* D. Don), but has been researching acetylation of other wood species such as southern yellow pine (USA), scots pine (EU), beech (EU) and masson pine from China. Also work was done on various tropical wood species of which tauari vermelho (*Cariniana micrantha*) was most promising (Bongers *et al.* 2008). Bollmus *et al.* (2015) acetylated boards of beech (*Fagus sylvatica*), alder (*Alnus glutinosa*) lime (*Tilia* spp.) and maple (*Acer* spp.) and the resistance to fungal decay and cyclic dimensional stability tests gave very promising results. Other species that have shown high prospects for acetylation are hornbeam (*Carpinus betulus*) (Fodor *et al.* 2017), scots pine (*Pinus sylvestris*) (Larsson and Tillmann 1989), Corsican pine (*Pinus nigra*) (Hill and Jones 1996), aspen / poplar (*Populus* spp.) (Beckers and Miltz 1994) and Southern pines (*Pinus* spp.) (Goldstein *et al.* 1961).

Chips and flakes

Whereas the permeability of wood is important for solid wood to obtain uniform acetylation throughout the board, this plays less a role in acetylation of smaller dimensions. Even less permeable wood species can be acetylated in the forms of chips, flakes or fibres. Over the years many research groups have studied acetylation of smaller elements to produce wood-based materials. Rowell *et al.* (1986) acetylated southern pine, aspen and Douglas-fir flakes. Hadi *et al.* (1995) made high dimensional stable composite boards from acetylated rubber wood (*Heavea brasillensis*) fibres, and

Rowell and Plackett (1988) produced flakeboards from acetylated radiata pine. Acetylated fibres also show improved resistance against fungal decay and dimensional stability when used in wood plastic composites (Segerholm 2012).

2.3. CONSISTENCE OF TREATMENT

To gain and maintain market acceptance, it is important that acetylated wood is manufactured in a uniform manner such that it will provide consistent, reliable and acceptable performance (Bongers and Van Zetten 2017). This is important since, the mechanism of protection of acetylated wood is not based on toxicity, unlike preservative treatment and highly durable wood species, and thus lower acetylated sections can be attacked by fungi (Emmerich *et al.* 2019). Therefore a board should be acetylated throughout the cross section, and be acetylated to a uniform sufficient level throughout the board's length. Furthermore the acetylation treatment should be sufficient for all boards within a batch (uniformity) and also the treatment process should be reproducible. Important for quality control is that the degree of acetylation can be quantitative determined reliably by a number of chemical analysis methods such as High Performance Liquid Chromatography (HPLC) and Gas Chromatography (GC) and spectroscopic methods like FTIR and NIR (Beckers *et al.* 2003, Schwanninger *et al.* 2011).

Accsys Group has developed a management system to warrant consistent day-to-day production. This is extended to National Level accreditations through several (private label) certification schemes which incorporate regularly independent third party audits, such as the KOMO[®] certification scheme of modified wood (Homan and Tjeerdsma 2005).

2.4. COMMERCIAL PRODUCTION

Over the last century several attempts to commercially produce acetylated wood were initiated on different locations worldwide (Rowell 2006, 2014). During the 1940's to 1960's the USDA Forest Product Laboratory developed an acetylation process by use of acetic acid anhydride where pyridine was used as catalyst (Tarkow 1946). In the 1960's Koppers (USA) made first attempt to introduce acetylated wood to the market by acetylation with a mixture of acetic anhydride and xylene without catalyst (Koppers 1961). Daiken started commercial production of acetylated wood for flooring called alpha-wood in the late 1980s in Japan. In the early 1990s a commercial attempt to acetylate fibres was made by a collaboration of British Petroleum (BP), A-Cell acetyl cellulose AB ("A-Cell"), and the BioComposites Centre (Sheen 1992). Due to technical and economic reasons these attempts were commercially unsuccessful.

Accsys Group introduced acetylated wood, named Accoya[®] wood (www.accoya.com), into the market in 2007. Accoya[®] wood is based on the acetylation of radiata pine (*Pinus radiata* D. Don) and is mainly used for applications such as joinery, cladding, decking and (light) civil works in the Netherlands, UK and Germany (Alexander 2007, Bongers *et al.* 2009, Kattenbroek 2007). In addition to solid wood acetylation, Accsys Technologies also developed a process for the acetylation of wood elements (under the brand name Tricoya[®]) for use within medium density fiberboard (MDF), particle board and wood plastic composites (Rowell 2014, Suttie *et al.* 2015).

3. PROPERTIES OF ACETYLATED WOOD

3.1. PHYSICAL PROPERTIES

Due to the acetylation the hydroxyl groups are replaced with acetyl groups which reduce directly the amount of moisture that can be bound to the cell wall (Hill 2008, Rowell 2015). The Equilibrium Moisture Content (EMC) and the Fibre Saturation Point (FSP) is reduced with increasing acetylation level. Water absorption within the cell wall is also accompanied by swelling of the wood. When the wood dries then the wood shrinks. Since the acetylation reduces the cell wall sorption behavior the swelling and shrinkage behavior in changing humidities is reduced. The higher the degree of acetylation the more dimensional stable the wood (Engelund 2013).

An Anti-Swelling-Efficiency (ASE) of circa 70-80% can be obtained by highly acetylating radiata pine (Bongers *et al.* 2008). Unmodified and acetylated radiata pine samples were conditioned at the following climates: oven dry, 25, 35, 50, 65, 80, 95% relative humidity and water saturated (all at a temperature of 20 °C). In this order (adsorption sequence), as well as in the reverse order (desorption sequence). The weight and dimensions (radial and tangential) of the samples were determined for each of the conditions. Based on the weight measurements, the relation between the relative humidity (of the air) and the corresponding equilibrium moisture content (EMC) of the wood was determined for both the adsorption and desorption sequence. The corresponding shrinking and swelling was measured in the radial and tangential orientations of the wood structure. The results are expressed in Figure 2. The results illustrate that the

equilibrium moisture content of acetylated radiata pine has been significantly reduced. Further the dimensional stability is improved considerably.

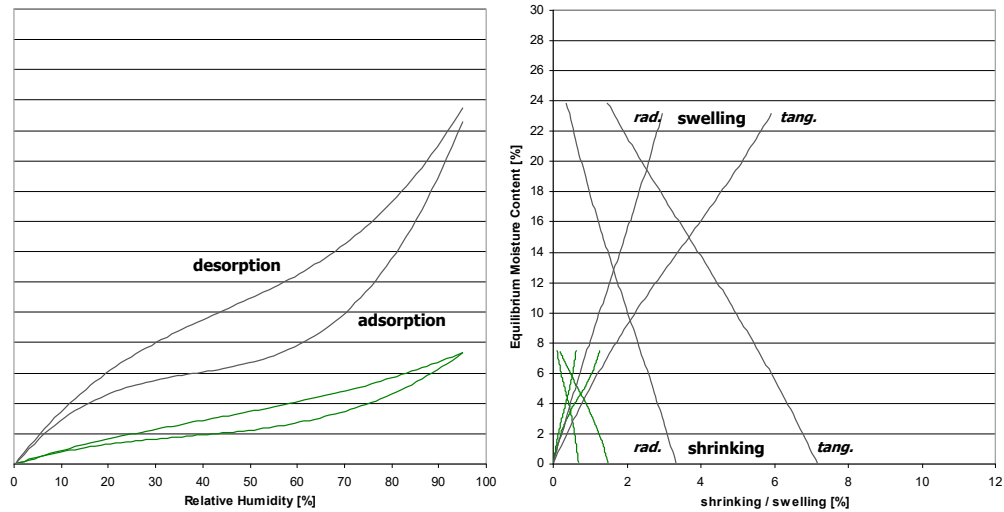


Figure 2: Hygroscopic behavior (left) of acetylated radiata pine (green line) and (unmodified) radiata pine (black line) under different moisture conditions and the corresponding swelling and shrinking behavior (Bongers *et al.* 2008).

3.2. DURABILITY

Fungi

Considerable research has been conducted to determine the effect of wood acetylation on the resistance to fungal degradation (Alexander *et al.* 2014, Alfredsen *et al.* 2013, Beckers *et al.* 1994, Militz 1991, Papadopoulos and Hill 2002, Peterson and Thomas 1978, Rowell and Dickerson 2014, Suttie *et al.* 1999, Takahashi *et al.* 1989). Bongers *et al.* (2008) studied the resistance of acetylated radiata pine, treated to different degrees, to brown-, white-, and soft rot fungi according to EN 113 and ENV 807. The higher degree of acetylation the better the resistance against fungal decay (see Figure 3). There is generally good agreement amongst researchers that, at least above weight percent gains (WPG) of 15-20%, acetylated wood shows marked resistance to attack by most wood destroying fungi. Long term in-ground stake testing (18 years) have confirmed that long term durability against fungal decay is achieved around 22% WPG (Larsson-Brelid and Westin 2010).

The 'mode of action' of acetylated wood to resistance of fungal decay is not fully understood. Recently Emmerich *et al.* (2019) confirmed that fungal hyphen can grow through acetylated wood and attack unmodified sections. Various hypotheses are linked with reduction of the moisture content of the cell wall (Alfredsen *et al.* 2013, Engelund *et al.* 2013, Hill 2009, Rowell 2015, Thygesen *et al.* 2010). The amount of bound water in the cell wall and Fiber saturation point (FSP) is significantly reduced by increasing degree of acetylation (Beck *et al.* 2018a, 2018b, Hill 2008). By extending the duration of laboratory testing up to 36 weeks under optimum condition with the highly aggressive brown rot fungus *Rhodonina (Poria) placenta*, Pilgård *et al.* (2012) found for the highly acetylated SYP no mass loss. Alfredsen *et al.* (2016) found that acetylated wood has a higher resistance against the first step in the decay process of this brown rot fungus (oxidative degradation of the cell wall).

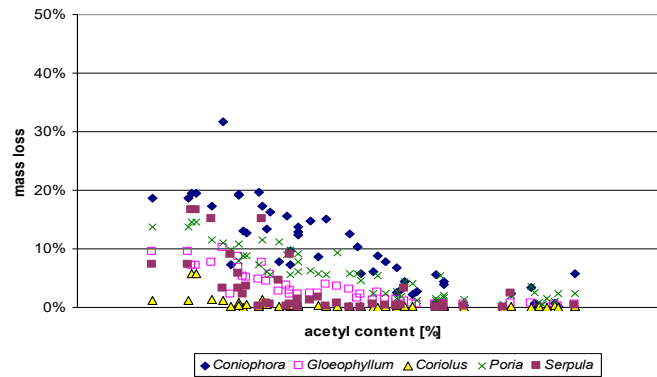


Figure 3: Mass loss of acetylated radiata pine caused by basidiomycetes (EN 113 test) in relation to the acetyl content (Bongers *et al.* 2008).

Marine organisms

A variety of studies on different locations have demonstrated that the resistance to marine borer attack of wood increases with increasing level of acetylation (Bongers *et al.* 2018, Johnson and Rowell 1988, Klüppel *et al.* 2010, Papadopoulos *et al.* 2008a), although the 'mode-of-action' is not fully understood as well as whether highly acetylated wood will be able to prevent marine-borer attack completely in all locations (Westin *et al.* 2016). With respect to the latter, running tests with highly acetylated radiata pine in Denmark, are showing no attack of marine borers after nine years of exposure (Bongers *et al.* 2018).

Termites and insects

Over the years a number of assessments have been made of the termite resistance of acetylated solid wood (Alexander *et al.* 2014, Bongers *et al.* 2015, Imamura and Nishimoto 1986, 1987, Miltz *et al.* 2009, Papadopoulos *et al.* 2008b, Rowell and Dickerson 2014). The various studies showed that in most forced feeding tests with acetylated wood the mortality of soldiers was far higher than that of workers, and that the acetylated wood is subjected to exploratory attack. Imamura and Nishimoto (1986) demonstrated that acetylated wood cannot be decomposed by the symbiotic protozoa in *Coptotermes formosanus* and *Reticulitermes speratus*, resulting in a kind of starvation effect. However, other factors that may affect the termite resistance for acetylated wood are suggested such as smell, hardness, reduced equilibrium moisture content, level and uniformity of acetylation (Bongers *et al.* 2015).

3.3. MECHANICAL PROPERTIES

Acetylation changes the cell wall chemistry that impacts the physical and mechanical properties of the wood (Rowell 1996). The overall mechanical properties of acetylated wood relate on varying increasing and decreasing effects resulting from the acetylation process (Bongers and Beckers 2013, Dreher *et al.* 1964, Larsson and Simonson 1994). Several mechanical properties such as compression strength and hardness are increased by acetylation due to 1) the lower equilibrium moisture content of acetylated wood, and 2) increase of density. On the other-hand, some mechanical properties such as tensile strength can be (slightly) reduced due to 1) the amount of fibres per volume being reduced compared to untreated wood, as acetylated wood is permanently in its 'swollen' dimension, and 2) the acetylation process being performed at elevated temperature that can create thermal degradation of cellulose, hemi-cellulose and lignin.

Many research has focussed on small clear samples, and mostly on bending stiffness and strength ((Bongers and Beckers 2003, Dreher *et al.* 1964, Larsson and Simonson 1994). Epmeier *et al.* (2007) investigated creep behaviour and found a significant reduction for acetylated wood. More recent large amount of research is done on large commercial sections of acetylated Radiata pine, and could a strength class of C22 as described in EN 338 be allocated for a defect free quality (Bongers and Alexander 2018). Furthermore Marcroft *et al.* (2013) found that the impact of high wood moisture content on reduction of the mechanical properties is less for acetylated radiata pine compared to untreated wood species. This has enabled to use acetylated radiata pine in load-bearing exterior applications (see paragraph 4.2).

3.4. BONDING AND FINISHING

Due to the acetylation process various material properties are altered that may influence bonding quality (Bongers *et al.* 2013, Brandon *et al.* 2006, Frihart *et al.* 2017, Hunt *et al.* 2007, Ormstad 2007, Treu *et al.* 2018, Vick & Rowell 1990):

- Acetylation replaces the hydrophobic hydroxyl groups with acetyl groups (see Figure 1). This has directly impact for adhesives on chemical bonding to hydroxyl groups.
- Increased hydrophobicity of the surface decreases the ability of water-based adhesive to wet, flow, and penetrate a bonding surface (Bryne and Wålinder 2010).
- Reduced equilibrium moisture content, improved dimensional stability and water uptake behaviour.
- Presence of small amount of acetic acid (by-product of the acetylation reaction) can impact the (surface) pH of the wood and its buffering capacity which play an important role for reaction and curing rates of several types of adhesives.
- Increased surface hardness and changed mechanical properties, especially increased wet strength resulting in different failure mechanisms in strength tests of laminated acetylated wood.

Lamination, finger-jointing and edge-glueing of acetylated wood is possible with various types of adhesives. Tjeerdsma and Bongers (2009) found good performance of acetylated Radiata pine with a PRF and PUR adhesive for structural applications. Vick and Rowell (1990) had good results with bonding acetylated Yellow poplar (*Liriodendron tulipifera* L.) with a water-borne non-polar high molecular weight and high solid content EPI adhesive, and with high viscosity PUR adhesives. The tested PVAc adhesive had difficulties to wet and penetrate acetylated wood and showed less performance in wet conditions. Bongers *et al.* (2016) tested several commercial available PUR adhesives and all showed good bonding with acetylated Radiata pine. In wet conditions Melamine Urea Formaldehyde (MUF) adhesive show a bad performance, but improvement is seen when a primer is used (Treu *et al.* 2018).

The increased dimensional stability of acetylated wood, and subsequent reduction in swelling and shrinkage of the wood in exterior applications, has a positive effect on reducing stresses in film-forming coating systems. This improves coating lifetime and thereby significantly extends maintenance intervals (Rowell and Bongers 2015, 2017, Uphill *et al.* 2018). Furthermore due to increased hardness, Uphill *et al.* (2018) found for acetylated radiata pine no negative impact on coating adhesion due to hail damage whereas other softwood species such as thermal modified pine, Scots pine, and Nordic Spruce were susceptible to coatings failure due to hail impact.

3.5. ENVIRONMENTAL ASPECTS

A series of methods are available to assess the environmental impact of a product such as Life Cycle Analysis (LCA following ISO 14040/44) and Environmental Product Declarations (EPD following ISO 14025 and EN 15804). Furthermore different Ecolabels exists worldwide.

Van der Lugt *et al.* (2014) performed a Cradle-to-Grave carbon footprint evaluated for acetylated radiata pine windows frames. The results of a similar evaluation for a pedestrian bridge was presented by Van der Lugt *et al.* (2016). In a carbon footprint assessment, the greenhouse gas emissions during the life cycle of a material can be measured, and compared to alternative products in terms of kg CO₂ equivalent. The results show that if lifespan considerations are included, acetylated wood has a considerably lower carbon footprint than non-renewable materials (such as concrete, PVC, steel, and aluminium) and unsustainably sourced hardwood, and is competitive in terms of carbon footprint with sustainably sourced hardwood. Because of the limited emissions during production and carbon credits related to temporary carbon storage and bio-energy production during End of Life, all sustainably sourced wood alternatives, including acetylated wood, are even CO₂ negative over the full life cycle. Van der Lugt *et al.* (2014, 2016) also indicate that several environmental issues cannot be caught by a carbon footprint, such as the high growing speed of species suitable for acetylation, compared to slow growing tropical hardwood species.

4. APPLICATIONS OF ACETYLATED WOOD

4.1. NON-LOAD BEARING APPLICATIONS

The material properties of acetylated wood; high dimensionally stability, extended coating performance and increased durability, make it very suitable for many applications such as joinery, cladding, decking, and non-structural civil works (such as canal lining). Applications and design, however, are not limited anymore to the traditional

concept but acetylated wood gives opportunity for new kind of designs and applications (Lankveld *et al.* 2014, 2015). It should be noted, that although more opportunities are available, standard design and building practise for wood structures still apply.

4.2. STRUCTURAL APPLICATIONS

Based on extensive research, the mechanical properties of acetylated radiata pine have been determined (see paragraph 3.3). Together with information on safety factors and the effect of service class, load-bearing constructions are possible (Bongers and Alexander 2018). Properties of glulam from acetylated radiata pine was investigated by Blaß *et al.* 2013. Already in 2008 and 2010 two heavy load-bearing traffic bridges were constructed in Sneek the Netherlands (Jorissen and Lüning 2010, Tjeerdsma and Bongers 2009). Encouraged by this success, several pedestrian bridges and various other column type structures situated in wet (Service Class 3) conditions have been completed over the last decade. Recent work by the University of Kaiserslautern, Germany on the mechanical properties of acetylated beech, indicated the potential for use in bridges and towers (Graf 2019).

4.3. MUSICAL INSTRUMENTS

For high quality music instruments superior quality wood is required that is dimensional stable, homogeneity of grain, hardness, flexibility and plasticity. The available wood for these instruments is getting more difficult to obtain, and modified wood could be an alternative (Ahmed and Adamopoulos 2018).

Acetylation of wood reduces the variability in the wood moisture content of the cell-wall throughout a board, and moisture contents are minor changing with different conditions (Yano *et al.* 1993). Thereby the physical and acoustic properties are stabilised and making acetylated wood suitable for music instruments such as violin, piano soundboard, guitar, recorder, bagpipe chanter, trumpet and trombone mouthpieces (Rowell 2013).

5. SUMMARY AND OUTLOOK

By acetylation, the resistance against fungal decay and insects as well as the dimensional stability of wood can be improved, thereby enabling the opportunity to upgrade and utilization of lower quality soft and hardwood species. Currently more than 10 years of experience with commercial acetylation of radiata pine, selling over 250.000 m³ of acetylated material world-wide (with the largest market being the UK and the USA), Accsys has confirmed the high potential of acetylated wood in many different applications across the globe. Independent inspection of 17 projects with acetylated wooden doors, windows, cladding, and decking built between 2007 and 2016 in the Netherlands showed that the use of acetylated wood increases the lifetime of timber products and decreases the intensity of maintenance (Klaassen *et al.* 2018), but special attention is needed to avoid fast water uptake in outdoor as well as in indoor (condensation) conditions by using appropriate design and application practises.

With expansion to other regions, local wood species will be explored . However, to be able to warrant uniform and reproducible products that meets the required performance, takes several years of development. Other opportunities are engineered acetylated wood products such as CLT and marine use.

Another field of opportunity is the acetylation of particles (such as acetylated MDF that is f.i. produced under the brand name Medite Tricoya®), and other engineered wood products such as lamella. Due to higher surface/volume ratio's, the acetylation process is much less dependent on the permeability of the wood species, thereby opening up the opportunity for many other wood species.

What is important with all these future opportunities is that the species and application are fully investigated and assessed such that the high quality of commercially available acetylated material continues.

REFERENCES

- Ahmed, S.A. and S. Adamopoulos. 2018. Acoustic properties of modified wood under different humid conditions and their relevance for musical instruments. *Applied Acoustics* 140: 92-99.
- Alexander, J. (2007). Accoya™ An Opportunity for Improving Perceptions of Timber Joinery. In: *Proceedings of the Third European Conference on Wood Modification*. Cardiff, UK, pp. 431-438.
- Alexander, J., J. Hague, M. Roberts, Y. Imamura, and F. Bongers. 2014. The resistance of Accoya® and Tricoya® to attack by wood-destroying fungi and termites. *The International Research Group on Wood Protection, IRG-WP 14-40658*.
- Alfredsen, G., A. Pilgård, and C.G. Fossdal. 2016. Characterisation of *Postia placenta* colonisation during 36 weeks in acetylated southern yellow pine sapwood at three acetylation levels including genomic DNA and gene expression quantification of the

- fungus. Holzforschung* 70(11): 1055–1065.
- Afredsen, G., P.O. Flaete, and H. Militz. 2013. Decay resistance of acetic anhydride modified wood: a review. *International Wood Products Journal* 4(3), 137-143.
- Beck, G., E.T. Englund, L.G. Thygesen, and C. Hill. 2018a. Characterization of moisture in acetylated and propionylated radiata pine using low-field nuclear magnetic resonance (LFNMR) relaxometry. *Holzforschung* 72(3): 225–233.
- Beck, G., S., Strohbush, E. Larnøy, H. Militz, and C. Hill. 2018b. Accessibility of hydroxyl groups in anhydride modified wood as measured by deuterium exchange and saponification. *Holzforschung* 72(1): 17-23.
- Beckers, E.P.J., H.P.M. Bongers, M.E. Van der Zee, and C. Sander. 2003. Acetyl content determination by different analytical techniques. In: Van Acker, J & C. Hill (eds.). *Proceedings of the First European Conference on Wood Modification. ECWM 2003, 3-4 April 2003, Ghent, Belgium*, pp. 83-101.
- Beckers, E.P.J. and H. Militz. 1994. Acetylation of solid wood. Initial trials on lab and semi industrial scale. In: *Second Pacific Rim Bio-Based Composites Symposium, Vancouver, Canada, November 6-9 1994*, pp. 125-133.
- Beckers, E.P.J, H. Militz, and M. Stevens 1994. Resistance of acetylated wood to basidiomycetes, soft rot and blue stain. *Proceedings IRG Annual Meeting, IRG/WP 94-40021*.
- Blaß, H.J., M. Frese, H. Kunkel, and P. Schädle, P. 2013. Brettschichtholz aus acetylierter Radiata Kiefer. (Glulam from acetylated radiata pine). *Karlsruher Berichte zum Ingenieurholzbau / Karlsruher Institut für Technologie, Holzbau und Baukonstruktionen (Band 25)*. KIT Scientific Publishing. ISBN: 978-3-7315-0007-0.
- Bollmus, S., F. Bongers, A. Gellerich, C. Lankveld, J. Alexander and H. Militz. 2015. Acetylation of German hardwoods. *European Conference on Wood Modification 2015*, pp. 164-173.
- Bongers, F. and J. Alexander. 2018. Strength classification of acetylated radiata pine. *European Conference on Wood Modification 2018*.
- Bongers, H.P.M. and E.P.J. Beckers. 2003. Mechanical properties of acetylated solid wood treated on pilot plant scale. In: Van Acker, J & C. Hill (eds.). *Proceedings of the First European Conference on Wood Modification. ECWM 2003, 3-4 April 2003, Ghent, Belgium*, pp. 341-350.
- Bongers, F., T. Meijerink, B. Lütke-meier, C. Lankveld, J. Alexander, H. Militz, and C. Lehringer. 2016. Bonding of acetylated wood, *International Wood Products Journal* 7(2): 102-106. DOI: 10.1080/20426445.2016.1161944
- Bongers, F., M. Kutnik, I. Paulmier, J. Alexander, and H. Militz. 2015. Termite and insect resistance of acetylated wood. *Proceedings IRG Annual Meeting, IRG/WP 15-40703*.
- Bongers, F., S. Palanti, A. Gellerich, J. Morrell, J. Creemers, and J. Hague. 2018. Performance of acetylated wood in aquatic applications. *The International Research Group on Wood Protection, IRG-WP 18-40822*.
- Bongers, F., R.M. Rowell, and M. Roberts. 2008. Enhancement of Lower Value Tropical Wood Species. *Acetylation for Improved Sustainability & Carbon Sequestration. FORTROP II International Conference, Bangkok, Thailand, November 17-20th, 2008. Volume 11*, pp. 29-45.
- Bongers, F., M. Roberts, H. Stebbins, and R. Rowell. 2009. Introduction of Accoya® wood on the market – technical aspects. *Forth European Conference on Wood Modification. ECWM 2009, 27-29 April 2009, Stockholm, Sweden*, p. 301-309.
- Bongers, F. and J. Van Zetten. 2017. Consistency of performance of acetylated wood. *The International Research Group on Wood Protection, IRG-WP 17- 20608*.
- Brandon, R., Ibach, R.E. and Frihart, C.R. (2006). Effects of Chemically Modified Wood on Bond Durability. In: C.R. Frihart (ed.). *Wood Adhesives. San Diego, 2005*, pp. 111-114.
- Bryne, L.E. and Wälinder, M.E.P. (2010). Ageing of modified wood. Part 1: Wetting properties of acetylated, furfurylated, and thermally modified wood. *Holzforschung*, 64, pp. 295–304.
- Dreher, W.A., I.S. Goldstein, and G.R. Cramer. 1964. Mechanical properties of acetylated wood. *Forest Products Journal*, 14(2): 66-68.
- Emmerich, L., S. Strohbush, C. Brischke, S. Bollmus, and H. Militz. 2019. Study on the ability of wood-destroying fungi to grow through chemically modified wood. *The International Research Group on Wood Protection, IRG 19-40858*.
- Englund, E.T. 2013. The decay resistance of modified wood influenced by moisture exclusion and swelling reduction. *Biodeterioration and Biodegradation* 82, pp. 87-95.
- Epmeier, H., M. Johansson, R. Klinger, and M. Westin. 2007. Bending creep performance of modified wood. *Holz als Roh- und Werkstoff*, 65: 343-351.
- Fodor, F., R. Nemeth, C. Lankveld, and T. Hofmann. 2017. Effect of acetylation on the chemical composition of hornbeam (*Carpinus betulus L.*) in relation with the physical and mechanical properties. *Wood Material Science & Engineering*.
- Frihart, C. R., R. Brandon, J. F. Beecher and R. E. Ibach (2017). "Adhesives for Achieving Durable Bonds with Acetylated Wood." *Polymers* 9(12).
- Goldstein, I.S., E.B. Jeroski, A.E. Lund, J.F. Nielson, and J.W. Weaver. 1961. Acetylation of wood in lumber thickness. *Forest*

- Products Journal*, 11(8): 363-370.
- Graf, J. 2019. *Potentiale zum Einsatz von acetyliertem Buchenholz in Brücken und Türmen. (Potential of using acetylated beech in bridges and towers). Deutsche Holzschutztagung 2019, 4-5 April, Dresden, Germany.*
- Hadi, Y.S., I.G.K.T. Darma, F. Febrianto, and E.N. Herliyana. 1995. *Acetylated rubberwood flakeboard resistance to bio-deterioration. Forest Products Journal 45(10): 64-66.*
- Hill, C.A.S. 2009. *Why does acetylation protect wood from microbiological attack? Wood Material Science & Engineering 4(1-2): 37-45.*
- Hill, C.A.S. 2008. *The reduction in the fibre saturation point of wood due to chemical modification using anhydride reagents: A reappraisal. Holzforschung 62: 423-428.*
- Hill, C.A.S. 2006. *Wood Modification: Chemical, Thermal and Other Processes. John Wiley and Sons, Chichester, Sussex, UK.*
- Hill, C.A.S. and D. Jones. 1996. *The dimensional stabilisation of Corsican pine sapwood by reaction with carboxylic acid anhydrides. The effect of chain length. Holzforschung 50: 457-462.*
- Homan, W.J. and B.F. Tjeerdsma. 2005. *Control systems, quality assessment and certification of modified wood for market introduction. The Second Conference on Wood Modification (ECWM), 6-7 October 2005, Göttingen, Germany, pp. 382-388.*
- Hunt, C., R. Brandon, R. Ibach and F. CR (2007). *What does bonding to modified wood tell us about adhesion? The 5th COST E34 International Workshop, Bled, Slovenia.*
- Imamura, Y., and K. Noshimoto. 1986. *Resistance of acetylated wood attack by subterranean termites. Wood Research 72: 37-44.*
- Imamura, Y. and K. Nishimoto 1987. *Some aspects on resistance of acetylated wood against biodeterioration. Wood Research, 74: 33-44.*
- Johnson, B.R. and R.M. Rowell. 1998. *Resistance of chemically modified wood to marine borers. Material und Organismen 23(2): 147-156.*
- Jorissen, A. and E. Lüning. 2010. *Wood modification in relation to bridge design in the Netherlands, Proceedings of 11th World Conference on Timber Engineering, 2010.*
- Kattenbroek, B. 2007. *The Commercialisation of Wood Acetylation Technology on a Large Scale. In: Proceedings of the Third European Conference on Wood Modification. Cardiff, UK, pp. 19-22.*
- Klaassen, R., B. Tjeerdsma, and R. Hillebrink. 2018. *Monitoring the performance of Accoya® in different applications. European Conference on Wood Modification 2018.*
- Klüppel, A, H. Militz, S. Cragg, and C. Mai. 2010. *Resistance of modified wood to marine borers. European Conference on Wood Modification, pp. 389-396.*
- Koppers Inc. 1961. *Dimensionally stabilized wood. New Materials Tech. Info. No. (RDW-400) E-106. Koppers Inc., Pittsburgh, PA, 23 p.*
- Lankveld, C., J. Alexander, A. Tangen, T. Olson, and F. Bongers (2014). *Accoya® wood flooring and decking in extreme environments. European Conference on Wood Modification 2014.*
- Lankveld, C., J. Alexander, F. Bongers, and H. Wiolders. 2015. *Accoya® and Tricoya® for Use in Innovative Joinery. European Conference on Wood Modification 2015, pp. 216-224.*
- Larsson, P. and R. Simonson. 1994. *A study of strength, hardness and deformation of acetylated Scandinavian softwoods. Holz als Roh- und Werkstoff 52: 83-86.*
- Larsson, P. and A.-M. Tillmann. 1989. *Acetylation of lignocellulosic materials. In: The International Group on Wood Preservation, Document No. IRG/WP/3516.*
- Larsson-Brelid, P and M. Westin. 2010. *Biological degradation of acetylated wood after 18 years in ground contact and 10 years in marine water. Proceedings IRG Annual Meeting, IRG/WP 10-40522.*
- Marcroft, J., F. Bongers, F. Perez, A. Alexander, and I. Harrison. 2013. *Structural performance of Accoya® wood under service class 3 conditions. In: RILEM Conference. Materials and Joints in Timber Structures – Recent Advancement of Technology, 2013.*
- Messner, K., A. Bruce, and H.P.M. Bongers. 2003. *Treatability of refractory wood species after fungal pre-treatment. In: Van Acker, J & C. Hill (eds.). Proceedings of the First European Conference on Wood Modification. ECWM 2003, 3-4 April 2003, Ghent, Belgium, pp. 389-401.*
- Militz, H. 1999. *The improvement of dimensional stability and durability of wood through treatment with non-catalysed acetic acid anhydride. Holz als Roh- und Werkstoff 49(4): 147-152.*
- Militz, H., B.C. Peters, and C.J. Fitzgerald (2009). *Termite resistance of some modified wood species. Proceedings IRG Annual Meeting, IRG/WP 09-40449.*
- Ormstad, E.B. 2007. *Gluing of treated Wood with Dynea Adhesives. In: Sernek, M. (ed.). Bonding of modified wood. In: Proceedings of the 5th COST E34 International Workshop. Bled, Slovenia, September 2007, pp. 11-18.*
- Papadopoulos A.N., P. Duquesnoy, S.M. Cragg, and A.J. Pitman. 2008a. *The resistance of wood modified with linear chain*

- carboxylic acid anhydrides to attack by the marine wood borer *Limnoria quadripunctata* Holthius. *International Biodeterioration & Biodegradation* 61(2): 199-202
- Papadopoulos, A.N., D.N. Avtzis, and N.D. Avtzis. 2008b. The biological effectiveness of wood modified with linear chain carboxylic acid anhydrides against the subterranean termites *Reticulitermes flavipes*. *Holz als Roh- und Werkstoff* 66(4): 249-252.
- Papadopoulos, A.N. and C.A.S. Hill. 2002. The biological effectiveness of wood modified with linear chain carboxylic acid anhydrides against *Coniophora puteana*. *Holz als Roh- und Werkstoff*, 60(5): 329-332.
- Pilgård, A., Alfreksen, G., Fossdal, C.G. & C.J. Long II (2012). The effects of acetylation level on the growth of *Postia placenta* over 36 weeks. *The International Research Group on Wood Protection IRG/WP 12-40589*.
- Rowell, R. 2015. Correlation between equilibrium moisture content and resistance to decay by brown-rot fungi on acetylated wood. *European Conference on Wood Modification 2015*, pp. 444-448.
- Rowell, R.M. 2014. Acetylation of wood – a review. *International Journal of Lignocellulosic Products* 1 (1): 1-27.
- Rowell, R.M. 2013. Acoustical properties of acetylated wood. *J Chem Chem Eng* 7(9): 834-841.
- Rowell, R.M. 2006. Acetylation of wood: journey from analytical technique to commercial reality. *Forest Product Journal* 56: 4-12.
- Rowell R.M. 1996. Physical and mechanical properties of chemically modified wood. In: *Chemical Modification of Lignocellulosic Materials*. Hon, D.N.S. (Ed.), Marcel Dekker, New York, USA, pp. 295-310.
- Rowell, R. and F. Bongers. 2015. Coating acetylated wood. *Coatings* 5: 792-801; doi:10.3390/coatings5040792.
- Rowell, R. and F. Bongers. 2017. Role of moisture in the failure of coatings on wood. *Coatings* 7: 219.
- Rowell, R.M. and J.P. Dickerson. 2014. Acetylation of wood. In: *Deterioration and protection of sustainable biomaterials*. Schultz, T.P., B. Goodell, and D.D. Nicholas (eds.). ACS Symposium series 1158. American Chemical Society. ISBN 978-0-8412-3004-0.
- Rowell, R.M. and D.V. Plackett. 1988. Dimensional stability of flakeboards made from acetylated *Pinus radiata* heartwood or sapwood flakes. *New Zealand Journal of Forestry Science* 18: 124-131.
- Rowell, R.M., A.-M. Tillman, and R. Simonson. 1986. Vapor phase acetylation of southern pine, douglas-fir, and aspen wood flakes. *Journal of wood chemistry and technology* 6(2): 293-309.
- Schwanninger, M., B. Stefke, and B. Hinterstoisser. 2011. Qualitative assessment of acetylated wood with infrared spectroscopic methods. *Journal of Near Infrared Spectroscopy* 19(5), pp. 349-357.
- Sheen, AD. 1992. The preparation of acetylated wood fibre on a commercial scale. *Chemical modification of lignocellulosics, FRI Bull. No. 176. 1st Pacific Rim Bin-Based Composite Symp., Forest Res. Inst., Rotorua, NZ*, pp. 14. Simonson, R. and R.M.
- Segerholm, K. 2012. Characteristics of wood plastic composites based on modified wood - moisture properties, biological resistance and micromorphology. *Doctoral Thesis KTH Building Materials Technology, Stockholm, Sweden*. ISBN 978-91-7501-554-5.
- Suttie, E., J. Alexander, and M. Maes. 2015. Durable fibre for durable MDF – testing Tricoya®. *The International Research Group on Wood Protection, IRG/WP 15-40704*.
- Suttie, E.D., C.A.S. Hill, D. Jones, and R.J. Orsler. 1999. Chemically modified solid wood. I. Resistance to fungal attack. *Material und Organismen* 32: 159-182.
- Takahashi, M., Y. Imamura, and M. Tanahashi. 1989. Effect of acetylation on decay resistance of wood against brown rot, white rot and soft rot fungi. *Proceedings IRG Annual Meeting, IRG/WP 89-3540*.
- Tarkow, H., A.J. Stamm, and E.C.O. Erickson. 1946. Acetylated wood. Report, Forest Products Laboratory, USDA Forest Service, 1593.
- Thygesen, L.G., Engelund, E.T., and P. Hoffmeyer (2010). Water Sorption in Wood and Modified Wood at High Values of Relative Humidity. Part 1: Results for Untreated, Acetylated and Furfurylated Norway Spruce. *Holzforshung* 64(3), pp. 315-323.
- Tjeerdsma, B. and F. Bongers. 2009. The making of: a traffic timber bridge of acetylated *Radiata* pine. In: *Proceedings of the Forth European Conference on Wood Modification*. Stockholm, Sweden, pp. 15-22.
- Treu, A., R. Bredesen, and F. Bongers. 2018. Potential solutions for gluing acetylated wood in load bearing constructions. *European Conference on Wood Modification 2018*.
- Uphill, S.J., F. Bongers, and S. Ashton. 2018. Coating performance of acetylated wood. *Timber 2018*.
- Van der Lugt, P., J. Vogtländer, J. Alexander, F. Bongers, and H. Stebbins. 2014. The Potential Role of Wood Acetylation in Climate Change Mitigation. *European Conference on Wood Modification 2014*.
- Van der Lugt, P., F. Bongers, and J. Vogtländer. 2016. Environmental impact of constructions made of acetylated wood. *World Conference on Timber Engineering, August 22-25, 2016, Vienna, Austria*.
- Vick, C.B. and Rowell, R.M. (1990). Adhesive bonding of acetylated wood. *International Journal of Adhesion and Adhesives*, 10(4),

pp. 263-272.

Yano, H., M. Norimoto, and R.M. Rowell. 1993. Stabilization of acoustical properties of wooden musical instruments by acetylation. *Wood and Fiber Science* 25(4): 395-403.

Westin, M., P. Larsson-Brelid, T. Nilsson, A.O. Rapp, J.P. Dickerson, S. Lande, and S. Cragg. 2016. Marine borer resistance of acetylated and furfurylated wood – results from up to 16 years of field exposure. *International Research Group on Wood Protection Document No. IRG/WP 16-40756*.

Life cycle inventory for currently harvested birch roundwood

Edgars Kuka^{1,2*}, Dace Cirule¹, Ingeborga Andersone¹, and Bruno Andersons¹

¹Laboratory of Wood Biodegradation and Protection
Latvian State Institute of Wood Chemistry
Riga, LV-1006, Latvia

²Faculty of Material Science and Applied Chemistry
Riga Technical University
Riga, LV-1048, Latvia

ABSTRACT

The knowledge of the environmental performance of different products and services is vital in the modern world because of the climate change and other environmental problems that we are facing. Life cycle assessment is a valuable tool that allows to determine the environmental performance and compare products and services with the same function. There is no doubt that the importance of forests is crucial in the environmental protection, despite that raw wood products (roundwood, pulpwood and fuelwood) are not carbon neutral as previously thought because of the human activities during forest management processes. Apart from climate change, production of raw wood products also contribute to other environmental impact categories: acidification, eutrophication, photochemical oxidant formation and abiotic resource depletion. Previous studies have shown that the life cycle inventory (LCI) data for raw wood products should be collected from the site-specific not from more generic sources because of the significant differences in several geography and technology related factors. However, less discussed are time-related factors, which should also be acknowledged especially because of the long growing time of trees.

*The main objective of the present study was to determine which forest management processes should be included in the LCI for currently harvested birch (*Betula* spp.) roundwood in Latvia and based on these results compile the required data for the LCI. The results of forest management history analysis showed that for currently produced birch roundwood only logging operations should be included in the system boundary. Subsystems such as seed production, seedling production and silvicultural operations were not practiced or had only minor impact due to low mechanization level in the past. By taking into account the time-related factors, the LCI was developed and can be used in further calculations of environmental impacts for different wood-based products that are manufactured from currently harvested birch roundwood.*

1. INTRODUCTION

Forest products are low emission raw materials and not carbon neutral as previously thought. The roundwood production/harvesting process can emit 2 to 60 kg CO₂-equiv. per m³ depending on wood species, geographical region, forest management practices, used technology, system boundary and assumptions of the life cycle assessment (LCA) study etc. (Klein et al. 2015, Cardellini 2018). These emissions contribute to climate change, which is the main concern nowadays. Besides that, the production of the forest products contribute also to other environmental impact categories: acidification, eutrophication, photochemical oxidant formation and abiotic resource depletion (Dias and Arroja 2012). LCA is the most accepted methodology that allows to quantify these environmental impacts for a specific product or service. The standardized methodology involves an extensive collection of relevant data and calculation of environmental impacts expressed as indicators for specific environmental impact category. The most critical and time consuming is the data collection or life cycle inventory (LCI) stage. The LCI gives a quantitative information about the inputs and outputs of the unit processes that concern the product system under study. The results and main conclusions of such studies are highly affected by the quality of the collected data. It has been pointed out that the LCI data for forest products should be taken from the site-specific not from more generic sources because of the major differences in several geography and technology related factors (Bosner et al. 2012, Gonzalez-Garcia et al. 2013, Klein et al. 2015, Cardellini 2018). Less discussed are time-related factors which should also be acknowledged especially because of the long growing time of trees. Most of the studies assume that roundwood is produced by using the current forest management practices and technologies, however that is not completely true (Berg and Lindholm 2005, Puettmann et al. 2012, Gonzalez-Garcia et al. 2013). When the time aspect is not taken into account the results do not represent nor currently harvested roundwood, nor roundwood that will be produced in the future. The only possibility to analyse the environmental impacts for currently produced roundwood is by interdisciplinary approach that involves analysis of forest management history followed by LCA study. By using the approach in our previous research, the

* Corresponding author: E-mail: edgars.kuka@edi.lv

results showed that for currently produced pine roundwood most of the forest management practices that are used presently were not implemented or these activities involved non-mechanized equipment (Kuka et al. 2019). Therefore, roundwood that is currently produced and used for wood-based material production have different impact on the environment than it is for roundwood, which is assumed to be produced according to the current forest management practices. Such studies that take into account the time aspect for hardwood species have not yet been published moreover hardwood species as whole have not yet been analysed by the LCA methodologies in the Baltic State region (Klein et al. 2015).

Practically no forest in Latvia is completely natural and unmanaged. Already in the middle of 19th century, forests were affected by human activities and only in particularly remote places some virgin forests were preserved (Susko 1997). Birch (*Betula* spp.) is the most dominant hardwood specie in Latvia taking around 30 % of the total forest area (Ministry of Agriculture of the Republic of Latvia 2018). Moreover, it is the most commercially important hardwood species in the Northern and Eastern Europe (Hynynen 2010). In the Soviet times, the importance of birch was only minor and the species was even considered as weed. Nowadays the notion have changed and because of the research and development in the field, the importance of birch have reached new heights. In 2015, birch was the most regenerated wood specie in Latvia. By being a pioneer species with prolific seeds and fast juvenile growth, birch mainly regenerated naturally (88 % by area) and often on former agricultural lands (Krustins 2000, Ministry of Agriculture of the Republic of Latvia 2016). It points to a predictable increase in birch timber resources after several years. Birch trees are mainly used for plywood, pulp, paper, chemical and ‘greener’ energy production (Ministry of Agriculture of the Republic of Latvia 2016, European Commission 2017). To analyse the environmental performance of these products the background information about the environmental burdens of raw wood products harvested from birch forests is vital. Therefore, the main objective of the present study was to determine which forest management processes should be included in the LCI for currently harvested birch roundwood in Latvia and based on these results compile the required data for the LCI.

2. METHODS

Life cycle inventory (LCI) study is carried out in compliance with the ISO 14040 and ISO 14044 standards. The standards provide overall guidelines for conducting LCI and life cycle assessment (LCA) studies.

2.1. GOAL OF THE LCI STUDY

The goal of the study is to carry out a cradle-to-gate LCI for currently produced birch (*Betula* spp.) roundwood in Latvia. The information will be useful as a background data for wood-based material manufacturers who uses birch roundwood as raw material. The data will also be used in further study in which LCA for double treated (thermal modification and impregnation with biocide) wood will be conducted. LCI will give all the necessary information (input and output data) for all the processes that should be considered based on the forest management history analysis. The present study is a part of the project aimed at improving wood bio-durability by combining thermal modification and impregnation with biocide.

2.2. PRODUCT SYSTEM

According to the legal acts of the Republic of Latvia, the final felling of birch trees is permitted when the age of trees reaches 51-71 years depending on the site index (Saeima of the Republic of Latvia 2000). Hence, birch trees that have reached the final felling age and are currently harvested started their life cycle in 1950s. At that time most of the forest managing operations that are in practice nowadays were not used or they involved non-mechanised equipment which can be excluded from the LCI system boundary because of the marginal impact on the environment. Production of birch roundwood (current practice) includes four subsystems (see Figure 1): seed production, seedling production, silvicultural operations and logging operations. All subsystems should be included in the system boundary for currently planted trees because most of the processes are mechanised and/or involve usage of different chemicals (fertilizers, repellents etc.), however for currently harvested birch trees the situation should differ. Therefore, analyses of forest management history in Latvia was done by using the accessible information about birch trees starting from 1950s. Assumptions were made based on the current forest management practices that each of the subsystem was done at specific time period: seed production and seedling production from 1950 till 1970; silvicultural operations from 1950 till 1980 and logging operations from 1970 till the present.

2.3. FUNCTIONAL UNIT

The functional unit (FU) for the present study was selected as 1 m³ of roundwood over bark. Bark is included in the FU because at this stage the bark is not removed from the roundwood and will or will not be removed depending

on the further uses. Gonzalez-Garcia et al (2013) had similar approach regarding the FU in their research. As the reference unit 1 ha of forest land was used. Afterwards, the collected inventory data was recalculated to 1 m³ of roundwood over bark by using the data about the total terrestrial biomass. The total underground biomass (stump and roots) was not included in the system boundary because all of it is left on the forest site.

2.4. SYSTEM BOUNDARY

The system boundary of the LCI study was set by analysing the literature about forest management history in Latvia as described in the paragraph about product system. This was one of the main objectives of the present research and therefore will be discussed in the results section of this paper. All of the forest processes were considered from seed production to loading of the produced roundwood into hauling trucks at the forest roadside.

2.5. ALLOCATION PROCEDURES

More than one product is produced in thinning and logging operations, therefore allocation by volume was used. The extracted products are roundwood, pulpwood and fuelwood. Roundwood in the present study is the main product, and pulpwood and fuelwood are co-products. Also in the process forest waste is produced, however it is left on the forest ground and not analysed as co-product, but as biogenic CO₂ emissions to air. Allocation by volume (mass) was used to allow better comparison between different studies as suggested by Klein et al (2015).

2.6. DATA REQUIREMENTS

The main data requirements for the present study were as follows:

- Geography coverage – the data primarily are collected, calculated or assumed by using sources that describe the situation in Latvia. If necessary, other sources are used for data that are not as dependent on location and that are not available for the studied location.
- Time and technology coverage – the data as much as possible represent the specific time period at which the relevant process was done. If such data were not available for the specific process assumptions were made based on the current forest management practices.

Precision, completeness, representativeness, consistency and reproducibility is considered when collecting the data.

2.7. ASSUMPTIONS

All assumptions in the present study are indicated and described when they are used. Nevertheless, if more appropriate alternatives are available assumptions are avoided as much as possible.

3. RESULTS

The forest management history was analysed by using several sources that describe the forest management practises in Latvia at the specific time period. Four main subsystems were analysed: seed production, seedling production, silvicultural operations and logging operations. Afterwards by considering the established system boundary the relevant data for the LCI was compiled and calculated.

3.1. DETERMINATION OF SYSTEM BOUNDARY

For seed production and seedling production the assumed time period is from 1950 till 1970. At the beginning of the 20th century, birch forests took only 9.8 % of the total forest area and with time the amount increased reaching 15 % in 1935. At that time and long after that most of the birch forests regenerated naturally and most often by replacing other tree species. Birch as a pioneer specie with more prolific seeds and more rapid juvenile growth outgrew softwood species (mainly spruce) in clear-cutted areas and young forest stands (Buss and Vanags 1987, Strods and Zunde 1999). Artificial regeneration was more frequently used for softwood species and until 1970s the process involved mainly non-mechanised equipment (Mangalis 1989, Salins 1999, Baumanis et al. 2014). The analysis suggest that the seed production and seedling production subsystems should not be included in the system boundary because birch forests mostly regenerated naturally and the part that regenerated artificially did not include the use of mechanised equipment.

For silvicultural operations the assumed time period is from 1950 till 1980. The processes included in the subsystem are the most labour-intensive and difficult to mechanise. The importance of the silvicultural operations increased steadily with time and the processes mainly involved the use of non-mechanised equipment (Mangalis

1989). The first mechanized equipment and machinery used in forest management activities were introduced in 1949. However, these devices were used only in logging operations. The first mechanized equipment (brush cutter) which was suitable for silvicultural operation was introduced in 1976, however at the beginning it was only tested in commercial thinnings (Buss and Vanags 1987, Salins 1999). Based on these facts the silvicultural operations can also be excluded from the system boundary because of the minor potential influence on the environment.

For logging operations the assumed time period is from 1970 till the present. The subsystem includes the following activities: commercial thinning, final cutting and loading in hauling trucks. Commercial thinning for birch forests is performed twice (at forest age 20 and 40) in a single forest rotation. The assumed time periods when these commercial thinnings were carried out are presented in Table 1. The beginning of forest thinning operations started in the late 1930s, because previously it was thought that pruning is negatively affected by thinning processes. The first mechanised equipment and machinery (chainsaw and farm tractor) in logging operations was introduced in 1949, however these devices were used only in final cutting. Almost ten years later in 1957 chainsaws and farm tractors were also introduced in commercial thinnings. In time more efficient forwarders replaced the farm tractors in final cuttings and later also in commercial thinnings. In 1994 forwarders were the most frequently used machinery for forwarding in commercial thinnings. Harvesters for thinning purposes were not used until 2005 due to restrictions in regulations of Republic of Latvia Cabinet of Ministers No. 217 (Buss and Vanags 1987, Salins 1999, Petersons 2010). In 2010 around 50 % of all commercial thinnings were done by harvesters (Petersons et al. 2010). Final cutting and loading are done currently and they involve the use of harvesters, forwarders and loading cranes. Overall situation about the use of equipment and machinery in logging operations is summarised in Table 1. These results were calculated based on the forest management history analysis and are used in further calculations regarding LCI.

Table 1: The use of equipment and machinery in logging operations for currently produced birch roundwood

Logging operations	Time period	Harvesting			Forwarding		
		Non-mechanized equipment, %	Chainsaw, %	Harvester, %	Non-mechanized equipment, %	Farm tractor, %	Forwarder, %
First thinning	1970-1990	0	100	0	0	100	0
Second thinning	1990-2010	0	87.5	12.5	0	15	85
Final cutting	present	0	0	100	0	0	100

From the forest management history analysis it can be concluded that only logging operations should be included in the system boundary for currently produced birch roundwood. The main differences between system boundaries for currently harvested and currently planted trees are shown in Figure 1. In addition, from personal communication with representative from JSC ‘Latvia’s State Forests’ (2018) it was established that fertilizers are not used in Latvian forests. Fertilizers are only used in seedling production.

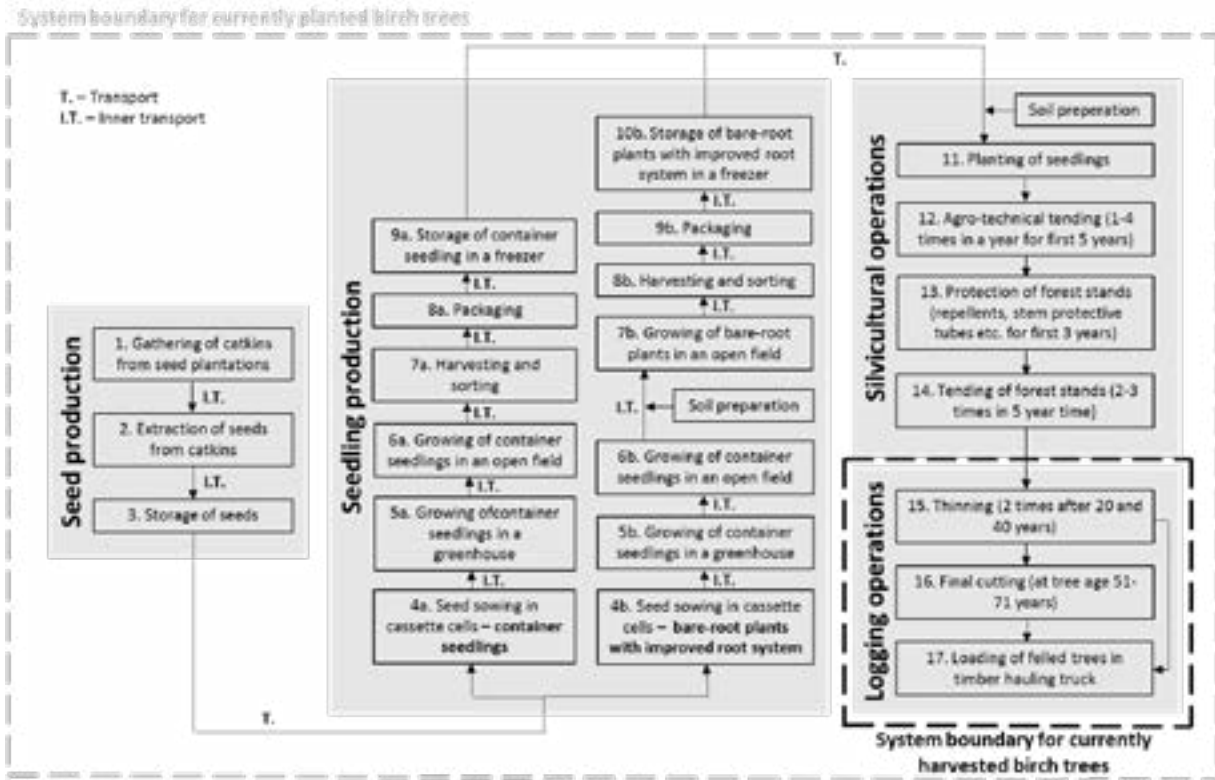


Figure 1: Subsystems included in the process chain of birch roundwood production in Latvia: system boundary for currently planted (grey dashed line) and for currently harvested (black dashed line) birch trees

3.2. INVENTORY ANALYSIS

As previously concluded only part of the processes should be considered when compiling LCI for currently produced birch roundwood in Latvia. For simplicity sake, processes that should be considered are included in the system boundary and the rest are excluded including processes with minor impact on the environment that involve the use of non-mechanized equipment, which technically should be included. All of the foreground unit processes that based on the system boundary are considered in the LCI are presented in Figure 2. The figure also shows the volume flow of timber which was calculated based on the LCI results. Solar energy inputs, all the ancillary inputs (equipment, machinery, land use, fuel, lubricating oil and transportation) and the emissions related to them are not presented in Figure 2, but are compiled in Table 4, where the input and output flows of each unit process are calculated according to 1 m³ of the specific intermediate product.

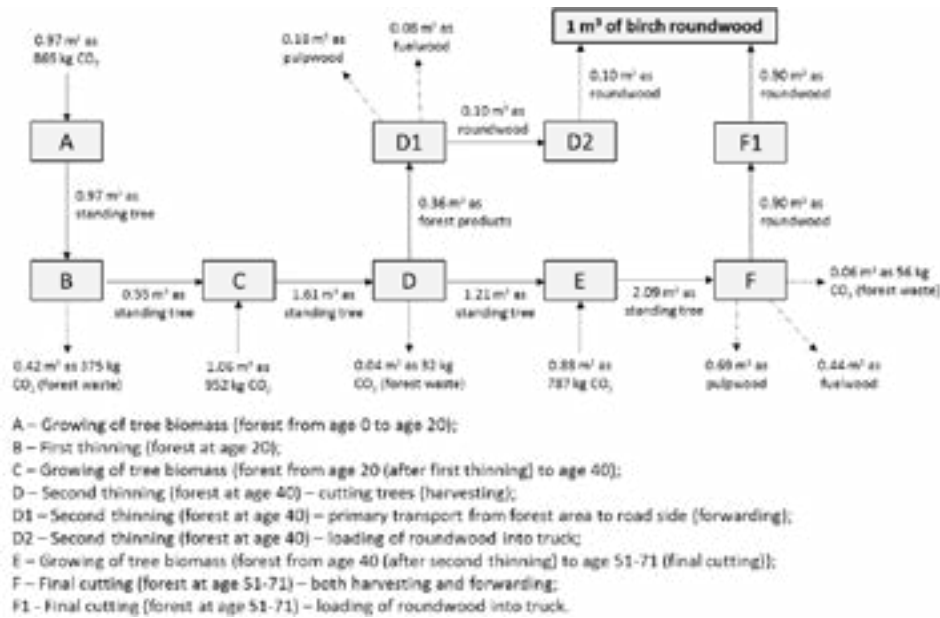


Figure 2: Volume flow of timber and foreground unit processes that are included in the system boundary for currently produced birch roundwood

The volume flow presented in Figure 2 is calculated and compiled based on the growth and thinning models for birch forests and the data about yield, removed biomass, amount of specific raw wood products and forest waste. The raw data are gathered from research papers, statistical information and from forest experts through surveys and personal communication. Most of the data were available in form of 1 ha of forest land (reference unit) and therefore the values afterwards were recalculated to comply with the functional unit (1 m³ of birch roundwood). The amount of captured CO₂ is calculated by taking into account that the specific density of birch is 470 kg/m³ and the carbon content is 52 wt. % of the dry wood biomass (Lazdins, 2015). Based on the growth models and statistical inventory of Latvian forest resources the total terrestrial biomass before the first commercial thinning is estimated around 137 ± 7 m³/ha and the removed biomass during thinning is around 59 ± 12 m³/ha (Grinvalds et al. 2008, Jansons 2017). The removed biomass is classified as forest waste that is left on the forest ground as stated by forest experts (JSC ‘Latvia’s State Forests’ 2018). Carbon in the forest waste was assumed to be released as CO₂ in the result of aerobic decomposition (Giunolia et al. 2016). The total terrestrial biomass before second thinning is estimated around 231 ± 12 m³/ha and the removed biomass is around 58 ± 11 m³/ha (Grinvalds et al. 2008, Jansons 2017). During second thinning only 9 % of all removed biomass is classified as forest waste and the rest is forest products that include roundwood, pulpwood and fuelwood (Lazdins et al. 2004). The share of each type of wood biomass formed during second thinning is presented in Table 2 (JSC ‘Latvia’s State Forests’ 2018). At the point when the birch forest reaches the final cutting age (forest at age 51-71) the total average terrestrial biomass is around 298 ± 16 m³/ha (Jansons 2017). For the final cutting it is assumed that it is a clear cut and 0 m³/ha of standing terrestrial biomass is left on the forest ground. From the removed biomass 3 % is classified as forest waste and the rest is forest products. The share of each type of wood biomass formed during final cutting is presented in Table 2 (Eurostat 2018). In total 142.6 m³/ha of roundwood is produced in one forest rotation. From that amount 10.2 % is produced during second thinning and 89.8 % during final cutting.

Table 2: Share of forest waste and products formed during thinnings and final cutting

SHARE OF FOREST WASTE AND PRODUCTS, %	Forest waste	Fuelwood	Pulpwood	Roundwood
First commercial thinning (removed wood biomass: 59 m ³ /ha)	100	0	0	0
Second commercial thinning (removed wood biomass: 58 m ³ /ha)	9	21	45	25
Final cutting (removed wood biomass: 298 m ³ /ha)	3	21	33	43

More detailed information regarding inputs and outputs for each unit process is presented in Table 4. The raw data are gathered in variety of forms and recalculated accordingly to comply with 1 m³ of the specific unit process intermediate product. Such approach is used to give a possibility to use each of the unit process separately in other studies if necessary. The solar energy was calculated by using the lower calorific value of birch wood biomass 18.9 MJ/kg and by assuming that the specific density is 470 kg/m³ (Dolacis et al. 2003, Lazdins 2015). The data required for characterization of used equipment and machinery are gathered by taking into account the results presented in

Table 1. It is assumed that the average fuel and lubricant consumption is not highly dependent on the tree diameter at breast height or the technology age. However, productivity and emissions are highly dependent on these previously mentioned factors, therefore these parameters significantly differ regarding commercial thinnings and final cutting. The data about productivity, fuel and lubricant consumption are presented in Table 3 (Kalejs et al. 2017, JSC ‘Latvia’s State Forests’ 2018).

Table 3: Productivity, fuel and lubricant consumption of mechanical equipment and machinery during thinnings and final cutting

PRODUCTIVITY, m ³ /h	Chainsaw	Harvester	Farm tractor	Forwarder	Loader-crane
First commercial thinning	0.75	-	-	-	-
Second commercial thinning	1.13	14.0	4.0	9.5	19.0
Final cutting	-	20.4	-	12.9	19.0
FUEL CONSUMPTION, L/h	0.40	12	6	12	17
LUBRICANT CONSUMPTION, L/h	0.08	0.84	0.18	0.36	0.025

The emissions from burning of fuel are calculated according to Tier 2 technology-dependent approach which is described in EMEP/EEA air pollutant emission inventory guidebook 2016 (Winther 2016). The approach is chosen because of the high importance of technology age in the present study. The technology age of specific equipment and machinery used in thinnings and final cutting is presented in Table 1. For calculation purposes the density of gasoline, diesel and lubricant was assumed to be 750 kg/m³, 830 kg/m³ and 850 kg/m³, respectively. The amount of sulphur and lead in fuel is taken from the relevant literature and by considering the time aspect (Blumberg et al. 2003, Needleman and Gee 2013, Sorusbay 2014, Transport policy 2018). The data are required for calculations of SO₂ and Pb emissions to air from burning of fuel. Lubricant is assumed to be partially burned in the process releasing CO₂ emissions to air and the rest of the amount is assumed to be emitted to soil. The CO₂ amount from lubricant is estimated according to Tier 1 for lubricants which is described in 2006 IPCC Guidelines for National Greenhouse Gas Inventories (Olivier et al. 2008). The data about the transportation distance and weight of the machinery are gathered from forest experts (JSC ‘Latvia’s State Forests’ 2018). Background data for transportation, land use, chainsaw, machinery, gasoline, diesel, and lubricant production are taken from ecoinvent 3 database.

Table 4: Life cycle inventory for currently produced birch roundwood presented as foreground unit process data sets calculated to 1 m³ of specific intermediate product

			Unit process								
			A	B	C	D	D1	D2	E	F	F1
Products and co-products	Products	Intermediate product, m ³	1.00	1.00	1.00	1.00	-	-	1.00	-	-
		D1 Roundwood (not loaded), m ³	-	-	-	-	1.00	-	-	-	-
		F Roundwood (not loaded), m ³	-	-	-	-	-	-	-	1.00	-
		Roundwood, m ³	-	-	-	-	-	1.00	-	-	1.00
Co-products	Co-products	Forest products, m ³	-	-	-	0.31	-	-	-	-	-
		Pulpwood, m ³	-	-	-	-	1.80	-	-	-	0.77
		Fuelwood, m ³	-	-	-	-	0.84	-	-	-	0.49
Inputs	Elementary flows	CO ₂ , kg	896	-	591	-	-	-	376	-	-
		Solar energy, MJ	8883	-	5863	-	-	-	3731	-	-
	Intermediate products	A intermediate product, m ³	-	1.76	-	-	-	-	-	-	-
		B intermediate product, m ³	-	-	0.34	-	-	-	-	-	-
		C intermediate product, m ³	-	-	-	1.34	-	-	-	-	-
		D intermediate product, m ³	-	-	-	-	-	-	0.58	-	-
		D Forest products, m ³	-	-	-	-	3.64	-	-	-	-
		D1 Roundwood (not loaded), m ³	-	-	-	-	-	1.00	-	-	-
		E intermediate product, m ³	-	-	-	-	-	-	-	2.33	-
	F Roundwood (not loaded), m ³	-	-	-	-	-	-	-	-	1.00	
	Equipment and machinery	Chainsaw production, p	-	4.05E-4	-	1.04E-4	-	-	-	-	-
		Harvester production, p	-	-	-	1.70E-7	-	-	-	-	6.48E-6
		Farm tractor production, kg	-	-	-	-	0.156	-	-	-	-
		Forwarder production, p	-	-	-	-	1.85E-5	-	-	-	9.9E-6
Loader-crane production, p		-	-	-	-	-	4.2E-6	-	-	4.2E-6	
Materials	Gasoline production, kg	-	0.304	-	0.78	-	-	-	-	-	
	Lubricant production, kg	-	0.069	-	0.03	0.121	0.001	-	0.13	0.001	
	Diesel production, kg	-	-	-	0.03	3.925	0.74	-	2.88	0.74	
Transportation	Transportation (EURO III), tkm	-	-	-	-	5.70	15.39	-	-	-	

Life cycle inventory for currently harvested birch roundwood

		Transportation (EURO IV), tkm	-	-	-	0.05	-	-	-	-	-	
		Transportation (EURO V), tkm	-	-	-	-	-	-	-	1.79	15.38	
	Land use	Transformation, from forest, m ²	73	-	-	-	-	-	-	-	-	
		Transformation, to forest, m ²	73	-	-	-	-	-	-	-	-	
		Occupation, forest, m ² a	1460	-	866	-	-	-	-	671	-	
Outputs	To air	CO ₂ (biogenic), kg	-	681.1	-	26.88	-	-	-	-	62.73	-
		BC, g	-	0.073	-	0.028	2.215	0.339	-	-	0.213	0.055
		CH ₄ , g	-	5.916	-	1.347	0.176	0.022	-	-	0.037	0.010
		CO, g	-	212.6	-	48.55	28.98	4.411	-	-	17.11	4.416
		CO ₂ , kg	-	1.018	-	0.356	12.48	2.347	-	-	9.182	2.347
		N ₂ O, g	-	0.005	-	0.005	0.544	0.103	-	-	0.400	0.103
		NH ₃ , g	-	0.001	-	0.000	0.031	0.006	-	-	0.023	0.006
		NMVOG, g	-	78.60	-	17.92	7.104	0.861	-	-	1.482	0.382
		NO _x , g	-	0.511	-	0.527	75.66	15.29	-	-	4.563	1.178
		PM ₁₀ , g	-	1.455	-	0.318	3.308	0.442	-	-	0.285	0.074
		PM _{2.5} , g	-	1.455	-	0.318	3.308	0.442	-	-	0.285	0.074
		TSP, g	-	1.455	-	0.318	3.308	0.442	-	-	0.285	0.074
		SO ₂ , g	-	1.216	-	0.103	11.10	1.789	-	-	0.069	0.018
		Lead, g	-	0.122	-	0.012	-	-	-	-	-	-
		Cadmium, mg	-	0.003	-	0.001	0.039	0.007	-	-	0.029	0.007
		Copper, mg	-	0.517	-	0.183	6.673	1.262	-	-	4.891	1.262
		Chromium, mg	-	0.015	-	0.005	0.196	0.037	-	-	0.144	0.037
		Nickel, mg	-	0.021	-	0.008	0.275	0.052	-	-	0.201	0.052
		Selenium, mg	-	0.003	-	0.001	0.039	0.007	-	-	0.029	0.007
		Zinc, mg	-	0.304	-	0.108	3.925	0.743	-	-	2.877	0.743
		Benz(a)anthracene, µg	-	22.80	-	8.226	314.0	59.41	-	-	230.2	59.41
		Benzo(b)fluoranthene, µg	-	12.16	-	4.606	196.3	37.13	-	-	143.9	37.13
		Dibenzo(a,h)anthracene, µg	-	3.040	-	1.077	39.25	7.426	-	-	28.77	7.426
		Benzo(a)pyrene, µg	-	12.16	-	4.010	117.8	22.28	-	-	86.31	22.28
		Chrysene, µg	-	45.60	-	17.65	785.0	148.5	-	-	575.4	148.5
		Fluoranthene, µg	-	136.8	-	48.46	1766	334.2	-	-	1295	334.2
	Phenanthrene, µg	-	364.8	-	168.0	9813	1857	-	-	7193	1857	
	To soil	Lubricant, kg	-	0.06	-	0.02	0.10	0.001	-	0.108	0.001	

4. CONCLUSIONS

By analysing forest management history it was possible to characterize the actual production process for currently produced birch roundwood in Latvia. The present study suggests that only logging operations should be included in the system boundary. Seed production, seedling production and silvicultural operations should be excluded because some of these subsystems were not practised at all or the activities included in the subsystems were performed with non-mechanized equipment. Based on these conclusions life cycle inventory (LCI) for birch roundwood was developed. The collected data for the LCI represent the actual production process taking into account the time aspect. These results are valuable for further calculations of environmental impacts and can be used as background data for evaluating different wood products. The interdisciplinary approach that considers forest management practice and technology development in time can give a more accurate characterization of environmental performance for currently produced roundwood. The study also suggest that currently manufactured wood products have lower environmental impacts than it is presented in their environmental product declarations due to these time related aspects. However, the environmental impacts for the future wood products will increase.

ACKNOWLEDGMENTS

The authors gratefully acknowledge the financial support by the European Regional Development Fund project No. 1.1.1.1/16/A/133.

REFERENCES

- Baumanis, I., A. Jansons, and U. Neimane. 2014. *Pine. Priede. Selection, genetics and seed production in Latvia (in Latvian)*. Daugavpils University academic publisher 'Saule', Daugavpils. 325 pp.
- Berg, S., and E. Lindholm. 2005. *Energy use and environmental impacts of forest operations in Sweden*. *J. Clean. Prod.* 13:33-42.
- Blumberg, K.O., M. P. Walsh, and C. Pera. 2003. *Low-sulfur gasoline & diesel: The key to lower vehicle emissions*. *The International Council on Clean Transportation (ICCT)*. 66 pp.
- Bosner, A., T. Porsinsky, and I. Stankic. 2012. *Forestry and life cycle assessment*. In: *Global Perspectives on Sustainable Forest Management, InTech*. pp. 139-160.
- Buss, M., and J. Vanags. 1987. *Latvian forests (in Latvian)*. Avots, Riga. 176 pp.
- Cardellini, G., T. Valada, C. Cornillier, E. Vial, M. Dragoi, V. Goudiaby, V. Mues, B. Lasserre, A. Gruchala, P. K. Rorstad, M. Neumann, M. Svoboda, R. Sirgmets, O. P. Nasaro, F. Mohren, W. M. J. Achten, L. Vranken, and B. Muys. 2018. *EFO-LCI: A new life cycle inventory database of forestry operations in Europe*. *Environ. Manage.* 61(6):1031-1047.
- Dias, A. C., and Arroja, L. 2012. *Environmental Impacts of eucalypt and maritime pine wood production in Portugal*. *J. Clean. Prod.* 37:368-376.
- Dolacis, J., E. Tomsons, and J. Hrols. 2003. *Fuelwood comparison with other kinds of fuel*. *Environment. Technology. Resources*. 67-72.
- European Commission. 2017. *Silver birch*. <https://ec.europa.eu/jrc/en/research-topic/forestry/qr-tree-project/silver-birch>. Accessed March 18, 2019.
- Eurostat. 2018. *Roundwood removals by type of wood and assortment (2010-2016)*. <https://ec.europa.eu/eurostat/data/database>. Accessed April 28, 2019.
- Giuntolia, J., A. Agostiniad, S. Caserinib, E. Lugatoc, D. Baxtera, and L. Marelli. 2016. *Climate change impacts of power generation from residual biomass*. *Biomass Bioenerg.* 89:146-158.
- Gonzalez-Garcia, D., I. Krowas, G. Becker, G. Feijoo, and M. T. Moreira. 2013. *Cradle-to-gate life cycle inventory and environmental performance of Douglas-fir roundwood production in Germany*. *J. Clean. Prod.* 54:244-252.
- Grinvalds, A., E. Linde, J. Gercans, M. Neicinieks, L. Sica, I. Brauners, and M. Gaigals. 2008. *Thinning handbook (in Latvian)*. JSC 'Latvia's State Forests'. 112 pp.
- Hynynen, J., P. Niemisto, A. Vihera-Aarnio, A. Brunner, S. Hein, and P. Velling. 2010. *Silviculture of birch (Betula pendula Roth and Betula pubescens Ehrh.) in northern Europe*. *Forestry* 83(1):103-119.
- Jansons, J. 2017. *National forest monitoring (in Latvian)*. Latvian State Forest Research Institute 'Silava'. <http://www.silava.lv/petijumi/nacionlais-mea-monitorings.aspx>. Accessed April 28, 2019.
- JSC 'Latvia's State Forests'. 2018. *Surveys and Personal Communication with Forest Experts*.
- Kaleja, S., A. Ziemelis, A. Lazdins, and P. O. Johansson. 2017. *Comparison of productivity of Kranman Bison 10000 forwarder in stands harvested with harvester and chainsaw*. In: *Proceedings of the 8th International Scientific Conference Rural Development 2017, November 23– 24, 2017, Kaunas, Lithuania*. pp. 319–323.
- Klein, D., C. Wolf, C. Schulz, and G. Weber-Blaschke. 2015. *20 years of life cycle assessment (LCA) in the forestry sector: state of the art and a methodical proposal for the LCA of forest production*. *Int. J. Life Cycle Assess.* 20:556–575.
- Krastins, O. 2000. *Century in Latvian forests (in Latvian)*. *Latvijas Vestnesis*. <https://www.vestnesis.lv/ta/id/3633>. Accessed April 28, 2019.
- Kuka, E., D. Cirule, I. Andersone, Z. Miklasevics, and B. Andersons. 2019. *Life cycle inventory for currently produced pine roundwood*. *J. Clean. Prod.* 235:613-625.
- Lazdans, V., E. Epalts, Z. Karins, V. Kaposts, J. Liepa, T. Blija, A. Abolina, S. Laivina, and D. Lazdina. 2004. *Forest management technique and technology influence on soil characteristics (In Latvian)*. Latvian State Forest Research Institute 'Silava', Salaspils. 59 pp.
- Lazdins, A. 2015. *Impact of forestry activities on greenhouse gas emissions and CO₂ capture (in Latvian)*. Latvian State Forest Research Institute 'Silava', Salaspils. 144 pp.
- Mangalis, I. 1989. *Forest cultures (in Latvian)*. Zvaigzne. Riga. 360 pp.
- Ministry of Agriculture of the Republic of Latvia. 2016. *Forest Sector in the 25 Years of Independence of Latvia*. Association 'Zalas majas', Riga. 47 pp.
- Ministry of Agriculture of the Republic of Latvia. 2018. *Latvian Forest Sector in Facts & Figures 2018*. Association 'Zalas majas', Riga. 54 pp.
- Needleman, H., and D. Gee. 2013. *Lead in petrol 'makes the mind give way', in: Late lessons from early warnings: science, precaution, innovation. Part A – Lessons from health hazards*. European Environment Agency, Copenhagen. pp. 46-75.
- Olivier, J. G. J., D. Gaudioso, M. Gillenwater, C. Ha, L. Hockstad, T. Martinsen, M. Neelis, H. Park, and T. Simmons. 2008. *Non-energy products from fuels and solvent use*. In: *2006 IPCC Guidelines for National Greenhouse Gas Inventories*. Institute for Global Environmental Strategies (IGES). pp. 5.1-5.18.

-
- Petersons, J. 2010. *Factors affecting harvester productivity in forest thinning in Latvia*. In: *Proceedings of the 16th International Scientific Conference Research for Rural Development, May 24-26, 2010, Jelgava, Latvia*. pp. 183-187.
- Petersons, J., A. Dreska, and A. Saveljevs. 2010. *Evaluation of removable tree reach factors and remaining standing tree quality during with machinery mechanised commercial thinning (in Latvian)*. *Mezzinatne*, 22(55), 116-128.
- Puettmann, M., E. Oneil, J. Wilson, and L. Johnson. 2012. *Cradle to gate life cycle assessment of softwood plywood production from the Southeast*. CORRIM, Technical Report, 35 pp.
- Saeima of the Republic of Latvia. 2000. *Law on Forests*. *Latvijas Vestnesis*, 98/99 (2009/2010), 16.03.2000. <https://likumi.lv/ta/en/en/id/2825>. Accessed April 28, 2019.
- Salins, Z. 1999. *Forest use in Latvia (in Latvian)*. LLU Department of Forest Use. Jelgava. 270 pp.
- Sorusbay, C. 2014. *Internal Combustion Engine Fuels*. Istanbul Technical University. http://web.itu.edu.tr/~sorusbay/ICE/index_files/LN04.pdf. Accessed April 28, 2019.
- Strods, H., and M. Zunde. 1999. *History of Latvian Forests until 1940 (in Latvian)*. WWF, Riga. 363 pp.
- Susko, U. 1997. *Natural forests in Latvia. Study on forest history, biodiversity structures and dependent species (in Latvian)*. WWF Latvian Program Office, Riga. 180 pp.
- Transport policy. 2018. *EU: Fuels: diesel and gasoline*. <https://www.transportpolicy.net/standard/eu-fuels-diesel-and-gasoline/>. Accessed April 28, 2019.
- Winther, M. 2016. *EMEP/EEA air pollutant emission inventory guidebook 2016 – Update May 2017. Non-road mobile sources and machinery*. European Environment Agency. 82 pp.



Session II

Laminated veneer lumber hollow cross-sections for temporary soil nailing

Testing and modelling of hardwood joints using beech and azobé

Use of northern hardwoods in glued-laminated timber: a study of bondline shear strength and resistance to moisture

PBlue gum: Assessment of its potential for load bearing structures

Experimental and numerical evaluation of the structural performance of Uruguayan Eucalyptus grandis fingerjoint

Mangium (*Acacia mangium*) and Sengon (*Falcataria moluccana*) Smoked Woods Resistance to Subterranean Termite Attack

French beech – a new opportunity in wood housing

Monitoring of Birch Veneer Moisture Content During the Drying Process by Single-Sided NMR technique

Laminated veneer lumber hollow cross-sections for temporary soil nailing

Sebastian Hirschmüller¹, Roman Marte² and Alexander Englberger¹

¹Research and Development
 Technical University of Applied Sciences Rosenheim
 Rosenheim, Bavaria, 83324, Germany

²Institute of Soil Mechanics
 Foundation Engineering and Computational Geotechnics
 Graz University of Technology
 8010 Graz, Austria

ABSTRACT

An innovative approach using laminated veneer lumber (LVL) hollow sections for temporary geotechnical slope stabilisation is being presented within this article. The use of circular laminated veneer lumber hollow sections as reinforcement elements in soil nailing walls demands load bearing elements, primarily loaded in tension, with a length up to 10 m. Thus finger-jointing was found to be an efficient method of a longitudinal load-carrying connection in combination with a minimized cross section reduction at the joint. This paper discusses the applicability of finger jointing on beech wood laminated veneer lumber hollow sections and presents the results of large scaled tensile under variation of the joint arrangement.

1. INTRODUCTION

Currently, soil nailing is a common way of slope stabilization in foundation engineering. Therefore, steel anchors are drilled into the soil and a reinforced shotcrete layer protects the slope surface. The gap around the steel rod is filled with cement grout. The hardened cement body ensures the necessary connection (force closure) between soil and anchor. For the stabilization of construction pit slopes, usually temporary soil nailing systems are used. In case of temporary soil nailing systems, the construction has a reduced service life of maximum two years. Thereafter, the anchors have no structural utility, but usually remain in the soil, because generally it is not possible to remove them due to their limited accessibility after their installation. The objective in this research topic is to replace the temporary steel nails by curved laminated hollow sections CLHS manufactured from European beech (*Fagus sylvatica L.*) in reinforced cut slopes.



Figure 1: Beech curved laminated hollow sections CLHS prototypes (left) and related cross section with 100 mm outer diameter and 18 mm wall thickness

The motivation is to develop a sustainable soil nailing system for temporary purposes in combination with a new way of using beech wood by combining both positive and negative beech material properties (high strength and low durability). The wooden soil reinforcement elements decompose in the soil after fulfilling their expected service life. Figure 2a shows a typical slope excavation supported by a shotcrete layer and steel nails, and Figure 2b illustrates the method using wood-based reinforcement elements.



a) Standard soil nailing system

b) Slope stabilisation using wooden hollow cross-sections

Figure 2: Current soil nailing system (a) and investigated temporary method (b)

Since the construction of the first reinforced soil walls (RSW), the first approaches of design methods were developed based on the results of large-scale field tests (Gäßler und Gudehus 1981; Gäßler 1987; Project National Clouterre 1991). Generally, the reinforced soil in combination with the soil facing is assumed to form a composite body, resisting externally-acting lateral and vertical forces. To ensure the internal bearing capacity of the reinforced soil body (internal stability), besides numerical methods, various other design concepts were developed based on mechanical limit equilibrium considerations of rigid body motions. Existing slope stability analysis methods, where external forces act on the rigid body, are compared to mobilised resistances in the soil and extended by reinforcement elements. Tensile elements were added to the equilibrium consideration, which increase the resistance to the external driving forces. However, these extended conventional slope analysis procedures based on LE considerations only assign axial forces to the nails to fulfill the equilibrium. The design concept following Gäßler 1987, considering two translation bodies and polygonal slip lines, is the theoretical concept of the internal stability design given in Design guide line RVS 09.01.41 for instance. Thus, based on current state of the art design methods, only tensile forces are considered as acting forces in the reinforcement elements.

Bar-shaped elements for load-bearing timber structures are usually made of solid wood or wooden engineered products like glue laminated timber (GLT), cross laminated timber (CLT) or LVL. With regard to production cutting losses, processing issues and the structural design of constructions and connections, rectangular cross-section geometries are usually preferred for load-bearing timber elements. However, cement grouted soil nails act as a composite element similar to reinforcement bars in concrete structures due to the force transformation from the soil into the bar. Therefore, the nail's tensile capacity and the bonding behaviour between the nail and the surrounding cement is essential and depends significantly from the available contact surface between the bar and the cement grout. Inspired by blades of grass, circular ring-shaped cross-sections offer a high stability performance due to the optimised proportion between moment of inertia $I_{Y,Z}$ and cross-section area A_t . Additionally, a circular cross-section of reinforcement members offers an improved proportion between outer periphery U_{out} and A_t compared to rectangular geometries (Figure 3) and is therefore preferably used for reinforcement elements primarily loaded in tension. Because of practical concerns, CLHS for soil nailing have to be installed by caused drillings. An installation similar to a self-drilling anchor is not possible from technical reasons at the moment. The outer diameter d_t of the LVL-nail is limited to about 100 mm due to a common bore hole diameter of about 140 mm and a minimum thickness of the surrounding cement body of 20 mm. The wall thickness t of the poles is given by the tensile force in the nail as well as the minimum possible curvature of the veneers in the inner diameter d_i without destruction of the veneer perpendicular to the fiber direction. A wall thickness of approximately 18 mm (6 layers of 3 mm thick veneers respectively) and an inner diameter d_i of 64 mm was found to be suitable for the manufacturing process without crushing the innermost veneers and had been adopted for all investigations. The fiber direction of all veneer layers corresponds with the pole axis.

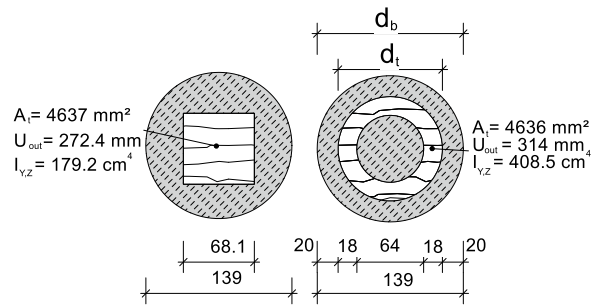


Figure 3: Cross-section of a cement-grouted bore hole with rectangular reinforcement member (left) and a circular hollow section member (right); all dimensions in millimeters

CLHS tensile and bending properties were determined on small and clear specimens and has been described in Hirschmüller et al. 2016, Hirschmüller et al. 2018b and Hirschmüller 2019. This part of the research work has been done primarily to investigate the influence of veneer thickness and curvature on LVL material properties and to define a proper CLHS layer structure. But for the definition of design values testing of structural sized members is inevitable, as brittle material strength is strongly influenced by a volume size effect, mainly caused by a higher probability of strength-reducing wood defects appearing in a larger material volume. Current soil nailing design methods based on limit equilibrium considerations mainly align tensile forces with the nail, wherefore the research focus was inter alia on the determination of CLHS tensile properties in structural dimensions. Temporary soil nailing walls with heights H_S up to about 6 to 7 m cover a large range of typically-practised geometries resulting in a nail length L_N not exceeding 6 m (corresponding to a guide value of $\sim 0,8 H_S$). Industrially-produced rotary cut veneers are available in lengths up to 3 m and therefore limit the length of available continuous CLHS without joints. Thus reliable and efficient longitudinal CLHS jointing without a significant cross-section reduction is a crucial factor for CLHS production of the required lengths. Various concepts have been suggested in the literature to produce long CLHS sections. Hara et al. 1994 used long veneer stripes, which were longitudinally connected by finger joints of the single veneers, for the production of moulded 1/6 round LVL. The moulded LVL were and connected in a high frequency heating press, suggesting a continuous roll forming process (as presented 14 years later in Srinivasan et al. 2008) for the production of long structural elements. Hata et al. 2001 proposed “spiral-winding” of veneer strips wrapped around a mandrel in an interlocking pattern for endless pole production. Gilbert et al. 2017 investigated three longitudinal jointing approaches of CLHS sections and compared the bending capacity, determined in four point bending tests, to reference sections without joints. The authors varied the longitudinal joint by

- inserting a sleeve at the inner CLHS wall with a bending stiffness and bending capacity similar to the continuous CLHS, resulting in a bending capacity of 50% relative to the reference section
- wrapping fibre-reinforced polymere around the longitudinal CLHS butt joint (94% bending capacity)
- longitudinal staggering of butt jointed veneers within the section in a similar process to that used to construct LVL products (83% bending capacity).

Nevertheless, all presented approaches for the production of longer, veneer based structural profiles are based on material jointing, either of veneers or of layered veneer members. However, finger jointing standardised in European standard EN 15497, is a high-performance jointing method mainly used for the longitudinal connection of timber boards as basic material in glulam processing. Youngquist et al. 1984 applied finger jointing to softwood LVL products and found a competitive method of LVL end jointing. But the finger joints in the LVL resulted in fast dulling of the cutterhead, especially if the finger joints were adjusted parallel to the adhesive plane with glue lines abrasing the cutters at one location on the tool. Biblis und Carino 1993 confirmed the strength influence of finger joint orientation and proposed an orientation perpendicular to the adhesive plane to generate reliable connections. Although these publications indicate that finger jointing is a promising way for a longitudinal softwood LVL-connection, several investigations report a limited loading capacity of finger jointed beech wood lamellas in glued laminated timber (Aicher 2001; Volkmer et al. 2017; Ehrhart et al. 2018). This paper discusses the applicability of finger jointing on beech wood laminated veneer lumber hollow sections and presents the results of large scaled tensile tests under variaton of the joint arrangement.

2. MATERIALS AND METHODS

2.1. CHLS MANUFACTURING AND SAMPLING

The tensile properties of full-sized CLHS with and without finger joints were determined in extensive test series of specimens conditioned in normal climate (NC) at 20°C and 65% relative humidity (RH) until reaching equilibrium moisture content $u_{gl} \approx 11.3\%$. The 2450 mm long CLHS specimens were made of four layers 3.1 mm thick and 2650 mm rotary cut beech veneers. The veneer basic population consisted of thirty 2650 mm long (in grain direction) and 1320 mm wide veneer sheets of quality class E (European Standard EN 635-2), delivered from a Swiss producer (HESS & Co AG). Subsequently to veneer conditioning in NC until weight constancy, the veneer gross density ρ_N was taken, whereby ρ_N of each CLHS was calculated as average mean of the single veneer layers.

To ensure a uniformly-distributed press stress for the production of circular half-sections with small radii, a three-stage production process has been developed using a fluid-filled fire hose for the press stress application.

1. Veneer preparation: Veneers are wetted on their open side (peeling crack side) for preliminary forming of 3 mm thick veneers to a minimum radius of 30 mm perpendicular to the fibre direction. The fixed form, using perforated PVC tubes, is stored in NC for drying at least until weight constancy of the veneers. Due to this wetting procedure, small veneer radii generally can be produced without crushing the veneers.
2. Adhesive application: After veneer drying, adhesive is applied on the right side (side with closed peeling cracks, log periphery) of each veneer to bond the circular half-sections, whereby the amount of resin is controlled by weighing.
3. Bonding process of half sections

For the production of half-sections, a system with an outer hard form and an inner elastic form is used (Figure 4). The outer hard form is made from insulated cast resin or steel and the inner elastic form consists of a 75 mm diameter fire hose with caps on both ends and connectors for compressed water. The use of an outer steel mould enabled the production of dimensionally consistent half-sections. Depending on the compressor unit and the bursting pressure of the fire hose, not more than 1.0 MPa radial press stress is applied. The fire hose is filled with water at 65°C and the outer cast resin form can be heated with externally-applied heating pads during the adhesive curing process. Thus, bonding at elevated temperatures of at least 30°C is ensured and controlled by a temperature sensor integrated within the cast resin form.



(a) Prototype of a pressing system with elastic fire hose and outer insulated cast resin form (b) Pressing system with steel moulded outer part

Figure 4: Compression moulding with optimum radial press stress

Subsequently the CLHS is formed by butt jointing the two matched and planed half-sections. For the production of longer CLHS, as demanded for the use in reinforced soil walls ($L_N = 0.6 \sim 1.0 H_S$), a prototype press was developed. The prototype press (Figure 5) is designed in C-shape for a manual loading from the front side. The main frame consists of four 160 mm thick C-shaped cross laminated timber (CLT) elements with an upper and lower pressure bar (HEB 160-S 235) placed in the recess of the CLT elements.

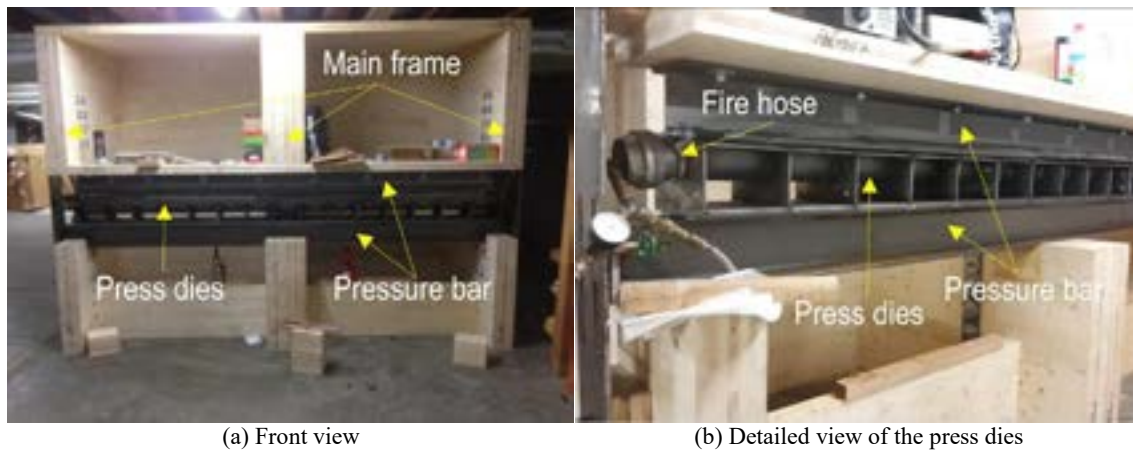


Figure 5: Prototype press

The steel moulded rigid outer part in the form of a half-pipe is placed on the bottom height-adjustable pressure bar, which is lowered during the material loading. After placing the adhesive wetted veneers in the rigid outer form (Figure 4b), the bottom pressure bar is raised until the fluid filled fire hose makes contact with the veneers. A hydraulic inflation system connected to the end caps of the fire hose generates the final press force. After the demanded adhesive curing time of at least 105 min, the half-sections are removed and equalised in a planing unit. To reach at least 30°C core temperature of the veneer layers, the fire hose is filled with water at 65°C. Additionally, 15 heating pads of 65 [W] capacity each are externally applied to the press dies in every single field (Figure 5b) and generate 65°C surface temperature for the acceleration of the MUF adhesive curing process. Subsequently, the equalised half-sections are butt jointed in a similar process and complete CLHS are formed (Figure 6).



Figure 6: CLHS prototype

Specimen geometry and clamping construction (Figure 7) was developed in several preliminary tests correlating the CLHS tensile loading capacity to the clamping system. For CLHS bonding (veneer surface bonding and butt-jointing) melamine formaldehyde resin (BASF Kauramin® 683 with Kauramin® 688 hardener) was used. Two additional 2 mm thick and 400 mm long veneers at the tube interior and six layers 1 mm thick and 600 mm long carbon fibre (FRP) reinforcement (one layer axially and five layers tangentially oriented) prevented the clamping section from splitting due to the high tangential forces caused by the wedge clamping system (Figure 8).



Figure 7: Longitudinal cut of the full-sized CLHS test setup including the wedge clamping construction

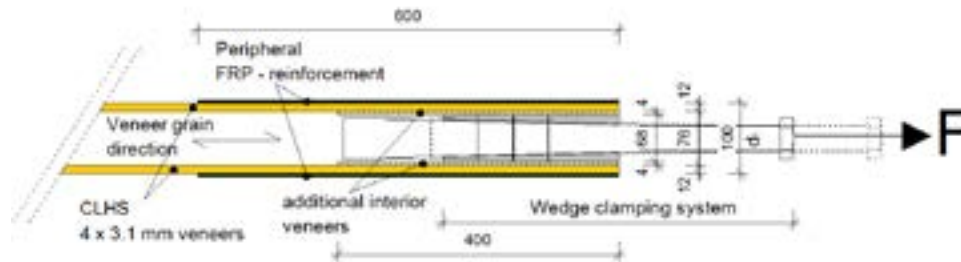


Figure 8: Clamping detail

Besides four CLHS for clamping system verification and estimation of the maximum load $F_{max,est}$, a further 20 CLHS (nominal outer diameter $d_o = 100$ mm and nominal inner diameter $d_i = 75$ mm) with 1250 mm free testing length between the FRP reinforcement were produced. Half of the produced samples were used for tensile testing of continuous CLHS without longitudinal joints (batch “CLHS”). The rest were used for the investigation of finger-jointed CLHS with a longitudinal joint. One additionally manufactured half section, produced from randomly-chosen veneer sheets of the same basic population, was cut into stripes and formed to 48 small bone-shaped specimens (batch “Bone”). This geometry is similar as described in Hirschmüller et al. 2016, Hirschmüller et al. 2018b or Hirschmüller et al. 2018a and was used to test tension strength after NC conditioning. The full-sized CLHS tensile tests (Figure 9) were performed compliant with European Standard EN 408 at *Technische Versuchs- und Forschungsanstalt der Universität Innsbruck* in a specially-developed steel frame using a 1 MN servohydraulic testing machine. The load was increased displacement controlled at 2 mm/s displacement rate, leading to testing cycles of 10 min per test. The application of higher displacement rates was not possible due to rough jerks occurring within the wedge clamping system. This resulted in a machine stroke up to 250 mm during loading, caused by slipping between the wedge clamping system’s cone and chucks. Three continuous samples without joints (batch “CLHS”) had to be adjusted during the tests as the maximum machine stroke of 250 mm was reached. The longitudinal strain was measured at the free testing length’s mid-section using two symmetrically-installed linear inductive displacement sensors with a measuring length of 500 mm. It were manually removed after a loading level of approximately 50% $F_{max,est}$. Each sensor placed upon a half section was positioned perpendicular to the butt joint for the evaluation of sample curvature during testing, due to possible different stiffnesses between the two half sections.



Figure 9: Test setup of a full-sized CLHS

2.2. CLHS FINGER JOINTING

The finger joints (FJ) were manufactured at a local glulam producer (*Grossman Bau GmbH&CoKG, Rosenheim, Germany*) using a common 15 mm finger-jointing profile (I 15/3.8; pitch = 3.8 mm, tip width 0.42 mm, 15 mm finger length and cross-section reduction factor $v = 0.11$) at a pressure level of 11 MPa. The adhesive used was of melamine type (BASF Kauramin® 683 with Kauramin® 688 hardener) and applied manually not later than six hours after cutting the fingers. For the jointing of curved geometries a special clamping model was developed to avoid CLHS crushing during the installation's clamping process. Two different FJ arrangements were produced, one to mimic a staggered arrangement of FJ within the CLHS section (batch "HFJ") and one with fully finger-jointed CLHS across the complete CLHS cross-section (batch "FFJ"). For the production of HFJ series, in a first step 2500 mm long half-poles were produced, cut into two pieces of equal length, and subsequently jointed again to a half-pole consisting of one finger joint in the mid-section of the free testing length.



Figure 10: Half section with milled finger cuts

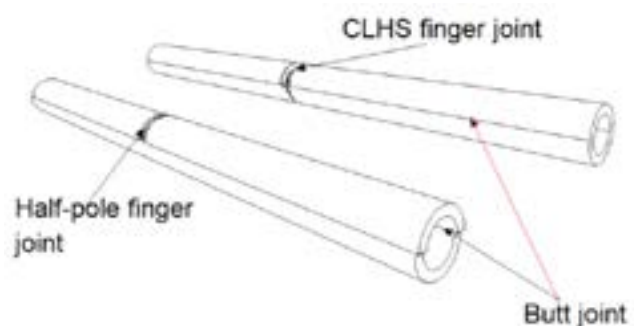


Figure 10: Schematic drawing of a half-pole finger joint HFJ (left) and finger jointing of the complete CLHS cross-section FFJ (right)

Thereby the finger edges were oriented parallel to the longitudinal CLHS butt joint (**Error! Reference source not found.**). After one hour of adhesive curing, the finger-jointed half-poles were equalised in a planing unit and butt jointed to continuous half-poles to form a complete CLHS (Figure 10).

FFJ series were produced similarly to HFJ series by cutting the CLHS in half, and the two halves were connected back together with finger jointing of the complete cross-section.



Figure 11: Half-pole finger joint HFJ (left) and complete cross-sectional finger joint (right)

After CLHS production and clamping section reinforcement, the finger jointed specimens were conditioned for two months at NC before testing. In total, ten continuous and ten longitudinally-jointed CLHS were produced, whereby five were half-section jointed (Figure 11 left) and five had a complete cross-sectional joint (Figure 11 right). One FFJ member failed during the installation, thus a number n of ten CLHS, five HFJ and four FFJ were tested in total.

3. RESULTS AND DISCUSSION

The tensile strength f_t of the samples is calculated using equation (1):

$$f_t = \frac{4 \cdot F_{max}}{\pi \cdot (d_t^2 - d_i^2)} \quad (1)$$

The modulus of elasticity MOE was determined by an averaged strain measurement of the displacement sensors placed in the mid-section of the sample with a linear regression analysis of the stress–strain diagram, with a correlation coefficient of $R > 0.99$ equation (2).

$$MOE = \frac{4 \cdot \Delta F}{\pi \cdot (d_t^2 - d_i^2) \cdot \Delta \varepsilon} \quad (2)$$

In a first step, the force-sensor displacement diagram (Figure 13) was evaluated for differences in sensor elongation. A slight curvature during testing was expected due to the reduced cross-section area of the jointed half section ($\nu = 0.11$) resulting in a differential axial stiffness between the components. But no significant difference in sample curvature between the three structural sized series evaluated was determined. The maximum observed differential strain of $\Delta \varepsilon = 0.9\%$ in batch HFJ was similar to the corresponding series FFJ and CLHS, and therefore the curvature was rather determined by different material stiffnesses of the butt-jointed half-poles. For simplification, the tensile results were applied to the full CLHS cross-section, neglecting the cross-section reduction factor ($\nu = 0.11$) of the finger joints.

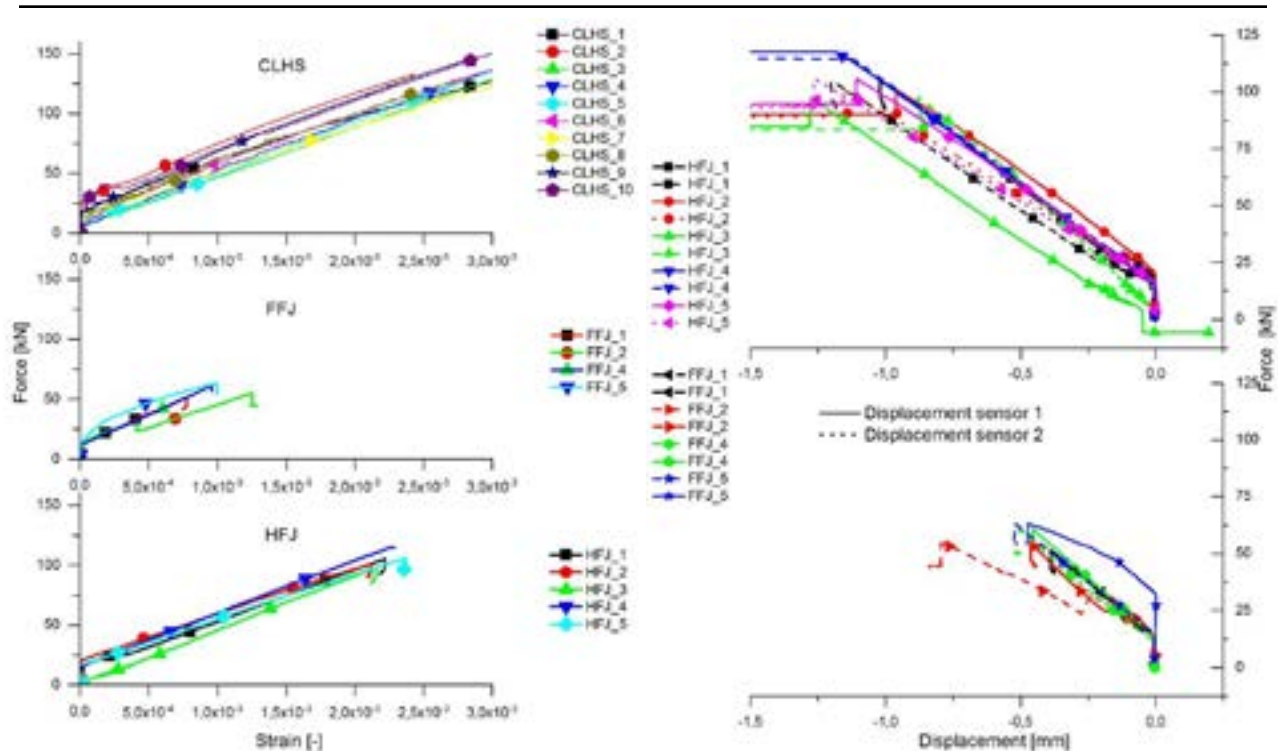


Figure 12: Force-strain diagram of finger jointed structural sized members (FFJ/HFJ) and continuous members without joints (CLHS); strain calculated as average between sensor 1 and sensor 2

Figure 13: Force-sensor displacement (elongation is plotted with negative values) diagram of *FFJ* fully finger jointed CLHS and members with finger jointed half sections HFJ; *solid line* displacement sensor 1, *dotted line* displacement sensor 2

Due to the high-grade veneers being almost free of defects, the tensile results show a high characteristic tensile strength $f_{t,k}$ of the structural sized CLHS sections without a longitudinal joint (

Table 1). Hereby moderate scattering values (coefficient of variation COV = 10%) were given. Nevertheless, the results obtained of the control batch “Bone”, consisting of $n = 48$ small sized and clear specimens are in accordance with published values of beech single veneer tensile properties (Buchelt und Pfriem 2011).

A comparison of the normal or lognormal distributed mean strengths \bar{x} of full finger-jointed members FFJ and sectional-jointed members HFJ by a t-test for two independent samples (including a Welch correction factor in case of unequal variances) at a level of significance of $\alpha = 0.05$ revealed no significant difference in means between both joining arrangements. However, the low test power ($P = 0.11$) obtained allows no statistically-sufficient assessment of the results (hypothetical sample size $n > 80$ for a test power $P \geq 0.7$, as Sachs 1993 demanded). This has also been reflected in a low characteristic tensile strength of batch FFJ ($f_{t,k} = 27$ MPa) due to the low number of tested samples ($n = 4$), in combination with a remarkable standard deviation (SD = 10.30 MPa).

Table 1: Tensile test results of structural sized series CLHS, HFJ and FFJ, compared to results of small, clear specimens (Bone) and literature values LIT 1 (Buchelt und Pfriem 2011), LIT 2 (Pollmeier Massivholz GmbH&CoKG 2018)

Group	Parameter	n	\bar{x}	SD	COV	\tilde{x}	$f_{t,k}$	u_{gl}	ρ_N
	Test		[MPa]	[MPa]	[%]	[MPa]	[MPa]	[%]	[kg/m ³]
CLHS	f_t	10	86.77	9.05	10	86.04	69	11.8	677
	MOE	10	12393	1053	8	12513	--	11.8	
HFJ	f_t	5	54.82	6.76	12	56.79	39	11.4	649
	MOE	5	12669	994	14	13016	--	11.4	
FFJ	f_t	4	49.80	10.30	21	51.83	27	11.5	719
	MOE	4	13677	1905	8	13938	--	11.5	
Bone	f_t	48	98.39	16.21	16	98.20	71	11.1	--
	MOE	48	12692	770	6	12832	--	11.1	
LIT 1	f_t	80	99.6	24.9	25	--	--	--	--
	MOE	80	12963	1687	13	--	--	--	
LIT 2	f_t	--	--	--	--	--	60	--	800
	MOE	--	16800	--	--	--	14900	--	

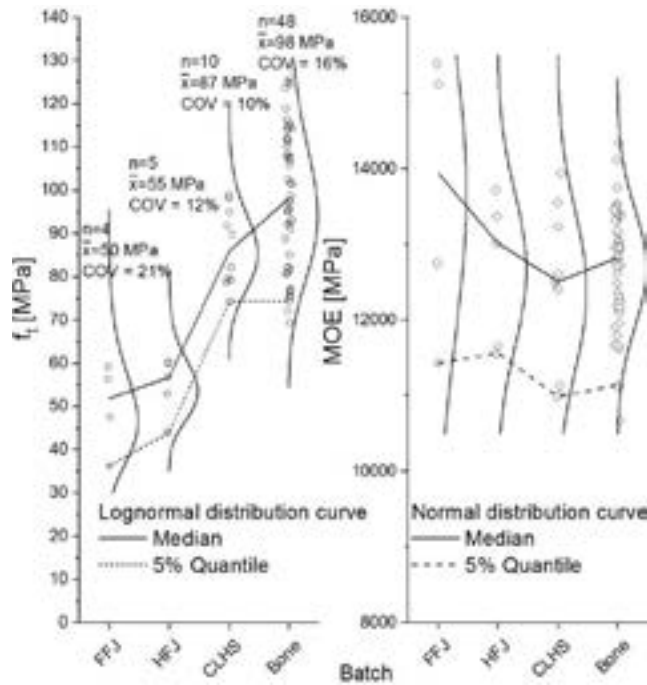


Figure 14: Scatter diagram of f_t (left) and MOE (right), comparing series FFJ, HFJ, CLHS and Bone

Similar to findings in small, clear specimens presented in Hirschmüller et al. 2018b, only a poor correlation was found between the common strength grading criteria MOE and f_t , and almost no correlation between ρ_N and f_t and MOE respectively (Figure 15). This findings emphasise the need for improved grading parameters for beech LVL, including a reliable determination of the veneer grain deviation as extensively described in (Ravenshorst 2015). The failure mechanism of jointed samples was determined by the reduced cross-section at the joint as expected. In all HFJ samples cracks initially occurred at the finger tip, leading to a brittle tensile failure of the jointed half section. After following a crack path along the butt joint, the complementary half section (without joint) failed at the weakest link in a short fibred fracture pattern typical for beech (Figure 16 left).

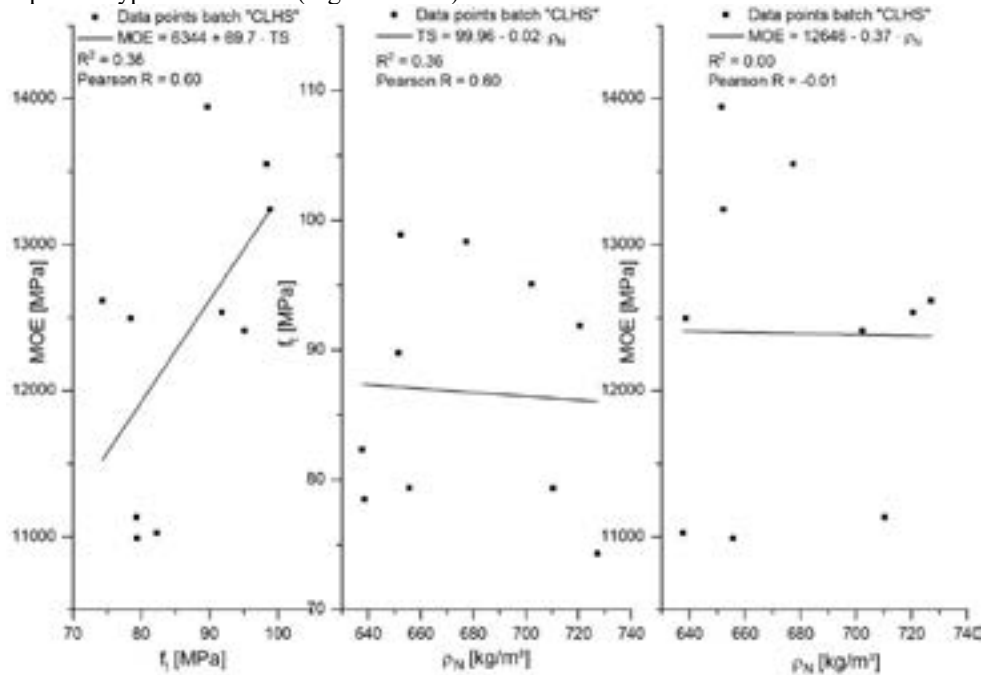


Figure 15: Correlation between f_t and MOE (left) and f_t and ρ_N (centre) and MOE and ρ_N (right) of batch "CLHS"

All FFJ samples failed at the finger joint, revealing a tensile failure at the finger tip or a shear failure at the finger sides, but always with fracture in the timber member (Figure 16 right). Just one member already failed during the clamping works due to an insufficient bond (FFJ_3) and had to be removed from further evaluation as no results could be obtained.



Figure 16: Exemplary fracture patterns of HFJ series (left) and FFJ series (right)

6. SUMMARY

However, NC conditioned beech CLHS achieve superior tensile properties, independent of the curved profile geometry. Finger jointing as an efficient and industrially well-established method of connecting plane timber members is also applicable for curved, layered veneer structures, although the abrasive bond lines require cutterhead modifications to achieve a service life similar to applications in solid timber elements. Despite a larger cross-section reduction of full finger-jointed sections, the difference in mean strength between FFJ sections (43% strength reduction compared to reference CLHS) and HFJ sections (37% strength reduction) is marginal, but still has to be improved and evaluated in further research. In half of the FFJ samples a shear failure on the finger sides was observed, resulting in lower strength, larger scattering and thus a low calculated characteristic strength.

In summary, based on the data presented it can be stated that

- even at a level of significance $\alpha = 1\%$ neither normal and lognormal nor Weibull distribution of f_t and MOE in batch CLHS could be rejected,
- no correlation was found between MOE (f_t) and ρ_N ,
- MOE and f_t correlate poorly positively and
- finger jointing is a promising alternative to staggered veneers for the production of curved and structural sized endless CLHS.

ACKNOWLEDGEMENTS

This work was supported by the Federal Ministry of Education and Research under Grant 13FH022IX4.

REFERENCES

Literaturverzeichnis

Aicher, Simon (Hg.) (2001): *Joints in timber structures. Proceedings of the international RILEM symposium* ; Stuttgart, Germany, 12 - 14 September 2001. *International Symposium on Joints in Timber Structures; Otto-Graf-Institut; International RILEM Symposium on Joints in Timber Structures. Cachan, France: RILEM Publications (RILEM proceedings PRO, 22).*

Biblis, Evangelos John; Carino, H (1993): *Factors influencing the flexural properties of finger-jointed southern pine LVL. In: Forest Products Journal 43 (1), S. 41–46.*

Buchelt, Beate; Pfriem, Alexander (2011): Influence of wood specimen thickness on its mechanical properties by tensile testing: solid wood versus veneer. In: *Holzforschung* (65), S. 249–252.

Ehrhart, Thomas; Steiger, René; Palma, Pedro; Frangi, Andrea (2018): Mechanical properties of European beech glued laminated timber. In: *International council for research and innovation in building and construction (Hg.): Working commission W18 - Timber structures, 51-12-04. Meeting fifty-one. Tallin, Estonia, 2018. Karlsruhe: Timber Scientific Publishing, KIT Holzbau und Baukonstruktionen.*

Gäßler, G.; Gudehus, G. (1981): Soil nailing – some aspects of a new technique. Volume 3, Session 12. In: *Publications Committee of X. ICSMFE. und X. ICSMFE. (Hg.): Proceedings of the 10th International Conference on Soil Mechanics and Foundation Engineering. 10th International Conference on Soil Mechanics and Foundation Engineering. Stockholm, Sweden, 15-19 June. Rotterdam: A.A. Balkema, S. 665–670.*

Gäßler, Günter (1987): *Vernagelte Geländespünge- Tragverhalten und Standsicherheit. (Nailed slopes- load-bearing behaviour and structural stability). PhD-thesis. Universität Fridericiana Karlsruhe, Karlsruhe. Institut für Bodenmechanik und Felsmechanik.*

Gilbert, Benoit P.; Underhill, Ian D.; Fernando, Dilum; Bailleres, Henri (2017): Structural solutions to produce long timber Veneer Based Composite hollow sections. In: *Construction and Building Materials* 139, S. 81–92. DOI: 10.1016/j.conbuildmat.2017.02.046.

Hara, Y.; Kawai, S.; Sasaki, H. (1994): Manufacture and mechanical properties of cylindrical laminated veneer lumber. In: *Wood Research* (81), S. 28–30.

Hata, Toshihiro; Umemura, Kenji; Yamauchi, Hidefumi; Nakayama, Akihiro; Kawai, Shuichi; Sasaki, Hikaru (2001): Design and pilot production of a “spiral-winder” for the manufacture of cylindrical laminated veneer lumber. In: *Journal of Wood Science* 47 (2), S. 115–123. DOI: 10.1007/BF00780559.

Hirschmüller, Sebastian (2019): *Beech circular hollow laminated veneer lumber sections for temporary soil nailing applications. PhD thesis. Graz University of Technology, Graz. Institute of Soil Mechanics, Foundation Engineering and Computational Geotechnics.*

Hirschmüller, Sebastian; Marte, Roman; Pravida, Johann (2016): Laminated veneer lumber poles for temporary soil nailing - investigation of material properties. In: *Josef Eberhardsteiner, Wolfgang Winter, A. Fadai und Martha Pöll (Hg.): WCTE 2016. Proceedings of the World Conference on Timber Engineering. World Conference on Timber Engineering. Vienna, 22.-25.08. Vienna: Vienna University of Technology.*

Hirschmüller, Sebastian; Marte, Roman; Pravida, Johann; Flach, Michael (2018a): Inhibited wood degradation of cement-coated beech Laminated Veneer Lumber (LVL) for temporary in-ground applications. In: *European Journal of Wood and Wood Products* 76 (5), S. 1483–1494. DOI: 10.1007/s00107-018-1325-9.

Hirschmüller, Sebastian; Pravida, Johann; Marte, Roman; Flach, Michael (2018b): Long-term material properties of circular hollow laminated veneer lumber sections under water saturation and cement alkaline attack. In: *Wood Material Science and Engineering* 81 (4), S. 1–15. DOI: 10.1080/17480272.2018.1434830.

European Standard EN 635-2, 1995: *Plywood - classification by surface appearance - Part 2: Hardwood.*

Pollmeier Massivholz GmbH&CoKG (2018): *BauBuche Beech laminated veneer lumber. Characteristic static strength values and dimensioning table. Hg. v. Pollmeier Massivholz GmbH&CoKG. Creuzburg.*

Project National Clouterre (1991): *Recommandation Clouterre 1991. Pour la conception, le calcul, l'exécution et le contrôle des soutènements réalisés par clouage des sols. (Recommendations CLOUTERRE 1991. Soil Nailing Recommendations-1991 for Designing, Calculating, Constructing and Inspecting Earth Support Systems Using Soil Nailing (English Translation, July 1993)). Paris: Presses de l'Ecole Nationale de Ponts et Chaussées.*

Ravenshorst, Gerard Johannes Pieter (2015): *Species independent strength grading of structural timber. Phd thesis. Delft University of Technology, Delft.*

Sachs, Lothar (1993): *Statistische Methoden; Planung und Auswertung. (Statistical methods; Planning and evaluation). 7th revised edition. Berlin, Heidelberg: Springer-Verlag Berlin Heidelberg.*

Srinivasan, Narayana; Jayaraman, Krishnan; Bhattacharyya, Debes (2008): Profile production in multi-veneer sheets by continuous roll forming. In: *Holzforschung* 62, S. 453–460.

European standard EN 15497, 2014: *Structural finger jointed solid timber — Performance requirements and minimum production requirements.*

European Standard EN 408, 2012: Timber structures - Structural timber and glued laminated timber - Determination of some physical and mechanical properties.

Design guide line RVS 09.01.41, 2013: Tunnelbau, offene Bauweise (Tunneling, Design Guide Lines, Cut and Cover Tunnel).

Volkmer, Thomas; Lehman, Martin; Clerc, Gaspard (2017): Brettschichtholz aus Buche: Keilzinkenverbindung und Flächenverklebung. (Glued laminated timber made of beech wood: Finger joints and surface bonding. In: Forum Holzbau (Hg.): 23. Internationales Holzbau-Forum IHF 2017. 23. Internationales Holzbau-Forum IHF 2017. Garmisch, 06.-08.12.2017: Author's edition.

Youngquist, J A; Laufenberg, T L; Bryant, B S (1984): End jointing of laminated veneer lumber for structural use. In: Forest Products Journal 34 (11-1), S. 25–32.

Testing and modelling of hardwood joints using beech and azobé

C. Sandhaas^{1*}, A. Khaloian Sarnaghi², and J.W.G. van de Kuilen^{2,3}

¹Timber Structures
Karlsruhe Institute of Technology
76131 Karlsruhe, Germany

²Wood Technology
Technical University of Munich
80797 Munich, Germany

³Biobased Structures and Materials
Delft University of Technology
2628 CN Delft, the Netherlands

ABSTRACT

Tests on double-shear steel-to-timber joints loaded parallel-to-grain were undertaken, using beech and azobé with one, three and five dowels in a row. The dowels were made of high strength steel (hss) and very high strength steel (vhss). The experiments have shown a significant difference in load-carrying capacity of joints with vhss and hss dowels. Joints with one dowel provided enough plastic deformation capacity to allow for ductile failure modes whilst this does not hold for joints with three or five dowels in a row. No correlation between load-carrying capacity and density within one wood species could be observed. Novel failure modes including steel failure of the dowels were observed. The observed effective number of fasteners was lower for the joints with vhss dowels. Also for the stiffness K_{ser} , an effective number of fasteners could be observed. The tested timber joints with their simultaneous ductile and brittle failure modes still present a major challenge for modelling. Wood is heterogeneous, highly anisotropic and shows ductile behaviour in compression and brittle behaviour in tension and shear. A bespoke 3D constitutive model for wood based on continuum damage mechanics was used to capture these effects. Eight stress-based failure criteria were defined in order to formulate piecewise defined failure surfaces. The damage development was controlled by nine damage variables that were inserted in the damage operator. The joint test results were compared to modelling outcomes. The failure modes could be identified and the general shape of the load-displacement curves agreed with the experimental outcomes.

1. INTRODUCTION

In timber joints with dowel-type fasteners, the preferred failure mode is combined failure of yielding of the fastener and embedment of the timber. Apart from the geometry, the load-carrying capacity is therefore defined by the embedment strength of the timber and the yield moment of the dowel-type fastener. The utilisation of very high strength steels (vhss) with subsequent higher yield moments is promising in order to optimise joints and get high performance connections. Thinner dowels and thinner member sections should lead to the same load-carrying capacity as have thicker mild steel dowels with bigger member cross sections – as long as failure modes with one or two plastic hinges per shear plane is reached. Another option is that with the same dimensions, fewer dowels could be used to obtain the same performance. This is especially valid and even more advantageous for high-density timber. The embedment strength of species with high densities is higher. Therefore, less member thickness would be needed when using vhss dowels in high-density timber in comparison to softwood. In the Netherlands, tropical hardwood with high densities is used for bridges and waterworks such as lock gates or mooring posts. The practical applicability is hence guaranteed

Tests have been carried out on double-shear steel-to-timber connections with vhss dowels using beech (*Fagus sylvatica*) and azobé (*Lophira alata*) (Sandhaas and van de Kuilen 2016). Comparative tests were done on the same connections, but with lower steel grade dowels. The dowel diameters were 12 and 24 mm. The number of dowels in a row was one, three and five. No other parameters such as further species, other dowel diameters or joint layout were experimentally evaluated. For this, in general, parametric studies applying finite element methods are used. However, timber joints are difficult to model. Apart from heterogeneity, two other main material-specific issues lead to numerical problems: anisotropy with different strength in tension and compression and ductile and brittle failure modes occurring simultaneously. Within the framework of continuum damage mechanics (CDM), a general approach combining the above-mentioned issues in one single 3D material model (Sandhaas 2012) was applied to predict the joint behaviour. Particularly, the capability of the models to capture failure modes was assessed.

* Corresponding author; E-mail: sandhaas@kit.edu

Testing and modelling of hardwood joints using beech and azobé

Table 1: Test series (5 tests per series) and results in terms of mean values (coefficients of variation are given in parentheses). t = thickness of timber members, u = moisture content, ρ_u = density at u , F_{max} = maximum load per joint (i.e. per two shear planes), v = displacement at F_{max} , k_s = initial stiffness acc. to EN 26891 (1991)

Diameter [mm]	Species	t [mm]	No. of dowels	Steel grade	ρ_u [kg/m ³]	u [%]	F_{max} [kN]	$F(vhss)/F(hss)$	v at F_{max} [mm]	k_s [kN/mm]
12	Beech	72	1	vhss	722 (2.5)	8.7 (3.1)	70 (6.0)	1.18	15.9 (14.6)	49 (44.2)
				hss	720 (1.6)	8.6 (3.4)	59 (3.6)		15.5 (7.2)	36 (40.6)
			3	vhss	732 (4.8)	8.7 (1.4)	173 (4.9)	1.10	6.5 (34.9)	67 (8.4)
				hss	730 (2.2)	8.5 (0.7)	157 (4.6)		5.9 (23.2)	61 (28.8)
			5	vhss	703 (2.3)	8.5 (1.0)	294 (2.5)	1.22	5.3 (17.4)	129 (13.3)
				hss	718 (3.1)	8.8 (12.6)	240 (2.5)		4.5 (8.8)	110 (4.2)
	Azobé	65	1	vhss	1115 (2.3)	22.0 (1.4)	72 (2.7)	1.26	7.9 (17.1)	53 (12.4)
				hss	1115 (2.3)	21.4 (1.4)	57 (6.5)		11.1 (41.1)	45 (29.5)
			3	vhss	1131 (4.0)	22.9 (3.1)	183 (7.9)	1.43	4.8 (23.4)	64 (11.2)
				hss	1117 (1.4)	21.8 (0.9)	128 (7.6)		3.7 (35.7)	39 (6.7)
			5	vhss	1130 (3.9)	17.2 (2.4)	281 (13.2)	1.21	2.9 (15.3)	158 (22.1)
				hss	1115 (1.6)	21.7 (0.8)	233 (14.1)		4.0 (56.1)	132 (6.0)
24	Beech	144	1	vhss	710 (1.0)	8.5 (2.0)	300 (2.4)	1.44	20.0 (21.8)	157 (7.7)
				hss	719 (2.2)	8.7 (8.0)	208 (3.6)		23.8 (16.2)	114 (20.4)
			3	vhss	724 (0.9)	8.3 (1.3)	659 (5.1)	1.29	4.2 (12.4)	205 (2.9)
				hss	711 (1.7)	8.4 (0.8)	510 (5.0)		6.0 (29.4)	202 (17.2)
			5	vhss	695 (2.3)	9.4 (4.5)	927 (3.5)	1.13	4.1 (13.5)	192 (6.3)
				hss	701 (1.0)	9.8 (2.9)	823 (5.3)		6.5 (24.0)	171 (7.2)
	Azobé	120	1	vhss	1154 (1.9)	21.5 (3.1)	306 (6.4)	1.69	5.3 (28.2)	201 (17.5)
				hss	1123 (3.1)	21.5 (5.9)	181 (10.6)		15.3 (36.8)	103 (15.1)
			3	vhss	1116 (1.9)	21.3 (6.6)	706 (5.5)	1.31	4.2 (14.7)	246 (13.8)
				hss	1104 (2.3)	22.6 (10.7)	539 (7.2)		5.0 (24.7)	186 (33.3)
			5	vhss	1111 (1.3)	15.9 (15.7)	1128 (16.0)	1.30	3.5 (36.9)	374 (40.9)
				hss	1118 (2.4)	22.5 (6.9)	868 (11.0)		4.9 (26.3)	321 (16.8)

Generally, dowels in joints with five dowels in a row were partly able to deform plastically before failure, especially when higher-density wood species were used. The displacement at the maximum load is however small. The joints with vhss dowels reached higher load-carrying capacities than the joints with hss dowels, see Table 1. The proportional limit of the joints with hss dowels is reached at lower loads than the one of the joints with vhss dowels. The ratios for the beech specimens with 12 mm dowels were however lower than expected. In order to consider all possible issues including the dowels, additional tension tests on 12 mm hss dowels were carried out. They showed that the hss dowels used for the beech specimens had 43% higher mechanical properties than the dowels for the azobé specimens, which explains why the trend of about 30% higher load-carrying capacity with vhss dowels was not found for this subseries. Finally, if the ordered mild steel grade dowels would have had a characteristic tensile strength of 360 MPa, the results given in Table 1 would have been more advantageous for the joints with vhss dowels. Then, an additional increase of the ratio of the load carrying capacities of about 40% would have been possible.

The joints with both species reach similar load-carrying capacities although the respective densities differ significantly. The moisture content of azobé was considerably higher than that of beech, which explains, at least partly, the similar values. Figures 3 and 4 show that the beech joints generally reach higher ultimate displacements compared to azobé, even though the differences disappear for three and five dowels in a row. For single dowel joints of beech, a large deformation capacity was observed with a consistent slight hardening. This also explains the relatively high load-carrying capacities of the beech joints. If for instance the load-carrying capacities of azobé and beech joints with one 12 mm vhss dowel are compared at the same displacement of 5 mm, i.e. 70 kN for beech joints and 72 kN for azobé joints, the ratio of the load-carrying capacities changes to 1.16 instead of $72/70 = 1.03$. Generally, beech is a ductile wood species that is able to support higher deformations before splitting than other species. This confirms earlier

research on the embedment strength of beech where high ductility, depending on the annual ring layout (reinforcement through rays), was observed (Sandhaas et al. 2013).

Figure 5 shows the dependency of the load-carrying capacity on the density of the timber members. A uniform load and stiffness distribution between the single dowels has been assumed. Generally, within species, density variations are such that hardly any correlation is found between the density of timber members and the load-carrying capacity of timber joints produced from them. Apparently, the scatter in load-carrying capacities is caused not only by density, but, probably more important, variations in shear and splitting strength around the fasteners which have higher coefficients of variation than density.

Figure 6 finally shows typical failure modes of joints where the shown plastic deformation of the dowel was much less for joints with three or five dowels in a row. As can be also seen in the load-displacement curves given in Figures 3 and 4, those multiple dowelled joints failed at small displacements through splitting of the timber members. Furthermore, novel failure modes were observed that do not occur when using softwoods (Blass et al. 2017).

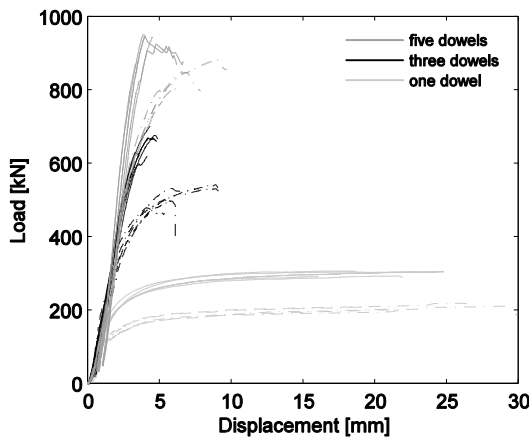


Figure 3: Mean load-displacement curves for beech joints with 24 mm dowels, solid line: vhss dowels, dashed line: hss dowels

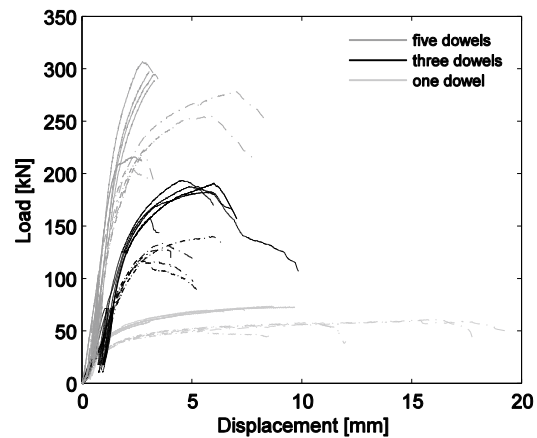


Figure 4: Mean load-displacement curves for azobé joints with 12 mm dowels, solid line: vhss dowels, dashed line: hss dowels

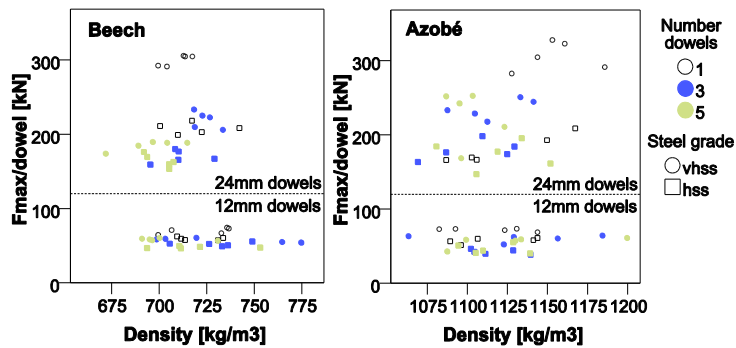


Figure 5: Density versus maximum load per dowel.

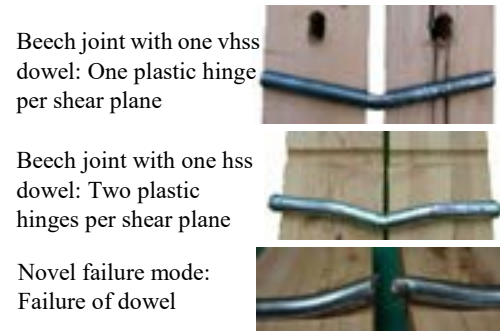


Figure 6: Failure modes of dowels.

3. MODELLING

3.1 CONSTITUTIVE MODEL

As stated in the introduction, timber joints are difficult to model due to material anisotropy, simultaneous ductile and brittle failure modes and complex stress states around fasteners. In order to investigate the potential of a constitutive model for wood based on continuum damage mechanics (Sandhaas 2012) to represent stress states and failure modes, the tests presented in section 2 were modelled using this constitutive model.

Continuum damage mechanics (CDM) is a nonlinear elastic approach where the nonlinear behaviour is obtained by modifying the stiffness matrix \mathbf{D} or its inverse, the compliance matrix \mathbf{C} . CDM can be implemented in an incremental-iterative FE framework. The stress increments are calculated from strain increments via a variable stiffness matrix. Therefore and as opposed to classical plasticity, the unloading in damage mechanics is following the secant stiffness and not following the elastic stiffness. In CDM, a damage variable d , $0 \leq d \leq 1$, is determined and inserted into the fundamental Hooke equation as follows:

$$\sigma_{ij} = (1-d) \cdot D_{ijkl} \cdot \varepsilon_{ij} \quad (1)$$

where σ_{ij} = stress matrix, d = damage variable, D_{ijkl} = stiffness matrix, ε_{ij} = strain matrix

If $d = 0$, no damage is present; if $d = 1$, the material has failed, where d is a scalar. However, anisotropic damage is observed for wood, which means that several damage variables d_{ij} must be defined to represent the 3D behaviour of wood. Therefore, three major mathematical definitions need to be established:

- Failure criteria to identify damage initiation;
- The post-elastic behaviour when $0 \leq d \leq 1$;
- A constitutive model linking the stresses to the strains.

Damage initiation of timber depends on the material directions. For instance, damage due to exceedance of tensile strength perpendicular to the grain starts at a much lower level than damage due to exceedance of tensile strength parallel to the grain. Therefore, **piecewise defined failure criteria** were used to identify damage initiation where maximum stress criteria were used in the directions parallel to the grain and quadratic criteria in the direction perpendicular to the grain. Apart from the anisotropy of timber, also failure modes differ. For instance, damage due to exceedance of tensile strength perpendicular to the grain is brittle whereas the exceedance of compressive strength perpendicular to the grain leads to ductile behaviour. Therefore, **two simplified damage laws** were defined as shown in Figure 7 and 8 where the elastic-perfectly plastic law was applied for behaviour in compression and the brittle law for behaviour in tension and shear. The final **constitutive model** is given in Eq. (2) where the damaged compliance matrix \mathbf{C}^{dam} is shown.

$$\mathbf{C}^{dam} = \begin{bmatrix} \frac{1}{(1-d_0)E_L} & -\frac{\nu_{RL}}{E_R} & -\frac{\nu_{TL}}{E_T} & 0 & 0 & 0 \\ -\frac{\nu_{LR}}{E_L} & \frac{1}{(1-d_{90})E_R} & -\frac{\nu_{TR}}{E_T} & 0 & 0 & 0 \\ -\frac{\nu_{LT}}{E_L} & -\frac{\nu_{RT}}{E_R} & \frac{1}{(1-d_{90})E_T} & 0 & 0 & 0 \\ 0 & 0 & 0 & \frac{1}{(1-d_\nu)G_{LR}} & 0 & 0 \\ 0 & 0 & 0 & 0 & \frac{1}{(1-d_\nu)G_{LT}} & 0 \\ 0 & 0 & 0 & 0 & 0 & \frac{1}{(1-d_r)G_{RT}} \end{bmatrix} \quad (2)$$

where:

Indices L , R and T refer to the longitudinal (L), radial (R) and tangential (T) material directions;

Indices 0, 90, ν and r identify damage parallel (0) and perpendicular (90) to the grain, in longitudinal (ν) and rolling shear (r),

E = moduli of elasticity

G = shear moduli

d = damage variables

ν = Poisson coefficients; were set to zero to avoid Poisson effects

For a through explanation of the constitutive model, please refer to Sandhaas (2012).

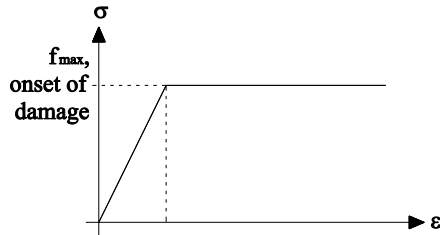


Figure 7: Elastic-perfectly plastic behaviour

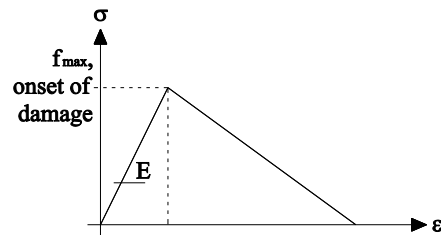


Figure 8: Brittle behaviour

3.2 MATERIAL PROPERTIES

A major issue of all material models is the need of mechanical input parameters such as stiffness and strength values that are usually based on test results. The developed model needs the mechanical input properties given in Table 2 per species. Generally, stiffness values are rather easily assembled with a satisfying reliability whereas already seemingly easy parameters as uniaxial strength values can be procured only with difficulty. This is due to two main issues. Firstly, the inherent large scatter of mechanical properties for timber and secondly, difficulties connected with testing and measuring. For instance, the uniaxial shear strength can hardly be assessed without triggering stress peaks or secondary stresses (Moses and Prion 2004). Furthermore, not always all parameters are measured, e.g. due to Poisson effect, or the positioning of the measuring instruments is not clear. In addition, the fracture energies suffer from a large scatter and they are usually derived from tests using small clear wood specimens which means that the heterogeneous nature of timber is not taken into account. Moreover, the needed material values are rather easily procurable for softwoods, but not for hardwoods.

Table 2: Material properties used in FE analysis

Parameters	Beech	Azobé	Parameters	Beech	Azobé
Stiffness in MPa			Strength in MPa		
E_L	13000	20000	$f_{i,0}$	86	72
$E_R = E_T$	860	1330	$f_{c,0}$	50	69
$G_{LR} = G_{LT}$	810	1250	$f_{i,90}$	1.0	1.0
G_{RT}	59	91	$f_{c,90}$	14.2	23.2
Fracture energy G_f in N/mm			f_v	13	16
$G_{f,parallel}$	100	180	f_r	1.0	1.6
$G_{f,perpendicular}$	0.71	0.71			
$G_{f,shear}$	1.2	1.5			
$G_{f,rolling\ shear}$	0.6	0.7			

3.3 JOINT MODELS

Double-shear steel-to-timber joint models with hss or vhss dowels have been created. Here, only models with one 12 mm dowel are presented. Von Mises plasticity with isotropic hardening has been used for all steel parts. Steel properties were a Poisson coefficient of 0.3, a modulus of elasticity of 21000 GPa, a yield strength of 570 MPa and a tensile strength of 600 for hss dowels and a yield strength of 1310 MPa and a tensile strength of 1350 MPa for vhss dowels. An exemplary joint model with one dowel is shown in Figure 9. The previously introduced constitutive model has been used only for the timber area surrounding the dowel (“UMAT” in Figure 9); in all other timber parts of the joint linear-elastic, orthotropic properties were used, applying the stiffness values given in Table 2. In the model, symmetry was used and only a quarter of the joint was modelled.

Joint models are complex models as they feature different contact regions; i.e. steel dowel/timber, steel plate timber and steel dowel/steel plate. Due to the significantly different moduli of elasticity of steel and timber, contact between these two materials is difficult to model. Deletion of the finite elements, after they have lost their stiffness, is making the damage propagation possible. However, as failure of the material generally occurs in the contact region between timber

and steel dowel, element deletion may lead to the deletion of the contact surface between steel and timber, which causes convergence problems. Therefore, element deletion in these models cannot be completed, and a tolerance needs to be defined, which reduces the stiffness of the elements without setting it to zero. Moreover, by restarting the mesh in every step, the failed elements in the contact region are removed and the contact surface is reactivated. Thus, the stiffness of the damaged elements is reduced, which deactivates the failed elements from taking the load and correspondingly prevents any stress transfer between these elements. Additionally, due to the contact problems in contact regions, the elements may get too rigid to deform flexibly to be able to reach a higher global displacement level. Therefore, the focus of this study is to overcome the problem of getting higher stiffness in the model and to come to a solution, which is able to predict the load-carrying capacity and the plastic behaviour of the material. General static solver and 3D linear hexahedral finite elements with reduced integration are used.

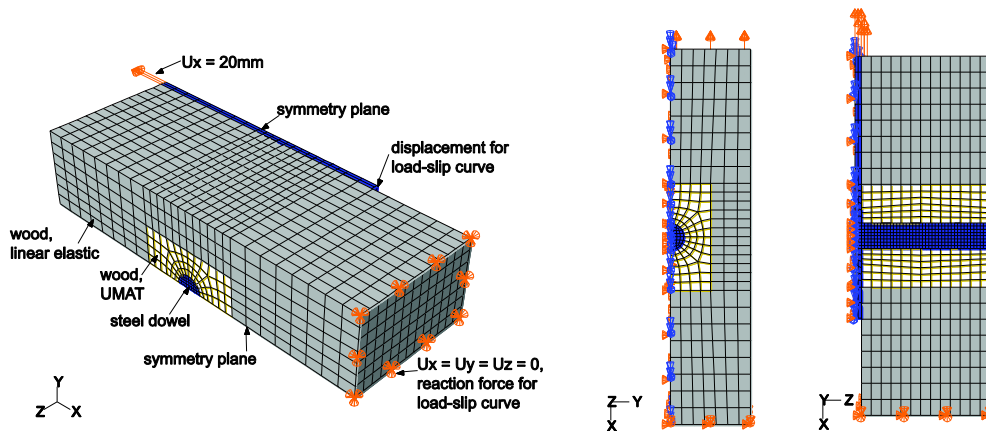


Figure 9: Typical model with one dowel, default mesh and boundary conditions.

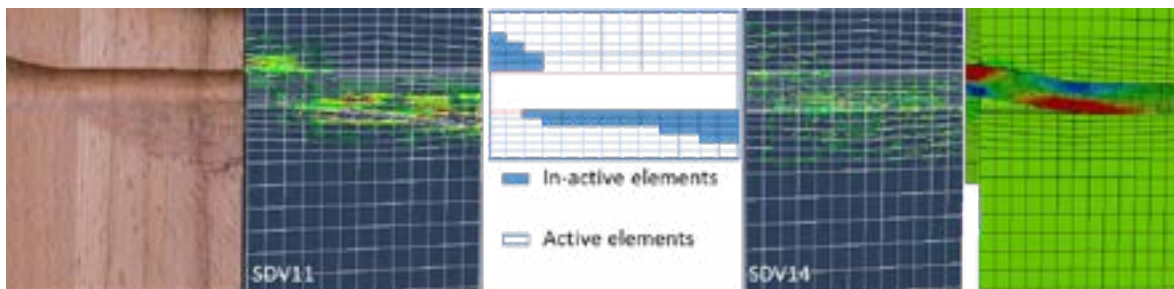


Figure 10: Typical modelling results for a joint with one hss dowel. From left to right: Photo after test, damage variable $d_{c,0}$ = compression parallel to the grain (SDV11), identification of active and deleted elements, $d_{t,90}$ = tension perpendicular to the grain (SDV14), stress in dowel axis direction

Figure 9 shows the sketch of the joint model with applied boundary conditions. Figure 10 shows results that help to judge the quality of the simulation. The results given in terms of damage variable $d_{c,0}$ (damage due to compression parallel to the grain) show the fibre crushing underneath the dowel. The test result in this figure illustrates the good phenomenological agreement between model and test. The deleted elements are also identified, and they fit well to the test result. Lastly, the normal stresses in dowel axis direction are shown to visualise dowel bending.

Figures 11 and 12 give some modelling results superposed with experimental results. The simulations were carried out for three grades of steel dowels; adding mild steel dowels with a tensile strength of 350 MPa to the analyses. The numerical results for both beech and azobé are in good agreement with the experimental results regarding the stiffness. Regarding the load-carrying capacity, the experimental results for azobé are in the same range as the numerical results if the used steel strength in the models is one grade lower than the one used in the tests. This means that the numerical results of timber joints with dowels of 600 MPa strength correspond well with the experimental results with dowels of 1350 MPa strength, and 350 MPa strength of steel dowels in numerical results correspond well with 600 MPa steel dowels in experiments. This is notable as not always tensile tests on fasteners are carried out and hence, numerical results using nominal values are compared to experimental results, which, in this case would lead to good overlap as mild steel dowels of grade S235 have been ordered.

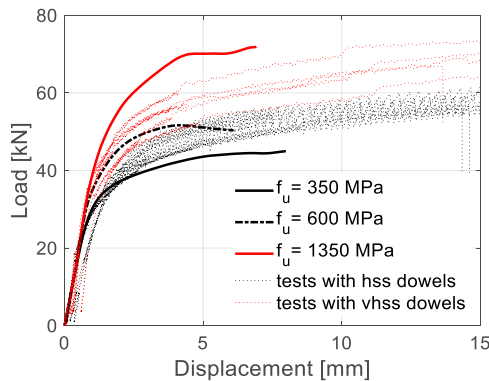


Figure 11: Overlap of numerical and experimental results for beech joints

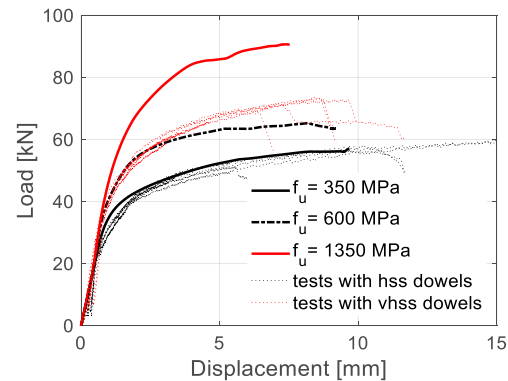


Figure 12: Overlap of numerical and experimental results for azobé joints

6. SUMMARY

The test results confirmed the feasibility of using very high strength dowels in timber joints. The load-carrying capacity of the joints with vhss dowels were increased by 10% to 69% in comparison to the same joints with hss steel dowels. Ductile failure modes with one or two plastic hinges per shear plane were possible. The tested joints were modelled using a bespoke constitutive model for the material timber that can identify failure modes and combine simultaneous ductile and brittle failures within one model. The mechanical material parameters needed for the constitutive relationship are clearly defined. The material model runs in a complex FE environment in combination with other material models and contact formulations. Modelling results were satisfying in terms of stiffness and load-carrying capacity. As for any other modelling approach, a major issue lies in the determination of the necessary mechanical properties. As the model performance and prediction capacity is highly dependent on these properties, methods to derive reliable values must be developed.

ACKNOWLEDGEMENTS

We thank the companies *Pollmeier Massivholz GmbH & Co KG* for donating the beech wood and *Groot Lemmer* for sponsoring and manufacturing the azobé specimens.

REFERENCES

- Blass, H.J., C. Sandhaas and N. Meyer. 2017. *Steel-to-timber connections: Failure of laterally loaded dowel-type fasteners. Proceedings INTER Meeting 49, Paper 50-7-1, Kyoto, Japan. Pages 67-79.*
- EN 1995 1-1:2010. *Eurocode 5. Design of timber structures - Part 1-1: General - Common rules and rules for buildings. Comité Européen de Normalisation (CEN), Brussels, Belgium.*
- EN 26891:1991. *Timber structures - Joints made with mechanical fasteners - General principles for the determination of strength and deformation characteristics (ISO 6891). Comité Européen de Normalisation (CEN), Brussels, Belgium.*
- Jorissen, A. 1998. *Double-shear timber connections with dowel-type fasteners. PhD thesis, Delft University of Technology, the Netherlands.*
- Moses, D.M. and H.G.L. Prion. 2004. *Stress and failure analysis of wood composites: a new model. Composites Part B Engineering, 35:251-261. DOI: 10.1016/j.compositesb.2003.10.002.*
- Sandhaas, C. 2012. *Mechanical behaviour of timber joints with slotted-in steel plates. PhD thesis, Delft University of Technology, the Netherlands.*
- Sandhaas, C., G. Ravenshorst, H.J. Blaß and J.W.G. van de Kuilen. 2013. *Embedment tests parallel-to-grain and ductility aspects using various wood species. European Journal of Wood and Wood Products, 71(5):599-608. DOI: 10.1007/s00107-013-0718-z*
- Sandhaas, C. and J.W.G. van de Kuilen. 2016. *Strength and stiffness of timber joints with very high strength steel dowels. Engineering Structures 131:394-404. DOI: 10.1016/j.engstruct.2016.10.046.*

Use of northern hardwoods in glued-laminated timber: a study of bondline shear strength and resistance to moisture

Alexandre Morin-Bernard^{1,2*}, Pierre Blanchet^{1,2}, Christian Dagenais^{1,2,3} and Alexis Achim²

¹ NSERC industrial chair on eco-responsible wood construction
Laval University
Quebec, QC, G1V 0A6, Canada

² Renewable materials research centre
Laval University
Quebec, QC, G1V 0A6, Canada

³ Building Systems
FPIInnovations
Quebec, QC, G1V 4C7, Canada

ABSTRACT

The growing demand for engineered wood products in the construction sector has resulted in the diversification of the product offer. Used marginally in structural products in North America, northern hardwoods are now attracting a growing interest from industry and policy makers because of their outstanding strength as well as their high availability and distinctive appearance. Currently, there is no standard in Canada governing the use of hardwoods in the manufacturing of glued-laminated timber. As part of a larger project aiming to assemble the basic knowledge that would lead to such standard, the specific objective of this study was to assess the shear strength in dry and wet conditions of assemblies made from different hardwood species and structural adhesives. Results suggest that a mean shear strength as high as 20.5 MPa for white oak, 18.8 MPa for white ash and respectively 18.2 MPa and 17.4 MPa for yellow birch and paper birch can be obtained in dry conditions. The choice of adhesive did not affect the dry shear strength of our specimens, but differences were observed in wet conditions. Specimens bonded with melamine-formaldehyde adhesive had generally the highest wet shear strength and wood failure values. Our results also highlight the important influence of wood density on the percentage of failure that occurs in wood and, to a lesser extent, on shear strength. Further investigations on finger joint strength and full-size bending tests will allow confirming the potential for the investigated species to be used in glued-laminated timber.

1 INTRODUCTION

The current growing demand for engineered wood products in the construction sector is largely attributable to their outstanding ecological performance. The substitution of materials having a larger ecological footprint, such as steel and concrete, by structural engineered wood products like glued-laminated timber have proven to be effective in minimizing the environmental impacts of the building sector (Thormark 2006). In addition to sustainability-related arguments, building designers also tend to choose wood products because of their aesthetics (Gaston 2014; Gosselin et al. 2016; Laguarda Mallo and Espinoza 2015; Markström et al. 2018). Aware of the market opportunities as well as of the lack of high value-added opportunities for some wood species, industry and policy makers from several jurisdictions have recently joined forces to develop products made from non-conventional species, especially with hardwoods. In addition to the possibility of creating products with a noble and distinctive appearance, the high mechanical properties of some hardwood species offers the opportunity to create engineered products of outstanding strength. Several glued-laminated timber products (DIBt 2009, 2013; ETA-13/0642-02646 2013) made from various hardwood species have been approved in the European union, which are largely exceeding the strength of their softwood counterparts. Hardwood glulam products are also available in the United states for over two decades. Work undertaken in this country in the early 1990s with red maple and red oak (Janowiak et al. 1995; Manbeck et al. 1993; Shedlauskas et al. 1996) led to the development of structural products now used in timber bridge design (Manbeck et al. 1996).

As the laminating effect in glued-laminated timber beams stems from the fact that laminations are bonded (Falk and Colling 1995), the integrity of the cross-section is a key factor in the overall product strength (Dietsch and Tannert 2015). For hardwood, the bonding quality and resistance to moisture remain issues that cannot be neglected. The thick cell walls and small lumens of hardwood species often lead to a limited penetration of the adhesive, and consequently to weakened bondlines (Frihart and Hunt 2010; Selbo 1975). Results from the work of Aicher et al. (2018), Konnerth et al. (2016), Jiang et al. (2014), Knorz (2014) and Lehmann (2018) with several European and Tropical hardwoods revealed that bond strength may greatly vary depending on the adhesive system and wood species. The low dimensional stability of hardwoods also induces important stresses on the bondlines when the moisture content fluctuates (Frihart and Hunt 2010). Several gluing tests (Ammann et al. 2016; Knorz et al. 2015; Konnerth et al. 2016; Vick and Okkonen 1998) conducted with dense hardwoods in wet conditions or after repeated moisture content

*Corresponding author: E-mail: alexandre.morin-bernard.1@ulaval.ca, Tel: 1-418 264-3265

variations confirmed the importance of this effect. Considering the inherent difficulties of bonding hardwoods, the achievable bondline strength of a given species and adhesive system must be carefully assessed in order to confirm the relevance of their use in a structural engineered wood product such as glued-laminated timber (GLT).

In Canada, no structural GLT products made from hardwood species are currently available on the market. The CSA O122 (2016) standard, governing the manufacturing and quality control testing of structural glued-laminated timber, does not include any provision regarding the use of hardwood species. Moreover, the resource is largely available. Each year in the province of Quebec, half of the annual allowable cut of deciduous trees remains unharvested (Durocher et al. 2019). As part of a project seeking to develop new opportunities for these species and promote the production of high value-added products such as GLT, the objective of this study was to assess the shear strength in dry and wet conditions of assemblies made from different hardwood species and structural adhesives.

2 MATERIALS AND METHOD

A preliminary test campaign was conducted prior to the main campaign. At the end of this first series of tests, species and adhesives that would be submitted to further investigations were selected and potential improvements in the experimental protocol were identified and integrated in the main test campaign.

2.1 MATERIALS

White oak (*Quercus alba* Linn.), white ash (*Fraxinus americana* Linn.), yellow birch (*Betula alleghaniensis* Britt.) and paper birch (*Betula papyrifera* Marsh.) lumber was purchased from various local merchants and sawmills. Birch trees were harvested in Duchesnay, near Quebec City, Canada, but the exact provenance of the white oak and white ash lumber is unknown.

All pieces used in this experiment showed a maximum slope of grain of 1 in 15, were free of knots and any other defects. Growth rings were making an angle of less than 45° with the wider face of the pieces. Lumber was conditioned at 20°C and 65% relative humidity until constant mass was reached. Density was measured by the volumetric method described in ASTM D2395 (2017). Mean values and standard deviation (SD) are presented in Table 1.

Two adhesive systems were used, approved both for interior and exterior exposure in structural applications. Names and specifications are shown in Table 2. Melamine-formaldehyde (MF) and two-component polyurethane (2C-PUR) adhesives were chosen amongst other products after preliminary trials.

Table 1 Mean density (ρ_{12}) values from preliminary trials and main test campaign

Species	Preliminary trials		Main campaign	
	Mean density ρ_{12} (kg/m ³)	SD	Mean density ρ_{12} (kg/m ³)	SD
Paper birch	634.6	30.6	613.3	13.7
Yellow birch	664.0	15.6	667.6	30.7
White ash	659.0	85.5	731.8	22.9
White oak	739.4	39.4	766.2	87.4

Table 2 Adhesives and gluing parameters

Adhesive type	Resin	Hardener	Glue spread (g/m ²)	Mixing ratio	Pressure (psi)	Press time (h)
Melamine-Formaldehyde (MF)	Cascomel™ 4720	Wonderbond™ 5025A	390	4:1	150	15
Two-component Polyurethane (2C-PUR)	Purbond® GT20	Purbond® GT205	340	100:15	200	2.3

2.2 BLOCK SHEAR TESTS

In glued-laminated timber quality-control process, block shear tests are widely used to assess the shear strength and wood failure of gluelines. In the United States, AINSI A190.1 (2017), the standard establishing performance

requirements for GLT products, relies on the block shear test method described in ASTM D905 (2013). Its counterpart in the European union, EN 14080 (2013), also relies on a block shear test method, described earlier in former standard EN 392 (1995). Block shear test is also the testing method prescribed by international standards ISO 6238 (2018) and ISO 12579 (2007) for determining the glue-line shear strength in glued-engineered wood products.

In Canada, block shear tests are an integral part of the quality control testing of glulam as specified in CSA O122 (2016), the standard governing the manufacturing of softwood GLT in Canada. Standard CSA O112.9 (2010) «*evaluation of adhesives for structural wood products (exterior exposure)*» is also largely based on block shear tests. In accordance with this standard, tests must be conducted in dry condition and in wet conditions, after the specimens are subjected to a vacuum-pressure cycle. Wet tests are used because they allow discriminating easily between performing and non-performing adhesives-species combinations in wet conditions.

2.2.1 PREPARATION OF TEST SPECIMENS

Lumber from the four species was cut into billets of 21 mm thick, 65 mm wide and 350 mm along the grain. All billets were planed to a final thickness of 19 mm on the same day when they were bonded, using a planer with a rotary cylindrical cutter. Knives were sharpened just before processing the pieces from the preliminary trial. In the main test campaign, it was decided not to do so, to make the surface preparation process more representative of a factory production.

For each combination of wood species and adhesive, six billets were grouped by pairs of similar density and assembled with the growth rings concave from the bondline. Adhesives application rates, assembly times, pressures and pressing times were specified after consulting the technical data sheets and the manufacturers (Table 2). After bonding, assemblies were placed in a conditioning room at 20°C and 65% relative humidity for at least two days before the preparation of test specimens. Five blocks of approximately 50 x 50 mm were cut from each assembly, as specified in standard CSA O112.9 (2010) and ASTM D905 (2013). A 5-mm notch extending to without going beyond the bondline was cut on each side of the test specimens. The bondline area was approximately 2000 mm². Figure 1 shows the configuration and measurements of test specimens. Specimens were returned in the conditioning chamber until tested. The exact contact surface was measured to the nearest 0.01 mm immediately before testing.

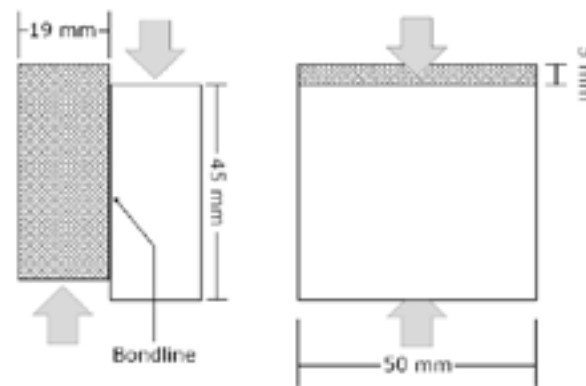


Fig. 1 Geometry and measurements of block shear test specimens from CSA O112.9 (2010)

2.2.2 TESTING PROCEDURE

Thirty test specimens were obtained for each species-adhesive combination. Fifteen specimens were randomly selected and subjected to a vacuum-pressure cycle as specified in CSA O112.9 (2010) standard before being tested. The cycle consisted of submerging specimens in water, holding a vacuum of 75 kPa ± 10 kPa for thirty minutes and then applying a pressure of 540 kPa ± 20 kPa for two hours. These specimens were tested in wet conditions, while the remaining fifteen specimens were tested in dry conditions.

Block shear tests were conducted on an MTS QTest load frame (Eden Prairie, USA) fitted with a 50 kN load cell and a compression shearing tool. The load was applied parallel to the grain direction in a continuous motion rate of 5 mm/minute. Wood failure percentage was visually estimated to the nearest 5%. The test apparatus and shearing tool shown in Figure 2 complied with ASTM D905 (2008). The maximum load was used to calculate the bondline shear strength with the following equation:

$$f_v = \frac{F_{max}}{A} \quad \text{in N/mm}^2$$

where

f_v : Shear strength (MPa), F_{max} : Maximum load applied (N) and A : Bondline area (mm²)



Fig. 2 Block shear testing device

2.3 DATA ANALYSIS

From the shear strength data, the mean value and standard deviation for each species-adhesive combination were calculated. A mixed-effects analysis of variance was conducted to compare means, using adhesive and wood species as fixed effects and the assembly from which specimens were cut out as a random effect. Assumptions were verified and confirmed. When a significant effect of one of the explanatory variables was detected, multiple comparisons were conducted using Tukey's test. Analyses were made using the *lme4* (Bates et al. 2015) and *emmeans* (Lenth et al. 2018) packages in the R software, version 3.5.2 (R Core Team 2018). Median and mean wood failure percentages were computed for each group as standards rely on either one or the other.

3 RESULTS AND DISCUSSION

3.1 RESULTS FROM THE PRELIMINARY TEST CAMPAIGN

Table 3 shows the results of the preliminary test campaign. The highest dry shear strength was achieved by yellow birch specimens glued with 2C-PUR adhesive (22.4 MPa) and was significantly higher ($p = 0.0095$) than the lowest strength value, which was observed with white ash specimens bonded with the MF adhesive (15.8 MPa). Strength of yellow birch specimens was also significantly higher ($p = 0.0416$) than that of paper birch specimens glued with MF adhesive. The differences between all other species-adhesive combinations were not statistically significant ($p > 0.05$).

In tests realized after the vacuum-pressure cycle, white oak specimens bonded with MF adhesive and white ash specimens bonded with 2C-PUR adhesive attained an equivalent strength of 10.0 MPa, which was significantly higher ($p = 0.0271, 0.0287$) than the strength of white oak specimens bonded with 2C-PUR (6.2 MPa). Specimens from the birch species and white ash specimens bonded with MF adhesive attained an intermediate strength varying between 8.1 and 9.5 MPa. Tukey's test did not reveal other statistically significant differences. In the dry test, the mean level of wood failure ranged from 59 to 98 % while it ranged from 2 to 99 % in the wet test. In both tests, the lowest wood failure percentage was observed on white oak specimens bonded with the 2C-PUR adhesive. In the wet test, wood failure of specimens bonded with 2C-PUR adhesive was always lower than those glued with the MF adhesive.

Table 3 Shear strength (MPa), mean density (kg/m³), median and mean wood failure percentage from the preliminary trials

Test	Species	Adhesive	n	Mean density (kg/m ³)	Mean f_v (MPa)	SD	Median WF (%)	Mean WF (%)
Dry	Paper birch	MF	15	615.4	16.9	0.9	80	81
		2C-PUR	15	653.2	19.5	1.7	100	97
	Yellow birch	MF	15	653.6	20.6	1.0	100	89
		2C-PUR	15	675.9	22.4	1.1	90	79
	White oak	MF	15	756.8	18.7	2.4	90	75
		2C-PUR	15	722.0	17.2	1.4	55	59
	White ash	MF	15	633.0	15.8	4.2	100	95
		2C-PUR	15	684.9	19.9	2.4	100	98
Wet	Paper birch	MF	5	626.8	8.3	0.3	90	93
		2C-PUR	5	644.0	9.3	0.4	75	78
	Yellow birch	MF	5	649.8	8.1	0.5	100	99
		2C-PUR	5	673.8	9.5	0.8	25	31
	White oak	MF	5	774.7	10.0	1.0	85	75
		2C-PUR	5	730.1	6.2	2.5	0	2
	White ash	MF	5	651.3	9.0	2.6	100	81
		2C-PUR	5	672.3	10.0	0.3	50	62

Consecutively to these tests, as density of the wood material between subsamples varied substantially and was most of the time lower than values stated in literature (Jessome 1977), it was decided to better control this parameter in the main test campaign. It was also decided to increase the number of repetitions for specimens tested after the vacuum-pressure cycle from five to fifteen to account for the variability observed in the first tests.

3.2 RESULTS FROM THE MAIN TEST CAMPAIGN

Figure 3 shows the mean dry bondline shear strength from the main test campaign for paper birch, yellow birch, white ash and white oak specimens, glued with MF and 2C-PUR adhesives. White oak specimens glued with MF adhesive exhibited the highest shear strength (20.5 MPa), followed by white oak specimens glued with 2C-PUR adhesive (19.3 MPa). White ash specimens had very similar values regardless of the adhesive used (18.6-18.8 MPa). Paper birch specimens glued with the MF adhesive attained the lowest strength (16.4 MPa). This value was significantly lower than the strength of MF ($p = 0.0001$) and 2C-PUR ($p = 0.0078$) bonded white oak specimens as well as that of white ash specimens bonded with the MF adhesive ($p = 0.0376$). Paper birch and yellow birch specimens bonded with the polyurethane adhesive (17.4-17.5 MPa) also achieved a significantly lower shear strength ($p = 0.0057$, 0.0059) than white oak specimens bonded with the melamine adhesive. Yellow birch specimens glued with the MF adhesive achieved the higher mean shear strength amongst birch samples, with 18.2 MPa, but this value was not significantly different from any other group ($p > 0.05$). No other statistically significant differences were unveiled by Tukey's multiple comparison test.

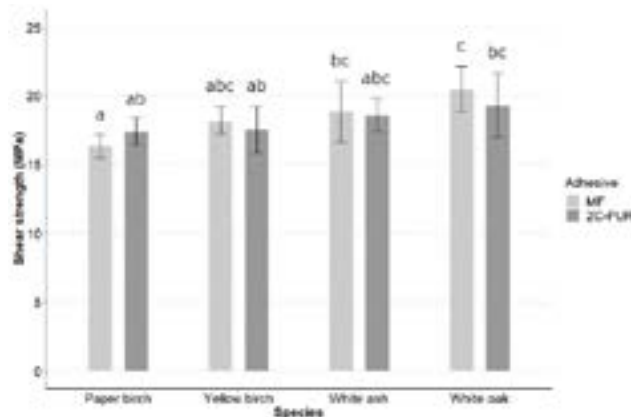


Fig. 3 Bondline shear strength (MPa) in dry conditions of paper birch, yellow birch, white oak and white ash specimens bonded with two adhesives

Figure 4 shows the mean bondline shear strength obtained from the wet test in the main test campaign. The shear strength achieved by the birches specimens was not significantly impacted by the adhesive choice ($p > 0.05$). Paper birch specimens attained a shear strength of 7,6 MPa with MF and 2C-PUR adhesives, corresponding to reductions of respectively 53.7 and 56.3 % compared to strength values from the dry test. Yellow birch specimens achieved slightly higher but not statistically different strengths ($p > 0.05$), with a mean value of 8.6 MPa for specimens glued with MF adhesive, and 7.8 MPa for specimens glued with 2C-PUR adhesive. The corresponding reductions from the dry shear strengths are respectively 52.8 and 55.4 %.

Oak and ash specimens glued with MF adhesive showed significantly higher shear strength than specimens from the same species glued with 2C-PUR adhesive, with values of 10.6 and 10.1 MPa for white oak ($p = 0.0001$) and white ash ($p = 0.0097$), which corresponded to reductions of 49.8 and 46.3 % from the dry shear strength, respectively. The strength of the oak and ash specimens glued with 2C-PUR was substantially lower with values of 7.3 MPa for white oak and 7.8 MPa for white ash, which corresponded to reductions of 62.2 and 58.1 %, respectively, compared to the dry test values. For specimens glued with the 2C-PUR adhesive system, differences between species were not significant according to Tukey's test ($p > 0.05$). However, strength of white oak and white ash specimens bonded with the MF adhesive was significantly higher than the strength of paper birch specimens bonded with the same adhesive ($p = 0.0009, 0.003$).

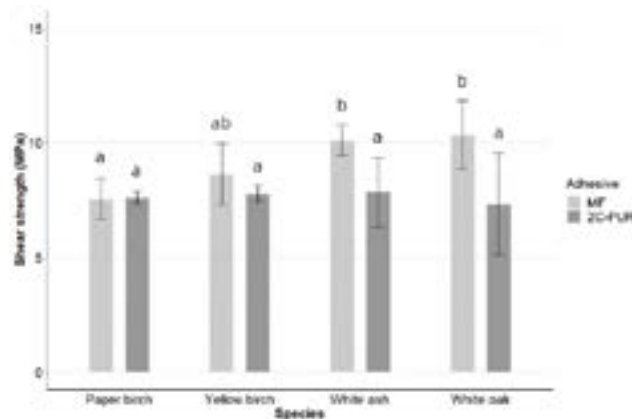


Fig. 4 Bondline shear strength (MPa) in wet conditions of white oak and white ash specimens bonded with two adhesives

Table 4 presents the detailed density values as well as mean and median wood failure percentages for every group from the main test campaign. In dry conditions, the mean wood failure levels of paper birch specimens were the highest amongst all species. Yellow birch specimens showed slightly lower levels, especially those bonded with the 2C-PUR adhesive. White ash and white oak groups followed in order and showed, for a given species, comparable wood failure levels irrespectively of the adhesive used, although 2C-PUR adhesive achieved slightly better results with white ash.

Compared to wood failure levels in dry conditions, wood failure in wet conditions was lower for all species-adhesive combination, exception made of the paper birch specimens bonded with the polyurethane adhesive and of the white ash specimens bonded with the melamine adhesive. Yellow birch, white oak and white ash specimens bonded with the 2C-PUR adhesive exhibited considerably lower wood failure levels in the wet test than their counterpart bonded with the MF adhesive, but this was not the case with paper birch specimens, for which the opposite trend was observed.

Table 4 Density and wood failure (WF) percentages of species-adhesive groups tested in dry and wet conditions

Test	Species	Adhesive	n	Mean density (kg/m ³)	Density SD	Median WF (%)	Mean WF (%)	WF SD
Dry	Paper birch	MF	15	617.7	13.9	95	94	7.0
		PUR2	15	614.4	11.0	100	95	8.3
	Yellow birch	MF	15	645.7	29.3	100	88	15.7

	PUR2	15	660.1	23.2	80	76	24.9
	MF	15	736.5	23.5	70	60	34.7
White ash	PUR2	15	729.3	23.0	75	78	17.3
	MF	15	783.0	91.1	60	56	38.3
White oak	PUR2	15	756.2	87.7	60	54	28.4
	MF	15	609.4	16.1	75	69	22.5
Paper birch	PUR2	15	611.7	13.1	95	94	10.2
	MF	15	691.9	30.5	70	53	32.6
Yellow birch	PUR2	15	672.5	20.1	30	32	31.7
Wet	MF	15	734.2	23.3	80	76	26.8
White ash	PUR2	15	727.4	23.0	15	29	27.0
	MF	15	777.9	94.0	50	47	32.5
White oak	PUR2	15	747.8	80.0	10	17	19.1

3.3 COMPARISON OF RESULTS WITH REQUIREMENTS FROM GLT STANDARDS AND COMPARABLE STUDIES

Various standards issued in different countries comprise shear strength and wood failure requirements for glued-laminated timber products. However, it is sometimes hazardous to use requirements of standards from other countries or that are not designed specifically for the investigated species. Indeed, it has been demonstrated that different block shear test methods can lead to discrepancies of up to 60 % in the results (Okkonen and River 1989). The testing device alone could cause significant differences (Steiger et al. 2010). For example, European standard EN 14080 (2013) relies on a different testing procedure and test apparatus and requirements for shear strength as well as wood failure are exclusively differentiated between softwoods and hardwoods by means of thresholds for the lowest single values.

In Canada, since no standards regulate the use of hardwoods in GLT, threshold values for shear strength and wood failure percentage are only available for softwood GLT in CSA O122 (2016). However, standard CSA O112.9 (2010) provides qualification requirements for adhesives used in products made from hardwoods and softwoods and intended for load-bearing applications in exterior conditions. However, requirements for hardwoods are based on tests conducted exclusively on hard maple (*Acer saccharum* Marsh., *Acer nigrum* Michx. f.). The minimum bondline shear strength requirements of 19 MPa in dry conditions and 11 MPa in wet conditions set out in this standard can therefore not be compared directly with our results.

In the United States, standard ANSI A190.1 (2017) defines the bond shear strength requirement as a ratio of the clear wood shear strength. In dry conditions, bonded specimens must reach at least 90 % of the strength of clear wood specimens as defined in ASTM D2555 (2006). In this study, all groups reached a shear strength considerably higher than the required 90 % of clear wood strength from ASTM D2555 (2006). However, the significance of this criterion should be interpreted with caution because values from this standard do not account for variation within species. As suggested by River et al. (1991) and Aicher (2018), comparing the bondline shear strength with a clear wood strength value obtained from the same sample of wood material would be more meaningful. Moreover, the shear strength should always be interpreted in conjunction with the level of wood failure. Shear strength values are a good indicator of the product's strength only if wood failure levels are sufficiently high (Frihart and Hunt 2010).

Any comparison of our results with reference values from other studies is difficult since very little literature on bonding of northern hardwood species is available. In a study of the impact of block shear test method on shear strength values, Okkonen and River (1989) conducted tests with bonded and clear wood white oak specimens using a phenol-resorcinol-formaldehyde (PRF) resin as adhesive. Amongst others, they used testing method ASTM D905 (2008) and a testing device comparable to that used in this study. White oak lumber had a mean density of 740 kg/m³ and clear wood specimens achieved a mean shear strength of 18 MPa, while bonded specimens reached 17 MPa. In addition to the difference in the adhesive used, the higher mean density of the white oak used in our study may explain why our bonded specimens reached higher strength than the clear wood specimens from Okkonen and River (1989). Unlike what we observed in our tests, almost all failures occurred entirely at the bondline in the case of their glued specimens. Our review of the literature did not lead to any results on the bondline shear strength of North American white ash. Even if shear strength values cannot be compared directly because of the different testing procedures and apparatus, experiments conducted in Europe with species related to those investigated in this study, namely common

ash (*Fraxinus excelsior* L.), common oak (*Quercus robur* L.) and sessile oak (*Quercus petraea* (Matt.) Liebl.) provide the best available basis for comparison. In that way, findings of the current study are not consistent with those of Aicher et al. (2018). In block shear tests conducted on specimens originating from industrially manufactured hardwood glued-laminated timber beams, common ash attained higher wood and bondline shear strengths than common/sessile oak with density of 695 kg/m³ and 752 kg/m³, respectively. No reference to shear strength of glued assemblies made from the investigated or related birch species was found in literature.

However, our results are consistent with the mechanical properties of the investigated species, as white oak is known to be slightly stronger in longitudinal shear than white ash, followed in decreasing order by yellow and paper birch (Jessome 1977). It must be noted, however, that mechanical properties from the work of Jessome (1977) were obtained from block shear tests conducted following standard ASTM D143, which involves a different specimen geometry and test apparatus to that used in this study.

In wet conditions, shear strength values were considerably lower. However, all species-adhesive combinations did not suffer an equivalent loss in strength. The observed loss ranged from 46,3 to 62,2 % depending on the adhesive and species. In comparison, the deemed-acceptable reduction in median shear strength for hard maple bonded specimens in CSA O112.9 (2010), when submitted to the vacuum-pressure cycle, is 42,1 % (i.e. 19 MPa to 11 MPa). The higher loss of strength observed in our experiment could be explained partially by the occurrence of bondline failures, mostly in the case of higher density specimens. Furthermore, the wet shear strength that was reached in paper birch specimens was similar to that of the yellow birch specimens bonded with the 2C-PUR adhesive. The lower wood failure level observed for the latter and the difference in density between the two species are the most likely factors explaining this result.

Wood failure percentage provides much information as it allows knowing if bonding took full advantage of the wood material's strength. In the dry test, wood failure percentages suggest that the maximum strength potential of the wood material was not always reached, particularly in the case of white ash and white oak specimens. With respect to wood failure requirements, ANSI A190.1 (2017) defines a specific category for dense hardwoods and different thresholds for Initial Type Testing (ITT) and Factory Production Control (FPC). Mean wood failure percentages in dry conditions must be at least 60 % for ITT and 50 % for FPC. Every combination of adhesive and wood species tested in the main test campaign reached the mean wood failure requirement in FPC for dense hardwoods from ANSI A190.1 (2017). For ITT however, white oak specimens bonded with MF and 2C-PUR adhesives did not reach the required mean wood failure percentage. Although requirements from CSA O112.9 (2010) apply to different species, our results in dry conditions are close to the minimum median wood failure requirement of 60 % set out in this standard, but only paper birch specimens glued with 2C-PUR adhesive and white oak specimens glued with MF adhesive fulfilled the threshold value of 80 % for the test in wet conditions. Since CSA O112.9 (2010) expects higher wood failure percentage in the wet test than in the dry test, our results are not entirely satisfactory. Only the white ash specimens bonded with the MF adhesive have met this criterion.

In comparable studies, Aicher et al. (2018) obtained higher mean wood failure percentages, with 89 % for the common/sessile oak sample bonded with melamine-urea-formaldehyde (MUF) and 79 % for the common ash sample bonded with a PRF adhesive. In block shear tests on bonded common ash specimens (661 kg/m³), Knorz et al. (2014) obtained a mean wood failure percentage of 63 % with a one-component polyurethane (1C-PUR) adhesive and 99 % with a MUF adhesive. In tensile shear tests with common ash (638 kg/m³) specimens bonded with MUF, PRF, 1C-PUR and emulsion polymer isocyanate adhesives, Jiang et al. (2014) obtained mean wood failure values of at least 70 % with all four adhesives tested. No reference to wood failure levels from shear strength tests on glued assemblies of paper birch or yellow birch was found in the literature. The difference between our results and comparable studies might be due to the adhesive system used, but also to the density of the wood material.

3.4 IMPACT OF WOOD DENSITY ON BONDLINE STRENGTH AND WOOD FAILURE

Differences observed in wood failure between the preliminary trials, the main test campaign and comparable studies tend to confirm the impact of wood density on the adhesive performance. For both white oak and white ash, the species showing the highest specific gravity, specimens made of higher density material showed most of the time lower wood failure percentage. In the first series of tests, average densities of white oak and white ash were lower. Some ash specimens had density as low as 522 kg/m³, which is far from the mean value of 690 kg/m³ stated in literature (Jessome 1977). Therefore, it was decided to increase the minimal density of the white oak and white ash sample to obtain more representative results. As a result, dry shear strengths for these species were higher in the main test campaign than in preliminary trials, even if for three of the four species-adhesive combinations, mean wood failure was considerably lower. The significant increase in the white ash sample density resulted in a 30 % reduction of mean wood failure percentage. The same effect is visible within the white oak sample from the main test campaign, where few specimens showed an extremely high density (i.e. 897-902 kg/m³) and very low wood failure. If those specimens

were excluded from the analysis, mean and median wood failure percentages would have been considerably higher, and thus closer to values obtained in preliminary trials.

When comparing all four species, the density of the wood material seemed to have a direct influence on the wood failure levels observed in the dry test, although other anatomical and chemical factors could also be responsible for the differences. Contrarily to white oak and white ash specimens, paper birch and yellow birch specimens had, except for a few exceptions, consistently high wood failure levels. Above a certain density value located somewhere between that of our yellow birch and white ash samples, the adhesive performance in dry conditions appears to be affected by an increase in the density of the adherent. This observation is in line with the threshold zone proposed by Frihart and Hunt (2010) of 700 to 800 kg/m³. In the wet test, the same general trend could be observed, especially for specimens bonded with the polyurethane adhesive.

These results show the interactions occurring between material density, shear strength and wood failure. To facilitate the use of hardwood species in structural glued-engineered wood products, it is important to consider the hardwoods intraspecies variability in the establishment of standardized shear strength and wood failure requirements. Grading requirements for lumber to be used in the manufacture of this type of product might also include provisions related to density. Nevertheless, if bonded satisfactorily, denser wood offers the possibility to increase the strength of the product.

3.5 IMPACT OF ADHESIVE ON WET CONDITIONS RESISTANCE

In dry conditions, no statistically significant differences between adhesive performance were detected for a given species. In wet conditions, wood failure percentage was particularly low for yellow birch, white ash and white oak specimens bonded with the 2C-PUR adhesive. The loss of strength induced by the vacuum-pressure cycle was also greater for specimens of these species bonded with the same adhesive. However, paper birch specimens showed higher wood failure levels when bonded with the 2C-PUR adhesive rather than with the MF adhesive. This inconsistent result coincides with the fact that paper birch is the least dense amongst all tested species. The magnitude of the stress induced on the glue-lines by wood swelling is thought to increase proportionally to the density of the material (Selbo 1975, River et al. 1991, Frihart and Hunt 2010). For paper birch specimens, this stress may have been contained under a certain threshold that is within the limits of the 2C-PUR performance. This could explain why despite showing similar wood failure levels in the dry test, yellow birch and paper birch performed differently in the wet test.

Thus, our findings are globally consistent with studies conducted in the past years on moisture resistance of several adhesive systems used to bond hardwood species. Work from Ammann et al. (2016) with common ash of a density of approximately 650 kg/m³ glued with six adhesive systems revealed that the two-component polyurethane adhesive was one of the least efficient in wet tensile shear tests and in resistance to delamination tests. In studies of structural bonding in common ash, Knorz et al. (2015, 2014) stated that polyurethane adhesives showed the highest delamination rates amongst multiple adhesive systems when submitted to repeated moisture content variations. In these studies, melamine-urea-formaldehyde (MUF) adhesives, which are recognized to have a lower moisture resistance than MF adhesives (Frihart and Hunt 2010), still offered a higher performance than polyurethane based adhesives. Melamine-formaldehyde adhesive therefore appears to be suitable for structural products exposed to weather. However, results in wet conditions with white oak and MF might have been better in regard to the results obtained with white ash. In the main test campaign, the fact that knives were not perfectly sharpened before planing may have limited adhesive penetration, as shown by Knorz et al. (2015). This effect could have been added to that of density, explaining the low wood failure percentage observed in some specimens. However, these conditions are more realistic in the context of an industrial production, since it is unlikely that knives would be sharpened as frequently as they were in our preliminary test campaign.

5 CONCLUSION

In this study, white oak and white ash specimens bonded with MF and 2C-PUR adhesives were submitted to block shear tests in dry and wet conditions. Results suggest that a mean shear strength as high as 20.5 MPa for white oak, 18.8 MPa for white ash and respectively 18.2 MPa and 17.4 MPa for yellow birch and white birch can be obtained in dry conditions. For a given species, results from the dry test were similar, regardless of the adhesive. The loss of strength induced by the vacuum-pressure cycle was considerable, especially for high-density specimens bonded with 2C-PUR adhesive. Therefore, the MF adhesive appears more suitable for such products exposed to weather. However, since the products investigated in this study are more likely to be used in a weather-protected environment, 2C-PUR adhesive may also be adequate.

The results also highlight the major influence of wood density on wood failure percentage and, to a lesser extent, on shear strength. In both test conditions, several bondline failures occurred in specimens of higher density. In this sense, it is important to account for extreme density values in the selection of lumber destined to the manufacture of structural glued engineered wood products made from hardwoods. A microscopic examination of the glue-lines could be carried out to better understand the impact of material density and specific anatomical features on the adhesive penetration.

Additional tests are required to confirm the potential use of the investigated species and adhesives in commercial glued-laminated timber production. For example, previous work with related species in Europe has pointed out the challenge that represents the fulfillment of delamination tests requirements. Such tests will be performed with the species and adhesives investigated in this study. Also in line with the aim of this project to assess the potential use of the investigated species in glued-laminated timber production, the next experiments will focus on determining the finger-joint strength and the bending strength of full-size beams.

ACKNOWLEDGMENTS

The authors are grateful to Natural Sciences and Engineering Research Council of Canada for the financial support through its IRC and CRD programs (IRCPJ 461745-18 and RDCPJ 524504-18) as well as the industrial partners of the NSERC industrial chair on eco-responsible wood construction (CIRCERB).

REFERENCES

- Aicher S, Ahmad Z, Hirsch M (2018) Bondline shear strength and wood failure of European and tropical hardwood glulams. *European Journal of Wood and Wood Products* 76(4):1205–1222. doi:10.1007/s00107-018-1305-0
- AINSI (2017) Standard for wood products—structural glued laminated timber. ANSI A190.1. APA—The Engineered Wood Association. <https://www.apawood.org/ansi-a190-1>. Accessed 12 January 2019
- Ammann S, Schlegel S, Beyer M, Aehlig K, Lehmann M, Jung H, Niemz P (2016) Quality assessment of glued ash wood for construction engineering. *European Journal of Wood and Wood Products* 74(1):67–74
- ASTM (2006). Standard Practice for Establishing Clear Wood Strength Values. ASTM D2555. ASTM International. <https://www.astm.org/Standards/D2555.htm>. Accessed 20 March 2019
- ASTM (2013). Test Method for Strength Properties of Adhesive Bonds in Shear by Compression Loading ASTM D905. <https://www.astm.org/Standards/D905.htm>. Accessed 16 March 2019
- ASTM (2017). Test Methods for Density and Specific Gravity (Relative Density) of Wood and Wood-Based Materials ASTM D2395. <https://www.astm.org/Standards/D2395.htm>. Accessed 25 February 2019
- Bates D, Maechler M, Bolker B, Walker S (2015) Fitting Linear Mixed-Effects Models Using lme4. *Journal of Statistical Software* 67(1):1–48
- CSA (2010) Evaluation of adhesives for structural wood products (exterior exposure) CAN/CSA O112.9-10. Etobicoke, Ontario: Canadian Standards Association
- CSA (2016) Structural glued-laminated timber CAN/CSA O122-16. Etobicoke, Ontario: Canadian Standards Association
- DIBt (2009) General technical approval Z-9.1-679. BS-Holz Glulam from beech and glulam from beech-hybrid. Wuppertal, Germany: Approval holder: BS-Holz
- DIBt (2013) German Technical Approval Z-9.1-821. Holz Schiller oak post and beam glulam. Germany: Approval holder: Holz Schiller GmbH
- Dietsch P, and Tannert T (2015) Assessing the integrity of glued-laminated timber elements. *Construction and Building Materials* 101:1259–1270
- Durocher C, Thiffault E, Achim A, Auty D, Barrette J (2019) Untapped volume of surplus forest growth as feedstock for bioenergy. *Biomass and Bioenergy* 120:376–386. doi:10.1016/j.biombioe.2018.11.024
- EN 392 (1995) Glued laminated timber — shear test of glue lines. European Committee for standardization (CEN). Brussels
- EN 14080 (2013) Timber structures — glued laminated timber — requirements. European Committee for standardization (CEN). Brussels
- ETA-13/0642 (2013) European Technical Approval, "VIGAM-Glued laminated timber of oak". Issued by Österreichisches Institut für Bautechnik (OIB). Vienna: Approval holder: Sierolam SA
- ETA-13/0646 (2013) European Technical Approval, "SIEROLAM— Glued laminated timber of chestnut". Issued by Österreichisches Institut für Bautechnik (OIB). Vienna: Approval holder: Grupo Gamiz SA

- Falk RH, Colling F (1995) *Laminating Effects in Glued-Laminated Timber Beams*. *Journal of Structural Engineering* 121(12):1857–1863. doi:10.1061/(ASCE)0733-9445(1995)121:12(1857)
- Frihart CR, Hunt CG (2010) Chapter 10: Adhesives with Wood Materials- Bond Formation and Performance. in : *Wood Handbook : Wood as an engineering material*. U.S. Department of Agriculture, Forest Service, Forest Products Laboratory. Madison, Wisconsin, pp 10-1 - 10-24
- Gaston CW (2014) *Visual Wood Product Trends in North American Nonresidential Buildings*. *Forest Products Journal*, 64(3–4):107–115. doi:10.13073/FPJ-D-13-00077
- Gosselin A, Blanchet P, Lehoux N, Cimon Y (2016) *Main Motivations and Barriers for Using Wood in Multi-Story and Non-Residential Construction Projects*. *BioResources* 12(1). doi:10.15376/biores.12.1.546-570
- ISO Standard 12579 (2007) *Timber structures—glued laminated timber—method of test for shear strength of glue lines*. International Organization for Standardization ISO. Geneva
- ISO Standard 6238 (2018) *Adhesives - Wood-to-wood adhesive bonds - Determination of shear strength by compressive loading*. International Organization for Standardization ISO. Geneva
- Janowiak JJ, Manbeck HB, Hernandez R, Moody RC, Blankenhorn PR, Labosky P (1995) *Efficient Utilization of Red Maple Lumber in Glued-Laminated Timber Beams*. Res. Pap. FPL–RP–541. U.S. Department of Agriculture, Forest Service, Forest Products Laboratory. Madison, Wisconsin
- Jessome AP (1977) *Resistance and Related Properties of Native Wood Species in Canada*. Eastern Forest Products Laboratory. Ottawa, Canada
- Jiang Y, Schaffrath J, Knorz M, Winter S, van de Kuilen J-W (2014) *Applicability of various wood species in glued laminated timber - Parameter study on delamination resistance and shear strength*. *Proceedings of the World Conference on Timber Engineering, Quebec, Canada, 10-14 August 2014*
- Knorz M (2014) *Investigation of structurally bonded ash (Fraxinus excelsior L.) as influenced by adhesive type and moisture*. Thesis submitted for the title of Doctor of Engineering. Technischen Universität München. <https://mediatum.ub.tum.de/1274270>. Accessed 6 December 2018
- Knorz M, Neuhaeuser E, Torno S, van de Kuilen J-W (2015) *Influence of surface preparation methods on moisture-related performance of structural hardwood–adhesive bonds*. *International Journal of Adhesion and Adhesives* 57:40–48. doi:10.1016/j.ijadhadh.2014.10.003
- Knorz M, Schmidt M, Torno S, and van de Kuilen J-W (2014) *Structural bonding of ash (Fraxinus excelsior L.): resistance to delamination and performance in shearing tests*. *European Journal of Wood and Wood Products* 72(3):297–309. doi:10.1007/s00107-014-0778-8
- Konnerth J, Kluge M, Schweizer G, Miljković M, Gindl-Altmatter W (2016) *Survey of selected adhesive bonding properties of nine European softwood and hardwood species*. *European Journal of Wood and Wood Products* 74(6):809–819. doi:10.1007/s00107-016-1087-1
- Laguarda Mallo MF, Espinoza O (2015) *Awareness, perceptions and willingness to adopt Cross-Laminated Timber by the architecture community in the United States*. *Journal of Cleaner Production* 94:198–210. doi:10.1016/j.jclepro.2015.01.090
- Lehmann M, Clerc G, Lehringer C, Strahm T, and Volkmer T (2018) *Investigation of the bond quality and the finger joint strength of beech glulam*. *Proceedings of the World Conference on Timber Engineering, Seoul, Republic of Korea, 20-23 August 2018*
- Lenth R, Singmann H, Love J, Buerkner P, Herve M (2018) *Emmeans: Estimated marginal means, aka least-squares means*. Henrik Singmann [ctb], Jonathon. <https://CRAN.R-project.org/package=emmeans>. Accessed 10 March 2019
- Manbeck HB, Janowiak JJ, Blankenhorn PR, Labosky P Jr (1996) *Standard Designs for Hardwood Glued-laminated Highway Bridges*. Ritter MA, Duwadi SR, Lee PDH, ed(s). Madison, Wisconsin. pp. 351–360
- Manbeck HB, Janowiak JJ, Blankenhorn PR, Labosky P. Jr, Moody RC, Hernandez R (1993) *Performance of Red Maple Glulam Timber Beams*. Res. Pap. FPL–RP–519. U.S. Department of Agriculture, Forest Service, Forest Products Laboratory. Madison, Wisconsin
- Markström E, Kuzman MK, Bystedt A, Sandberg D, Fredriksson M (2018) *Swedish architects view of engineered wood products in buildings*. *Journal of Cleaner Production* 181:33–41. doi:10.1016/j.jclepro.2018.01.216
- Okkonen EA, River BH (1989) *Factors affecting the strength of block-shear specimens*. *Forest Products Journal*, 39(1):43-50
- R Core Team (2018) *R: A language and environment for statistical computing*. <http://www.R-project.org/>. Accessed 3 December 2018
- River BH, Vick CB, Gillespie RH (1991) *Wood as an adherend. Treatise on adhesion and adhesives. Vol 7*. Marcel Dekker Inc., New York. 230 p.
- Selbo ML (1975) *Adhesive bonding of wood*. Tech. Bull. No. 1512. U.S. Department of Agriculture, Forest Service. Washington D.C.
- Shedlauskas JP, Manbeck HB, Janowiak JJ, Hernandez R, Moody RC, Labosky P Jr, Blankenhorn PR (1996) *Efficient Use of Red Oak for Glued-laminated Beams*. *Transactions of the ASAE*, 39(1):203–209. doi:10.13031/2013.27499

Blue gum: Assessment of its potential for load bearing structures

Carlos Martins^{1*}, Alfredo M. P. G. Dias², and Helena Cruz³

¹ISISE, Department of Civil Engineering
University of Coimbra
Coimbra, 3030-788, Portugal

³Department of Structures
LNEC
Lisboa, 1700-066, Portugal

ABSTRACT

*Portuguese Forest is mainly composed of hardwoods which represented 69% of the forest area in 2010, being Blue gum (*Eucalyptus globulus* Labill.) the most abundant species (26%) (INCF 2013). The suitability of Blue gum species for structural application was demonstrated in previous studies. However, the most common uses are still related to pulp and paper industry as well as energy applications. The present paper describes a preliminary study on the potential application of non-destructive tests and analytical methods to predict the most important mechanical properties of glued laminated timber (glulam) beams made of Blue gum. The potential of mixed beams made of Blue gum and Poplar (mix of Hybrid Poplar, White Poplar and Black Poplar) was also analysed. Longitudinal vibration method (LVM) and the transformed section method (TSM) were considered. A total of 7 full-scale glulam beams (4 of Blue gum and 3 mixed) were manufactured in laboratory and tested for determination of modulus of elasticity and bending strength. After the bending tests their density and moisture content were determined, and the bonding performance was checked by delamination and shear strength tests. Correlation coefficients were established between the predicted values (LVM and TSM) and the mechanical properties, indicating a huge potential. The determined mechanical properties were above the typical values found in the literature for the most common hardwoods available in European Forest.*

1. INTRODUCTION

Blue gum is a fast growing hardwood species that presents interesting physical and mechanical properties. Besides, this is the dominant species in the Portuguese forest, occupying 26% of the Forest area (ICNF 2013). The most common uses are the pulp and paper industry as well as energy applications, being largely unknown its potential for other valuable application, like furniture, floors or load bearing structures. The little use of Blue gum as structural material is typically associated with difficulties regarding sawing and drying processes (Franke and Marto 2014).

Nevertheless, some studies have been performed in the last two decades to promote the use of Blue gum in structural applications. Touza Vásquez and P. Saavedra (2002) presented a proposal for drying Blue gum down to 12% moisture content based on two phases, ensuring good quality of the material in terms of absence of cross section collapse. Also Franke and Marto (2014) studied the drying process of Blue gum suggesting radio-frequency pre-treatments for the improvement of the permeability of the wood.

The study of physical and mechanical properties of Blue gum grown in Spain was reported in Alvite et al. (2002) both for sawn wood and glued laminated timber. Average values of 760 kg/m³, 20580 MPa and 130 MPa were presented respectively for density, modulus of elasticity and bending strength for sawn wood, while for glued laminated timber the average values obtained were 20300 MPa and 125 MPa, for modulus of elasticity and bending strength respectively. A recent study carried out by Martins (2015) on Blue gum grown in Portuguese forest revealed lower mechanical properties for sawn wood (75x75 mm²): average values of 18150 MPa for modulus of elasticity and 75 MPa for bending strength, yet reasonable bending properties. Previous test results obtained from clear wood specimens are presented in M6 sheet (LNEC 1997) with average values of 127 MPa for bending strength and 17500 MPa for modulus of elasticity.

The study of innovative applications, such as glued laminated timber, was performed by Lopez-Suevos (2009). This study focused on the use of primers to enhance the bond durability of Blue gum, through delamination and shear strength tests, being observed a significant improvement of the bonding performance in the case of the PUR adhesive. Another genus of Eucalyptus, *Eucalyptus grandis*, was considered for glued laminated timber production, considering also the combination with Poplar (*Populus x euramericana*, 'Neva' Clone) (Castro and Paganini 2003).

* Corresponding author: Carlos Martins; E-mail: carlosmartins86@gmail.com

The present research focuses on the use of Blue gum and its combination with Poplar (both grown in Portuguese forest) for glued laminated timber. The use of non-destructive methods (longitudinal vibration method and transformed section method) was considered for the prediction of static bending properties, since previous studies have demonstrated high accuracy of both methods (Hodousek et al. 2017 and Martins et al. 2018). A total of 7 glulam beams were produced in laboratory, non-destructively tested through longitudinal vibration method and destructively tested following EN 408 requirements (CEN 2012). Finally, the bonding performance of the PUR adhesive was evaluated through delamination and shear strength tests according to EN 14080 (CEN 2013).

2. MATERIALS AND METHODS

2.1. CHARACTERIZATION OF RAW MATERIAL AND ASSEMBLY PROCESS OF GLULAM BEAMS

A total of 35 timber boards, 26 of Blue gum (BG) and 9 of Poplar (BP) were chosen from larger samples. The selected boards were measured to determine their cross sectional dimensions, length, weight and moisture content (using a moisture meter device) resulting in average dimensions of 36 x 125 x 2479 mm³ and 38 x 118 x 2573 mm³ for BG and BP samples, respectively. The average value and standard deviation of density and moisture content were 905±55 kg/m³ and 13.9±0.6% and 417±25 kg/m³ and 14.2±1.9%, for BG and BP samples, respectively.

In a first step, all boards were non-destructively assessed through the longitudinal vibration method (LVM). A rubber mat between the steel plate and the board was used to ensure minimal attenuation of passing waves. Average values of 20450 MPa (COV = 13.4%) and 10100 MPa (COV = 4.9%) were determined, for BG and BP respectively.

2.2. ASSEMBLY PROCESS OF GLULAM BEAMS

Each glulam beam was composed of five lamellas. Boards were sorted to place the lowest E_{dyn_b} in the central lamella then increasing stiffness towards the external layers, ensuring similar values between tension and compression sides. For the mixed glulam beams of Blue gum and Poplar (HBGBP), Poplar was used in the 3 central layers, to maximize the density reduction of the cross section.

Before assembly the boards were planed to the final thickness of 24 mm and trimmed to 100 mm wide and to the shortest length of each group of five lamellas (between 2300 mm and 2500 mm). Each lamella in its final dimensions was non-destructively assessed through LVM, providing a new value of dynamic modulus of elasticity (E_{dyn_l}). Re-arrangement of the lamellas was made when necessary. Figure 1 presents the distribution of E_{dyn_l} values of all 7 glulam beams, the respective average value, $E_{dyn_l_av}$ and the density of each beam. From each group of five columns the left one corresponds to the compression layer and the right one to the tension layer.

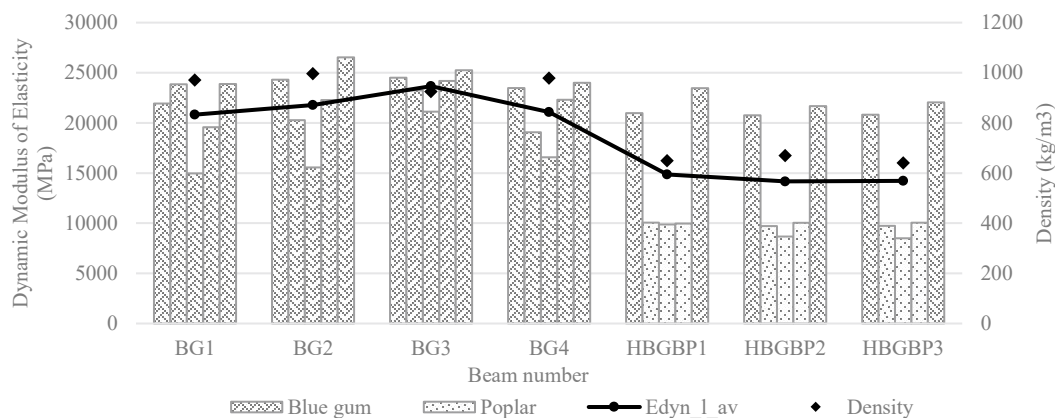


Figure 1: Summary of E_{dyn_l} values and their distribution within each glulam beam.

The assembly of lamellas was made with a one component polyurethane adhesive, commercially available for load bearing structures. Previous studies on Maritime pine (Martins 2018) and Poplar (Martins et al. 2017) with the reference Purbond HB S 709, showed the need of a primer. PR 3105 primer especially developed for bonding Blue gum was used. Based on those results an amount of adhesive of 180 g/m² was considered and 20 g/m² of primer. The adhesive was applied with a manual roller spreader and primer was sprayed. Both amounts were controlled by weighing.

The clamping pressure was 1.2 MPa (maximum recommended at the adhesive TDS) applied by a series of hydraulic jacks spaced by 500 mm and with a maximum load capacity of 5 tons each, under controlled conditions of temperature ($20 \pm 2^\circ\text{C}$) and relative humidity ($65 \pm 5\%$). After the pressing process (7 hours), beams stayed in controlled conditions for a minimum curing period of 7 days. Later on the beams were planed to final dimensions of 92 mm x 120 mm x 2300 mm (width x height x length).

2.3. MECHANICAL PROPERTIES: NON-DESTRUCTIVE AND DESTRUCTIVE CHARACTERIZATION

Non-destructive prediction of mechanical properties

Prediction of mechanical properties of glulam beams is essential to ensure the quality of the material. In the present paper two methods were considered: i) LVM and ii) Transformed Section Method (TSM).

The LVM method was applied to all glulam beams, following the same procedure adopted for boards/lamellas. Each glulam beam was measured (width, height, length) and weighted. The moisture content of each glulam beam was determined based on average value of the respective lamellas. From the application of LVM it was determined the dynamic modulus of elasticity ($E_{\text{dyn_LVM}}$).

The TSM is a simple analytical method fully described in annex A4 of ASTM D 3737 (ASTM 2005), used to predict the static modulus of elasticity and bending strength properties. It is based on the conversion of a section with three well defined stiffness zones (symmetrically displayed) into a section with homogeneous properties through a transformed section factor. The predicted values of modulus of elasticity ($E_{\text{dyn_TSM}}$) were determined through the multiplication of the transformed section factor by the average modulus of elasticity of the outer stiffness zone.

Static tests

Modulus of elasticity (local E_{local} and global E_{global}) and bending strength (f_m) were determined through four-point bending tests of full scale glulam beams according to EN 408 (CEN 2012). Both tests were performed with a total span of 2.16 m and 0.72 m of load span. Both supports and loading points had a piece of timber between glulam beam and steel elements to minimize local indentation on the glulam beams.

Modulus of elasticity tests were done in displacement control (10 mm/min) recording load-deformation data between 10% and 40% of the predicted failure load at every second. Deflection was measured with linear variable differential transformer (20-50 mm maximum capacity) and loads were measured using a load cell (200 kN maximum capacity).

After failure, moisture content of each glulam beam was determined by the oven-dry method following EN 13183-1 (CEN 2002). At least one specimen (representative of the full cross section) per beam was collected, free from defects and at least 0.3 m away from the ends. The same specimens were used for density calculation. Density and modulus of elasticity were adjusted to a reference moisture content of 12% according to EN 384 (CEN 2004). Bending strength values were multiplied by a factor to account for a reference depth of 600 mm and by a factor to account for a reference lamella thickness of 40 mm as mentioned in EN 14080 (CEN 2013). Test results and the adjusted values are summarized at Table 1.

2.4. QUALITY CONTROL OF BONDING PROCESS

The bonding quality of glue lines was assessed through delamination and shear strength tests following the procedures described in EN 14080 (CEN 2013). At least one specimen per glulam beam was collected for delamination and one for shear strength test. Delamination tests followed Method A of Annex C, involving the full cross section (92 mm x 120 mm) and 75 mm of length. Shear strength tests followed Annex D considering specimens of $50 \times 50 \times 120 \text{ mm}^3$ (length x width x height). The test was performed in displacement control with a speed rate of 0.06 mm/s. Table 2 presents the results both for delamination and shear strength tests.

3. RESULTS AND DISCUSSION

3.1. MECHANICAL PROPERTIES

Table 1 presents the individual results of non-destructive tests ($E_{\text{dyn_LVM}}$ and $E_{\text{dyn_TSM}}$) as well as of static tests (E_{local} , E_{global} and f_m), moisture content (w) and density (ρ) and the adjusted values of density ($\rho_{12\%}$), modulus of elasticity ($E_{12\%}$) and bending strength (f_{m_adj}).

Table 1: Summary of non-destructive and static test results of Blue gum beams (BG) and mixed beams of Blue gum and Poplar (HBGBP)

Beam number	w (%)	ρ (kg/m ³)	E _{dyn_LVM} (MPa)	E _{dyn_TSM} (MPa)	E _{local} (MPa)	E _{global} (MPa)	f _m (MPa)	$\rho_{12\%}$ (kg/m ³)	E _{12%} (MPa)	f _{m_adj} (MPa)
BG1	13.2	978	21545	22593	24577	21885	125.8	972	22417	118.8
BG2	13.0	996	22167	24480	28803	24829	130.7	991	25310	123.5
BG3	13.1	938	24062	24605	28394	24805	131.9	933	25367	124.7
BG4	12.6	980	21400	23044	27132	23332	127.6	977	23602	120.6
Average	13.0	973	22294	23680	27226	23713	129.0	968	24174	121.9
Minimum	12.6	938	21400	22593	24577	21885	125.8	933	22417	118.8
Maximum	13.2	996	24062	24605	28803	24829	131.9	991	25367	124.7
COV (%)	2.2	2.5	5.5	4.3	7.0	5.9	2.2	2.6	5.9	2.1
HBGBP1	13.6	654	15304	19615	22638	20010	107.0	649	20663	101.1
HBGBP2	12.8	678	14409	18754	29815	18768	88.9	675	19064	84.0
HBGBP3	13.1	657	14438	18934	27835	18601	93.6	653	19006	88.5
Average	13.2	663	14717	19101	26763	19126	96.5	659	19578	91.2
Minimum	12.8	654	14409	18754	22638	18601	88.9	649	19006	84.0
Maximum	13.6	678	15304	19615	29815	20010	107.0	675	20663	101.1
COV (%)	3.3	2.0	3.5	2.4	13.9	4.0	9.7	2.2	4.8	9.9

Very good mechanical properties were obtained for BG glulam beams. Mean static modulus of elasticity was approximately 16.6% higher compared to the results presented by Alvite et al. (2002) (20300 MPa) whereas for bending strength the results were 2.9% higher in the present study (Alvite et al. (2002) - 125 MPa). A comparison with previous studies on Blue gum sawn wood revealed even higher differences. The technical data sheet M6 published by LNEC (1997) for Blue gum indicates a range of densities between 750 kg/m³ and 850 kg/m³, average modulus of elasticity of 17500 MPa (35.5% lower) and bending strength of 127 MPa (1.2% lower).

The combination of Blue gum with Poplar resulted in a significant decrease of the average density (31.9%). Also the mechanical properties registered a decrease of 19.3% and 25.2% for modulus of elasticity and bending strength, respectively. The comparison of HBGBP results with glulam beams fully made of Poplar tested by Martins et al. (2018) showed an increase of 53.9%, 77.8% and 73.3% for density, modulus of elasticity and bending strength, respectively, based on the adjusted values. Castro and Paganini (2003) studied the combination of Poplar (“Neva” clone) with several clones of *Eucalyptus grandis* (“358”, “7”, “329” and “330”). The clone “330” provided the highest mechanical properties; therefore, the mixed glulam beams made of Poplar are compared with clone “330” of *Eucalyptus grandis*, being observed higher values with the combination of the present study, namely 35.6%, 31.4% and 61.6% for density, modulus of elasticity and bending strength. This shows the potential of Blue gum species for load bearing structures as glulam beams.

Failure of the glulam beams occurred in the central third span and were triggered by tension failure of the bottom lamination. In all glulam beams it was observed a ductile behavior (Figure 2) associated with the presence of compression folds on the top laminations (Figure 3).

The structural efficiency (relation between a specific mechanical property and the density) was determined for each group of beams. For HBGBP glulam beams the highest values were determined, 29.7 for modulus of elasticity and 0.138 for bending strength. On the other hand, BG glulam beams had 25.0 and 0.125 for modulus of elasticity and bending strength, respectively. The values determined for modulus of elasticity are in line with the ones presented by Castro and Paganini (2003): for mixed glulam beam Poplar/*E. grandis* “330” the structural efficiency for bending strength was significantly lower (0.129).

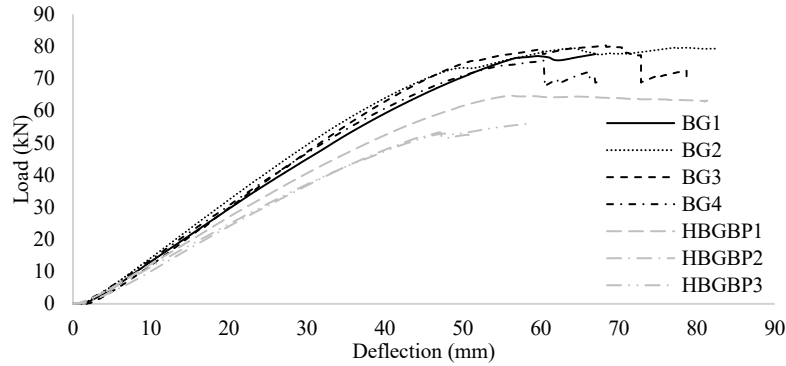
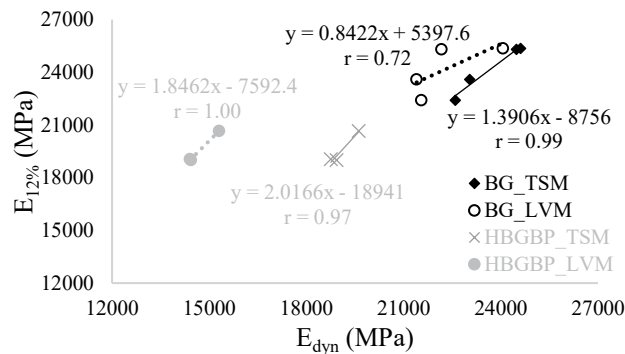


Figure 2: Load-deflection curves of BG and HBGBP glulam beams



Figure 3: Load-deflection curves of BG (left) and HBGBP (right) glulam beams

The analysis of non-destructive values showed a better accuracy of TSM to predict the static values of modulus of elasticity both for BG and HBGBP glulam beams. It could be also mentioned that LVM underestimated static modulus of elasticity especially for HBGBP glulam beams with a difference about 4000 MPa. A linear regression analysis between the non-destructive methods (E_{dyn_TSM} and E_{dyn_LVM}) and static modulus of elasticity ($E_{12\%}$) results was performed (Figure 4). Correlation coefficients close to 1.0 for TSM (both BG and HBGBP glulam beams) and for LVM (HBGBP glulam beams) were determined. The prediction of bending strength through non-destructive methods showed similar values as for static modulus of elasticity. The prediction considering the E_{dyn_LVM} provided a correlation coefficient of 0.83, significantly higher if compared to the prediction of $E_{12\%}$ (0.72). It should be noted that the number of glulam beams tested was and the size of sample should be increased to prove these results.


 Figure 4: Correlation coefficients between non-destructive tests (E_{dyn_TSM} and E_{dyn_LVM}) and static modulus of elasticity ($E_{12\%}$)

3.2. QUALITY CONTROL OF GLUE LINES

Table 2 presents a summary of delamination and shear strength results. Delamination test results (Method A) evidence an inadequate performance of the bonding procedure followed considering the maximum limits defined for

softwoods in EN 14080 (CEN 2103) both for 2nd and 3rd test cycles, 5% and 10%, respectively. Even HBGBP beams presented excessive values, with only one specimen showing total delamination below 10%. Figure 5 shows that the inadequate performance was observed at the glue lines between Blue gum lamellas and between Blue gum and Poplar. Glue lines between Poplar lamellas presented a good performance, as previously demonstrated by Martins et al. (2017).

Table 2: Summary of non-destructive and static test results from Blue gum beams (BG) and mixed beams of Blue gum and Poplar (HBGBP)

Beam number	Total delamination (%)			Shear strength tests		
	Specimens	2 nd cycle	3 rd cycle	Specimens	Shear strength (MPa)	WFP (%)
BG1	D1 / D2	89 / 88	92 / 91	S1 / S2	15.4 / 15.1	63 / 79
BG2	D1 / D2	91 / 93	93 / 94	S1 / S2	16.8 / 15.4	65 / 44
BG3	D1 / D2	64 / 62	68 / 70	S1 / S2	16.8 / 17.0	84 / 84
BG4	D1 / D2	88 / 86	91 / 91	S1 / S2	16.2 / 15.7	78 / 89
HBGBP1	D1 / D2	9 / 6	10 / 6	S1 / S2	9.4 / 9.5	99 / 80
HBGBP2	D1	34	35	S1	9.9	80
HBGBP3	D1	21	22	S1	11.2	88



Figure 5: Delamination specimens after 3rd test cycle (Method A): BG3-D1 specimen (left) and HBGBP2-D1 specimen (right)

The analysis of average values of shear strength showed significant differences between BG and HBGBP glulam beams. According to Vick (1999), shear strength values increased for higher densities (up to a certain point) as it was observed for BG glulam beams compared to HBGBP glulam beams. Figure 6 presents the individual shear strength and wood failure percentage (WFP) values both for BG and for HBGBP glulam beams. HBGBP glulam beams had two different responses of their glue lines, namely BG/BP and BP/BP. From all the tests, three glue lines (2 BG and 1 HBGBP-BG/BP) did not fulfilled the minimum requirements of EN 14080 (CEN 2013). A comparison between HBGBP-BG/BP and HBGBP-BP/BP clearly shows that Poplar species conditioned the shear strength values and Blue gum was responsible for the lowest values of wood failure percentage measured.

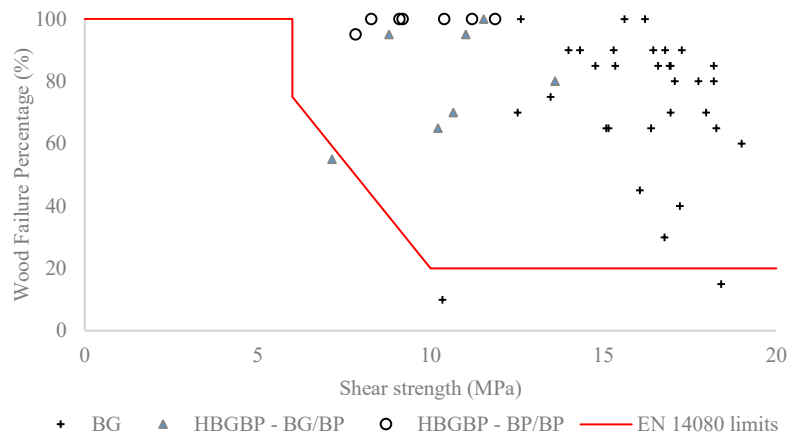


Figure 6: Individual values of shear strength and wood failure percentage

4. CONCLUSIONS

The research performed had as main goal the assessment of the potential of Blue gum timber for load bearing structures as glulam beams made of a single species or mixed with Poplar. To accomplish the established aims, an experimental campaign was carried out. A total of 7 glulam beams (4 of BG and 3 HBGBP) were produced with five lamellas each of 24 mm of thickness and tested at SerQ laboratory to assess the most important mechanical properties in bending as well as the respective density and the bonding performance (delamination and shear strength). Assembling followed the specifications of EN14080 for softwoods and the technical data sheet from the adhesive used. Two non-destructive methods were considered to predict the mechanical properties, namely: i) longitudinal vibration method (also applied to raw material characterization) and ii) transformed section method. Delamination and shear strength tests were performed to assess the bonding quality of glue lines. The main conclusions from this study are as follows.

- Very high mechanical properties were obtained both for BG and HBGBP glulam beams with average values of 23700 MPa and 19100 MPa for static modulus of elasticity and 121 MPa and 91 MPa for bending strength, respectively.
- The comparison of the present results with similar studies confirm the potential of Blue gum or its combination with Poplar for load bearing structures.
- Transformed section method predicted accurately the mechanical properties of both BG and HBGBP glulam beams (correlation coefficients above 0.97). Longitudinal vibration method also showed potential to be used namely on the non-destructive characterization of the raw material.
- High correlation coefficients were obtained both for static modulus of elasticity and bending strength considering both non-destructive methods applied.
- An inadequate bonding performance was observed in delamination tests, for glue lines between BG lamellas and on the interface between Blue gum and Poplar with the adhesive and bonding procedure adopted.
- Future work should focus on the bonding performance improvement, and the increase of the number of glulam beams tested to validate the present results. Also the finger-joint performance should be considered (tensile and bending tests), namely its influence on bending strength values of glulam beams.

ACKNOWLEDGEMENTS

This work was partly financed by FEDER funds through the Competitiveness Factors Operational Programme – COMPETE and by national funds through FCT – Foundation for Science and Technology, within the scope of the Project POCI-01-0145-FEDER-007633. The authors acknowledge the financial support of the Operational Program Competitiveness and Internationalization R&D Projects Companies in Co-promotion, Portugal 2020, within the scope

of the project OptimizedWood – POCI-01-0247-FEDER-017867. The authors wish to thank Foundation for Science and Technology for the PhD grant (PD/BD/52656/2014) given to Carlos Martins, to Henkel for providing the adhesives and finally to Pedrosa & Irmãos Lda for the collaboration given concerning the timber.

REFERENCES

- Alvite, J. D. B., M. C. Touza Vázquez and F. S. Infante (2002). *White Eucalyptus Species manual (in Spanish)*. Ourense, Fundación para o Fomento da Calidade Industrial e Desenvolvemento Tecnológico de Galicia.
- ASTM (2005). *ASTM D 3737 - Standard Practice for Establishing Allowable Properties for Structural Glued Laminated Timber (Glulam)*.
- Castro, G. and F. Paganini (2003). "Mixed glued laminated timber of poplar and Eucalyptus grandis clones." *Holz Als Roh-Und Werkstoff* 61(4): 291-298.
- CEN (2002). *EN 13183-1 - Moisture content of a piece of sawn timber - Part 1: Determination by oven dry method*. Brussels.
- CEN (2004). *EN 384 - Structural timber - Determination of characteristic values of mechanical properties and density*. Brussels.
- CEN (2012). *EN 408 - Timber structures - Structural timber and glued laminated timber - Determination of some physical and mechanical properties*. Brussels.
- CEN (2013). *EN 14080 - Timber structures - Glued laminated timber and glued solid timber - Requirements*. Brussels.
- Franke, S. and J. Marto (2014). *Investigation of Eucalyptus globulus wood for the use as an engineered material*. WCTE 2014 - World Conference on Timber Engineering. Quebec City, Canada.
- Hodousek, M., A. M. P. G. Dias, C. Martins, A. F. S. Marques and M. Bohm (2017). "Comparison of Non-Destructive Methods Based on Natural Frequency for Determining the Modulus of Elasticity of Cupressus lusitanica and Populus x canadensis." *Bioresources* 12(1): 270-282.
- ICNF (2013). *IFN6 – Areas land use and forest species in mainland Portugal in 1995, 2005 and 2010 (in Portuguese)*. I. d. C. d. N. e. d. Florestas. Lisboa: 34.
- LNEC (1997). *M6 – Common Eucalyptus (in Portuguese)*. Lisbon, Portugal
- Lopez-Suevos, F. and K. Richter (2009). "Hydroxymethylated Resorcinol (HMR) and Novolak-Based HMR (n-HMR) Primers to Enhance Bond Durability of Eucalyptus globulus Glulams." *Journal of Adhesion Science and Technology* 23(15): 1925-1937.
- Martins, C. (2018). *Health Assessment of Glued Laminated Timber Elements (in Portuguese)*. PhD thesis, University of Coimbra.
- Martins, C., A. M. P. G. Dias and H. Cruz (2017). *Glulam made by Poplar: delamination and shear strength tests*. ISCHP 2017 - International Scientific Conference on Hardwood Processing. Lahti, Finland.
- Martins, C., A. M. P. G. Dias and H. Cruz (2018). "Using non-destructive testing to predict the mechanical properties of glued laminated poplar." *Proceedings of the Institution of Civil Engineers – Structures and Buildings*.
- Martins, M. (2015). *Eucalyptus globulus characterization for structural applications (in Portuguese)*. MSc, University of Coimbra.
- Vick, C. B. (1999). *Adhesive Bonding of Wood Materials - Chapter 9*. Wood Handbook - Wood as an engineering material. Madison, Forest Products Laboratory.
- Touza Vázquez, M. C. and F. Pedras Saavedra (2002). *An industrial proposal for drying timber of Eucalyptus white (Eucalyptus globulus) from Galicia (in Spanish)*. CIS-Madera.

Experimental and numerical evaluation of the structural performance of Uruguayan *Eucalyptus grandis* finger-joint

Abel Vega¹, Vanesa Baño^{1*}, Andrea Cardoso², Laura Moya³

¹Instituto de Estructuras y Transporte. Facultad de Ingeniería. Universidad de la República. Montevideo, 11300, Uruguay

²Laboratorio Tecnológico del Uruguay-LATU Montevideo, 11500, Uruguay

³Facultad de Arquitectura Universidad ORT Uruguay Montevideo, 11300, Uruguay

ABSTRACT

The aim of this study was to evaluate the structural performance of finger-joints made of Uruguayan Eucalyptus grandis and two types of adhesives. A numerical model for bending strength and stiffness prediction was developed. Model inputs were experimentally determined from tests on wooden specimens and from literature. Finger-joints glued with two types of adhesives (one-component polyurethane -PUR- and emulsion polymer isocyanate-EPI-) were tested in bending and the failure modes were evaluated. Results show that adhesive type did not influence the stiffness of the finger-joint, while did influence the bending strength. Specimens glued with PUR showed higher strength than those glued with EPI. A 3D model, using Comsol Multiphysic software, was developed to simulate the finger-joint behavior. Adhesive-wood interaction in the finger-joints was modeled using the Comsol Thin Elastic Layer module, defined by the elastic properties of the adhesives. The numerical results showed no differences on the stiffness of the joints regardless of adhesive type. Results agreed with those obtained from experimental tests, with a maximum error of 7%. Models predicted the bending strength with an error of 6% with respect to the experimental values. Different finger configurations were analyzed, and the optimal geometry (20 mm-length, 6.2 mm-pitch and 1.0 mm-tip-thick) to attain the maximum strength for Uruguayan Eucalyptus was found.

1. INTRODUCTION

Glued laminated timber (GLT or glulam) is one of the most important engineered wood products (EWP) used at present, in architecture and civil engineering. The manufacturing process is complex and involves many factors, such as species, adhesive type and applied pressure, among others. Optimum parameter combinations, both in glulam and lamella production, must be tailored to meet end-product's requirements. The efficiency of the longitudinal union of lamellas through suitable finger-joints is crucial for the overall structural performance of GLT and is close related to the manufacturing process. Production requirements, for GLT and finger-joint have been well documented, and for softwood species and poplar are established in EN 14080 (CEN 2013). However, there are still several unknowns regarding finger jointing for hardwoods, or for new species/adhesives combinations. The influence of the manufacturing process on the mechanical properties of finger-joint hardwoods has been approached with emphasis on the production conditions such as timber conditioning (Raknes 1980), curing time and end pressure (Bourreau et al. 2013), finger-joint geometry (Ahmad et al. 2017; Özçifçi 2008; Ayarkwa et al. 2000) and other several interlinked factors (Vrazel 2004). In addition, an extensive literature related to the gluing performance and adhesive evaluation is available (Ayarkwa et al. 2000; Vassiliou et al. 2006; Volkmer et al. 2014).

The principal criterion for structural finger-joint assessment is the load bearing strength, usually evaluated by static bending test. The test is considered as the most convenient for a preliminary study of finger joints and is commonly employed for quality control as well. Frequently, experimental programs are complemented with numerical simulations with the aim of modelling the mechanical behavior of finger joints. Finite element method (FEM) has been used for simulation in analyses of wooden materials for over 30 years, due to the ability for dealing with the structural complexity of wood (Sebera et al. 2015), and has been reported as a convenient approach to model wooden materials when limited experimental data is available (Tran et al. 2014). Several researchers have successfully applied FEM to simulate the stress distribution in finger joints of softwood (HR and E 1991; Serrano et al. 2001; Khelifa et al. 2015) and hardwood species (Smardzewski 1996; Tran et al. 2014; Franke and Marto 2014).

The main difficulty of finger-jointing hardwoods lies in the uncertainties of the wood-adhesive interaction. In particular, some species of *Eucalyptus* are not fully characterized, and therefore their interaction with some adhesives

is still unknown. Such is the case of Uruguayan fast growing *Eucalyptus* spp., one of the most important renewable genres cultivated in Uruguay that covers more than 600,000 ha and annually produce approximately 11.2 million m³ of roundwood. The major part is consumed by pulp and energy production, and 1.2 million m³ from the annual average supply is intended for mechanical transformation (Dieste 2012). Having growth rates of 30m³ha⁻¹yr⁻¹, *Eucalyptus grandis* is a promising raw material for GLT production in Uruguay. Information on suitable adhesives for finger-jointing *Eucalyptus grandis* is scarce. The most commonly adhesive used for *Eucalyptus* glulam are phenoplast or aminoplast adhesives (Piter et al. 2007a). However, in the last years, one-component polyurethane (PUR) and emulsion polymer isocyanate (EPI) adhesives are gaining acceptance for structural applications, and recently, they have been included in the European standards EN 14080 (CEN 2013) and EN 16351 (CEN 2015). Recently, few studies on glulam made of *Eucalyptus globulus* (Lara-Bocanegra et al. 2017; Franke and Marto 2014), *Eucalyptus grandis* (Moya et al. 2019; Bourscheid et al. 2015; Calil Neto et al. 2014) and a hybrid of two *Eucalyptus* species (Pereira et al. 2016), showed the potential of PUR with this genus. In general, the mechanical properties of glulam achieved values above those of the corresponding solid wood; however certain difficulties related to the integrity of the glue line were also reported in these works. Literature on glulam made of hardwoods and EPI is limited; few works report on tropical species such as teak (Iwakiri et al. 2014), and beech (Volkmer et al. 2014). A study by Franke et al. (Franke et al. 2014) comparing the finger joint performance of beech and PUR or beech and EPI, revealed no substantial difference in strength results. In general, the mechanical properties of glulam achieved values above those of the corresponding solid wood; however certain difficulties related to the integrity of the glue line were also reported in these works. Literature on glulam made of hardwoods and EPI is limited; few works report on tropical species such as teak (Iwakiri et al. 2014), and beech (Volkmer et al. 2014). A study by Franke et al. (Franke et al. 2014) comparing the finger joint performance of beech and PUR or beech and EPI, revealed no substantial difference in strength results.

Knowing the influence of the gluing quality on the successful performance of the finger-joint, several works have focused on analyzing the adhesive-wood connection by models that simulate its behavior (Franke et al. 2014; Tran et al. 2014; Camú and Aicher 2018).

This study aims to evaluate the mechanical performance of finger-joints made of *Eucalyptus grandis* and two different adhesives, EPI and PUR, focusing on the bending properties and the glue line behavior. In addition, a numerical model to predict the modulus of elasticity and the bending strength of the finger-joints is presented.

2. MATERIALS AND METHODS

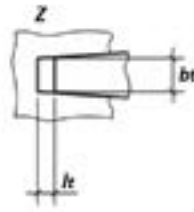
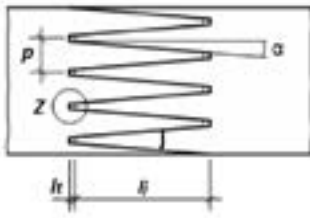
The study is divided in two phases: i) an empirical testing program on physical sections cut from lamellas, subjected to bending, and ii) numerical modeling of the finger-jointed sections using input data from phase i) tests.

2.1. SAMPLING

The material used in this study came from *Eucalyptus grandis* sawn boards that have been previously graded as Class 1 (IRAM 9662-2 2015), with corresponding values of 30 N/mm² for bending strength (f_{mk}), 18 N/mm² for tension parallel to grain strength ($f_{t,0,k}$), 14.000 N/mm² for longitudinal modulus of elasticity ($E_{0,mean}$), and 430 Kg/m³ for density (ρ^k).

A total of 80 specimens with nominal cross section of 70 mm x 22 mm, and 400 mm long, were prepared from the selected boards, and divided in three groups: i) 40 with one finger-joint in the mid-span bonded with EPI; ii) 20 with one finger-joint bonded with PUR; and iii) 20 control (without finger-joint). The last group was prepared to determine input values for the FE modelling, and to compare the effect of the finger-joint with different adhesives, on the structural behavior of tested specimens.

All specimens were conditioned at 20°C/65% RH until they reach 12% moisture content. Finger-joints were then manufactured following the production requirements described on EN 14080 (CEN 2013), with manual application of the adhesive and with a finger profile as shown in Figure 1.



l_j	Finger length	15 mm
p	Pitch	4 mm
l_t	Tip gap	0,1 mm
b_t	Tip thickness	0,5 mm

Figure 1: Finger-joint parameters (CEN 2013)

2.2. TESTING

The specimens were tested in flatwise bending following the recommendations of EN 14080 (CEN 2013) and EN 408 (CEN 2010). Modulus of elasticity and bending strength were calculated by Equations 1 and 2.

$$E_m = \frac{3al^2 - 4a^3}{2bh^3 \left(2 \frac{w_2 - w_1}{F_2 - F_1} \right)} \quad (1)$$

$$f_m = \frac{3Fa}{bh^2} \quad (2)$$

where

h and b, are the height and width of the specimen, respectively, in mm

a, is the distance between one support and the nearest loading point (6h), in mm

l, is the span (18h), in mm

$F_1 - F_2$, is an increment of the load on the straight-line portion of the load deformation curve, in kN

$w_1 - w_2$, is the increment of deformation corresponding to $F_2 - F_1$, in mm

F is the maximum load at the failure, in kN

In addition, the failure mode of the finger joints was visually evaluated and roughly assigned to one of the following types: i) mode 1, fracture occurs 100% by wood; ii) mode 2, fracture partially occurs by wood and partially by adhesive; and iii) mode 3, failure occurs 100% by adhesive. Figure 2 shows an example of each failure mode.



Figure 2: Failure modes of finger-joint lamellas: Mode 1 (left), Mode 2 (center) and Mode 3 (right)

2.3. FE MODELING

A 3D model, using Comsol Multiphysics software (Comsol Inc., USA), was developed to simulate the finger joint behavior of the lamellas in bending tests depending on the adhesive type. Variable mesh size, with a gradient ranging from 30 to 3 mm (decreasing close to the finger-joint proximities) at a maximum growth rate of 1.45, was employed (Figure 3). Typical 4-point bending test following EN 408 specifications (CEN 2010) was simulated using geometrical models of lamellas with dimensions of 70 mm- width, 22 mm-depth, and 396 mm-length. The applied loads were located on the central third and separated at a distance of 132 mm.

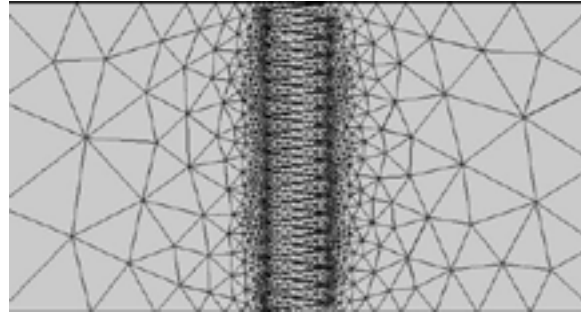


Figure 3: Meshing of sample on the Finite Element model

Timber was considered as an orthotropic and non-linear material, whose elasto-plastic behavior was modeled through the Comsol *hardening function* obtained from control tests. Input data of the physical and mechanical properties were obtained from the experimental tests on the control samples (see 3.1.), and other relevant properties derived from the empirical equations established in EN 384 (CEN 2016a) for deciduous species (Eqs. 3, 4, 5, 6, 7, 8 and 9).

$$E_{90} = E_0/15 \quad (3)$$

$$G = E_0/16 \quad (4)$$

$$f_{t,0} = 0,6 \cdot f_m \quad (5)$$

$$f_{t,90} = 0.6 \quad (6)$$

$$f_{c,0} = 5 \cdot (f_m)^{0,45} \quad (7)$$

$$f_{c,90} = 0,015 \cdot \rho \quad (8)$$

$$f_v = 4 \quad (9)$$

where,

E_{90} is the modulus of elasticity perpendicular to the grain

E_0 is the modulus of elasticity parallel to the grain, obtained from experimental bending tests

G is the shear modulus

$f_{t,0}$ is the strength in tension parallel to the grain

$f_{c,0}$ is the strength in compression parallel to the grain

$f_{c,90}$ is the strength in compression perpendicular to the grain

f_v is the shear strength

f_m is the bending strength, obtained from experimental bending tests

Adhesive-wood interaction in the finger joints was modeled through the Comsol *Thin Elastic Layer* module, defined by the elastic properties of the adhesives, shown in Table 1. Young modulus and Poisson coefficients were taken from Stoeckel et al. (Stoeckel et al. 2013) and de Castro (de Castro San Román 2005), and Konnerth and Muller (Konnerth et al. 2007), respectively. Shear modulus was determined by Equation 10 (Konnerth et al. 2007).

$$G = E_{ad}/2 * (1 + \nu_{ad}) \quad (10)$$

where

E_{ad} is the Young modulus of the adhesive

ν_{ad} is the Poisson coefficient of the adhesive

Table 1: Adhesive properties used in FE simulations

	Property/Adhesive type	PUR	EPI
Young modulus (GPa)	E_{ad}	0.50	3.50
Poisson coefficient	ν_{ad}	0.30	0.30
Shear modulus (GPa)	G_{ad}	0.19	1.35

3. RESULTS AND DISCUSSION

3.1. CONTROL SAMPLES

Experimental data of bending properties and density (E_0 , f_m , and ρ), plus other derived mechanical properties (G , $f_{t,0}$, $f_{c,0}$, $f_{c,90}$ and f_v) from control samples, are shown in Table 2. Control samples were used as input data for FE modeling to predict the load-deflection curve in the elastic phase, without influence of the finger joints or the adhesive type. Control sample also provided input data to define the hardening function used in Comsol for the elastoplastic phase.

Table 2: Wood properties used in FE simulations. Mean values

E_0^1	f_m^1	$\rho^{1,2}$	E_{90}	G	$f_{t,0}$	$f_{c,0}$	$f_{t,90}$	$f_{c,90}$	f_v
15363 (15%)	91.9 (19%)	556 (12%)	1024	960	55.1	38.2	0.6	8.3	4.0

Values in parentheses indicate COV

Property values are in N/mm², with the exception of ρ in kg/m³

¹Experimental values from control samples

²Derived values from eq. (3), (4), (5), (6), (7), (8) and (9)

3.2. EXPERIMENTAL RESULTS OF FINGER-JOINT LAMELLAS

Mean values of modulus of elasticity and bending strength recorded for each failure mode (i.e., 1, 2, and 3, as described in 2.2), were obtained from the three experimental samples: i) control lamellas without finger joints (hereinafter referred to as “controls”); ii) glued finger joints with EPI (herein after referred to as “fj-EPI”); and iii) glued finger joints with PUR (hereinafter referred to as “fj-PUR”). Table 3 shows mean properties and failure modes under bending tests for the three samples.

Table 3: Experimental bending results of the three samples (mean values)

Sample	i) Control	ii) fj-EPI	iii) fj-PUR
Specimens per sample (n)	20	40	20
Moisture content (%)	11.02 (±4 %)	9.12 (±3 %)	9.09 (±3 %)
$E_{0,mean}$ (N/mm²)	15363 ^a (±15 %)	12394 ^b (±19 %)	13326 ^b (±22 %)
Failure mode 1 (wood)	$E_{0,mean_1}$	$E_{0,mean_1}$	$E_{0,mean_1}$
	15363 ^a (±15 %)	10786 ^b (±20 %)	11619 ^b (±15 %)
Failure mode 2 (mixed)	$E_{0,mean_2}$	$E_{0,mean_2}$	$E_{0,mean_2}$
	--	12784 ^a (±20 %)	12332 ^a (±21 %)
Failure mode 3 (adhesive)	$E_{0,mean_3}$	$E_{0,mean_3}$	$E_{0,mean_3}$
	--	13483 ^a (±13 %)	15525 ^b (±17 %)
f_m (N/mm²)	91.88 ^a (±19 %)	59.96 ^a (±15 %)	72.13 ^b (±14 %)
Failure mode 1 (wood)	f_{m_1}	f_{m_1}	f_{m_1}
	91.88 ^a (±19 %)	56.47 ^b (±14 %)	60.88 ^b (±5 %)

Failure mode 2 (mixed)	f_{m_2}	--	58.51 ^a (±13 %)	69.48 ^b (±9 %)
Failure mode 3 (adhesive)	f_{m_3}	--	65.38 ^a (±13 %)	79.18 ^b (±11 %)
Failure mode percentage				
Failure mode 1 (wood)		100 %	30%	20%
Failure mode 2 (mixed)			40%	35%
Failure mode 3 (adhesive)			30%	45%

NOTES: Values in parentheses indicate the coefficient of variation (CoV)
 Different uppercase letters denote significant differences between control, EPI and PUR values with a confidence level of 95%.
 Failure mode 1: 100% wood; Failure mode 2: mixed; Failure mode 3: 100% adhesive

Within fj-EPI, specimens showed similar percentages of failure for the three modes; within fj-PUR, percentage of failure in mode 1 was inferior to those corresponding to modes 2 and 3. In both samples, low percentages (30% in fj-EPI and 20% in fj-PUR) of failure in mode 1 (i.e., 100% wood) were observed.

Controls presented a significantly higher mean value of modulus of elasticity compared to those of fj-EPI and fj-PUR, being these last two, similar to each other. Focusing on the failure mode, significant differences between fj-EPI and fj-PUR were observed, but just for specimens that failed by adhesive (mode 3). Note that the modulus of elasticity, evaluated in the elastic phase of the load-deflection curve it is not affected by the ultimate load, which in modes 1 and 2, occurs once the elastic-plastic phase has been reached in the compressed area of the specimen. However, failure by adhesive (mode 3) can occur in the elastic phase, affecting the modulus of elasticity depending on the adhesive type.

Typical load-deflection curves for lamellas glued with EPI or glued with PUR, against controls (i.e., without finger joint) are depicted in Figure 4.

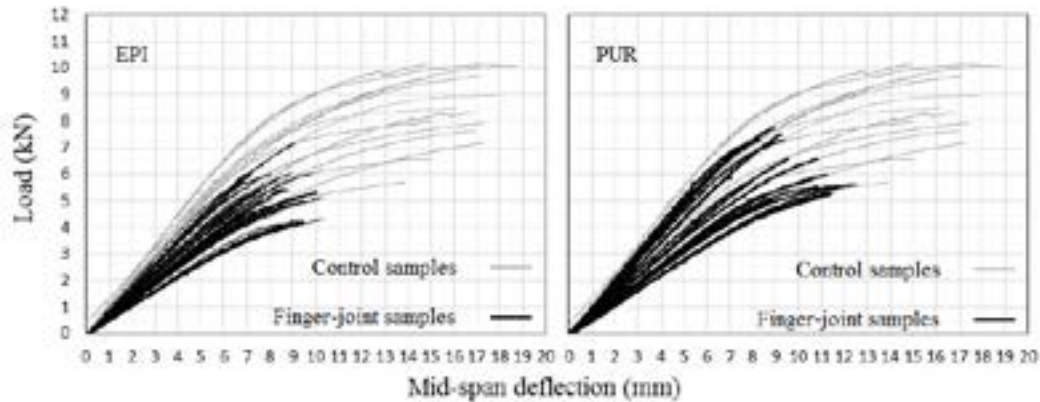


Figure 4: Load-mid-span deflection curves of finger-jointed samples with EPI (left) and PUR (right) adhesive compared to control samples curves (grey color)

As can be observed, the peak load attained in finger-jointed lamellas was lower than in controls. While failure of controls occurred in the elasto-plastic phase, failure of finger-jointed appeared close to the yield limit, shown in Figure 4 as the inflection point of the curves. Bending strength were significantly higher in fj-PUR ($f_m=72.13 \text{ N/mm}^2$) compared to those observed in fj-EPI ($f_m=59.96 \text{ N/mm}^2$), being both, lower than controls ($f_m=91.88 \text{ N/mm}^2$). These findings were higher than those presented by Piter et al. (Piter et al. 2007b) for finger joint lamellas of Argentinean *E. grandis* glued with melamine-urea-formaldehyde adhesive (f_m between 46.9 and 49.7 N/mm^2).

Boxplots of bending properties by failure mode for controls and finger-jointed samples are shown in Figure 5.

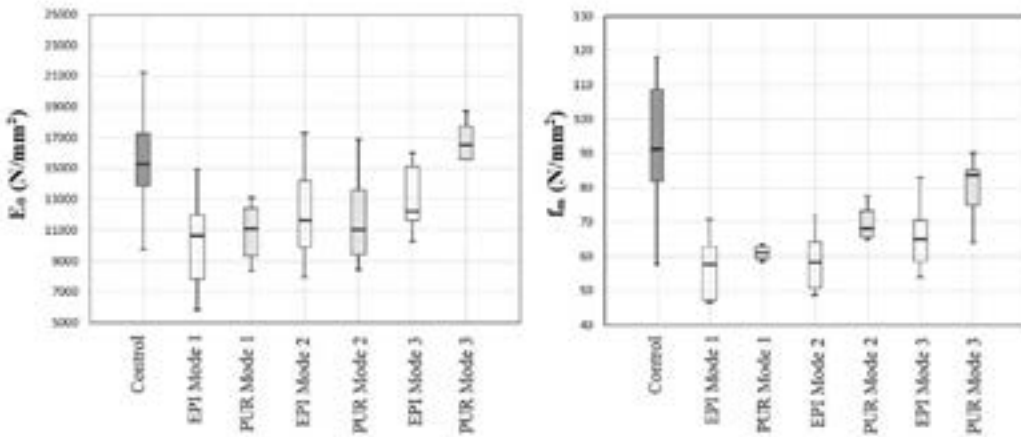


Figure 5: Modulus of elasticity and bending strength by adhesive type and failure mode

Analysis of $E_{0,mean}$ by failure mode within each fj-EPI and fj-PUR samples, reveals an increasing trend of mean values from mode 1 to mode 3 (Figure 5).

Similarly, bending strength in regard to failure mode within each fj-EPI and fj-PUR samples, shows an increase in f_m from failure mode 1 to failure mode 3. The lowest bending strengths observed in specimens that failed 100% by wood (mode 1) could mislead interpretations by contradicting the premise that the finger joint is a weak point. However, this behavior could be attributed to wood heterogeneity, masking its influence on the bending strength and showing failure modes by adhesive.

Comparison of strength values between fj-EPI and fj-PUR, for failure mode 1 (56.47 and 60.88 N/mm², respectively), showed no significant differences, agreeing with the fact that the limiting factor was the wood strength rather than the glue line. On the other hand, significant superior values of f_m in fj-PUR compared to fj-EPI for failure modes 2 and 3 were observed.

3.3. VALIDATION OF FE MODEL

Typical load-deflection curves comparing the experimental results and the numerical predictions for control samples are presented in Figure 6.

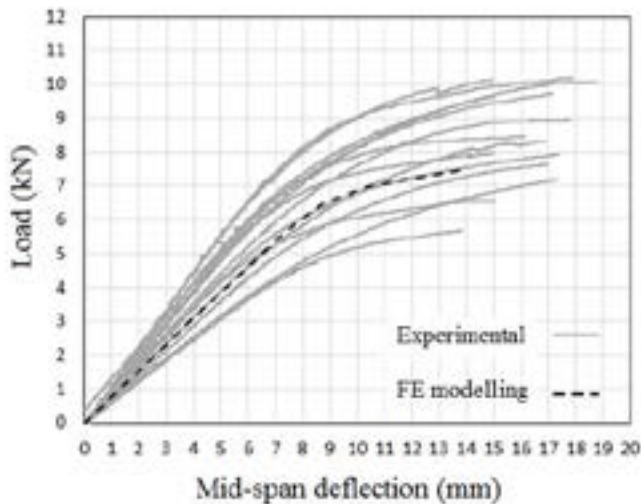


Figure 6: Load-mid-span deflection curves for experimental and numerical control samples

As can be seen, the load-deflection curve obtained from the FE simulation matches the experimental curves. The numerical modulus of elasticity in the elastic phase resulted in 13442 N/mm^2 , 12.5% lower than the experimental mean value, yet in between the minimum-maximum experimental range.

In addition, two numerical models to simulate the experimental behavior of finger-jointed lamellas, one glued with EPI (fj-EPI), and one glued with PUR (fj-PUR), under bending tests were developed. Figure 7 presents the load-deflection curves obtained from the models in comparison with the experimentals.

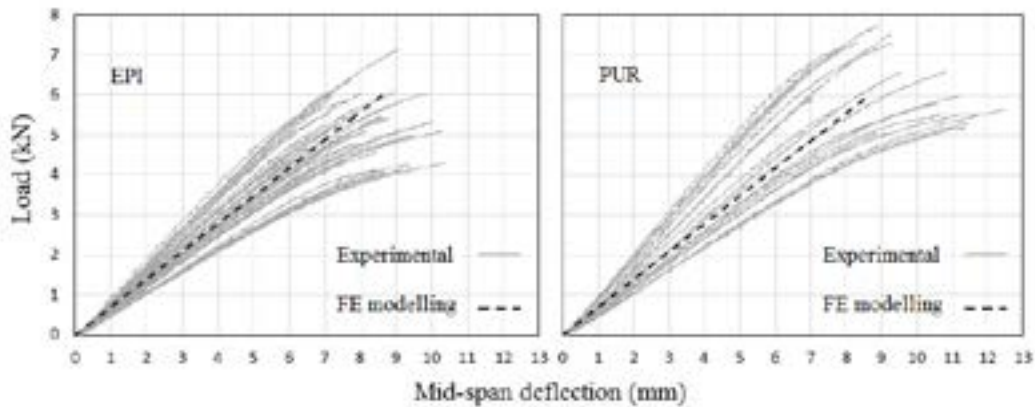


Figure 7: Load-mid-span deflection curves of experimental samples vs. FE models

The different adhesive (EPI and PUR) properties considered in the model had no significant influence on the numerical deflections and therefore, neither on the numerical modulus of elasticity. The adjustment of the numerical models was in good agreement with the experimental data. Table 4 shows the relative differences between the modulus of elasticity obtained from the numerical models and the mean values from experimental tests. A maximum error of 7.5% was observed for fj-PUR sample.

Table 4: Modulus of elasticity (E_0) of finger-jointed lamellas obtained from numerical modeling and experimental testing

	FE model	fj-EPI ¹	fj-PUR ¹	[fj-EPI+fj-PUR] ¹
E_0 (mean value, N/mm^2)	12321	12394	13326	12805
Error (%)	---	0.59	7.54	3.78

¹values obtained in experimental testing

Once the model was validated for stiffness prediction, the next step involved applying the model to predict the bending strength of finger-jointed lamellas. In doing so, based on the experimental results and considering an ideal behavior with proper adhesion of the finger-joints, two assumptions were alleged: i) the glue line is stronger than the wood leading to a 100%-wood failure (mode 1); and ii) the 5th percentile (characteristic value that reflect material variability) is similar for the whole sample, even in a hypothetical scenario in which every finger-joint fails by mode 1 (leading to an increase of the f_m mean value).

Bearing in mind that failure of lamellas under bending typically occurs in the tensile side, the bending strength was estimated by evaluation of the tensile stress distributions of wood, in the vicinity of the finger-joints. The predicted strengths were compared with experimental results of specimens that failed in mode 1.

Figure 8 shows the distribution of tensile stresses, parallel and perpendicular to the grain, in the proximities of the finger joints, obtained from the numerical models. The maximum stresses were observed close to the bottom of the fingers, coinciding with the rupture zone of the experimental specimens.

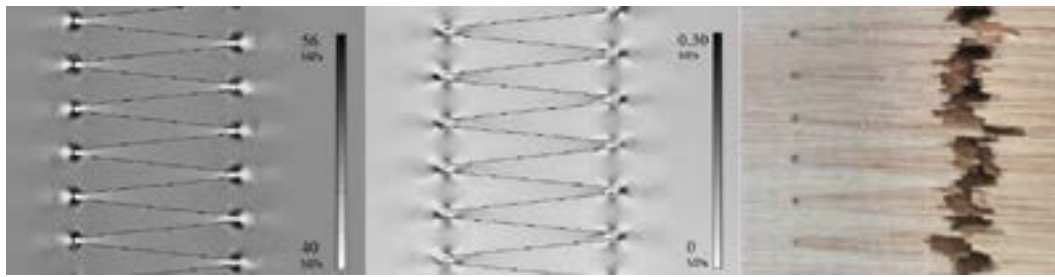


Figure 8: Stress distributions (N/mm²) parallel (left) and perpendicular (center) to the grain from FE modeling, and experimental failure (right) under bending load

As expected, the tensile strength was higher in the direction parallel- than perpendicular- to the grain and therefore, the finger-joints failure occurred when the longitudinal tension stress at the bottom of the finger exceeded the estimated strength in tension parallel to the grain ($f_{t,0}=55.13$ N/mm²) of *Eucalyptus grandis* (see section 3.1). The peak load was determined for the first node that reached the value of $f_{t,0}$, and the numerical bending strength was calculated by equation 2. Table 5 shows the error in the prediction of the bending strength by FEM in comparison with the experimental values.

Table 5: Bending strength (f_m) of finger-jointed lamellas obtained from numerical modelling and experimental testing

	FE model	fj-EPI	fj-PUR	[fj-EPI+fj-PUR]	[fj-EPI+fj-PUR]	
f_m (mean value, N/mm ²)	50.26	56.47	60.88	56.48	f_{05} (5 th percentile)	47.29
Error (%)	---	10.99	17.44	11.01		6.28

The numerical bending strength showed 11 to 17% lower values than the experimental means. Comparing the numerical results with the 5th percentile of experimental f_m , the estimation error is reduced to 6%. This decrease could be attributed to the way in which $f_{t,0}$ was calculated, *i.e.*, by the equation specified in EN 338 (CEN 2016b), which, due to safety reasons is conservative oriented, instead of using experimental data. Nevertheless, it is worth noting that employing the mechanical properties derived by EN 338 (CEN 2016b) equations leads to a reasonably prediction of the bending strength from *Eucalyptus grandis* finger-joints.

Since the finger geometry has a relevant effect on the performance of the structural joints (Bustos et al. 2003; Tran et al. 2015), several finger-joint geometries were considered in FE modeling. The strength performance of the different geometries were evaluated just for mode 1, where failure occurs due to tension stresses in wood, rather than to adhesive (failure modes 2 and 3) where the modeling of the wood-adhesive interaction becomes unpredictable. Table 6 shows the finger-joint geometries evaluated:

Table 6: Finger joint geometries evaluated by FEM

Finger code	Finger length l (mm)	Pitch p (mm)	Tip thickness b_t (mm)
10/4/0.5	10	4.0	0.5
11/4/0.5	11	4.0	0.5
13/4/0.5	13	4.0	0.5
15/4./0.5	15	4.0	0.5
20/5/0.5	20	5.0	0.5
20/6/1.0	20	6.2	1.0
30/6/1.0	30	6.2	1.0

Finger lengths of 15, 20 and 30 mm (with their corresponding values of pitch and tip thickness) indicated in EN 14081 and, lengths of 10, 11 and 13 mm, usually employed in Uruguayan industries, were considered. The modeling parameters were similar to those defined in 2.3. The estimated bending strength obtained for each finger-joint geometry is shown in Figure 9:

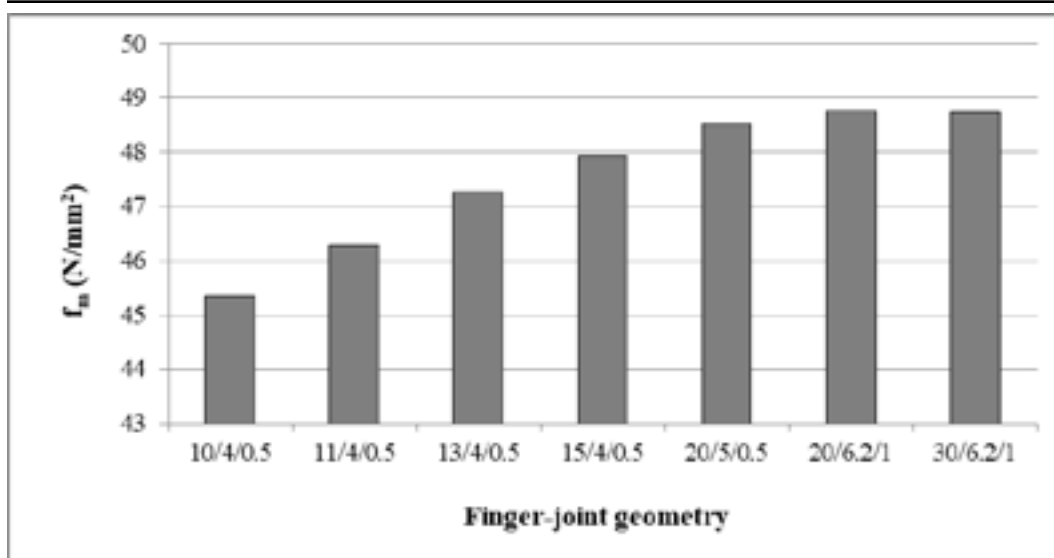


Figure 9: Bending strength f_m (N/mm²) of different finger-joint geometry estimated by FEM

As can be seen, the numerical bending strength slightly improved by increasing the finger length, results that compare relatively well with those obtained from tests for fingers with codes 10/4/0.5, 11/4/0.5 and 13/4/0.5. As was previously mentioned, the improvement in strength is related to the different distribution of tensile stresses near the bottom of the finger, being valid just for failure mode 1. Increasing the length of the finger entails an augmentation of the contact area between wood and adhesive, which in turn should improve modes 2 and 3 results. Results showed that lower bending strength values (and therefore defining the characteristic values) were obtained in samples with failure mode 1. Under this premise, the evaluation of different geometries by FEM indicates that a finger length of 20 mm is optimal for maximizing the bending strength for failure mode 1.

3. CONCLUSIONS

Eucalyptus grandis finger-joints glued with different adhesives (PUR and EPI) were tested in bending to obtain their mechanical properties and to evaluate the failure mode. Additionally, numerical simulations were developed to model the finger-joints and to estimate their strength and stiffness.

The experimental tests showed not significant differences in the modulus of elasticity (E_0) for lamellas with finger-joints glued with EPI and with PUR, being both significantly lower than those from controls (lamellas without finger-joint). However, the bending strength (f_m) of finger-joints was significantly higher for PUR than for EPI, being both lower than controls. The lowest bending properties obtained in samples with failure mode 1 (failure 100% by wood) suggests that the characteristic strength value of finger joints defined by the wood and not by the adhesive.

Despite the relative high values of bending strength reached in the finger-joints, high percentages of undesirable failure type, *i.e.*, in the glue line (modes 2 and 3) for both adhesives (70% in EPI samples and 80% in PUR samples), were found. This observation suggests that the wood-adhesive interphase has yet to be improved, probably by optimizing the manufacturing parameters or evaluating the performance of new adhesives.

There were no differences on the numerical results for the modeling of the lamellas in function of the type of adhesives used for the gluing of the finger joints. The numerical modulus of elasticity of finger-joint lamellas was estimated by with a maximum error of 7.54% with respect to the experimental mean values. From these models, bending strength could be predicted in a conservative way, with an error of 6.28% compared with the experimental value of the 5th percentile.

FEM modeling showed that optimum finger geometry is 20 mm length, with a gap of 6.2 mm and tip thickness of 1 mm. This finger configuration maximizes the bending strength in failure modes 1 and, therefore, the characteristic value.

In further works, the accuracy of the numerical models for bending strength prediction could be improved by using experimental data as input values for the entire set of elastic and mechanical properties needed. In addition, more

complex FE models considering the interaction between wood and adhesive for modeling failure modes 2 and 3, should be developed.

REFERENCES

- Ahmad Z, Lum WC, Lee SH, Razlan MA, Mohamad, WHW (2017) Mechanical properties of finger jointed beams fabricated from eight Malaysian hardwood species. *Constr Build Mater* 145:464–473. doi: 10.1016/j.conbuildmat.2017.04.016
- Ayarkwa J, Hirashima Y, Sasaki Y (2000) Effect of finger geometry and end pressure on the flexural properties of finger-jointed tropical African hardwoods. *For Prod J* 50:53
- Ayarkwa J, Hirashima Y, Sasaki Y Ando K (2000) Effect of glue type on flexural and tensile properties of finger-jointed tropical African hardwoods. *For Prod J* 50:59
- Bourreau D, Aimene Y, Beauchene J, Thibaut, B (2013) Feasibility of glued laminated timber beams with tropical hardwoods. *Eur J Wood Wood Prod* 75:653–662
- Bourscheid CB, Terezo RF, Stüpp AM, Vanzella DA (2015) Desempenho mecânico de madeira laminada colada de *Eucalyptus* spp. In: *Anais do II Congresso Brasileiro de Ciencia e Tecnologia da Madeira - CBCTEM*. Belo Horizonte, Brazil
- Bustos C, Mohammad M, Hernández RE, Beauregard R (2003) Effects of curing time and end pressure on the tensile strength of finger-jointed black spruce lumber. *For Prod J* 53:85
- Calil Neto C, Christoforo AL, Ribeiro Filho SM, Moni S., Rocco Lahr F.A., Calil Junior C (2014) Evaluation of strength to shear and delamination in glued laminated wood. *Ciência Florest* 23:989–996
- Camú CT, Aicher S (2018) A stochastic finite element model for glulam beams of hardwoods. In: *World Conference on Timber Engineering*. Seoul, South Korea
- CEN (2013) EN 14080. Timber structures. Glued laminated timber and glued solid timber. Requirements
- CEN (2015) EN 16351. Timber structures. Cross laminated timber. Requirements
- CEN (2010) EN 408. Timber structures. Structural timber and glued laminated timber. Determination of some physical and mechanical properties.
- CEN (2016a) EN 384. Structural timber. Determination of characteristic values of mechanical properties and density
- CEN (2016b) EN 338. Structural timber. Strength classes
- de Castro San Román J (2005) Experiments on Epoxy, Polyurethane and ADP Adhesives: Composite construction laboratory, Technical Report Nr. CCLab2000.1b/1
- Dieste A (2012) Program to promote exports of wood products [Programa de promoción de exportación de productos de madera]. Technical Report 1. Dirección Nacional de Industrias. Ministerio de Industrias, Energía y Minería. Consejo Sectorial Forestal-Madera. Montevideo, Uruguay. pp 35
- Franke B, Schusser A, Müller A (2014) Analysis of finger joints from beech wood. In: *World Conference on Timber Engineering*. Quebec, Canada
- Franke S, Marto J (2014) Investigation of *Eucalyptus globulus* wood for the use as engineered wood material. In: *Proceedings of the World Conference on Timber Engineering*. Quebec, Canada
- IRAM 9662-2 (2015) Structural glued laminated timber. Visual grading of boards by strength. Part 2. Boards of *Eucalyptus grandis* [Madera laminada encolada estructural. Clasificación visual de las tablas por resistencia. Parte 2. Tablas de *Eucalyptus grandis*]
- Iwakiri S, Monteiro Matos JL, Prata JG, Trianoski R, Parchen CF, Gomes Castro V, Teixeira Iwakiri V (2014) Characteristics of glued laminated beams made of teak wood (*Tectona grandis*). *Floresta e Ambient* 21:269–275
- Khelifa M, Auchet S, Méausoone PJ, Celzard A (2015) Finite element analysis of flexural strengthening of timber beams with Carbon Fibre-Reinforced Polymers. *Eng Struct* 101:364–375
- Konnerth J, Gindl W, Müller U (2007) Elastic properties of adhesive polymers. I. Polymer films by means of electronic speckle pattern interferometry. *J Appl Polym Sci* 103:3936–3939. doi: 10.1002/app.24434
- Lara-Bocanegra AJ, Majano-Majano A, Crespo J, Guaita M (2017) Finger-jointed *Eucalyptus globulus* with IC-PUR adhesive for high performance engineered laminated products. *Constr Build Mater*. doi: 10.1016/j.conbuildmat.2017.01.004
- Millner HR, Yeoh E (1991) Finite element analysis of glued timber finger joints. *J Struct Eng* 117(3):755–766
- Moya L, Pérez-Gomar C, Vega A, et al (2019) RELATIONSHIP BETWEEN MANUFACTURING PARAMETERS AND STRUCTURAL PROPERTIES OF EUCALYPTUS GRANDIS GLUED LAMINATED TIMBER. *Maderas Cienc y Tecnol* 21:21
- Özçiğci A, Yapici F (2008) Structural performance of the finger-jointed strength of some wood species with different joint configurations. *Constr Build Mater* 22(7):1543–1550

- Pereira MC, Calil Neto C, Icimoto FH, Calil Junior C (2016) Evaluation of tensile strength of a *Eucalyptus grandis* and *Eucalyptus urophylla* Hybrid in wood beams bonded together by means of finger joints and polyurethane-based glue. *Mater Res* 19:1270–1275
- Piter JC, Cotrina AD, Sosa Zitto MA, Stefani PM, Torr n EA (2007) Determination of characteristic strength and stiffness values in glued laminated beams of Argentinean *Eucalyptus grandis* according to European standards. *Holz als Roh - und Werkst* 65:261–266. doi: 10.1007/s00107-006-0161-5
- Raknes E (1980) The influence of production conditions on the strength of finger-joints (of sawnwood in Norway). In: Transmitted by the Government of Norway in FAO, Geneva (Switzerland). Joint ECE/FAO Agriculture and Timber Div. Seminar on the Production, Marketing and Use of Finger-Jointed Sawnwood. Hamar (Norway)
- Sebera V, Muszyński L, Tippner J, Noyel M, Pisaneschi T, Sundberg B (2015) FE analysis of CLT panel subjected to torsion and verified by DIC. *Mater Struct* 48(1-2):451–459. doi: 10.1617/s11527-013-0195-1
- Serrano E, Gustafsson J, Larsen HJ (2001) Modeling of finger-joint failure in glued-laminated timber beams. *J Struct Eng* 127(8):914–921
- Smardzewski J (1996) Distribution of stresses in finger joints. *Wood Sci Technol* 30(6):477–489
- Stoeckel F, Konnerth J, Gindl-almutter W (2013) Mechanical properties of adhesives for bonding wood — A review. *Int J Adhes Adhes* 45:32–41
- Tran VD, Oudjene M, M ausoone PJ (2015) Experimental and numerical analysis of the structural response of adhesively reconstituted beech timber beams. *Compos Struct* 119:206–217
- Tran VD, Oudjene M, M ausoone PJ (2014) FE analysis and geometrical optimization of timber beech finger-joint under bending test. *Int J Adhes Adhes* 52:40–47. doi: 10.1016/j.ijadhadh.2014.03.007
- Vassiliou V, Barboutis I, Karasterogiou S (2006) Effect of PVA bonding on finger-joint strength of steamed and unsteamed beech wood (*Fagus sylvatica*). *J Appl Polym Sci* 103:1664–1669
- Volkmer T, Franke B, Schusser A (2014) Analysis of the penetration of adhesives at finger-joints in beech wood. In: In World Conference on Timber Engineering-WCTE. Quebec, Canada
- Vrazel M, Sellers Jr T (2004) The effects of species, adhesive type and cure temperature on the strength and durability of a structural finger-joint. *For Prod J* 54:66

Mangium (*Acacia mangium*) and Sengon (*Falcataria moluccana*) Smoked Woods Resistance to Subterranean Termite Attack

Yusuf Sudo Hadi^{1*}, Muh Yusram Massijaya¹, Imam Busyra Abdillah¹, Gustan Pari², Wa Ode Muliastuty Arsyad²

¹) Bogor Agricultural University, Bogor, Indonesia;

²) Forest Products Research and Development Centre.

Corresponding author: yshadi@indo.net.id

ABSTRACT

Indonesian logs production is mostly cut from plantation forest at young age. The timbers contain a lot of sapwood, juvenile wood, and not resistant to termite attacks. Smoked wood has improved to be more resistant to termite attack. Wood specimens of mangium (*Acacia mangium*) and sengon (*Falcataria moluccana*) were exposed during one-, two-, and three-week to smoke produced from pyrolysis of salam (*Syzygium polyanthum*) wood. All treated-wood specimens were exposed to subterranean termite (*Coptotermes curvignathus* Holmgren) under laboratory conditions according to Indonesian standard SNI 7207-2014. For comparison purposes untreated wood was also prepared. The results showed that untreated wood of mangium was moderate resistance or resistance class III, and sengon was poor resistance or resistance class IV. Smoke of salam wood could improve wood resistance to subterranean termite attack. Smoke treatments during one week for mangium and two weeks for sengon could enhance the woods becoming very resistance or resistance class I.

1. INTRODUCTION

The Indonesian wood industry processed 43 million m³ of logs in 2017, and 87% of the wood was harvested from plantation forests (Ministry of Environment and Forestry, 2018). Fast-growing tree species, such as mangium (*Acacia mangium*) and sengon (*Falcataria moluccana*), are commonly planted to achieve a short cutting rotation, typically only 6 to 10 years. Fajriani *et al.* (2013) and Hadi *et al.* (2010) reported that wood from young plantation forests contains a lot of sapwood and juvenile wood, which have low physical-mechanical properties and low resistance to termite attack. Production of better physical-mechanical properties and resistance to termite attack, requires ongoing development of methods to improve wood quality.

To lengthen the service life of wood or make it more resistant to termite attack without preservative agents, chemically modifications have been used to produce furfurylated wood (Hadi *et al.*, 2005) and acetylated wood (Hadi *et al.*, 2015). In addition, bulking plastic into wood void has yielded polystyrene-impregnated wood (Hadi *et al.*, 2016a), methyl methacrylate-impregnated wood (Hadi *et al.*, 2018), and acetylated rubber-wood flakeboard (Hadi *et al.*, 1995).

Smoke treatment of wood has also been investigated to preserve both wood (Hadi *et al.*, 2012) and glulam (Hadi *et al.*, 2016b, 2016c). Smoke from wood contains a large number of polycyclic aromatic hydrocarbons, which are predominantly phenols, aldehydes, ketones, organic acids, alcohols, esters, hydrocarbons, and various heterocyclic compounds (Stołyhwo and Sikorski, 2005).

To determine the effect of smoke on wood resistance to termite attack, cold to warm smoking, temperature held at 15-45 °C, was more sharply giving needed information. This work has done by Hadi *et al.* (2016b) on mindi (*Melia azedarach*), sengon (*Falcataria moluccana*), sugi (*Cryptomeria japonica*), and pulai (*Alstonia* sp.) wood as well as glulam from fast-growing wood species. Overall, the results showed that cold smoking improved wood resistance against termite attacks.

Salam wood (*Syzygium polyanthum*) has a medium specific gravity and a high number of chemical compounds, especially extractive substances (Martawijaya *et al.*, 2004). It can be processed for charcoal production, and the smoke produced as a byproduct could be used in the smoking process of wood. The purpose of the current study was to determine how smoke from salam wood could improve resistance to subterranean termite attack of mangium and sengon wood. Imidacloprid-preserved wood was prepared for comparative purposes.

2. MATERIALS AND METHODS

2.1. WOOD PREPARATION

Mangium and sengon were harvested in Bogor, West Java, Indonesia, and wood samples were used for smoked wood experiments. The densities of mangium and sengon wood were 0.56 ± 0.02 and 0.36 ± 0.03 g/cm³, respectively. The measured response was resistance to subterranean termite attack in laboratory tests according to Indonesian standard SNI 7207-2014 (SNI, 2014). Wood was cut into specimens of 0.5×2.5 cm in cross section by 2.5 cm in the longitudinal direction for the testing. Wood specimens were divided into three categories: untreated wood, smoked wood, and imidacloprid-preserved wood. Salam wood was pyrolyzed to produce charcoal, and the smoke released as a byproduct was used for the smoking process, which lasted 1, 2, and 3 weeks (Hadi *et al.*, 2010).

For purposes of comparison, wood preserved with imidacloprid 3% was also prepared. The samples were dried to reach 12% moisture content, weighed, and then placed under vacuum at 5 atmospheres for 30 minutes, and during vacuum released the imidacloprid solution was inserted, and then pressure at 5 atmospheres for 30 minutes was applied (Hadi *et al.*, 2018). The samples then underwent conditioning for 2 weeks. Five replications were done for each treatment.

2.2. SUBTERRANEAN TERMITE TEST

The laboratory subterranean termite test was based on Indonesian standard SNI 7207-2014. Each test specimen was placed in a glass container with 200 g of sterilized sand, 50 mL of water, and 200 healthy and active workers of *Coptotermes curvignathus* subterranean termites from a laboratory colony. The containers were put in a dark room at a temperature of 25 °C to 30 °C and 80% to 90% relative humidity for 4 weeks and weighed weekly. If the moisture content of the sand decreased by 2% or more, water was added to achieve a 25% moisture content. At the end of the 4-week test, the wood samples were oven-dried. Wood weight loss and termite mortality were determined using the following formulae 1 and 2:

$$\text{Weight loss (WL)} = (W1 - W2)/W1 \times 100\% \quad \dots\dots\dots (1)$$

where W1 is the weight (g) of oven-dried samples before the test, and W2 is the weight (g) of oven-dried samples after the test.

$$\text{Termite mortality} = (T1 - T2)/T1 \times 100\% \quad \dots\dots\dots (2)$$

where T1 is the number of live termites before the test, and T2 is the number of live termites after the test.

We assumed that termites died linearly with time, and we calculated the feeding rate according to the following equation (3):

$$\text{Feeding rate (FR)} (\mu\text{g/termite/day}) = (\text{weight of wood eaten; } \mu\text{g})/(\text{average number of living termites})/(\text{number of days in the test period}) \quad \dots\dots\dots (3)$$

Wood resistance class against subterranean termites was determined by referring to SNI 7207-2014 as shown in Table 1.

Table 1: Resistance class against subterranean termite

Resistance class	Sample condition	Mass loss (%)
I	Very resistant	<3.52
II	Resistant	3.52–7.50
III	Moderately resistant	7.50–10.96
IV	Poorly resistant	10.96–18.94
V	Very poorly resistant	>18.94

2.3. DATA ANALYSIS

To analyze the effect of treatments upon all responses, we used a 2×5 factorial completely randomized design for data analysis. The first factor was wood species (mangium and sengon), and the second factor was treatment (untreated, smoke 1 week, smoke 2 weeks, smoke 3 weeks, and imidacloprid preservation). Duncan's multiple range test was used for further analysis if a factor was significantly different at $p \leq 0.05$.

3. RESULTS AND DISCUSSION

Wood resistance to subterranean termite attack is described with weight loss and it could be classified to resistance class according to Indonesian standard. The other responses are termite mortality and termite feeding rate. All responses are described as followed:

3.1. WEIGHT LOSS

Results for weight loss (WL) of wood samples, wood resistance class, termite mortality, and termite feeding rate are shown in Table 2. Untreated mangium wood was more resistant than untreated sengon wood as indicated by the lower WL and higher resistance class of mangium. Mangium wood had a higher density (0.56 g/cm^3) than sengon wood (0.36 g/cm^3), resulting in mangium potentially being more resistant than sengon. In a previous study, Arango *et al.* (2006) analyzed six hardwood species and found that wood with a higher specific gravity had more resistance to *Reticulitermes flavipes* Kollar termites. Mangium and sengon wood in the current study had similar resistance classes as found by Arinana *et al.* (2012). With regard to retention of the imidacloprid preservative, mangium reached 6.12 kg/m^3 and sengon 7.89 kg/m^3 . With its lower density, sengon is usually more easily penetrated by a chemical solution because there is more void space in its structure.

Table 2: Wood loss, resistance class, mortality, and feeding rate.

Wood species	Treatment	WL (%)	Resistance class	Mortality (%)	Feeding rate ($\mu\text{g/termite/day}$)
Mangium	Untreated	10.86 (3.78)	III	23.9 (9.2)	41.8 (13.3)
	Smoke 1-Week	2.90 (1.33)	I	100 (0)	18.9 (9.4)
	Smoke 2-Week	2.63 (1.25)	I	100 (0)	16.6 (8.0)
	Smoke 3-Week	2.12 (0.85)	I	100 (0)	14.7 (5.9)
	Preserved	2.93 (0.97)	II	100 (0)	18.8 (6.1)
Sengon	Untreated	19.32 (3.91)	V	22.3 (7.2)	42.11 (6.7)
	Smoke 1-Week	5.01 (1.90)	II	100 (0)	23.5 (7.8)
	Smoke 2-Week	3.24 (1.10)	I	100 (0)	15.2 (5.1)
	Smoke 3-Week	2.06 (0.72)	I	100 (0)	10.1 (3.6)
	Preserved	4.59 (1.98)	II	100 (0)	23.0 (10.7)

Remarks: Values in parentheses are standard deviations.

Table 3: Variance analysis of weight loss, mortality, and feeding rate

Source	Weight loss	Mortality	Feeding rate
Wood species	**	ns	ns
Treatment	**	**	**
Interaction	**	ns	ns

Remarks: **p \leq 0.01; ns = not significant.

Table 4: Duncan's multiple range test for weight loss, mortality, and feeding rate

Respond	Wood species	Untreated	Smoke 1-Week	Smoke 2-Week	Smoke 3-Week	Imidacloprid
Weight loss	Mangium	10.86d	2.90ab	2.63ab	2.12a	2.93ab
	Sengon	19.32e	5.01c	3.24abc	2.06a	4.59bc
Mortality		20.62a	100b	100b	100b	100b
Feeding rate		41.96c	21.18b	16.03ab	12.39a	20.89b

Remarks: Values followed by the same are not statistically different.

The analysis of variance in Table 3 shows that wood species, treatment, and the interaction of both factors highly affected WL. Based on Duncan's multiple range test of WL in Table 4, the untreated mangium and sengon wood had the largest WL values compared to treated wood, and they were significantly different from all treated wood. These results indicate that all treatments significantly enhanced wood resistance to subterranean termite attack. Furthermore, the results show that all mangium wood samples were not significantly different from each other. In the case of sengon wood, the 3-week smoking period was associated with the lowest WL, but it was not significantly different from the 2-week smoking period.

With reference to Table 1, untreated mangium wood was classified as resistance class III, or moderately resistant, based on the WL values. However, untreated sengon wood was class V, or very poorly resistant to subterranean termite attack. For mangium wood, all smoking periods resulted in class I resistance, or very resistant, but sengon wood required at least 2 weeks of smoking to get the same results. In other words, a 1-week smoking period for mangium and a 2-week smoking period for sengon were sufficient to obtain the best results. These results were better than those found for imidacloprid-preserved wood, which got resistance class II, or resistant to subterranean termite attack.

3.2. MORTALITY

Based on data presented in Table 2, termite mortality was much lower for untreated wood, with a rate that was approximately one-fourth that found for treated wood. These findings indicate that both the smoking treatment and imidacloprid preservation were effective in enhancing wood resistance to subterranean termite attack. According to the analysis of variance in Table 3, only treatment affected termite mortality, and based on Table 4, smoke treatment and preservation both resulted in all termites dying. This result aligns with Hadi *et al.* (2012), who found that smoke treatment applied to sengon, sugi, and pulai wood for 2 weeks resulted in 100% termite mortality at the end of the experiment. The presence of acetic acid and phenolic compounds in the smoke has been suggested to increase wood resistance to subterranean termite attack (Oramahi *et al.*, 2014).

3.3. FEEDING RATE

The daily termite feeding rate, or daily wood consumption of each termite, reached 41.82 ± 13.29 $\mu\text{g}/\text{termite}$ for untreated sengon, which was lower than for untreated mangium, with 42.11 ± 6.66 $\mu\text{g}/\text{termite}$. These results were similar to those of Arinana *et al.* (2012), but lower than those of Hadi *et al.* (2014). According to the analysis of variance in Table 3, only treatment affected the termite feeding rate; the other factors did not have an effect on it. Based on data shown in Table 4, smoke treatment and preservation both substantially reduced the termite feeding rate. Untreated wood clearly had the highest daily feeding rate, while wood smoked for 3 weeks had the lowest. Rates for other samples between these extremes. The daily feeding rate was determined by mass (g) loss and the number of living termites, with the assumption that the termites died linearly over time. However, this assumption was not based on observation, and for future research, methods are needed for how to recognize living termites at any time during an experiment.

4. CONCLUSIONS

Based on the findings in this work, we were able to make the following conclusions:

1. Untreated mangium wood, with a density of 0.56 g/cm^3 and resistance class III, was more resistant than untreated sengon wood, with a density of 0.36 g/cm^3 and resistance class V.
2. Smoking treatment enhanced wood resistance to subterranean termite attack. A smoking period of 1 week for mangium and 2 weeks for sengon resulted in resistance class I wood, that is, very resistant to subterranean termite attack. These results were better than those for imidacloprid-preserved wood, which was resistance class II, or resistant to subterranean termite attack.

ACKNOWLEDGMENTS

This research was a part of Competency Research 2018 Granted by the Ministry of Research, Technology, and Higher Education of the Indonesian Republic.

REFERENCES

- Arango, R.A., F. Green, K. Hintz, P.K. Lebow and R.B. Miller. 2006. Natural durability of tropical and native woods against termite damage by *Reticulitermes flavipes* (Kollar). *International Biodeterioration & Biodegradation* 57: 146–150.
- Arinana, A., K. Tsunoda, E.N. Herliyana and Y.S. Hadi. 2012. Termite-susceptible species of wood for inclusion as a reference in Indonesian standardized laboratory testing. *Insects* 3: 396–40.
- Fajriani, E., J. Rulle, J. Dlouha, M. Fournier, Y.S. Hadi and W. Darmawan. 2013. Radial variation of wood properties of sengon (*Paraserianthes falcataria*) and jabon (*Anthocephalus cadamba*). *Journal of the Indian Academy of Wood Science* 10(2): 110–117.
- Hadi, Y.S., I.G.K.T. Darma, F. Febrianto and E.N. Herliyana. 1995. Acetylated rubber-wood flakeboard resistance to bio-deterioration. *Forest Products Journal* 45(10): 64–66.
- Hadi, Y.S., M. Westin and E. Rasyid. 2005. Resistance of furfurylated wood to termite attack. *Forest Products Journal* 55(11): 85–88.
- Hadi, Y.S., T. Nurhayati, J. Jasni, H. Yamamoto and N. Kamiya. 2010. Smoked wood resistance against termite. *Journal of Tropical Forest Science* 22(2): 127–132.
- Hadi, Y.S., T. Nurhayati, J. Jasni, H. Yamamoto and N. Kamiya. 2012. Smoked wood resistance to subterranean and dry wood termites attack. *International Biodeterioration & Biodegradation* 70: 79–81. doi: 10.1016/j.ibiod.2011.06.010.
- Hadi, Y.S., A. Arinana and M.Y. Massijaya. 2014. Feeding rate as a consideration factor for successful termite wood preference tests. *Wood and Fiber Science* 46(4): 590–593.
- Hadi, Y.S., M.Y. Massijaya, D. Hermawan and A. Arinana. 2015. Feeding rate of termites in wood treated with borax, acetylation, polystyrene, and smoke. *Journal of Indian Academy Wood Science* 12(1): 74–80. DOI: 10.1007/s13196-015-0146-2.
- Hadi, Y.S., M.Y. Massijaya and A. Arinana. 2016a. Subterranean termite resistance of polystyrene-treated wood from three tropical wood species. *Insects* 7(3): pii: 37; doi:10.3390/insects7030037.
- Hadi, Y.S., M. Efendi, M.Y. Massijaya, A. Arinana and G. Pari. 2016b. Subterranean resistance of smoked glued laminated lumber made from fast-growing tree species from Indonesia. *Wood and Fiber Science* 48(3): 211–216.
- Hadi, Y.S., M. Efendi, M.Y. Massijaya, G. Pari and A. Arinana. 2016c. Resistance of smoked glued laminated lumber to subterranean termite attack. *Forest Products Journal* 66(7/8): 480–484. doi: 10.13073/FPJ-D-15-00085.
- Hadi, Y.S., M.Y. Massijaya, L.H. Zaini, I.B. Abdillah and W.O.M. Arsyad. 2018. Resistance of methyl methacrylate-impregnated wood to subterranean termite attack. *Journal of the Korean Wood Science and Technology* 46(6): 748–755.
- Martawijaya, A., I. Kartasujana, K. Kadir and S.A. Prawira. 2004. *Atlas kayu Indonesia, jilid III [Indonesian Wood Atlas]*. Forest Products Research Institute, Forestry Department, Bogor, Indonesia.
- Ministry of Environment and Forestry. 2018. *Statistic of forestry production*. Ministry of Environment and Forestry, Jakarta, Indonesia.
- Oramahi, H.A., F. Diba and Nurhaida. 2014. New bio preservatives from lignocelluloses biomass bio-oil for anti termites *Coptotermes curvignathus* Holmgren. *Procedia Environmental Science* 20: 778–784.
- SNI 7207-2014 (Standar Nasional Indonesia, Indonesian National Standard). 2014. Uji ketahanan kayu terhadap organisme perusak kayu [Test for resistance of wood on wood deterioration organism]. National Standardization Bureau, Jakarta, Indonesia.
- Stolyhwo, A. and Z.E. Sikorski. 2005. Polycyclic aromatic hydrocarbons in smoked fish: a critical review. *Food Chemistry* 91: 303–311.

French beech – a new opportunity in wood housing

LANVIN Jean-Denis*, REULING Didier, LEGRAND Guillaume

FCBA
Allée de Boutaut BP 227
Bordeaux, 33028, FRANCE

ABSTRACT

Hardwood housing especially from beech is one item of possible added value products based on solid wood and / or wood reconstituted in Europe. However, design of structures requires structural product with a certified strength according to regulatory framework of CE marking. French beech forest occupies about 1.4 Mha lead mainly in regular high forests and coppices with standards with an annual volume of harvested wood (1 million m³) for a sawn timber estimated at 400000 m³. FCBA has launched since in 2011 a study to characterize the French beech as a raw material and its structural bonding. To qualify French beech species as solid wood, a national representative sampling was performed to collect 2400 lumbers (6 French areas, 21 stands, 99 trees, 3 cross-sections) and to establish visual grading rule (NF B 52 001-1 2017) for assessment in D40-D24 or D35-D18. A new table of strength classes of European hardwood (EN 338) will be proposed according to experimental results. Grading machine could be done for D50 with a good yield (38-47%). A general work plan has been developed to reach requirements for beech glulam in two steps. Firstly, the compatibility of different type I adhesives technology was studied by the way of lab tests usually performed in the field of common adhesives approval (EN 302-2). On the other hand, full scale tests according to EN 14080 have been done to characterize glulam beams (58 beams - GL32h) with verification of finger joint performance. French beech data could be merged with other hardwood data to develop a GLT CE marking standard as EN 14080 part 2 specifically devoted to hardwoods. The construction market in the future could provide an important alternative for French beech, particularly in the form of reconstituted products.

1. INTRODUCTION

For twenty years, production of hardwood sawn timber fell sharply in France. Today, industrials are rediscovering the immense potential of these species in the construction, especially in structure. Traditionally used for carpentry, furniture, stud, packaging, French hardwoods are used to new techniques such as finger jointing, panelling or by high-temperature treatment, enabling them to meet requirements and open to new markets.

In France, French Beech species occupies about 1.4 Mha [MEMENTO FCBA 2018] conducted mainly in regular high forests and coppices with standards for a volume of harvested wood estimated at 1 million m³ for 0.4 Mm³ in sawn timber. French beech occupies the second forest surface after oaks and some softwood like spruce and pine.

The essential characteristics of the beech are its hardness and facility of impregnation. It's easy to prevent stain if drying done as quickly as possible after sawing and this species lends itself well to gluing and is easy to transform (bending). Its qualities have made it a popular wood for the interior design and furniture, but these sectors have seriously declined over the past two decades.

The construction market could provide an important alternative for beech, particularly in the form of reconstituted products. Some recent initiatives have also demonstrated the importance of this species in building in France as the example of school of Tendon (88) using widely beech in structural part of the building. Other examples of beech species in structure make up a “showroom” for architects (Tisserand 2016).

Whatever technical solution used, development of structural beech requires lumber (solid or laminated wood) with a certified strength grading required in the regulatory framework of CE marking. Therefore, FCBA has launched in

* Corresponding author: LANVIN JD ; E-mail: jean-denis.lanvin@fcba.fr

2011 a study to characterize the French beech and its structural bonding in the perspective of CE marking into the following phases:

- Identify the mechanical behaviour of French beech lumber as solid wood,
- Validate the structural bonding ability of beech through laboratory tests,
- Conduct a mechanical characterization and classification of beech GluLam Timber (GLT).

2. BEECH SOLID WOOD CHARACTERIZATION

The knowledge of the capability of hardwood in structure has been based for two decades on the realization of experimental campaigns respectively for oak (Lanvin & Al 2007) and chestnut (Lanvin & Al 2015) on full size specimens coming from forest as opposed to a direct sampling in sawmill what was commonly practiced in Europe. This approach allowed:

- To know the mechanical properties of solid woods, as well as the influence of defects,
- To establish relationships between mechanical properties and silviculture (France is the only European country to perform this kind of sampling),
- To propose optimized classification rules by visual and/or machine grading.

2.1. METHODOLOGY AND DESCRIPTION OF TREES SAMPLING

Based on current volume provided by French Ministry, eight areas were selected to provide a representative sample of trees. The sample selected must indeed have at least 65% of the country's diversity to ensure the representativeness of national resource. Four trees are chosen by stand around mean DbH of the stand. An additional tree was selected in case of log splits during felling. The table 1 summarizes the sampling made by areas and the total number of collected trees. All the harvesting was made over the year 2013 and 2014. The whole logs were regrouped in log yard of sawmiller's partners for analysis (EN 1316-1) by FCBA before sawing.

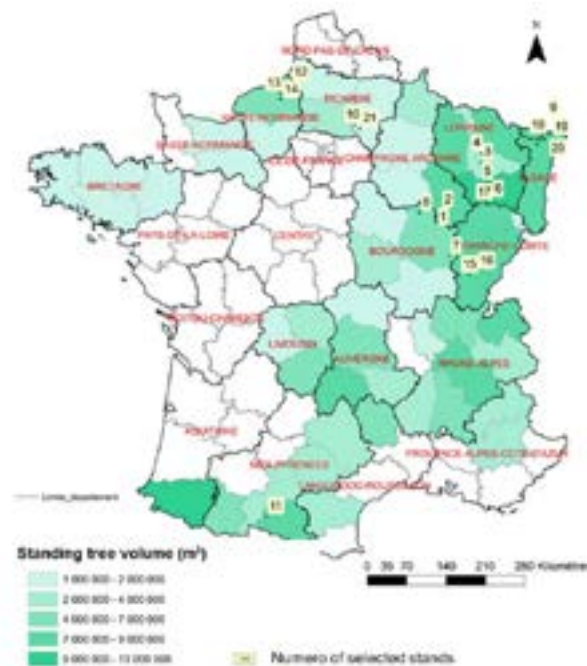


Figure 1: Localization of 21 selected stands according to the French beech resource (2012).

Table 1: description of trees by sub-samples

Area	sub sample	Stand number	Number of Trees	Mean height (m) of tree and CoV	Mean Age of tree and CoV	Mean DbH (cm) of tree and CoV
Alsace	1	9 ;18 ;19 ;20	20	27,4 - 5%	95,2 - 12%	61,7 - 18%
Bourgogne	2	7 ;8	10	18,8 - 5%	126,4 - 13%	61,6 - 8%
Champagne-Ardenne		1 ;2	7	NA	112 - 17%	70,5 - 14%
Franche-Comté	3	15 ;16 ;17	15	30,6 - 8%	110,2 - 21%	65,6 - 17%
Lorraine	4	3 ;4 ;5 ;6	20	34,1 - 15%	132,8 - 7%	56,3 - 17%
Midi-Pyrénées	5	11	5	36,2 - 4%	124,9 - 20%	53,3 - 8%
Normandie	6	12,13,14	12	36,8 - 11%	114,2 - 20%	65,1 - 13%
Picardie		10 ;21	10	32,5 - 10%	95,2 - 12%	62,4 - 13%
Total		21	99	31,9 - 20%	126,4 - 13%	61,1 - 17%

2.2. DESCRIPTION OF BENDING TESTS

Logs were sawed in 6 sawmills following the geographical localization of the sampled stands. Logs were transformed into sawing in three different cross section (48*112 ; 58*162 ; 78*220 mm²) and were dried in 14 % +/-2 % in sawmill. The difference between 2400 collected boards and the 1872 mechanical results correspond to the boards moved away because they break out of the centre part of the bending tests (122 pieces) or lack of traceability, broken piece, too distorted during drying which represent 406 pieces. On each lumber, defect measurements have been made as following to establish the visual grading criteria tables:

- Measurement of the projection of maximum knots on edge and face of lumber,
- Measurement of the other singularities (slope of grain, decay, wane, distortions),
- Annual growth rings.

All pieces were tested in bending test according to EN 408. The tests of modulus of elasticity were done according to clause number 10 in EN 408 and be calculated from the EN 384 equation, which includes an adjustment to a pure bending modulus of elasticity. The bending strength values were adjusted to a width of 150 mm (k_b -factor) and the modulus of elasticity to moisture content (U) of 12%. The following Table summarizes the mean value and the coefficient of variation of bending strength (f_m) modulus of elasticity in bending test (E_m) and density (ρ_{12}) for each sub-sample.

Table 3: Mechanical properties of French beech per sub-samples.

Sub sample	N	Moisture content		f_m		E_m		ρ_{12}	
		Mean (%)	COV (%)	Mean (MPa)	COV (%)	Mean (GPa)	COV (%)	Mean (kg/m ³)	COV (%)
1	372	10,8	11,2	79,6	32,1	14,7	15,8	723	4,9
2	275	11,6	13,5	70,0	30,6	11,7	20,1	681	6,2
3	251	9,4	17,4	69,2	37,0	12,2	24,8	711	6,1
4	524	10,3	10,6	80,2	27,2	14,5	16,1	699	5,3
5	123	10,9	13,7	70,6	30,9	14,0	15,9	715	8,3
6	327	9,0	16,7	80,2	30,9	16,1	16,9	698	5,9
Mean value	1872	10,3	15,7	76,5	31,5	14,1	20,6	704	6,1

2.3. FRENCH BEECH STRENGTH GRADING

To be used for housing market, beech lumber must be CE marked (EN 14081-1), and thus a mechanical assessment of lumber must be done by sorting through visual method (see NF B 52-001) or machine using non-destructive methods (EN 14081 (parts 2 to 4) Whatever method, a representative sample of the resource lumber will be ranked from the qualification of its intrinsic defects in several categories called mechanical classes defined in EN 338. Analysis has shown that the measurement of the defect of beech allowed a classification of wood in two mechanical ranges classes with visual method as following:

- Solid wood in carpentry and stud
 - Combination 1 : D40 & D24 or
 - Combination 2 : D35 & D18

- Solid wood for GLT
 - Combination 0 : D45

French mechanical strength classes reach German ones (DIN 4074-5). The following figure shows yields obtained by strength grading methods

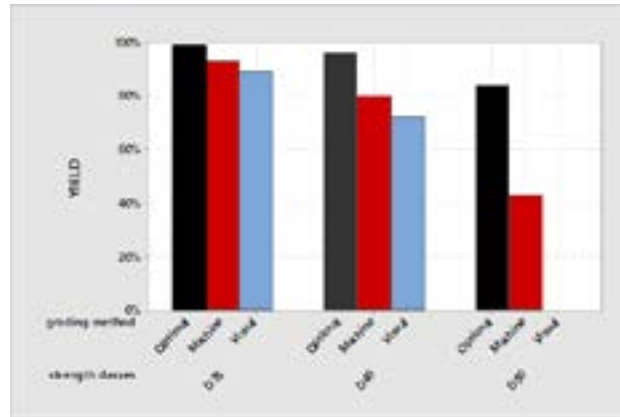


Figure 2: percentage of French beech graded lumbers per methods for EN 338 strength classes.

3. VALIDATION OF STRUCTURAL BONDING OF FRENCH BEECH

The feasibility of beech GLT structural beams relies on studying the potential of adhesive systems to fulfil the requirements of the conventional approvals for timber structures. The results of this study could be transferred, in the end, to the production of GLT beams. The compatibility of different adhesives technologies was studied by way of lab tests usually performed in the field of usual adhesives approval (EN 301, EN 15425, EN 16254) for load bearing timber structures (according to EN 302-2) on Melamine Urea Formaldehyde (MUF), Polyurethane (PUR), Resorcinol Phenol Formaldehyde (RPF) and Emulsion Polymerized Isocyanates (EPI).

Delamination requirements according to EN301 (2013) must be 5% at the maximum. The tests configurations can take into account the wood “reality” and can be performed with the lamination and glulam cross-sections and sawing patterns of the laminations conforming to the maximum sizes and the lamination sawing patterns used in the respective glued product.

PRF and MUF adhesives systems fulfil the EN301 requirements regarding resistance to delamination (Konnerth & Al 2016). It is important to emphasize that these conclusions are valid only for the adhesives tested and are not necessarily indicative of the performance of similar products. As the industrial transfer (premix or separate application, pressing time, mixing ratio) should be more convenient with the MUF adhesive system, regarding working properties, it was decided with the adhesives producers to scale up the study on MUF adhesive solutions, especially since most of French GLT plants use MUF adhesives.

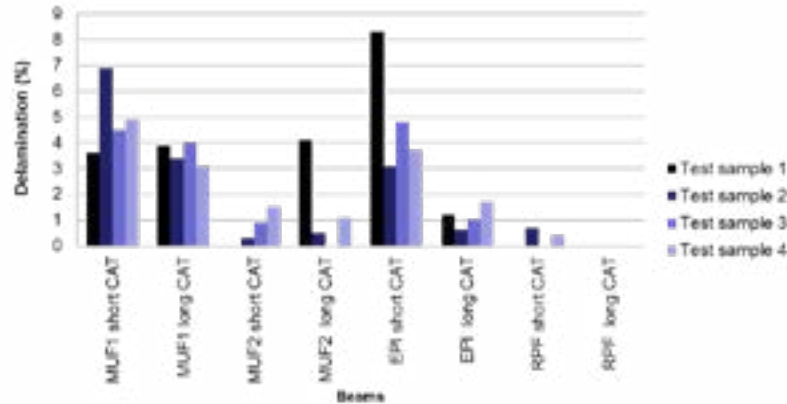


Figure 3: Delamination of beech EN 302-2 GLT for 4 kind of type I glues (cross section 24*150 mm²).

4. CHARACTERISATION OF BEECH GLT

4.1. PROTOTYPE GLT BEAMS MANUFACTURING STEP

The third step was to study the production of a large volume of two different cross sections of beams in one French plant usually producing structural glulam beams made from Spruce. Production settings should consider reduced lamellae thicknesses as compared to usual sawing from sawmills (20 mm thick raw lamellae) from D35 wood quality and one single lamellae width (115 mm).

The challenge for this study is to use length of lamellae between 500 to 960 mm in order to reduce price of beech GLT. Initial price has been found to 1500 €/m³ (Ressel 2005), the idea is to reduce by two final prices with small length solid wood. By the way, only one of French glulam manufacturer was able to produce GLT with smaller length of lamellae but the length of finger jointing is smallest too.

This production step was divided in 2 main parts as:

- One production step of beams during 2 working days, focusing on lamellae finger jointing and face gluing to lead to 2 different cross sections of beams. Have been produced in 6 m length pieces in 2016 :
 - 36 final section beams of 100 x 100 mm² in 5 lamellae
 - 22 final section beams of 100 x 260 mm² in 13 lamellae.
- One first small production of finger jointed (20 x 105 mm) samples made for defining production parameters and mechanical properties in flat bending.

This step was also finely studied according to the requirements of EN 385 and EN 386 (replaced in 2013 by EN 14080) and validated the production process applied for beech finger jointing and faces gluing for structural glulam application as following.

- Good feedback in general with the integration of the beech wood in the full production chain, by limitation of defects suppression only at the board ends (minimum distance from the base of the finger joint and a knot = 3 times diameter of knot). Due to the beech properties, it would have been better to reduce the profile machining head speed for the 10 x 3.8 x 0.6 mm profile to avoid damage on the finger joint and optimize final strength.
- Measures performed on each lamellae to control the wood planning quality, fulfil EN 386 standard requirements.

Pressure applied to the beam assembly has been increased for the use of beech to the maximal level allowed by the device. The probability to get thicker joints exists and could induce some local delamination during further tests on the beams.

4.2. TENSILE AND BENDING TESTS OF FINGER JOINTS ACCORDING TO EN 408

Due to the good performance of solid wood, the bending test quality lamella Finger jointing remains a key element of the overall mechanical performance of GLT beams tested by way of 4-point bending tests, since the failure occurs most often at the last lamella when the finger joints are in the central third highly stressed in tension.

Finger-jointed samples were tested in 4 point bending and tensile tests at initial state. The finger jointing profile used (finger length = 10 x pitch = 3.8 mm * tip width 0.6 mm) was chosen according to standardized profiles (EN 14080) and still demonstrates a very satisfactory level of performance. The final characteristic value (EN 14358) reaches 41.4 MPa, higher than the requirement for graded wood as shown below rather than for tensile results probably due to smallest length of finger joints.

Table 3: Mechanical performance on beech finger joints samples (cross section = 20*105 mm²)

	Bending	Tensile
Mean $f_{m,j}$ or $f_{t,j}$	64.5 MPa	34.0 MPa
CV%	12%	20%
$f_{m,j,k}$ or $f_{t,j,k}$ (MPa)	51.5 MPa	22.9 MPa
Number of specimens	80	27
Requirements EN 14080	41.4 MPa	25 MPa ($f_{m,k}$ (D35)/1.4)

4.3. CHARACTERISATION OF BEECH GLT

The last step was to characterize all beams produced, regarding bonding quality of gluing and overall strength of the beams. The quality of the bonded beams, proven by means of bending tests on finger jointed lamellae and delamination of glue lines, should compare to general requirements of the EN 14080 standard dedicated to softwood species and poplar.

Four point bending tests were performed in accordance with EN 408. Loads are applied perpendicular to the glue line. The following table presents results for nominal and adjusted dimension. If the overall height or depth of the glued laminated timber is less than 600 mm the 4 points bending strength parallel to the grain $f_{m,g,k}$, determined by testing, shall be multiplied by k_h . As the lamination thickness is less than 40 mm, the bending strength may be divided by k as given in formula.

$$k = \min \left\{ \left(\frac{40}{t} \right)^{0.1}, 1.05 \right\} \quad \text{and} \quad k_h = \max \left\{ \left(\frac{h}{600} \right)^{0.1}, 0.9 \right\} \quad (1)$$

Compression test have been performed on prototype beams according to the methodology given by EN 408 to estimate compressive strength as shown in the following figure.



Figure 4: Compressive test apparatus and facies of failure on beech GLT.

Table 4: Bending Mechanical behaviour for French beech GLT (MC%=12%)

Nominal Cross section	100*100 mm	100*260 mm ²	All sampling
Mean $f_{m,g}$ (MPa)	47.1	38.5	43.9
CV %	15.4%	16.1%	18.8%
$f_{m,g,k}$ (MPa)	37.5	31.5	31.8
$E_{0,g,mean}$	14230	15480	14700
CV %	6.2%	2.8%	5.4%
$E_{0,g,05}$	12300	13400	12150
$\rho_{0,05}$	670	650	655
Nb of specimen	36	22	58

 Table 5: Compression performance on beech GLT (cross section = 100*100 mm²) * softwood

	Compression strength parallel to grain	Compression strength perpendicular to grain
Mean $f_{c,0,g}$ or $f_{c,90,gt}$	55.8 MPa	10.0 MPa
CV%	7%	13%
$f_{c,0,g,k}$ or $f_{c,90,g,k}$ (MPa)	49.7 MPa	8.4 MPa
Requirements EN 14080* GL32c	32	2.5
Number of specimens	35	35

5. NEW TABLE OF STRENGTH CLASSES OF EUROPEAN HARDWOOD (EN 338)

More and more, industrial manufacturers of glulam beams classify their woods in tension (Ehrhart & Al 2018) according to methodology given by EN 14080 for softwood. At equal visual quality, we get better yield in tensile due to coefficients between the tensile values from the classes of flexural strengths with EN 384 formulas. For instance, tensile grade T21 gives characteristic bending strength equal to 29 MPa, grade D35 allow a tensile strength equal to 21 MPa.

A new French beech sample benchmarked with MTG device has been created from threes visual grades in 2019 and performed into flexion and tensile tests. The statistical analysis of curves can convert bending data to obtain tensile data using a coefficient as :

$$f_{t,0} = 0,85 * f_{m,0} \quad (2)$$

$$E_{t,0} = 0,85 * E_{m,0} \quad (3)$$

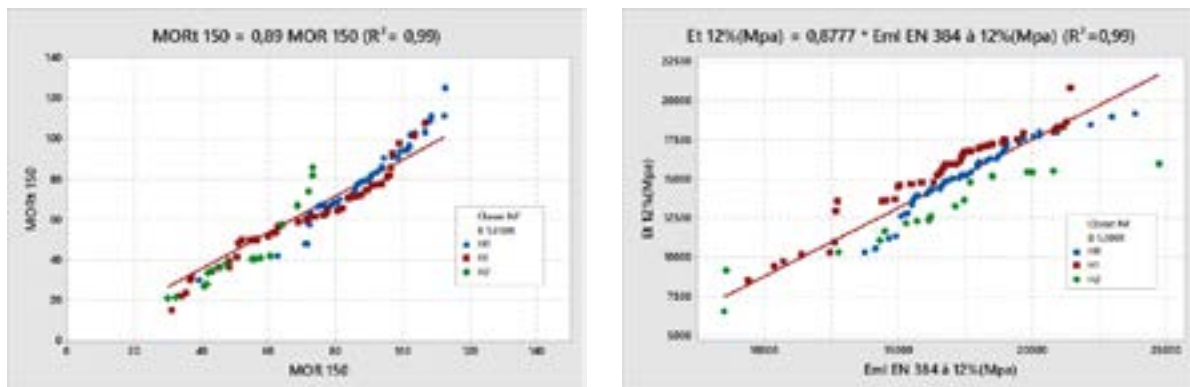


Figure 5: Correlation between mechanical properties in tensile and bending test on a specific sub-sample.

The following table summarized results and corresponding strength classes between bending and tensile but additional data could be merged to improve regression.

Table 6: Mechanical strength classes for French beech (* for softwood; + for hardwood)

French Beech visual strength classes		Test results.	Bending		Test results.	Tensile		New EN 338 strength classes+ $f_{t,k}/0.85$
			EN 338 graded	Tensile strength class from EN 384* 0.6 fm,k		EN 338 graded	Bending strength class from EN 384* 3,66+1,213ft,0,k	
LHO-D45	MOR _{0.05} MPa	68.7			47.9			
	MOE _{0.5} GPa	17.5	D50	TD27	15.1	TD45	D58	TD45-D50
	$\rho_{0.05}$ kg/m ³	620			625			
	NB	54			54			
H2-D35	MOR _{0.05} MPa	35.0			27			
	MOE _{0.5} GPa	16.8	D35	TD21	15.7	T27	D36	TD27-D32
	$\rho_{0.05}$ kg/m ³	660			645			
	NB	52			52			
H4-D18	MOR _{0.05} MPa	31.5			21.4			
	MOE _{0.5} GPa	16.3	D18	TD11	12.7	T21	D29	TD21-D24
	$\rho_{0.05}$ kg/m ³	690			645			
	NB	17			17			

6. DISCUSSIONS AND CONCLUSIONS

French Beech forest occupies about 1.4 Mha lead mainly in regular high forests and coppices with standards with an annual volume of harvested wood (1 million m³) for a sawn timber estimated at 400000 m³. The goal of French industry is to extend the knowledge of mechanical properties of French beech (already initiated in Germany), thus promoting its use in construction applications (sawn timbers, glulam beams).

A national representative sampling protocol was created in order to reach 1872 lumbers (6 French areas, 21 stands, 93 trees, 3 cross-sections) which were being bent until failure. French beech sawn timber could be graded 60% in D40 (95% in optimal) according to new visual rules published in NF B 52-001 (2017). However, strength grading machines as XYLOCLASS, MTG or ViSCAN allow also classification in D50 (37 - 48%).

A general work plan has been developed to reach requirements for hardwood glulam. On one hand, the compatibility of different type I adhesive technologies was studied by the way of lab tests usually performed in the field of structural adhesives approval according to EN 302-2. On the other hand, full scale tests have been performed to characterize glulam beams (more than 50 beams – 2 cross sections) in GL32_h according to EN 14080 requirements on glue bonding (bending tests of finger-joints, shear tests of glue lines and autoclave delamination tests) and strength (bending and compressive). Weakest point is due to smaller length for finger joints due to short length of lamellae between 500 to 960 mm in order to reduce price of beech. It is to be noted that compression strengths are very important, this characteristic is fundamental for high-rise timber construction.

French beech data will be merged with other hardwood studies in order to create a new GLT CE making standardisation devoted to hardwoods (EN 14080-2) and to upgrade EN 338 with specific thresholds.

ACKNOWLEDGEMENTS

The authors are pleased to thank on one hand Ministry of Agriculture (MINAGRI), France Bois Forêt for financial support and ONF for trees as well their come from public forest, on the other hand, Manubois, Avivés de l'Est, Scierie

et Caisserie de Steinbourg, Akzo Nobel Industrial Finishes (Antony, France), Simonin respectively for collecting the sawn timber, glue and plant for GLT part of the study.

REFERENCES

- Ehrhart T., Fink G., Steiger R., Frangi A. « Strength grading of European beech lamellas for the production of GLT & CLT » INTER/49-05-1 2016*
- Ehrhart T., Palma P., Steiger R., Frangi A. « numerical and experimental studies on mechanical properties of glued laminated timber beams made from european beech wood » WTCE 2018.*
- Konnerth, J; Kluge, M; Schweizer, G; Miljkovic, M; Gindl-Altmutter, W, Survey of selected adhesive bonding properties of nine European softwood and hardwood species, European Journal of Wood and Wood Products, 2016, vol. 74, n° 6, pp. 809-819)*
- Lanvin JD, Reuling D, Costrel Y, Ducerf J “Evaluation of French oak for structural use” Proceedings of 1st International Scientific Conference on Hardwood Processing, Quebec September 2007, pp 61-65*
- Lanvin JD, Legrand G, Simon F, Prince C, Lemaire J “Strength Assessment and Potential for Use as Glulam of French Chestnut Lumber” 5th International Scientific Conference on Hardwood Processing QUEBEC Sept. 15-17, 2015.*
- Ressel JB “High Quality Beech Glulam Production – Properties – Limitations – Prospects” COST Action E44 Wood Processing Strategy, 14-15 June of 2005*
- Tisserand F. “Valorisation des feuillus – plateforme technologique de Xertigny : un premier atelier en hêtre ». Le Bois international samedi 17 décembre 2016*

Monitoring of Birch Veneer Moisture Content During the Drying Process by Single-Sided NMR technique

Anti Rohumaa¹, Ekaterina Nikolskaya¹, Jyrki Pesonen² and Yrjö Hiltunen¹

¹FibreLaboratory,
South-Eastern Finland University of Applied Sciences,
57200 Savonlinna, Finland

²Raute Oyj,
Mecano Business,
87400 Kajaani, Finland

ABSTRACT

The evaluation of veneer moisture content before and after drying is an important issue for veneer-based product industry. Moisture content affects many veneer properties, e.g. veneer dimensional changes, bonding quality. Controlling moisture content is critical in order to be able to produce a high-quality product with the required properties and quality. However, traditionally evaluation of moisture content of wood bases on oven-drying method, which is time-consuming and sample-destructive.

*Moisture content measurement in wood and wood-based materials is a process that could be handled by nuclear magnetic resonance (NMR) technique. In present study, single-sided NMR was used in order to evaluate the moisture content of rotary cut birch (*Betula pendula* Roth.) veneer during drying process at ambient conditions. The results show that the NMR signal correlates well with moisture content of veneer obtained by oven-drying method. Hence, the single-sided NMR technique can be used for the robust and rapid determination of water content in veneer during the drying process, and that it can be considered as being a routine instrument for testing veneer quality in the production of veneer-based products.*

1. INTRODUCTION

The moisture content of wood material is an important factor affecting many properties of wood-based products and its processing. Hence, proper drying of wood veneers plays a crucial role in successful production of veneer and veneer-based products. The control of drying process and its parameters is critical in order to produce a high-quality product.

Traditionally in research, oven drying method has been used in order to measure the total moisture content of wood and wood-based products as the most accurate method. However, it is time-consuming and sample-destructive. In veneer-based products industry, several methods are in use (mainly based on microwave techniques or measurement of the electrical resistance of wood) for online measurement of veneer moisture content. Unfortunately, the described methods do not give information where the moisture locates, in cell wall or lumens. This information could provide understanding in order to optimise industrial drying process and veneer behaviour during drying.

Several researchers have shown that water in wood and wood-based products can be measured with nuclear magnetic resonance (NMR) technique, e.g. from untreated, acetylated and furfurylated wood (Labbé et al. 2002, Thygesen and Elder 2008, Thygesen and Elder 2009). NMR can distinguish water-bound hydrogen located in different physical and chemical environments and allows measuring the total wood moisture content and the distribution of water in cell walls and lumens (Labbé et al. 2002). According to Menon et al. (1987) NMR evidence indicates, that the ¹H NMR signal from water in wood may be separated on the basis of spin-spin T₂ relaxation times into the bound water (associated with wood cell walls) and lumen water (associated with free water in the cell lumens). Hence, the T₂ relaxation times provide detailed and quantitative information. However, time-domain NMR has shown to be very robust approach for measuring water content in wood (Nikolskaya et al., 2012). These NMR methods are non-invasive and non-destructive, however, they could need some simple sample preparation procedures. The technology based on single-sided NMR, has all above-mentioned advantages. Moreover, it does not require any preliminary sample

preparation, there is no limitation towards the sample size and it could measure water content at different depths inside the sample.

In this study the moisture content of green and rewetted veneer was measured with the help of single-sided NMR in order to evaluate the natural variability of moisture content inside of veneer prepared under the industrial conditions. Obtained information will be utilised in the future by veneer processing industry and technology companies in order to develop optimized process control systems.

2. MATERIALS AND METHODS

2.1. WOOD MATERIAL

Industrially prepared birch (*Betula pendula* Roth) veneer sheets were used in the present study. Logs were felled during winter and spring season. The storage of logs was conducted for approximately 1-2 months in log yard before soaking process at 40 °C was performed. After peeling the five wet veneer sheets by 100 x 100 mm and 1.5 mm thickness were obtained for NMR measurements. Additionally, five similar 100 x 100 mm pieces were directly sent to the oven for drying in order to verify the initial moisture content.

NMR measurements were made for all five samples continuously one after other by placing the NMR sensor above the sample, so the deformations of veneers that might occur during drying would not affect the measurements. NMR measurements of samples were done immediately after preparation and afterwards in every 30 min during the first 3 h of air-drying. The last NMR signals were obtained in 4 h of air-drying. Between the NMR measurements samples were kept in the special rack, in order to secure even drying process for each veneer sheet.

After 4 hours of drying, the samples were photographed and oven dried at 103 °C in order to obtain the moisture content 0%. This procedure was conducted four times at different days in order to obtain information about the natural variability of material used in plywood mill during springtime. Additionally, three oven-dried samples from first, second and third experiments were rewetted and then measured during air-drying again.

2.1. NMR TECHNIQUE

NMR measurements were made by a single-sided NMR sensor from Resonance Systems Ltd (Fig. 1). Single-sided NMR sensor consists of a set of magnet bars of special geometry and organization, that a magnetic field is generated in nearly parallel plane to the surface of the sensor (X-Y plane in Figure 1). The maximum depth of penetration for this sensor is approximately 3 mm. The sensitive slice is about 20 x 20 mm² in the central area of the sensor. The NMR sensor was tuned and calibrated so that the maximum sensitivity was at the thin slice, at about 1.3 mm over the surface. This corresponds to the frequency of ¹H protons of 19.4 MHz. A standard pulse sequence CPMG was used to measure NMR magnetisation decays. After removing of first obtained 10 signal points, measured decays were fitted by mono-exponential functions, and the spin-spin relaxation time T₂ values were solved.

Average amplitude (A_{mean}) was calculated between 8th and 12th points with subtracting the noise

$$A_{\text{mean}} = A_{\text{mean signal}} - A_{\text{mean noise}} \quad (1)$$

The moisture contents (mc) of the veneers were calculated:

$$mc = \frac{(W_{\text{wet}} - W_{\text{dry}})}{W_{\text{dry}}} * 100\% \quad (2)$$

where W_{wet} is the original weight of wet sample, W_{dry} is the weight of dried sample, determined by drying for 24 h at 103 °C in an oven. W_{wet} was measured before and after each NMR measurement, and mc for each experimental point was calculated as average between these two values.

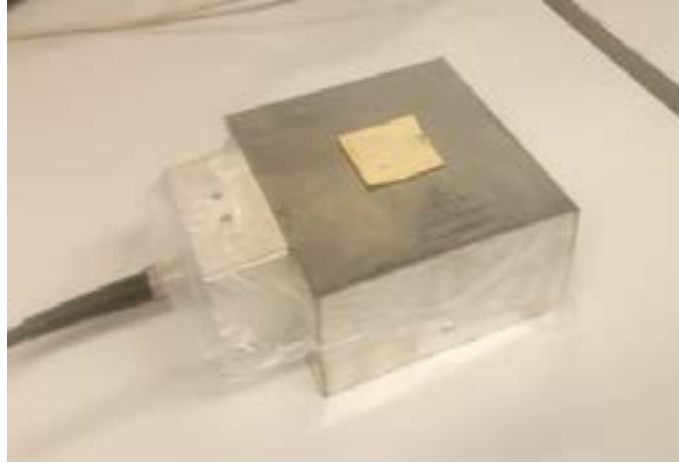


Figure 1: Single-sided NMR sensor with wood sample on top of it.

4. RESULTS AND DISCUSSION

The results of the study show that there are variations in the initial mc of veneer measured from the separate sheets (Fig 2). This is mainly caused by moisture evaporation during the sample preparation process. However, the results clearly show that this process was quick since the initial mc was still around 65-75%. According to the literature, the average moisture content of freshly felled birch varies between 71 - 80% (Jalava 1932, Hakkila 1962, Kärkkäinen 2007)

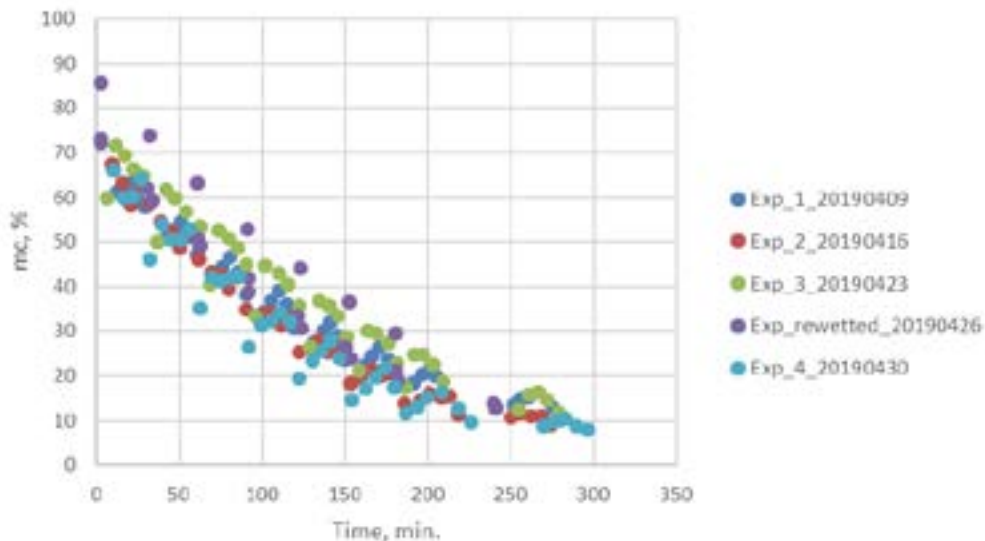


Figure 2: Air-drying curves of veneers delivered from the industry to laboratory on four different days (Experiments 1 to 4) and curve received from oven-dried and rewetted veneers samples.

The results also show (Fig 2.), that the final mc of veneers after air-drying at ambient conditions for 4 h reached 10%. Rewetted samples had higher initial moisture content, but after 4 h drying quickly reached similar values as initially wet samples.

Measured signals were fitted by mono-exponential functions, and the spin-spin relaxation time T_2 values were solved. The fastest decaying signal with the shortest T_2 corresponds to the driest sample. It is consistent with the NMR relaxation theory, according to which, T_2 is the characteristic of mobility of ^1H protons. A longer T_2 value corresponds to a higher molecular mobility. When veneers samples are saturated with water, large fraction of free water is contained

in the porous system, and this water is highly mobile, so the observed T_2 is longer. When the sample is dried, water remains in the smaller pores, and its mobility is restricted, so T_2 is shorter.

Interestingly, different sets of samples obtained at different days act differently at the same testing and measurement conditions. Fig 3 shows, that Exp 1 and Exp 4 data shows similar trends. However, Exp 2, Exp 3 and rewetted samples had different trend. This is related to mobility of free water in veneers. In Exp 1 and Exp 4 water is more mobile.

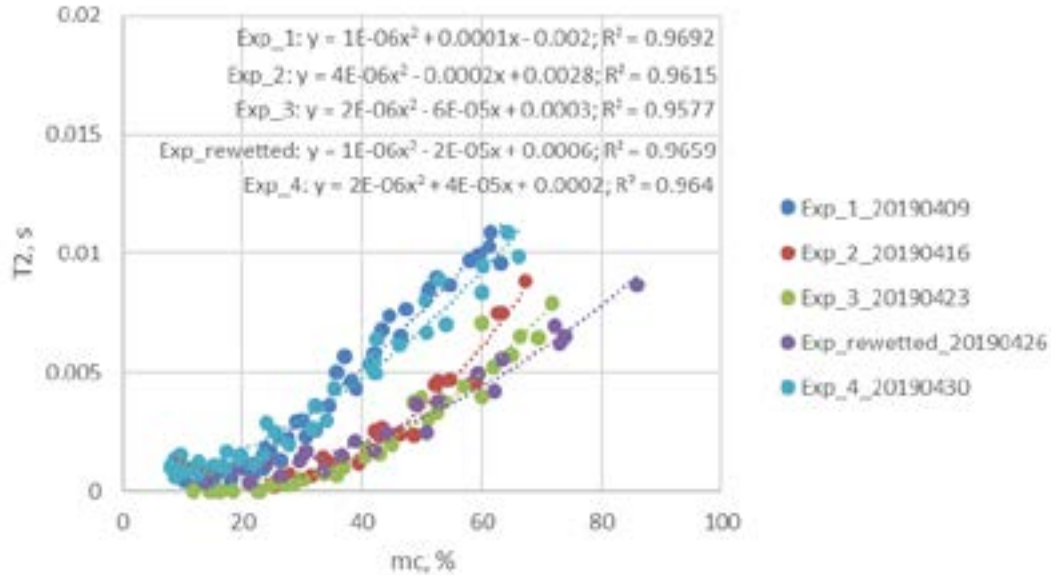


Figure 3: Dependence of T_2 on moisture content for different experiments.

Prior to the drying tests, a calibration between water contents and NMR parameter (spin-spin relaxation time) was performed. Several NMR pulse sequences and measurement settings were tested for finding the best measurement conditions. The spin-spin relaxation time T_2 showed linear correlation with water content with very high correlation coefficient ($R^2 = 0.9172$). The calibration between water content and relaxation time T_2 is given in Fig 4.

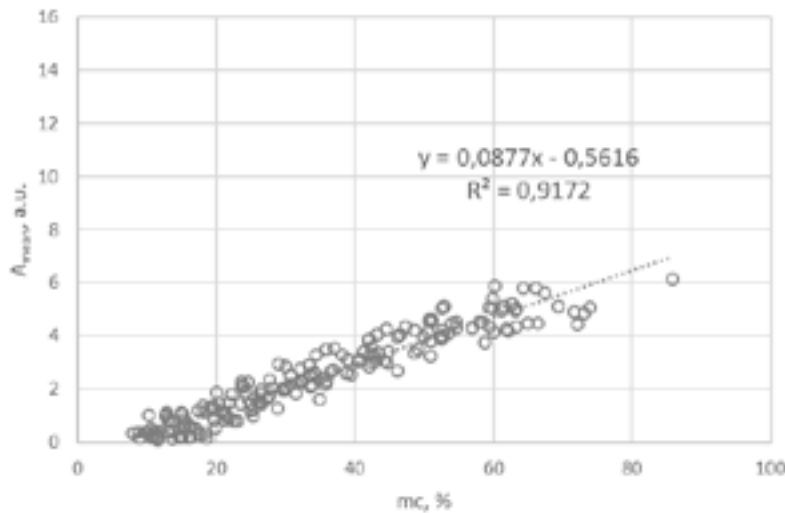


Figure 4: Dependence of average signal magnitude A_{mean} on moisture content. All points from all conducted experiments are presented in this correlation

For the development of a real application based on this NMR technology to monitor the drying process precise sensor calibration, finding of a proper measurement and fitting conditions giving minimal errors, and accurate models between NMR parameters and water contents of different wood types would be required.

6. CONCLUSIONS

The acquired preliminary results show, that single-sided NMR is a promising technique for analyzing water content in wood veneer and observation its drying process. However, more studies should be conducted using different wood materials to get more general calibration models between water content and NMR parameters.

The results show that the NMR could detect differences in moisture behavior in different sets of veneers. This is hardly possible to measure with traditional methods used in veneer-based products industry. Understanding veneer moisture relation more accurately allows developing new and optimized processes for veneer-based product industry.

ACKNOWLEDGEMENTS

This research was funded by The Regional Council of South Savo (Finland), European Regional Development Fund (ERDF), and partner companies.

REFERENCES

- Hakkila, P. 1962. Forest seasoning of wood intended for fuel chips. *Metsätutkimus laitoksen julkaisuja, Helsinki* 54:1-82.
- Jalava, M. 1932. Changes in the moisture content, volume and form of wood. *Valtioneuvoston kirjapaino, Helsinki* 18:1-57.
- Kärkkäinen, M. 2007. *Wood structure and properties*. Karisti Oy, Hämeenlinna: 468.
- Labbé, N., B. Jéso1, J-C. Lartigue1, G. Daudé1, M. Pétraud, M. Ratier. 2002. Low Field 1H NMR Analysis of Maritime Pine Wood. *Holzforschung*. 56, pp. 25–31.
- Menon, R.S., A.L. MacKay, J.R.T. Hailey, M. Bloom, A.E. Burgess and J.S. Swanson. 1987. An NMR determination of the physiological water distribution in wood during drying. *J. Appl. Pol. Sci.* 33, 1141–1155
- Nikolskaya E., Y. Hiltunen, L. Grunin. 2012. Time-domain NMR Method of Water Content Determination of Wood and Peat Based Fuels for On-line Process Control. *The 53rd ENC Experimental Nuclear Magnetic Resonance Conference, Miami, Florida, April 15-20, 2012*.
- Thygesen, L.G. and T. Elder. 2008. Moisture in untreated, acetylated, and furfurylated Norway spruce studied during drying using Time Domain NMR. *Wood Fiber Sci* 40:309–320
- Thygesen, L.G. and T. Elder. 2009. Moisture in untreated, acetylated, and furfurylated Norway spruce monitored during drying below fiber saturation using time domain NMR. *Wood Fiber Sci* 41:194–200
- Wang, P.C. and S.J. Chang. 1986. Nuclear Magnetic Resonance Imaging of Wood. *Wood and Fiber Science*. 18(2), pp. 308-314.



Session III

Wood coloring by reactive stains

Study on the wettability of Pannónia poplar (*P.x euramericana* Pannónia) from two Hungarian plantations: Győr and Soltvadkert

Use of northern hardwoods in glued-laminated timber: a study of bondline shear strength and resistance to moisture

Lathe Checks Formation, Measurement and Effect on Plywood Quality - European Hardwoods

High-value composite products from fast growing Eucalyptus trees

Mechanical performance of wood-based products fabricated with Portuguese Poplar

Vertical Forest Engineering: Applications of Vertical Forests with Self-Growing Connections in High-Rise Buildings

Biodynamic timber sheet pile – vegetation retaining structure

Wood coloring by reactive stains

Roberta Dagher^{1*}, Tatjana Stevanovic², and Véronique Landry³

¹NSERC/Canlak Industrial Research
Chair in interior wood-product
finishes
Renewable Materials Research
Center (CRMR)
Quebec Center for Advanced
Materials
Department of Wood and Forest
Sciences
Laval University
Quebec, Quebec, G1V0A6, Canada

²Renewable Materials Research
Center (CRMR)
Quebec Center for Advanced
Materials
Department of Wood and Forest
Sciences
Laval University
Quebec, Quebec, G1V0A6, Canada

³NSERC/Canlak Industrial Research
Chair in interior wood-product
finishes
Renewable Materials Research
Center (CRMR)
Quebec Center for Advanced
Materials
Department of Wood and Forest
Sciences
Laval University
Quebec, Quebec, G1V0A6, Canada

ABSTRACT

The appearance of interior wood products (e.g.: furniture and floors) is often the first criteria that affects customer's interests while making a purchase. One way to diversify the colors and appearances of wood products is by using reactive stains. These coloring systems, consisting of aqueous solutions of metal salts, can penetrate wood and react with its phenolic compounds by forming metal complexes. The color of wood obtained depends on the type of phenolic compounds, type of metal salt, wood surface preparation, temperature, wood humidity, and others. In order to determine the relationship between the structural characteristics of the phenolic compounds and the color developed on wood surface, the polyphenols of two North American hardwood species were extracted and analyzed by different spectrophotometric methods and by liquid state phosphorus-31 nuclear magnetic resonance (NMR) spectroscopy. The chromatic coordinates (CIELAB system) of wood colors obtained after application of reactive stains were compared for these hardwood species. A better knowledge of the reaction mechanisms and the factors influencing them, will allow the optimal use of these systems in wood finishing industries. Since the colored products are present in the wood structure, the wood grain appearance will be preserved or even be accentuated. Enhancing the natural and warm aspect of wood used in buildings interiors can contribute to the well-being of the consumers and promote furthermore the use of this biosourced material.

1. INTRODUCTION

Wood's natural appearance is perceived by the consumers as being warm, welcoming and relaxing (Rice 2006). Therefore, the wood finishing industries seek to diversify wood's color and appearance while preserving or enhancing its natural traits. Wood coloring systems that are most commonly used in industries consist of solvent- or water-based dispersions containing dyes and/or pigments that are applied to wood's surface.

Alternative dyeing systems that can modify wood's color instead of depositing colored substances on its surface, have been developed and discussed in the literature. Two well known methods for wood color's darkening are wood fuming with ammonia (Miklečić, Španić, and Jirouš-Rajković 2012; Weigl et al. 2012; Čermák and Dejmál 2013) and heat treatments of wood at high temperatures (Čermák and Dejmál 2013; Kučerová et al. 2016; Ayadi et al. 2003). The color modification of wood resulting from these treatments is related to changes in the chemical composition of the structural and extractables substances in wood (Barcák, Gašparík, and Razumov 2015; Matsuo, Umemura, and Kawai 2012; Weigl, Pöckl, and Grabner 2009; Kučerová et al. 2016). Both treatments are limited by the shifting of wood color toward brown and black shades (Ayadi et al. 2003; Weigl et al. 2012; Miklečić, Španić, and Jirouš-Rajković 2012). A larger variety of color hues have not been obtained on wood by these treatments.

Heat treatments influence several mechanical properties of wood (Tjeerdma et al. 1998; Del Menezzi et al. 2009; Kučerová et al. 2016). Kučerová et al. (2016) have reported a slight increase in the bending strength (MOR) and the modulus of elasticity (MOE) with the initial increase of temperatures for heat-treated Fir wood but both properties showed reduced values following the treatment at higher temperatures. Esteves et al. (2008) have also investigated the changes in mechanical properties of heat-treated pine wood and have reported the decrease of the MOR and MOE. They also reported the decrease in wettability which influences the gluing and finishing of wood.

* Corresponding author: E-mail: roberta.dagher.1@ulaval.ca 144

The decrease in moisture content of heat-treated wood resulted in improved dimensional stability and durability. Ammonia treatment does not influence significantly the mechanical properties of wood while it improves the aesthetic properties and is considered therefore a milder treatment than heat treatment (Weigl et al. 2012). Due to the possible health and environmental risks associated to ammonia exposure, researchers have investigated alternative methods for wood color modification (Machová et al. 2019).

Another possible method for wood coloring is the application of metal salts aqueous solutions to wood's surface (Figure 1) (Leach 1988). These solutions, when applied on wood's surface, can react with the polyphenols present naturally in wood by forming colored complexes (Krilov and Gref 1986; Andjelkovic et al. 2006; McDonald, Mila, and Scalbert 1996). Therefore, the color of wood is modified due to the formation of new colored products and the resulting color depends on the structures of the complexes formed (Malesev and Kuntic 2007; Perron and Brumaghim 2009; Hider et al. 1981). According to Malesev and Kuntic (2007), the intensity and the hue of the colored complexes depend on the chemical structure of the polyphenols and the properties of the metal ion. More precisely, the number and the position of the hydroxyl groups present in polyphenols structure influence the length of the conjugated Pi-bond system and consequently influence the absorption intensity of the complexes. Due to the variation of the quantity and type of polyphenols from one species to another (Stevanović and Perrin 2009), the color of wood obtained by metal salt treatment is strongly dependent on the type of species treated. Other factors, such as wood's surface preparation and drying temperatures can also influence the resultant colors of wood.



Figure 1: Wood coloring by reactive stains

The objective of this study was to determine the phenolic substitution patterns of the polyphenols present in two North American hardwood species, that can be responsible of the differences in colors obtained following the treatment by metal salts solutions. Liquid state phosphorus-31 nuclear magnetic resonance (NMR) spectroscopy was used to analyze the crude ethanolic extracts of the heartwood and sapwood of White oak and Yellow birch.

2. MATERIAL AND METHODS

2.1 EXTRACTIONS

Lumber of two North American species White oak (*Quercus alba* Linnaeus) and Yellow birch (*Betula alleghaniensis* Britton) that do not include any defects were used for these experiments. Sapwood and heartwood of the two wood species were separately milled with a Fritsch cutting mill (Model PULVERSISSETTE 19) then sieved. The fractions with particle size between 250 μm and 425 μm were selected and then stored in darkness at -5 °C.

For each type of wood, 15 g of ground wood were extracted at room temperature with 150 mL of 95% aqueous ethanol with continuous shaking (250 RPM) on an orbital shaker (Barnstead Lab Line model 4633) for 24 h. After filtration on a Büchner funnel by vacuum through a Whatman No. 4 paper, the wood powder was additionally washed with 75 mL of 95 % aqueous ethanol. Ethanol was evaporated by vacuum on a rotatory evaporator at 40 °C and the extract was then dried in a vacuum oven at 40 °C until the weight remained constant. All extracts were stored at -20 °C in darkness prior to experiments. The moisture content was determined following the standard method by oven drying at 104°C.

2.2 PHENOL CONTENT

The total phenol content was quantified by the spectrophotometric method of Folin Ciocalteu as described by Royer et al. (2011). The extract solutions were prepared at 200 $\mu\text{g/mL}$ in methanol and the Folin Ciocalteu reagent was diluted 10 times in distilled water. 2.5 mL of Folin reagent was added to 500 μL of the extract solution followed by 2 mL of sodium carbonate solution (75 g/L). The mixture was heated to 50 °C for 10 min. A Varian Cary 50 UV-Vis spectrophotometer was used to read the absorbance at 760 nm. Gallic acid was used to prepare the calibration

curve ($y = 0,0103x + 0,0263$; $R^2 = 0,9982$). The results are expressed as mg equivalent of gallic acid per gram of dry extract (mg GA/g dry extract).

2.3 TANNIN CONTENT

The polyvinyl polypyrrolidone (PVPP) method was used to quantify the total tannin content (Royer, Diouf, and Stevanovic 2011). The PVPP was added to the extract solutions (200 $\mu\text{g/mL}$ in methanol) to precipitate the tannins. The mixture was centrifuged (3000 g, 10 min, 4 °C) and the supernatant was collected and analyzed by the Folin Ciocalteu method. The total tannin content corresponds to the difference between the total phenol content of the extract and the phenols remaining in the supernatant.

2.4 ^{31}P NMR ANALYSIS

^{31}P NMR analysis were performed according to the method described by Melone et al. (2013b). The solvent used was a mixture of pyridine d_5 and CDCl_3 (1.6/1, v/v). For each extract, 10 to 15 mg is weighed and dissolved in 500 μL of the solvent mixture. 100 μL of the standard solution was added followed by addition of 100 μL of the phosphorylating agent 2-chloro-4,4,5,5-tetramethyl-1,3,2-dioxaphospholane (Cl-TMDP). The internal standard used was endo-*N*-hydroxy-5-norbornene-2,3-dicarboximide (0.1 mol/L). Cr (III) acetylacetonate (5 mg/mL) was added as a relaxation agent. The liquid phase ^{31}P NMR analyses were performed on a NMR Agilent DD2 spectrophotometer 500 MHz with a relaxation time of 15 s, a pulse width of 45° and application of line broadening of 4 Hz. The signal at 132.2 ppm corresponding to the reaction product of water with Cl-TMDP was used as a reference for all the chemical shifts reported in this study.

2.5 COLOR MEASUREMENTS

Color measurements were performed with a X-rite spectrophotometer (model Ci6x) used in SPIN mode. The standard illuminant D65 was chosen with an angle of observation of 10° . Colors were expressed in the CIELab color space (Figure 2) with the coordinates a^* , b^* and L^* respectively defining the red/green, yellow/blue and lightness values.

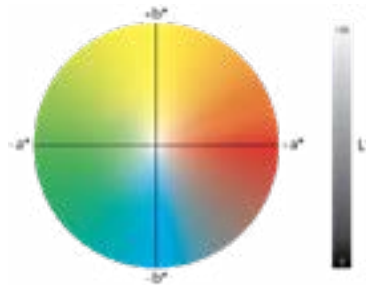


Figure 2 : CIELab color space (Image prepared by Jeremy Winninger)

Ten color measurements were taken on each wood sample. The following equations were used to calculate the color differences of wood surface before and after application of metal salts:

$$\Delta a^* = a_1 - a_2 \quad (1)$$

$$\Delta b^* = b_1 - b_2 \quad (2)$$

$$\Delta L^* = L_1 - L_2 \quad (3)$$

Where a_1 , b_1 et L_1 are the chromatic coordinates of the untreated wood samples. The a_2 , b_2 and L_2 are the chromatic coordinates of the samples after treatment with reactive dyes. The total color change of the sample after treatment with reactive dyes compared to the colors of the untreated wood are expressed as ΔE :

$$\Delta E = \sqrt{(\Delta a^*)^2 + (\Delta b^*)^2 + (\Delta L^*)^2} \quad (4)$$

3. RESULTS AND DISCUSSION

3.1 COLOR MEASUREMENTS

The application of reactive dyes on the surface of wood boards of white oak and yellow birch modified the natural wood color for both wood species. The values of the chromatic coordinates L^* , a^* and b^* (Figure 3) decreased for both wood species. The decrease of L^* ($\Delta L^* > 0$) indicates a darker wood color after application of reactive dyes. The decrease of a^* ($\Delta a^* > 0$) indicates a shift in wood's color to green shade and the decrease of b^* ($\Delta b^* > 0$) value indicates a shift toward blue shades. The total color change is higher for white oak ($\Delta E = 29.44 \pm 2.71$) than for yellow birch ($\Delta E = 8.31 \pm 0.66$).

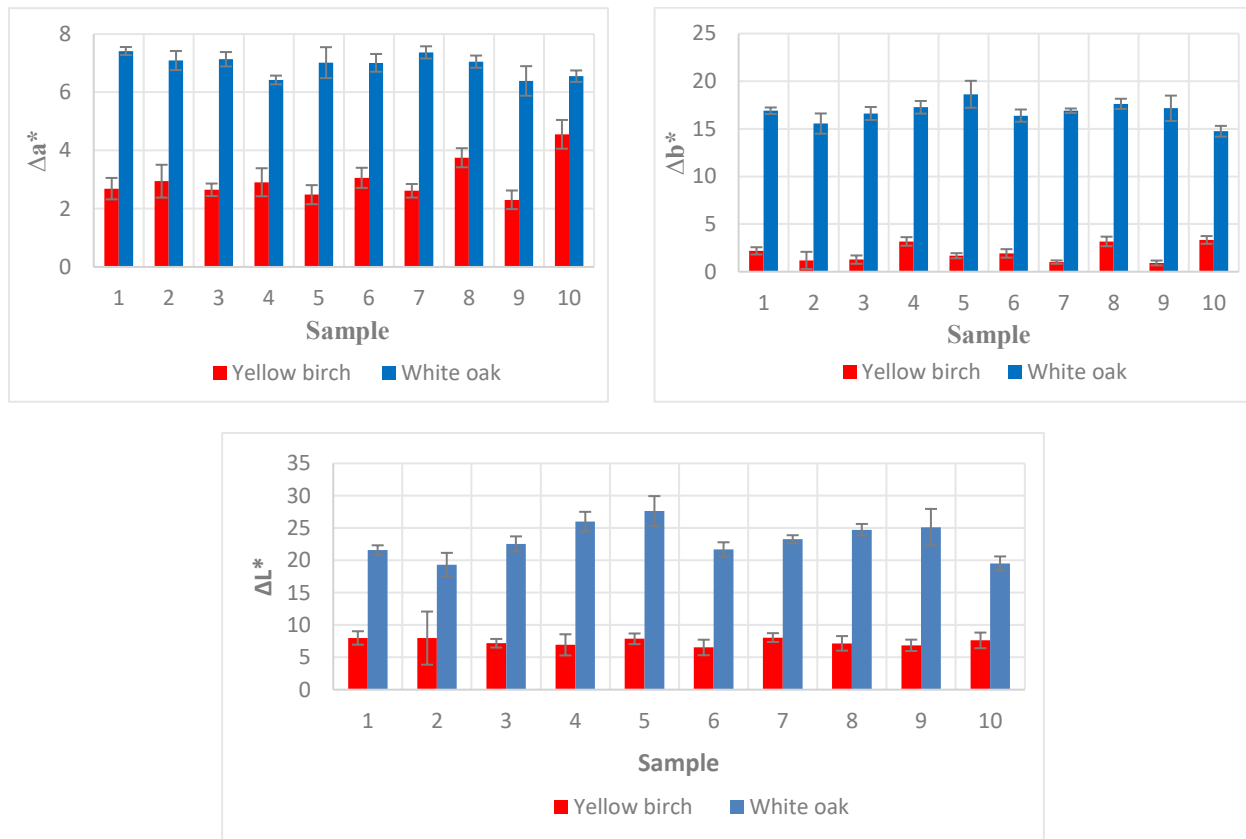


Figure 3 : Chromatic coordinates difference for wood's color before and after application of reactive dyes

3.2 POLYPHENOLS ANALYSIS

The extraction yields and the results of the total phenol and tannin content of the heartwood and the sapwood of white oak and yellow birch are presented in Table 1. The yield obtained for the heartwood of yellow birch was higher than for the sapwood. As for white oak, the yield obtained was higher for the sapwood than the heartwood. Although it was mostly demonstrated in the literature that the heartwood contains a higher amount of extractives than the sapwood (Panshin and Zeeuw 1980), multiple factors can influence the results for different wood species. In the case of white oak, the presence of tyloses in the heartwood (Pallardy 2008) can limit the penetration of the solvent and therefore result in a lower yield of extractives.

Table 1: Extraction yield and polyphenolic composition of extracts of the heartwood and sapwood of white oak and yellow birch

Wood coloring by reactive stains

Extracts		Yield (%)	Phenol content (mg GA/g dry extract)	Tannin content (mg GA/g dry extract)
White oak	Heartwood	2.6 ± 00	443 ± 21	367 ± 23
	Sapwood	3.9 ± 0.1	208 ± 14	155 ± 12
Yellow birch	Heartwood	1.7 ± 0.0	258 ± 12	128 ± 7
	Sapwood	1.4 ± 0.0	153 ± 6	82 ± 7
Oligopin®		-	682 ± 4	625 ± 1

Results are presented as means of triplicates with standard deviation

The ethanolic extracts of the heartwood and the sapwood of the two wood species were analyzed by ³¹P NMR after phosphorylation with Cl-TMDP. This technique has been widely used to study the structure of lignin (Pu, Cao, and Ragauskas 2011; Argyropoulos 1994; Koumba-Yoya and Stevanovic 2017; Crestini and Argyropoulos 1997). Melone et al. (2013) have demonstrated the possibility of using this analytical technique for the chemical characterization of tannins. In this study, we have applied this method to analyze the crude extracts of wood and to determine quantitatively the different OH substitutions in the structures of the polyphenols present in the extracts. The signals obtained in the spectra were attributed to aliphatic OH, phenolic OH and OH from carboxylic acids according to the chemical shifts presented in Table 2. The quantitative analysis was done by the integration of different signals and the calculation according to the precise quantity of internal standard added to the sample.

Table 2: Signals attribution for ³¹P NMR spectra (Melone et al. 2013a, 2013b; Pu, Cao, and Ragauskas 2011)

Signals	Chemical shifts (ppm)
Aliphatic OH	150.0 – 145.4
Phenolic OH	144.0 – 137.0
Ortho di-substituted OH	142.46 – 141.06
Ortho substituted OH	140.6 – 137.59
Ortho substituted OH (catechol)	140.2 – 138.3
Ortho unsubstituted OH	137.72 – 137.4
COOH	135.5 – 134.0

The total phenol content determined by the spectrophotometric method of Folin Ciocalteu (Table 1) and by ³¹P NMR (Table 3) showed that the heartwood of oak wood has a higher phenol content than the heartwood of yellow birch. The sapwood of white oak also has a higher phenol content than the sapwood of yellow birch. The phenol content obtained for the sapwood was lower than the heartwood for the two wood species. The ³¹P NMR spectra of the ethanolic extracts of the heartwood and the sapwood of the two species (Figures 4 and 5) showed signals in the aliphatic OH, phenolic OH and COOH regions. The comparison of the signals corresponding to the specific types of substitutions of OH showed remarkable differences between the two wood species. The ortho-disubstituted OH signals were present intensely in the spectra of the heartwood of white oak (Figure 4a) and barely present in the spectra of the heartwood of yellow birch (Figure 5a). As for the non-substituted OH, the signals were more intense in the heartwood of yellow birch (Figure 5a) than for white oak (Figure 4a). The signals corresponding to the substituted OH signals were present in the spectra of the two wood species.

The quantitative analysis (Table 3) of the signals showed that the quantity of di-substituted OH present in the ethanolic extract of the heartwood of white oak wood (1.42 ± 0.09 mmol/ g extract) was almost 10 times higher than in the heartwood of yellow birch (0.15 ± 0.03 mmol/ g extract). As for the non-substituted OH, the quantity present in the ethanolic extract of yellow birch (1.01 ± 0.16 mmol/ g extract) was almost 10 times higher than for white oak (0.11 ± 0.01 mmol/ g extract). These results show the presence of di-substituted phenolic compounds in white oak's extracts that can stabilize the metal complexes formed and be responsible of the more intense color change compared to yellow birch (Fiuza et al. 2004).

Moreover, the comparison of the signals in the phenolic OH region of the ³¹P NMR spectra obtained for the crude ethanolic extract of the heartwood of white oak with the signals obtained for different model compounds in the study of Melone et al. (2013b) showed that the two most intense signals in this region at 139.15 ppm and 141.6

ppm correspond to the ortho-substituted and di-substituted OH specific to the ellagic phenolics. The signals at 138.4 ppm and 141.4 ppm are typical of gallate residues. These results can confirm the presence of ellagitannin, a specific type of hydrolysable tannin in the heartwood of white oak.

Table 3: OH content of phosphorylated ethanolic extracts of the heartwood and sapwood of white oak and yellow birch

Extracts		OH (mmol / g extract)					
		Aliphatic	Phenolic	Ortho di-substituted	Ortho-substituted catechol	Ortho-unsubstituted	COOH
White oak	Heartwood	7.41 ± 0.7	4.74 ± 0.34	1.42 ± 0.09	1.54 ± 0.11	0.11 ± 0.01	0.74 ± 0.18
	Sapwood	14.88 ± 0.1	2.84 ± 0.12	0.57 ± 0.02	0.97 ± 0.03	0.06 ± 0.01	0.42 ± 0.01
Yellow birch	Heartwood	5.43 ± 0.42	3.61 ± 0.45	0.15 ± 0.03	0.56 ± 0.08	1.01 ± 0.16	0.52 ± 0.06
	Sapwood	8.77 ± 0.27	2.11 ± 0.07	0.19 ± 0.00	0.79 ± 0.04	0.14 ± 0.01	0.55 ± 0.01

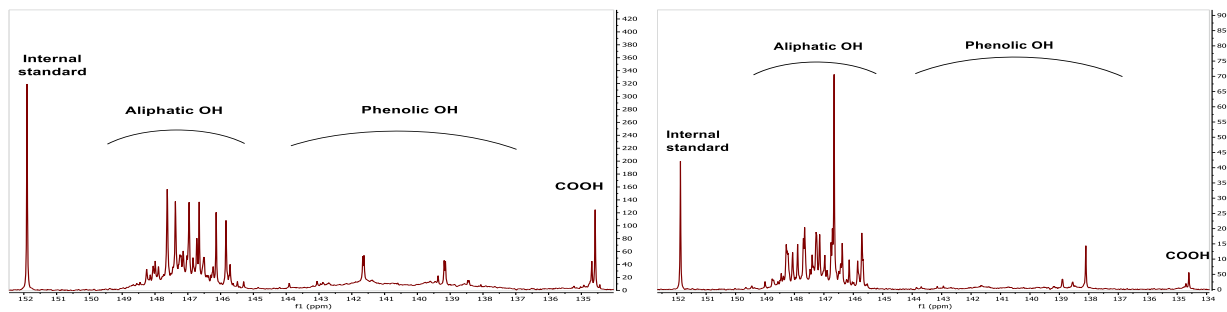


Figure 4: ^{31}P NMR spectrum of the phosphorylated ethanolic extract of the heartwood (a) and softwood (b) of white oak

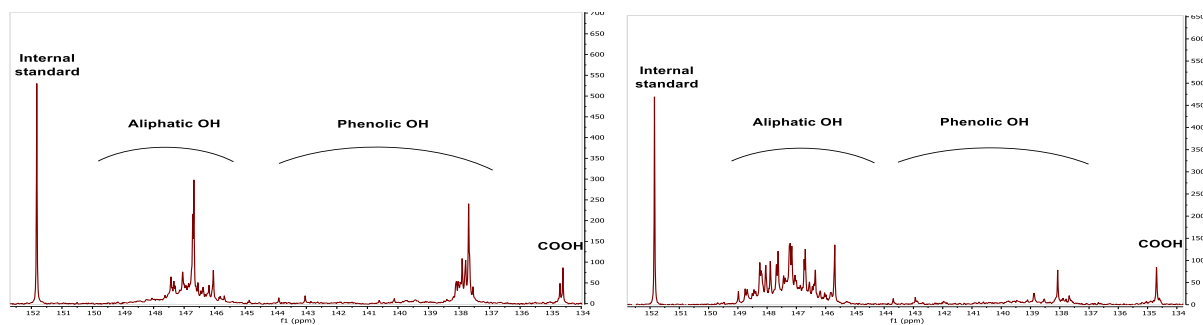


Figure 5: ^{31}P NMR spectrum of the phosphorylated ethanolic extract of the heartwood (a) and softwood (b) of yellow birch

4. CONCLUSION

The chemical characterization of ethanolic extracts of Yellow birch and White oak wood, after phosphorylation with Cl-TMDP by ^{31}P NMR spectroscopy, indicate the differences in the OH substitution patterns of their polyphenols. The presence of OH ortho di-substituted, OH ortho-substituted or OH ortho-unsubstituted can influence the capacity of polyphenols in forming metal complexes. Therefore, the intensity and hue obtained on wood's surface following the application of reactive stains will be dependent on the wood species treated. The better

understanding of the reaction of polyphenols with metal salts and the factors influencing them, will allow the optimal control of the colors obtained in wood finishing industries while using reactive stains.

ACKNOWLEDGEMENTS

This project was funded by NSERC and our industrial partners Canlak, Boa-Franc, EMCO-Inortech, Portes Lambton and Canadel. Thank you to Yves Bédard for assistance with the lab work, Luc Germain, Daniel Bourgault David Lagueux for assistance in wood samples preparation and to Stéphanie Vanslambrouck for assistance with the NMR analyses.

REFERENCES

- Andjelkovic, M, J Vancamp, B Demeulenaer, G Depaemelaere, C Socaciu, M Verloo, and R Verhe. 2006. 'Iron-Chelation Properties of Phenolic Acids Bearing Catechol and Galloyl Groups'. *Food Chemistry* 98 (1): 23–31. <https://doi.org/10.1016/j.foodchem.2005.05.044>.
- Argyropoulos, Dimitris. 1994. 'Quantitative Phosphorus-31 NMR Analysis of Lignins, a New Tool for the Lignin Chemist'. *Journal of Wood Chemistry and Technology* 14 (1): 45–63. <https://doi.org/10.1080/02773819408003085>.
- Ayadi, N., F. Lejeune, F. Charrier, B. Charrier, and A. Merlin. 2003. 'Color Stability of Heat-Treated Wood during Artificial Weathering'. *Holz Als Roh- Und Werkstoff* 61 (3): 221–26. <https://doi.org/10.1007/s00107-003-0389-2>.
- Barčík, Štefan, Miroslav Gašparík, and Evgeny Y Razumov. 2015. 'EFFECT OF TEMPERATURE ON THE COLOR CHANGES OF WOOD DURING THERMAL MODIFICATION', 10.
- Čermák, Petr, and Aleš Dejmal. 2013. 'THE EFFECT OF HEAT AND AMMONIA TREATMENT ON COLOUR RESPONSE OF OAK WOOD (*Quercus Robur*) AND COMPARISON OF SOME PHYSICAL AND MECHANICAL PROPERTIES'. *Maderas. Ciencia y Tecnología*, 16.
- Crestini, Claudia, and Dimitris S. Argyropoulos. 1997. 'Structural Analysis of Wheat Straw Lignin by Quantitative ³¹P and 2D NMR Spectroscopy. The Occurrence of Ester Bonds and α-O-4 Substructures'. *Journal of Agricultural and Food Chemistry* 45 (4): 1212–19. <https://doi.org/10.1021/jf960568k>.
- Del Menezzi, C.H.S., I. Tomaselli, E.Y.A. Okino, D.E. Teixeira, and M.A.E. Santana. 2009. 'Thermal Modification of Consolidated Oriented Strandboards: Effects on Dimensional Stability, Mechanical Properties, Chemical Composition and Surface Color'. *European Journal of Wood and Wood Products* 67 (4): 383. <https://doi.org/10.1007/s00107-009-0332-2>.
- Esteves, Bruno M, Idalina J Domingos, and Helena M Pereira. 2008. 'PINE WOOD MODIFICATION BY HEAT TREATMENT IN AIR', 14.
- Fiuza, S.M., E. Van Besien, N. Milhazes, F. Borges, and M.P.M. Marques. 2004. 'Conformational Analysis of a Trihydroxylated Derivative of Cinnamic Acid—a Combined Raman Spectroscopy and Ab Initio Study'. *Journal of Molecular Structure* 693 (1–3): 103–18. <https://doi.org/10.1016/j.molstruc.2004.02.019>.
- Hider, Robert C, A Rahirn Mohd-Nor, Jack Silver, and Wivenhoe Park. 1981. 'Model Compounds for Microbial Iron-Transport Compounds. Part I. Solution Chemistry and Mossbauer Study of Iron(Ii) and Iron(Iii) Complexes from Phenolic and Catecholic Systems', 14.
- Koumba-Yoya, Georges, and Tatjana Stevanovic. 2017. 'Study of Organosolv Lignins as Adhesives in Wood Panel Production'. *Polymers* 9 (12): 46. <https://doi.org/10.3390/polym9020046>.
- Krilov, A., and R. Gref. 1986. 'Mechanism of Sawblade Corrosion by Polyphenolic Compounds'. *Wood Science and Technology* 20 (4): 369–75. <https://doi.org/10.1007/BF00351589>.
- Kučerová, Viera, Rastislav Lagaňa, Eva Výboňová, and Tatiana Hýrošová. 2016. 'The Effect of Chemical Changes during Heat Treatment on the Color and Mechanical Properties of Fir Wood'. *BioResources* 11 (4): 9079–94. <https://doi.org/10.15376/biores.11.4.9079-9094>.
- Leach, Robert M. 1988. '[54] PROCESS FOR COLORING WOOD WITH IRON SALT IN WATER', 7.
- Machová, Dita, Jan Baar, Zuzana Paschová, Petr Pařil, Jana Křenková, and Jozef Kúdela. 2019. 'Color Changes and Accelerated Ageing in Oak Wood Treated with Ammonia Gas and Iron Nanoparticles'. *European Journal of Wood and Wood Products*, April. <https://doi.org/10.1007/s00107-019-01406-x>.
- Malesev, Dusan, and Vesna Kuntic. 2007. 'Investigation of Metal-Flavonoid Chelates and the Determination of Flavonoids via Metal-Flavonoid Complexing Reactions'. *Journal of the Serbian Chemical Society* 72 (10): 921–39. <https://doi.org/10.2298/JSC0710921M>.
- Matsuo, Miyuki, Kenji Umemura, and Shuichi Kawai. 2012. 'Kinetic Analysis of Color Changes in Cellulose during Heat Treatment'. *Journal of Wood Science* 58 (2): 113–19. <https://doi.org/10.1007/s10086-011-1235-5>.

- McDonald, Mark, Isabelle Mila, and Augustin Scalbert. 1996. 'Precipitation of Metal Ions by Plant Polyphenols: Optimal Conditions and Origin of Precipitation'. *Journal of Agricultural and Food Chemistry* 44 (2): 599–606. <https://doi.org/10.1021/jf950459q>.
- Melone, Federica, Raffaele Saladino, Heiko Lange, and Claudia Crestini. 2013a. 'Tannin Structural Elucidation and Quantitative 31 P NMR Analysis. 1. Model Compounds'. *Journal of Agricultural and Food Chemistry* 61 (39): 9307–15. <https://doi.org/10.1021/jf401477c>.
- . 2013b. 'Tannin Structural Elucidation and Quantitative 31 P NMR Analysis. 2. Hydrolyzable Tannins and Proanthocyanidins'. *Journal of Agricultural and Food Chemistry* 61 (39): 9316–24. <https://doi.org/10.1021/jf401664a>.
- Miklečić, Josip, Nikola Španić, and Vlatka Jirouš-Rajković. 2012. 'WOOD COLOR CHANGES BY AMMONIA FUMING', 12.
- Pallardy, Stephen G. 2008. 'CHAPTER 3 - Vegetative Growth'. In *Physiology of Woody Plants (Third Edition)*, edited by Stephen G. Pallardy, 39–86. San Diego: Academic Press. <https://doi.org/10.1016/B978-012088765-1.50004-X>.
- Panshin, A. J., and C. de Zeeuw. 1980. 'Textbook of Wood Technology.' *Textbook of Wood Technology*. <https://www.cabdirect.org/cabdirect/abstract/19810669130>.
- Perron, Nathan R., and Julia L. Brumaghim. 2009. 'A Review of the Antioxidant Mechanisms of Polyphenol Compounds Related to Iron Binding'. *Cell Biochemistry and Biophysics* 53 (2): 75–100. <https://doi.org/10.1007/s12013-009-9043-x>.
- Pu, Yunqiao, Shilin Cao, and Arthur J. Ragauskas. 2011. 'Application of Quantitative 31 P NMR in Biomass Lignin and Biofuel Precursors Characterization'. *Energy & Environmental Science* 4 (9): 3154. <https://doi.org/10.1039/c1ee01201k>.
- Rice, Jennifer. 2006. 'APPEARANCE WOOD PRODUCTS AND PSYCHOLOGICAL WELL-BEING'. *WOOD AND FIBER SCIENCE* 38: 16.
- Royer, Mariana, Papa Niokhor Diouf, and Tatjana Stevanovic. 2011. 'Polyphenol Contents and Radical Scavenging Capacities of Red Maple (*Acer Rubrum* L.) Extracts'. *Food and Chemical Toxicology* 49 (9): 2180–88. <https://doi.org/10.1016/j.fct.2011.06.003>.
- Stevanović, Tatjana, and Dominique Perrin. 2009. *Chimie Du Bois*. Presses polytechniques et universitaires romandes.
- Tjeerdsma, B. F., M. Boonstra, A. Pizzi, P. Tekely, and H. Militz. 1998. 'Characterisation of Thermally Modified Wood: Molecular Reasons for Wood Performance Improvement'. *Holz Als Roh- Und Werkstoff* 56 (3): 149–53. <https://doi.org/10.1007/s001070050287>.
- Weigl, Martin, Ulrich Müller, Rupert Wimmer, and Christian Hansmann. 2012. 'Ammonia vs. Thermally Modified Timber—Comparison of Physical and Mechanical Properties'. *European Journal of Wood and Wood Products* 70 (1–3): 233–39. <https://doi.org/10.1007/s00107-011-0537-z>.
- Weigl, Martin, Johannes Pöckl, and Michael Grabner. 2009. 'Selected Properties of Gas Phase Ammonia Treated Wood'. *European Journal of Wood and Wood Products* 67 (1): 103–9. <https://doi.org/10.1007/s00107-008-0301-1>.

Study on the wettability of Pannónia poplar (*P.x euramericana* Pannónia) from two Hungarian plantations: Győr and Soltvadkert

L. Rábai^{1*}, N. Horváth², and Cs. Csiha³

¹Institute of Wood based Products
and Technologies
University of Sopron
Sopron, 9400, Hungary

²Institute of Wood Science
University of Sopron
Sopron, 9400, Hungary

³Institute of Wood based Products
and Technologies
University of Sopron
Sopron, 9400, Hungary

ABSTRACT

*In Hungary large stocks of plantation poplar reached their cutting age. In frame of an OTKA project a comprehensive study of psychico-mechanical properties of both the poplar samples and poplar glulam has been conducted to evaluate the suitability of Pannónia poplar (*P.x euramericana* Pannónia) hybrid, from different plantations, for load bearing applications, especially for glulam production. The present paper is a parttime report of the project, on the wettability of Pannónia poplar samples originating from two Hungarian plantations: Győr and Solt (Soltvadkert), with the main question, that are the different sites with significant influence on the properties of the boards? Samples from the two plantation sites have been collected from different trunks and laboratory samples with tangential cut, have been prepared by planing. Wettability has been measured by sessile drop method, both with distilled water and diiodo-methan, using a PGX Goniometer. Surface tension has been calculated according to the Fowkes method.*

1. INTRODUCTION

The spruce and other coniferous species generally involved in glulam production usually manifest densities between a 300-700 kg/m³. In Hungary in current years large stocks of plantation poplar reach the cutting age, and improving its utilization became a major goal, as poplar is first of all used by the paper industry. Pannónia poplar (*P.x euramericana* Pannónia) has been developed by F. Kopecky in 1961, in a forestry research center at Sárvár, Hungary. It is a fast growing species similar to the I-214 Italian poplar (*P.x euramericana* „I-214”), but its density is similar to the Robust poplar (*P.x euramericana robust*). The Pannónia poplar is the most frequent planted poplar hybrid nowadays (Molnár 2004). Its growth properties make it suitable for short, medium or long term (10-25 years) cultivation as well (Dr. Halupa-Dr.Tóth 1988).

The Hungarian poplar species can be classified in 3 density classes: very low density: $\rho \leq 360$ kg/m³, semi low density: $\rho = 361-400$ kg/m³, not that low density $\rho \geq 401$ kg/m³. The Pannónia poplar hybrid, regarding its density, belongs to this latest class. As Pannónia poplar (*P.x euramericana* Pannónia) has a density around 411 kg/m³, raises the question whether would it be suitable for glulam production.

In frame of OTKA K 116216 project a comprehensive study of psychico-mechanical properties (including the analysis of MOE, MOR, bending strength, compressive strength, etc.) of both the poplar samples and poplar glulam has been conducted to evaluate the suitability of Pannónia poplar (*P.x euramericana* Pannónia) hybrid, from different plantations, for load bearing applications, especially for glulam production.

The aim of the actual study is to find answer whether is the plantation with a relevant influence on the wettability of the boards and furthermore are there sites which could be favored due to the good wettability (and thus a supposed good adhesion) of their samples.

* Corresponding author: ; E-mail: csiha.csilla@uni-sopron.hu

2. MATERIAL AND METHOD

Pannónia poplar boards have been collected from different poplar trunks of two plantations: Győr and Solt and kiln dried to $8 \pm 1,2\%$ MC. The boards have been planed and 20 defect free samples of 400 mm x 70 mm x 20 mm size, with tangential cut surface, have been prepared. All the samples have been conditioned for 30 days prior to measurements at $20 \pm 2^\circ\text{C}$ temperature and 65% RH (Fig.1).



Fig. 1 Conditioning the Pannónia poplar samples

After conditioning the samples have been freshly planed in order to enable the detection of the contact angle of the freshly machined surface, as in practice freshly machined surfaces are glued in course of glulam production. Although the samples have been prepared in the same way, their surface roughness also has been measured, to enable an eventual comparison of these results with other researcher's data.

Surface roughness of the samples has been determined based upon 5 consecutive stylus tip measurements, performed on each sample, along a 17,5 mm trace, using a Mahr Perthen SP3 instrument, equipped with a stylus, with diamond head of $2 \mu\text{m}$ radius. Both R_a and R_z roughness parameters, considered widely used to describe the status of the surface (Magoss, 2000) have been calculated.



Fig. 2 Goniometer PGX equipped with dozier

Study on the wettability of Pannónia poplar (*P.x euramericana* Pannónia) from two Hungarian plantations: Győr and Soltvadkert

Contact angle of the surfaces has been measured using a PGX Goniometer (FIBRO SYSTEMS AG, Sweden) (Fig. 2), dynamic method, and a 5 µl test liquid volume. The contact angle has been determined in the 1st second after release, as by this time the drop consolidated and 3 measurements have been performed on each sample. Contact angle has been determined both with distilled water (DW) and with diiodo-methane (DIM). The measurements have been performed with two different tube sets for distilled water and diiodo-methane.

In order to evaluate wettability, Young's equation (Eq. 1) has been considered and the Fowkes model (Eq. 3) has been used for surface tension (also quoted surface free energy) calculation.

$$\gamma_{SL} + \gamma_{LV} \cos\theta - \gamma_{SV} = 0 \quad (\text{Eq. 1})$$

$$\gamma_{SL} + \gamma_{LV} = \gamma_{SV} \quad (\text{Eq. 2})$$

$$W_{sl}^d + W_{sl}^p = \gamma_l * (1 + \cos\theta) \quad (\text{Eq. 3})$$

$$(\gamma_l^d)^{\frac{1}{2}} * (\gamma_s^d)^{\frac{1}{2}} + (\gamma_l^p)^{\frac{1}{2}} * (\gamma_s^p)^{\frac{1}{2}} = \frac{\gamma_l * (\cos\theta + 1)}{2} \quad (\text{Eq. 4})$$

$$\gamma_s^d = \frac{\gamma_l * (\cos\theta + 1)^2}{4} \quad (\text{Eq. 5})$$

According to Fowkes the surface tension of the solid results as the sum of the polar and dispersive component

$$\gamma_s = \gamma_s^p + \gamma_s^d \quad (\text{Eq. 6})$$

First the calculation of the dispersive component of the surface tension of the solid has been performed with a liquid which manifests dispersive forces, and in a second step the polar component has been calculated as well. Contact angle measurements thus have been performed both with distilled water (as polar component $\gamma_l^p = 46,4$ mN/m) and diiodo-methane (dispersive component 50,8 mN/m).

3. RESULTS AND DISCUSSION

The results of the surface roughness measurements, the contact angle measurements (performed with distilled water and diiodo-methane) and the calculated values of the surface tension are represented in Table 1.

	R _a (µm)/SD	R _z (µm)/SD	Contact angle (DW)/SD	Contact angle (DIM)/SD	Surface tension (mN/m)
GYŐR	7,15/1,14	53,52/11,36	72,32/4,51	31,08/7,27	47,17
SOLT	8,2/2,37	56,38/15,47	68,58/4,88	28,17/5,11	49,97

Table 1. Results of the Pannónia poplar samples from two plantations: Győr and Solt

The results of the roughness measurements indicate that whilst the average roughness Ra is not significantly different, the Rz values show significant difference (t test, p=0,05). Since Rz is more sensitive to the real status of the surface than Ra (Csiha. 2003), and since the samples have been machined and treated in the same way, this difference in the roughness values suggests that there is an effect of the plantation on the quality of the timber. The samples have been investigated under microscope also, but no relevant difference in the anatomical structure could be identified. In the same time the samples originating from Solt, when exposed for short time soaking in water, manifested higher swelling than the ones from Győr, leading to the conclusion, that the differences in their anatomical structure need further investigation.

The contact angle values measured with distilled water are roughly two times higher than the one measured with diiodo-methane, and with both test liquids show significant difference (t test, p=0,05) between plantations. The higher

the contact angle the worse the wettability of the surface is. The samples from Győr show higher contact angle both with distilled water and diiodo-methane, than the samples from Solt, indicating that the samples from Solt have better wettability. The trend of the contact angle's behavior has been the same with both test liquids: in case of Solt samples both the contact angle of distilled water and the contact angle of diiodo-methane have been lower than the same contact angles of Győr samples. The surface free energy calculated according to the Fowkes model has been also significantly different for the two plantation samples: the samples from Soltvadkert resulted significantly higher (t test, $p=0,05$) surface tension than the samples from Győr. According to the Young-Dupré equation, high surface tension of the solid indicates good wetting. The better adhesion with the same adhesive can be expected on samples originating from Solt plantation, but it is still a question how these results relate to the values of coniferous species frequently used in glulam production. In a parallel study F.Z. Brahmia et al. (2019) when investigating the wettability of some wood species with different fire retardants, published data on the contact angle of planed Scots pine surfaces, measured with distilled water, and they have found that the average contact angle is 63,7°. This value is significantly lower than the contact angle values measured on Pannónia poplar samples originating from Győr and Soltvadkert (72,32 and 68,58), leading to the conclusion, that Scots pine's wettability (and consequently the expected adhesion) is better than the wettability of the Pannónia poplar samples originating from the two investigated sites.

As these preliminary results show uncertainty regarding the suitability of Pannónia poplar samples for glulam production, it is necessary to test the glulam performance itself, with known load bearing adhesive. On the other hand the surface tension of these boards also may need to be increased (by choosing a different machining type (for ex. sanding), or by chemical pretreatment, for example by nano- agents etc.).

4. SUMMARY

Wettability of Pannónia poplar samples originating from two different Hungarian plantations Győr and Soltvadkert has been investigated in order to evaluate their suitability for glulam production. The samples from Győr show higher contact angle both with distilled water and diiodo-methane, than the samples from Solt, indicating that the samples from Solt have better wettability. The surface free energy calculated according to the Fowkes model has been also significantly different for the two plantation samples: the samples from Soltvadkert resulted significantly higher (t test, $p=0,05$) surface tension than the samples from Győr, indicating that the site of origin may have a significant effect on the quality of the boards. The better adhesion with the same adhesive can be expected on samples originating from Solt plantation. In the same time both sample batches manifested higher contact angle values measured with distilled water than the same way treated and machined Scots pine samples, meaning that their expected adhesion doesn't reach the adhesion of Scots pine, - a frequently used species in glulam production.

As these preliminary results show uncertainty regarding the suitability of Pannónia poplar samples for glulam production, it is necessary to test the glulams performance itself, with known load bearing structural adhesive. On the other hand the surface tension of these boards also may need to be increased (by choosing a different machining type (for ex. sanding), or by chemical pretreatment, for example by nano- agents etc.).

ACKNOWLEDGEMENTS

We acknowledge the support gained from the NKFIH - National Research, Development and Innovation Office Hungary, within the frame of „ OTKA 116216: Complex analysis of the physico-mechanical and surface-physical properties of wood material with low density”.

REFERENCES

- F.Z. Brahmia, T. Alpár, P.Gy. Horváth, Cs. Csiha (2019): *Comparative analysis of wettability with fire retardants of Poplar (Populus cv. euramericana I214) and Scots pine (Pinus sylvestris). (In press)*
- S. Molnár (2004): *Faanyagismeret. (Wood species) Szaktudás Kiadó Ház Rt.*
- L. Halupa, B. Tóth (1998): *A nyár termesztése és hasznosítása. (Cultivation and utilization of poplar). Mezőgazdasági Kiadó*
- Cs. Csiha (2003): *Faanyagok felületi érdességének vizsgálata „P” és „R” profilon, különös tekintettel a nagyedényes fajokra. (Analysis of wood surface roughness of large porous species with special regard to “P” and “R” profile) Dissertation.pp 7.*
- E. Magoss (2000): *Természetes faanyag anatómiai felépítésének hatása a felületi minőségre (The effect of the anatomical structure*

Lathe Checks Formation, Measurement and Effect on Plywood Quality - European Hardwoods

Anti Rohumaa¹, Louis Denaud², Joffrey Viguiet², Stéphane Girardon², Guillaume Pot²

¹FibreLaboratory,
South-Eastern Finland University of Applied Sciences,
57200 Savonlinna, Finland

² Arts et Metiers ParisTech,
LaBoMaP,
71250 Cluny, France

ABSTRACT

Lathe check formation and measurement have received a lot of attention in the past. Reliable results about the lathe checks properties have been obtained mainly by using microscopy techniques, measuring the check depth and the frequency. However, microscopic measurements are time-consuming and laborious. Moreover, only a limited amount of specimens could be evaluated during the study, which often leads to high dispersion of obtained results.

In order to automatize the lathe check depth and frequency measurement several methods have been introduced, e.g. ultrasound, acoustic, however these methods do not give high quality information about the check properties. During the present study, the SMOF was used in order to measure high quantity of samples and evaluate the effect of processing parameters on check formation and properties. This method will enable to evaluate remarkable amount of checks immediately after the peeling process, from the wet veneer at microscopic level.

In this study the effect of peeling temperature and compression ratio on lathe checks properties were evaluated from European hardwoods. The results of the study show that at higher temperature, shallower and more frequent checks are formed compared to lower temperature. Moreover, higher compression ratio produced veneer with shallower and more frequent lathe checks. The results also reveal that the rays could affect the propagation direction of lathe check in veneer, hence the anatomical structure plays remarkable role in check formation.

1. INTRODUCTION

In veneer-based products, adhesive bond formation and performance highly depends on processing parameters, but also the quality of used veneer plays crucial role. It has been shown, that veneer and veneer-based products quality is affected by the lathe checks properties, which in turn are affected by processing parameters during soaking and peeling. Generally, at higher soaking temperature during peeling process the formation of deep lathe checks will be reduced (Meriluoto 1965; Dupleix et al. 2013; Rohumaa et al. 2018). This will improve the integrity of the veneer (Rohumaa et al. 2016a), bonding quality (Rohumaa et al. 2013, 2014, 2016b) and veneer-based products shape stability (Blomqvist et al. 2014) and mechanical properties (Pot et al. 2015). Moreover, positive effect of higher soaking and peeling temperature is not the only way to reduce the lathe checking of veneer, but also it has been noted that the compression ratio affects the depth and frequency of lathe checks (Lutz 1974, Rohumaa et al. 2018). According to available literature, the lathe check phenomenon is almost constant and periodical for homogeneous wood species (Denaud et al. 2012; Palubicki et al. 2010). It is also shown, that lathe check depth and frequency correlate with each other, where the deeper checks tend to be less frequent than shallower checks (McMillin 1958; Denaud et al. 2007; Palubicki et al. 2010, Rohumaa et al. 2018). However, some studies show opposite results (Darmawan et al. 2015). These contradictions in published results highlight that there are still open questions about the lathe check formation and their role on product quality. The variation of results and contradiction in literature could be caused by many factors, e.g. different measuring techniques for lathe checks, processing parameters and anatomy of wood species.

Lathe check formation and measurement have received a lot of attention in the past as well as more recently (Denaud et al. 2007, 2012; Tomppo et al. 2009; Palubicki et al. 2010; Dupleix et al. 2013; Antikainen et al. 2015; Darmawan et al. 2015; Rohumaa et al. 2018). Mostly the lathe check depth and the frequency have been measured

under the microscope from dry veneer. However, microscopic measurements are time-consuming and laborious. In order to automatize the lathe check depth measurement process, the checks have to be measured from the green veneer since accurate measurement of checks from the dry veneer is complicated due to the waviness of the veneer (Tomppo et al. 2009). During this study a semi-automated lathe checks measurement device (SMOF), described by Paľubicki et al. (2010), was used. SMOF will enable to measure precisely all checks and their parameters through the whole mat of peeled veneer. Moreover, this method also provides information on veneer microscopical structure.

This paper shows how lathe checks are formed on birch and beech during veneer processing and how anatomical structure affects lathe check formation.

2. MATERIALS AND METHODS

2.1. WOOD MATERIAL

In this paper, European beech (*Fagus sylvatica* L.) and Silver birch (*Betula pendula* Roth) logs were used. The material was selected carefully and only material without visual defects was used. The logs were soaked and peeled at different temperatures from 20 to 80°C. This range of temperature corresponds to the common distribution also used in industry. Following soaking, the logs were immediately peeled at different compression ratio (0, 5, 10, or 15%). Immediately after peeling, veneer ribbons were cut and the checks were measured.

2.1. MEASUREMENT METHODS

In LaBoMaP a specific apparatus has been developed in order to measure the lathe check parameters, called SMOF (Système de Mesure d'Ouverture des Fissures) and this apparatus is described more in detail by Paľubicki et al. (2010). The SMOF (Fig 1.) enables to measure automatically and precisely the position and the depth of a large number of checks by slightly bending the veneer on a wheel with previously approved diameter.

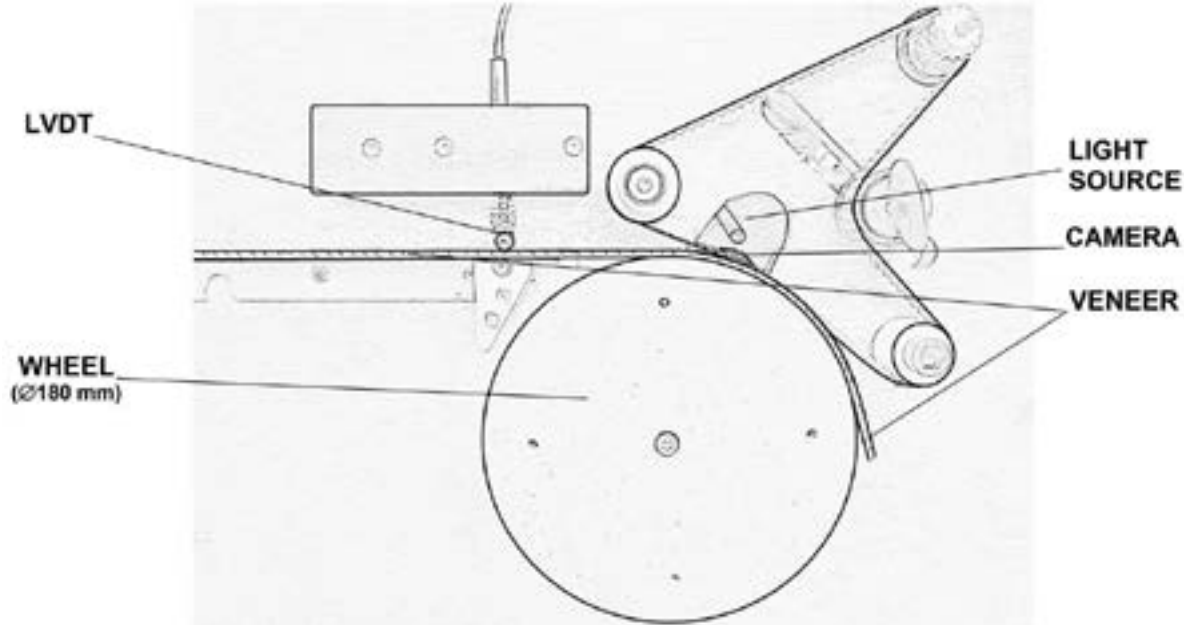


Figure 1: The SMOF (optical lathe check measuring system). LVDT is the linear variable differential transformer.

3. RESULTS AND DISCUSSION

The lathe check depth is highly influenced by compression ratio and by soaking temperature, which softens the logs prior peeling process. Higher compression ratio will form shallower checks, which could be sometimes hard to detect visually (Fig 2). The results show (Fig. 2), that at higher soaking temperature and higher compression ratio checks are visually almost undetectable. This could cause often non-periodical detection of checks. At lower soaking temperature and at higher compression ratio deeper and periodical checks are formed as demonstrated in Fig 2. These images also support previously described finding, where some of the checks could not be revealed for visual or automatic detection and therefore, increase variability in measured results.

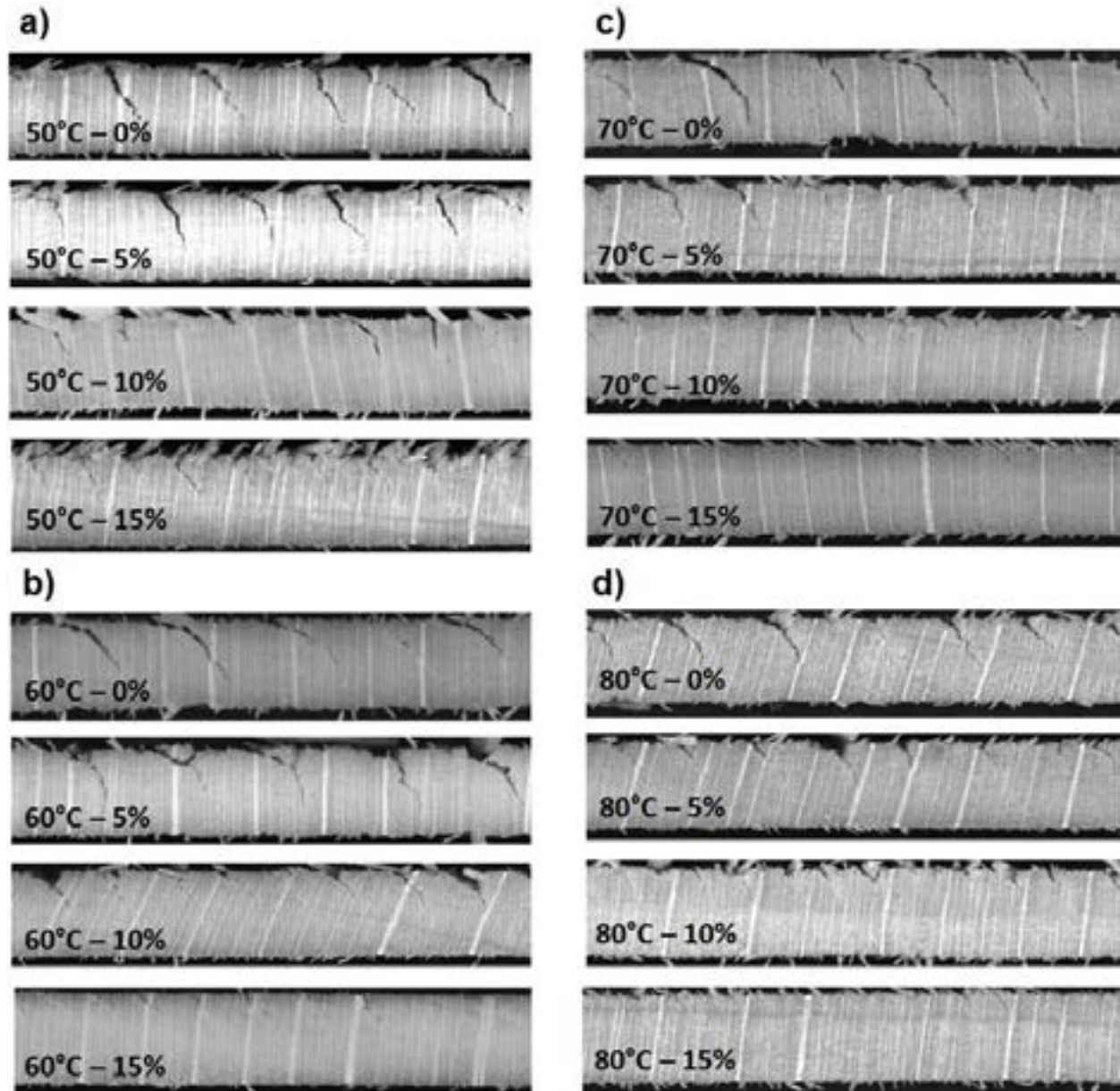


Figure 2: The effect of soaking temperature and compression ratio on lathe check properties. Where the compression ratio varies from 0% to 15% of the veneer thickness for a) soaking at 50°C, b) soaking at 60°C, c) soaking at 70°C, d) soaking at 80°C (Rohumaa et al. 2018)

The comparison of obtained results with other studies conducted under similar conditions (Dupleix et al. 2013; Rohumaa et al. 2016a), shows that the rise of soaking temperature from 50°C to 80°C will have a decreasing effect on lathe check depths, which is approximately 15-20%. Interestingly, soaking temperature has a much more significant effect on birch than on beech veneer by decreasing the depth of lathe checks approximately by 30-35% in the same range of soaking temperature (Dupleix et al. 2013; Rohumaa et al. 2016a). The reason might be found in the different anatomical structures, where beech has much higher volume of rays (approx. 20%) compared to birch (approx. 10%). According to literature, rays could resist crack growth in tangential direction, but act as weak planes in radial direction (Boatright and Garrett 1983; Ashby et al. 1985). This is also supported by present study, where the lathe checks will more favorably propagate along the rays at lower temperature (Fig. 3a) and will pass through the rays at higher temperature (Fig. 3b). This weaker plane caused by rays in radial direction could also explain the deeper checks compared to the results on birch wood obtained by Dupleix et al. (2013) and Rohumaa et al. (2016a).

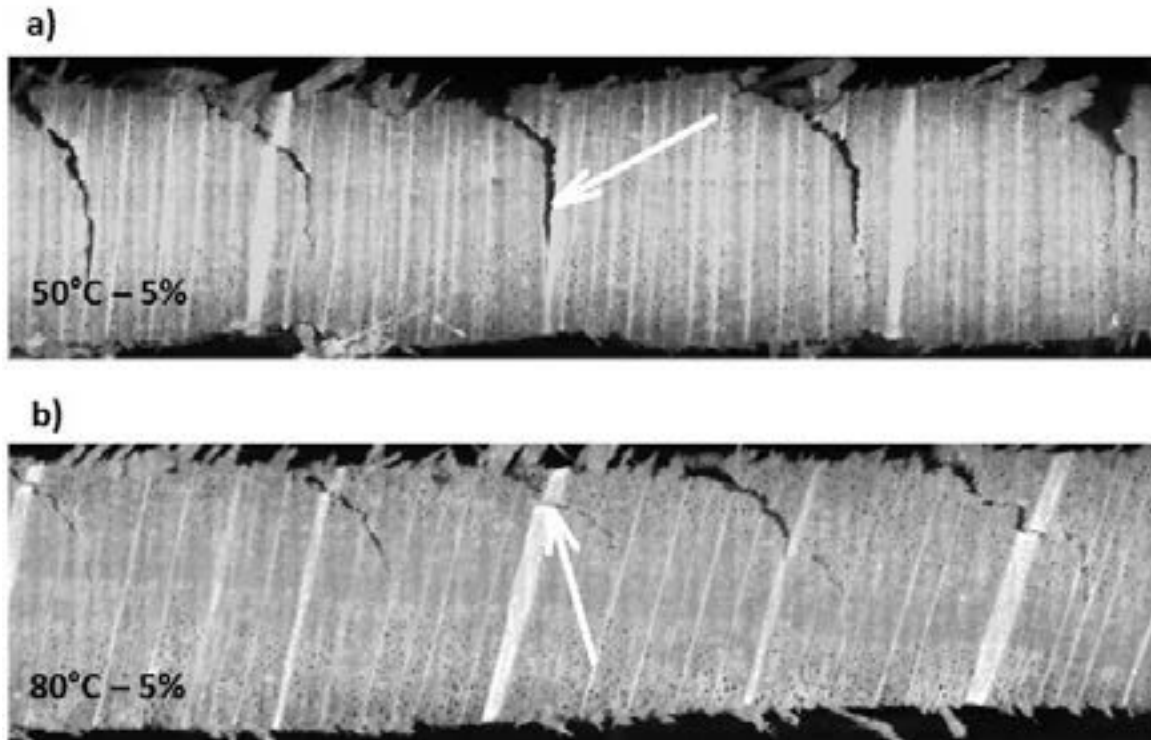


Figure 1: The effect of temperature and anatomical structure on lathe check propagation. Arrows show check propagation a) along and b) through the ray (Rohumaa et al. 2018).

4. CONCLUSIONS

The results of the study show, that the higher the soaking temperature the shallower and more frequent lathe checks are. However, the effect of compression ratio during peeling is much greater than the effect of soaking temperature on veneer checking. The results show, that the higher compression creates veneer with shallower and more frequent checks.

The results also show that the anatomical structure of wood material most probably will have effect on check formation. In beech veneer, lathe check propagation is affected by rays, which resist crack growth in tangential direction, but act as weak planes in radial direction. Moreover, in birch veneer lathe checks are uniform and not affected by rays to such an extent.

ACKNOWLEDGEMENTS

The authors gratefully acknowledge the financial support from the Bourgogne Franche-Comté region and thank the Xylomat Technical Platform from the Xylomat Scientific Network funded by ANR-10-EQPX-16 XYLOFOREST.

REFERENCES

- Antikainen, T., J. Eskelinen, A. Rohumaa, T. Vainio, M. Hughes. 2015. Simultaneous measurement of lathe check depth and the grain angle of birch (*Betula pendula* Roth) veneers using laser trans-illumination imaging. *Wood Sci Technol* 49:591-605
- Ashby, M.F., K.E. Easterling, R. Harrysson, S.K. Maiti. 1985. The fracture and toughness of woods. *Proc Roy Soc* 398:261-280
- Blomqvist, L., D. Sandberg, J. Johansson. 2014. Influence of veneer orientation on shape stability of plane laminated veneer products. *Wood Mat Sci Eng* 9:224-232
- Boatright, S.W.J and G.G. Garrett. 1983. The effect of microstructure and stress state on the fracture behaviour of wood. *J Mater Sci* 18:2181-2199
- Darmawan, W., D. Nandika, Y. Massijaya, A. Kabe, I. Rahayu, L.É. Denaud, B. Ozarska. 2015. Lathe check characteristics of fast growing sengon veneers and their effect on LVL glue-bond and bending strength. *J Mater Process Tech* 215:181-188
- Denaud, L.É., L. Bléron, F. Eyma, R. Marchal. 2012. Wood peeling process monitoring: A comparison of signal processing methods to estimate veneer average lathe check frequency. *Eur J Wood Prod* 70:256-261
- Denaud, L.É., L. Bléron, A. Ratle, R. Marchal. 2007. Online control of wood peeling process: acoustical and vibratory measurements of lathe checks frequency. *Ann Forest Sci* 64:569-575
- Dupleix, A., L.É. Denaud, L. Bléron, R. Marchal, M. Hughes. 2013. The effect of log heating temperature on the peeling process and veneer quality: beech, birch, douglas-fir and spruce case studies. *Eur J Wood Prod* 71:163-171
- Lutz, J.F. 1974. Techniques for Peeling, Slicing, and Drying Veneer. *US For. Prod. Lab. Rep. No 228, Madison, Wise.*
- McMillin, C.W. 1958. The relation of mechanical properties of wood and nosebar pressure in the production of veneer. *Forest Prod J* 8:23-32
- Meriluoto, J. 1965. The Influence of Raw Material Factors on the Quantity and Quality of Rotary Cut Brick Veneer. *Acta Forestalia Fennica*, 80:1-155
- Pot, G, L.É. Denaud, R. Collet. 2015. Numerical study of the influence of veneer lathe checks on the elastic mechanical properties of laminated veneer lumber (LVL) made of beech. *Holzforschung*, 69:337-345
- Palubicki, B., R. Marchal, J.C. Butaud, L.É. Denaud, L. Bléron, R. Collet, G. Kowaluk. 2010. A Method of Lathe Checks Measurement; SMOF device and its software. *Eur J Wood Prod* 68:151-159
- Rohumaa, A., J. Viguier, S. Girardon, M. Krebs and L. Denaud. 2018. Lathe check development and properties: effect of log soaking temperature, compression rate, cutting radius and cutting speed during peeling process of European beech (*Fagus sylvatica* L.) veneer. *Eur. J. Wood Prod* 76:1653-1661
- Rohumaa, A., T. Antikainen, C.G. Hunt, C.R. Frihart, M. Hughes. 2016a. The influence of log soaking temperature on surface quality and integrity performance of birch (*Betula pendula* Roth) veneer. *Wood Sci Technol* 50:463-474
- Rohumaa, A., A. Yamamoto, C.G. Hunt, C.R. Frihart, M. Hughes, J. Kers. 2016b. Effect of log soaking and the temperature of peeling on the properties of rotary-cut birch (*Betula pendula* Roth) veneer bonded with phenol-formaldehyde adhesive. *BioResources* 11:5829-5838
- Rohumaa, A., C.G. Hunt, C.R. Frihart, P. Saranpää, M. Ohlmeyer, M. Hughes. 2014. The influence of felling season and log-soaking temperature on the wetting and phenol formaldehyde adhesive bonding characteristics of birch veneer. *Holzforschung* 68:965-970
- Rohumaa, A., C.G. Hunt, M. Hughes, C.R. Frihart, J. Logren. 2013. The influence of lathe check depth and orientation on the bond quality of phenol-formaldehyde-bonded birch plywood. *Holzforschung* 67:779-786
- Tomppo, L., M. Tiitta, R. Lappalainen. 2009. Ultrasound evaluation of lathe check depth in birch veneer. *Eur J Wood Prod* 67:27-35.

High-value composite products from fast growing *Eucalyptus* trees

C. B. Wessels¹, M. Nocetti^{1,3}, M. Brunetti³, P.L. Crafford¹, M. Pröller¹, M.K. Dugmore¹, C. Pagel^{1,2}, R. Lenner², Z. Naghizadeh¹

¹Department of Forest and Wood
Science
Stellenbosch University
Stellenbosch, 7600, South Africa

²Department of Civil Engineering
Stellenbosch University,
Stellenbosch, 7600, South Africa

³CNR-IVALSA
Istituto per la Valorizzazione del
Legno e delle Specie Arboree
Sesto Fiorentino, Italy

ABSTRACT

The objectives of the work described in this paper were to develop concept processing pathways for manufacturing high value, green-glued Eucalyptus composite products, review existing research on this topic, and identify critical knowledge gaps that need to be addressed in future research. A review of research showed that structural grading on green Eucalyptus grandis, boards using dynamic MOE as a predictor, proved to be as effective as dry grading. Green finger-jointing seem to provide good quality bonds but the finger-jointed lumber have very different properties to existing softwood resources – which will make it more resource efficient to define new stress grades for this wood resource. Material and processing variables for green edge lamination has been investigated and it has been found that high strength bonds are possible. Face bonding quality of dry Eucalyptus grandis for CLT has also been investigated and it was found that excellent face-bonding quality could be achieved when using a clamping pressure of 0.7 MPa and with no stress relief grooves present. A composite product where green Eucalyptus grandis was finger-jointed and then face-laminated before drying to equilibrium moisture content had much lower levels of checks, splits, and twist than products that were not face laminated. Both green finger-jointed as well as face-laminated Eucalyptus grandis that was dried had lower strength and stiffness variation than currently used pine structural lumber resources. A higher material resistance factor can therefore be used for this resource than the current value prescribed in the South African national timber design code.

1. INTRODUCTION

The *Eucalyptus* genus is the most widely planted hardwood in the world due, mainly, to its adaptability and high growth rates. There are *Eucalyptus* plantations in more than 100 countries across six continents covering over 20 million ha (Myburg et al. 2014). Most *Eucalyptus* species, however, are rarely processed into sawn lumber due to processing problems associated with poor dimensional stability, splitting, brittle heart, excessive shrinkage, cell collapse, and checking after drying (Jacobs 1955, Malan 1984, Malan 1993, Vermaas and Bariska 1994, Yang and Waugh 2001, Malan 2003, Crafford and Wessels 2016). The result is that the vast majority of the world's commercial *Eucalyptus* plantations are used for low value applications such as pulp, board and energy products.

The development of structural adhesives that can be applied to unseasoned wood above fibre saturation point (so-called “green gluing”) created opportunities for new manufacturing processes of composite wood products. This is of special interest to *Eucalyptus* solid wood product manufacturing since some of the problems associated with processing this genus can be overcome or at least be minimised by joining the wood into composite products before the drying process (Crafford and Wessels, 2016; Pröller et al. 2018; Pagel 2018; Dugmore et al. 2019). The two defects with arguably the highest value implications viz. splitting and warp, both develop or increase during the drying process and can be reduced by joining green lumber into composite components. Additionally, harvesting *Eucalyptus* trees when they are relatively young can mitigate some of the effects of high growth stresses (Yasin and Raza 1992). Growth stresses are one of the main causes of splitting in logs and lumber from *Eucalyptus* and often manifest in freshly felled trees and sawn boards (Malan and Gerischer 1987; Yang and Waugh 2001; Washusen et al. 2003; Kojima et al. 2012). Another consequence of growth stresses is a condition known as brittle heart. Wood with brittle heart contains numerous fractures and splits, are unattractive, low in strength, and impossible to machine to a smooth surface (Malan 2003). Brittle heart only manifests in large older trees (Yang and Waugh 2001). A combination of harvesting young *Eucalyptus* trees, sawmill processing, and joining lumber into composite products before drying the wood therefore provide a chance of mitigating some of the problem properties associated with this hardwood.

The concept of green gluing *Eucalyptus* wood into composite products including investigation of several individual processing steps, has received considerable attention over the last few years from researchers at Stellenbosch University, South Africa and IVALSA, Italy (Crafford and Wessels, 2016; Nocetti et al. 2017; Touffie 2017; Pröller et al. 2018; Pagel 2018; Dugmore et al. 2019; Mathenjwa et al. 2018). The focus was on *Eucalyptus grandis* which is an economically very important species in countries such as South Africa, Brazil, Argentina, Uruguay, Paraguay, Mozambique, and Tanzania. The objectives of the work described in this paper were to (1) develop concept processing pathways for manufacturing green-glued *Eucalyptus* composite products, (2) review existing research on green-glued *Eucalyptus* processing relevant to the concept processing pathways, and (3) identify critical knowledge gaps that need to be addressed in future research.

2. PROCESSING PATHWAYS FOR MANUFACTURING GREEN-GLUED *EUCALYPTUS* COMPOSITE PRODUCTS

The most common way for producing sawn lumber and solid composites (from both softwoods and hardwoods) involve sawmill processing of logs into green lumber, seasoning of the lumber in drying kilns, and grading the lumber before preparation for joining pieces into composite products. The objective of green gluing *Eucalyptus* lumber into a composite before drying is mainly to (1) reduce formation of splits and cracks during the drying process, where joined pieces prohibit the neighbouring pieces from splitting and (2) reduce warp due to neighbouring pieces restraining each other. Composites (green or dry glued) in general also reduce the variability of the mechanical properties of wood products. Potential processing pathways for *Eucalyptus* trees into four different end products are depicted schematically in Figure 1. These products have been selected specifically with the South African market in mind and also for their suitability to absorb different quality regions of *Eucalyptus* trees into final products.

The first processing pathway, production of green roof trusses from young *Eucalyptus* wood, is described in Crafford and Wessels (2016). This process has been commercialised and the product has been well established in the South African market (see www.biligom.co.za). The product is fundamentally different to existing roof truss products in South Africa since manufacture and installation of the trusses occur while the lumber is unseasoned and above fibre saturation point. Natural air drying occur after erection of the roof structure. The initial processing steps of this pathway (sawmilling, cross-cutting, green finger-jointing) is common to all the pathways defined in Figure 1. Cross-cutting of freshly sawn lumber into short laminates is important mainly to remove the bow and crook in wet lumber pieces present as a result of growth stresses in the trees. Large knots (which is not common in young *Eucalyptus* wood) and other defects can also be removed during this step. Green finger-jointing, planing, and manufacture of roof trusses occur directly afterwards.

The second processing pathway is the production of dry CLT panels (Figure 1). This involves edge-laminating the green finger-jointed lumber into panels, and kiln drying of these panels. The reason for producing panels while the wood is still green and drying panels instead of individual lumber pieces is mainly for suppression of excessive deformation. As the research of Crafford and Wessels (2016) illustrated, when green finger-jointed *Eucalyptus grandis* is dried as individual pieces, nearly 30% of the lumber did not conform to warp specifications of structural lumber. CLT as a product is also attractive in the context of *Eucalyptus* raw materials since the centre layers could absorb material that might be visually unacceptable and have some splitting and checking whilst being structurally sound in the parallel to grain direction.

The third processing pathway involve green face gluing of finger-jointed lumber into beams which is then kiln-dried into dry face laminated beams (Figure 1). This product could potentially compete against higher grade structural softwood lumber – the product class with the largest lumber market share in South Africa. Green face lamination is intended to reduce warp and splitting during drying. Using only two laminations in the face direction also allow kiln drying which could potentially be a problem when more laminations are glued together as is customary with traditional glued laminated timber (GLT). The intention was also that the laminated beams could potentially increase the structural reliability of the product.

The fourth processing pathway is dry edge laminated planks and panels (Figure 1). As with dry face-laminated beams the product could potentially compete against structural softwood lumber and additionally it could also be used as a panel product such as shelving or components for furniture or other wood products.

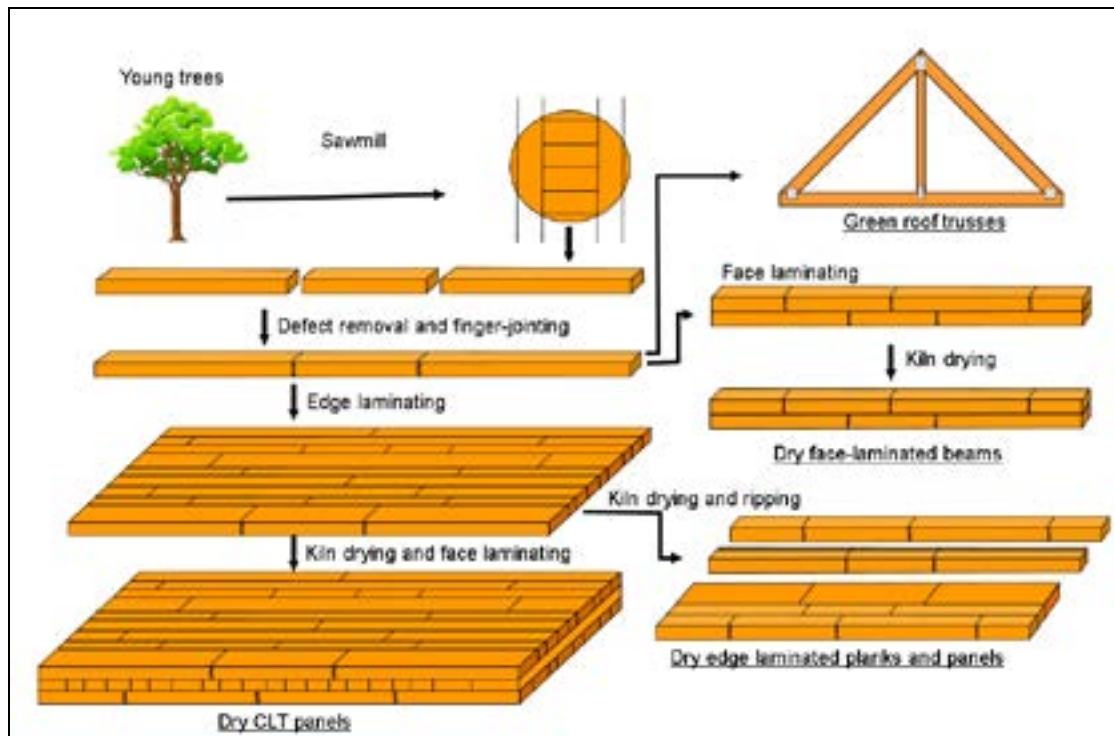


Figure 1: Schematic diagram of processing pathways for young *Eucalyptus* trees into high value end products with green gluing as a central processing step. End products are underlined.

3. A REVIEW OF RESEARCH ON GREEN-GLUED *EUCALYPTUS* PROCESSING AND PRODUCTS

The processing pathways as defined in Figure 1 were developed for the various reasons discussed in the previous section. In this section research that were performed specifically on the processes and products described in Figure 1 will be reviewed. It will focus on the research on *Eucalyptus grandis* processing at Stellenbosch University, South Africa and IVALS in Italy but will also include, to a lesser extent, relevant work on other species and from other researchers.

3.1. GREEN STRUCTURAL GRADING OF *EUCALYPTUS GRANDIS*

One of the challenges of processing wet hardwood lumber into structural lumber is that the structural grading need to occur on the unseasoned lumber. Structural grading of hardwood and especially *Eucalyptus* is not very common but some research has been performed on dry Argentinean grown *Eucalyptus grandis* by Piter et al. (2004a and 2004b). They found the highest coefficient of determination for the prediction of strength was with modulus of elasticity and that inclusion of knots in strength prediction models only increased the model slightly. Vega et al. (2012) and Riesco Munoz and Remacha Gete (2012) similarly found that for chestnut and oak respectively, the best models only include modulus of elasticity and that including knot variables were not justifiable. Similarly, in work on green South African grown *Eucalyptus grandis*, using multi-sensor grading technology, Nocetti et al. (2017) found that only measuring the dynamic modulus of elasticity was the best approach and that including other parameters such as knots did not improve the model sufficiently to warrant its measurement. Research results for hardwoods including *Eucalyptus grandis*, therefore, seems to be fairly consistent in suggesting that only modulus of elasticity need to be measured and that, unlike softwoods, knot parameters do not add sufficient value to predictive models to justify its measurement. Nocetti et al. (2017) also found that green grading of the *Eucalyptus grandis* lumber proved to be as effective as dry grading and that there was close correlation between the green and dry dynamic modulus of elasticity results.

3.2 GREEN FINGER-JOINTED *EUCALYPTUS GRANDIS* LUMBER

Research results on the bonding quality of green finger-jointed wood were generally very positive on both softwoods (Pommer and Elbez 2006, Sterley et al. 2014) and hardwoods (Karastergiou et al. 2008). Crafford and Wessels (2016) evaluated green finger-jointed *Eucalyptus grandis* lumber (using one-component PUR adhesive) of different ages and dimensions. The intention was to evaluate the use of this lumber for possible application in roof truss structures while the lumber is still in the green, unseasoned state. One group of finger-jointed lumber was tested while green, and another group of lumber was tested after drying to equilibrium moisture content. The study showed that the young finger-jointed *Eucalyptus grandis* lumber had very good flexural, tensile parallel to grain, and shear properties in both the green and dry state. The mean and characteristic MOE and MOR values of the finger-jointed *Eucalyptus grandis* product were higher and the variation lower in comparison to currently used SA pine sources. The tensile perpendicular to grain and compression perpendicular to grain strength did not conform to SANS requirements for the lowest structural grade (S5). Both tree age and product dimension were sources for variation in the physical and strength properties. The strength properties of this resource is clearly very different to that of the currently used softwood resources in South Africa in terms of both the absolute magnitude as well as the ratio between different properties. As also mentioned by Nocetti et al. (2017), it will be more resource efficient to define new stress grades for finger-jointed *Eucalyptus grandis* lumber instead of using existing grades developed based on pine resources.

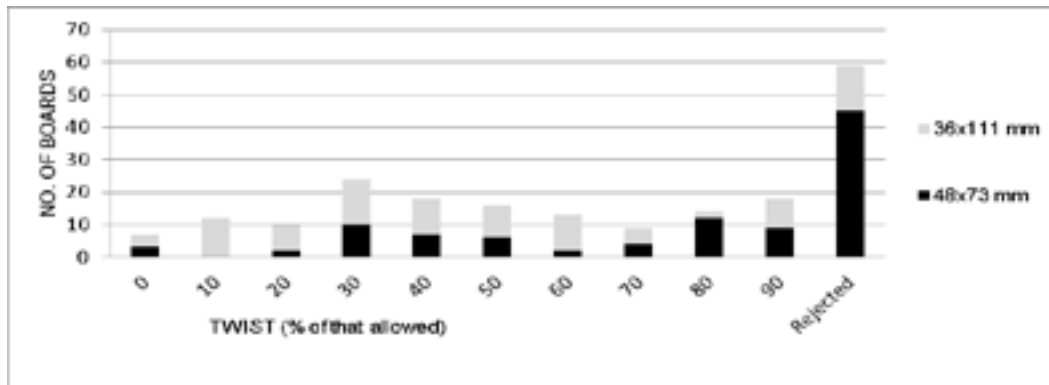


Figure 2: The distribution of twist of the two dimension classes, expressed as a percentage of that allowed according to SANS 1783-2 (2012). Adapted from Crafford and Wessels (2016).

For the group of lumber that was dried to equilibrium moisture content after the finger-jointing process, it was interesting to note that twist was a major problem, with about 45% of all the boards having unacceptable levels of twist (Figure 2). Checking was also fairly high with 35.5% of the boards having checking levels above the national standard (Table 1) while end-splitting due to the drying process was surprisingly low. These defects (twist, checking) during the drying process emphasize the need for further processing of the lumber while still green into new products (roof trusses, edge glued components, face glued components) – where the wood can be restrained during the drying process.

Table 1. The percentage of boards from the dry sample rejected according to the checking and end-splitting requirements of SANS 1783-2 (2012). Adapted from Crafford and Wessels (2016).

Dimension (mm)	Checks			End-splits		
	Combined	48x73	36x111	Combined	48x73	36x111
Reject (%)	35.5	54	17	1.5	1	2

3.3 EDGE GLUING OF GREEN EUCALYPTUS GRANDIS WITH A ONE-COMPONENT PUR ADHESIVE AND THE PRODUCTION OF LAMINATED PLANKS AND PANELS

Edge gluing of *Eucalyptus grandis* lumber in its wet state, before kiln-drying, is considered a potential inhibiting factor for warp and splitting of lumber. Pröller et al. (2018) conducted a study where the objective was to determine how certain material and processing variables influence the bond quality of unseasoned, edge-glued, *Eucalyptus*

grandis, using a moisture-curing one-component polyurethane adhesive. The study considered the effect of four parameters, namely wood density, moisture content, adhesive spread rate and pressure, on the shear strength of bondlines. They found the bonding quality to be satisfactory proving the feasibility of edge gluing *Eucalyptus grandis* in the wet state. Multiple ANOVA showed that generally better results were obtained for samples with a higher moisture content of roughly 60% compared to specimens with a lower moisture content around fibre saturation point. Results indicated that the lower spread rate tested (150 g m^{-2}) should be preferred to the higher one (250 g m^{-2}), since it will likely give more stable shear strength results and it would be preferable from an economic point of view. Increasing pressure from 0.6 MPa to 1 MPa did not increase the shear strength significantly.

Compton et al. (1977) described a sawmill processing system called EGAR (edge-glue-and rip) where small diameter logs were cut into slabs which were seasoned, edged to maximum width, edge-glued into wider panels and again ripped into lumber of required width. The main aim of this system was to increase volume recovery but it was never really commercially implemented. Bergman et al. (2010) tested the same system but in this case edge-gluing occur on wet ponderosa pine and the objective was to reduce warp during the drying stage. Pröller (2016) used the same concept to test the potential of edge gluing green *Eucalyptus grandis* boards before kiln drying in order to inhibit the development of warp and splitting. Edge-glued panels were produced from wet material above fibre saturation point and kiln-dried together with non-edge-bonded control boards from the same material source. After drying, the panels were sawn apart into single boards, graded regarding the development of check, split, bow, cup and twist and compared to the results obtained for the control boards. The ability of stress-relief grooves in boards to reduce the development of defects was also investigated. The results showed that the edge gluing of green *Eucalyptus grandis* lumber before kiln drying could not decrease the number of board rejections according to the SANS 1707-1 (2010) requirements for sawn *Eucalyptus* timber. Cup could be significantly decreased, while twist was only reduced for boards without pith. Stress-relief grooves did not have a significant influence on the development of any of the investigated defects but caused severe deformation and damage in some of the boards. Pröller (2016) suggested that ripping the kiln dried panels back into dimension lumber of structural sizes probably did not reduce defects to such an extent to make this process economically viable. However, use of the wider panels as a product or a component for other products such as CLT might be an attractive option since the whole panel exhibited relatively little warp.

3.4 BONDING QUALITY AND DIMENSIONAL STABILITY OF *EUCALYPTUS GRANDIS* CLT

Eucalyptus grandis has very high shrinkage and expansion coefficients and there is concern that acceptable cross-grain face bonding quality such as that in CLT manufacturing might be a challenge. There is, however, also some concerns that the present test methods for CLT bonding quality, based on tests for GLT, might be too severe (Betti et al., 2016; Knorz et al., 2017). Dugmore et al. (2019) conducted a study to analyse different testing methods for evaluating face-bonding quality of cross-laminated timber from *Eucalyptus grandis* timber bonded with a one component polyurethane adhesive and to evaluate the effect of different processing variables on the face-bonding quality of cross-laminated panels. The effect of clamping pressure, wood density, and presence of stress relief grooves on the bonding quality were evaluated. Two existing test methods from the EN 16351 standard and two recently developed test methods were used in the evaluation. Among them a combined delamination and shear test seems to have potential to determine bond quality of cross-laminated timber panels since it evaluates both the durability and shear strength of a joint while minimising the effect of rolling shear. Complex failure behaviour in the different tests and various interactions between the factors evaluated (density, grooves, pressure) made it difficult to reach firm conclusions on the effect of each factor. In general though, the presence of grooves had a negative effect, both increasing the delamination and decreasing the shear strength (whatever the pressure and density used during processing). High clamping pressure was preferable, particularly when high density material was used. Wood density had a positive effect on shear strength when determined on dry specimens, and a negative effect on delamination. Results indicated that the production of *Eucalyptus grandis* cross laminated timber could be possible and that excellent face-bonding quality could be achieved when using a clamping pressure of 0.7 MPa and with no stress relief grooves present.

Another possible effect of the large shrinkage and expansion coefficients on *Eucalyptus grandis* CLT might be the possibility of warp in panels when a moisture gradient is introduced through the cross section of the panel. Gereke et al. (2008, 2009, and 2010) conducted several studies on the stresses and deformation that is introduced in spruce and beech wood when a moisture gradient is present in CLT panels. Touffie (2017) and Mathenjwa et al. (2019) investigated development of warp in *Eucalyptus grandis* CLT when a moisture gradient was introduced. In a comparative study with European grown spruce, Mathenjwa et al. (2019) found that spruce CLT had significantly less warp in both the parallel and the perpendicular to grain directions than *Eucalyptus grandis*. Touffie (2017) found that density played a role in the magnitude of warp and that stress-relief grooves might reduce the amount of warp slightly. The method of CLT building construction might restrain most warp due to joints at all the edges of a panel. However,

deformation at the centre of large panels might occur when a high moisture gradient develop – the possibility and magnitude of such an occurrence will have to be further investigated in different test setups.

3.5 MATERIAL RESISTANCE FACTORS AND PROPERTIES OF GREEN FINGER-JOINTED LUMBER AS WELL AS DRY FACE-LAMINATED *EUCALYPTUS GRANDIS* LUMBER

Green finger-jointed *Eucalyptus grandis* lumber has become an acceptable product for roof trusses in South Africa in a relatively short time period. However, high moisture content prevent the use of this product for many other applications and it has been shown that drying of the boards result in excessive deformation and checking of a large proportion of the raw material (Crafford and Wessels, 2016). One possibility to manufacture kiln-dried *Eucalyptus grandis* structural lumber is face lamination of two finger-jointed boards in the wet state and subsequent kiln drying. Since only one face of each laminate is joined by adhesive there should be enough open surface area available for successful drying whilst the joined laminates restrain the product from excessive warp, checking and splitting. Additionally, the finger-jointing and face lamination of many different laminates could possibly also result in less variation in strength properties resulting in the use of higher material resistance factors to be used in the designing of structures from this material. Pagel (2018) conducted a study to calculate the material resistance factors for (a) green finger-jointed *Eucalyptus grandis* lumber, (b) green finger-jointed lumber that has been dried to equilibrium moisture content, and (c) green finger-jointed and green face-laminated lumber that has been dried to equilibrium moisture content. He also measured and quantified the warping, checking and splitting associated with each process. The material resistance factor for green finger-jointed *Eucalyptus grandis* was found to be higher than that for South African pine resources and as well as the value used in the national timber design code. It was found that the face lamination process did not further reduce the variation in strength results to a significant extent but significantly lower rejection rates due to defects were recorded for the laminated set (Figure 3). Based on reliability theory, a material reduction factor of 0.77 is proposed in this study for both green finger-jointed *Eucalyptus grandis* as well as dry face-laminated *Eucalyptus grandis* in contrast to the current factor of 0.68 stipulated by the national code.

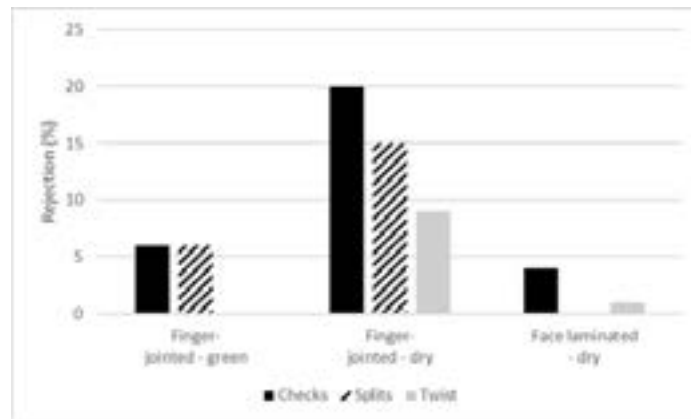


Figure 3: Rejection rates due to defects of (a) green finger-jointed *Eucalyptus grandis* in the green state (b) green finger-jointed lumber that has been dried and (c) green finger-jointed and green face-laminated lumber that has been dried (adapted from Pagel 2018).

4. DISCUSSION AND CONCLUSIONS

Processing pathways for new *Eucalyptus grandis* composite products has been defined and several research projects on the products and processes involved has been completed. Structural grading on green boards using dynamic MOE as a predictor proved to be as effective as dry grading. Green finger-jointing seem to provide good quality bonds but the finger-jointed lumber have very different properties to existing softwood resources – which will make it more resource efficient to define new stress grades for this wood resource. Material and processing variables for green edge lamination has been investigated and it has been found that high strength bonds are possible. Face bonding quality of dry *Eucalyptus grandis* for CLT has also been investigated and it was found that excellent face-bonding quality could be achieved when using a clamping pressure of 0.7 MPa and with no stress relief grooves present. A composite product where green *Eucalyptus grandis* was finger-jointed and then face-laminated before drying to equilibrium moisture content had much lower levels of checks, splits, and twist than products that were not face laminated. Both green finger-jointed *Eucalyptus grandis* and face-laminated *Eucalyptus grandis* that was dried had lower strength and

stiffness variation than currently used pine structural lumber resources. A higher material resistance factor can therefore be used for this resource than the current value prescribed in the South African national timber design code.

The following areas has been identified as critical knowledge gaps for future research which will hopefully advance the use of *Eucalyptus* for processing into high value composite products:

- Process economics: Research into the economics of the different products and processes involved is critical to understand the potential of successful commercialisation;
- Process integration: Integrated primary and secondary manufacturing could potentially result in improved process efficiencies. This might specifically be an advantage for CLT manufacturing where a single process from primary log breakdown to final panel production could potentially lead to higher recoveries of wood. Research using simulation methods could shed light on improvements in this regard.
- Durability treatment of CLT: The durability treatment of structural wood products is compulsory in certain parts of South Africa. This is not a problem for products with relatively small dimensions but is a challenge for CLT that is much larger than current treatment facilities. Research into the durability treatment of laminates before joining into panels and specifically the interaction between adhesive systems and treatment chemicals is required.

ACKNOWLEDGEMENTS

We gratefully acknowledge the following organisations for funding this research and contributing research materials and assistance: Hans Merensky Foundation, Hans Merensky Timbers, Biligom International, Safcol, the Italian Ministry of Foreign Affairs and the South African Department of Science and Technology.

REFERENCES

- Bergman, R.D., W.T. Simpson, C. Turk. 2010. Evaluating Warp of 2 by 4s Sawn from Panels Produced through Green Gluing Dimension Lumber from Small Ponderosa Pine Logs, *Forest Products Journal*, 60(1): 57 – 63.
- Betti, M., M. Brunetti, M.P. Lauriola, M. Nocetti, F. Ravalli, B. Pizzo, 2016. Comparison of newly proposed test methods to evaluate the bonding quality of cross laminated timber (CLT) panels by means of experimental data and finite element (FE) analysis, *Construct. Build. Mater.* 125: 952–963.
- Compton, K. C., H. Hallock, C. Gerhards, and R. Jokerst. 1977. Yield and strength of softwood dimension lumber produced by EGAR system. *Research Paper FPL-RP-293. USDA Forest Service. Forest Products Laboratory, Madison, Wisconsin.* 12 pp.
- Crafford, P.L. and C.B. Wessels CB. 2016. A potential new product for roof truss manufacturing: Young, green finger-jointed *Eucalyptus grandis* lumber. *Southern Forests: a Journal of Forest Science* 78(1):61-71.
- Dugmore, M., M. Nocetti, M. Brunetti, Z. Naghizadeh, and C.B. Wessels. 2019. Bonding quality of cross-laminated timber: Evaluation of test methods on *Eucalyptus grandis* panels. *Construction and Building Materials* 211: 217–227
- Gereke, T., P.J. Gustafsson, K. Persson and P. Niemz. 2009. Experimental and numerical determination of the hygroscopic warping of cross-laminated solid wood panels. *Holzforschung* 63(3): 340-347.
- Gereke, T., Schnider, T., Hurst, A. and Niemz, P. 2009. Identification of moisture-induced stresses in cross-laminated wood panels from beech wood (*Fagus sylvatica* L.). *Wood Science and Technology* 43:301
- Gereke, T., P. Hass, and P. Niemz. 2010. Moisture-induced stresses and distortions in spruce cross-laminates and composites laminates. *Holzforschung* 64(1): 127-133.
- Jacobs, M.R. 1955. *Growth habits of the Eucalypts. Commonwealth Forestry and Timber Bureau, Canberra.*
- Karastergiou, S., G.I. Matanis, K. Skoularakos. 2008. Green gluing of oak wood (*Quercus conferta* L.) with a one-component polyurethane adhesive. *Wood Material Science and Engineering* 3–4: 79–82
- Kojima, M., T. Nakai, K. Saegusa, F.M. Yamaji, H. Yamamoto, S. Yamashita. 2012. Anatomical and chemical factors affecting tensile growth stress in *Eucalyptus grandis* plantations at different latitudes in Brazil. *Canadian Journal of Forest Research* 42(1): 134.
- Knorz, M., S. Torno, J.W. van de Kuilen. 2017. Bonding quality of industrially produced cross-laminated timber (CLT) as determined in delamination tests, *Constr. Build. Mater.* 133: 219–225
- Malan, F.S. 1984. *Studies on the phenotypic variation in growth stress intensity and its association with tree and wood properties of South African grown Eucalyptus grandis (Hill ex Maiden). Dissertation, University of Stellenbosch.*

- Malan, F.S., and G.F.R. Gerischer. 1987. Wood property differences in South African grown Eucalyptus grandis trees of different growth stress intensity. *Holzforschung* 41(6): 331–335.
- Malan, F.S. 1993. The wood properties and qualities of three South African-grown Eucalypt hybrids. *South African Forestry Journal* 167: 35-44.
- Malan, F.S. 2003. The wood quality of the South African timber resource for high-value solid wood products and its role in sustainable forestry. *Southern African Forestry Journal* 198: 53-62.
- Mathenjwa A., Z. Naghizadeh, C.B. Wessels. 2019. A comparison of moisture-related dimensional behaviour of Pinus, Eucalyptus and Picea Cross-Laminated Timber. Stellenbosch University. Special report as part of post graduate diploma. Copy obtainable from cbw@sun.ac.za.
- Myburg AA et al. 2014. The genome of Eucalyptus grandis. *Nature* 510: 356–362.
- Nocetti, M., M. Pröller, M. Brunetti, G.P. Dowse, and C.B. Wessels. 2017. Investigating the potential of strength grading green Eucalyptus grandis lumber using multi-sensor technology. *Bioresources* 12(4):9273-9286.
- Pagel, C. 2018. Investigation into material resistance factors and properties of young, engineered Eucalyptus grandis timber. Thesis, Department of Civil Engineering, Stellenbosch University.
- Piter J.C., R.L. Zerbino, H.J. Blaß. 2004a. Visual strength grading of Argentinean Eucalyptus grandis. Strength, stiffness and density profiles and corresponding limits for the main grading parameters. *Holz als Roh- und Werkstoff*, 62(1): 1-8.
- Piter J.C., R.L. Zerbino, H.J. Blaß. 2004b. Machine strength grading of Argentinean Eucalyptus grandis. *Holz als Roh- und Werkstoff*, 62(1): 9-15.
- Pommer, R., G. Elbez. 2006. Finger-jointing green softwood: Evaluation of the interaction between polyurethane adhesive and wood, *Wood Material Science and Engineering* 1: 127-137.
- Pröller, M. 2016. An investigation into the edge gluing of green Eucalyptus grandis lumber using a one-component polyurethane adhesive. MScFor (Wood Products Science) thesis. Department of Forest and Wood Science, Stellenbosch University.
- Pröller, M., Nocetti, M., Brunetti, M., Barbu, M-C., Blumentritt, M., and C.B. Wessels. 2018. Influence of processing parameters and wood properties on the edge gluing of green Eucalyptus grandis with a one-component PUR adhesive. *European Journal of Wood and Wood Products* 76:1195-1204.
- Riesco Muñoz G, Remacha Gete A. 2012. Prediction of bending strength in oak beams on the basis of elasticity, density, and wood defects. *Journal of Materials in Civil Engineering*, 24(6), 629–634.
- Sterley, M., E. Serrano, B. Enquist, J. Hornatowska. 2014. Finger Jointing of Freshly Sawn Norway Spruce Side Boards – A Comparative Study of Fracture Properties of Joints Glued with Phenol-Resorcinol and One-Component Polyurethane Adhesive, *Materials and Joints in Timber Structures* 9: 325-339
- Touffie, A-D. 2017. Moisture induced deformations in Eucalyptus grandis cross laminated timber. Final year bachelors project report. Stellenbosch University. Copy obtainable from cbw@sun.ac.za.
- Vega, A., Dieste A, Guaita M, Majada J, Baño V. 2012. Modelling of the mechanical properties of Castanea sativa Mill. structural timber by a combination of non-destructive variables and visual grading parameters. *European Journal of Wood and Wood Products*, 70(6): 839-844.
- Vermaas, H.F., and M. Bariska. 1994. Collapse during low temperature drying of Eucalyptus grandis W. Hill and Pinus silvestris L. *Proceedings IUFRO Wood Drying Conference, Rotorua, New Zealand* 141-150.
- Washusen, R., J. Ilic, and G. Waugh. 2003. The relationship between longitudinal growth strain and the occurrence of gelatinous fibers in 10- and 11-year-old Eucalyptus globulus Labill. *Holz als Roh- und Werkstoff*, 61(4): 299-303.
- Yang, J.L., and G. Waugh. 2001. Growth stress, its measurement and effects. *Australian Forestry* 64(2): 127-135.
- Yasin, S.M., and S.M. Raza. 1992. Improving the quality of wood produced from eucalyptus trees. Technical note WQ TN1. Pakistan Forest Institute, Peshawar.

Influence of slope of grain on the mechanical properties of hardwoods and the consequences for grading

Geert Ravenshorst^{1*}, Wolfgang Gard¹, and J.W.G van de Kuilen^{1,2}

¹Biobased Structures and Materials
Delft University of Technology
Delft, The Netherlands

²Chair of Wood Technology
Technical University of Munich
Munich, Germany

Abstract

The main parameter that influences the bending strength of timber from tropical hardwood is the slope of grain. Although in the grading rules a specific threshold value is given, in these hardwoods the global slope of grain is very difficult to quantify by a visual assessment. The slope of grain measured after testing gives a better indication, but still it can only poorly describe the Hankinson relations. By rewriting the Hankinson relations, the slope of grain can be determined from the bending strength test values and from the MOE test value, both in combination with the density values and constants derived by non-linear regression analysis. These two values correlate very well and the average value is designated as the theoretical slope of grain. With the theoretical slope of grain 5 test samples of tropical wood species were evaluated and slope of grain values of 0.3 were observed where 0.1 is the limit value. Because all pieces passed the normal visual grading method in practice, slope of grain values should be incorporated in the strength class assignment test program, when these qualities cannot be ruled out for coming on the market. The (dynamic) modulus of elasticity can be used to evaluate the occurrence of desired range of slope of grain values in the test samples.

1. INTRODUCTION

To assign a timber beam to a strength class, this beam has to be graded. With visual grading, the grader assesses the most important strength reducing characteristics and designates the visual grade of the beam. In a previously performed laboratory research the relationship between the visual characteristics and the strength is determined, and based on that the strength class connected to that specific visual grade was established. This is documented in grading reports and for a number of species there is a European standard (EN 1912) that provides information of strength classes that can be assigned to visual grades of a number of species from different growth areas. In Europe there is a harmonised standard (EN 14081) that provides guidance how strength assignments should be performed, to ensure that the same method is followed over Europe. The harmonised standard is referring to the standard EN 384 that gives guidelines on sampling in connection with visual grading. This paper discusses the influence of the strength reducing characteristic slope of grain in combination with visual grading.

EN 384 states how the characteristic value of for instance the bending strength can be determined based on the number of samples and specimen within a sample for a visual grade. That means that before the laboratory testing is performed, the material has to be subdivided in visual grades, that are defined in visual grading standards. For softwoods, the knot ratio (the size of the knots related to the width of the beam) is the most governing strength reducing parameter. It is possible to distinguish between different values of knot ratios during grading in practice, therefore it is possible to divide softwood in 2 or 3 visual grades. For tropical hardwoods however, the slope of grain (the deviation of the grain angle with the longitudinal beam axis) is the most important strength reducing characteristic (since in most cases, no knots are present). Because the value of the slope of grain is more difficult to determine in practice, for tropical hardwoods only one visual grade defined is for a species. For instance in the Europeans standard EN 16737 or in the Dutch standard EN 5493. For these visual grades the slope of grain is limited to a value of 1:10. Beams with higher slope of grain should be rejected. Figure 1 shows the definition of slope of grain according to EN 1310. The slope of grain is the tangent of the angle of the grain to the beam axis. Sometimes multiplied by 100 to express it as a percentage. In this paper slope of grain (SoG) is given as the tangent of the angle of the grain to the beam axis (x/y in figure 1).

* Corresponding author: ; E-mail: g.j.p.ravenshorst@tudelft.nl

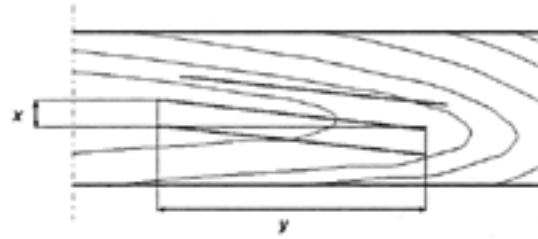


Figure 1: Definition of slope of grain according to EN 1310.

However, related to the requirements for visual grading of tropical hardwoods for slope of grain there are two assumptions that are important in this process. The visual grading for slope of grain is assumed to be correctly performed in practice and related to that: the sampling for the laboratory research for the strength class assignment is representative. These two assumptions will be investigated in this paper.

2. INFLUENCE OF THE SLOPE OF GRAIN ON THE BENDING STRENGTH

The influence of the grain angle on the strength is described in EC 5 (EN 1995-1-1) by the so called Hankinson equation. However, in EC 5 this is used for a stress verification as the result of a force acting under an angle with the longitudinal beam axis, thereby assuming that the grain direction is parallel to the longitudinal beam axis.

Hankinson (1932) based his equation on compression tests. From a theoretical point of view the Hankinson equation describes the interaction between stresses parallel and perpendicular to the grain. This has proven to be also valid for tension under an angle with the grain, and also for bending properties with varying slope of grain. Equation (1) gives Hankinson equation for the bending strength and equation (2) for the Modulus of Elasticity.

$$f_{m,\alpha} = \frac{f_{m,0}}{\left(\frac{f_{m,0}}{f_{m,90}}\right) * \sin^2(\alpha) + \cos^2(\alpha)} \quad (1)$$

$$MOE_{\alpha} = \frac{MOE_0}{\left(\frac{MOE_0}{MOE_{90}}\right) * \sin^2(\alpha) + \cos^2(\alpha)} \quad (2)$$

Figures 2 show results of tests performed on specifically prepared specimens of the tropical hardwood species massaranduba with a depth of 50 mm as described in Ravenshorst (2015). These graphs show that the effect of increasing slope of grain is not linear with bending strength. Through a non-linear regression analysis the values for $f_{m,0}$ and $f_{m,90}$ were determined (And also MOE_0 and MOE_{90}) and inserted in equation (1) and (2). The lines of equation (1) and (2) are shown in the figures together with the original data. The graphs shows the limit value of 1:10 that is used for the visual grade of tropical hardwood. This shows that the reduction in bending strength when the slope of grain increases from SoG =0 to 0.1 is 85% % and when the slope of grain increases from 0 to 0.2 the reduction in bending strength is 50 % . That shows the importance of limiting the slope of grain.

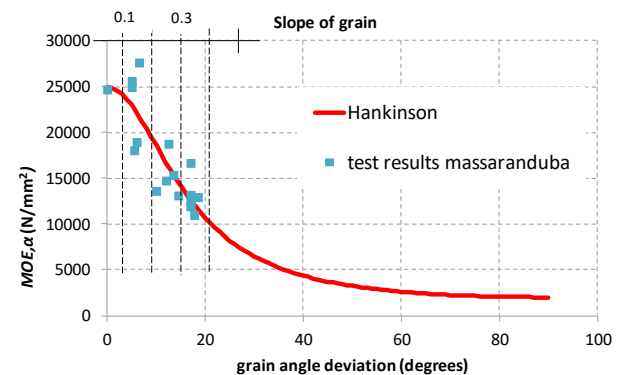
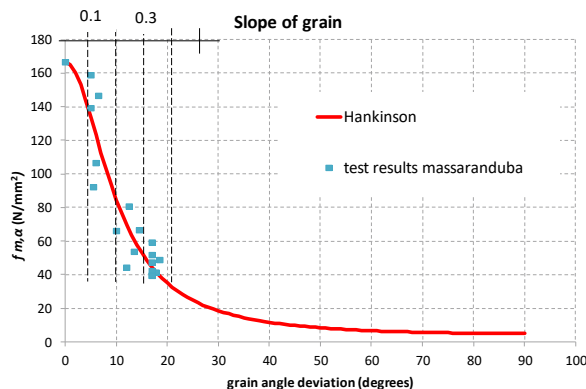


Figure 2: Influence of slope of grain on bending strength (left) and Modulus of Elasticity (right) of specimens of massaranduba according to Ravenshorst (2015)

3. MEASURING OF SLOPE OF GRAIN

3.1. INTRODUCTION

The slope of grain is evaluated in the grading process but can also be studied in the laboratory. Figure 3 shows on the left the measurement of the slope of grain on a timber beam before testing and after a bending test. On the right two beams of tropical hardwood species okan are shown that have to be graded.

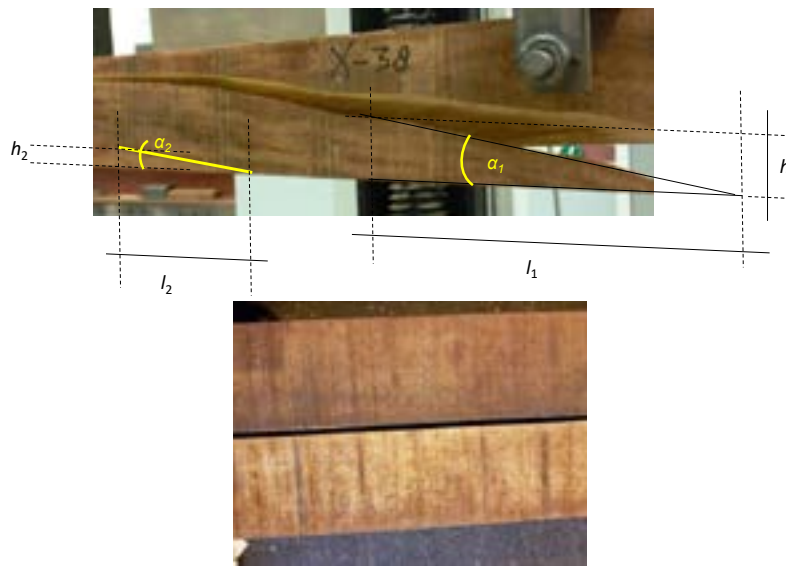


Figure 3: Angle of the grain and associated slope of grain measured before (α_2) and after (α_1) the bending test (left) and two okan beams that have to be graded (right)

3.2. MEASURING THE SLOPE OF GRAIN IN THE GRADING PROCESS

For tropical hardwoods there is only one visual class with the requirement to limit to the slope of grain of 1:10 according to grading standards NEN 5493 or EN 16737. In contrast with visual grading on the basis of knots, to determine the exact slope of grain in practice is very difficult. Therefore in practice, graders will judge the slope of grain as within or without the required limits. When the slope of grain is assessed to be out of the limits, the beam will be rejected. The right picture in figure 3 shows how difficult the determination of the slope of grain in practice can be.

3.2. MEASURING THE SLOPE OF GRAIN AFTER TESTING

After testing in the laboratory the slope of grain can be measured based on the failure cracks that follow the grain (although this also sometimes is difficult). See figure 3 on the left. EN 384 states that in the report for visual grading assignments histograms showing samples distributions of knot size measurements, rate of growth and density. This is clearly focused on softwoods, and in practice, in reports dealing with tropical hardwoods, distributions of the slope of grain are required, to give insight in the distribution in the strength reducing characteristics. EN 384 does not state if these distributions should be measured before or after testing. However, to get insight in the actual influence it is more valuable to give the slope of grain values after testing. In Ravenshorst (2015) was shown that when beams from a large number of species are evaluated the influence of the slope of grain is visible, but with much more scatter than when specimens are specifically prepared as was described in section 2.

3.3. COMPARISON OF SLOPE OF GRAIN MEASUREMENTS BEFORE AND AFTER TESTING

To evaluate the predicting capability of the slope of grain after failure on measurements before testing two samples of hardwood timber species were investigated. All pieces were visually graded as in practice with the result that the slope of grain was acceptable and the piece did not have to be rejected. Then the slope of grain was measured in the

laboratory before and after testing according to figure 3 (left). Figure 4 (left) shows the results for a sample of okan and figure 4 (right) shows the results for a sample of greenheart. Figure 4 shows that is very difficult to predict the slope of grain after failure before testing with measurements before testing, that there is a large scatter, and that it also depends on the species or sample. For the okan sample (left) is was much more difficult than for the greenheart sample. The slope of grain often exceeds the maximum value of 0.1 according to the visual grading standards. Once again, all pieces passed the normal visual grading process.

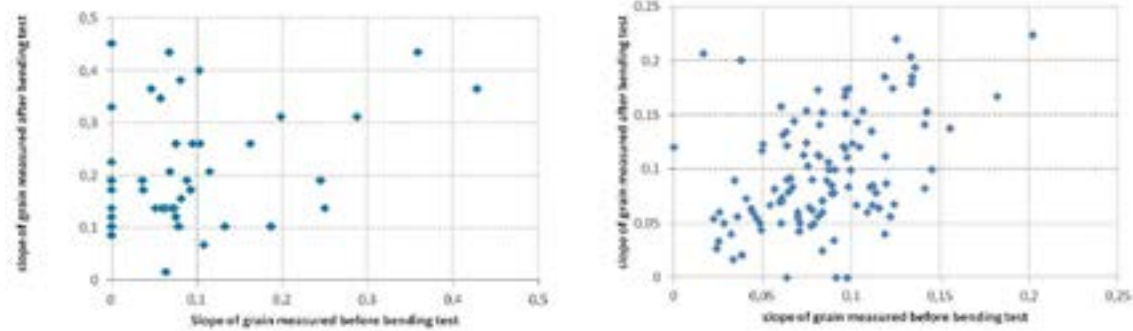


Figure 4: Slope of grain measured before and after testing for a sample of okan (left) and a sample of greenheart (right)

4. THEORETICAL DERIVATION OF THE SLOPE OF GRAIN.

According to section 2 the slope of grain has an effect on both the bending strength and the Modulus of Elasticity. That explains why the Modulus of Elasticity and the bending strength are well correlated. In Ravenshorst (2015) the Hankinson equations were rewritten according to equations (3) and (4).

$$f_{m,\alpha} = \frac{(\rho C_1)}{(C_3 - 1)\sin^2(\alpha) + 1} \quad (3)$$

$$MOE_\alpha = \frac{(\rho C_2)}{(C_4 - 1)\sin^2(\alpha) + 1} \quad (4)$$

Where ρ is the density, α the grain angle and C_1 , C_2 , C_3 and C_4 are constants. Equations (12) and (13) can be rewritten to respectively equations (5) and (6) to calculate $\sin^2(\alpha)$ when the actual values of the density, the bending strength and MOE are known.

$$\sin^2(\alpha) = \left[\frac{(\rho C_1)}{f_{m,\alpha}} - 1 \right] \frac{1}{(C_3 - 1)} \quad (5)$$

$$\sin^2(\alpha) = \left[\frac{(\rho C_2)}{MOE_\alpha} - 1 \right] \frac{1}{(C_4 - 1)} \quad (6)$$

For this paper a dataset of 5 samples of timber species okan as described in Ravenshorst and van de Kuilen (2018) was studied. The constants C_1 , C_2 , C_3 and C_4 were determined through a non-linear regression analysis with the precondition that the slope of the regression line of the values of $\sin^2(\alpha)$ calculated with equation (5) and (6) should be 1. The correlation graph is show in figure 6. The found values of the constants were $C_1 = 0.12$, $C_2 = 25.9$, $C_3 = 27.8$ and $C_4 = 15.0$. From the calculated values of $\sin^2(\alpha)$ the square root is taken to calculate $\sin(\alpha)$. For negative values of $\sin^2(\alpha)$ the value of $\sin(\alpha)$ is taken as 0. From the values of $\sin(\alpha)$ derived from equation (5) and (6) in this way the average was taken. Then the angle was calculated from this average $\sin(\alpha)$. The tangent of angle α was calculated and this value was designated as the theoretical slope of grain.

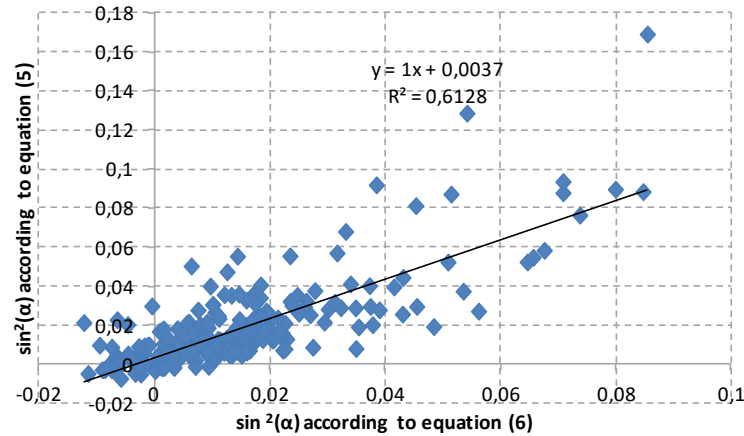


Figure 6: Relationship between $\sin^2(\alpha)$ calculated with equations (5) and (6).

5. ANALYSIS

In figures 7 and 8 the slope of grain measured after the bending test and the theoretical slope of grain, determined according to section 4 are compared with the theoretical Hankinson equations according to equations (3) and (4) with the average density of all 5 samples of okan as input value, and the C-factors determined in section 4.

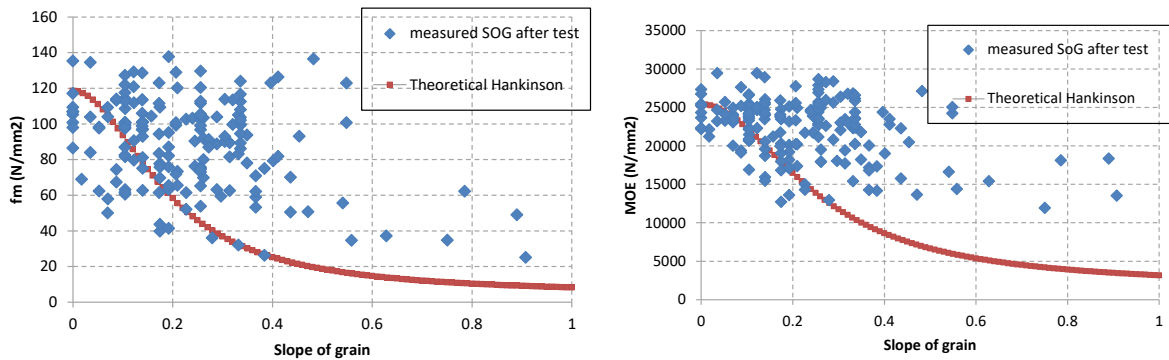


Figure 7: Bending strength (left) and MOE (right) against for slope of grain measured after testing and theoretical Hankinson line 5 samples of okan

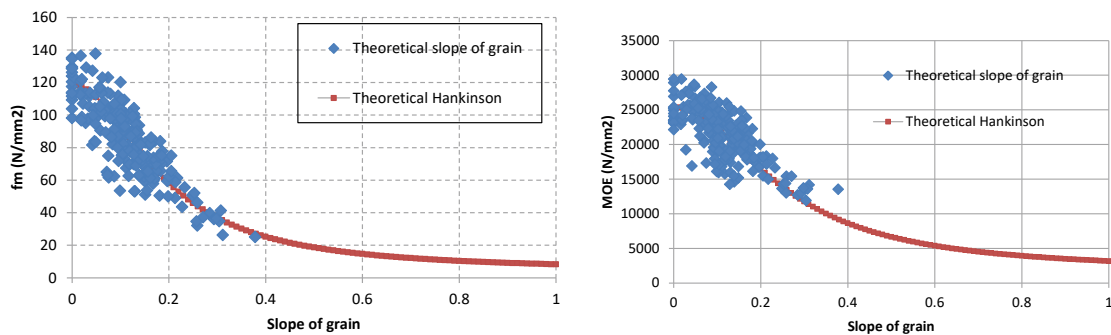


Figure 8: Bending strength (left) and MOE (right) against theoretical slope of grain and theoretical Hankinson line for 5 samples of okan

Figures 7 and 8 show that the theoretically determined slope of grain follows the theoretical Hankinson lines much better for both bending strength and MOE than the slope of grain measured after the test. This can be explained by two things. Firstly, also after the bending test the slope of grain is not always very clear to measure. Secondly, it is difficult to capture the 3D effect that is present in timber beams. These two effects show different in test results of full size compared to the specifically prepared specimens described in section 2. Figure 8 shows that the theoretical slope of grain values can capture the 3D effect for bending strength and MOE.

With the theoretical slope of grain the influence different samples on the classification of samples can be investigated. Figure 8 shows that for pieces that pass the normal grading procedure for visual grading, can have a theoretical slope of grain up to 0.3. Figure 9 shows the bending strength against the theoretical slope of grain values for okan samples 4 and 5 (left) and the bending strength against the MOE (right). When only samples with the quality of sample 4 would be incorporated in the testing program and the strength class assignments would be based on these samples, then when in practice a sample with the quality of sample 2 is used in practice (this would pass the current grading method for visual grading as explained) this would be unsafe.

Therefore, when the presence of samples with higher slope of grain values cannot be ruled out, for strength class assignments the range of slope of grain values should be more than the threshold value of 0.1, a range between 0 and 0.3 seems reasonable. To be sure that these pieces are incorporated the (dynamic) MOE of pieces can be determined and based on these values a selection can be made. The MOE for straight grained pieces (SoG of 0) is expected to be the density (for the okan samples an average value of 980) multiplied by constant C_2 ($=25.9$) which gives a value around 25400 N/mm². Therefore, sample 4 can be regarded as high quality. For a slope of grain of 0.3 a value of 11000 N/mm² can be expected.

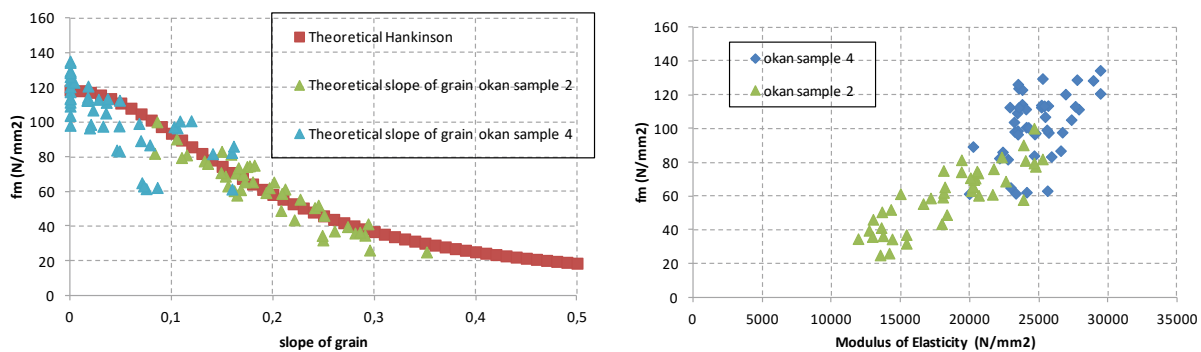


Figure 9: Bending strength against theoretical slope of grain and theoretical Hankinson line for okan samples 2 and 4 (left) and bending strength against MOE for okan samples 2 and 4 (right).

6. CONCLUSIONS AND RECOMMENDATIONS CONCERNING THE SLOPE OF GRAIN IN THE STRENGTH CLASS ASSIGNMENT S OF TROPICAL HARDWOODS

For tropical hardwoods the slope of grain is the most important parameter that influence the bending strength and the Modulus of Elasticity. The relation of the slope of grain with these parameters can be described with Hankinson equations. Because the slope of grain is more difficult to assess than the size of knots for softwoods, only one visual grade is possible for tropical hardwoods. In practice it is assessed if the beams complies with the required limit of 1:10 for the slope of grain or not. The actual value of the slope of grain is not measured. However, it is shown that slope of grain values measured after testing can be much higher than the limit of 1:10, but also these values do not follow the Hankinson relations very well. This can be explained by the 3D effect that is difficult to capture visually.

The theoretical slope of grain can be determined with the measurements of the bending strength, the MOE and the density. The theoretical slope of grain follow the Hankinson relations very well. For 5 samples of okan species values for the theoretical slope of grain were found in the range from 0 to 0.3 for pieces that pass the normal visual grading assessment.

It is therefore advised that in the testing program for the strength class assignments specimens with values for the slope of grain up to 0.3 are incorporated in the testing program, when it cannot be ruled out, that these pieces might come on the market. The selection of the specimens can be made of the expected MOE for the range of slope of grains.

The slope of grain should be measured after testing and the theoretical slope of grain can be calculated. These distributions should be incorporated in the strength class assignment reports. For historical data where no slope of grain data are available the theoretical slope of grain can be calculated from the density, bending strength and MOE, to evaluate if the sampling was representative and not consisted of unique high quality samples.

REFERENCES

- EN 384 (2016). *Structural Timber- Determination of characteristic values of mechanical properties and density*. Brussels. CEN.
- EN 1912 . 2012. *Structural Timber – Strength classes- Assignment of visual grades and species*. Brussels. CEN.
- EN 1310 . 2012. *Structural Timber – Strength classes- Assignment of visual grades and species*. Brussels. CEN.
- EN 14081-1 (2016). *Timber Structures- Strength graded structural timber with rectangular cross section-Part1-1. General requirements*.
- NEN 5493 (2010). *Quality requirements for hardwoods in civil engineering works and other structural applications*. Delft. NEN
- EN 16737:2016 *Structural timber. Visual strength grading of tropical hardwood*. Brussels. CEN.
- NEN-EN 1995-1-1 (2005) . *Eurocode 5. Design of timber structures - Part 1-1: General- Common rules and rules for buildings*. Delft. NEN.
- Hankinson.,R.L., (1921) 'Investigation of crushing strength of spruce at varying angles of grain.', U.S. Air Service , Inform. Cir.3 no.259.
- Ravenshorst G.J.P. 2015. *Species independent strength grading of structural timber*, PhD thesis, Delft University of Technology.
- Ravenshorst G.J.P. Van de Kuilen J.W.G. (2016). *Species independent strength modeling of structural timber for machine grading*. WCTE 2016, Vienna.
- Ravenshorst G.J.P. Van de Kuilen J.W.G. (2018). *Relationships between non-destructive measurements and mechanical properties of tropical hardwoods*. WCTE 2018, Seoul.

Mechanical performance of wood-based products fabricated with Portuguese Poplar

S.R.S. Monteiro^{1*}, C. Martins¹, A.M.P.G. Dias¹, and H. Cruz²

¹Department of Civil Engineering
University of Coimbra,
Coimbra, 3030-788, Portugal

²Structures Department
LNEC – National Laboratory of Civil Engineering
Lisbon, 1700-066, Portugal

ABSTRACT

*Due to its mechanical properties, Poplar, a fast grown species, was deprecated in relation to stronger species, for several decades. Wood-based products help to change that point of view and Poplar has been gaining its space for structural uses. A state-of-the-art review concerning the use of Poplar to produce glued laminated products, with special focus on the use of Portuguese Poplar, is presented. The Portuguese forest is constituted by a great variety of species. The most common Poplar species found here are *Populus x Canadensis*, *P. nigra* L., and *P. alba* L.. Despite the limited availability, and the general hesitation on its structural application, recent studies on Poplar grown in the Portuguese forest showed its suitability for structural purposes. The use of this species to produce Glued Laminated Timber (GLT) beams revealed a very promising mechanical behavior. Bending strength tests evidenced a ductile behavior of most beams, which led to deepening the study on the raw material used to produce those beams which is described in detail elsewhere. Aiming at predicting the mechanical behavior of such beams, a 3D numerical model was developed, and the results compared with the experimental ones. A very good agreement between both approaches was found.*

1 INTRODUCTION

The Poplar paradigm, once regarded as a weed tree unwanted in timber stands, has changed, mostly in the last decades. Lack of the usual timber raw material (e.g. Pine timber) or the need to import it, associated with the available resources and/or the excessive demand of timber, contributed to this (Balatinecz et al., 2001; Bier, 1985; Fraanje, 1998). The uneven worldwide distribution of Poplar, among plantations (about 31.4 MH) and indigenous forests (about 54.5 MH), has varied over time due to numerous factors, from the economic to the biological ones. Despite the fact that North America, Europe and Asia concentrate about 98% the Poplar natural resources, currently they spread essentially over four countries: Canada with more than 39 MH (21.8 MH of plantations and 17.3 MH of indigenous forests); Russian Federation with 25 MH (indigenous forests); and U.S.A. and China with about 10 MH each (FAO, 2016). Back to the beginning of the last century, while Poplar wood of good quality was abundant in Canada, there was a shortage in some European countries. This was the chance to take advantage of crossing Poplar species, e.g. European silver poplar (*Populus alba* L.) with some Canadian native aspens (*P. tremuloides* Michx. and *P. grandidentata* Michx.) (Heimbürger, 1936). The timber demand in the second half of the last century, in countries as the U.S.A., Denmark, Sweden or Norway, increased the interest in Poplar wood. In addition, the easy hybridization (that in some cases can occur naturally) made the *Populus* genus the subject of genetics forest studies, promoting the emerging and the investigation of several Poplar hybrid clones (Beaudoin et al., 1992; Farmer, 1970; Farmer and Wilcox, 1968; Hernández et al., 1998; Koubaa et al., 1998; Schreiner, 1959).

The list of uses for this hardwood is rather diverse and includes pulp and paper, furniture, pallets, and biomass energy. However, its structural application raised doubts among producers and possible buyers. Some of its intrinsic characteristics are the susceptibility to discoloration or to decay, which diminishes the value of wood, and some manufacture problems; its lightness and softness with a relatively low density (280–520 kg/m³ for a moisture content of 12% (FAO, 1979)). These, together with the lack of knowledge on its mechanical properties, limited its worldwide acceptance for structural uses. The drying process was always a critical point since an inappropriate technique could lead to warp. Distortion is the consequence of different shrinkage coefficients in different directions within each piece, and in Poplar it is frequently associated with intrinsic factors like the presence of wet wood pockets, tension wood,

* Corresponding author: S. R. S. Monteiro; E-mail: sandra@dec.uc.pt

juvenile wood or longitudinal growth stress (Balatinez et al., 2014; Bier, 1985; Maeglin, 1985). However, government pressure to use the whole resource at the time of harvesting, together with technological advances and the will to add value to this fast grown species led to increasing its use, specifically in the development of engineered wood products, such as oriented strand board (OSB), in the last decades of the last century in North America (Morley and Balatinez, 1993). At the beginning of this century, in Northern Europe, applications different from those of low quality and short life span were also sought, by using solid and Poplar-based products as purlins (Fraanje, 1998).

2 POPLAR AS RAW MATERIAL FOR WOOD-BASED PRODUCTS

The wood-based products intend to improve the “natural resource” on its mechanical properties and performance, on its geometrical characteristics, such as length and shape, and at the same time to minimize wastage of raw material. The development of these products increased the structural applications of Poplar. Besides OSB, mentioned above, Poplar is used in other products, such as laminated veneer lumber (LVL), parallel strand lumber (PSL), laminated strand lumber (LSL), oriented strand lumber (OSL), glued laminated timber (GLT), laminated scrimmed lumber (Scrimber), among others, (Balatinez and Kretschmann, 2001; Castro and Fragnelli, 2006; De Boever et al., 2007; He et al., 2016; Sheriff, 1998; Van Acker et al., 2016). The manner in which these products are obtained includes combining timber or wood components, in flakes, strands, veneers, or laminations, with adhesives (e.g. Phenol-formaldehyde resins, usually used in OSB and Plywood; or Melamine-Urea-Formaldehyde used in GLT) and in some cases with additives (e.g. wax, to improve water resistance; or preservatives and fire retardants, among others, depending on the purpose of the wood-based product) (American Wood Council, 2018; Bolden and Greaves, 2008; Forest Products Laboratory, 2010; Martins et al., 2017).

GLT, also known as glulam, is part of this category and is the oldest wood-based product made. The first records of its use date back to the early 1890s, in Europe, with its patenting in 1906 by a German master carpenter (Rinke, 2015). This composite is obtained by gluing together two or more lamellae of lumber (about 45 mm maximum thickness (EN14080, 2013)), with their grain aligned with the length direction of the structural piece. The lamellar constitution combined with the manner in which the lamellae are coupled to each other (end-to-end, edge-to-edge, and face-to-face) allows a customized cross-section with a virtually unlimited width and height multiple of the individual thickness of the lamella. A broad range of sizes and shapes, straight or curved, can be achieved with this composite. A great revolution associated with GLT production and use happened when the synthetic adhesives developed for gluing the lamellae allowed its application in exterior environment conditions. All these characteristics make GLT suitable for numerous structural applications (APA, 2017; EN14080, 2013; Forest Products Laboratory, 2010; Yeh, 2002).

3 ADVANTAGES OF USING POPLAR IN THE PRODUCTION OF GLUED LAMINATED TIMBER BEAMS

As explained above, Poplar was not always a species of choice for structural applications. With the advent of composite materials, thus diminishing the variability on the mechanical properties when compared with the natural resource, the mind state started to change. This paper intends to present the advantageous properties - specifically mechanical properties - of GLT beams produced using Portuguese Poplar species. The use of Poplar species to produce this composite is not new, with the first scientific references dating back the second half of the 1980's. According to (Lepper and Keenan, 1986), investigation of the use of Poplar species to produce GLT was a consequence of supply problems associated with the usual raw material, Douglas-fir, in Canada by that time, which threatened the economic competitiveness of this composite. These authors studied the strength and stiffness of a set of Poplar (*P. tremuloides Michx.* and *P. balsamifera L.*) laminations through experimental tests and the collected results were used as input data to analytically model GLT beams made with this material. Also, the strength and stiffness of those beams were obtained and analyzed, which results indicated that the species of Poplar studied are suitable to produce GLT beams, but further studies are suggested. In the following years, various studies were developed concerning the use of Yellow Poplar¹ (*Liriodendron tulipifera*) to produce glulam, reaching similar conclusions (Hernandez et al., 1997; Moody et al., 1993).

Although the following decades were not very productive regarding studies about Poplar species, as Lepper and Keenan had foreseen, several studies were developed since then, using this species to produce glued laminated timber, as the following paragraphs show. Some others, using Poplar as raw material, focused reaching a final composite with improved mechanical properties, and the overall behavior when subjected to bending, through its association with wood treatments (preservative or hydrothermal (De Boever et al., 2016; Han et al., 2018; Marcon et al., 2018; Mirzaei

¹ Although Yellow Poplar is not of the *Populus* genus, given its similar characteristics, such as lightness, smoothness, and tree shape and growth rate, it is often assumed as Poplar. In fact, it is usually known only by the name Poplar (omitting the “Yellow”).

et al., 2017)), as well as inner or outer reinforcement, such as e.g. steel, fiber-reinforced polymers (FRP), carbon fiber-reinforced polymers (CFRP) or glass fiber-reinforced polymers (GFRP) (Cheng and Hu, 2011; Lu et al., 2015; Osmannezhad et al., 2014; Tomasi et al., 2009).

To produce a GLT beam, a homogenous or combined cross-section can be assembled. The second option, also known as combined glulam, is only suitable for horizontally laminated members. When the element is subjected to bending stresses, the outer lamellae will be the ones subjected to higher compressive (upper lamella) and tensile (lower lamella) stresses, thus those will be the ones with the higher timber grade, while the inner lamellae will be of lower grade. This is a procedure particularly efficient and economical concerning the flexural response of the GLT beam (Forest Products Laboratory, 2010). Following this reasoning, some studies arose focusing on the use of different species in the same cross-section, aiming to balance the structural response of the combination with weight, cost and/or performance (such as (Castro and Paganini, 2003)). The use of Poplar on these combinations allows taking advantage of characteristics that, in a solid section of this species, could be seen as disadvantages. Some examples are its lightness when using Poplar in the inner lamellae in combination with heavier stronger species, like, for instance, *Eucalyptus* (e.g. *Eucalyptus grandis* (Castro and Paganini, 1999)). On the other hand, positioning the Poplar lamellae on the compression side and the stronger species on the lamellae subjected to tension intends to induce the development of deformations on the most compressed lamella outside the elastic domain, associated with a ductile behavior. Additionally, the ratio between strength and density of Poplar species results in a high structural efficiency ratio, which is another advantage, especially when concerning the behavior of the GLT beam under dynamic actions (Del Senno et al., 2003).

In Portugal, given the limited availability of this raw material, only recently some studies took place, like those developed by Hodoušek et al. and Martins et al. (Hodoušek et al., 2017; Martins et al., 2018, 2017). Those studies investigated Poplar grown in the Portuguese forest, specifically *P. x Canadensis*, *P. nigra L.*, and *P. alba L.* showing its suitability for structural purposes. On the study (Martins et al. 2018), the authors produced and experimentally studied several GLT beams. Bending strength mechanical tests evidenced a ductile behavior associated with two-thirds of the produced set of beams. This led to deepening the study on the material used to produce those beams, aiming to analyze their mechanical properties (Monteiro et al., 2019). Therefore, more Poplar GLT beams were produced and tested, and from the tests' remains, several samples were collected in order to perform a mechanical characterization, in tension and in compression, of clear wood specimens. Also, these tests showed a significant ductile behavior associated with compression parallel-to-grain, suggesting the potential advantages associated with the use of these species for the production of GLT beams.

4. MECHANICAL BEHAVIOR OF WOOD

Despite, in general, timber be assumed as a brittle material, and the only possible ductile structural behavior be associated with the steel connections, this is not completely true since wood under compression may present a ductile behavior. (Pirinen, 2014) states that this behavior is a consequence of some factors at the wood structure level, specifically the inelastic buckling deformations of the cell walls, which also depends on the angle between the compressive ultimate load and the grain directions. When the grain and compression load have the same direction there is a strain-hardening following the elastic phase. Regarding the radial and the tangential compression, slight hardening and almost perfectly plastic behavior occur, respectively. In the latter case, the ultimate strain is essentially limited by splitting when wood deforms, due to tension perpendicular-to-grain.

Concerning GLT beams, the general consideration of a linear behavior until failure remains. From the studies using Poplar species to produce GLT beams, some focused the numerical modeling. Different goals led to different approaches by their authors, namely concerning the manner in which wood mechanical behavior was modeled. Aiming at obtaining a numerical model capable to predict the mechanical behavior of these beams, also studies using different wood species were considered, in order to gather as much information as possible. In general, authors sought for describing the GLT beams behavior, considering the effect of several parameters (e.g. defects, finger joints connections, delamination, combination of species, among others), and/or sought for their mechanical properties (Frese et al., 2010b, 2010a; Frese and Blaß, 2007, 2005; Gao et al., 2015; Kandler et al., 2018, 2015; Kessel and Guenther, 2006; Serrano et al., 2001), with focus on the elastic phase. Studies like those from Frese and Blaß, Kandler et al. and Frese et al. (Frese et al., 2010b, 2010a; Frese and Blaß, 2007, 2005; Gaspar et al., 2005; Kandler et al., 2018, 2015) follow a common approach: to establish equations able to estimate properties such as bending strength, based on parameters as the mechanical properties of the boards that constitute them, the mechanical properties of the finger joints, and the cross-section dimensions.

There are, however, some studies, like the ones developed by (Čizmar et al., 2014; Del Senno et al., 2004; Tomasi et al., 2009) which sought to consider the ductile capability of GLT beams, with the latter two focusing the use of Poplar together with other species in the same cross-section, with the Poplar located in the compression zone. The three works sought to define the constitutive law of timber in bending, listing some of the existing approaches to do so, as for the elastic phase, as for the post-elastic phase, considering ductility.

5. NUMERICAL ANALYSIS

5.1. EXPERIMENTAL DATA

A set of twenty-one Poplar GLT beams was produced and their bending properties, namely modulus of elasticity (local, $E_{m,l}$ and global, $E_{m,g}$) and bending strength parallel to grain (f_m), were obtained. Each beam was composed of five lamellae, 24 mm thick, resulting on a $92 \times 120 \text{ mm}^2$ (width \times height) cross-section. They were experimentally tested subjected to four-point static bending tests, following the (EN408, 2012). An experimental average value of bending strength of 55.3 MPa was found (with a coefficient of variation, COV, of 17.9%) at the ultimate deformation (average value of 68.7 mm). The load-deflection curves were obtained and gathered in Figure 1 and Figure 2. This allows identifying two sets concerning the behavior of the beam: a tendentially elastic behavior (Figure 1); a non-linear behavior where the ductile phase can be clearly identified (Figure 2)). More than two-thirds of the sample fall in the latter set. Taking into account that stated in section 4, this is undoubtedly a very interesting and promising behavior, concerning the use of these structural elements made from Portuguese Poplar. Aiming at better understanding and characterizing the material associated with this behavior, experimental clear wood tests were performed, in tension and in compression parallel-to-grain, in order to mechanically characterize the species used to produce the GLT beams. From the beams subjected to bending test until failure, the upper and lower lamellae were collected taking into consideration the maximum undamaged length of the lamella, the available length clear from defects, such as knots, cracks or other defects, aiming at producing the specimens for compression and tension tests, respectively. A set of twenty clear wood tests in tension parallel-to-grain and the same amount in compression parallel-to-grain were performed. Linear elastic behavior was found for all the specimens subjected to tension tests, and a non-linear ductile behavior was found for those subjected to compression tests. The data collected from both sets of tests allow obtaining a stress-strain curve which characterizes the typical (average) behavior of the Portuguese Poplar species in both loadings (Monteiro et al., 2019).

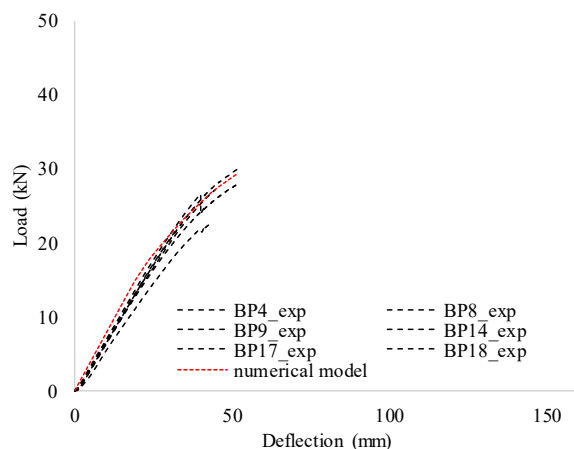


Figure 1: Experimental and numerical load-deflection curves from linear elastic behavior set of beams.

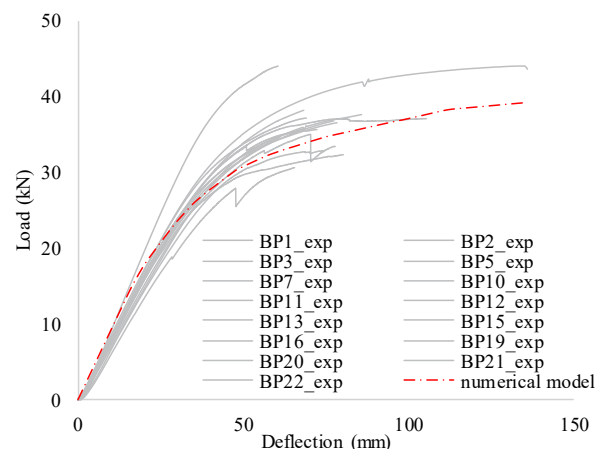


Figure 2: Experimental and numerical load-deflection curves from non-linear behavior set of beams.

The first group is identified by lower values of strain, when compared with the average maximum strain values, from Poplar mechanical characterization in tension parallel-to-grain, 0.683%, with an average bending strength of 42.9 MPa (COV = 12.0%) and an average ultimate deformation of 44.3 mm. Expressive differences were found for the non-linear behavior set, with an average bending strength of 60.3 MPa (COV = 10.1%), and a significantly higher

average ultimate deformation of 78.5 mm. Among the beams of this group, significant deformation was observed in four beams (BP3, BP5, BP20, and BP21), which approaches its mechanical behavior to elastic-perfectly plastic.

5.2. NUMERICAL MODELLING

Aiming at obtaining a numerical model which predicts adequately the behavior of GLT beams subjected to bending, a three-dimensional model was developed using Abaqus CAE (Simulia, 2017) software. The GLT beam considered intends to simulate those produced with the Portuguese Poplar species and described in (Martins et al., 2018) subjected to a static bending test, as described in the previous subsection. The same dimensions were considered. A 3D solid finite element continuum and hexahedral (C3D8R) was chosen. This kind of element is a height-node brick element with reduced integration, hourglass control, and first-order interpolation. It has three degrees of freedom per node, each one corresponding to a translation in each of the three directions (x, y, and z). In order to obtain an efficient mesh, as regards to accuracy versus computing time, a mesh with approximately 12 mm (half thickness of each lamella) was adopted. In a simplified manner, the contact interaction between adjacent lamellae was considered as rigid. This was achieved through connection nodes between the surfaces of both lamellas, assuming a Master-Slave relation, with the dominant surface (Master) corresponding to the lamella with a higher dynamic modulus of elasticity (E_{dyn_1}). Concerning the test layout, a simply supported beam loaded at thirds was considered. Therefore, a pinned support with no translations was associated with one of the supports, and a second one was defined using a pinned support with all the translations blocked but the one parallel to beam' longitudinal axis. The load procedure defined in the model followed the procedure defined in the experimental test, as well as the loading conditions recommended in EN 408 (2012). Therefore, an imposed displacement of 100 mm was adopted for both load points. There were cases in which the ultimate deformation of the beams exceeded 100 mm, for those a displacement of 200 mm was assumed.

In order to model the material mechanical behavior three parameters were taken into account: i) density, ii) elastic behavior, and iii) plastic behavior. Wood is an anisotropic material. Nevertheless, simplified approaches modeled it as orthotropic, with three axes of symmetry, defined by the three main directions: longitudinal (L), radial (R) and tangential (T). Aiming at defining the elastic phase of the material behavior, three properties were considered, namely: i) modulus of elasticity (E), ii) shear modulus (G), and iii) Poisson coefficients (ν). The definition of these elastic constants passed through an iterative procedure which details can be found in (Martins, 2018; Martins et al., 2019). The values adopted are listed in Table 1, wherein E_{dyn_1} corresponds to the values obtained experimentally for the longitudinal dynamic modulus of elasticity (detailed information can be found in (Martins, 2018)). The numerical definition of the wood behavior, in tension and in compression, was based on five stress-strain pairs, corresponding to the values of 10%, 50%, 70%, 90% and 100% of the maximum strength of each specimen, in tension and in compression, respectively. Aiming at considering the ductile behavior in compression, an extra stress-strain pair was used, corresponding to 90% of the maximum stress value (90%_d) in the descending branch (see Table 2).

Table 1: Poplar elastic constants

Modulus of Elasticity		Shear Modulus		Poisson' Coefficients	
Longitudinal, E_L	E_{dyn_1}	G_{LR}/E_L (%)	7.55	VLR	0.331
				VL T	0.406
E_R/E_L (%)	8.75	G_{LT}/E_L (%)	6.05	VRT	0.789
				VTR	0.311
E_T/E_L (%)	4.50	G_{RT}/E_L (%)	1.10	VRL	0.037
				VTL	0.019

Table 2: Numerical mechanical behavior of wood

Stress %	Tension		Compression	
	Stress (MPa)	Strain (%)	Stress (MPa)	Strain (%)
10%	6.9	0.065	3.3	0.030
50%	34.6	0.333	16.3	0.160
70%	48.4	0.470	22.9	0.248
90%	62.2	0.609	29.4	0.360
100%	69.2	0.683	32.7	0.456
90%_d	-	-	33.0	2.418

As Figure 1 and Figure 2 have already shown, two sets of beams with different behavior were identified: one, composed of 6 beams, with linear elastic behavior up to failure (BP4, BP8, BP9, BP14, BP17, and BP18), and a second one, of 15 beams, with non-linear behavior. In addition to the experimental curves, these figures also present two numerical curves representative of the two types of behavior. For the first set, a numerical average bending strength of 46.3 MPa (COV = 9.9%), and for the second set, a value of 57.9 MPa (COV = 7.2%) were found. In general, there is a very good agreement between the numerical and the experimental results, concerning the maximum tensile stress of the GLT beam, with a mean absolute error of 7.3% and a coefficient of determination, R^2 , of 0.73. As for the maximum

compressive stress values, in 81% of the beams, numerical compressive stresses were higher or very close to the mean experimental values of clear wood tests (33 MPa). This work is described in detail elsewhere (Monteiro et al., 2019).

6. CONCLUSIONS

Poplar, a light wood with a fast growth rate, which mechanical properties and durability were once brought into question, has been conquering its space on structural applications. This is, in part, a consequence of the development of wood-based products, which allow diminishing the effect of concentrated defects (such as knots) in the product properties, creating a more uniform material when compared with the raw solid wood pieces. The oldest wood-based product, glued laminated timber or GLT, was the focus of this study, specifically addressing the use of Portuguese Poplar species to produce GLT. A sample composed of *Populus x Canadensis*, *P. nigra L.*, and *P. alba L.* was used to produce twenty-one GLT beams. When subjected to static bending tests, most of the sample showed a clear ductile behavior. With the purpose to analyze these beams mechanical behavior, when subjected to bending, a 3D numerical model was developed. Each beam was modeled and its numerical results compared with the experimental ones. A mean absolute error of 7.3%, concerning the maximum tensile stress, was found, which corresponds to a coefficient of determination of 0.73.

ACKNOWLEDGMENTS

This work was partly financed by FEDER funds through the Competitiveness Factors Operational Programme – COMPETE and by national funds through FCT – Foundation for Science and Technology, within the scope of the Project POCI-01-0145-FEDER-007633 as well as, by the Operational Program Competitiveness and Internationalization R&D Projects Companies in Co-promotion, Portugal 2020, within the scope of the project OptimizedWood – POCU-01-0247-FEDER-017867. The authors wish to thank Foundation for Science and Technology for the Ph.D. grant (PD/BD/52656/2014) given to Carlos Martins, to Dynea AS and Henkel for providing the adhesives and finally to Pedrosa Irmãos for the collaboration given concerning the timber.

REFERENCES

- American Wood Council, 2018. *Manual for Engineered Wood Construction*.
- APA, 2017. *Glulam Product Guide (No. Form No.X440)*. APA – The Engineered Wood Association.
- Balatinecz, J., Mertens, P., De Boever, L., Yukun, H., Jin, J., Van Acker, J., 2014. *Properties, Processing and Utilization*, in: *Poplars and Willows: Trees for Society and the Environment*. FAO and CABI, pp. 527–561.
- Balatinecz, J.J., Kretschmann, D.E., 2001. *Properties and utilization of poplar wood*, in: *Poplar Culture in North America, Part A*. NRC Research Press, National Research Council of Canada, Ottawa, ON KIA OR6, Canada, pp. 277–291.
- Balatinecz, J.J., Kretschmann, D.E., Leclercq, A., 2001. *Achievements in the utilization of poplar wood – guideposts for the future*. *The Forestry Chronicle* 77, 265–269. <https://doi.org/10.5558/tfc77265-2>
- Beaudoin, M., Hernández, R.E., Koubaa, A., Poliquin, J., 1992. *Interclonal, Intraclonal and Within-Tree Variation in Wood Density of Poplar Hybrid Clones*. *Wood and Fiber Science* 24, 147–153.
- Bier, H., 1985. *Structural Properties of Timber from Two Poplar Varieties*. *New Zealand Journal of Forestry Science* 15, 223–32.
- Bolden, S., Greaves, H., 2008. *Guide to the specification, installation and use of preservative treated engineered wood products*, *Market Knowledge & Development*. Forest & Wood Products Australia.
- Castro, G., Fragnelli, G., 2006. *New technologies and alternative uses for poplar wood*.
- Castro, G., Paganini, F., 2003. *Mixed glued laminated timber of poplar and Eucalyptus grandis clones*. *Holz als Roh- und Werkstoff* 61, 291–298. <https://doi.org/10.1007/s00107-003-0393-6>
- Castro, G., Paganini, F., 1999. *Poplar-Eucalyptus glued laminated timber*. Presented at the EUROWOOD Technical Workshop “Industrial end-uses of fast-grown species,” Florence, Italy.
- Cheng, F., Hu, Y., 2011. *Nondestructive test and prediction of MOE of FRP reinforced fast-growing poplar glulam*. *Composites Science and Technology* 71, 1163–1170. <https://doi.org/10.1016/j.compscitech.2011.04.007>
- Čizmar, D., Damjanović, D., Pavković, K., Rajčić, V., 2014. *Ductility analysis of laminated timber beams of small section height*. *GRADEVINAR* 66, 395–406. <https://doi.org/10.14256/JCE.874.2013>
- De Boever, L., Van den Bulcke, J., Van Acker, J., 2016. *Potential of thermally modified poplar wood for construction products*, in:

- Proceedings of the 2nd Conference on Engineered Wood Products Based on Poplar/Willow Wood. León, Spain, pp. 107–112.*
- De Boever, L., Vansteenkiste, D., Acker, J., Stevens, M., 2007. *End-use related physical and mechanical properties of selected fast-growing poplar hybrids (Populus trichocarpa × P. deltoides). Annals of Forest Science 64, 621–630.* <https://doi.org/10.1051/forest:2007040>
- Del Senno, M., Paganini, F., Piazza, M., Tomasi, R., 2003. *Investigation on Failure Behavior of Mixed-Species Glued Laminated Timber Beams. Architectural Engineering, Proceedings 1–4.* [https://doi.org/10.1061/40699\(2003\)41](https://doi.org/10.1061/40699(2003)41)
- Del Senno, M., Piazza, M., Tomasi, R., 2004. *A pseudo-ductile approach design of glued laminated timber beams, in: WCTE 2004. Presented at the 8th World Conference on Timber Engineering, Lahti, Finland, pp. 517–522.*
- EN408, 2012. *Timber structures - Structural timber and glued laminated timber - Determination of some physical and mechanical properties. CEN - European Committee for Standardization, Brussels.*
- EN14080, 2013. *Timber structures - Glued laminated timber and glued solid timber - Requirements. CEN - European Committee for Standardization, Brussels.*
- FAO, 2016. *Poplars and Other Fast-Growing Trees - Renewable Resources for Future Green Economies: Synthesis of Country Progress Reports - Activities Related to Poplar and Willow Cultivation and Utilization- 2012 through 2016 (Working Paper IPC/15). FAO, IPC, Rome, Italy.*
- FAO, 1979. *Poplars and Willows in Wood Production and Land Use, FAO Forestry Series. FAO, Rome.*
- Farmer, R.E., 1970. *Genetic Variation Among Open-Pollinated Progeny of Eastern Cottonwood. Silvae Genetica 19(5-6):149-151* 19, 149–151.
- Farmer, R.E., Wilcox, J.R., 1968. *Preliminary testing of eastern cottonwood clones. Theoret. Appl. Genetics 38, 197–201.* <https://doi.org/10.1007/BF00935267>
- Forest Products Laboratory, 2010. *Wood handbook: wood as an engineering material (No. General Technical Report FPL-GTR-190). USDA, Forest Service, Forest Products Laboratory, Madison, WI.*
- Fraanje, P.J., 1998. *Poplar wood for purlins; an evaluation of options and environmental aspects. Holz als Roh- und Werkstoff 56, 163–169.* <https://doi.org/10.1007/s001070050291>
- Frese, M., Blaß, H.J., 2007. *Characteristic bending strength of beech glulam. Mater Struct 40, 3–13.* <https://doi.org/10.1617/s11527-006-9117-9>
- Frese, M., Blaß, H.J., 2005. *Beech Glulam Strength Classes, in: Working Commission W18 - Timber Structures, Meeting Thirty-Eight. Presented at the International Council for Research and Innovation in Building and Construction, Karlsruhe, Germany, p. 11.*
- Frese, M., Chen, Y., Blaß, H.J., 2010a. *Tensile strength of spruce glulam. Eur. J. Wood Prod. 68, 257–265.* <https://doi.org/10.1007/s00107-010-0449-3>
- Frese, M., Hunger, F., Blaß, H.J., Glos, P., 2010b. *Verification of strength models for glulam bending strength (Verifikation von Festigkeitsmodellen für die Brettschichtholz-Biegefestigkeit). Eur. J. Wood Prod. 68, 99–108.* <https://doi.org/10.1007/s00107-009-0384-3>
- Gao, Y., Wu, Yuxuan, Zhu, X., Zhu, L., Yu, Z., Wu, Yong, 2015. *Numerical Analysis of the Bending Properties of Cathay Poplar Glulam. Materials 8, 7059–7073.* <https://doi.org/10.3390/ma8105362>
- Gaspar, F., Cruz, H., Nunes, L., Gomes, A., 2005. *Glued-laminated structures made with autoclaved Pine wood (Fabrico de estruturas lameladas-coladas com madeira de Pinho bravo tratada em autoclave), in: Proceedings do 5.o Congresso Florestal. Viseu.*
- Han, Z., Zhang, R., Song, B., 2018. *Evaluation of the Bending Properties of Modified Fast-growing Poplar Glulam Based on Composite Mechanics. BIORESOURCES 13, 7071–7085.*
- He, M.-J., Zhang, J., Li, Z., Li, M.-L., 2016. *Production and mechanical performance of scrimber composite manufactured from poplar wood for structural applications. Journal of Wood Science 62, 429–440.* <https://doi.org/10.1007/s10086-016-1568-1>
- Heimburger, C., 1936. *REPORT ON POPLAR HYBRIDIZATION 1936.*
- Hernandez, R., Davalos, J.F., Sonti, S.S., Kim, Y., Moody, R.C., 1997. *Strength and stiffness of reinforced yellow-poplar glued-laminated beams 30.*
- Hernández, R.E., Koubaa, A., Beaudoin, M., Fortin, Y., 1998. *Selected mechanical properties of fast-growing poplar hybrid clones. WOOD AND FIBER SCIENCE 30, 10.*
- Hodoušek, M., Dias, A.M.P.G., Martins, C., Marques, A., Böhm, M., 2017. *Comparison of Non-Destructive Methods Based on Natural Frequency for Determining the Modulus of Elasticity of Cupressus lusitanica and Populus x canadensis. BioResources 12, 270–282.* <https://doi.org/10.15376/biores.12.1.270-282>
- Kandler, G., Füssl, J., Serrano, E., Eberhardsteiner, J., 2015. *Effective stiffness prediction of GLT beams based on stiffness*

- distributions of individual lamellas. *Wood Sci. Technol.* <https://doi.org/10.1007/s00226-015-0745-5>
- Kandler, G., Lukacevic, M., Füssl, J., 2018. Experimental study on glued laminated timber beams with well-known knot morphology. *Eur. J. Wood Prod.* 76, 1435–1452. <https://doi.org/10.1007/s00107-018-1328-6>
- Kessel, M.H., Guenther, M., 2006. Assessment of the load bearing capacity of defectively glued laminated timber, in: *WCTE 2006. Presented at the 9th World Conference on Timber Engineering, Portland, OR, U.S.A.*
- Koubaa, A., Hernández, R.E., Beaudoin, M., Poliquin, J., 1998. Interclonal, Intraclonal, and Within-Tree Variation in Fiber Length of Poplar Hybrid Clones. *Wood and Fiber Science* 30, 40–47.
- Lepper, M.M., Keenan, F.J., 1986. Development of poplar glued–laminated timber. I: Tensile strength and stiffness of poplar laminating stock. *Canadian Journal of Civil Engineering* 13, 445–459. <https://doi.org/10.1139/186-069>
- Lu, W., Ling, Z., Geng, Q., Liu, W., Yang, H., Yue, K., 2015. Study on flexural behaviour of glulam beams reinforced by Near Surface Mounted (NSM) CFRP laminates. *Constr Build Mater* 91, 23–31. <https://doi.org/10.1016/j.conbuildmat.2015.04.050>
- Maeglin, R.R., 1985. Using Poplar Wood for Structural Lumber: the SDR Process. Presented at the 22nd Annual Meeting of the Poplar Council of the United States, Lawrence, KS, p. 10.
- Marcon, B., Goli, G., Matsuo-Ueda, M., Denaud, L., Umemura, K., Gril, J., Kawai, S., 2018. Kinetic analysis of poplar wood properties by thermal modification in conventional oven. *iForest* 11, 131–139. <https://doi.org/10.3832/ifor2422-010>
- Martins, C., 2018. Structural Evaluation of Glued Laminated Timber Elements (Avaliação Estrutural de Elementos de Madeira Lamelada Colada) (PhD Thesis). University of Coimbra, Coimbra.
- Martins, C., Dias, A.M.P.G., Cruz, H., 2019. Numerical and experimental analysis of glulam modulus of elasticity. (unpublished).
- Martins, C., Dias, A.M.P.G., Cruz, H., 2018. Using non-destructive testing to predict the mechanical properties of poplar glued laminated timber. *Proceedings of the ICE – Structures and Buildings.* <https://doi.org/10.1680/jstbu.18.00060>
- Martins, C., Dias, A.M.P.G., Cruz, H., 2017. Glulam made by Poplar: Delamination and shear strength tests. Presented at the 6th ISCHP, Lahti, Finland, pp. 222–231.
- Mirzaei, G., Mohebbi, B., Ebrahimi, G., 2017. Glulam beam made from hydrothermally treated poplar wood with reduced moisture induced stresses. *Constr Build Mater* 135, 386–393. <https://doi.org/10.1016/j.conbuildmat.2016.12.178>
- Monteiro, S.R.S., Martins, C.E.J., Dias, A.M.P.G., Cruz, H., 2019. Mechanical Characterization of Clear Wood from Portuguese Poplar. *BioResources* (unpublished).
- Moody, R.C., Hernandez, R., Davalos, J.F., Sonti, S.S., 1993. Yellow Poplar Glulam Timber Beam Performance (Research Paper), FPL-RP-520. United States Department of Agriculture, Forest Service, Forest Products Laboratory, Madison, WI.
- Morley, P.M., Balatinecz, J.J., 1993. Poplar utilization in Canada: Past, present and future. *The Forestry Chronicle* 69, 46–52. <https://doi.org/10.5558/tfc69046-1>
- Osmannezhad, S., Faecipour, M., Ebrahimi, G., 2014. Effects of GFRP on bending strength of glulam made of poplar (*Populus deltoids*) and beech (*Fagus orientalis*). *Constr Build Mater* 51, 34–39. <https://doi.org/10.1016/j.conbuildmat.2013.10.035>
- Pirinen, M., 2014. Ductility of Wood and Wood Members Connected with Mechanical Fasteners (MSc). Aalto University, Espoo, Helsinki, Finland.
- Rinke, M., 2015. Terner & Chopard and the new timber –Early development and application of laminated timber in Switzerland. Presented at the 5th International Congress on Construction History, Chicago, p. 8.
- Schreiner, E.J., 1959. Production of Poplar Timber, in Europe and Its Significance and Application in the United States, *Agriculture Handbook*. USDA Forest Service.
- Serrano, E., Gustafsson, P.J., Larsen, H.J., 2001. Modeling of Finger-Joint Failure in Glued-Laminated Timber Beams. *Journal of Structural Engineering* 127, 914–921. [https://doi.org/10.1061/\(ASCE\)0733-9445\(2001\)127:8\(914\)](https://doi.org/10.1061/(ASCE)0733-9445(2001)127:8(914))
- Sheriff, D.W., 1998. Productivity and Economic Assessment of Hardwood Species for Scrimber Production (No. 98/4 RIRDC Project No. CSF–38A).
- Simulia, 2017. AbaqusCAE, Abaqus 6.14. Dassault Systèmes, USA.
- Tomasi, R., Parisi, M.A., Piazza, M., 2009. Ductile Design of Glued-Laminated Timber Beams. *Practice Periodical on Structural Design and Construction* 14, 113–122. [https://doi.org/10.1061/\(ASCE\)1084-0680\(2009\)14:3\(113\)](https://doi.org/10.1061/(ASCE)1084-0680(2009)14:3(113))
- Van Acker, J., Defoirdt, N., Van den Bulcke, J., 2016. Enhanced potential of poplar and willow for engineered wood products, in: *Proceedings of the 2nd Conference on Engineered Wood Products Based on Poplar/Willow Wood*. León, Spain, pp. 187–210.
- Yeh, B., 2002. Structural Glued Laminated Timber (Glulam), in: *APA Engineered Wood Handbook*. McGRAW-HILL.

Vertical Forest Engineering: Applications of Vertical Forests with Self-Growing Connections in High-Rise Buildings

Xiuli Wang^{1*}, Wolfgang Gard¹, and J.W.G van de Kuilen^{1,2}

¹Biobased Structures and Materials
Delft University of Technology
Delft, The Netherlands

²Chair of Wood Technology
Technical University of Munich
Munich, Germany

ABSTRACT

Living architecture is thriving. The integration of buildings with vegetation has become a necessity in many metropolitan areas of the world today, including Singapore, New York City, Shanghai and Milan, to name a few. It expands the potential of vertical and horizontal, exterior and interior, exposed and enclosed spaces in a building that can be used to accommodate plants. Green infrastructures have benefits both on urban and building scales. They can be categorized into green roofs and vertical greenery systems that can be divided further into green façade, green/living wall, green terraces, elevated forests and vertical forests. There are many design and planting considerations for architects, structural engineers and botanists when using living architectures to mimic natural systems, such as climatic and regional considerations, primary functions and design objectives, structural support systems, maintenance, irrigation and so on. Plants used for vertical greenery are more likely to be hardwood species to adjust solar radiation during cooling and heating periods, and also for aesthetic pleasure. Take Bosco Verticale, which is located in Milan, as an example to look into engineering methods when trees grow on balconies of high rise buildings. It could be concluded that planting restraint safety system and regular maintenance are necessary for trees growing in the sky. But the change of growing conditions causes various problems such as stability and growth of trees. Instead of using steel cages and bracings to prevent falling off of trees in the sky, the concept of self-growing connections is proposed to provide the stability of vertical forests. This paper is meant to generate awareness of the possibilities of the integration of greenery vertically with buildings, show application considerations, and inspire future developments in typologies and integration with forests.

1. INTRODUCTION

Cities are getting bigger and denser while buildings are getting bigger and taller. There is a growing significance of environmental issues such as urban island effects and reduction of energy consumption which are relevant to dense urbanization.

While high-rise buildings as a typology have evolved to become predominant nowadays, there are several challenges to meet. One is that buildings should be more in tune with their locations in term of both sustainability and design (Wood, 2008). Another challenge is that buildings should minimize the usage of non-renewable energy, pollution, with increased comfort, health, and safety of people who live and work in them (Sheweka & Magdy, 2011). With increasing building height, it is challenging to provide a high-quality work environment with natural ventilation. Because of higher and irregular wind speeds, this leads to a closing-off and dislocation of their natural surroundings.

Vegetation plays an important role by its special properties with energy balance and human health in urban areas. The benefits of vegetation in buildings are similar to ordinary vegetation in cities. It has become an important new construction principle to increase the livability and sustainability of modern buildings both outdoor and indoor (Feng & Hewage, 2014). Positive climatic effects can be created by combining green cover on walls, roofs, and in open spaces in the vicinity of buildings (Wilmers, 1990). Indoor plants can provide comfort by means of purification (Wolverton & Wolverton, 1993), humidification and psychological relaxation (Raji, Tenpierik, & van den Dobbelen, 2015), and indoor greening technology such as indoor vertical green walls has been proved to be one effective way to improve indoor air quality (Wang, Er, & Abdul-Rahman, 2016). While comparing outdoor plants with blinds in buildings,

* Corresponding author: Xiuli Wang; E-mail: X.Wang-16@tudelft.nl

plants create more effective shading performance than blinds, which should be considered as a way of construction with building envelope (Stec, van Paassen, & Maziarz, 2005).

In densely populated regions, where green areas are scarce and open ground space is limited, the concept of integrating nature with high rise buildings represents an innovative and sustainable opportunity for green infrastructure in cities (Medl, Stangl, & Florineth, 2017). Greening technology can protect building façades which are under permanent environmental influences such as sun and rain which may damage the facades and reduce their service life (Köhler, 2008). Roofs of buildings are suitable spaces to accommodate vegetation. At the same time, greening of walls of high-rise buildings can also be feasible since the difference between surface area of walls and roofs can reach roughly 20 times (Pérez, Coma, Martorell et al., 2014). Numerous countries in the world, such as USA (Susorova, Angulo, Bahrami et al., 2013), Italy (Giacomello, 2015) and Singapore (Yok, 2013) have shown great interests in green infrastructures. The technologies of green infrastructures extend the potential of horizontal and vertical, exterior and interior spaces in a building that can accommodate plants (Tan, Köhler, Peck et al., 2014).

In this study, an identification and a classification of vertical greenery systems are proposed. Then some recommendations are given for design considerations and planting strategies that should be studied in depth. Based on the system of vertical forests, an innovative concept of self-growing connections is proposed to provide reliability and stability to a vertical forest. In the end, this study gives an overview on current debates and state-of-the-art technologies as a basis for further development of vertical forest engineering.

2. GREEN INFRASTRUCTURE

2.1. CLASSIFICATION

Greenery can be inserted on buildings in many forms including horizontal and vertical, exterior and interior spaces. Green infrastructure can be considered to comprise all natural, semi-natural and artificial networks of multifunctional ecological systems within, around and between urban areas, at all spatial scales (Tzoulas, Korpela, Venn et al., 2007). But because of the diversity of disciplines, application contexts, methods, terminologies, purposes and valuation criteria, there is no consensus on a comprehensive classification for green infrastructure (Koc, Osmond, & Peters, 2017). In this study, green infrastructures are organized into two main categories: green roofs and elevated forests which are considered horizontal greenery and vertical greenery systems which include green façades, green/living walls, green terraces and vertical forests.

2.2. HORIZONTAL GREENERY

Green roof is one of the earliest forms of green infrastructures. Green roofs can be defined as roofs with a vegetated surface and substrate which can be divided into intensive and extensive green roof depending on substrate depths, roof dimension and intensity of use. It can provide ecosystem services in urban areas, including improved storm-water management, better regulation of building temperatures, increased sound insulation (Dunnett & Kingsbury, 2008), reduces urban heat-island effects (Besir & Cuce, 2018), and increased urban wildlife habitat (Bass, Rowe, Oberndorfer et al., 2007). Its relative lightweight nature allows its use on many roofs without the need for structural strengthening and it has seen a surge in installations worldwide (Tan et al., 2014). Another form of horizontal greenery is elevated forests which refers to trees growing in the sheltered horizontal spaces which form into forests in the sky. While horizontal spaces provide accommodations for plants, vertical spaces offer more possibilities. Apart from the development on the horizontal surface, vertical spaces provide opportunities to integrate vegetation with buildings.

2.3. VERTICAL GREENERY SYSTEMS

The vertical greenery system can be defined as structures that spread vegetation that may or may not be attached to a building façade or to an interior wall (Pérez-Urrestarazu, Fernández-Cañero, Franco-Salas et al., 2015). It is also named as vertical garden (Peck, Callaghan, Kuhn et al., 1999), green wall, vertical green and sky-rise greenery (Blanc & Lalot, 2008; Tan et al., 2014; Timur & Karaca, 2013). According to the strategies of development of vertical greenery systems, they can be categorized as green façade, green/living wall, green terraces, elevated and vertical forests (Marugg, 2018; Ottelé, 2011; Serra, Bianco, Candelari et al., 2017; Sheweka & Magdy, 2011) (see Figure 1). But there are some differences between the definitions in various fields. Within this study, the characteristics and definitions can be seen in Figure 1 and Table 1.

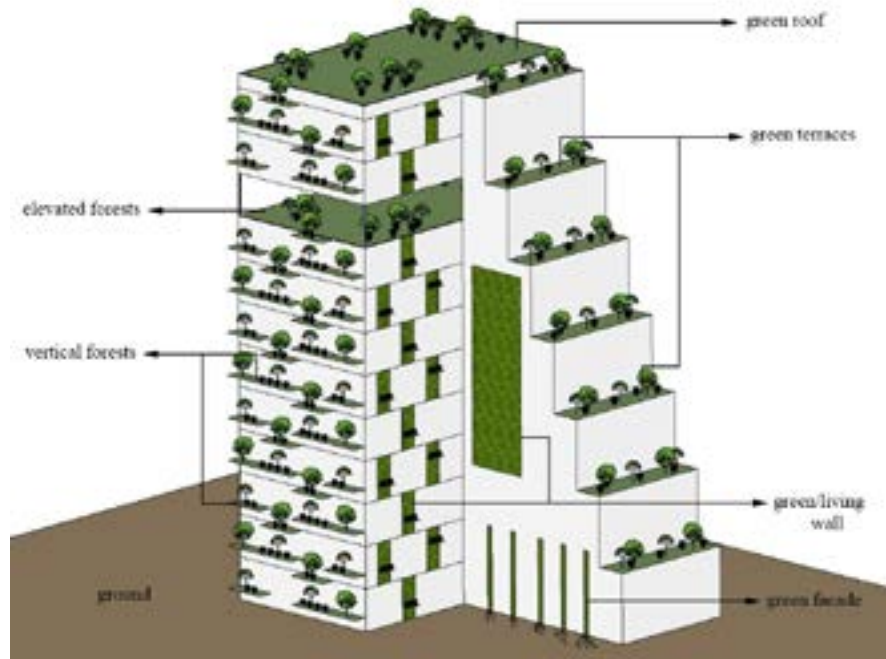


Figure 1 Classification

Table 1 Identification and classification of vertical greenery systems

Typologies	Plants	Characteristics
green façade	climbing plants	plants rooted on the ground and climbing on the façades of building themselves or with the support of other structures
green/living wall	modular plants or plants with hanging-down branches	supporting structures such as steel nets, modular rails and planter boxes that should be built on façades for hanging and placing plants
green terraces	short, medium and tall plants	planting in the planting media which is located on the horizontal terraces at different levels
elevated forest	trees	trees growing in the sheltered horizontal open spaces
vertical forest	trees	trees growing on cantilevering balconies

There are four main elements in the vertical greenery systems: plants, planting media such as substrate and containers, supporting systems which can hold plants, and irrigation systems (Wood, Bahrami, & Sfarik, 2014).

- **Green façade** refers to vegetation rooted on the ground, which makes use of either the wall itself for climbing (traditional direct systems) or independent supporting systems, such as trellis, wires, cables or meshes (double-skin indirect system) affixed to walls (Fernández-Cañero, Pérez Urrestarazu, & Perini, 2018).
- **Green or living walls** have been made using geotextile, pots, panels, boxes or modular nets where pre-cultivated vegetation has been planted and subsequently suspended and fixed to a larger vertical structure (Bartesaghi Koc, Osmond, & Peters, 2017). Living walls demand more complex constructions and imply higher installation and maintenance costs in comparison to green façades (Dunnett & Kingsbury, 2008).
- **Green terraces** are defined as plants growing on the horizontal terraces, which are built on different heights and levels.
- **Vertical forest** means when using cantilevered balconies around the envelop of a building to act as an accommodation for trees to grow, this group of trees is formed into vertical forests.

Vertical forest engineering is a relatively new field for architects, botanists and structural engineers to study deeper with respect to plant and tree species, nutrition and growth conditions (e.g. root system development) as well as engineering aspects with regard to wind loads, earthquake, tree stability and development of these over time.

3. BENEFITS

3.1. ENVIRONMENTAL BENEFITS

Integration nature with buildings has become a necessary for buildings in densely populated urban areas. It is widely admitted that the proper arrangement of plants around buildings not only has psychological effects but also improves unfavorable microclimatic conditions around these buildings (Hoyano, 1988). Advantages of vertical greenery systems relate to environmental practices, economic and social benefits.

Regarding to environmental benefits, many studies have shown that using the technologies of vertical greenery systems can effectively mitigate the urban island effects. Because vegetation provides shading and evapotranspiration services that cool and regulate surface and atmospheric temperatures (Price, Jones, & Jefferson, 2015). Vegetation has the capacity of evapotranspiration. By evapotranspiration, large amounts of solar radiation can be converted into latent heat, which prevents temperature to rise rapidly during the day. With the increase of wind speed, evapotranspiration of vegetation increases too. Consequently, an efficient way to increase the evapotranspiration surface area in big cities is to cover buildings with vegetative greenery (Takakura, Kitade, & Goto, 2000). This can also be basically explained by decreasing wall temperature depending on variation of the effect of the wind on buildings, thermal insulation impact of vegetation and growth substrate (Besir & Cuce, 2018).

3.1.1. WIND BARRIER

Wind speed and air temperature grow with increasing building height. Water vapor pressure is reduced by the combination of higher wind speed and higher air temperature. When evaluating the thermal performance of building façades, wind effect is one of the most notable factors which should be taken into consideration (Besir & Cuce, 2018).

The wind barrier effect refers to the capacity of the vertical green system, plants and support structure to modify direct wind effect over the building façade (Pérez et al., 2014). By affecting the wind speed with plants around building vertical spaces, a reduction of exterior wall temperature can be reached. According to a study by Perini et al. (2011) found that the wind speed within the foliage decreases nearly 0.43 m/s in comparison to 10cm distance from a bare wall and the wind speed inside vegetation is found to be close to zero. Franco et al. (2012) used wind tunnel test to evaluate the water volume retained, pressure drop, saturation efficiency and water consumption for three types of synthetic substrates used in active living walls to give recommendations for further research. By changing wind direction and wind speed with a vertical greenery system, the energy performance of the building could be optimized.

3.1.2. SHADING EFFECT

Vegetation could provide direct shade to buildings and protect them from direct solar radiation. At the same time, it can absorb solar radiation for photosynthesis and evapotranspiration, therefore this can reduce solar reflection and re-radiation to atmosphere (Perini, Ottel , Haas et al., 2013b; Sunakorn & Yimprayoon, 2011). Leaf area index is an important factor to provide energy saving through evapotranspiration and solar shading. Wong et al. (2009) conducted experiments on vertical greenery systems and found an equation showing that shading coefficient has a linear correlation with the leaf area index. However, shading effect may have both positive and negative effects depending on cooling and heating seasons. In summer seasons, plant canopies strategically integrated to building façades can act as sun screen devices to filter solar radiation and air with high temperature (Ip, Lam, & Miller, 2010). When using perennial plants both cooling and heating periods influenced by plant coverage whereas using deciduous plants only the cooling period is affected since the solar radiation will pass during the heating period (leafless period) (P rez et al., 2014). During the summer months, vertical greenery systems would have the twofold effect of reducing incoming solar energy into the interior through shading and reducing heat flow into the building (Wong, Kwang Tan, Chen et al., 2010). Studies have shown that with proper and appropriate design and selection strategies of plants in vertical greenery systems, the positive effect of shading is obviously higher than negative effect, which can improve the energy performance of high-rise buildings (Marugg, 2018; Raji et al., 2015). In other words, to make full use of advantages of vertical greenery systems, the planting strategy is needed to take into consideration when vertical greenery system is applied.

3.1.3. THERMAL INSULATION

Vertical greenery systems recognize vegetation as having a larger impact in heat reduction when compared to artificial cooling (Price et al., 2015). The use of climbing plants and other vegetation types as a part of building enclosures has been shown to improve facade thermal performance during summer in Chicago (Susorova, Azimi, & Stephens, 2014). By evapotranspiration of vegetation, Besir and Cuce (2018) found that the external surface temperature of vertical greenery systems reduce in the range of 3.7 to 11.3°C while increasing the percentage of foliage in the system between 13% and 54%. Reductions in external surface temperatures of the building façades were considerable in warm temperate climate, ranging from 12 to 20.8°C in the summer period and 5 to 16°C in autumn (Pérez et al., 2014). Cuce (2017) studied green walls with about 10cm thick *Hedera helix* in sunny sky conditions of temperate climates like Nottingham. Results revealed that an average of 2.5°C reduction in internal wall temperature can be achieved. A case study in Hong Kong found that vertical greenery wall saved as much as 16% of the electricity consumption for air-conditioning in August and September with typical daily temperatures of 25 to 30°C (Pan & Chu, 2016). Inside urban canyons, results showed that the wind direction does not have any significant effect on temperature decreases due to vegetation (Alexandri & Jones, 2008). In the tropical climate, a study pointed out a reduction of surface temperature of building façades by a maximum of more than 11°C in the wall surface temperature on clear days (Wong, Kwang Tan, Chen, et al., 2010). Experiments on investigating the energy behavior on buildings in a Mediterranean temperate climate were conducted by Mazzali et al. (2013). The results showed that during sunny days, differences in temperature between the bare wall and the covered wall range from 12°C to 20°C. In different light conditions, the leaf orientation varies and leaves of plants move. Based on TLiDAR, a movement parameterization of leaf can be quantified (Herrero-Huerta, Lindenbergh, & Gard, 2018). The thermal benefits of vertical greenery systems highly depend on vegetation intensity and its orientation with respect to the sun, possible intermediate air layers and plant characteristics such as growth rate, coverage, height, leaf area index and substrate thickness.

3.1.4. MISCELLANEOUS

Apart from that, acoustic performance of vertical greenery systems has been proven well at low to middle frequencies due to the absorbing effect of substrate while a smaller attenuation is observed at high frequencies due to scattering from greenery (Wong, Kwang Tan, Tan et al., 2010).

Urban vegetation has been shown to improve air quality by increasing air flow (Dunnett & Kingsbury, 2008; Perini et al., 2011) and depositing dust (Perini, Ottelé, Giulini et al., 2017). The air quality improvement due to vegetation is related to the absorption of fine dust particles and the uptake of gaseous pollutants (Perini, Ottelé, Haas et al., 2013a).

Vertical greening systems are especially important in dense urban areas as they create a habitat for urban plants and native wildlife by supporting biodiversity (Francis & Lorimer, 2011; Perini et al., 2013a). The benefits of biodiversity for human wellbeing are generally determined by the diversity of habitats and species in and around urban areas (Loreau, Naeem, Inchausti et al., 2001). However, biodiversity in sky gardens may not be as high as that at ground level, because of the thinner depth of soil, and more severe living environment on roofs and podiums such as higher temperature and stronger wind (Tian & Jim, 2011).

3.2. SOCIAL BENEFITS

Plants give beauty unstintingly and remains steadfast. It is known that people are more likely to suffer from a range of medical and mental health problems if they are living in areas without green nature. By providing a more comfortable living and working environment, it has also been proved that visual and physical contacts with plants can result in direct health benefits. Plants can generate restorative effects leading to decreased stress and improve work productivity (Sheweka & Magdy, 2011). Interacting with green plants regularly has a positive impact on human wellbeing.

3.3. ECONOMIC BENEFITS

By changing the energy performance of buildings with vertical greenery systems, energy saving is one among multiple benefits that a greenery system can offer to buildings (Coma, Pérez, de Gracia et al., 2017; Raji et al., 2015). The energy performance of a building in terms of the building envelope can be described as minimizing energy requirements for heating and cooling owing to the structural properties of the envelope (Besir & Cuce, 2018). The energy loss as a crucial issue for energy performance entirely depends on building age and type, climate, the materials of a building envelop, dweller behavior and geographic location. Irradiance reductions due to plants can reduce energy use for space cooling, and increase energy use for space heating. Plant canopies that shade buildings move the active heat absorbing surface from the building envelop to leaves (McPherson, Herrington, & Heisler, 1988).

In wet and cold climates in Hunan Province in China, an energy saving rate of 18% was achieved during the heating experiment owing to the extra thermal insulation provided by the vertical greening system (Xing, Hao, Lin et al., 2019). But planting strategies have adverse and beneficial effects on building energy performance. For energy effectiveness, tree arrangements provide shade, for instance, in Hong Kong primarily for east and west walls and roofs providing wind protection from the direction of prevailing winter winds, and this arrangement may vary depending on regions.

Because of a lack of technical information, maintenance instructions, and information on plants suitable for vertical greenery system locally, the adoption of vertical greenery systems is hindered. Similarly, the lack of awareness of long term economic benefits for building owners. Also grants and subsidies of the new system should also be considered for implementation. Economic benefits may be obtained by lower heating costs, reduction of air and noise pollution, improvement of human wellbeing by closure to nature which is a potential economic benefit, but may be negatively influenced by increased building and greenery maintenance costs during service life, and higher upfront costs for construction as structural detailing for cantilevering balconies with soil provisions may be more complex.

In general, the main benefits connected to vertical greenery systems include environmental, economic, and social aspects on both building and urban scales. But it also reflects that there is still a long way to go for the application of vertical forests.

4. PLANTING STRATEGIES

The species used in outdoor living walls vary to a great extent, depending on the location, on the exposure to the sun and wind and on the height of the building (Pérez-Urrestarazu, Fernández-Cañero, Franco-Salas et al., 2015). There are some factors that can influence the growth of vegetation. These can be moisture stress and severe drought, extreme elevated temperatures, high light intensities and high wind speeds. They all increase the risk of desiccation and physical damage to vegetation and substrate (Dunnett & Kingsbury, 2008). Similarly, various plant physiological parameters such as leaf area index, average leaf dimension, and leaf absorptivity can improve facade thermal performance by reducing the exterior wall surface temperatures and heat flux through the façade (Susorova et al., 2013). For green façades, the number of useable plant species in the tropical area is between 300 and 500 climber species. This is around 10 times than in Europe (Köhler, 2008). Selection of suitable plant species depend upon many factors such as climatic conditions, building and plant orientation, wind effect, type of the soil, characteristics of container, requirement of water and nutrient, neighboring plant materials and preferred visual effect. Native plants should be given priority in selecting plant species as they are well adapted to local weather condition (Dahanayake & Chow, 2015). Strategies for selecting the most suitable plants are given in Table 2.

Table 2 Plants selection

Considerations	Strategies
plant arrangement	climatic consideration, orientation, wind effect, trees anchorage and fall off protection
plant species	aesthetic appreciation, foliage, density, growth rate, tolerance of high height condition maintenance and repair activities
planting media	properties such as thickness, moisture content and density
maintenance and inspection	pruning, weeding, watering, fertilization, plant replacement
irrigation and drainage system	accessible and well equipped for regular watering, water consumption waterproofing work

By combining engineered structures and botanical technologies, planting designs for cold climates preferably should reduce winter winds and provide solar access to south and east walls. For temperate climates, vegetation should be able to avoid blocking summer winds. In hot climates, high-branching shade trees and low ground covers should be used to promote both shade and wind (McPherson et al., 1988). However, some trade-off discussions can also be identified. For instance, from a structural viewpoint it would be advantageous to have the thickness of substrate as small as possible for weight reduction, but plants may grow less well and can require soil layers that are sufficiently thick to grow healthy in the long run. Similarly, with higher elevation it might become more advantageous to use low plants, reducing the cooling capacity of vertical forests.

5. DESIGN CONSIDERATIONS

As vertical greenery systems are relatively new applications in construction, there seem to be a lack of standard technical guidelines and maintenance specifications (Köhler, 2008; Tian & Jim, 2011). Singapore's Design for Safety for Rooftop Greenery (Parks, 2012) provides the only recommended guidelines for worker safety with a focus on design. During phases of design, installation and maintenance, many factors need to be taken into consideration before any decisions are taken, dealing with architectural and structural design, plant and environmental aspect.

5.1. DESIGN PHASE

During design phase, designers should take into consideration of many aspects including a suitable planting strategy, a sustainable material choice, the environmental impact, the interaction between the growing medium and vegetation (Perini et al., 2013a). Designers also should consider that the mechanical performance which might need to be characterized with technological support in the laboratory. An evaluation of the biometric parameters of the plants is also important. By analyzing the energy performance of buildings such as thermal behavior and acoustic performance with various vertical greenery systems, the most suitable one should also take local conditions into consideration. Before construction, technological issues that should be looked at are as follows.

- Making comparisons between different planting options according to structural performance of high-rise buildings, including additional loads by plants, the substrate and influences from extreme weather conditions;
- Applying proper ways of structural supports to prevent plants from falling down;
- Studying the influence of integrating greenery systems on energy saving for buildings ;
- Taking accessibility for regular and proper irrigation and maintenance activities into consideration;
- Checking whether a life cycle analysis (Perini et al., 2013a) can provide insights into an integral balance and discuss on cost effectiveness of different greening systems.

In order to optimize and balance all aspects involved, a multidisciplinary approach is needed and people from different fields should be joined together to make decisions during the early design phase.

5.2. INSTALLATION PHASE

Vertical greenery systems need to be designed in such a way that workers are able to maintain, re-plant, and provide overall care for the plants, which should be able to get free access to systems and avoid damage or fall off (Behm & Choon Hock, 2012). Vertical greenery systems present more potential access and fall protection issues compared to the rooftop greenery. Vegetation hanging over the edge of a building's roof (trees, creeper plants, etc.), presents additional safety challenges (Behm & Choon Hock, 2012). Such challenges will be considerable to façade cleaning teams.

Therefore, fall prevention and protection should be provided with special considerations for ledges. For vertical plants above ground level on roofs, terraces, and other upper surfaces, the height of the greenery should not exceed its horizontal distance from the roof edge or top of parapet unless fall protection measures are provided. In other words, the greenery should be set back from the edge of the building so that if equipment fails or a fall occurs, the distance is limited (Behm & Choon Hock, 2012). When a greenery system is designed onto building ledges, both fall protection and safe access options must be provided and consequently considered in the design phase when planning installation and maintenance.

5.3. MAINTENANCE PHRASE

An optimal system will provide benefits with respect to human comfort and environmental impact with less additional maintenance costs. While living plants bring life to a building, they also add to the risk of failure through death of plants, an unsuccessful installation will cause additional costs of rectification. On the other hand, poor growing and dying as well as distorted plants will create an unsightly view that can affect the image of the building. However, there will be a trade-off between extra maintenance costs compared to a traditional building. With precise design and successful installation, improved environmental impact, jobs for maintenance workers and ecological services and improvement of social wellbeing have great values for buildings and societies in the long term.

6. VERTICAL FORESTS

An appropriate selection of tree species and a proper placement of trees around buildings are important to improve benefits of trees on reducing building energy use. The presence of trees acts as a barrier and blocks the thermal radiation emitted by the surface of the building façade (Berry, Livesley, & Aye, 2013). Trees can reduce external solar irradiance loads when they are close enough and tall enough to shade the majority of the wall (Berry et al., 2013). The characteristics of vertical forests include tree height, locations and spacing between the trees (both horizontal and vertical), distance between tree and the hard building envelope, canopy density and tree species. There are two cases (Table 3) collected where vertical forests have been applied as a way of improving the quality of high-rise buildings (Blanc & Lalot, 2008; Giacomello, 2015). All the plants and tree species growing on balconies of Bosco Verticale are selected according to the context, its climate conditions, orientation, solar exposition and height, which is shown in Table 3.

Table 3 Characteristics of cases

Cases	Pictures	Tree Species	Location and containers
Bosco Verticale Milan, Italy (Giacomello, 2015)		Acer Campestre Fagus Sylvatica Mafnolia Stellata Quercus Ilex Prunus Subhirtella Laburnum Alpinum (3-6-9 m high)	four sides of the envelop, around 1-meter-deep planter boxes with restraint systems to prevent fall off
Newton Suites Singapore (Blanc & Lalot, 2008)		Plumeria Palm trees	north and south sides with 900mm deep planter boxes

As for Bosco Verticale, small-scale wind load assessment was carried out using wind tunnel test to understand the aerodynamic and structural performance (Argentini, Fossati, & Muggiasca, 2010). Full-scale trees were investigated at a large open-jet facility in a local-effect study to account for the wind-tree interaction. Results show that at relatively high wind speeds the load coefficients tend to be reduced, limiting the wind loads on trees (Mousaad ALY, Fossati, Muggiasca et al., 2013). Trees planted on the balconies of Bosco Verticale classified as “large” and “medium” are secured to the structure of the terraces by means of temporary, basic and redundant binds. As is known, trees grow on the ground and their root systems develop freely, preventing trees from turning over in high winds. This change of growing conditions will have an influence on the development of root systems as they are restraint within the containers on the cantilever balconies.



Figure 2 Trees in the corner (Giacomello, 2015)



Figure 3 Growth of trees



Figure 4 A tree with different dense branches



Figure 5 Trees with different dense foliage

By observing trees (Figure 2-6) in Bosco Verticale, there are several aspects that need to pay attention to:

- It is observed that the orientation of branches and density of foliage are different between four sides of buildings due to the phototropism of the trees.
- If trees are applied to a horizontal forces frequently, it is likely that they grow with bended shape, which means trees that is under the effect of wind, especially for trees at corners and high levels will not grow straight vertically.
- With the development of time, trees grows both above and in ground. When the uprooting resistance of roots system ($F_{wind} > F_{res}$, $M_{wind} > M_{res}$) is not sufficient, it may lead to stability problems(Figure 6).

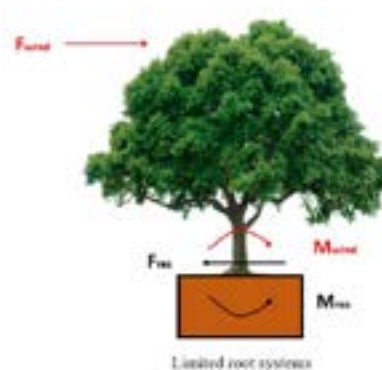


Figure 6 Stability of a single tree

Instead of using steel bracings and cages to hold trees for stability, self-growing connections between multiple trees is a possible way to provide the sufficient stability and resistance. Trees are growing organisms that can be manipulated in a natural way to grow into structures that can be useful in the built environment. The use of trees as structural

elements is possible for tree houses, where they act as a support structure (Nelson, 1997; Nuijten, 2011). Within the framework of a Building with Nature program, a self-growing tree structure has been created by the research group Biobased Structures and Materials of the Faculty of Civil Engineering and Geosciences of TU Delft, in cooperation with the Botanical Garden of the university. The structure is a study object that has been growing over the last 9 years. The trees are planted in such a way that young branches can be tied together at an early stage. Having tied branches together with a flexible tape, the trees are now interconnected by these naturally grown nodes (Figure 7,8), forming a structural entity by itself. In the Botanical Garden, the trees will be able to support a look-out platform within a couple of years. The nodes are the connections in natural tree structures that ensure the stability of a structural tree network. The advantages that are envisaged are a reduced need of tying the trees to the main structure, and reducing the effect of high wind loads on individual trees, avoiding excessive tree deformations. Three different node types are identified as shown in Figure 9. Each branch will probably retain its own biological and physiological structures but improved mechanical strength and stiffness will be created. The structure is the starting point for research into the internal structure of the nodes in order to address biological growth, structural performance of both trees and nodes, and the future development of such structures for use in the built environment, vertical forests and urban forests in particular (Borská, 2018).



Figure 7 Crosswise connection



Figure 8 parallel-surface connection



Figure 9 Typical nodes for interconnected trees: Three natural node types are studied: parallel-surface, crosswise and parallel-pith (Nuijten, 2011)

By using self-growing connections within vertical forests, it is possible to keep trees stable and less deformed as a result of high wind loads. The trees will grow more naturally shaped, effectively making the vertical forest more appealing.

7. CONCLUSIONS AND OUTLOOK

Classified types of vertical and horizontal greenery with definitions are given in this study. Greenery inserted on buildings can be organized into two main categories: horizontal greenery and vertical greenery systems. Green roofs and elevated forests are horizontal greenery which makes use of space horizontally. While integrating vegetation vertically is vertical greenery systems. They include green façade, green/living wall, green terraces and vertical forests. In this study, vertical forests mean when using cantilevered balconies around the envelop of a building to act as an accommodation for trees to grow. This group of trees is formed into vertical forests.

The main benefits related to vertical greenery systems include environmental, economic and social aspects. Environmentally, vertical greenery systems have a positive impact by wind barrier and shading effect, providing thermal insulation, reducing air pollution and noise. By getting closer to nature, human wellbeing can be improved.

Economic benefits may be obtained by lowering energy costs, reduction of air and noise pollution and improvement of living quality.

By combining engineered structures and botanical technologies, planting strategies and plants selection should be considered based on different regions usages.

For vertical forest engineering it is essential that criteria and design guidelines need to be developed including guidance for multi-criteria analyses. From design to maintenance phases, considerations for designers, engineers and relative workers are proposed.

The majority of recent studies mainly focuses on the evaluation of energy performance of buildings with vertical greenery systems. Fewer studies point out the importance of planting strategies. There is still a lack of knowledge on how to deploy high growing plants such as trees with high-rise buildings. From literature review, vertical greenery systems are primarily considered as a passive cooling option, and thermal studies need to compare it to other passive cooling options. Its potentials and magnitude of benefits, however, may not be the same across all seasons, climates and building designs (Hunter, Williams, Rayner et al., 2014; Pérez et al., 2014).

The success of a vertical greenery system relies partly on the ability to select suitable plant species that can maximize the capacity and performance of vertical greenery system. Plant selection, morphology, design and maintenance will differ from one climate to another. Advancement in research and technologies will aim to maximize benefits of application of vertical greenery system to suit a climate and building (Bustami, Belusko, Ward et al., 2018). There are very little research that has been focused on the analysis of the substrate or on the role of the growing media on root and plant growth (Serra et al., 2017). An extensive plant selection which may involve quality of foliage, color, texture, leaf shape, plant size, vigor, growth habits (Dunnett & Kingsbury, 2008) and its cost and effectiveness should be investigated.

Relevant guidelines and specifications for structural engineers should be developed with the effort from multidisciplinary approaches. Structural performance of buildings with vertical greenery systems should be looked into deeply especially for the wind performance of plants and high-rise buildings.

Vertical forest engineering with self-growing connections can be implied in the future. The mechanical properties of connections require further analyses but first inspections (Borská, 2018) indicate high stiffness and strength, similar to normal tree sections.

REFERENCES

- Alexandri, E., & Jones, P. (2008). Temperature decreases in an urban canyon due to green walls and green roofs in diverse climates. *Building and Environment*, 43(4), 480-493. doi:<https://doi.org/10.1016/j.buildenv.2006.10.055>
- Argentini, T., Fossati, F. V., & Muggiasca, S. (2010). *The vertical forest: wind loads on trees, pedestrian comfort, and net pressure distributions on facades*. Paper presented at the 9th UK Conference on Wind Engineering WES-2010.
- Bartasaghi Koc, C., Osmond, P., & Peters, A. (2017). Towards a comprehensive green infrastructure typology: a systematic review of approaches, methods and typologies. *Urban Ecosystems*, 20(1), 15-35. doi:10.1007/s11252-016-0578-5
- Bass, B., Rowe, B., Oberndorfer, E., Doshi, H., Lundholm, J., Liu, K. K. Y., et al. (2007). Green Roofs as Urban Ecosystems: Ecological Structures, Functions, and Services. *BioScience*, 57(10), 823-833. doi:10.1641/B571005 %J BioScience
- Behm, M., & Choon Hock, P. (2012). Safe design of skyrise greenery in Singapore. *Smart and Sustainable Built Environment*, 1(2), 186-205.
- Berry, R., Livesley, S. J., & Aye, L. (2013). Tree canopy shade impacts on solar irradiance received by building walls and their surface temperature. *Building and Environment*, 69, 91-100. doi:<https://doi.org/10.1016/j.buildenv.2013.07.009>
- Besir, A. B., & Cuce, E. (2018). Green roofs and facades: A comprehensive review. *Renewable and Sustainable Energy Reviews*, 82, 915-939. doi:<https://doi.org/10.1016/j.rser.2017.09.106>
- Blanc, P., & Lalot, V. r. (2008). *The vertical garden : from nature to the city*. New York: W.W. Norton.
- Borská, H. (2018). *Structural performance of the self growing structure in the TU Delft Botanical Garden*. (M.Sc), Delft University of Technology,
- Bustami, R. A., Belusko, M., Ward, J., & Beecham, S. (2018). Vertical greenery systems: A systematic review of research trends. *Building and Environment*. doi:<https://doi.org/10.1016/j.buildenv.2018.09.045>
- Coma, J., Pérez, G., de Gracia, A., Burés, S., Urrestarazu, M., & Cabeza, L. F. (2017). Vertical greenery systems for energy savings in buildings: A comparative study between green walls and green facades. *Building and Environment*, 111, 228-237. doi:<https://doi.org/10.1016/j.buildenv.2016.11.014>

- Cuce, E. (2017). Thermal regulation impact of green walls: An experimental and numerical investigation. *Applied Energy*, 194, 247-254. doi:<https://doi.org/10.1016/j.apenergy.2016.09.079>
- Dahanayake, K., & Chow, C. (2015). *A brief discussion on current vertical greenery systems in Hong Kong: the way forward*. Paper presented at the 14th Int. Conf. Sustain. Energy Technol.(SET2015), 25–27 August 2015.
- Dunnett, N., & Kingsbury, N. (2008). *Planting green roofs and living walls*: Timber press Portland, OR.
- Feng, H., & Hewage, K. (2014). Lifecycle assessment of living walls: air purification and energy performance. *Journal of Cleaner Production*, 69, 91-99. doi:<https://doi.org/10.1016/j.jclepro.2014.01.041>
- Fernández-Cañero, R., Pérez Urrestarazu, L., & Perini, K. (2018). Vertical Greening Systems: Classifications, Plant Species, Substrates. In G. Pérez & K. Perini (Eds.), *Nature Based Strategies for Urban and Building Sustainability* (pp. 45-54): Butterworth-Heinemann.
- Francis, R. A., & Lorimer, J. (2011). Urban reconciliation ecology: The potential of living roofs and walls. *Journal of Environmental Management*, 92(6), 1429-1437. doi:<https://doi.org/10.1016/j.jenvman.2011.01.012>
- Franco, A., Fernández-Cañero, R., Pérez-Urrestarazu, L., & Valera, D. L. (2012). Wind tunnel analysis of artificial substrates used in active living walls for indoor environment conditioning in Mediterranean buildings. *Building and Environment*, 51, 370-378. doi:<https://doi.org/10.1016/j.buildenv.2011.12.004>
- Giacomello, E. (2015). *Case study: Bosco verticale, milan: A new urban forest rises in Milan*.
- Herrero-Huerta, M., Lindenbergh, R., & Gard, W. (2018). Leaf Movements of Indoor Plants Monitored by Terrestrial LiDAR. 9(189). doi:10.3389/fpls.2018.00189
- Hoyano, A. (1988). Climatological uses of plants for solar control and the effects on the thermal environment of a building. *Energy and Buildings*, 11(1), 181-199. doi:[https://doi.org/10.1016/0378-7788\(88\)90035-7](https://doi.org/10.1016/0378-7788(88)90035-7)
- Hunter, A. M., Williams, N. S. G., Rayner, J. P., Aye, L., Hes, D., & Livesley, S. J. (2014). Quantifying the thermal performance of green façades: A critical review. *Ecological Engineering*, 63, 102-113. doi:<https://doi.org/10.1016/j.ecoleng.2013.12.021>
- Ip, K., Lam, M., & Miller, A. (2010). Shading performance of a vertical deciduous climbing plant canopy. *Building and Environment*, 45(1), 81-88. doi:<https://doi.org/10.1016/j.buildenv.2009.05.003>
- Koc, C. B., Osmond, P., & Peters, A. (2017). Towards a comprehensive green infrastructure typology: a systematic review of approaches, methods and typologies. *Urban Ecosystems*, 20(1), 11.
- Köhler, M. (2008). Green facades—a view back and some visions. *Urban Ecosystems*, 11(4), 423.
- Loreau, M., Naeem, S., Inchausti, P., Bengtsson, J., Grime, J., Hector, A., et al. (2001). Biodiversity and ecosystem functioning: current knowledge and future challenges. *science*, 294(5543), 804-808.
- Marugg, C. (2018). *Vertical Forests: The Impact of Green Balconies on the Microclimate by Solar Shading, Evapotranspiration and Wind Flow Change*. Delft University of Technology, Retrieved from <http://resolver.tudelft.nl/uuid:f6498f91-83ea-4223-b25a-246da71db4a7> WorldCat.org database.
- Mazzali, U., Peron, F., Romagnoni, P., Pulselli, R. M., & Bastianoni, S. (2013). Experimental investigation on the energy performance of Living Walls in a temperate climate. *Building and Environment*, 64, 57-66. doi:<https://doi.org/10.1016/j.buildenv.2013.03.005>
- McPherson, E. G., Herrington, L. P., & Heisler, G. M. (1988). Impacts of vegetation on residential heating and cooling. *Energy and Buildings*, 12(1), 41-51. doi:[https://doi.org/10.1016/0378-7788\(88\)90054-0](https://doi.org/10.1016/0378-7788(88)90054-0)
- Medl, A., Stangl, R., & Florineth, F. (2017). Vertical greening systems - A review on recent technologies and research advancement. *Building and Environment*, 125, 227-239. doi:10.1016/j.buildenv.2017.08.054
- Mousaad ALY, A., Fossati, F., Muggiasca, S., Argentini, T., Bitsuamlak, G. T., Franchi, A., et al. (2013). Wind loading on trees integrated with a building envelop. *Wind and Structures*, 17(1).
- Nelson, B. P. (1997). *Be in a Treehouse*.
- Nuijten, A. (2011). *Living tree buildings*. Delft University of Technology,
- Ottelé, M. (2011). *The green building envelope : vertical greening*. TU Delft, Delft. Retrieved from http://repository.tudelft.nl/assets/uuid:1e38e393-ca5c-45af-a4fe-31496195b88d/Proefschrift_The_green_building_envelope_17-06-2011.pdf WorldCat.org database.
- Pan, L., & Chu, L. (2016). Energy saving potential and life cycle environmental impacts of a vertical greenery system in Hong Kong: a case study. *Building and Environment*, 96, 293-300.
- Parks, N. (2012). Trees on Rooftop. In.
- Peck, S. W., Callaghan, C., Kuhn, M. E., & Bass, B. (1999). *Greenbacks from green roofs: forging a new industry in Canada*: Citeseer.
- Pérez-Urrestarazu, L., Fernández-Cañero, R., Franco-Salas, A., & Egea, G. (2015). Vertical greening systems and sustainable cities. *Journal of Urban Technology*, 22(4), 65-85.

- Pérez-Urrestarazu, L., Fernández-Cañero, R., Franco-Salas, A., & Egea, G. (2015). Vertical Greening Systems and Sustainable Cities. *Journal of Urban Technology*, 22(4), 65-85. doi:10.1080/10630732.2015.1073900
- Pérez, G., Coma, J., Martorell, I., & Cabeza, L. F. (2014). Vertical Greenery Systems (VGS) for energy saving in buildings: A review. *Renewable and Sustainable Energy Reviews*, 39, 139-165. doi:<https://doi.org/10.1016/j.rser.2014.07.055>
- Perini, K., Ottel , M., Fraaij, A. L. A., Haas, E. M., & Rahim, A. M. (2011). Vertical greening systems and the effect on air flow and temperature on the building envelope. *Building and Environment*, 46(11), 2287-2294. doi:<https://doi.org/10.1016/j.buildenv.2011.05.009>
- Perini, K., Ottel , M., Giuliani, S., Magliocco, A., & Roccotiello, E. (2017). Quantification of fine dust deposition on different plant species in a vertical greening system. *Ecological Engineering*, 100, 268-276. doi:<https://doi.org/10.1016/j.ecoleng.2016.12.032>
- Perini, K., Ottel , M., Haas, E., & Raiteri, R. (2013a). Vertical greening systems, a process tree for green fa ades and living walls. *Urban Ecosystems*, 16(2), 265-277.
- Perini, K., Ottel , M., Haas, E., & Raiteri, R. J. U. E. (2013b). Vertical greening systems, a process tree for green fa ades and living walls. 16(2), 265-277.
- Price, A., Jones, E. C., & Jefferson, F. (2015). Vertical Greenery Systems as a Strategy in Urban Heat Island Mitigation. *Water, Air, & Soil Pollution : An International Journal of Environmental Pollution*, 226(8), 1-11. doi:10.1007/s11270-015-2464-9
- Raji, B., Tenpierik, M. J., & van den Dobbelsteen, A. (2015). The impact of greening systems on building energy performance: A literature review. *Renewable and Sustainable Energy Reviews*, 45, 610-623. doi:<https://doi.org/10.1016/j.rser.2015.02.011>
- Serra, V., Bianco, L., Candelari, E., Giordano, R., Montacchini, E., Tedesco, S., et al. (2017). A novel vertical greenery module system for building envelopes: The results and outcomes of a multidisciplinary research project. *Energy and Buildings*, 146, 333-352. doi:<https://doi.org/10.1016/j.enbuild.2017.04.046>
- Sheweka, S., & Magdy, A. N. (2011). The Living walls as an Approach for a Healthy Urban Environment. *Energy Procedia*, 6, 592-599. doi:<https://doi.org/10.1016/j.egypro.2011.05.068>
- Stec, W. J., van Paassen, A. H. C., & Maziarz, A. (2005). Modelling the double skin fa ade with plants. *Energy and Buildings*, 37(5), 419-427. doi:<https://doi.org/10.1016/j.enbuild.2004.08.008>
- Sunakorn, P., & Yimprayoon, C. (2011). Thermal Performance of Biofa ade with Natural Ventilation in the Tropical Climate. *Procedia Engineering*, 21, 34-41. doi:<https://doi.org/10.1016/j.proeng.2011.11.1984>
- Susorova, I., Angulo, M., Bahrami, P., & Brent, S. (2013). A model of vegetated exterior facades for evaluation of wall thermal performance. *Building and Environment*, 67, 1-13. doi:<https://doi.org/10.1016/j.buildenv.2013.04.027>
- Susorova, I., Azimi, P., & Stephens, B. (2014). The effects of climbing vegetation on the local microclimate, thermal performance, and air infiltration of four building facade orientations. *Building and Environment*, 76, 113-124. doi:<https://doi.org/10.1016/j.buildenv.2014.03.011>
- Takakura, T., Kitade, S., & Goto, E. (2000). Cooling effect of greenery cover over a building. *Energy and Buildings*, 31(1), 1-6. doi:[https://doi.org/10.1016/S0378-7788\(98\)00063-2](https://doi.org/10.1016/S0378-7788(98)00063-2)
- Tan, P. Y., K hler, M., Peck, S., Velazquez, L., Urban Redevelopment, A., & National Parks, B. (2014). *Vertical garden city : Singapore*. Singapore: Straits Times Press.
- Tian, Y., & Jim, C. Y. (2011). Factors influencing the spatial pattern of sky gardens in the compact city of Hong Kong. *Landscape and Urban Planning*, 101(4), 299-309. doi:<https://doi.org/10.1016/j.landurbplan.2011.02.035>
- Timur,  . r. B., & Karaca, E. (2013). Vertical gardens. In *Advances in Landscape Architecture*: IntechOpen.
- Tzoulas, K., Korpela, K., Venn, S., Yli-Pelkonen, V., Ka mierczak, A., Niemela, J., et al. (2007). Promoting ecosystem and human health in urban areas using Green Infrastructure: A literature review. *Landscape and Urban Planning*, 81(3), 167-178. doi:<https://doi.org/10.1016/j.landurbplan.2007.02.001>
- Wang, C., Er, S.-S., & Abdul-Rahman, H. (2016). Indoor vertical greenery system in urban tropics. *Indoor and Built Environment*, 25(2), 340-356.
- Wilmers, F. (1990). Effects of vegetation on urban climate and buildings. *Energy and Buildings*, 15(3), 507-514. doi:[https://doi.org/10.1016/0378-7788\(90\)90028-H](https://doi.org/10.1016/0378-7788(90)90028-H)
- Wolverton, B., & Wolverton, J. D. (1993). Plants and soil microorganisms: removal of formaldehyde, xylene, and ammonia from the indoor environment. *Journal of the Mississippi Academy of Sciences*, 38(2), 11-15.
- Wong, N. H., Kwang Tan, A. Y., Chen, Y., Sekar, K., Tan, P. Y., Chan, D., et al. (2010). Thermal evaluation of vertical greenery systems for building walls. *Building and Environment*, 45(3), 663-672. doi:<https://doi.org/10.1016/j.buildenv.2009.08.005>
- Wong, N. H., Kwang Tan, A. Y., Tan, P. Y., Chiang, K., & Wong, N. C. (2010). Acoustics evaluation of vertical greenery systems for building walls. *Building and Environment*, 45(2), 411-420. doi:<https://doi.org/10.1016/j.buildenv.2009.06.017>

- Wong, N. H., Tan, A. Y. K., Tan, P. Y., & Wong, N. C. (2009). Energy simulation of vertical greenery systems. *Energy and Buildings*, 41(12), 1401-1408. doi:<https://doi.org/10.1016/j.enbuild.2009.08.010>
- Wood, A. (2008). Trends and challenges in high-rise buildings in the 21st century. In C. o. T. B. a. U. Habitat (Ed.). Chicago.
- Wood, A., Bahrami, P., & Sfarik, D. (2014). *Green Wall in High-Rise Buildings: An output of the CTBUH Sustainability: Council on Tall Buildings and Urban Habitat*: Chicago.
- Xing, Q., Hao, X., Lin, Y., Tan, H., & Yang, K. (2019). Experimental investigation on the thermal performance of a vertical greening system with green roof in wet and cold climates during winter. *Energy and Buildings*, 183, 105-117. doi:<https://doi.org/10.1016/j.enbuild.2018.10.038>
- Yok, T. P. (2013). *Vertical Garden City: Singapore*. Singapore: Straits Times Press.

Biodynamic timber sheet pile – vegetation retaining structure

Abhijith Kamath¹, Wolfgang Gard¹ and Jan-Willem Van de Kuilen^{2,1}

¹Biobased structures and Materials
Delft university of technology
Delft, The Netherlands

²Chair of Wood Technology
Technical University of Munich
Munich, Germany

ABSTRACT

Timber sheet pile walls are widely used for the protection of stream banks in different parts of the world. However, there is tendency of creating more sustainable types of stream banks not only because exploitable wood is more difficult to obtain, but also because of disturbance to the natural habitat of plants and animals due to hard embankments. In The Netherlands alone, about 2500 km of engineered timber sheet pile wall embankments exist, primarily made with tropical hardwood, apart from an even much larger amount of 'non-engineered' small size timber based embankments. As an alternative, the authors propose to use a mixed timber sheet pile-vegetation system, where locally available timber can be applied in combination with natural vegetation. Unlike the usual bioengineering scheme, vegetation is not seen as an element, which could replace the timber sheet piles. Instead a new perspective is tested, where the vegetation is included as a 'structural' element which will reduce or even counteract the consequences time dependent biological degradation of the timber sheet pile. By doing so, both long term durability as well as reliability of the stream bank are improved. We have developed a comprehensive design model, based on well-established sub- models from the literature on plant growth as well as timber service life. The timber sheet pile wall-vegetation system is illustrated in an example case study. Preliminary analysis including only the mechanical reinforcement of vegetation shows that the durability of timber sheet piles is enhanced. Thus, using vegetation in combination with highly degradable timber could possibly negate the need for using hardwood timber, or more generally, save resources that are currently used for these structures.

1. INTRODUCTION

A study of the evolution of bioengineering techniques by (Evette et al., 2009) shows evidence of the use of woody species to stabilize river banks dating back from 16th century. Prominent examples include that of King Frederick William I of Prussia who ordered to plant willow on river banks and that of Dugied in France, who suggested to plant exotic species like Chinese Varnish Tree (*Toxicodum verriciflum* (Stokes) F. Barkley) and White Mulbery (*Morus alba* L.) to form dense barriers (Evette et al., 2009; Dugied, 1819). Ecological engineering techniques have being well recognized and implemented in many riverbank restoration and protection projects (Li et al., 2006; Anstead and Boar, 2010; Anstead et al., 2012; Evette et al., 2009). The first and second principles of ecological engineering as stated by (Bergen et al., 2001) requires that the designs produced mimic natural structures and are site specific. The concepts of energy efficiency, independence of design and functional requirements are addressed in the third and fourth principle.

Ecological bioengineering involves the use of live plants in combination with inert material to protect and conserve soil. The plant roots are expected to provide mechanical reinforcement to the soil while the evapo-transpiration provides hydrological reinforcement. Mickovski and Tardío (2016) used live plants in combination with wood to develop a dynamic soil bioengineering scheme, which was validated on a slope stabilized by crib wall and willow. Ollauri and Mickovski (2014) developed an integrated model taking into account the hydrological and mechanical effects of vegetation that could be used with easy input parameters. Different types of bioengineered structures were analysed by Fernandes and Guiomar (2016) some 20 years after construction. The effect of riparian vegetation in stabilizing streambanks was studied and quantified in the pioneering works of Thomas and Pollen-Bankhead (2010), Simon and Collison (2002), Pollen-Bankhead and Simon (2009) etc.

Riverbank degradation has societal and environmental impacts. Timber sheet piles are often used as stream bank protection structure. Timber sheet piles are considered environmental friendly compared to other conventional solutions like concrete walls or steel sheet piles. Sometimes, tropical hardwoods which have better resistance to decay may not be locally available, and have to be imported. For example, The Netherlands has about 2400 km of engineered timber sheet pile, while it has very less exploitable tropical hardwoods (Van de Kuilen and Linden, 1999). Thus, there is a need for an alternative solution, which involves locally available material and at the same time fits into the scope of ecological engineering. A timber sheet pile –vegetation composite stream bank protection structure is proposed in

this paper an alternative to currently employed conventional methods. The mechanical reinforcement of the soil with growth of vegetation could result in a reduction of bending moments and shear stresses acting on the sheet pile over time, thereby decreasing the duration of load effect in the timber and counteracting the effects of slow biological degradation of wood in air-water-soil conditions. Researchers have pointed out the need for including dynamic nature of vegetation roots in slope stability analysis, Stokes et al., (2009). To the best knowledge of the authors, there exist no study focusing on a bio-engineered stream bank retaining structure, which takes into account the specific characteristics of the riparian vegetation root growth, dynamic nature of the roots, variation in moment and shear acting on the sheet pile and the reduction of time dependent damage in the sheet pile. The basic methodology adopted in any bio-engineered structure is the design of stress transfer between the inert material and the vegetation. This eventually leads to the vegetation supporting the slope and the inert material decaying away. The authors would like to see the effect of vegetation from a different perspective. As mentioned earlier, one of the key issues faced in countries like the The Netherlands is the non-availability of high decay resistance hardwood. Thus, in this study vegetation reinforcement is hypothesised as an element which reduces the damage accumulated on the low decay resistance sheet pile, thus providing a valuable alternative.

2. MATERIALS AND METHODS

2.1 MODEL COMPONENTS

We attempt to understand the development of a timber sheet pile-vegetation system and characterize the effect of vegetation on the time dependent load carrying capacity of vegetation - timber sheet pile system. After introducing the components of the model, first, a conventional sheet pile without anchor is evaluated (Case 1), see Fig 1. Second, the timber sheet pile –vegetation system is analysed in a time framework with growth of vegetation and damage accumulation on the sheet pile (Case 2).

A root distribution model suitable for riparian ecosystems is employed in the model. Knowing the root distribution at each time period Δt_i , the root cohesion is estimated for that time period. Any change in cohesion of the backfill would reflect as a change in lateral earth pressure and hence as a change in bending moment and shear forces acting on a sheet pile. The variation in bending moment and shear stresses experienced by the timber sheet pile are the key parameters in the evaluation of the effect of vegetation on the sheet pile. Any change in moment would in turn result in a change in the required thickness of the sheet pile structure. Thus, the required thickness of sheet pile would become a time dependent parameter. On the other hand, the sheet pile is subjected to biological degradation and effects of load duration, especially when locally available less durable softwoods are used. This would result in a reduction of thickness of the sheet pile and hence the moment carrying capacity and shear resistance. All the component models are described briefly in the next section. The behaviour and evolution of the timber sheet pile-vegetation system is illustrated through an example application.

2.2 ROOT GROWTH MODEL

The models for root distribution proposed by Laio et al., (2006), Preti et al., (2010), Schenk (2008) are mainly intended to use in situations where the vegetation uptake relies on water infiltrating into soil (Tron et al., 2015). In riparian regions, ground water is the main source of nutrients and water for vegetation (Zeng et al., 2006), unlike in other situations where the nutrient availability decreases with depth. The roots can concentrate in top regions due to lack of oxygen resulting from high water table or can grow deep to reach the water table to exploit necessary nutrients and water. To model the effects of riparian vegetation on soil reinforcement, it is required to adopt a root distribution model, which takes into account the above mentioned situations. Tron et al., (2014) developed a stochastic analytical model for finding the vertical root distribution in ecosystems where rainfall infiltration is not the main source of plant water uptake, see equations 1 to 4:

Subsequently the CLHS is formed by butt jointing the two matched and planed half-sections. For the production of longer CLHS, as demanded for the use in reinforced soil walls ($LN = 0.6 \sim 1.0$ HS), a prototype press was developed. The prototype press (**Error! Reference source not found.**) is designed in C-shape for a manual loading from the front side. The main frame consists of four 160 mm thick C-shaped cross laminated timber (CLT) elements with an upper and lower pressure bar (HEB 160-S 235) placed in the recess of the CLT elements.

$$\bar{r}(z) = \frac{2\theta(z)k(z)}{\theta(z) + \theta(z)K(z) + 1 - k(z)} \quad (1)$$

$$\theta(z) = \frac{\beta(z)}{\gamma} \quad (1)$$

$$k(z) = \begin{cases} \frac{\Gamma\left(\frac{\lambda}{\eta}, \frac{h_1 - z - L}{\alpha}\right) - \Gamma\left(\frac{\lambda}{\eta}, \frac{h_1 - z}{\alpha}\right)}{\Gamma\left(\frac{\lambda}{\eta}\right)}, & \text{if } -\infty < z < h_1 - L \\ 1 - \frac{\Gamma\left(\frac{\lambda}{\eta}, \frac{h_1 - z}{\alpha}\right)}{\Gamma\left(\frac{\lambda}{\eta}\right)} & \text{if } h_1 - L < z < h_1 \end{cases} \quad (3)$$

$$\alpha = \frac{\check{\alpha}}{h_2} \quad (4)$$

$\bar{r}(z)$ is the quantity of roots one expects to find at depth z ,
 $k(z)$ is the probability that a depth z falls in the optimal root growth zone,
 L is the width of root box,
 $\theta(z)$ is the ratio of growth rate of roots,
 $\beta(z)$ to decay rate of roots γ ,
 λ is the mean rate of stochastic instantaneous rise of water level,
 $\check{\alpha}$ is the mean depth of the pulses,
 h_2 is the depth of water table at driest periods,
 η is the water level decrease in time,
 h_1 is depth of the root box.

According to this model, the roots concentrate on the upper layers if the variability of the water table is high and deeper roots are found when the variability of water table is less.

2.3 ROOT COHESION MODEL

The most widely used Wu & Waldron model developed by Wu (1976) assumes that all roots grow perpendicular to shear surface and they all break simultaneously. With the availability of root distribution and tensile strength, this model can be easily implemented and is applied here. Even though this model results in overestimation (Pollen and Simon, 2005; Thomas and Pollen-Bankhead, 2010) of the assessed additional cohesion, successful application and observation has been reported (Mickovski et al., 2008; Ollauri et al., 2014). Parameters k' and k'' are used to correct the overestimation. k'' is the ratio between “W&W” model and the fiber bundle model developed and Pollen and Simon (2005).

$$C_r(z) = k' * k'' * RAR(z) * T_r \quad (5)$$

$C_r(z)$ is the additional cohesion due to vegetation,
 $RAR(z)$ is the root are ratio,
 T_r is the average tensile strength of the root.

2.4 SHEET PILE MODEL

D-Sheet piling (Visschedijk and Trompille, 2011) is a tool with graphical interactive interface used to design sheet pile walls and horizontally loaded piles. The sheet pile is modelled as an elasto-plastic beam and uniform or variable stiffness could be defined along the beam axis. Initial horizontal stress is estimated using Jaky's equation and additional stresses using Boussinesq's stress distribution theory. Soil stiffness is modelled as a series of discrete, independently acting multi linear springs, forming an elastic foundation for a beam. Options to optimize length are also included in the standard module. The elastic stiffness and an estimated depth of the sheet pile are given as input parameter's for the sheet pile. Cohesion, internal friction angle, density are given as input parameters for the soil. It is possible to define different soil layers with different properties.

2.5 TIMBER SERVICE LIFE MODEL

Timber service life modelling is generally conducted for time dependent structural safety evaluation. The prediction of rate of decay of wooden members and hence their structural strength is key to any bioengineered structure. For an ideal bioengineered structure, herein timber sheet pile-vegetation combination, the load transfer and load sharing design depends on the ability to accurately predict the contribution of sheet pile to the system with time. Effects due to variation in load and resistance determine the time dependent behaviour of the sheet piles. Timber service life models are also referred to as damage accumulation models and a number of approaches can be found in literature (Van der Put, 1986, Foschi and Yao, 1986, Gerhards and Link, 1987). These models assume that cross sections do not change over time, for instance by assuming that over time the wood material properties are not influenced by decay and the cross section is constant. A modification of exponential damage model of Gerhards (1987), for changing material properties and cross sections can be found in Van de Kuilen (2007) and Van de Kuilen and Gard (2012) for deteriorating timber piles and cracked timber beams respectively. To include the time dependent reduction in load carrying capacity of the timber when physical and biological deterioration takes place, as given in equation (6).

$$\frac{d\alpha}{dt} = \exp \left[-a + \frac{b\sigma(t)}{f_s(t)} \right] \quad (6)$$

Where $\frac{d\alpha}{dt}$ is rate of damage and α can take value of 0 to 1, 0 representing no damage and 1 representing structural failure, $\sigma(t)$ represents the history of load variation (N or Nmm), $f_s(t)$ represents the variation in load carrying capacity with time (N or Nmm). Often, instead of plotting the development of α , $1-\alpha$ is plotted, indicating the residual load carrying capacity. The moment carrying capacity varies with time due to reduction of cross section, but also because the strength of the outer layers may be reduced because of biological decay. Thus, the total rate of change of the effective sectional moment of area W_t and change in effective cross sectional area ϵ_A resisting shear can be written as:

$$\epsilon_t = \left(1 - \frac{2\delta}{b}\right) \left(1 - \frac{2\delta}{t}\right)^2 \quad (7)$$

$$\epsilon_A = \left(1 - \frac{2\delta}{b}\right) \left(1 - \frac{2\delta}{h}\right) \quad (8)$$

Where δ is the rate of decay per year, b is the width and h is the thickness of the sheet pile.

Thus, time dependent area and moment of area could be written as:

$$W_t = W_0 \epsilon_t \quad (9)$$

$$A_t = A_0 \epsilon_A \quad (10)$$

The time dependent sectional moment of inertia, area resisting shear, moment carrying capacity and shear resistance can be evaluated from the above equation while the bending moment and shear acting on the sheet pile could be obtained from the D-sheet piling software.

2.6 CASE STUDY

To illustrate the model and understand the effect of vegetation on the damage induced on the sheet pile a case study at the stream bank location in Huairou District, Beijing China is chosen. This location is ideal for the case study, due to readily available biomass measurements of *Salix alba* L. for 5 and 7 years from the experimental study by Zhang et al., (2018). The detailed soil description is also available for the location. A 3 meter high stream bank made of sandy loam and loamy sand is to be retained. The internal friction angle of the soil is chosen to be 30° with no cohesion. The density of the embankment is taken as 18kN/m^3 . A timber sheet pile retaining structure (Case 1) is compared with a timber sheet pile-vegetation structure (Case 2) for a design life of 20 years, see Fig 1.

3. RESULTS & DISCUSSIONS

3.1 ROOT DISTRIBUTION MODEL

For any location the root distribution model given by Tron et al., (2015) needs to be calibrated for prediction of the root distribution with depth. The temporal variation of *Salix alba* L. ‘Tristis’ for 5 years given by Zhang et al., (2018) was used to calibrate the parameters of the root distribution model. A preliminary assessment of the root distribution and root growth rates given by Zhang et al., (2018) implies that significant root growth (about 12 percent of the maximum root growth) is observed to a depth of 0.9 meters. Also, it should be noted that the root density is higher at 0.2-0.4 meters, which implies the availability of water for plants at these depth and that the water table fluctuates sharply. Thus a relatively higher root growth window ($L=0.5$) and $\alpha=0.3$ is chosen to represent these conditions. A value of 2.0 is chosen for λ to fit the calibration better for the first 5 years. The root growth rate given by Zhang et al., (2018) is input as such in the model for the prediction of the root distribution for the 7 year period. Tron et al., (2015) suggested that the impact of $\theta(z)$ on the root profile is low and for the prediction of root biomass after 7 years a constant value of 1 is assumed throughout the depth.

The parameters of the root distribution model are calibrated with the abovementioned parameters for the root distribution of 5 years. With the calibrated model parameters and growth rates for the 6th and 7th year, a prediction of the root distribution is made. The observed and the predicted root distributions show good conformity, which implies that the adopted parameters and the model are able to capture the root distribution at the location with good accuracy.

To estimate the root distribution in the future, it is necessary to know the temporal increase in maximum root biomass. This parameter will not be known to the designer during the design stages. Thus, like in many soil engineering problems, estimation of maximum root biomass or root growth rate will rely on the experience, understanding and judgement of the designer. Future research needs to be directed in this regards in estimating the growth rate and field data is necessary for the literature. In this case study a steady growth rate of 30 grams per year is assumed for the first 20 years. This assumption falls within the range of minimum biomass of willow root balls

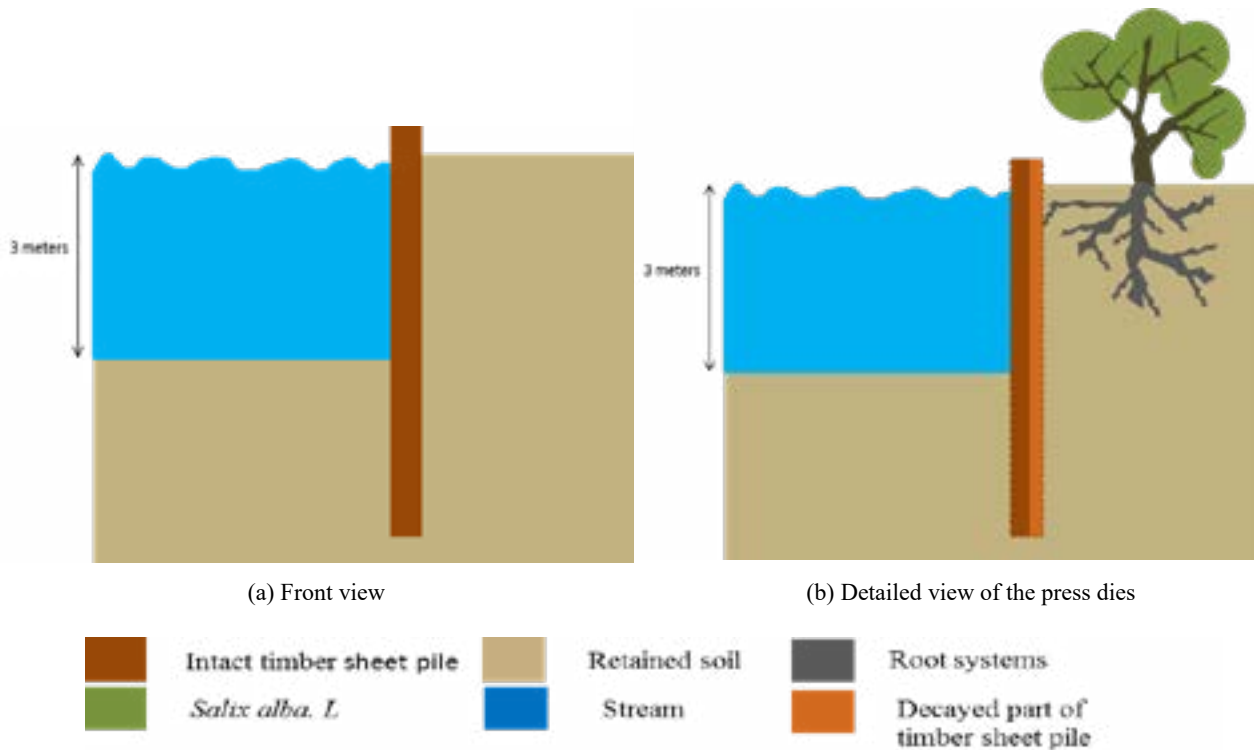


Figure 1: Case 1, a 3 meter high stream bank retained by sheet pile made of timber which has low resistance to decay. Case 2, the same stream bank retained by low resistance to decay timber sheet pile-vegetation system. A decayed sheet pile and grown vegetation is shown in Case 2.

reported in Juliszewski et al., (2015). How this assumption of 30 grams per year of root biomass growth and how its variation propagates to the safety of the whole system is out of scope of this article. The root distribution as expected is different from the water limited ecosystems, they don't decrease exponentially with depth, instead show a peak at 0.3 meters. The distribution variation is dependent on vegetation parameters, like the growth rate and hydraulics of water table.

3.2 MECHANICAL STRENGTH MODEL

The root distribution obtained is input into the mechanical reinforcement model. Even though some studies (Smyth et al., 2013) used analytical models to estimate the fine and coarse roots from the total root biomass, they are not used in here due to lack of proof of applicability of these models in all conditions. Hence average tensile strength as used by other researchers (Mickovski and Tardío, 2016; Ollauri and Mickovski, 2014) in analytical modelling is adopted here. An average tensile strength of 32 MPa for *Salix alba L.* 'Tristis' is input. For this case study the values of k' (Range: close to 1, Thomas and Pollen-Bankhead (2010)) and k'' (range: 0.32-1.00, Bischetti et al., (2010)) are assumed as unity.

The variation of the root mechanical strength is shown in Fig 2. The variation of mechanical strength with depth follows the same as the variation of root biomass. The calculated root cohesion of 7 years is more conservative compared with the experimental results obtained by Zhang et al., (2018). The mechanical reinforcement at 20 years due to the plant growth is estimated, see Fig 2.

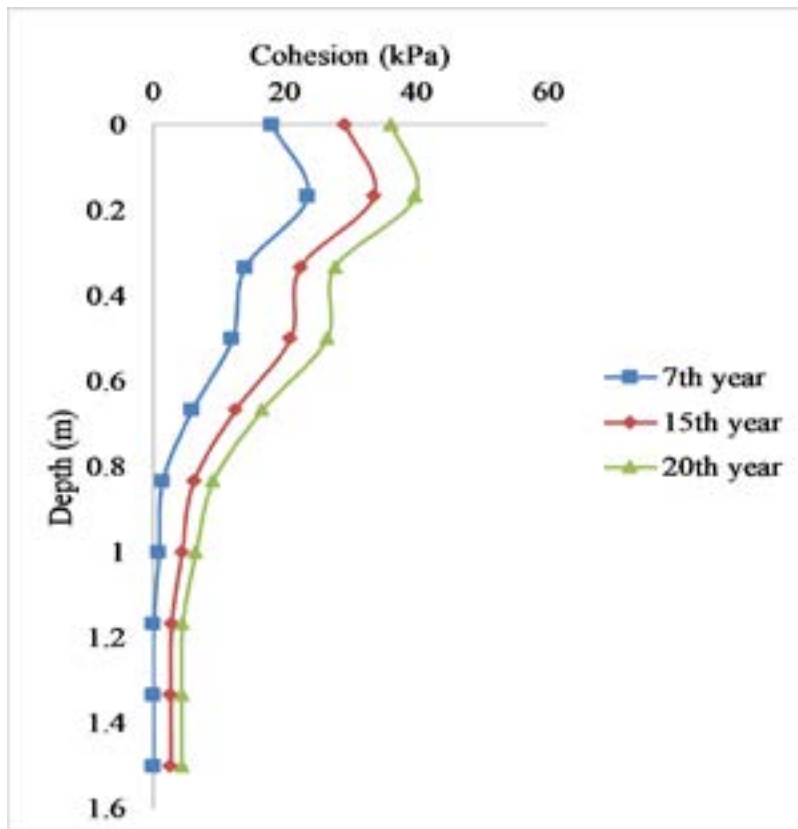


Figure 2: Variation of mechanical contribution of vegetation. Increase in cohesion due to the roots with time is shown

3.3 TIMBER SERVICE LIFE MODEL

The maximum bending moment (M) acting on the sheet pile was taken from the output of D-sheet piling (Visschedijk and Trompille., 2011). This will be the initial bending moment ($M_0=21.54\text{kNm}$) experienced by the sheet pile before the growth of vegetation. Sheet piles are often made of wood species azobé (*Lophiara alata*) which is assigned to strength class D70 of European standard EN 338, (Van de Kuilen and Blass, 2006). This corresponds to a characteristic bending strength of $f_m = 49.5\text{MPa}$ after taking into account the safety factors for material property, ($\gamma_M = 1.3$ EC5, $k_{is}=1.15$) modification factor and a shear strength of 1.5N/mm^2 , but excluding the influence of long term loading, as this is now incorporated in the damage model. A sheet pile with width of 1 m, and thickness 0.075 m was chosen to retain the soil. The decay rate of the entire timber sheet pile was assumed to be -0.001 m (1 mm/year). The parameters of the timber damage accumulation model, $a=21$, $b=24.63$ were adopted for the estimation of the time to failure line for timber beams (Gerhards and Link, 1987). To estimate the contribution of decayed section modulus, there exist two options. The more conservative approach is to neglect the contribution of the decayed section completely. For more realistic estimation the decayed section can be assumed to have a certain percentage of the initial strength (f_0), (Van de Kuilen, 2007). In this paper two conditions are checked (i) decayed section has a remaining strength f_r which is 20% of the initial strength, $f_r=0.2 \cdot f_0$ (ii) decayed section has no contribution at all: $f_r=0$.

With the assumed decay rate of 1 mm/year, the sectional modulus is estimated to decrease by more than 48% in 20 years. This results in a decrease of moment carrying capacity of the sheet pile. When the decayed area is assumed to have no contribution, the damage coefficient reaches a value of 1 in the 18th year. Thus, the residual moment carrying capacity of the sheet pile system is expected to reduce to zero in 18 years. When the decayed section is assumed to have a remaining strength of $0.2f_0$, the damage coefficient reaches a value of 1 in the 23rd year, see Fig 4. Thus when, $f_r=0.2 \cdot f_0$, it can be seen that complete damage does not occur in 20 years.

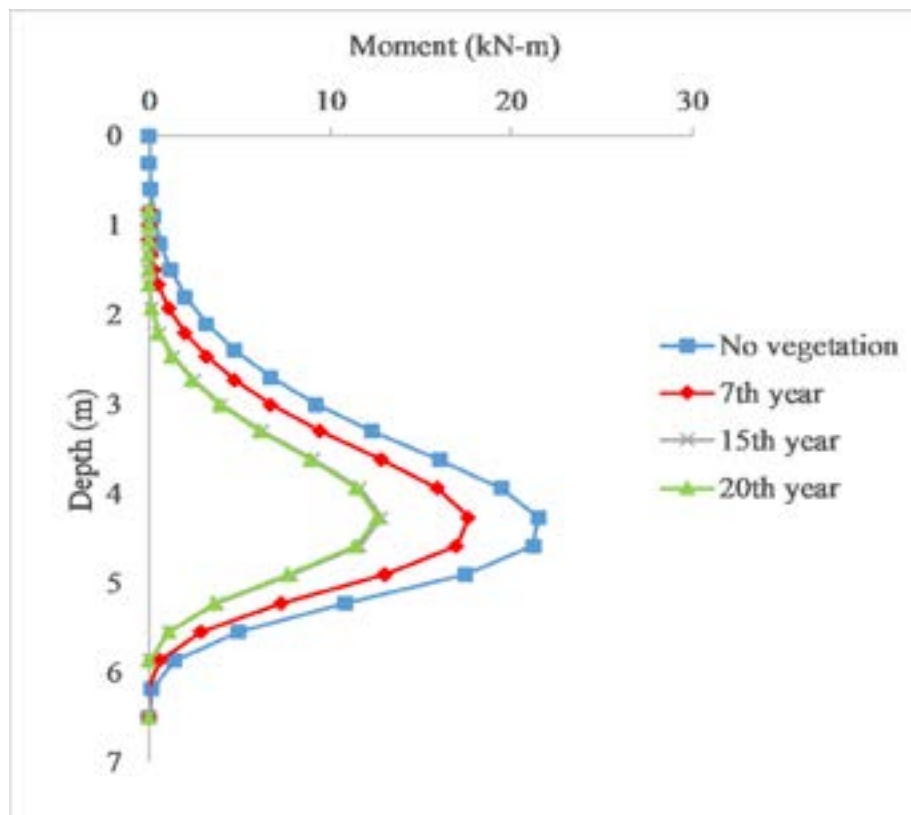
The cross sectional area resisting shear reduces by over 28% in 20 years. The residual shear carrying capacity is seen to reduce to zero in 47th year when no contribution of the decayed part is assumed. Under the condition $f_r=0.2 \cdot f_0$,

the sheet pile will fail completely by the 59th year (see Fig 4). It can be concluded that the bending moment thus becomes the critical parameter in this case of a design life of 20 years.

3.4 SHEET PILE-VEGETATION SYSTEM

The increase in cohesion was represented as layers of soil of increased cohesion in the stream bank. A total of 10 layers of thickness 0.16 meter each was created and assigned the corresponding cohesion value obtained from the mechanical model. The moment distribution in each year from the 7th year to 20th year was calculated and it can be seen that the moment acting on the sheet pile decreases with the growth of the vegetation. The bending moment without vegetation, Case 1, is 21.54 kNm, reduces to 17.6 kNm in 7 years and further reduces to 12.62 kNm after 20 years (Case 2), see Figure 3. The shear load in Case 1, is 21.44 kN and it reduces to 13.36 kN by 20 years in Case 2. This reduction in bending moment and shear could be included as the time dependent loading in the timber damage model. The new damage coefficient and subsequent residual moment and shear carrying capacity after inclusion of the time dependent loading $\sigma(t)$ has been estimated. Applying $f_r=0.2 f_0$, and the new time dependent loading (bending moment and shear), the damage coefficient α at 20 years is $6e-04$ in bending and $6e-06$ in shear. Further, when $f_r=0$, the damage coefficient α takes a value of 0.0018 in bending and $7e-06$ in shear. This implies that the sheet pile-vegetation system has only very minor damage. As compared to the sheet pile only system, the residual moment and shear carrying capacity of the sheet pile-vegetation system does not reduce to zero in the intended service life of 20 years. In other words, the effect of vegetation is such that a longer service life could be expected.

For instance for the condition $f_r=0$ the sheet pile-vegetation system is estimated to be damaged completely or the damage coefficient reaches the value of one in 31 years, in case $f_r=0.2 f_0$ it reaches 43 years in bending. Consequently, a prolonged service life of approximately 13 years and 20 years is expected when the vegetation reinforcement is included in the calculations. In shear an extra service life of 10 years ($f_r=0$) and 14 years ($f_r=0.2 f_0$) is expected in a timber sheet pile-vegetation compared to the retaining structure of timber sheet pile alone.



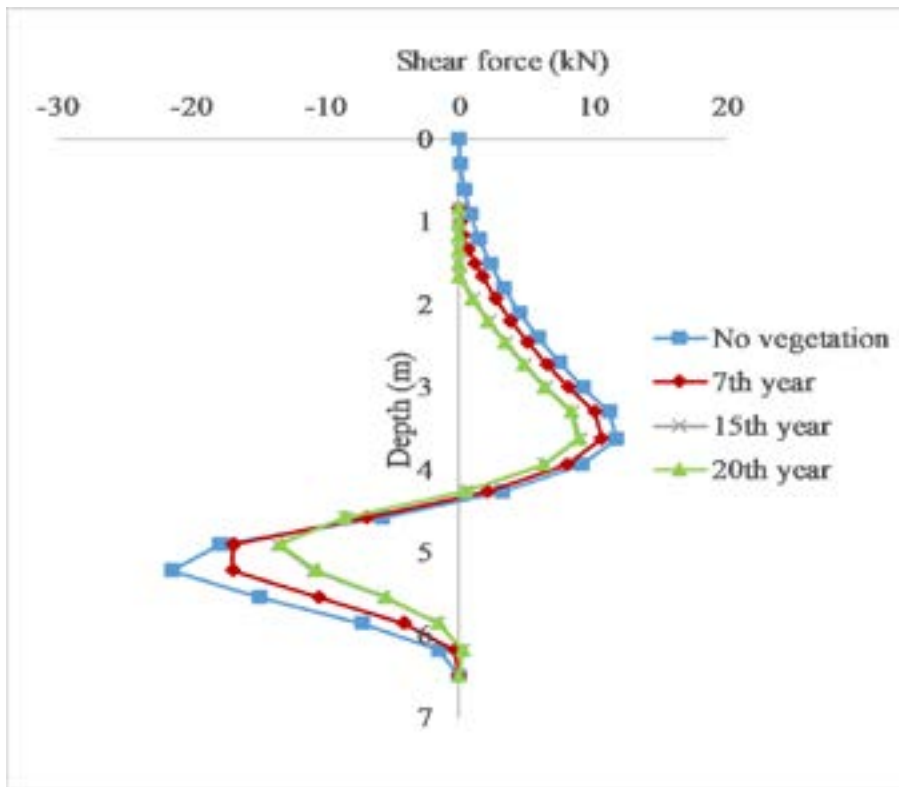
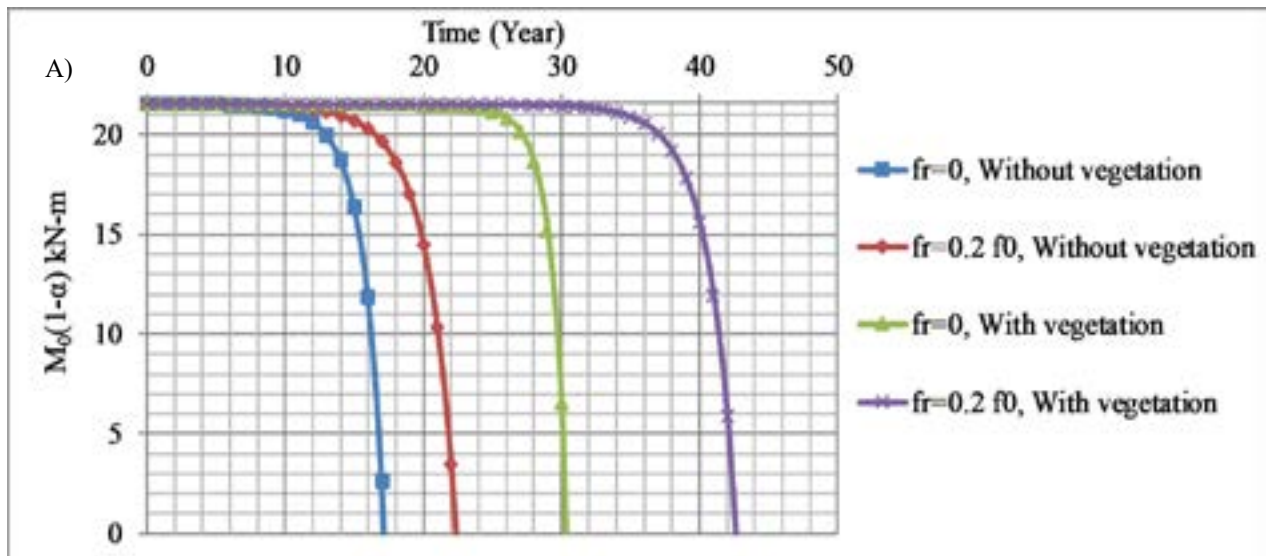


Figure 3: Time-dependent variation of bending moment and shear force acting on the entire length of the timber sheet pile in a timber sheet pile-vegetation system.



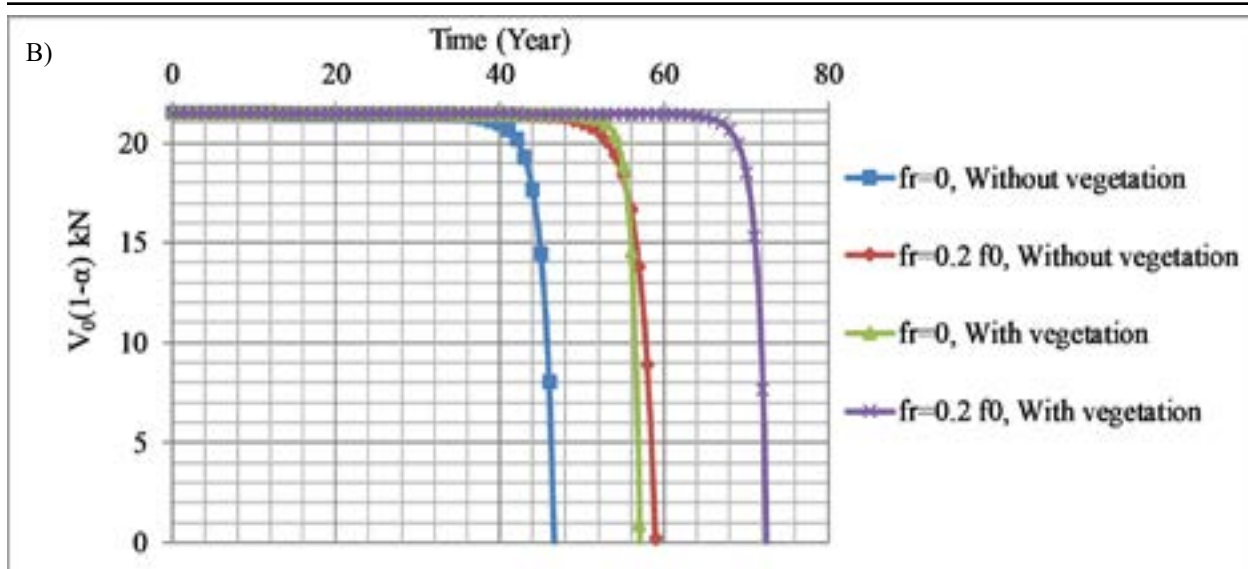


Figure 4: Evolution of damage accumulation on the timber sheet pile with and without vegetation. The variation when a contribution to the resistance is assumed from the decayed section is shown. A) Gives the variation of $M_0(1-\alpha)$ with time due to change in bending moment B) Gives variation of $V_0(1-\alpha)$ with time due to change in shear load

4. CONCLUSIONS

The research in the field of soil bio-engineering is focussed on designing the structure in such a way that the vegetation takes over the inert material like timber in the long term. Realizing the fact that the strength degradation of timber is dependent on the variation of load acting on it with time, an integral model is proposed taking the vegetation development as well as duration of load effects in timber and its biological degradation into account. With decreasing load acting on the timber sheet pile with the growth of vegetation, the damage accumulation on the sheet pile decreases, thereby increasing the design life of the timber sheet pile. This is illustrated through a case study, where the vegetation is seen to increase the durability of the timber sheet pile by decreasing the load acting on it with time. The system leads to the possibility of designing timber sheet pile walls with smaller dimensions, or with less durable material. The structural safety of the 'combined' system of sheet pile and vegetation can be estimated using the proposed procedure.

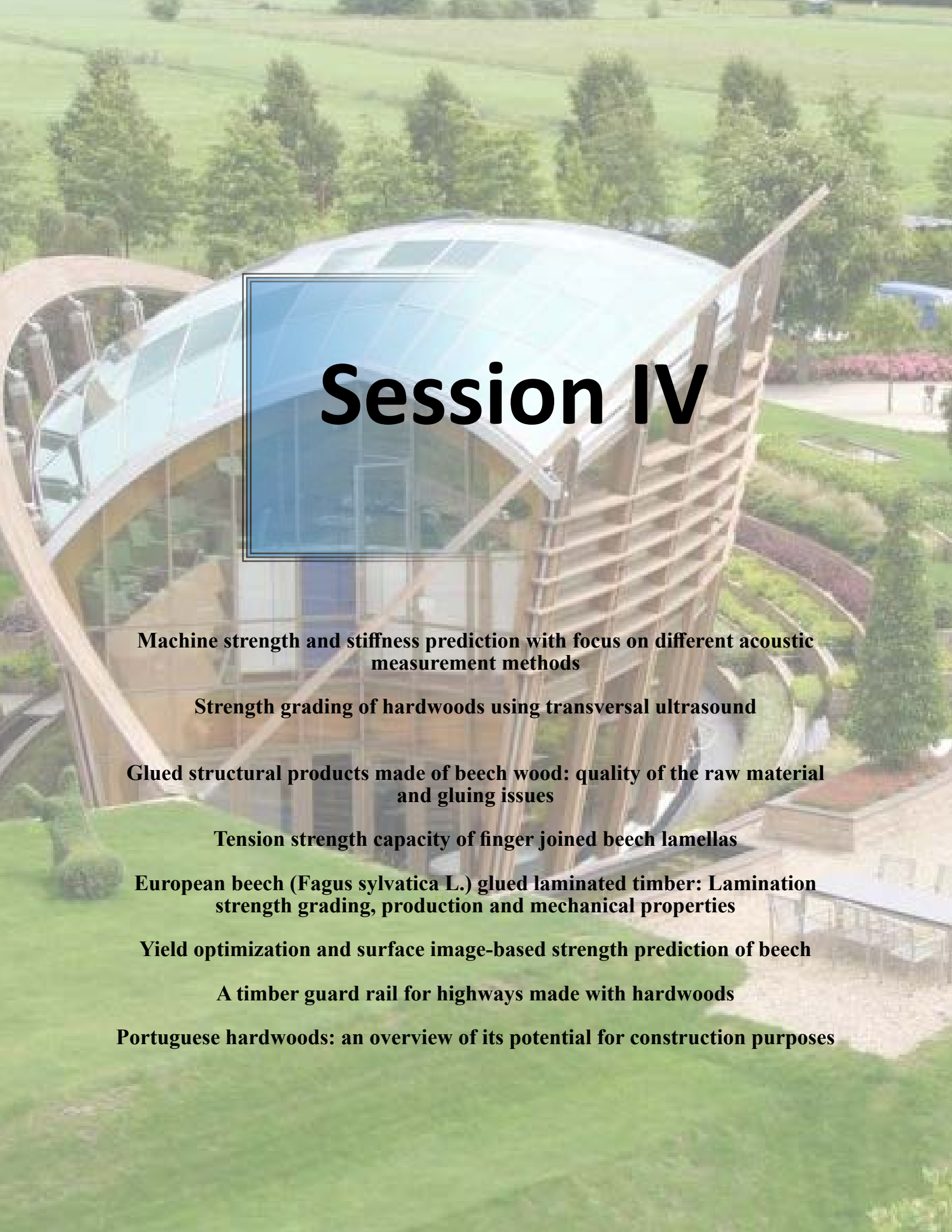
ACKNOWLEDGEMENTS

The work described in this publication was supported by the European Commission H2020 Framework Programme through the grant to the budget of the Marie Skłodowska-Curie European Training Networks (ETN) project TERRE, Contract H2020-MSCA-ITN-2015-675762.

REFERENCES

- Anstead, L., & Boar, R. R. (2010). Willow spiling: review of streambank stabilisation projects in the UK. *Freshwater Reviews*, 3(1), 33-48.
- Anstead, L., Boar, R. R., & Tovey, N. K. (2012). The effectiveness of a soil bioengineering solution for river bank stabilisation during flood and drought conditions: two case studies from East Anglia. *Area*, 44(4), 479-488.
- Bergen, S. D., Bolton, S. M., & Fridley, J. L. (2001). Design principles for ecological engineering. *Ecological Engineering*, 18(2), 201-210.
- Dugied, P. H. (1819). *Projet de boisement des Basses-Alpes... Imprimerie royale.*
- Evette, A., Labonne, S., Rey, F., Liebault, F., Jancke, O., & Girel, J. (2009). History of bioengineering techniques for erosion control in rivers in Western Europe. *Environmental Management*, 43(6), 972.
- Fernandes, J. P., & Guiomar, N. (2016). Simulating the stabilization effect of soil bioengineering interventions in Mediterranean environments using limit equilibrium stability models and combinations of plant species. *Ecological Engineering*, 88, 122-142.
- Foschi R. O. and Yao Z. C. (1986). Another look at three duration of load models. CIB-W18, *Proceedings of the 19th Meeting, Paper 19-9-1, Florence, Italy.*
- Gerhards, C. C., & Link, C. L. (1987). A cumulative damage model to predict load duration characteristics of lumber. *Wood and Fiber Science*, 19(2), 147-164.
- González-Ollauri, A., & Mickovski, S. B. (2014). Integrated model for the hydro-mechanical effects of vegetation against shallow landslides. *EQA-International Journal of Environmental Quality*, 13(13), 37-59.
- Juliszewski, T., Kwaśniewski, D., Pietrzykowski, M., Tylek, P., Walczyk, J., Woś, B., & Likus, J. (2015). Root biomass distribution in an energy willow plantation. *Agricultural Engineering*, 19(4), 43-49.
- Laio, F., D'Odorico, P., & Ridolfi, L. (2006). An analytical model to relate the vertical root distribution to climate and soil properties. *Geophysical Research Letters*, 33(18).
- Li, X., Zhang, L., & Zhang, Z. (2006). Soil bioengineering and the ecological restoration of riverbanks at the Airport Town, Shanghai, China. *Ecological engineering*, 26(3), 304-314.
- Mickovski, S. B., Hallett, P. D., Bengough, A. G., Bransby, M. F., Davies, M. C. R., & Sonnenberg, R. (2008). The effect of willow roots on the shear strength of soil. *Advances in GeoEcology*, 39, 247-262.
- Pollen, N., & Simon, A. (2005). Estimating the mechanical effects of riparian vegetation on stream bank stability using a fiber bundle model. *Water Resources Research*, 41(7).
- Pollen-Bankhead, N., & Simon, A. (2009). Enhanced application of root-reinforcement algorithms for bank-stability modeling. *Earth Surface Processes and Landforms*, 34(4), 471-480.
- Preti, F., Dani, A., & Laio, F. (2010). Root profile assessment by means of hydrological, pedological and above-ground vegetation information for bio-engineering purposes. *Ecological Engineering*, 36(3), 305-316.
- Qin, S., & Yang, N. (2018). Strength degradation and service life prediction of timber in ancient Tibetan building. *European Journal of Wood and Wood Products*, 76(2), 731-747.
- Schenk, H. J. (2008). The shallowest possible water extraction profile: a null model for global root distributions. *Vadose Zone Journal*, 7(3), 1119-1124.
- Simon, A., & Collison, A. J. (2002). Quantifying the mechanical and hydrologic effects of riparian vegetation on streambank stability. *Earth Surface Processes and Landforms*, 27(5), 527-546.
- Stokes, A., Atger, C., Bengough, A. G., Fourcaud, T., & Sidle, R. C. (2009). Desirable plant root traits for protecting natural and engineered slopes against landslides. *Plant and soil*, 324(1-2), 1-30.
- Tardío, G., & Mickovski, S. B. (2016). Implementation of eco-engineering design into existing slope stability design practices. *Ecological Engineering*, 92, 138-147.
- Thomas, R. E., & Pollen-Bankhead, N. (2010). Modeling root-reinforcement with a fiber-bundle model and Monte Carlo simulation. *Ecological Engineering*, 36(1), 47-61.
- Tron, S., Laio, F., & Ridolfi, L. (2014). Effect of water table fluctuations on phreatophytic root distribution. *Journal of theoretical biology*, 360, 102-108.
- Tron, S., Perona, P., Gorla, L., Schwarz, M., Laio, F., & Ridolfi, L. (2015). The signature of randomness in riparian plant root distributions. *Geophysical Research Letters*, 42(17), 7098-7106.
- Van de Kuilen, J.W.G., Blass, H.J. (2005), Mechanical properties of azobé (*Lophira alata*), *Holz- als Roh- und Werkstoff*, 63: 1–10, DOI 10.1007/s00107-004-0533-7

-
- Van de Kuilen, J.W.G. (2007). Service life modelling of timber structures. Materials and Structures, 40(1), 151-161.*
- Van de Kuilen, J. W. G., & Gard, W. F. (2012). Residual service life estimation using damage accumulation models. In World conference on timber engineering, Auckland, New Zealand, 15-19 juli 2012.*
- Van de Kuilen, J. W. G., M. L. R. Van Der Linden, M. (1999). Reliability Based Design Of Timber Sheet Pile Walls. New Zealand Timber Design Journal. 1.*
- CIB-W18 Timber Structures, Proceedings of the 19th Meeting, Paper 19-9-3, Florence, Italy.*
- Visschedijk, M. A. T. and V. Trompille (2011). D-Sheet piling Version 9, design of diaphragm and sheet pile walls. Delft, Deltrares.*
- Waldron, L. J. (1977). The Shear Resistance of Root-Permeated Homogeneous and Stratified Soil 1. Soil Science Society of America Journal, 41(5), 843-849.*
- Wang, X. L. (2008). Research on evaluation method of reliability-based residual life of historic timber structure(Doctoral dissertation, Ph. D. thesis, Wuhan University of Technology, Wuhan, China).*
- Wu, T. H. (1976). Investigations of landslides on Prince of Wales Island: geotechnical engineering report.*
- Zeng, F., Bleby, T. M., Landman, P. A., Adams, M. A., & Arndt, S. K. (2006). Water and nutrient dynamics in surface roots and soils are not modified by short-term flooding of phreatophytic plants in a hyperarid desert. Plant and Soil, 279(1-2), 129-139.*
- Zhang, D., Cheng, J., Liu, Y., Zhang, H., Ma, L., Mei, X., & Sun, Y. (2018). Spatio-Temporal Dynamic Architecture of Living Brush Mattress: Root System and Soil Shear Strength in Riverbanks. Forests, 9(8), 493.*



Session IV

Machine strength and stiffness prediction with focus on different acoustic measurement methods

Strength grading of hardwoods using transversal ultrasound

Glued structural products made of beech wood: quality of the raw material and gluing issues

Tension strength capacity of finger joined beech lamellas

European beech (*Fagus sylvatica* L.) glued laminated timber: Lamination strength grading, production and mechanical properties

Yield optimization and surface image-based strength prediction of beech

A timber guard rail for highways made with hardwoods

Portuguese hardwoods: an overview of its potential for construction purposes

Machine strength and stiffness prediction with focus on different acoustic measurement methods

A. Kovryga¹, J. O. Chuquin Gamarra^{1*}, and J-W. G. van de Kuilen^{1,2}

¹ Wood Research Munich
Technical University of Munich
80797 Munich, Germany

² Faculty of Civil Engineering
and Geosciences
Technical University of Delft, The Netherlands

ABSTRACT

*Strength grading is an important step for the production of homogenous and high-quality solid wood material. In particular, for hardwoods, the use of non-visible characteristics is indispensable. Dynamic MOE (MOE_{dyn}) is an important parameter widely used for grading of softwoods and applicable to hardwoods as well. There are two common ways to measure MOE_{dyn} – ultrasound (US) wave propagation and longitudinal stress wave (LSW) propagation. Both methods are used in practice, however, due to the different measurement techniques behind them, the results differ. Current paper analyses the stiffness and strength prediction accuracy for several temperate European hardwood specimens and stress the differences between the two measurement systems. The performance was analysed with regard to grading techniques, testing modes for the mechanical properties (tension and bending) and wood qualities. For more than 2861 pieces of European ash (*Fraxinus excelsior*), European beech (*Fagus sylvatica*), European oak (*Quercus spp.*) and maple (*Acer spp.*), the MOE_{dyn} was measured using both techniques, and destructive tests (tension and edgewise bending) were applied. The results show that LSW has higher prediction accuracy compared to the US MOE_{dyn} . The prediction accuracy for both methods and tensile application can be increased by calculating MOE_{dyn} with average density. Furthermore, the results support the species independent strength grading of hardwoods. Further research on the effect of different wood qualities and sawing pattern is required.*

1. INTRODUCTION

Temperate hardwoods are very well known for excellent mechanical properties, which make them favourable for structural purposes. As a renewable material, wood shows high variation in mechanical properties. Strength grading is a crucial step for the production of homogenous and high-quality solid wood material with defined material properties. Whereas the research on softwoods has led to the high acceptance of the machine strength grading methods, the application of those methods to the hardwoods is less frequent. The research activities of the recent years in the field of strength grading and engineered wood products aimed to bridge knowledge gaps with regard to hardwoods.

The recent research activities have been focused on applying the established methods of machine strength grading for softwoods to hardwoods, as well as novel methods of non-destructive testing. In focus of the mechanical strength grading, the dynamic MOE (MOE_{dyn}) can be highlighted as a major criterion of interest. MOE_{dyn} is a mechanical property of the material and describes the elastic behaviour of wood under dynamic cyclic stress and has been used to characterize wood material for decades (Kollmann and Côté 1968). The MOE_{dyn} application for the strength grading of structural timber dates back to Goerlacher (1990) and is currently one of the most frequent methods for the machine strength grading of wood. Generally, there are two possibilities to determine MOE_{dyn} , which are: ultrasound (US) wave propagation and longitudinal stress wave (LSW) propagation. Both methods are related to the acoustic properties of wood. In the first case, the ultrasound wave signal is generated and the propagation in wood is measured, whereas in the other case, a stress wave is induced using a hammer and the eigenfrequency of wood is determined. Nowadays, the eigenfrequency has established itself as a very robust and is the most frequently used method. The characteristic vibrations in the board can be detected contact-free using laser vibrometer (Giudiceandrea 2005).

As a grading parameter, MOE_{dyn} shows a high correlation to static MOE, for both softwoods (Bacher 2008) and hardwoods (Frühwald und Schickhofer 2005). The prediction accuracy for the strength is high, especially for the softwoods. For the hardwoods, the prediction accuracy of both methods seems to be less high. The reported R^2 values for the strength prediction range from 0.18 to 0.36 for temperate hardwoods (Nocetti et al. 2016, Ravenshorst 2015).

* J. O. Chuquin Gamarra: E-mail: gamarra@hfm.tum.de

And are lower for the tensile strength prediction of temperate hardwoods shown for a variety of species ($R^2 < 0.25$) (Ehrhart et al. 2016, Glos and Lederer 2000, Green and McDonald 1993). For tensile strength, the prediction accuracy depends on the quality of the material, (Westermayr et al. 2018) reports of high R^2 value of 0.48 for low-quality beech lamella, compared to the value achieved for high quality with 0.22 (Ehrhart et al. 2016). This should imply that timber of rejectable quality shows higher grading accuracy. In most publications, the MOE_{dyn} is determined using the LSW. Therefore, the question arises regarding the performance of both methods and the differences between tension and bending strength prediction accuracy. Frühwald and Hasenstab (2010) mention that the accuracy of the method is higher for LSW.

The present study aims to investigate the differences in the prediction accuracy between US and LSW method on a large data pool of hardwood specimens tested at TU Munich in recent years. Both methods are compared regarding the prediction accuracy for the tensile strength and stiffness measurement. Special focus is given to the differences between the species, the ability to apply species independent strength grading, and the ability for the bending and tensile strength prediction. The species ash, beech, maple and oak that represent the hardwood species with different anatomical structure (ring-porous and diffuse porous) are investigated.

2. MATERIALS

For the current study, in total 2681 specimens of European hardwoods – European ash (*Fraxinus excelsior*), European beech (*Fagus sylvatica*), oak (*Quercus spp.*) and maple (*Acer spp.*) were used. Table 1 gives an overview of the specimens and dimensions used. The length of the specimens varied between 3 and 5.5 m. The specimens originated from different projects run at TU Munich over two decades. Beech and oak were tested by Glos and Lederer (2000) within the hardwood strength grading project. Ash and maple tested in bending originate from the project on the assignment of those species to the bending strength classes (D-Classes) by Glos and Torno (2008a, 2008b). Tension test data of ash and maple were obtained by Kovryga et al. (2019) within the project on hardwood strength grading. For details, please refer to the publications.

Table 2 summarizes the mechanical properties of the tested hardwoods. The tested specimens are representative for the tested wood species and, particularly, for the growth region in Central Europe. The mechanical property values are comparable to the values given in publications. So for ash, the mean tensile strength values are comparable to the values reported by Frühwald and Schickhofer (2005). For beech, the values are lower compared to the ungraded tensile strength of beech ($f_{t,mean} = 62.2$ MPa, Erhart et. al. 2016) and by Frühwald and Schickhofer. On the other side, the values considerably exceed the values reported by Westermayr et al. (2018) ($f_{t,mean} = 35,9$ MPa) for low-quality beech lamella. The bending strength of oak is lower compared to beech and maple particularly due to the high moisture content, which was on average 31.9%. Therefore, the values are adjusted to the reference moisture content of 12% m.c. as described in section 3.

Table 1: Overview of specimens and dimensions

Species	Bending			Tension		
	Cross-section (<i>b</i> <i>x</i> <i>h</i>) [mm x mm]	<i>N</i>	Reference	Cross-section (<i>b</i> <i>x</i> <i>h</i>) [mm x mm]	<i>N</i>	Reference
Europeanash (<i>Fraxinus excelsior</i>)	50x100, 50x150	324	Glos and Torno (2008a)	50x100; 50x150	259	
				25x85; 30x100; 30x125; 35x125	35x160; 35x100;	481 Kovryga et al. (2019)
Europeanbeech (<i>Fagus sylvatica</i>)	35x70;60x120; 60x120 60x180	224	Glos and Lederer (2000)	30x120;30x160;30x165	217	Glos & Lederer (2000)
Maple (<i>Acer spp.</i>)	50x100;50x150; 50x175	459	Glos and Torno (2008b)	25x125;30x100; 30x125; 35x100; 25x100	381	Kovryga et al. (2019)
Oak (<i>Quercus spp.</i>)	40x80;60x120; 60x180	336	Glos and Lederer (2000)			
TOTAL		1343			1338	

Table 2: Descriptive statistics of grading characteristics and mechanical properties from tension and bending test for European ash (*Fraxinus excelsior*), European beech (*Fagus sylvatica*), oak (*Quercus* spp.) and maple (*Acer* spp.) species

Species		Bending				Tension		
		ash	beech	maple	oak	ash	beech	maple
N		324	224	459	336	740	217	381
$tKAR$ [-]	μ	0.055	0.102	0.075	0.175	0.067	0.146	0.119
	s	0.074	0.106	0.082	0.141	0.092	0.107	0.135
$E_{dyn,us,12}$ [GPa]	μ	16.1	18.1	15.1	13.4	16.5	17.7	16.7
	s	1.9	1.9	2.0	2.3	2.5	2.2	1.9
$E_{dyn,freq,12}$ [GPa]	μ	14.0	14.3	12.8	11.0	14.7	14.7	14.4
	s	1.8	2.8	1.7	2.1	2.4	2.0	1.7
$m.c.$ [%]	μ	10.6	11.6	8.4	31.9	10.6	10.2	11.2
	s	0.9	0.6	0.9	9.5	1.0	0.4	0.6
ρ_{12} [kg/m ³]	μ	678	742	635	714	685	723	664
	s	49	38	41	55	57	41	45
$E_{0,12}$ [GPa]	μ	12.7	14.6	12.0	10.9	14.1	13.8	13.8
	s	1.8	2.4	1.9	2.8	2.7	2.5	2.2
f [MPa]	μ	69.8	65.3	56.3	56.1	59.0	48.2	53.4
	s	16.1	20.7	18.7	17.2	28.2	22.1	26.2

3. METHODS

3.1 NON-DESTRUCTIVE MEASUREMENTS

For all the specimens, the grading characteristics and the mechanical properties from tension and bending test were determined. The MOE_{dyn} was measured in two ways - using the ultrasound wave and stress wave propagation. The longitudinal US measurement was done using sylvatest device with the frequency of 20 kHz. During the non-destructive measurement, the runtime of the wave is measured longitudinal to the grain direction between the transmitter and receiver transducer. The MOE_{dyn} is calculated as a product of density and ultrasound wave using Eq. 1:

$$E_{dyn,us} = v^2 \cdot \rho \quad (1)$$

For the longitudinal stress wave (LSW), measurement hammer is used to generate stress wave. The signal is recorded by means of a microphone or an accelerometer. Both measurements are done at the laboratory of the TU Munich for consistency check, as they provide similar results. In industrial facilities laser, vibrometer can be used to record vibrations contact-free. By applying the FFT-transformation, the eigenfrequency is calculated. The $E_{dyn,freq}$ is calculated by combining the eigenfrequency (f) with length (l) of the specimen and density (ρ) measurement using the following equation:

$$E_{dyn,freq} = 4 \cdot l^2 \cdot f^2 \cdot \rho \quad (2)$$

The density is measured by weighting the specimen.

For temperate hardwoods, density shows usually no correlation to the tensile and bending strength (Erhart et al. 2016, Westermayr et al. 2018, Frühwald & Schickhofer 2005). Therefore, the MOE_{dyn} was calculated using constant density value to study the effect of eigenfrequency and ultrasound velocity on the strength properties. For each wood species, the average density from Table 2 was taken into account. The difference between the MOE_{dyn} calculated with individual readings and MOE_{dyn} with an average density of the wood species are discussed in the paper.

To separate with low and high-quality specimens, the knottiness parameter $tKAR$ (total knottiness area ratio) is used. $tKAR$ is a parameter frequently used in scientific publications and is calculated as the area of knots appearing in 150mm large window, projected on the cross-sectional area. The overlapping areas are counted once.

3.2 DESTRUCTIVE TESTS

The hardwoods specimens were tested in tension and in bending according to the test specification of EN 408 (2010). The bending strength and local MOE were measured in four-point bending test. The test span between the two loading points was six times the depth of cross-section. For local MOE the deformation was measured over the length

of five times the depth. The tension strength was determined with the free test length of nine times the height and the gauge length for the tensile MOE measurement was five times the height.

3.3. MOISTURE CONTENT ADJUSTMENT

The mechanical properties were adjusted to the reference conditions 20° and 65 relative humidity. For all species, the equation derived by Nocetti et al. (2015) on chestnut has been used to adjust dynamic and static MOE. The procedure in EN 384 does not specify any adjustment factors for m.c. above 18%. For MOE below FSP the eq. 3

$$E_{12} = \frac{E_u}{1-0.005(u-12)} \quad (3)$$

For changes in MC above fiber saturation point (FSP) the eq. 4 has been used:

$$E_{12} = \frac{E_u}{0.9} \quad (4)$$

The equation assumes constant MOE value above FSP also shown by Unterwieser and Schickhofer (2011).

The bending strength (f_m) values are adjusted to the reference conditions by assuming a 1.4% increase in strength per 1% m.c. decrease up to the fiber saturation point (Hernández et al. 2014). The selected factor is supported by the findings of Glos and Lederer (2000) for the tested sample who found the difference in bending strength between green and dry specimens of about 21%. The selected factor is designated on the safe side, as in some publications higher change rate is reported. Wang and Wang (1999) report 3.9% per % m.c for red oak.

Table 3: Coefficient correlation (R^2) between the MOE_{dyn} determined using LSW and US method for both data sets tested in bending and tension for European ash (*Fraxinus excelsior*), European beech (*Fagus sylvatica*), oak (*Quercus spp.*) and maple (*Acer spp.*) species

	Bending				Tension			
	$E_{dyn,us,12}$	$E_{dyn,freq,12}$	$E_{dyn,us,\overline{dens},12}$	$E_{dyn,freq,\overline{dens},12}$	$E_{dyn,us,12}$	$E_{dyn,freq,12}$	$E_{dyn,us,\overline{dens},12}$	$E_{dyn,freq,\overline{dens},12}$
European ash								
ρ_{12}	0.450	0.346	0.005	0.001	0.476	0.414	0.057	0.042
$E_{dyn,us,12}$	1.000	0.866	0.617	0.469	1.000	0.878	0.749	0.594
$E_{dyn,freq,12}$		1.000	0.576	0.683		1.000	0.664	0.773
$E_{dyn,us,\overline{dens},12}$			1.000	0.796			1.000	0.807
$E_{dyn,freq,\overline{dens},12}$				1.000				1.000
European beech								
ρ_{12}	0.303	0.190	0.007	0.003	0.413	0.301	0.050	0.022
$E_{dyn,us,12}$	1.000	0.639	0.771	0.423	1.000	0.824	0.792	0.561
$E_{dyn,freq,12}$		1.000	0.491	0.849		1.000	0.689	0.824
$E_{dyn,us,\overline{dens},12}$			1.000	0.549			1.000	0.752
$E_{dyn,freq,\overline{dens},12}$				1.000				1.000
Maple								
ρ_{12}	0.187	0.138	0.003	0.007	0.366	0.189	0.005	0.008
$E_{dyn,us,12}$	1.000	0.877	0.768	0.634	1.000	0.768	0.693	0.391
$E_{dyn,freq,12}$		1.000	0.704	0.795		1.000	0.647	0.730
$E_{dyn,us,\overline{dens},12}$			1.000	0.864			1.000	0.739
$E_{dyn,freq,\overline{dens},12}$				1.000				1.000
Oak								
ρ_{12}	0.067	0.069	0.068	0.051				
$E_{dyn,us,12}$	1.000	0.746	0.743	0.561				
$E_{dyn,freq,12}$		1.000	0.520	0.770				
$E_{dyn,us,\overline{dens},12}$			1.000	0.750				
$E_{dyn,freq,\overline{dens},12}$				1.000				

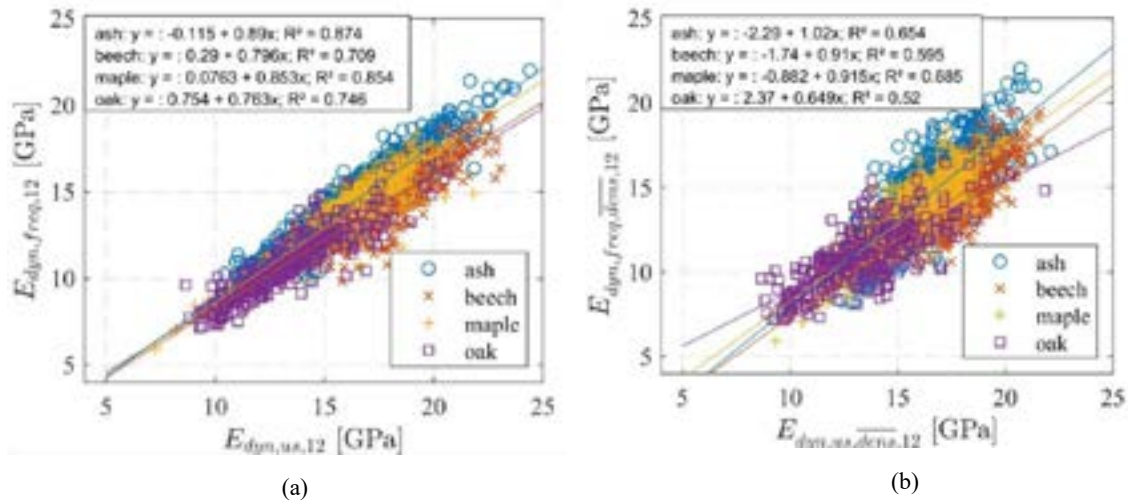


Figure 1: Relationship between MOE_{dyn} from US measurement and MOE_{dyn} measured using LSW method with MOE_{dyn} calculated (a) with individual density reading and (b) calculated with constant density value, grouped by the hardwood species

Table 4: Coefficient of determination (R^2) for the prediction of density, modulus of elasticity and strength from bending test and tension test for European ash (*Fraxinus excelsior*), European beech (*Fagus sylvatica*), oak (*Quercus spp.*) and maple (*Acer spp.*) species

	Bending			Tension		
	ρ_{12}	$E_{0,12}$	f_m	ρ_{12}	$E_{0,12}$	f_t
European ash						
ρ_{12}	1	0.234	0.036	1	0.298	0.034
$E_{dyn,us,12}$	0.415	0.651	0.119	0.424	0.658	0.148
$E_{dyn,freq,12}$	0.312	0.778	0.282	0.386	0.749	0.270
$E_{dyn,us,\overline{dens},12}$	0.008	0.467	0.092	0.054	0.509	0.149
$E_{dyn,freq,\overline{dens},12}$	0.002	0.568	0.269	0.047	0.591	0.296
mc	0.116	0.009	0.009	0.012	0.059	0.009
European beech						
ρ_{12}	1	0.066	0.034	1	0.172	0.010
$E_{dyn,us,12}$	0.369	0.386	0.202	0.475	0.625	0.188
$E_{dyn,freq,12}$	0.287	0.699	0.407	0.351	0.847	0.386
$E_{dyn,us,\overline{dens},12}$	0.038	0.350	0.187	0.103	0.575	0.246
$E_{dyn,freq,\overline{dens},12}$	0.039	0.661	0.393	0.054	0.772	0.471
mc	0.191	0.053	0.070	0.020	0.025	0.002
Maple						
ρ_{12}	1	0.078	0.017	1	0.031	0.029
$E_{dyn,us,12}$	0.238	0.666	0.163	0.364	0.319	0.007
$E_{dyn,freq,12}$	0.201	0.792	0.312	0.207	0.598	0.142
$E_{dyn,us,\overline{dens},12}$	0.005	0.573	0.144	0.009	0.348	0.054
$E_{dyn,freq,\overline{dens},12}$	0.002	0.674	0.285	0.002	0.558	0.263
mc	0.000	0.077	0.085	0.067	0.002	0.000
Oak						
ρ_{12}	1	0.007	0.009			
$E_{dyn,us,12}$	0.209	0.554	0.312			
$E_{dyn,freq,12}$	0.192	0.572	0.398			
$E_{dyn,us,\overline{dens},12}$	0.022	0.482	0.252			
$E_{dyn,freq,\overline{dens},12}$	0.025	0.521	0.345			
mc	0.083	0.000	0.028			

4. RESULTS

4.1. LONGITUDINAL STRESS WAVE METHOD VS. ULTRASOUND MEASUREMENT

Figure 1 shows the relationship between MOE_{dyn} from the US and LSW measurement. Generally, high consistency between both measurements across the wood species can be observed. The prediction accuracy between ultrasound MOE_{dyn} and eigenfrequency MOE_{dyn} ranges between 0.7 for beech and 0.87 for ash. If the MOE_{dyn} is calculated using average density (Figure 1b), the overall R^2 value drops and the scatter shows significantly higher variation. Therefore, individual density values provide a homogenizing effect on the relationship between the MOE_{dyn} . Major differences in the prediction of grade determining properties, like strength and stiffness, are, therefore, expected for the MOE_{dyn} without considering the density.

4.2. STIFFNESS PREDICTION

The prediction accuracy for the tensile and bending MOE is shown in Table 4. MOE_{dyn} from LSW measurement shows higher R^2 values compared to the US measurement. Whereas for ash the difference is less pronounced, the difference for oak and maple accounts approximately 0.3. The prediction strength of static MOE drops for both MOE_{dyn} ($E_{dyn, freq, dens, 12}$ and $E_{dyn, us, dens, 12}$) calculated with average density.

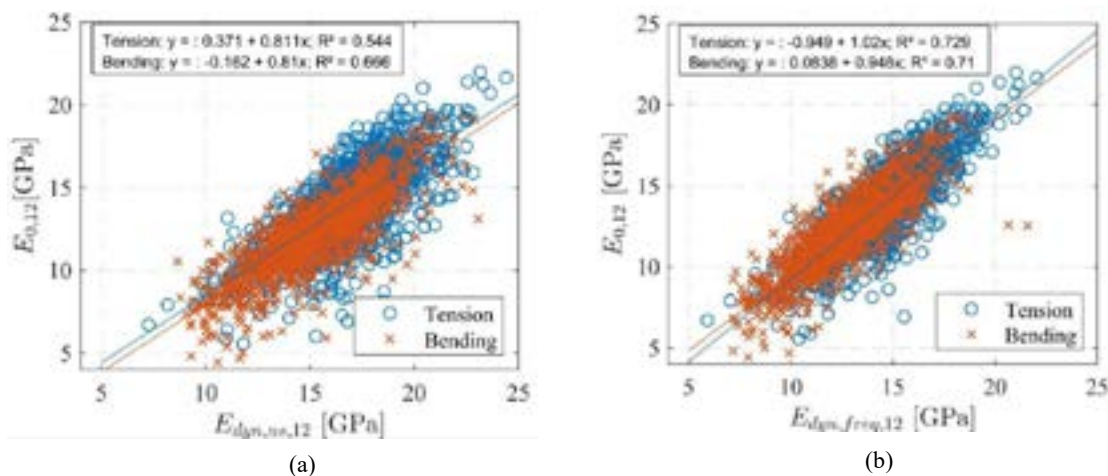


Figure 2: Scatterplot between (a) MOE_{dyn} measured using US device and static MOE and (b) MOE_{dyn} measured using LSW method and static MOE for all investigated hardwood species, split by the testing mode (bending, tension)

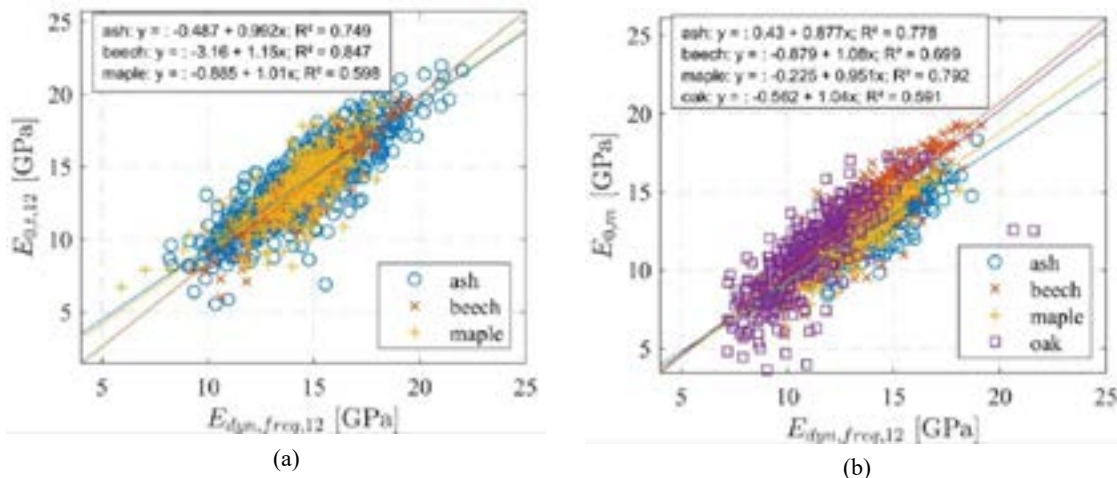


Figure 3: Relationship between (a) MOE_{dyn} measured using LSW method and tension MOE and (b) MOE_{dyn} measured using LSW method and bending MOE, grouped by the hardwood species (bending, tension)

The prediction accuracy between US MOE_{dyn} and LWS MOE_{dyn} is compared for a combined hardwood species data set in Figure 2 dependent on the testing mode. The LWS MOE_{dyn} scatters less compared to the US measurement. For both measurements, the regression equation seems to predict tensile and bending MOE equally well. Furthermore,

no difference in scatter is observable between the two testing modes. For the specimens tested in tension, E_t shows larger scatter with values ranging up to 22 GPa.

The possibility of combining the wood species for the species independent strength grading is visualized in Figure 3. For both testing modes (bending and tension) the population of temperate European hardwoods show homogenous scatter. The values scatter within the same range. Furthermore, specimens show, especially for tension test specimens, almost parallel slope of the regression line. The observation supports the approach of Ravenshorst (2015) regarding the applicability of the species independent strength grading on the example of tensile data.

4.3. STRENGTH PREDICTION

The bending and tensile strength are predicted with US ($E_{dyn,us,12}$) less accurately compared to the LSW. The accuracy ranges between 0.007 and 0.279 for US and 0.142 and 0.405 for the LSW. The R^2 values between $E_{dyn,freq,12}$ and strength (f_i and f_m) is approximately two times higher compared to the values between $E_{dyn,us,12}$ and strength. These findings support the results of Frühwald and Hasenstab (2010) who came to the conclusion that MOE_{dyn} from LSW is a better predictor for the tensile strength.

The scatter between MOE_{dyn} calculated with average density and tensile strength is visualized for the frequency measurement in Figure 4. The scatter for the US shows a similar pattern but higher variation (not shown here). The species range similar to the stiffness in the same values range. Especially, for the tensile strength, the scatter is uniform. The slopes of the regression lines are almost equal, allowing for a species-independent strength grading.

The use of ultrasound and eigenfrequency MOE_{dyn} depends on the density value used for the calculation of the MOE_{dyn} . If the average density value of the wood species is used for the calculation of MOE_{dyn} and not the individual density value, the strength prediction accuracy increases for some samples. For specimens tested in tension, a clear increase in prediction accuracy is observable, for the specimens tested in bending, the exclusion of density value leads to a slight drop in R^2 values (0.015 on average). Same results have been shown by (Nocetti et al. 2016) on chestnut timber tested in bending. The prediction accuracy decreased from 0.24 to 0.15. This behaviour is attributed most likely not only to the testing mode but rather to specimens dimensions and sawing pattern used, as shown below.

Figure 5 visualizes exemplarily the difference in prediction accuracy of the tensile strength using MOE_{dyn} calculated with average and individual density. For the relationship between MOE_{dyn} calculated with average density and tensile strength, a scatter with less variation and steeper regression line can be observed. As a consequence, higher R^2 value can be achieved. By calculating with an average density, the variation in MOE_{dyn} is reduced. The density is a part of MOE_{dyn} calculation that show either low correlation or no correlation to the timber strength. In the case of maple, the correlation is even negative ($r = -0.120$).

Figure 4: Relationship between (a) MOE_{dyn} measured using LSW and tensile strength and (b) MOE_{dyn} measured using LSW and bending strength, grouped by hardwood species

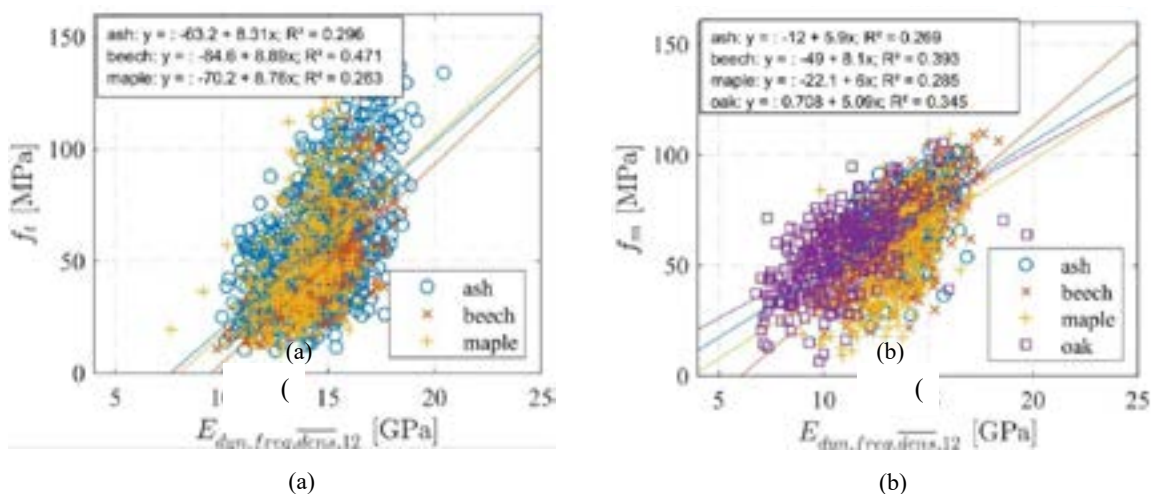


Figure 5: Relationship between tensile strength and MOE_{dyn} measured by using LSW and calculated with the individual (a) and average density (b) for ash sample tested by Kovryga et al. (2019) ($N = 481$)

The observable differences in strength prediction accuracy are attributed most likely to the cross-section size and the sawing pattern used. This can be observed clearly on the ash tested in tension. Ash specimens with cross-sections 50x100 and 50x150 were cut with “cutting all around” (without pith) and indicate no significant difference in prediction accuracy using $E_{dyn, freq, 12}$ and $E_{dyn, freq, dens, 12}$. Other tensile test samples, except beech, were sawn with pith. The juvenile wood is known for hardwoods for slightly higher density compared to the mature wood. Therefore, a higher share of pith specimens could affect the applicability of the density for strength prediction. Especially as between density and strength no or low correlation is present. So for the smaller ash dimensions, the prediction accuracy increased from 0.265 to 0.334. To make general conclusions and study the causes, the special testing program is required.

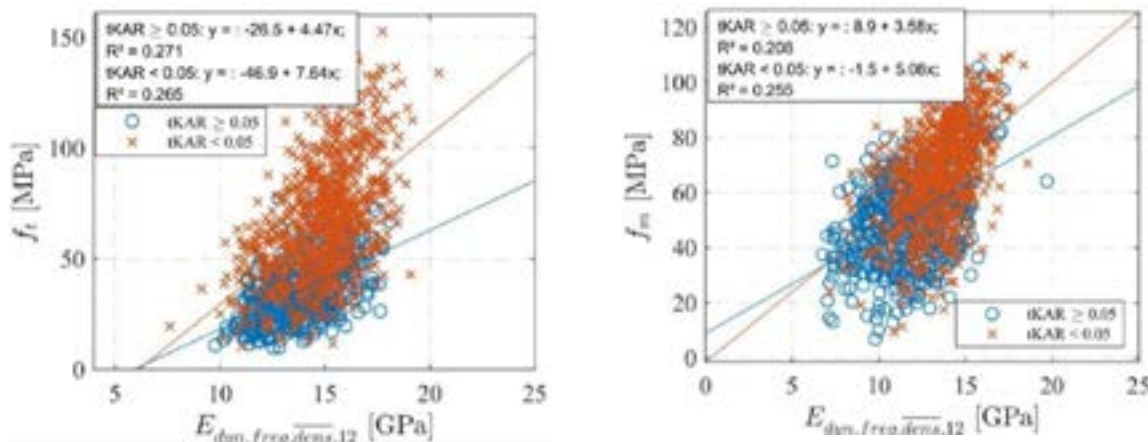
Additionally, the effect of the wood quality on the relationship between MOE_{dyn} and strength can be observed in Figure 6. The wood quality was defined as knot free specimens and specimens with $tKAR > 0.05$. For the tensile and bending strength prediction, the greater slope of the regression line is visible on the knot free specimens. In the case of tensile strength, the difference is much more pronounced. Although the R^2 value does not differ significantly between knot free ($tKAR < 0.05$) and specimens with knots, the variation of residuals in case of knot free specimens is greater. For bending strength the prediction accuracy is slightly higher.

(a)

Figure 6: Relationship between (a) MOE_{dyn} measured using LSW and tensile strength and (b) MOE_{dyn} measured using LSW and bending strength, for a combination of hardwood species, grouped in knot free specimens ($tKAR < 0.05$) and specimens with knots ($tKAR > 0.05$)

6. CONCLUSIONS

In this paper, the differences between the prediction accuracy of the dynamic MOE measured by using US and LSW methods were studied. The MOE_{dyn} measured by using LSW allows higher prediction accuracy for the strength and stiffness. Nevertheless, the accuracy of the ultrasound (US) MOE is high as well, especially for the MOE measurements. The results also support the findings of Ravenhorst (2015) for the species independent strength grading for both bending strength and tensile strength. The same regression equation can be used to predict both tensile MOE and bending MOE with MOE_{dyn} . Furthermore, the effect of quality on the grading accuracy could be observed. Whereas for tensile specimens the prediction accuracy did not differ much, the slope of the regression line and the scatter differ significantly. The prediction accuracy of strength grading with LWS and US is dependent on the cross-section. For smaller cross-sections, the use of average density in MOE_{dyn} calculation is likely to reduce the variation and increase the prediction accuracy. Further research on these specimens is required.



REFERENCES

- Bacher M (2008) Comparison of different machine strength grading principles. In: Proc. of Conference COST E53, 29–30 October, Delft, The Netherlands.
- Ehrhart T, Fink G, Steiger R, Frangi A (2016) Experimental investigation of tensile strength and stiffness indicators regarding European beech timber. In: Proc. of WCTE 2016, Vienna, Austria. August 23–25

- EN 408 (2010) *Timber structures - Structural timber and glued laminated timber - Determination of some physical and mechanical properties*. CEN European Committee for Standardization, Brussels
- Frühwald K, Hasenstab A (2010) *Zerstörungsfreie Prüfung von Laubholz in Holzbauprodukten und im eingebauten Zustand*. In: *Fachtagung Bauwerksdiagnose*, Berlin, 17.-18. Februar
- Frühwald K, Schickhofer G (2005) *Strength grading of hardwoods*. 14th International Symposium on Nondestructive testing of wood: 198–210
- Giudiceandrea F (2005) *Stress grading lumber by a combination of vibration stress waves and Xray scanning*. In: 11th International Conference on Scanning Technology and Process Optimization in the Wood Industry (ScanTech 2005), pp 99–108
- Glos P, Lederer B (2000) *Sortierung von Buchen- und Eichenschnittholz nach der Tragfähigkeit und Bestimmung der zugehörigen Festigkeits- und Steifigkeitskennwerte*. Bericht Nr. 98508, München
- Glos P, Torno S (2008a) *Allocation of ash and poplar of German origin to EN 1912*. TU München (TG1 / 0508 / 16).
- Glos P, Torno S (2008b) *Allocation of maple of German origin to EN 1912*. TU München (TG1 / 1108 / 26)
- Goerlacher R (1990) *Klassifizierung von Brettschichtholzlamellen durch Messung von Longitudinalschwingungen*, Dissertation, Universität Karlsruhe
- Green DW, McDonald KA (1993) *Mechanical properties of red maple structural lumber*. *Wood and Fibre Science* 25(4):365–374
- Hernández RE, Passarini L, Koubaa A (2014) *Effects of temperature and moisture content on selected wood mechanical properties involved in the chipping process*. *Wood Sci Technol* 48(6):1281–1301. doi: 10.1007/s00226-014-0673-9
- Kollmann FFP, Côté WA (1968) *Principles of Wood Science and Technology. I. Solid wood*. Springer-Verlag, Berlin
- Kovryga A, Schlotzhauer P, Stapel P, Militz H, van de Kuilen, Jan-Willem G. (2019) *Visual and machine strength grading of European ash and maple for glulam application*. *Holzforschung*. doi: 10.1515/hf-2018-0142
- Nocetti M, Brunetti M, Bacher M (2015) *Effect of moisture content on the flexural properties and dynamic modulus of elasticity of dimension chestnut timber*. *Eur. J. Wood Prod.* 73(1):51–60. doi: 10.1007/s00107-014-0861-1
- Nocetti M, Brunetti M, Bacher M (2016) *Efficiency of the machine grading of chestnut structural timber: prediction of strength classes by dry and wet measurements*. *Mater Struct* 49(11):4439–4450. doi: 10.1617/s11527-016-0799-3
- Ravenshorst GJP (2015) *Species independent strength grading of structural timber*. Technische Universiteit Delft, Delft
- Unterwieser H, Schickhofer G (2011) *Influence of moisture content of wood on sound velocity and dynamic MOE of natural frequency- and ultrasonic runtime measurement*. *Eur. J. Wood Prod.* 69(2):171–181. doi: 10.1007/s00107-010-0417-y
- Wang S-Y, Wang H-L (1999) *Effects of moisture content and specific gravity on static bending properties and hardness of six wood species*. *J Wood Sci* 45(2):127–133. doi: 10.1007/BF01192329
- Westermayr M, Stapel P, van de Kuilen JWG *Tensile strength and stiffness of low quality beech (Fagus sylvatica) sawn timber*. In: *Proc. of WCTE 2018, Seoul, South Korea*. August 20–23

Strength grading of hardwoods using transversal ultrasound

A. Kovryga^{1*}, A. Khaloian Sarnaghi¹, J-W. G. van de Kuilen^{1,2}

¹ Wood Research Munich
Technical University of Munich
80797 Munich, Germany

² Faculty of Civil Engineering and Geosciences
Technical University of Delft
Delft, Netherlands

ABSTRACT

*Detection of local wood inhomogeneities is important for accurate strength and stiffness prediction. In hardwood specimens, visual characteristics (e.g. knots or fibre deviation) are difficult to detect, either with a visual surface inspection or by the machine. Transversal ultrasound scan (TUS) is a non-destructive evaluation method with high potential for hardwoods. The method relies on differences in ultrasound wave propagation in perpendicular to the grain direction. The aim of this study is to estimate and analyse the capabilities of TUS for defect detection in hardwoods and prediction of mechanical property values. In the current paper, the TUS was applied to the hardwood species European ash (*Fraxinus excelsior*) and European maple (*Acer sp.*). In total, 16 boards of both specimens were completely scanned perpendicular to the grain using a laboratory scanner with dry-coupled transducers. The measurements were processed to 2D scan images of the boards, and image processing routines were applied to further feature extraction, defect detection and grading criteria calculation. In addition, as a reference for each board, all relevant visual characteristics and mechanical properties from the tensile test were measured. Using the TUS global fibre orientation, the size and the position of the knots can be detected. Knottiness correlates to the strength properties similarly or even better compared to the manual knottiness measurement. Between the global fibre orientation (measured using TUS and measured on the failure pattern) no correlation could be found. The ultrasound MOE perpendicular to the grain does not show any meaningful correlation to the elastic-properties parallel to the grain. In overall, TUS shows high potential for the strength grading of hardwoods.*

1. INTRODUCTION

Temperate European hardwoods, such as ash, beech and oak are known for excellent mechanical properties, which also make them attractive for structural applications. In order to utilize the advanced mechanical properties, the high variation of this naturally grown material needs to be reduced. For the strength of wood and, especially of hardwoods, visible local wood inhomogeneities are important. The same characteristics are more difficult to detect and measure with the available techniques compared to softwood (Olsson et al. 2018; Schlotzhauer et al. 2018).

The relationship between the grading criteria and the mechanical properties, as well as application of grading methods, differ between softwoods and hardwoods. The most accurate strength prediction method, at least for softwoods, is achieved by the means of the machine strength grading. The grading machines can explain up to 62% of the strength variation (Bacher 2008). For hardwoods machine grading allows only limited prediction accuracy. Models based on dynamic MOE (MOE_{dyn}), most common criterion for the strength prediction, show R^2 values between 0.18 and 0.36 (Nocetti et al. 2016; Ravenshorst 2015). Higher prediction accuracy can be achieved only if dynamic MOE is combined with visually measured knottiness (Frühwald and Schickhofer 2005; Kovryga et al. 2019). Machine detection of the knottiness works currently less accurate for hardwoods compared to softwoods. Grading machines that use x-ray for the knot detection are limited due to the low contrast between the knots and clear wood (Giudiceandrea 2005). Other methods are currently not available for the strength grading purposes.

Fibre deviation is another important criterion for the grading of hardwoods if strength is regarded. For defect free specimens with high variation in strength values fibre angle has major impact on the strength. Visible fibre angle provides no reliable results for the strength prediction (Frühwald and Schickhofer 2005). The machine detection of the fibre deviation by means of different non-destructive techniques has been recently in the scope of the study. For softwoods the multi-sensory systems able to detect the fibre deviation by the means of tracheid effect are available

* Andriy Kovryga: Tel.: +49 89 2180 6473; E-mail: kovryga@hfm.tum.de

(Olsson et al. 2013). Application of other NDT techniques on hardwoods, such as thermal conductivity measurement (Daval et al. 2015). 2015) and automated visual analysis of the spindle patterns (Ehrhart et al. 2018) has been on the research agenda.

A possible technology for cost-efficient and precise strength grading of timber is transversal ultrasound scan (TUS). The common way to use ultrasound for strength grading is to determine velocity of the ultrasound wave in longitudinal to the grain direction and therefore MOE_{dyn} (Sandoz 1989). By applying ultrasound perpendicular to the grain direction defects in wood can be detected. TUS has been reported to detect the knots in softwoods and some Northern American hardwoods in pallet parts (Kabir et al. 2002; Kabir et al. 2003) and structural timber (Machado et al. 2004). Ultrasound provides also information on the growth ring alignment. Propagation of the ultrasound wave differs between the radial and tangential growth ring orientation e.g. (Bucur 2006). Yaitskova and van de Kuilen (2014) provides analytical model that links ultrasound wave propagation and growth ring orientation, so called radial-tangential profile (RT-profile) and also highlights the possible application of TUS for the strength grading.

The aim of the present study is to analyze the potential of TUS for the grading of European hardwoods ash and maple. Particularly, is the definition and application of the novel grading criteria of interest. The possibility to detect the major grading criteria - knots and the fibre deviation – and relate them to the mechanical properties are within the scope of the study.

2. MATERIALS

To study the potential of ultrasound scan in overall 16 lamellas of European softwoods and hardwoods were used. Table 1 gives an overview of the selected specimens of the species European ash (*Fraxinus excelsior*), maple (*Acer spp.*). The selected specimens are part of a larger sampling presented in Kovryga et al. (2019) for hardwoods. The material can be considered representative for the selected species grown in central Europe. The boards were selected in a way that different wood features such as presence of the pith, knots, fibre deviations, as well as defect free specimens were present in a sample. The growth ring orientation affects the propagation time of the ultrasound wave.

Table 1: Number, dimensions and mechanical properties of scanned European ash (*Fraxinus excelsior*) and maple (*Acer spp.*) boards

Wood species	Number (n)	Cross-sections <i>b</i> x <i>h</i> [mm x mm]	Scan length [mm]	tKAR [-]		ρ [kg/m ³]		E_0 [GPa]		f_t [MPa]	
				μ	s	μ	s	μ	s	μ	s
Ash	3	30 x 125	1125	0.090	0.081	692	43	16.9	1.5	71.0	17.8
	4	35 x 125	1125								
Maple	2	25 x 125	1125	0.208	0.117	664	23	14.1	1.8	39.1	15.8
	3	30 x 125	1125								
	4	35 x 125	1125								
	63*	35 x 100	900								
Total	80										

3. METHODS

3.1. TRANSVERSAL ULTRASOUND SCAN (TUS)

The hardwood specimens were scanned using laboratory scanner developed at the TU Munich (Figure 1). The measuring unit (ultrasound transducers) are moved along the specimen in x and y-direction within the scan area. Measuring unit used to measure and generate ultrasound signal included Pundit Lab+ with two dry-contact piezoceramic transducers, with a central frequency of 54 kHz from PRECEQ.

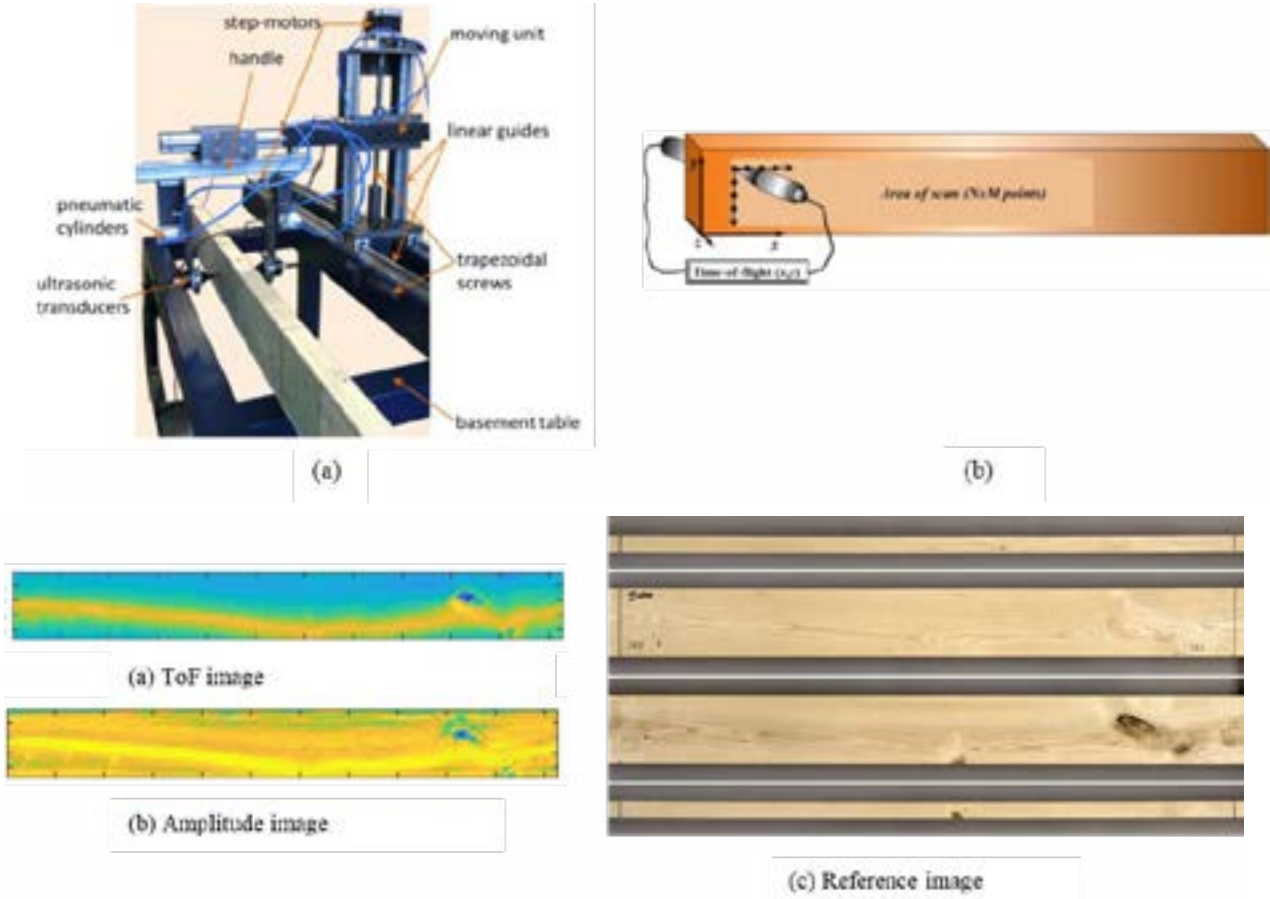
For each specimen, the area of 9 times the width was scanned by the device resulting in total of 82800 measuring points. For each measuring points different parameters of us signal – ToF, amplitude, energy, and spectral density – were calculated. For each parameter, a 2D image was generated and used to distinguish between the wood features and clear wood using image processing algorithms and optimization routines (Figure 2). For the current analysis only ToF is used. The ToF was calculated using threshold value of the signal amplitude. When the signal exceeds the threshold, the time is measured as ToF. Based on cluster-analysis we came to the conclusion that for 54 kHz transducer

*scanned with a coarse grid to evaluate relationship between $E_{us,90}$ to E_0

only time-of-flight provides sufficient results for the defect detection. Other parameters (such as amplitude in Figure 2b) did not provide any additional information on the defects.

Figure 1: Mechanical structure of TUS (a) and the measuring geometry (b) (Yaitskova et al. 2015)

Figure 2: Scan images for the European ash (*Fraxinus excelsior*) specimen Nr. 263 (a) time-of-flight (ToF) and (b) amplitude in



comparison to the images of the scan area acquired on all four surfaces (c)

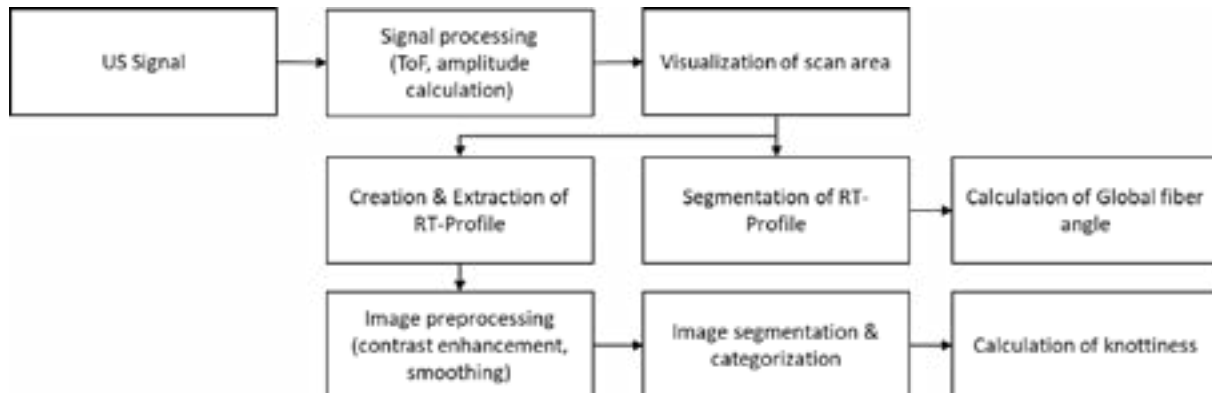


Figure 3: Algorithm for the processing of the ultrasound images

3.2. PROCESSING OF ULTRASOUND IMAGES

3.2.1 IMAGE PROCESSING

In current study the feature detection includes two major targets: the detection of the global fibre deviation (minimum of RT-profile) and the detection of defects such as knots. Figure 3 visualizes major steps in processing of ultrasound signal starting with the measurement of ultrasound signal, over signal processing to the visualization and image processing steps required to segment the selected wood features (knots and alignment of fibres) out of the image. Each board is processed separately. For the implementation the MATLAB Image Processing Toolbox ver. 2016a with image were used. The major steps are highlighted in following:

1. RT-profile extraction. In original time of flight (ToF) image beside the wood features the macroscopic growth ring orientation can be observed. The speed of ultrasound wave differs dependent on the propagation direction and is greater in radial than in tangential direction. These differences between radial and tangential orientation, named RT-profile, is shown in Figure 2a as gradient. This alignment coincides with the position of the knots and needs to be filtered. Yaitskova and van de Kuilen (2014) suggested analytical approach to extract the profile. However, this approach requires fitting the polynomial to each tested specimen. In the current study the RT-profile was restored by applying the median filter with the 3x10 mask to the ToF image and extracting it (Eq. 1). Applying filter over the length allowed to exclude local wood features, such as knots. Similar approach was chosen by Machado et al. (2004) to normalize the wave parameters and reduce the influence of structural features from timber pieces.

$$D(x, y) = M_{tof}(x, y) - F(x, y) \quad (1)$$

where D is a filtered image, M_{tof} is original image and F is medium filter applied to it.

2. Image preprocessing. Extraction of the profile increased the noise level in the image. To improve the segmentation performance blurring using “wiener filter” was applied to the images after RT-profile extraction. Wiener filter provides good solution for noisy images by adaptively tailoring itself to the local image variance. Where the variance is large only little smoothing is done; where the variance is little more smoothing is performed. The mask of 3x10 pixels was chosen for the filtering. This means that the filter was applied in 10 pixels over the length of the board and 3 pixels in the height.

3. Segmentation. Segmentation is the process of objects extraction out of the image. Various algorithms, such as threshold techniques, texture-based algorithms, wavelet-based techniques, are available. Algorithms are suitable to some specific use cases. Threshold technique are the most common and frequently used techniques for low noise levels. For the current study, the segmentation was done using global threshold value. Binary map is created by the global thresholding technique. By exceeding certain threshold value pixels are either assigned to defects or clear wood. Map is created as follows:

$$B_{tof}(x, y) = \begin{cases} 1 & \text{if } D(x, y) \geq T, \text{ defect} \\ 0 & \text{if } D(x, y) < T, \text{ clear wood} \end{cases} \quad (2)$$

Threshold (T) is a threshold value calculated for each single board as follows:

$$T = \mu \pm s \quad (3)$$

Where μ is the mean value and s standard deviation of values in filtered image D.

4. Classification. Classification is an important step to assign the object to the specific defect type based on the features of the segmented region. The boards included mostly knots and drying cracks in knots. No cracks were observed within the boards. Due to the low number of defect classes (clear wood vs knots) and only limited number of boards no specific classification routine has been applied. Applying classification routines such as kNN-classifier (k- nearest neighbor) or Neuronal networks might improve the classification result, would, however, require larger data set.

3.2.2 DETECTION OF RT-PROFILE

Each measurement of the ultrasound wave between the sender and receiver integrates both macroscopic profile and the effect of wood features. Such overlapping may lead to unreliable defect detection and classification, as well difficulties in profile detection.

Different solutions were tested for the RT-profile detection. One possibility to detect the RT-profile is to calculate the minima of the ToF at each single crosscut over the length of the test sample. In this case, for some crosscuts instead of the minimum of the RT-profile, the wood inhomogeneities were detected. Also image processing techniques, and particularly edge detection algorithm, were tested for the fibre alignment detection. Edge detection uses discontinuities in brightness to detect the boundaries of the object. Such contrast is observable at the minima of the RT-profile.

However, presence of the knots and in some cases low contrast did not allow for the continuous and consistent fibre alignment identification.

The best solution was to detect the RT-Profile by calculating the weighted minimum of ToF at a given point over the length of the board. The weight assured that abrupt changes in RT-profile do not occur. The minimum of RT-Profile in position x is calculated using following equation:

$$P_x = \min(W(x, y) \cdot M_{tof,x}) \quad (4)$$

The weights W at the length coordinate x are calculated using Eq. 5.

$$W(x, y) = \left(1 + \frac{|P_{(x,y)} - P_{x-1}|}{z} \right) \quad (5)$$

where P_{x-1} position of the minimum of the RT-profile in previous x position and z – distance between the RT-profile and board edge.

The calculation procedure is performed stepwise from the beginning of the board to the end. The selected approach ensures continuous path of RT-Profile within the board.

The grain angle is calculated as follows:

$$\alpha_{us} = \tan\left(\frac{\Delta y}{\delta}\right) \quad (6)$$

Where δ is window size used for the calculation of the fibre angle and Δy is the distance in y plane (width of the specimen between the beginning (P_x) and the end of the window ($P_x + \delta$)). Window size was set to 150mm.

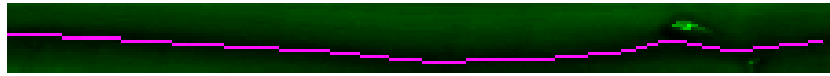


Figure 4: Minimum of the RT profile representing the fibre for the ash specimen 263

3.2.3 KNOTTINESS

Ultrasound knottiness was calculated based on the processed ToF images (B_{tof}) and is defined as an area of the knot related to the reference area. Knottiness value at the location x is calculated using Eq. 7.

$$KAR_{us}(x) = \frac{\int_0^w B_{tof}(x, y) dy}{w} \quad (7)$$

Where w is the width of the board.

The knottiness of the board is calculated as maximum of running average in a 150 mm window (δ) over the length of the board or within a tension range as a maximum of a running average.

$$KAR_{us} = \max \frac{1}{\delta} \int_{x=\bar{x}-\delta/2}^{x=\bar{x}+\delta/2} KAR_{us}(x) dx \quad (8)$$

3.2.4 MOE PERPENDICULAR TO THE GRAIN

Additionally, the Modulus of elasticity perpendicular to the grain has been calculated. With knowledge of density and ultrasound velocity the MOE perpendicular to grain ($E_{us,90}$) has been calculated:

$$E_{us,90} = v_{us} \cdot \rho \quad (9)$$

For the large maple sample ($N = 63$) the ultrasound velocity (v_{us}) was measured in 150 mm distance over the length of the board in four rows, with space 22.5 mm in between. In total 28 measurement points were measured for each board.

3.4 REFERENCE MEASUREMENTS

As the reference to the TUS, the visual quality of boards was assessed by measuring size and location of knots ($d > 5$ mm), cracks and fibre deviation. To quantify the knottiness, the $tKAR$ (*total Knottiness Area Ratio*) parameter was used. $tKAR$ is calculated as area of knots appearing in 150mm large window, projected on the cross sectional area. The overlapping areas are counted once. Additionally, the fibre deviation was determined after the destructive test on the failure pattern. Fibre deviation is defined as an angle with the longitudinal axis of the sawn piece and is measured in % (grain angle). Furthermore, each scanned board was tested destructively in tension parallel to the grain in acc. with EN 408 (2010), with tensile strength and stiffness determined after conditioning under the reference conditions 20 °C and 65 % rel. humidity.

4. RESULTS & DISCUSSION

Ultrasound transversal to the grain scan allows the detection of characteristics relevant for the strength of hardwoods. As already mentioned knots and global fibre orientation can be detected and extracted from the ultrasound scan images. The results and some pre-processing steps can be observed in Figure 4 for ash specimen. The knots can be visualized in ultrasound scan images. Furthermore, the global fibre-deviation can be observed and detected. The visibility of the fibre orientation is referred to the differences in the ultrasound wave propagation in radial and tangential direction. The knot detection works not smooth in every case.

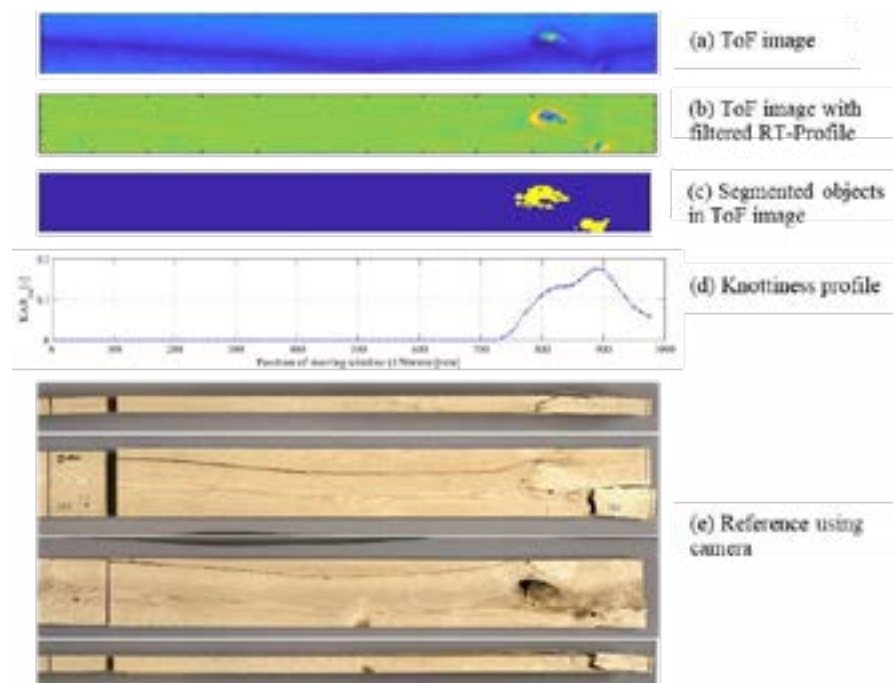


Figure 5: Ultrasound scan of ash specimen nr. 263 with (a) Original ToF image; (b) ToF image with extracted RT-Profile; (c) segmented objects in image; (d) Knottiness profile; (e) Reference image

Table 2: Correlations between ultrasound parameters, visual properties and mechanical properties for combined sample of European ash (*Fraxinus Excelsior*) and maple (*Acer spp.*) ($N = 16$)

	KAR_{us}	α_{us}	$tKAR$	α_{break}	ρ	E	f_i
KAR_{us}	1	0.353	0.791**	0.235	-0.177	-0.401	-0.781**
α_{us}		1	0.459	0.814**	-0.171	-0.462	-0.388
$tKAR$			1	0.516*	0.019	-0.469	-0.737**
α_{break}				1	-0.170	-0.484	-0.341
ρ					1	0.508*	0.178
E						1	0.619**
f_i							1

Note: * $p < 0.05$, ** $p < 0.01$

4.1. KNOTTINESS

The knottiness from ultrasound image shows high correlation to the visually measured knottiness ($r = 0.791$). The scatter shows positive relationship between KAR values from TUS measurement and $tKAR$ and the clear trend line can be registered (Figure 6). It also appears that for one specimen the knottiness has been detected, although no knots were visually observable within the specimen. By studying the test specimen carefully, we detected pith on the surface of the board with groove that has led to an increase in time of flight value due to the missing contact between the surface and transducer. Applying classification routine would allow to avoid such misclassification and/or classify such features separately. Selected approach would allow applying the classification on the detected object and not to the single measurement. This spatial information would allow to increase the accuracy.

The relationship between the knottiness parameters and tensile strength can be observed in Figure 7. For both TUS knottiness and manually measured knottiness $tKAR$ the tensile strength decreases with an increase in knottiness values. The prediction accuracy is in both cases high ($R^2 > 0.5$). TUS knottiness shows significantly higher R^2 values compared to the $tKAR$. The residuals scatter less around the regression line in case of the TUS knottiness compared to the visually determined knottiness. The results should be taken indicative only, as only limited number of specimens are scanned.

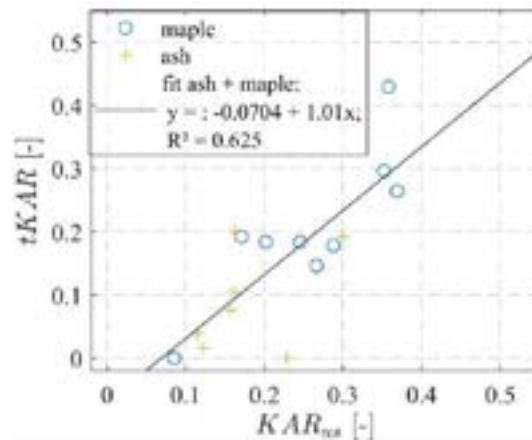


Figure 6: Scatter plot between knottiness parameter KAR_{us} estimated from the ultrasound scan and the manually measured knottiness $tKAR$

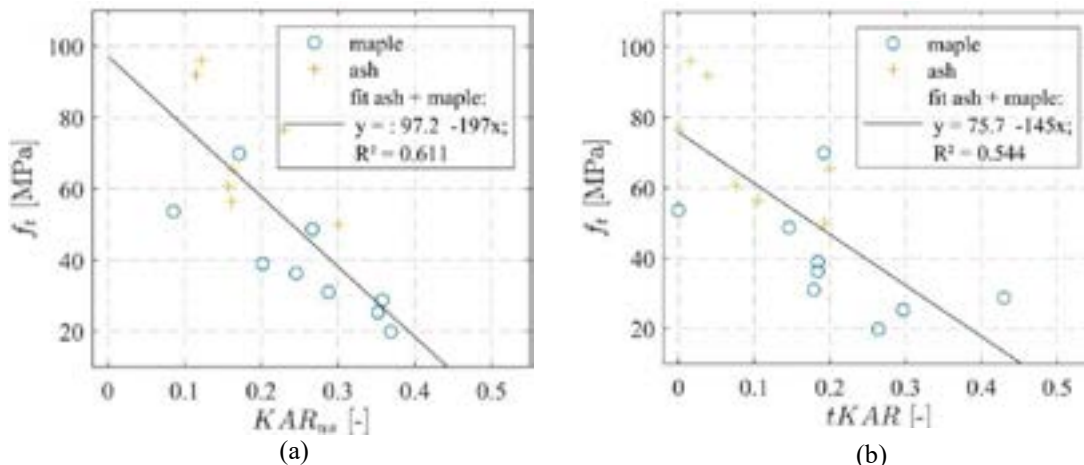


Figure 7: Relationship between (a) knottiness measured using ultrasound device and tensile strength and (b) manually measured knottiness ($tKAR$) and tensile strength for European ash and maple

4.2 GLOBAL FIBRE DEVIATION DETECTION

Fibre deviation is an important grading parameter for hardwoods. As shown previously the ultrasound is able to detect the minimum of the so-called RT-Profile that indicates the alignment of fibres in board. The ultrasound wave propagates in radial direction faster than in tangential direction. Figure 8 shows the relationship between fibre deviation measured using ultrasound and the fibre deviation detected manually by observing the failure pattern. The relationship is linear, between the two measurement methods. For most of the specimens, the fibre angle ranged between 3 to 10 %. For two boards greater fibre deviation was indicated using both methods. The small sample allows only indicative conclusions. The difference between the two measurements arises from the nature of the measurement. In case of ultrasound, the fibre angle measurement is an integral over the depth of the board.

Relationship between fibre angle and tensile strength is similar for both measurements. Clear decrease in tensile strength for decreasing fibre angle can be observed (Figure 9). However, there is no significant correlation between the fibre angle (measured using TUS device and measured manually on the failure pattern) and strength. For fibre deviations of 10% and lower the residuals scatter large around the regression line. In case of low fibre angle values, other criteria, such as knots or local fibre deviations limit the mechanical properties. Local aberrations of fibres aren't detected using ultrasound, as the detection is based on the RT-Profile. In case of local fibre deviation, other methods, such as thermal conductivity measurement, might be more attractive.

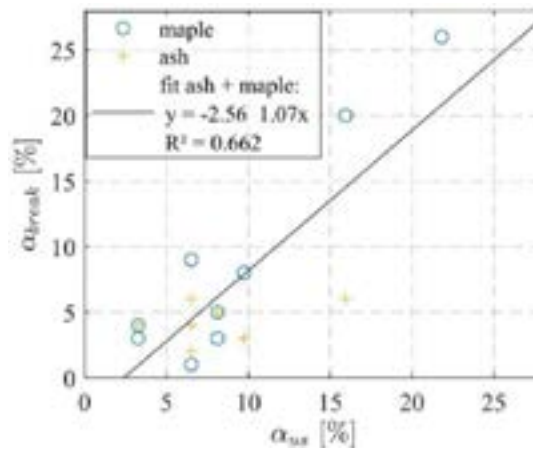


Figure 8: Relationship between grain angle determined from the ultrasound image and the grain angle after the failure

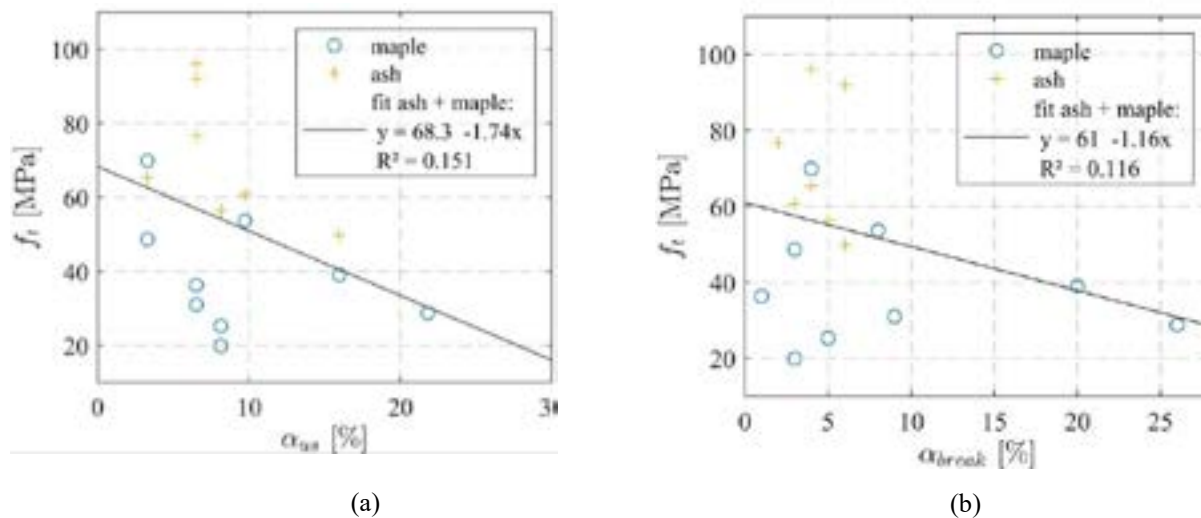


Figure 9: Relationship between (a) grain angle measured using ultrasound device and tensile strength and (b) manually measured grain angle after failure and tensile strength for European ash and maple

4.3 MODULUS OF ELASTICITY PERPENDICULAR TO THE GRAIN

The relationship between ultrasound MOE perpendicular to the grain and tensile MOE longitudinal to the grain has been observed on the small (ash and maple) and on the large dataset (maple only). For small sample, no relationship between MOE_{dyn} perpendicular to the grain and mechanical properties (strength, stiffness) could be found. For the larger data set, measured with coarse grid, the ultrasound parameters - ultrasonic MOE perpendicular to the grain ($E_{us,90}$) the velocity of ultrasound wave (v_{us}) - show low to medium correlation to the tensile strength (Table 3). Maximum value shows the best correlation to tensile strength. Density improves the correlation of ultrasound velocity only slightly. Between $E_{us,90,max}$ and E_0 (Figure 10) no correlation can be found. The negative correlation and especially higher correlation of max. value of ultrasound velocity/ ultrasound MOE perp. to the grain can be explained as the values rather represent the local defects. The max. value of ultrasound velocity coincides with the presence of the knots (if any are present in a board), as the velocity in sound knots is greater compared to the clear wood.

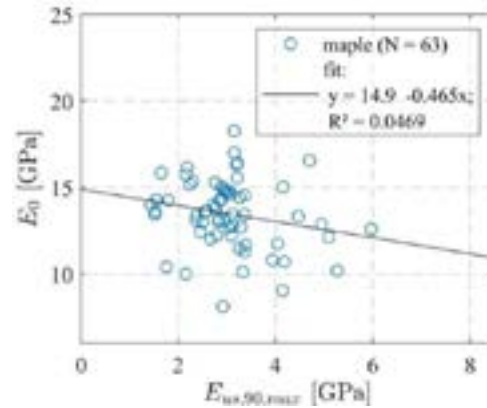


Figure 10: Relationship between the ultrasound MOE perpendicular to the grain and E_0 for maple (*Acer spp.*) specimens ($N = 63$)

Table 3: Correlations between parameters of ultrasound wave and mechanical properties for maple (*Acer spp.*) ($N = 63$)

	$E_{us,90,mean}$	$E_{us,90,min}$	$E_{us,90,max}$	$v_{us,mean}$	$v_{us,max}$	ρ	E_0	f_i
$E_{us,90,mean}$	1	0.780**	0.778**	0.977**	0.777**	0.451**	-0.087	-0.344**
$E_{us,90,min}$		1	0.510**	0.763**	0.500**	0.510**	-0.004	-0.207
$E_{us,90,max}$			1	0.735**	0.986**	0.350**	-0.217	-0.417**
$v_{us,mean}$				1	0.764**	0.289**	-0.038	-0.282*
$v_{us,max}$					1	0.255**	-0.189	-0.391**
ρ						1	-0.101	-0.268*
E_0							1	0.705**
f_i								1

Note: * $p < 0.05$, ** $p < 0.01$

5. SUMMARY

Current study examined the opportunities of the ultrasound for defect detection in hardwood species ash and maple. Ultrasound is able to detect the strength-reducing characteristics, fibre orientation, the knot position and its size. Especially knottiness parameter shows high compliance with the manually measured knottiness. Also high correlation between knottiness and strength values could be achieved. Fibre deviation is an important parameter especially for the knot-free hardwood specimens. For a sample with knot and knot-free specimens tested in current study, no correlation between global fibre orientation (visually determined and using ultrasound) and strength could be found as in Frühwald and Schickhofer (2005). MOE perpendicular to the grain shows no relationship to the tensile MOE properties parallel to the grain. Due to the small sample size here, further tests on a large number of specimens are required. Further investigations are necessary, not only regarding the different wood species but also regarding the technical aspects of meeting industrial requirements.

ACKNOWLEDGEMENTS

This research was supported by the German Federal Ministry of Food and Agriculture (BMEL), grant no.: 22011913.

REFERENCES

- Bacher M (2008) Comparison of different machine strength grading principles. In: Proc. of Conference COST E53
- Bucur V (2006) *Acoustics of Wood*, 2nd Edition. Springer Series in Wood Science. Springer-Verlag Berlin Heidelberg, Berlin, Heidelberg
- Daval V, Pot G, Belkacemi M, Meriaudeau F, Collet R (2015) Automatic measurement of wood fiber orientation and knot detection using an optical system based on heating conduction. *Opt Express* 23(26):33529–33539. doi: 10.1364/OE.23.033529
- Ehrhart T, Steiger R, Frangi A (2018) A non-contact method for the determination of fibre direction of European beech wood (*Fagus sylvatica* L.). *Eur. J. Wood Prod.* 76(3):925–935. doi: 10.1007/s00107-017-1279-3
- EN 408 (2010) *Timber structures - Structural timber and glued laminated timber - Determination of some physical and mechanical properties*. CEN European Committee for Standardization, Brussels
- Frühwald K, Schickhofer G (2005) Strength grading of hardwoods. 14th International Symposium on Nondestructive testing of wood:198–210
- Giudiceandrea F (2005) Stress grading lumber by a combination of vibration stress waves and Xray scanning. In: 11th International Conference on Scanning Technology and Process Optimization in the Wood Industry (ScanTech 2005), pp 99–108
- Kabir MF, Schmoldt DL, Araman PA, Schafer ME, Lee S-M (2003) Classifying defects in pallet stringers by ultrasonic scanning. *Wood and Fiber Science* 35(3):341–350
- Kabir MF, Schmoldt DL, Schafer ME (2002) Time domain ultrasonic signal characterization for defects in thin unsurfaced hardwood lumber. *Wood and Fiber Science* 34
- Kovryga A, Schlotzhauer P, Stapel P, Militz H, van de Kuilen J-WG (2019) Visual and machine strength grading of European ash and maple for glulam application. *Holzforschung* 0(0):329. doi: 10.1515/hf-2018-0142
- Machado J, Sardinha R, Cruz H (2004) Feasibility of automatic detection of knots in maritime pine timber by acousto-ultrasonic scanning. *Wood Sci Technol* 38(4). doi: 10.1007/s00226-004-0224-x
- Nocetti M, Brunetti M, Bacher M (2016) Efficiency of the machine grading of chestnut structural timber: prediction of strength classes by dry and wet measurements. *Mater Struct* 49(11):4439–4450. doi: 10.1617/s11527-016-0799-3
- Olsson A, Oscarsson J, Serrano E, Källsner B, Johansson M, Enquist B (2013) Prediction of timber bending strength and in-member cross-sectional stiffness variation on the basis of local wood fibre orientation. *Eur. J. Wood Prod.* 71(3):319–333. doi: 10.1007/s00107-013-0684-5
- Olsson A, Pot G, Viguier J, Faydi Y, Oscarsson J (2018) Performance of strength grading methods based on fibre orientation and axial resonance frequency applied to Norway spruce (*Picea abies* L.), Douglas fir (*Pseudotsuga menziesii* (Mirb.) Franco) and European oak (*Quercus petraea* (Matt.) Liebl./*Quercus robur* L.). *Annals of Forest Science* 75(4):33529. doi: 10.1007/s13595-018-0781-z
- Ravenshorst GJP (2015) *Species independent strength grading of structural timber*. PhD. Technische Universiteit Delft, Delft.
- Sandoz JL (1989) Grading of construction timber by ultrasound. *Wood Sci Technol* 23(1):95–108. doi: 10.1007/BF00350611
- Schlotzhauer P, Wilhelm F, Lux C, Bollmus S (2018) Comparison of three systems for automatic grain angle determination on European hardwood for construction use. *Eur. J. Wood Prod.* 40:118. doi: 10.1007/s00107-018-1286-z
- Yaitskova N, Nadkernychmy Y, Franjga R, Monroy R (2015) TUS: a breadboard for development of new wood grading algorithms using ultrasound
- Yaitskova N, van de Kuilen JW (2014) Time-of-flight modeling of transversal ultrasonic scan of wood. *J Acoust Soc Am* 135(6):3409–3415. doi: 10.1121/1.4873519

Glued structural products made of beech wood: quality of the raw material and gluing issues

Michele Brunetti¹, Michela Nocetti^{1,2}, Benedetto Pizzo¹, Giovanni Aminti¹, Corrado Cremonini³, Francesco Negro³, Roberto Zanuttini³, Manuela Romagnoli⁴, and Giuseppe Scarascia Mugnozza⁴

¹CNR-IBE
Sesto Fiorentino (FI),
50019, Italy

²Department of
Forest and Wood
Science
Stellenbosch
University
Stellenbosch, 7600,
South Africa

³Department of
Agricultural, Forest
and Food Sciences
University of
Torino
Grugliasco (TO),
10095, Italy

⁴Dipartimento per
l'Innovazione nei
Sistemi Biologici,
Agroalimentari e
Forestali
University of
Tuscia
Viterbo, 01100,
Italy

ABSTRACT

Hardwoods are becoming increasingly important in Europe for the use as structural material, both as solid wood and engineered structural products. The recent constitution of a new standardization working group at European level (CEN TC124 / WG3 / TG1) for the drafting of a harmonized standard regulating the production and characterization of glulam beams made of hardwoods proves this growing interest.

In Italy, the great abundance of beech forests has led to the demand of a research project to investigate the use of this species in construction. Specifically, the study, among other things, deals with the production of structural glued products made of beech. The research starts with the characterization of the raw material, developing the strength grading of the beech boards, both by visual and machine methods. At the same time, the study addresses the comparison of different gluing parameters, such as the pressing process and the adhesive used to achieve an adequate structural bonding between lamellas.

The paper reports the results concerning the mechanical characterization of beech sawn wood from different Italian Regions and the first outcomes encountered during the selection of the different structural gluing parameters for the production of CLT.

1. INTRODUCTION

Increasing the use of hardwoods in structural applications is a relevant topic in Europe (Aicher et al. 2014). Several factors contribute to promoting the use of hardwoods in construction: Europe is rich in large, underused hardwoods forests; various European countries are encouraging re-afforestation with hardwood species to face forest disturbances such as windstorms; for this reason use of hardwoods falls within the growing interest in timber as a sustainable material for bio-building. Overall, new perspectives for European hardwoods, namely ash, beech, sweet chestnut, and oak, can arise in the coming years in the construction sector.

In this context, beech wood is particularly interesting given the abundance of European beech forests that can regularly supply large-scale productions. The load-bearing attitude of beech wood has long been exploited by producing plywood for the transport sector or by using solid wood for heavy-load packaging. Conversely, the structural bonding of beech wood is known to be difficult. This is strictly related to its density and requires a fine-tuning of the bonding systems (Aicher and Ohnesorge 2011).

Nowadays, in Europe, glued laminate timber (GLT) and cross laminated timber (CLT) can only be made from coniferous or poplar wood according to the standards EN 10480 (EN 14080 2013) and EN 16351 (EN 16351 2015). Anyway, the growing interest in the structural use of hardwoods is confirmed by the recent constitution of a working group within the European Committee for Standardization (CEN-TC124/WG3/TG1). The group is currently working on the project “Timber structures - Glued laminated timber and glued solid timber made from hardwood species – Requirements”. The aim is to draft a standard setting out provisions regarding the production glue laminated timber (GLT) made from hardwood and characterizing its mechanical properties. Over the years, the potential of beech wood in construction fostered several scientific studies that investigated the mechanical performance of sawn wood (Glos et al. 2004; Frese and Blass 2005; Aicher and Ohnesorge 2011; Cibecchini et al. 2016; Ehrhart et al. 2016a, b) and the gluing of boards (Aicher and Reinhardt 2007; Ohnesorge et al. 2010; Schmidt et al. 2010; Luedtke et al. 2015). A recent study (Ehrhart et al. 2018) showed that beech GLT can reach strength classes up to GL 55 (characteristic bending strength of 55 MPa), with mean values of local bending Modulus of Elasticity (MoE) of 16,200 MPa. Considering that coniferous GLT is commonly used in Class GL 24, it can be seen how beech wood can broaden the applications of GLT and CLT in construction. Presumably, beech GLT and cross laminated timber (CLT) could compete with steel and concrete in heavy-load bearing uses. The increased mechanical performance could also be exploited for reducing the cross sections, allowing new architectural prospects and limiting the amounts of material used.

On the other hand, the high variability of the raw material requires an in-depth study of the characteristics that influence its mechanical performance and a careful analysis of the different strength grading methods in order to select the starting material at best (Ehrhart et al. 2016a; Westermayr et al. 2018a). Currently the attention of glulam manufacturers is mainly addressed to materials of high structural quality, but this involves a high waste of the raw material (Torno et al. 2013). Only few studies investigated the low quality beech timber (Westermayr et al. 2018b), which on the other hand can be present on the market and can be better used if selected effectively.

To make the use of structural wooden products safe, but at the same time efficient, these basic steps must be followed: (1) characterization of the raw material with the development of strength grading systems; (2) for the glued products, whether they are glulam beams or structural panels, the evaluation of the bonding quality.

Regarding the second point, most of the studies found in the literature concern the evaluation of the bonding for glulam production (Ohnesorge et al. 2010; Schmidt et al. 2010; Konnerth et al. 2016); here a first attempt is made comparing different gluing parameters to manufacture CLT made of beech wood.

Therefore, the present study focuses on the characterization of the beech raw material that can be found in Italy and the development of visual and machine strength grading methods; preliminary results about the gluing process for CLT production are also briefly presented. The aim is laying the basis for the production of structural engineered products made from Italian beech wood, which can have positive effects on the national wood sector.

2. MATERIALS AND METHODS

2.1 QUALITY OF THE RAW MATERIAL: STRENGTH GRADING

2.1.1 SAMPLING

The collection of the raw material was defined in order to sample the distribution of beech in the Italian territory. Overall, 465 boards were sampled, divided into four origins as described in Table 1. The variability of the sample was obtained by collecting the timber from different geographical areas, covering the whole latitude of the country. Sub-samples were collected in the regions with high national percentages of beech forest area: 2 sub-samples (NE and NW) were collected in Northern Italy, Chiusaforte (Sella Nevea, Friuli Venezia Giulia) and Chianocco (Val di Susa, Piemonte); 1 sub-sample in the centre (C), Val Cervara (Monti Simbruini, Lazio) and 1 in the South (S), Serra San Bruno (Vibo Valentia, Calabria).

The specimens were mostly boards, with squared cross sections and thicknesses ranging from 20 to 60 mm and widths from 100 to 150 mm, since the intended final use was the manufacturing of glued structural products.

Table 1 - Number of pieces sampled by cross-section size (thickness x width) and Italian geographical origin.

Cross section (mm)	Length (mm)	Provenance				TOT
		South (S)	North-East (NE)	North-West (NW)	Central (C)	

20x100	3100	53		29		82
25x100	4200		30			30
30x100	3200				44	44
20x120	3100	66				66
40x120	3700			39		39
45x120	4200		44			44
50x120	3800				34	34
50x150	3700			38		38
55x150	4200		45			45
60x150	3800				43	43
TOT		119	119	106	121	465

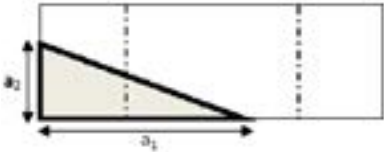
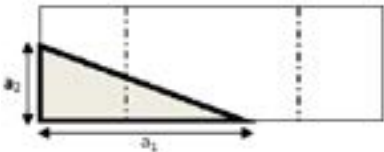
2.1.2 VISUAL AND MACHINE MEASUREMENTS AND LABORATORY TESTS

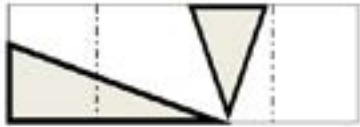
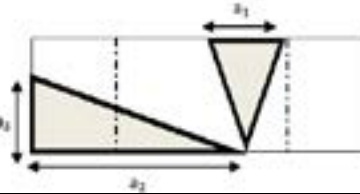
As a first step, each board was examined by its visual characteristic: the main features visually detectable were measured and noted. Then the boards passed through a grading machine for the machine property measurement and afterward they were destructively tested to determine their physical and mechanical properties.

Concerning the visual inspection, it focused on what can be considered a strength-reducing characteristic: knots, slope of grain, ring width and presence of pith included in the cross section.

The knots were mapped in order to calculate several parameters: the position of each knot, as well as the minimum diameter and its projection on the side of the board were registered, and the calculations listed in Table 2 were made. For each board, the highest value of each knot parameter was selected for the further statistical analysis.

Table 2 – Description of the knot parameters.

Symbol	Description	Scheme*	Equation ⁽¹⁾
Single Knot			
KAR	Knot Area Ratio: ratio of the projected cross-sectional area of the knot to the cross sectional area of the piece.		$KAR = \frac{A}{wt} \quad (1)$
Dm/S	Ratio of the minimum diameter of the knot to the dimension of the side.		$Dm/S = \max \left\{ \frac{d}{t}; \frac{d}{w} \right\} \quad (2)$
Pr/S	Ratio of the knot projection on the side to the dimension of the side itself.		$Pr/S = \max \left\{ \frac{a_2}{t}; \frac{a_1}{w} \right\} \quad (3)$
sPr/2W	Ratio of the sum of the projections of the knot on the sides to the double width.		$sPr/2w = \frac{\sum a_i}{2w} \quad (4)$
Grouped knots			

tKAR	Ratio of the sum of total projected cross-sectional areas of all knots in a length of 150 mm to the cross sectional area of the piece.		$tKAR = \frac{\square}{wt} \quad (5)$
tPr/2W	Ratio of the sum of the projections of all knots in a length of 150 mm to the double width.		$tPr/2w = \frac{\sum a_i}{2w} \quad (6)$

⁽¹⁾ w = width; t = thickness

* schemes of knots by Microtec WebKnot Calculator <http://knots.microtec.eu/>

The slope of grain was measured as the general inclination of the wood fibres to the longitudinal axis of the timber piece. The measurement was made on a length of one metre following the fissures if present or by means of a swivel handle scribe, and expressed as a percentage (EN 1310 1997). The same measure was also executed after the destructive tests, taking advantage of the failure fissures to detect the grain direction. Local fibre deviations, for example close to knots, were ignored.

The presence of the pith included in the cross section was also registered and the average ring width was measured on the transversal section of the piece along the longest straight line normal to the growth rings (EN 1310 1997).

As for the machine measurement, the natural frequency of vibration in the longitudinal direction was measured by means of an industrial device (ViSCAN) for each specimen. The piece was placed on supports and percussion provided the excitation necessary to cause vibration; the natural frequency of vibration was measured by a non-contact laser interferometer.

The weight and dimensions of each piece were also measured and the dynamic modulus of elasticity was calculated by the following formula (Eq. 7):

$$E_{dyn} = IP_{MOE} = 4f^2 L^2 \rho \quad (7)$$

where f is the natural frequency of vibration, L the length of the timber piece and ρ is the density, calculated by the timber weight divided by its volume.

As a next step, four point edgewise bending tests were carried out in accordance with the European standard EN 408 (EN 408 2012), in order to measure the global and local static modulus of elasticity. The total span was 18 times the nominal depth and the shear span was 6 times the nominal depth. The local deformation was measured in the neutral axis on both sides of the timber piece and the mean of the two measures was used to calculate the local modulus (Eq. 8). In the same test setup, the total deformation was measured in the central point on the tension edge of the beam and used to calculate the global modulus of elasticity (Eq. 9). Then the load was applied until failure and the bending strength (f_m) was computed (Eq. 10).

$$E_{lo} = \frac{3al_1^2 \Delta F}{4bh^3 \Delta w_{local}} \quad (8)$$

$$E_{gl} = \frac{l^3 \Delta F}{bh^3 \Delta w_{global}} \left[\left(\frac{3a}{4l} \right) - \left(\frac{a}{l} \right)^3 \right] \quad (9)$$

$$f_m = \frac{3aF_{max}}{bh^2} \quad (10)$$

With ΔF : the applied load increment, F_{max} : the load at failure, l : the length between the two supports, b : the thickness of timber piece, h : the width, a : the distance between the load point and the nearest support, l_f : the central gauge length, Δw_{local} and Δw_{global} : the deformation increments.

After testing, density and moisture content were determined in accordance with ISO 13061-1 (ISO 13061-2 2014) and EN 13183-1 (EN 13183-1 2002) (oven dry method) respectively, cutting a small specimen of full cross section from each timber piece. Density and modulus of elasticity values were corrected to a moisture content of $u = 12\%$ according to the adjustment equations suggested in EN 384 (EN 384 2016).

Measured values of bending strength were adjusted to a reference depth (h) of 150 mm using the $k_h = (150/h)^{0.2}$ factor calculated in accordance with EN 384 (2016).

2.1.3 DATA ANALYSIS

Descriptive statistics were calculated for all the properties measured visually, by the machine and during the laboratory tests. Correlations between properties were determined by means of Pearson correlation coefficient and linear regression analysis.

Finally, machine and visual grading were performed according the European standardization and the yields were compared.

Derivation of machine settings

According to the machine grading system described in the EN 14081-2 (EN 14081-2 2018), before it can grade, a machine must be “calibrated” to the specific timber species and provenance. This means that the proper settings have to be derived through appropriate statistical procedures. The methods used in the present work were those specified in the EN 14081-2 (2018) and summarized below.

The basic approach is to set thresholds for the property measured by the machine (called Indicating Property, IP) so to group the sampled pieces into strength classes. Subsequently, a series of verifications are applied to validate such thresholds. Firstly, the required characteristic values of the grade determining properties (GDP, read bending strength, modulus of elasticity and density determined in laboratory by destructive tests) for the strength class assigned to the timber pieces shall be met both for the entire sample and for each provenance (sub-sample). Then, a cost analysis performed as already described in a previous paper (Nocetti et al. 2016). Briefly, the cost analysis compares the assignment to a class made by the machine based on the IP with the optimum grading, that is the assignment based on timber mechanical properties determined by laboratory tests. Specific weighting factors are applied for wrongly graded pieces; particularly adverse factors are given for incorrectly upgraded pieces.

The IP used here was the dynamic modulus of elasticity; the k_v factor provided by the EN 384 (2016) for machine grading was not applied (Stapel and Van De Kuilen 2013; Nocetti et al. 2016).

The required characteristic values of the strength classes are reported in the EN 338 (EN 338 2016), while the methods to calculate the characteristic values are described in the EN 14358 (EN 14358 2016) and EN 384 (2016). For the calculations, the local modulus of elasticity was used, since it does not need any adjustment for shear stresses as global does (Nocetti et al. 2013).

When all the verifications were met, the thresholds constituted the settings used by the machine for grading.

Visual grading rule and strength class assignments

The visual grading approach is based on the set up of specific limitation to the visual characteristics, in order to group the timber pieces into quality groups (grades). Afterwards, the characteristics values of the GDPs are calculated for each grade to assign it to a strength class as defined in the EN 338 (2016).

Here, the limitation to the visual properties was set in order to get two grades and the rejects (pieces not suitable to structural use). For the assignment to the strength classes, the provision of the EN 384 (2016) was applied: for each grade, the characteristics values of the GDPs were calculated according to the EN 14358 (2016) separately by provenance (sub-sample) and only for the sub-samples with at least 40 pieces. Then they were weighted averaged

and the adjustment (k_n) for the number of the sub-samples was applied. According to the k_n factor, the less is the number of the sub-samples and the highest is the reduction of the characteristic values.

The assignment of a grade to a strength class was achieved when the characteristic values of that grade calculated as above met the requirement of the class.

2.2 GLUING PROCESS FOR CLT PRODUCTION

2.2.1. CLT MANUFACTURE

3-layered CLT experimental panels were assembled with nominal dimensions of 450x450x60 mm³ (the thickness of the layers was 20 mm). The boards were kiln-dried until the achievement of the equilibrium moisture content of about 12%.

Three different adhesive systems, commonly available on the market, were used for producing the experimental CLT panels: polyurethane (PUR), polyurethane plus primer (PUR+P), and melamine-urea-formaldehyde (MUF).

The PUR spread rate was 150 g/m² and, when used, the primer amounted to 20 g/m²; MUF spread was of about 300 g/m². The open assembly time was ≤5 minutes and the closed assembly time ranged from 20 to 25 minutes.

Two pressing types were used: by hydraulic press, the pressure of 1.2 MPa was applied at 15°C and held for at least 2 h for PUR and 24 h for MUF; by membrane-vacuum press, the pressure of 0.09 MPa was applied at 12 °C for at least 2 h for PUR and 4.5 h for MUF. After manufacturing, CLT panels were stored for 30 days at 20 °C and 65% of relative humidity.

2.2.2 DELAMINATION TEST

The delamination test was performed according to Annex C of EN 16351 (2015). The cross section of tested specimens was of 100x100 mm². Grain formed an angle of 90° with the sides of the specimens. These were immersed in water at 20°C applying for 30 min a vacuum between 15 and 30 kPa. Following, a pressure of 600-700 kPa was applied for 2 h. The specimens were then dried at 75°C for 10-15 h until their mass reached the 100-110% of the initial value. After the above pre-treatment, the length of delaminations was measured. The total delamination D_{tot} and the maximum delamination D_{max} were calculated as:

$$D_{tot} = 100 \times \frac{l_{tot,delam}}{l_{tot,glueline}} \quad (11)$$

$$D_{max} = 100 \times \frac{l_{max,delam}}{l_{glueline}} \quad (12)$$

where $l_{tot,delam}$ is the total delamination length in the specimen, in mm; $l_{tot,glueline}$ is the sum of the perimeters of all glue lines in the specimen, in mm; $l_{max,delam}$ is the maximum delamination length, in mm; $l_{glueline}$ is the perimeter, in mm, of the glue line in which the maximum delamination occurred. Openings between adjacent layers were considered as delamination only when presenting the criteria described in Annex C of EN 16351.

After testing, the specimens were split by hammer and chisel and the percentage of wood failure (WFP) was visually assessed by an experienced operator and rounded to the nearest 5%.

3. RESULTS AND DISCUSSIONS

3.1 QUALITY OF THE RAW MATERIAL

The average values and the variability of the mechanical and physical properties as a result of the destructive tests are reported in Table 2. The dynamic modulus of elasticity measured by the grading machine is also shown for each sub-sample and for the whole dataset. The visual characteristics are summarized in Table 3.

Considering the two tables together provides a complete description of the raw material. As a first observation the sub-sample NE had by far the worst quality: the boards had the lowest mechanical properties (both strength and stiffness) and the knots were more and bigger. Also the variability of the mechanical properties is higher than in the

other sub-samples. Very high variability was earlier observed in low quality material tested in Germany (Westermayr et al. 2018b).

On the other hand, the three other provenances had a very similar average bending strength, comparable to what was previously observed for Italian beech (Cibecchini et al. 2016), but differentiated by stiffness and knottiness. The sub-sample S had the highest modulus of elasticity (both static and dynamic), but higher values of the knot parameters if compared to NE and mainly NW, the last with the smallest values of knot parameters among the four provenances. This does not mean that the knots of S boards were larger, but that their size, compared to the size of the boards, was higher. It should be remembered, in fact, that all the pieces in the sub-sample S had the minimum tested thickness of 20 mm.

Besides, looking at the number of knots (Kn in Table 3) and the percentage of pieces with the pith included in the cross section, sub-sample S and NW showed the lowest average values. This indicates that the boards were probably cut from the outer part of the logs (due for instance to larger stems) or that in the sawing pattern the pith was often discarded. On the contrary, in the sub-samples NE and C more than the 20% of the pieces had the pith included, denoting that also the inner part of the logs was kept during sawing.

As for density, S had the heaviest timber (and the widest rings), while the other provenances did not differ from each other. Anyhow, the variability of density was extremely low, with a coefficient of variation less than 6%. The same was already noticed and reported for beech (Glos et al. 2004).

As a whole, the analyzed sample has a high variability, useful for verifying the effectiveness of different grading methods.

Table 3 – Average values of the mechanical and physical properties measured during destructive bending tests and of the machine measurement. Coefficient of variation between brackets.

Property	Symbol	Unit	Provenance				all
			S	NE	NW	C	
Bending strength	$f_{m,mean}$	(MPa)	74.3 (29.7)	58.5 (39.1)	74.2 (31.3)	74.6 (31.3)	69.4 (34.6)
Global MoE	$E_{g,0,mean}$	(GPa)	14.6 (13.9)	10.8 (17.3)	13.4 (15.8)	12.6 (14.2)	12.8 (18.7)
Local MoE	$E_{l,0,mean}$	(GPa)	15.2 (17.6)	10.9 (21.9)	13.9 (19.3)	13.3 (17.0)	13.3 (22.2)
Dynamic MoE	$E_{dyn,mean}$	(GPa)	15.2 (11.3)	12.6 (15.3)	13.8 (12.1)	14.0 (12.7)	13.9 (14.5)
Density	ρ_{mean}	(kg/m ³)	752 (6.0)	701 (4.7)	714 (4.5)	700 (4.4)	716 (5.8)

Table 4 – Average values of the visual properties. Symbols of the knots explained in Table 2.

Property	Symbol	Unit	Provenance				all
			S	NE	NW	C	
Knottiness (n. of knots)	Kn	(-)	1.63	2.23	1.58	1.85	1.83
Single knot	KAR	(-)	0.17	0.19	0.08	0.11	0.14
	Dm/S	(-)	0.32	0.45	0.22	0.22	0.30
	Pr/S	(-)	0.36	0.48	0.25	0.26	0.34
	sPr/2W	(-)	0.20	0.23	0.12	0.14	0.17
Knot cluster	tKAR	(-)	0.18	0.21	0.09	0.12	0.15
	tPr/2W	(-)	0.21	0.26	0.13	0.16	0.19
Slope of grain (visual)	SGv	(%)	2.6	1.7	2.1	2.3	2.2
Slope of grain (after test)	SGa	(%)	5.4	2.8	4.5	2.8	4.0
Ring width	W	(mm)	3.5	2.8	3.0	2.2	2.87
Pith (boards with pith)	P	(%)	6.7	24.4	8.5	23.1	15.9

3.2 CORRELATIONS BETWEEN PROPERTIES

The relationships between the several properties were investigated by linear regression analysis and the results are presented in Table 5.

In general, for the whole sample, correlations between strength and stiffness's (both static and dynamic modulus of elasticity, fig. 1) have shown trends and values similar to those found in similar works for softwoods and higher to what was observed in the past for other hardwoods (Nocetti et al. 2010; Vega et al. 2012; Nocetti et al. 2016). For beech, Ehrhart et al. (2016a) found a lower correlation between tensile strength and dynamic modulus of elasticity ($R^2 = 0.22$), while Westermayr et al. (2018) for the same properties reported a correlation similar to our findings ($R^2 = 0.5$)

Density was not correlated neither with bending strength nor with the modulus of elasticity, as reported in several previous works on beech (Cibecchini et al. 2016; Ehrhart et al. 2016a; Westermayr et al. 2018b); neither the ring width showed any significant correlation with density. This is not unusual for hardwoods, so that the sorting of structural quality material is difficult to base on density (Nocetti et al. 2010, 2016).

The relationships of the knot parameters with the mechanical properties were again as good as what observed for softwood, and much better than the results previously achieved for hardwoods (Nocetti et al. 2010). Among the several knot parameters calculated, the higher values of the coefficient of determination were detected for sPr/2W and tPr/2W (Fig. 2), even if also the values for the other parameters were not very far. Earlier studies reported a correlation value $r = -0.67$ between KAR and tensile strength (Glos et al. 2004) or coefficient of determination $R^2 = 0.53$ again between KAR and tensile strength and $R^2 = 0.52$ between DEB (the same parameter here called sPr/2W) and strength (Ehrhart et al. 2016a). On the contrary, Westermayr et al. (2018) for low quality beech reported lower correlations between knots and tensile strength ($R^2 = 0.15$ for KAR and $R^2 = 0.18$ for DEB)

Concerning the remaining visual features measured, the slope of grain was not related to any of the mechanical properties, neither the grain deviation measured before testing, nor the one determined after failure. The explanation could be found in the well-known difficulties in detecting and therefore measuring the real grain deviation (Cibecchini et al. 2016; Westermayr et al. 2018b), but also keeping in mind that here the general direction of the grain is considered, and not the local deviation due to the presence of knots or other defects.

Finally, the presence of the pith included in the timber piece was a significant factor affecting both bending strength and the modulus of elasticity, but not density (Westermayr et al. 2018b). Pieces with the pith included had a mean strength of 61.1 MPa and a local modulus of elasticity of 12.2 GPa against the values of 70.9 MPa and 13.5 GPa for the same properties for the boards with the pith not included.

Table 5 – Coefficient of determination (R^2) of the relationship between bending strength (f_m) and local modulus of elasticity (E_l) and the other mechanical, physical and visual properties. Symbols are explained in Tables 2 and 3.

		$E_{l,0}$	$E_{g,0}$	E_{dyn}	ρ	KAR	Dm/S	Pr/S	sPr/2W	tKAR	tPr/2W
f_m	S	0.33	0.34	0.30	0.05	0.33	0.24	0.26	0.40	0.30	0.36
	NE	0.63	0.64	0.48	0.08	0.42	0.39	0.38	0.49	0.44	0.51
	NW	0.59	0.59	0.45	0.04	0.56	0.55	0.50	0.56	0.55	0.52
	C	0.73	0.68	0.55	0.00	0.55	0.46	0.55	0.59	0.58	0.63
	all	0.57	0.54	0.47	0.00	0.44	0.43	0.44	0.51	0.45	0.51
E_l	S	-	0.78	0.53	0.07	0.16	0.14	0.17	0.20	0.15	0.19
	NE	-	0.83	0.64	0.02	0.44	0.31	0.31	0.47	0.45	0.49
	NW	-	0.92	0.72	0.02	0.37	0.40	0.32	0.35	0.39	0.36
	C	-	0.91	0.76	0.01	0.47	0.41	0.49	0.53	0.50	0.56
	all	-	0.89	0.71	0.05	0.27	0.29	0.29	0.31	0.28	0.34

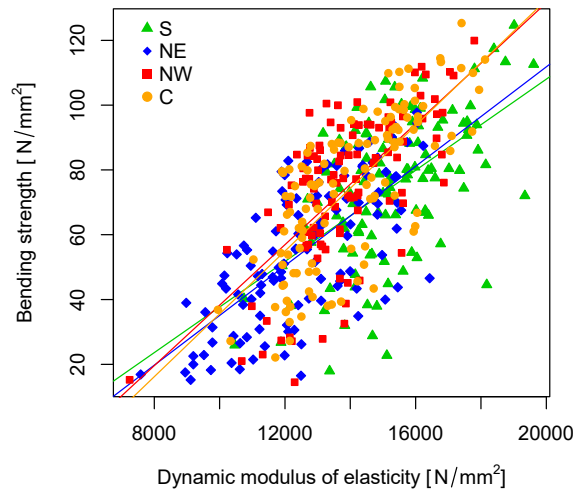


Figure 1 – Relationship between bending strength and dynamic modulus of elasticity ($R^2 = 0.47$).

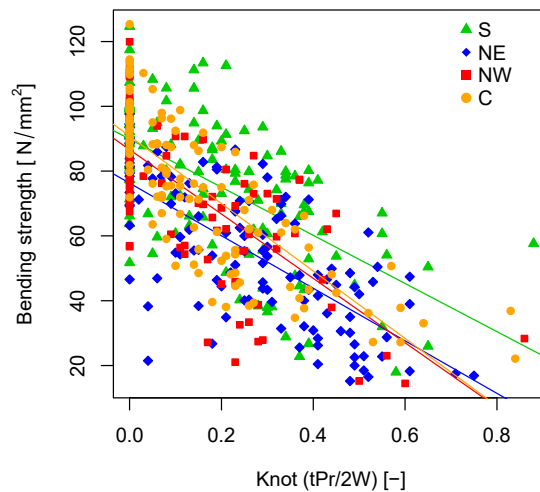


Figure 2 – Relationship between bending strength and knot parameter ($R^2 = 0.51$).

3.3 STRENGTH GRADING

In view of the results above described, the parameters used for the development of visual grading rules were the knots and the presence of pith, as the only characteristics that affected significantly the mechanical quality of the material. Regarding the knots, only limitations for the single knot were established while the knot clusters have been disregarded. This decision was supported by the relatively poor presence of grouped knots: the ratio of KAR to tKAR was on average 0.96 and the ratio of sPr/2W to tPr/2W was 0.98, an indication of the infrequent presence of more than one knot within a distance of 150 mm.

Four grading rules were developed (Table 6): in the visual grading rules 1 (V1), the Dm/S parameter was used; in the visual grading rules 2 (V2), sPr/2W was the knot parameter taken into account. The choice was due on one hand to the determination of the minimum knot diameter, which is a very common measure in many grading rules already established (included the Italian one), and on the other hand to the selection of the sPr/2W parameter as the one with the highest correlation with mechanical properties.

The grading rules were developed to maximize the timber quality (D45-D24-R) or, alternatively, to minimize the rejects (D45-D18-R). Two grades were always selected by each grading rule (S1 the better grade and S2 the lowest); the limitation for the knot parameters for each grade are reported in Table 6. The presence of the pith was permitted only in the pieces to be assigned to grade S2, while the presence of any kind of damage was never permitted.

Table 6 – Description of the visual grading rules: limitation for the parameter used, characteristics values achieved and assignment to strength classes for the visual grades. NP = Not Permitted; P = Permitted

	Visual grading rules							
	V1_D45-D24-R		V1_D45-D18-R		V2_D45-D24-R		V2_D45-D18-R	
Grade	S1	S2	S1	S2	S1	S2	S1	S2
Knot parameter	Dm/S	Dm/S	Dm/S	Dm/S	sPr/2W	sPr/2W	sPr/2W	sPr/2W
Knot limitation	≤0.2	≤0.7	≤0.2	≤0.8	≤0.2	≤0.4	≤0.2	≤0.7
Pith	NP	P	NP	P	NP	P	NP	P
Damage	NP	NP	NP	NP	NP	NP	NP	NP
f_{mk} (MPa)	47.9	25.3	47.9	20.7	47.9	24.6	47.9	18.3
$E_{0,mean}$ (GPa)	15.1	11.8	15.1	11.3	14.9	11.5	14.9	10.9
ρ_{mean} (kg/m ³)	610	623	610	624	615	613	615	615
Assignment	D45	D24	D45	D18	D45	D24	D45	D18

In order to compare the visual and the machine grading, the machine settings were developed for the same combinations of strength classes achieved with the visual grading. The obtained settings (thresholds of dynamic modulus of elasticity) were: 14200 / 10400 MPa for the combination D45-D24-R and 14200 / 9120 MPa for D24-D18-R.

Both the machine and the visual grading were applied to the beech boards and a strength class was assigned to each piece. The yields achieved with the different grading methods are shown in figure 3.

As first observation, beech is confirmed to be a species with high mechanical performance, since almost 50% of the pieces analysed could be assigned to the class D45 and another 45% to the class D24.

Comparing the machine to the visual grading, the machine allowed to minimize the number of rejects (4.3% for the combination D45-D24-R and 1.1% for D45-D18-R), as already determined for softwood (Brunetti et al. 2016); but the percentage of pieces graded as D45 were comparable.

Next, comparing the grading rules V1 and V2, the two knot parameters allowed for the same assignments of the visual grades, but the rules using sPr/2w had better yields, both in terms of the number of pieces in the higher class and in terms of fewer rejects (almost equalling the machine grading).

However, the Dm/S parameter seemed more versatile despite having slightly lower correlations with the mechanical properties: raising the limitation for the grade S1 from 0.2 to 0.25 the assignment could be D40, while raising the same limitation to 0.33 the assignment to D35 was possible. This could not be achieved with sPr/2W.

Focusing on the single provenances, the sub-sample NE displayed the lowest yields, reflecting the quality of the raw material and confirming the effectiveness of the strength grading on beech. For the other provenances the yields were comparable, even if differences were noticed between machine and visual grading mainly in the sub-sample S, for which the machine selected a higher number of D45 in respect to the visual grading, and in the sub-sample NW, for which the opposite was noticed, with the visual grading selecting a far higher number of D45. The explanation could be found in the characteristics of the raw material: the two sub-samples had the same mean bending strength (the limiting property for the assignment to the strength classes), but S showed higher stiffness (i.e. high yields with machine grading) and worse values of the knot parameter (i.e. low yields with visual grading). The contrary could be observed for NW, with lower values of modulus of elasticity and low values of knot parameter.

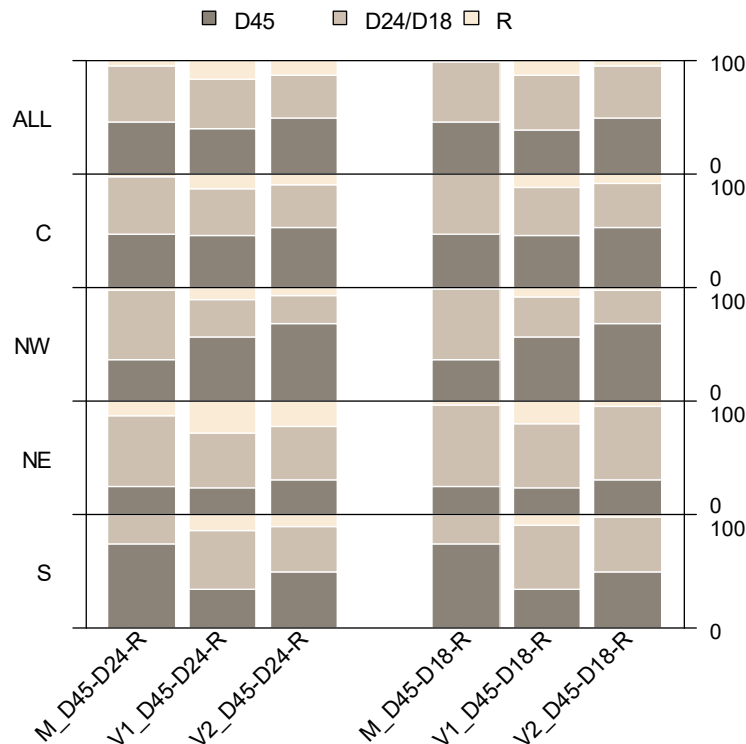


Figure 3 – Yields (%) achieved by means of the machine grading (M) and the visual grading rules described in Table 6. The yields are reported for each provenance and for the whole sample.

Finally, here are few remarks on the development of the grading methods. During the development of the settings for the machine, the sub-sample NE penalized the achievement of very high strength classes because of the verification prescribing that the characteristics values of the strength class shall be met for each provenance. This verification was introduced in the new version of the standard EN 14081-2 (2018).

In the same way, the assignments of the visual grades to strength classes were penalized by the number of sub-sample: at least 5 sub-samples are required to avoid reductions in the characteristics values because of the application of the k_n . Therefore, with a bigger sample, higher assignment for the grades or more permissive limitation for the visual characteristics could be achieved.

3.2 GLUING PARAMETERS

When preparing assemblies, boards were selected to not include knots, considering that this parameter was shown to be the most important for structural grading and that knot presence is known to affect gluing characteristics of wood joints. In this way, the obtained results have to be considered valid only at a laboratory scale.

The results of the delamination tests for the different adhesives and press systems are summarized in figure 4 and 5. According to the standard on CLT (EN 16351 2015) the bonding requirements are met if the total delamination does not exceed 10% and the maximum delamination 40%. It is clear that none of the gluing systems fulfilled such requirements. However, delamination test is known to be disadvantageous for CLT (Betti et al. 2016; Dugmore et al. 2019), so that the splitting of the specimen and the evaluation of the wood failure percentage was added. The additional requirement provides a WFP of at least 70%, which was not fulfilled either by specimens.

Undoubtedly, the structural bonding of hardwoods is the critical point to produce glued products, but some evidences can be retrieved from the test results. As concerns the adhesives, PUR was definitely the one to not use pure, while the addition of the primer increased the performance to the level of MUF. Very similar results were obtained by means of the hydraulic press and the vacuum one, even if the pressures used were very different.

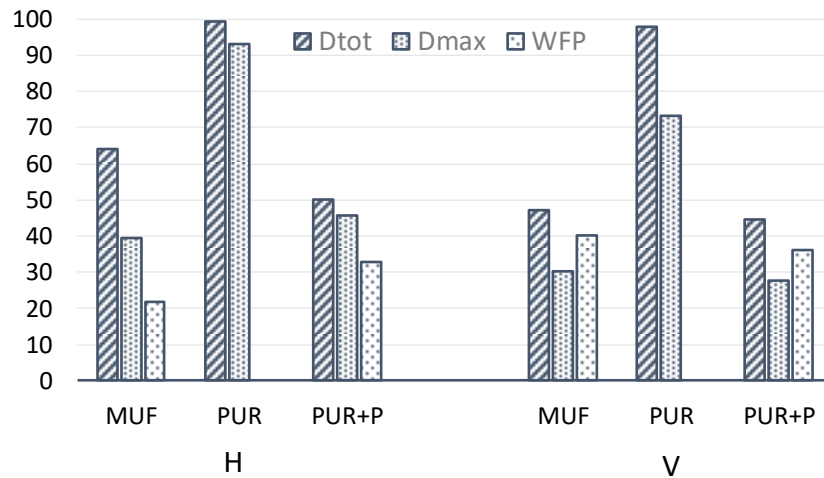


Figure 4 – Mean values of delamination and wood failure percentage for the different adhesives and press methods (H = hydraulic; V = vacuum).

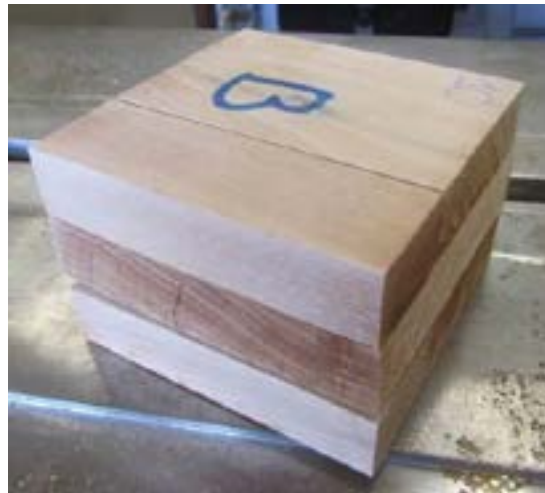


Figure 5 – Example of an extensive opening after the delamination cycles.

4. CONCLUSIONS

The quality of the raw material can be very variable with beech. At time, most of the attention is paid to the high quality pieces to produce very high performing structural products, therefore, a suitable grading system could reduce waste and increase yields with a view of a more sustainable and efficient use of the wood resource.

The strength grading was very effective for beech timber: machine grading, as well as visual grading, worked properly both with good quality boards and with weaker pieces and the yields reflected the quality of the raw material. Currently, no grading machine is certified at European level to grade beech timber, while few visual grading rules exists: in Germany the national standard (DIN 4074-5 2008) allows the assignment of the higher grade (LS13) to D40 and the second one (LS10 & better) to D35 (EN 1912 2012). Our results were in line with the German grading, with the possibility to assign the best grade to the higher class D45.

The grading yields for the best class (D45) were very similar for machine and visual grading, while the machine permitted to reduce the rejects, if two grades are selected at the same time. Moreover, correlations between machine and visual properties with the mechanical properties of beech timber were similar to what often observed for softwood, with the exception of density that does not correlated neither with strength or stiffness nor with ring width. Hence, the suggestion to exclude density from the grading of hardwood seems reliable.

Since strength grading demonstrated to be effective, the issue of structural bonding remains the one to be solved for the production of glued structural beam or panels made of beech. None of the adhesive tested met the requirements for delamination tests provided by the actual standardization for softwood. However, it was possible to see room for improvement, and further investigation on the reasons of such performance.

ACKNOWLEDGEMENTS

This study was realized in the framework of the PRIN2015 project (no. 2015YW8JWA) “Short chain in the biomass-wood sector: supply, traceability, certification and carbon sequestration. Innovations for bio-building and energy efficiency”, coordinated by G. Scarascia-Mugnozza.

The authors want to thank the companies Pagano Costruzioni in Legno, Domini Legnami Srl, La Foresta Soc. Coop. and Gruppolegno Srl for the strong collaboration and support to the research because of the supplying of the raw material; Paolo Burato, Paolo Pestelli and Graziano Sani for the support during laboratory tests. Dr. Marco Lelli for the support in finding the site and the raw material of the research and the organization of the logistic transport in Monti Simbruini.

REFERENCES

- Aicher S, Christian Z, Dill-langer G (2014) *Hardwood Glulams – Emerging Timber Products of Superior Mechanical Properties. In: Proceedings of the World Conference on Timber Engineering - WCTE 2014. Québec City, Canada*
- Aicher S, Ohnesorge D (2011) *Shear strength of glued laminated timber made from European beech timber. Eur J Wood Wood Prod 69:143–154. doi: 10.1007/s00107-009-0399-9*
- Aicher S, Reinhardt H-W (2007) *Delamination properties and shear strength of glued beech wood laminations with red heartwood. Holz als Roh- und Werkst 65:125–136. doi: 10.1007/s00107-006-0135-7*
- Betti M, Brunetti M, Lauriola MP, et al (2016) *Comparison of newly proposed test methods to evaluate the bonding quality of Cross-Laminated Timber (CLT) panels by means of experimental data and finite element (FE) analysis. Constr Build Mater 125:952–963. doi: 10.1016/j.conbuildmat.2016.08.113*
- Brunetti M, Burato P, Cremonini C, et al (2016) *Visual and machine grading of larch (Larix decidua Mill.) structural timber from the Italian Alps. Mater Struct 49:2681–2688. doi: 10.1617/s11527-015-0676-5*
- Cibecchini D, Cavalli A, Goli G, Togni M (2016) *Beech sawn timber for structural use: A case study for mechanical characterization and optimization of the Italian visual strength grading rule. J For Sci 62:521–528. doi: 10.17221/93/2016-JFS*
- DIN 4074-5 (2008) *Strength grading of wood - Part 5: Sawn hardwood. DIN, Berlin*
- Dugmore M, Nocetti M, Brunetti M, et al (2019) *Bonding quality of cross-laminated timber: Evaluation of test methods on Eucalyptus grandis panels. Constr Build Mater 211:217–227. doi: 10.1016/j.conbuildmat.2019.03.240*
- Ehrhart T, Fink G, Steiger R, Frangi A (2016a) *Experimental Investigation of Tensile Strength and Stiffness Indicators Regarding European Beech Timber. Proc World Conf Timber Eng WCTE 22-25 August, Vienna, Austria 600–607*
- Ehrhart T, Fink G, Steiger R, Frangi A (2016b) *Strength grading of European beech lamellas for the production of GLT & CLT. Int Netw Timber Eng Res INTER, Meet 49, Graz, Austria 29–42*
- Ehrhart T, Steiger R, Frangi A (2018) *Mechanical properties of European beech glued laminated timber. In: Proceedings of the International Network on Timber Engineering Research, INTER, Meeting 51, Tallin, Estonia. paper 51-12-4*
- EN 1310 (1997) *Round and sawn timber. Method of measurement of features. CEN - European Committee for Standardization, Brussels*
- EN 13183-1 (2002) *Moisture content of a piece of sawn timber. Determination by oven dry method. CEN - European Committee for Standardization, Brussels*
- EN 14080 (2013) *Timber structures - Glued laminated timber and glued solid timber - Requirements. CEN - European Committee for Standardization, Brussels*
- EN 14081-2 (2018) *Timber structures - Strength graded structural timber with rectangular cross section - Part 2: Machine grading; additional requirements for type testing. CEN - European Committee for Standardization, Brussels*

- EN 14358 (2016) *Timber structures - Calculation and verification of characteristic values*. CEN - European Committee for Standardization, Brussels
- EN 16351 (2015) *Timber structures - Cross laminated timber - Requirements*. CEN - European Committee for Standardization, Brussels
- EN 1912 (2012) *Structural Timber. Strength classes. Assignment of visual grades and species*. CEN - European Committee for Standardization, Brussels
- EN 338 (2016) *Structural timber. Strength classes*. CEN - European Committee for Standardization, Brussels
- EN 384 (2016) *Structural timber – Determination of characteristic values of mechanical properties and density*. CEN - European Committee for Standardization, Brussels
- EN 408 (2012) *Timber structures - Structural timber and glued laminated timber - Determination of some physical and mechanical properties*. CEN - European Committee for Standardization, Brussels
- Frese M, Blass HJ (2005) *Beech glulam strength classes*. CIB-W18
- Glos P, Denzler JK, Linsenmann PW (2004) *Strength and stiffness behaviour of beech laminations for high strength glulam*. In: *Proceedings of the CIB W18, Meeting 37, Edinburgh, Scotland*. paper 37-6-3
- ISO 13061-2 (2014) *Physical and mechanical properties of wood - Test methods for small clear specimen. Part 2: Determination of density for physical and mechanical tests*. ISO - International Organization for Standardization, Geneva
- Konnerth J, Kluge M, Schweizer G, et al (2016) *Survey of selected adhesive bonding properties of nine European softwood and hardwood species*. *Eur J Wood Wood Prod* 74:809–819. doi: 10.1007/s00107-016-1087-1
- Luedtke J, Amen C, van Ofen A, Lehringer C (2015) *1C-PUR-bonded hardwoods for engineered wood products: influence of selected processing parameters*. *Eur J Wood Wood Prod* 73:167–178. doi: 10.1007/s00107-014-0875-8
- Nocetti M, Bacher M, Brunetti M, et al (2010) *Machine grading of Italian structural timber: Preliminary results on different wood species*. In: *Proceedings of the World Conference on Timber Engineering, WCTE 2010, Riva del Garda, Italy*
- Nocetti M, Brancheriau L, Bacher M, et al (2013) *Relationship between local and global modulus of elasticity in bending and its consequence on structural timber grading*. *Eur J Wood Wood Prod* 71:297–308. doi: 10.1007/s00107-013-0682-7
- Nocetti M, Brunetti M, Bacher M (2016) *Efficiency of the machine grading of chestnut structural timber: prediction of strength classes by dry and wet measurements*. *Mater Struct* 49:4439–4450. doi: 10.1617/s11527-016-0799-3
- Ohnesorge D, Richter K, Becker G (2010) *Influence of wood properties and bonding parameters on bond durability of European Beech (Fagus sylvatica L.) glulams*. *Ann For Sci* 67:601–610. doi: 10.1051/forest/2010002
- Schmidt M, Glos P, Wegener G (2010) *Verklebung von Buchenholz für tragende Holzbauteile*. *Eur J Wood Wood Prod* 68:43–57. doi: 10.1007/s00107-009-0382-5
- Stapel P, Van De Kuilen JWG (2013) *Effects of grading procedures on the scatter of characteristic values of European grown sawn timber*. *Mater Struct Constr* 46:1587–1598. doi: 10.1617/s11527-012-9999-7
- Torno S, Knorz M, Kuilen J van de (2013) *Supply of beech lamellas for the production of glued laminated timber*. In: *Proceedings of the International Scientific Conference on Hardwood Processing, ISCHP 2013, Florence, Italy*, pp 210–217
- Vega A, Dieste A, Guaita M, et al (2012) *Modelling of the mechanical properties of Castanea sativa mill. structural timber by a combination of non-destructive variables and visual grading parameters*. *Eur J Wood Wood Prod* 70:839–844. doi: 10.1007/s00107-012-0626-7
- Westermayr M, Stapel P, Kuilen JW Van De (2018a) *Tensile strength and stiffness of low quality beech (Fagus sylvatica) sawn timber*. In: *Proceedings of the World Conference on Timber Engineering WCTE, Seoul, Rep. of Korea*
- Westermayr M, Stapel P, Kuilen JW Van De (2018b) *Tensile strength and stiffness of low quality beech (Fagus sylvatica) sawn timber*. In: *Proceedings of the World Conference on Timber Engineering WCTE, 20-23 August, Seoul, Rep. of Korea*

Tension strength capacity of finger joined beech lamellas

Barbara Fortuna^{1*}, Mitja Plos¹, Boris Azinovic², Tamara Šuligoj¹ and Goran Turk¹

¹University of Ljubljana
Faculty of Civil and Geodetic Engineering
Ljubljana, Slovenia

²Slovenian national Building and
Civil Engineering Institute
Ljubljana, Slovenia

ABSTRACT

Beech wood has high mechanical properties, therefore the production of high quality beech glulam beams is one of our main objectives. Finger joints with standard geometries and adhesives used for joining coniferous wood are not sufficient in terms of strength when gluing beech wood. A hybrid glulam beam was produced and tested in a standard four point bending test. The beam was produced from finger joined beech lamellas on the outer sides and finger joined spruce lamellas in the middle. The results from the bending test showed a lack of tensile strength of the finger joints of beech lamellas on the bottom middle part of the beam, where the rupture occurred. We prepared a numerical model of finger joined beech lamellas and simulations of tension tests, parallel to the lamella. We performed parametric studies with multiple variables referring to geometrical properties of finger joints and two different types of applied adhesives. The results showed a high influence of the finger joint geometrical parameters. Experimental tests on the tension strength of the finger joints were performed. Two finger joint lengths were tested, 10 and 20 millimetres. The results showed a clear influence of the finger joint geometry where highest strengths were obtained with longer and thinner fingers.

1. INTRODUCTION

Finger joints were primarily designed for use in softwood bonding. Since hardwoods usually have higher mechanical properties than softwood, the currently used finger joint design might pose a problem for joining beech. This was observed during the hybrid glulam bending test and also in other research (Ehrhart et al., 2018). To address the issue, we decided to perform analytical and numerical calculations and try to find a finger joint design better suited for beech wood. To evaluate the simulations, samples were made and tested using different adhesives and finger joint lengths .,

The strength of a finger joint is essentially determined by three factors, the strength of the joined boards, the quality of the production and the finger joint profile (Aicher and Radovic, 1999; Collin and Ehlbeck, 1992). The type of glue used also plays an important role in the strength of the finger joint (Konnerth et al., 2006). We tried to take into account as many of the significant variables as we could, excluding the production process. The main focus was the finger joint profile. We expected that the finger joint length would play a major role in the strength of the joints. This was shown in the study of Franke, Schusser and Müller (2014), where longer (50 mm) finger joints resulted in a higher flat-wise bending strength and in the study of Tran, Oudjene and Méausoone (2014) where maximal finger joint length and minimal pitch produced the best results in edge-wise bending tests.

Our primary focus was to find a solution for finger joints in beech wood, that could withstand the higher tension strengths. This could enable the glulam producers to manufacture beech or hybrid glulam with a much higher strength than the most commonly used softwood glulam.

2. METHODS

In the first part of the study, a preliminary assessment of finger joint tension strength was made based on simple equilibrium equations for scarf joints that are, in terms of achieving the highest strength, known as the most effective joint profile, although its use is due to extensive timber loss, highly uneconomical (Aicher 2003). The profile is shown

* Corresponding author: Barbara Fortuna; E-mail: barbara.fortuna@fgg.uni-lj.si

in Figure 1 (left). The shear stress $\sigma_{\xi\eta}$ and normal stress $\sigma_{\eta\eta}$ in the inclined plane were calculated by the following Equations (1)

$$\sigma_{\xi\eta} = \sigma_0 \cdot \sin \alpha \cdot \cos \alpha \quad \text{and} \quad \sigma_{\eta\eta} = \sigma_0 \cdot \sin^2 \alpha, \quad (1)$$

where σ_0 is the normal stress in the longitudinal direction ($\sigma_0 = F / A$), F is the axial force and A is the area of the cross section. The stresses were assumed to be constant along the glue line and shear strength τ_1 and normal peel strength σ_u were calculated based on the assumption of the quadratic strength criteria by the Equation (2) (Aicher and Klöck, 2001) and the assumed ratio $\tau_1/\sigma_u = 6$

$$\left(\frac{\sigma_{\xi\eta}}{\tau_1} \right)^2 + \left(\frac{\sigma_{\eta\eta}}{\sigma_u} \right)^2 = 1. \quad (2)$$

With the determined strength properties, the obtained nominal tension strength f_t was observed. When calculating the effective length of the glue line, the tip width b_t was neglected.

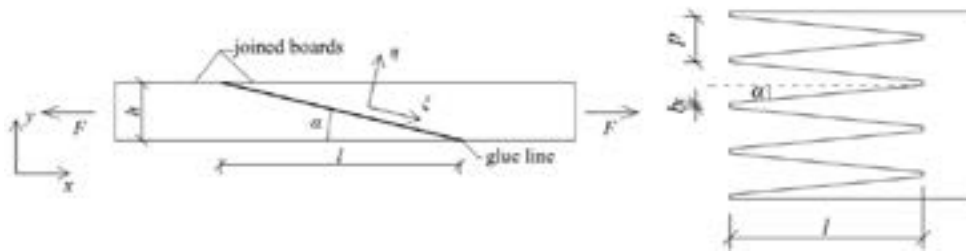


Figure 1: Scarf joint (Aicher, 2003) (left) and finger joint geometry (right).

In the second part of the study, a numerical model was used to estimate the response of the finger joints in tension. The main aim of the parametric studies was the optimization of the finger joint geometry for beech boards.

The tension test was simulated with a 2D numerical model in Abaqus. The model takes into account the symmetrical response along the longer axis of the lamination. Therefore, only a small section of the lamination with one half of the finger was analyzed (Figure 2). The lamination was fixed at one end, while on the other end, a displacement (u_x) was induced until failure. The model is supported in transverse direction (u_y) due to the symmetry. The eight node biquadratic plane stress quadrilateral elements were used in the finite element. The mesh is condensed in the local area next to the cohesive elements and the cohesive surface (the maximum size of the element was approximately 0.5×0.5 mm²).



Figure 2: 2D numerical model of the finger joint.

The model consisted of parts with linear elastic and orthotropic behavior for beech, where the wood fibers were oriented in the longitudinal direction. The mean values for the elastic behavior of beech (Table 1) were assumed according to the literature (Desch and Dinwoodie, 2016; Sandhaas, 2012). The nonlinear behavior was presumed in the finger's adhesive layer (failure of the joint, modelled by a cohesive surface) and along the weakened area of the pitch (wood failure, modelled by cohesive elements). To model the adhesive layer a cohesive zone model (CZM) approach was used, where the input parameters were based on experiments with melamine urea formaldehyde adhesive (MUF) and beech performed by Khelifa et al. (2016) and Tran et al. (2014). Damage initiation was assumed by a quadratic traction criterion and the evolution of damage was considered according to the energy law.

Tension strength capacity of finger joined beech lamellas

Table 1: Mean elastic properties of beech.

E_1 [MPa]	E_2 [MPa]	ν_{12} [-]	G_{12} [MPa]
13700	11400	0.51	1060

Note: E_1, E_2 ... elastic moduli in the longitudinal and radial directions of the wood; ν_{12} ...Poisson's ratio, where the first index refers to the direction of the applied stress and the second index to the direction of lateral deformation; G_{12} ... shear moduli in the 12 plane.

Table 2: Cohesive zone model properties used for the cohesive surface and cohesive elements.

	σ_u [MPa]	τ_1 [MPa]	K_{nn} [MPa/mm]	$K_{tt,1}$ [MPa/mm]	G_f [mm]	η [-]
Timber adhesive bond-line (cohesive surface)	1.6	9.6	default contact enforcement method (high stiffness)		0.50	0.001
Beech along the pitch (cohesive elements)	70	100	13700	1610	10	$5 \cdot 10^{-6}$

Note: σ_u ... strength in the normal direction, τ_1 ... shear strength; K_{nn} ... stiffness in the normal direction; $K_{tt,1}$... stiffness in the shear direction; G_f ... fracture energy (mode independent); η ... viscosity coefficient

In the parametric study, three different parameters were varied; pitch (p), tip thickness (b_t) and length of fingers (l). Parameters were changed in the range of; (i) $\alpha = 2 - 6^\circ$, (ii) $b_t = 1 - 2$ mm and (iii) $l = 10 - 50$ mm.

3. MATERIAL

The experiments were carried out on beech wood gathered from Southeastern part of Slovenia. Boards were air dried and then sawn and planned to the nominal cross sections of 70×20 mm² for the 10 mm long finger joints and 120×20 mm² for the finger joints with the length of 20 mm. The density was determined measuring the weight and actual dimension of each board. The average density of the material was 695 kg/m³. The moisture content was measured with the resistance moisture meter Brookhuis FME. The average moisture content was 9.6 %.

Finger joints were produced in two production companies. The shorter length of 10 mm was produced by a Slovenian window and door manufacturer M Sora d.d. The profile of the finger joints isn't in compliance with the EN 14080:2010+A1:2012 demands for structural finger joints, where self-interlocking is required. Nevertheless, we decided to include the geometry in the testing program to evaluate the influence of the adhesive type on the strength properties. The geometry is illustrated in Figure 3A. The pitch is $p = 6$ mm and tip width is $b_t = 2$ mm. The application of the glue and the joining of the boards were handled manually. Joined boards were then placed in a press for curing for 24 hours. The longer finger joints (20 mm) were produced in a Slovenian glulam producer Hoja d.d., using the cutting knives that are otherwise used for longitudinal joining of spruce lamellas. The configuration is in accordance with the standard for structural finger joints. The pitch was $p = 6$ mm and the tip width $b_t = 1$ mm. The cutting, glue application and pressing were automatized. The majority of the joints were pressed under a pressure of 5 MPa while one third of the specimens were joined under 10 MPa of pressure.

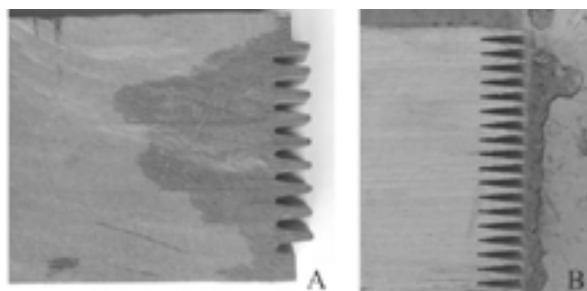


Figure 3: Finger joint profile for 10 mm (A) and 20 mm (B) finger length.

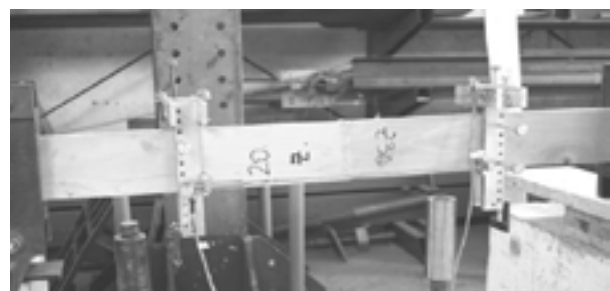


Figure 4: Measurements of modulus of elasticity in tension.

Two types of adhesives were used. Melamin-urea formaldehyde (MUF) as one of the most commonly used adhesive for spruce timber among the Slovenian glulam producers and Phenol-resorcinol Formaldehyde (PRF) as one of the adhesives with the highest tensile shear strength (Konnerth et al. 2016).

The length of the boards before gluing was 1.2 m for the 10 mm and 1.5 m for the 20 mm finger joints. The boards were selected in a way that there were no knots within 300 mm from the joint line. Before cutting the finger joint, all the boards were non-destructively tested. The dynamic modulus of elasticity (E_{dyn}) from longitudinal vibrations was determined with the STIG strength grading machine. The measurements were carried out with a microphone, capturing sound oscillations from a hammer impact on the board's end. In order to assess the influence of joining on the non-destructive testing, the measurements of E_{dyn} were repeated after the cutting and gluing process.

Glued specimens were then tested in tension. The experiments were carried out according to the EN 408:2010+A1:2012 standard. The test length, clear of the clamping, was 1.20 m and the finger joint was positioned in the middle, between the clamps. For the 10 mm finger joints, only the tension strength was measured, while for the longer finger joints the static modulus of elasticity was also determined. Deformations of the glue line are rather difficult to measure since it is hard to exclude the timber deformation within the length of the measurement. Therefore, we decided to measure the deformations in the same way as it is usually done in tension tests, that is with linear variable displacement transformers (LVDTs) and at a reference length $l_0 = 600$ mm. Knowing that the obtained deformations are a combination of glue and timber deformation, we wanted to assess the quality of the whole joint. In our previous measurements of moduli of elasticity, we observed increased accuracy of the measurements if the loading cycle was repeated three times. When calculating the modulus of elasticity, the last displacement measurement was taken into account. Before further loading, the LVDTs were removed and the specimen was tested to failure. The position of the clamping system remained the same.

A pilot hybrid beech-spruce-beech glulam beam was produced at HOJA d.d. with a cross section of 140×300 mm² and a length of 5 m. The glulam had two layers of 6 lamellas of beech wood and 8 spruce lamellas in the middle with a thickness of 13 mm and 18 mm, respectively. MUF glue was used. The beam was tested in bending according to EN 408:2010+A1:2012. Bending strength, modulus of elasticity and shear modulus were measured.

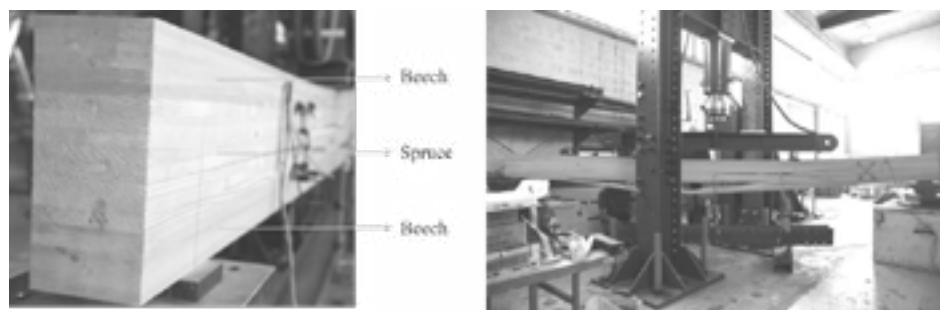


Figure 5: Bending test on hybrid glued laminated timber made of spruce and beech.

4. RESULTS

For preliminary calculations, a reference shear strength of 8.8 MPa and normal peel strength of 1.5 MPa were used. Both were determined from the average tension strength of the 20 mm finger joints according to the quadratic strength criteria. For a series of different finger joint profiles, we made the estimation of tension strength, shown in Figure 6. The tension strength is linearly correlated to the effective glue line area. On the graphs, the pitch p is expressed indirectly through the slope of the fingers and the influence of each geometry parameter can be seen. The graphs show that longer finger joints produce higher tension strength. The increase of the strength can also be achieved by decreasing the slope α and decreasing the tip width b_t . In order to achieve higher strengths, for example 80 MPa which is about 10 % above the average tension strength of Slovenian beech wood, it would be necessary to increase the length to at least 30 mm, having a rather small slope and tip width compared to the most common geometry profiles (Aicher, 2003).

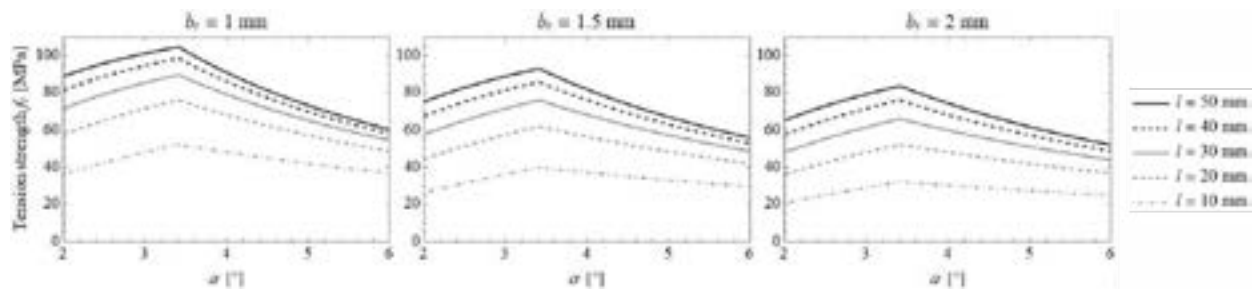


Figure 6: Graphical demonstration of the influence of the geometrical parameters on the tension strength of finger joints - analytical model.

4.1. NUMERICAL MODEL

Although the obtained strengths were lower, the results from the numerical simulations were similar. The results of the parametric study are shown in Figure 7. An optimal pitch dimension (p) can be found for each curve on the graphs (with a constant b_f and l). In the first part of the curve (low values of p), the ultimate load capacity of the joint increases until the optimal p is reached. For smaller values of p (smaller slope of the fingers), the failure occurs in the cohesive elements simulating the failure of wood. After reaching the optimal pitch, the failure mode changes and the load capacity decreases with further increase of p since the area of the glued surface decreases correspondingly. The optimal slope of the fingers proved to be approximately $3-4^\circ$ for the analyzed numerical model with MUF adhesive and the assumed failure mechanisms. One can observe that the results from the numerical simulation are always lower than those from the analytical analysis. The differences increase with increased length. We believe that tension strength is considerably overestimated by the analytical analysis. This stems from the stresses distribution along the glue line which were assumed to be constant in the analytical model and is not the case in reality, where peaks of the shear stresses occur at the beginning and the end of the glue line.

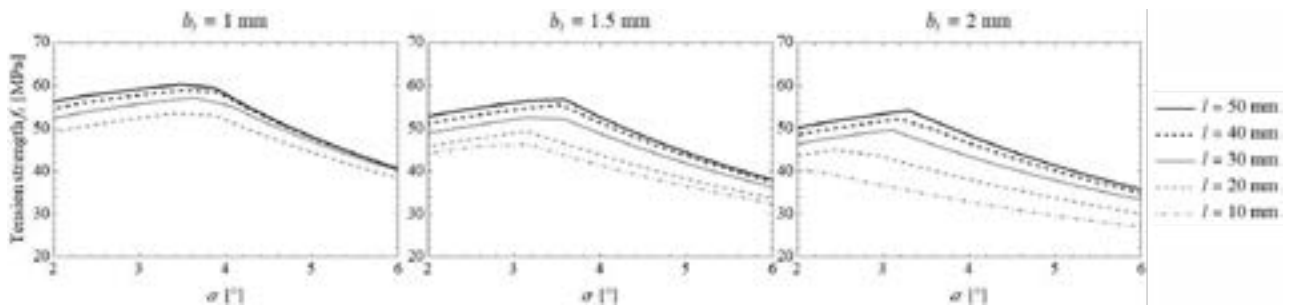


Figure 7: Ultimate capacity of the finger joint dependent on different geometric parameters - numerical model.

4.2. EXPERIMENTAL TESTING

The results from the tension tests of the 10 mm finger joints showed a significant difference in tension strength between both adhesives. The PRF adhesive clearly had a higher strength than MUF. On average, the ratio between the adhesives was approximately 1:2.25. The obtained tension strengths were very low, which can be explained with the lack of finger joints interlocking in this type of the profile and lack of control of the applied pressure in the curing time. The statistical values are shown in Table 3. In general, the rupture of the specimens occurred along the glue line (Figure 8A), only two specimens, glued with PRF, failed in wood (Figure 8B).

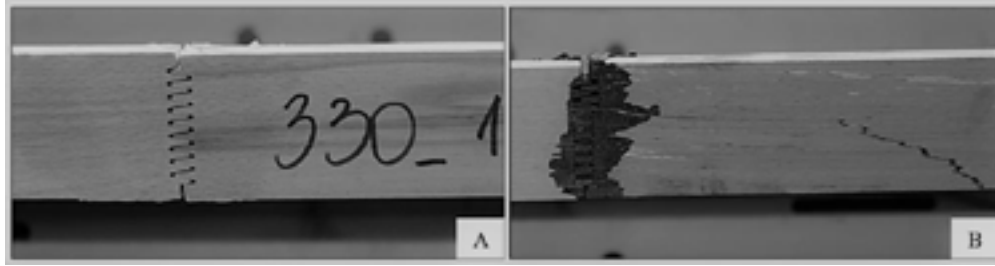


Figure 8: Failures of finger joints (10 mm) glued with PRF (A) and MUF (B).

As expected, the 20 mm long finger joints proved to have a much higher tension strength (Table 3). The average value for all specimens was 51.0 MPa and the 5th percentile was 15.9 MPa. The values are still relatively low compared to another study (Aicher, Hoffelin and Behrens, 2014) where they tested 20 mm long finger joints on beech wood with Melamin type of adhesive. One of the reasons for the difference could be in the different production precision and applied pressure. In our study, quite a few of the specimens cracked in the joint area during the gluing and pressing procedure. Though boards weren't visually graded, we observed the obvious slopes of grain and some discolorations, therefore the boards were of a rather low quality and more exposed to cracking.

When comparing the two types of the adhesives, the mean tension strength is no longer higher for joints glued with PRF as was the case with the short joints. The average value was almost 15 % lower than in the case of the MUF adhesive. In the case of PRF adhesive, a high percentage of wood failure was observed. This means that the measured strengths represent the timber tension strength and one can notice they are quite low. Previous research indicates much higher strength properties for European beech timber (Ehrhart et al. 2018; Fortuna et al. 2018). In Figure 8 the strengths for the specimens that failed in the glue line are shown separated by groups of joint length, glue and pressure used. The PRF specimens have the highest values, but the difference is not statistically significant as in the case of 10 mm finger joints. This confirms the results from the preliminary assessment of tension strengths with numerical simulations, where the influence of the adhesive type decreased with the increasing length of the finger joints and the selected finger joint profile became the influential parameter for increasing the strength.

Table 3: Statistical values for tension strength, modulus of elasticity in tension and dynamic modulus of elasticity for specimens divided into six groups by the type of adhesive, assembling pressure and type of failure.

f_t [MPa]	10 mm		20 mm					
	Joint failure		Wood failure			Joint failure		
	MUF (-)	PRF (-)	MUF (5 MPa)	MUF (10 MPa)	PRF (5 MPa)	MUF (5 MPa)	MUF (10 MPa)	PRF (5 MPa)
5 th percentile	3.6	8.1	20.2	13.7	9.8	20.6	32.0	36.1
Mean	6.5	14.1	36.8	31.1	28.1	41.5	43.9	46.4
St. Deviation	1.4	3.8	10.6	12.7	13.0	14.1	7.0	9.0
N	28	25	13	9	17	14	17	9
$E_{t,mean}$ [MPa]	-	-	17500	16600	16500	17900	18300	17800
$E_{dyn,mean}$ [MPa]	-	-	15900	14500	15300	16900	16300	16900

The dynamic modulus of elasticity was measured on each board separately and then on joined boards with the STIG. The correlation between the measured E_{dyn} and the tension strength was analyzed. With all the specimens included, the correlation factor R was 0.40 for tension strength f_t and 0.48 for the static modulus of elasticity E_t . When analyzing the specimens, grouped by type of failure, those correlations changed significantly.

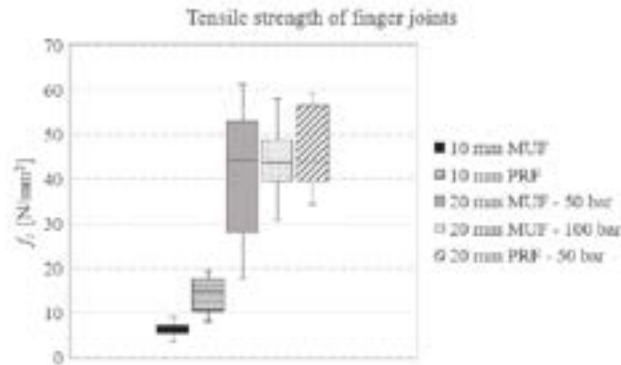


Figure 9: Box plots of tension strengths for five groups of finger joints that failed in the glue line.

In the case of the joint failure group, the correlation factor was not significant and negative. In the case of wood failure, the correlation factor was 0.52 which is a relatively high correlation for a non-destructive measured property, that can be easily and quickly obtained and could possibly be included into the glulam production as part of the manufacturing process of structural elements.

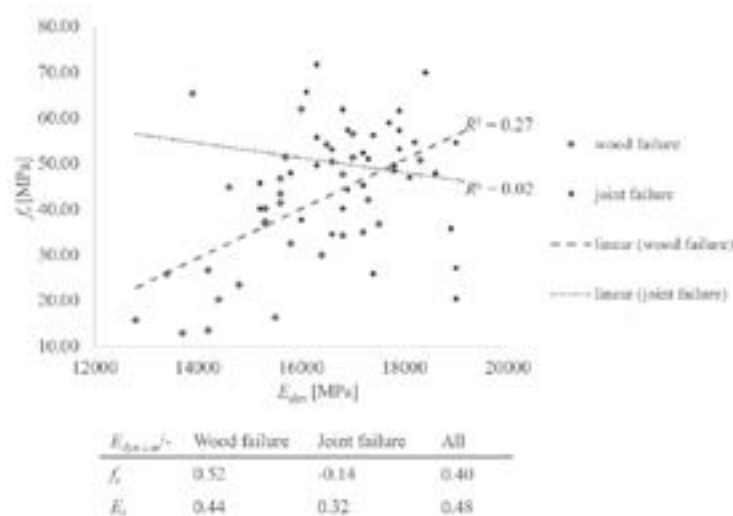


Figure 2: Correlation of dynamic modulus of elasticity measured on joined boards and tension strength of all boards.

The hybrid glulam beam was tested in bending. As expected, the rupture occurred in the finger joint in the lower beech lamella. The static global modulus of elasticity $E_{m,g}$ was 14900 MPa. The ultimate force F_{max} was 133 kN, corresponding to a bending strength f_m of 47.6 MPa. A shear modulus $G = 630$ MPa was also measured between the loading point and the supports. Since beech was only on the outer part of the beam, mostly spruce lamellas were influential on the shear modulus.

5. CONCLUSIONS

The results of experimental tension testing of the finger joints are highly influenced by the specimens that failed in wood. However, based on the studies performed on European beech (Ehrhart et al. 2018) and also specifically on Slovenian beech (Fortuna et al. 2018), higher tension stresses can be expected. The results showed, that with the use of standard finger joint cutting heads used in spruce glulam production, it is not possible to achieve the high strengths that are required for joining beech wood. A new, nonstandard finger joint profile should be constructed. Analytical, numerical and experimental research shows that longer and thinner finger joints produce higher tension strengths. This was confirmed also by the geometrical optimization process of finger joints, performed by Tran, Oudjene and

Méausoone (2014), where the best results were obtained with the maximal length and minimal pitch within the selected optimization limits. In order to achieve a strength of at least 80 MPa, which is around 10 percent above the mean value for Slovenian beech, some suitable profiles would be $l = 30$ mm, $p = 5.8$ mm and $b_i = 1$ mm; $l = 40$ mm, $p = 7.1$ mm and $b_i = 1$ mm or $l = 50$ mm, $p = 8.4$ mm and $b_i = 1$ mm. The production of the proposed cutting head has its limits and would be somewhat challenging. Another finger joint profile that could be used and was presented in EN 385:2001 with $l \cdot p \cdot b_i = 32 \cdot 6.2 \cdot 1.0$ mm. According to the analytical model, a tension strength of approximately 70 MPa could be expected, where the strength parameters were obtained from the experiments with the assumption of the quadratic strength criteria. The numerical model exhibits somewhat lower strengths (approximately 55 MPa) than the analytical model, but we have to emphasize that the strength parameters were obtained from the literature and are probably slightly underestimated. The expected tension strength for a 32 mm finger joint is higher than the strength that was obtained with the hybrid glulam beam where 20 mm finger joints were used. Using finger joints that can withstand 55 to 60 MPa in tension will have a considerable influence on the bending strength of the glued laminated beam made of beech wood.

6. ACKNOWLEDGEMENTS

We would like to acknowledge the national TIGR4smart project funded by the Slovenian Ministry of education, science and sport and the Cohesion fund of the European Commission.

REFERENCES

- Aicher, S., L. Hofflin, W. Behrens. 2001. *A study on tension strength of finger joints in beech wood laminations*. *Otto-Graf Journal* 12:169-186.
- Aicher, S., Klöck, W. 2001. *Linear versus quadratic failure criteria for inplane loaded wood based panels*. *Otto-Graf Journal* 12: 187-199.
- Aicher, S. 2003. *Structural adhesive joints including glued-in bolts*. In: Thelandersson, S. (ed), Larsen, H. J. (ed) *Timber Engineering*, Wiley, Chichester, England. pp. 333-363.
- BS EN 385:2001. *Finger joined structural timber – Performance requirements and minimum production requirements*.
- Desch, H. E., J. M. Dinwoodie. 2016. *Timber: structure, properties, conversion and use*. *Macmillan International Higher Education*.
- EN 408:2010+A1:2012. *Timber structures – Structural timber and glued laminated timber – Determination of some physical and mechanical properties*.
- EN 14080:2013. *Timber structures – Glued laminated timber and glued solid timber – Requirements*.
- Ehrhart, T., R. Steiger, P. Palma, A. Frangi. 2018. *Estimation of tensile strength for European beech timber boards based on density, dynamic modulus on density, dynamic modulus of elasticity and local fibre orientation*. In: *Proceedings of the 2018 World Conference on Timber Engineering, August 20-23, 2018, Seoul, Republic of Korea*.
- Ehrhart, T., R. Steiger, P. Palma, A. Frangi. 2018. *Mechanical properties of European Beech glued laminated timber*. *International Network on Timber Engineering Research (INTER), 5th meeting, August 13-16, 2018, Tallin, Estonia*.
- Fortuna, B., M. Plos, T. Šuligoj, G. Turk. 2018. *Mechanical properties of Slovenian structural beech timber*. In: *Proceedings of the 2018 World Conference on Timber Engineering, August 20-23, 2018, Seoul, Republic of Korea*.
- Franke, B., A. Ashusse, A. Müller. 2014. *Analysis of finger joints from beech wood*. In: *Proceedings of the 2014 World Conference on Timber Engineering, August 10-14, 2014, Quebec City, Canada*.
- Hibbitt, H. D., B. I. Karlsson, E. P. Sorensen. 2016. *ABAQUS/standard: User's Manual*. Hibbitt, Karlsson & Sorensen.
- Khelifa, M., A. Celzard, M. Oudjene, J. Ruelle. 2016. *Experimental and numerical analysis of CFRP-strengthened finger-jointed timber beams*. *International Journal of Adhesion and Adhesives* 68:283–297.
- Konnerth, J., W. Gindl, M. Harm, U. Müller. 2006. *Comparing dry bond strength of spruce and beech wood glued with different adhesives by means of scarf- and lap joint testing method*. *Holz als Roh- und Werkstoff* 64:269-271.
- Konnerth, J., M. Kluge, G. Schweizer, M. Miljkovic, W. Gindl-Altmutter. 2016. *Survey of selected adhesive bonding properties of nine European softwood and hardwood species*. *European Journal of Wood and Wood Products* 74(6):809-819.
- Sandhaas, C. 2012. *Mechanical behaviour of timber joints with slotted-in steel plates*. PhD Thesis. Technical University Delft, Netherlands.
- Tran, V.-D., M. Oudjene, P. J. Méausoone. 2014. *FE analysis and geometrical optimization of timber beech finger-joint under bending test*. *International Journal of Adhesion and Adhesives* 52:40–47.

European beech (*Fagus sylvatica* L.) glued laminated timber: Lamination strength grading, production and mechanical properties

Thomas Ehrhart ^{1) 2)}* (ORCID ID: 0000-0001-9551-4714), René Steiger ²⁾ (0000-0002-0096-098X), Martin Lehmann ³⁾, Andrea Frangi ¹⁾ (0000-0002-2735-1260)

¹⁾ ETH – Swiss Federal Institute of Technology, Institute of Structural Engineering, Stefano-Franscini-Platz 5, 8093 Zurich, Switzerland

²⁾ Empa – Swiss Federal Laboratories for Materials Science and Technology, Structural Engineering Research Laboratory, Ueberlandstrasse 129, 8600 Duebendorf, Switzerland

³⁾ Bern University of Applied Sciences, Institute for Materials and Wood Technology, Solothurnstrasse 102, 2504 Biel, Switzerland

* corresponding author: ehrhart@ibk.baug.ethz.ch; +41 44 633 9150

ABSTRACT

*This paper presents the results of extensive investigations on the lamination strength grading, the production and the mechanical properties of European beech (*Fagus sylvatica* L.) glued laminated timber (GLT). Based on the analysis of potential influencing parameters on strength and stiffness as well as subsequent tension tests parallel to the grain on single boards, a combined visual/machine approach for grading the raw material into tensile strength classes T50, T42, T33 and T22 was developed. Boards strength graded with the developed procedure were then finger-jointed by a Swiss GLT producer and the strength of the finger joints was investigated by means of tensile and bending tests. The strength and durability of the bonding was investigated and verified by means of tensile-shear and delamination tests. It could be shown that the required finger-joint and bondline strengths for GLT of strength classes GL40, GL48 and GL55 can be achieved. Finally, an extensive experimental testing campaign was performed to investigate the mechanical properties of European beech GLT produced based on the strength grading rules and production techniques developed before. Bending, tensile and compressive parallel to the grain, as well as shear tests were carried out on GLT specimens of strength classes GL40, GL48 and GL55 in different sizes in terms of cross-section and length. Based on these investigations and complementing numerical simulations, characteristic strength and stiffness values and formulae for consideration of size effects in bending, tension and shear were determined.*

1 INTRODUCTION

To date the share of European beech (*Fagus sylvatica* L.) amounts to 18.1% of the total timber stock in the Swiss forests. Along with Norway spruce (*Picea abies* Karst., 43.7%), European beech is the second most common tree species and by far the most common hardwood species in Switzerland, followed by ash (*Fraxinus excelsior* L., 4.1%), maple (*Acer pseudoplatanus* L., 3.1%), and oak (*Quercus robur* L., 1.9%) (BAFU, 2018). Hardwoods in general are expected to benefit from the changing climatic conditions in Central Europe and their share of the forests is predicted to increase further in future (Lindner et al., 2010). However, the long-term goal of sustainable forest management, a balance between growth and harvest, cannot be achieved today, especially regarding hardwoods. In 2017, an increase in forest stock of 3.5 million m³ could have hardly been balanced by commercial use and mortality of only 2.6 million m³. Additionally, the actually still predominant use of hardwood for energy purposes (70% of the hardwood harvested in 2017) is rated unfavourable by the Swiss economy, forestry agencies and federal offices.

The construction sector has been identified as an economically and climate-politically interesting option for using beech wood with its excellent mechanical properties. Numerous ongoing or completed research projects in Austria (e.g. Frühwald & Schickhofer, 2004, Hübner, 2013, Linsenmann, 2016), Germany (e.g. Glos & Lederer, 2000, Frühwald et al., 2003, Blaß et al., 2005, Westermayr et al., 2018), Slovenia (e.g. Plos et al., 2018) and Switzerland contribute to a steadily growing knowledge of the characteristics and peculiarities of this wood species with regard to its application for construction purposes.

In Switzerland, the *Swiss Federal Office for the Environment (FOEN)* launched the programme *Aktionsplan Holz*. The main objective of the programme is to ensure that wood from Swiss forests is provided, processed and recycled in a sustainable and resource-efficient manner. Resource policy thus makes a major contribution to forest,

climate and energy policy (BAFU, 2017). As part of this research and innovation programme, a project was launched in 2015 under the lead of the *Structural Engineering Research Laboratory of Empa*, in collaboration with *ETH Zurich* and the *Bern University of Applied Sciences BFH/AHB* in Biel. The aim of the project was to investigate the entire production chain of glued laminated timber (GLT) made of European beech wood, as well as to determine the mechanical properties of the product and to contribute to the implementation of the findings in relevant standards. Highly stressed columns, beams and trusses in residential, office and industrial buildings have been identified as providing the biggest potential for the application of beech GLT in load-bearing structures. The present paper gives an overview on the results of this extensive research project and shows that the GLT strength classes GL40, GL48 and GL55 targeted in the project offer the possibility to expand the currently increasing share of modern timber construction at the expense of mineral and metallic building materials.

2 LAMINATION STRENGTH GRADING

2.1 RELEVANT INDICATORS

Naturally grown wood has to be strength graded when intended to be used for structural purposes, i.e., the mechanical properties have to be estimated based on the assessment of non-destructively measurable indicators. Indicators applicable to strength grading (i) shall be highly correlated with the target parameters (strength and stiffness), (ii) shall be easily and reliably identifiable by appropriate non-destructive means, and (iii) shall be quantifiable (Ehrhart, 2019). All investigations described in the following were conducted on boards with cross-section dimensions of 160×25 mm².

2.1.1 VISUAL INDICATORS

The following visual indicators were investigated, i.e., their presence, location and dimension were documented and their influence on the tensile strength and stiffness of single laminations was evaluated:

- Knot area ratio (KAR) & total knot area ratio (tKAR) (e.g. BS 4978, 1996);
- Fibre deviation (Fig. 1a);
- Wavelike annual ring pattern (Fig. 1b);
- Redheart.

Whereas the size of knots and knot groups was quantified by means of the parameters knot area ratio KAR and the total knot area ratio tKAR respectively, the indicators fibre deviation (Fig. 1a), wavelike annual ring pattern (Fig. 1b) and redheart were only documented qualitatively. A more detailed description of the visual indicators evaluated during the strength grading process can be found in Ehrhart et al. (2016).

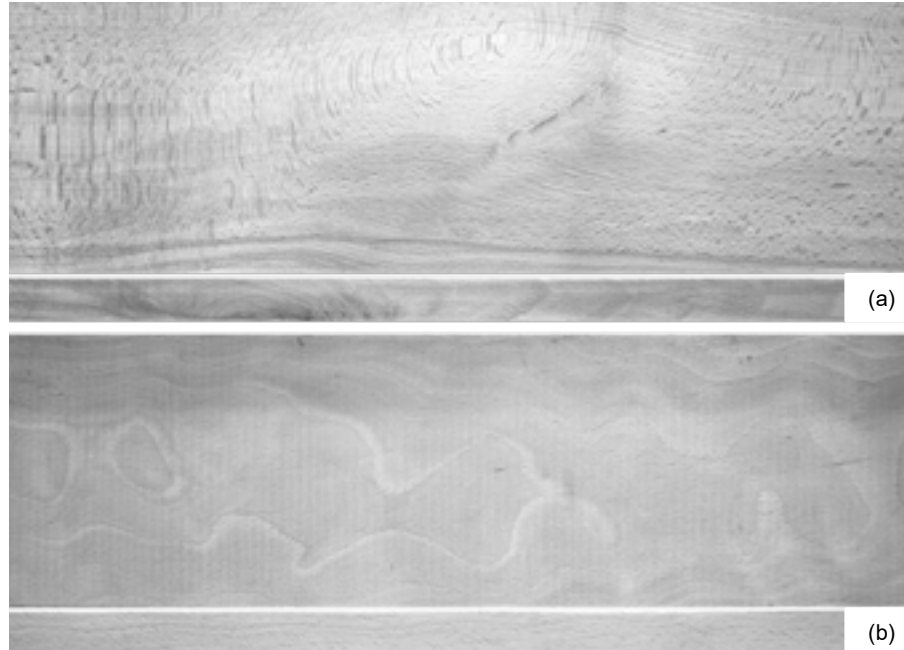


Fig. 1 Examples boards with fibre deviation (a) and wavelike annual ring pattern (b).

2.1.2 PHYSICAL INDICATORS

The bulk density (ρ) and the first natural frequency (f_0) were measured in order to be able to determine the dynamic modulus of elasticity MOE (E_{dyn}). The two devices *ViScan V2.8* (by *MiCROTEC*) and *MTG Timber Grader* (by *Brookhuis*) were used. Based on the first natural frequency f_0 , the length of the lamination l_ℓ , and the board's bulk density ρ , the dynamic MOE E_{dyn} was calculated with Equation 1. Depending on the actual wood moisture content (u), the resulting densities and dynamic moduli of elasticity were adjusted to the reference moisture content, which had been set to $u_{\text{ref}} = 8\%$ (EN 384, 2019) in this study due to the primarily intended application of beech GLT for indoor construction.

$$E_{\text{dyn}} = 4 \cdot f_0^2 \cdot l_\ell^2 \cdot \rho \quad (1)$$

2.2 VERIFICATION BY MEANS OF TENSION TESTS

Tension tests according to EN 408 (2012) were carried out on 294 European beech timber boards and the influence of the visual and physical indicators determined during the strength grading process on the tensile strength ($f_{t,0}$) and the static tensile MOE ($E_{t,0}$) parallel to the grain was evaluated. The tensile strength was calculated based on the ultimate force (F_{max}) and the lamination's width (w_ℓ) and thickness (t_ℓ) by means of Equation 2. The tensile MOE was calculated using Equation 3 based on the displacements (d) measured over a length of $l_{\text{meas}} (= 5 \times w_\ell = 800 \text{ mm})$ at force levels corresponding to 10% (F_1) and 40% (F_2) of the expected ultimate force F_{max} .

$$f_{t,0,1} = \frac{F_{\text{max}}}{w_\ell \cdot t_\ell} \quad (2)$$

$$E_{t,0,1} = \frac{l_{\text{meas}} \cdot (F_2 - F_1)}{w_\ell \cdot t_\ell \cdot (d_2 - d_1)} \quad (3)$$

The resulting tensile MOE was adjusted to the reference moisture content ($u_{\text{ref}} = 8\%$) according to EN 384 (2019). For the tensile strength, no equation for adjustment is specified in EN 384 (2019) since the tensile strength parallel to the grain is not subject to marked changes with changing moisture content (Hoffmeyer, 1995). Further information on the test setup and the applied measurement data recording system is available in Ehrhart et al. (2016).

2.3 STRENGTH GRADING CRITERIA

European beech (*Fagus sylvatica* L.) glued laminated timber: Lamination strength grading, production and mechanical properties

Based on correlation analyses, the knots, the fibre deviation and the dynamic MOE were identified to have largest influence on the target parameters tensile strength and MOE. Consistent with findings of Frühwald & Schickhofer (2004) and Aicher & Ohnesorg (2011), no significant influence of redheart was found.

Based on the analysis of the indicators relevant for strength and stiffness, criteria for the combined visual/machine strength grading of European beech timber boards into the strength grades T50, T42, T33 and T22 were developed. The criteria were calibrated based on the 294 European beech timber boards tested. In Tab. 1, the visual and physical criteria are summarised. Additional criteria regarding curvature, cracks and wane, which are mainly of importance for the production of GLT, may be adopted from DIN 4074-5 (2008).

Tab. 1 Criteria for combined visual and machine strength grading of European beech boards into strength classes T22, T33, T42 and T50.

Visual criteria	Visual grade			
	Vis. 1	Vis. 2	Vis. 3	Vis. 4
Knot and bark inclusion	tKAR \leq 0.05	tKAR \leq 0.1	tKAR \leq 0.2	tKAR \leq 0.3
Fibre deviation	Not perm.	Permitted	Permitted	Permitted
Wavelike annual ring pattern	Not perm.	Permitted	Permitted	Permitted
Redheart	Permitted	Permitted	Permitted	Permitted
Discolouration				
<i>Hardness not reduced</i>	Permitted	Permitted	Permitted	Permitted
<i>Hardness reduced</i>	Not perm.	Not perm.	$\leq 0.2 w_\ell$	$\leq 0.2 w_\ell$
Insect damage	Not perm.	Not perm.	Not perm.	Not perm.
Pith	Not perm.	Not perm.	Not perm.	Not perm.
Minimum MOE E_{dyn} (GPa)	Strength grade (based on visual grade and E_{dyn})			
Visual grade	T50	T42	T33	T22
Vis. 1	≥ 16.5	≥ 14.0	≥ 12.0	≥ 10.0
Vis. 2	-	≥ 16.5	≥ 14.0	≥ 10.0
Vis. 3	-	≥ 18.0	≥ 16.5	≥ 10.0
Vis. 4	-	-	-	≥ 15.0

The resulting 5%-fractile values of tensile strength ($f_{t,0.05}$) and mean values of MOE ($E_{t,0,mean}$) parallel to the grain for the strength grades are summarised in Tab. 2. It can be seen that the actual 5%-fractile values of tensile strength are very close to the targeted values. Further information on the correlation analyses performed when developing the strength grading rules are available in Ehrhart (2019).

It could be shown that strength grades up to T50 can be achieved with European beech timber boards when applying the visual and physical indicators presented in Tab. 1. For a better estimation of strength and a more efficient strength grading, information on the (local) fibre orientation with higher precision is necessary. However, as mentioned, e.g., by Aicher et al. (2001), Frühwald & Schickhofer (2004) and Schlotzhauer et al. (2018), so far no method for the automated detection and documentation of fibre orientation had been available for European beech wood. Hence, in the course of the project a new non-contact method for the determination of fibre direction in European beech wood, based on the analysis of the wood rays, was developed (Ehrhart et al., 2017, 2018a and 2018b). This method allows for highly accurate predictions of the fibre orientation, especially for flat-sawn and semi-rift-sawn boards. Thus, the method can contribute to a more efficient strength grading of the raw material and the implementation of strength grades even higher than T50.

Tab. 2 Mean and 5%-fractile values of lamination tensile strength ($f_{t,0,\ell}$) and MOE ($E_{t,0,\ell}$) and finger joint bending ($f_{m,j}$) and tensile strengths ($f_{t,i}$) grouped by strength grade.

Property		Symbol	Unit	T50	T42	T33	T22
Lamina tion	Number of tension tests	n	-	64	82	45	60
	Tensile strength, mean value	$f_{t,0,\ell,mean}$	MPa	90.3	71.1	61.0	47.4
	Tensile strength, 5%-fractile value	$f_{t,0,\ell,05}$	MPa	55.1	43.8	32.6	21.8

European beech (*Fagus sylvatica* L.) glued laminated timber: Lamination strength grading, production and mechanical properties

	Number of MOE measurements	n	-	43	43	19	37
	Tensile MOE, mean value	$E_{t,0,\ell,\text{mean}}$	GPa	16.8	15.4	14.4	13.7
	Tensile strength, 5%-fractile value	$E_{t,0,\ell,05}$	GPa	15.0	12.6	12.0	11.3
Finger joints	Number of bending tests	n	-	29	30	31	-
	Bending strength, mean value	$f_{m,j,\text{mean}}$	MPa	85.9	83.3	78.9	-
	Bending strength, 5%-fractile value	$f_{m,j,05}$	MPa	66.8	66.1	65.2	-
	Number of tension tests	n	-	36	46	48	-
	Tensile strength, mean value	$f_{t,j,\text{mean}}$	MPa	73.4	62.0	59.1	-
	Tensile strength, 5%-fractile value	$f_{t,j,05}$	MPa	52.2	43.7	43.5	-
	Ratio between $f_{m,j,\text{mean}}$ and $f_{t,j,\text{mean}}$	-	-	1.17	1.34	1.34	-
	Ratio between $f_{m,j,05}$ and $f_{t,j,05}$	-	-	1.28	1.51	1.50	-

3 PRODUCTION OF EUROPEAN BEECH GLT

In general, the process steps in the production of beech GLT do not differ from those for softwood GLT: Logs are sawn, the boards are dried, strength graded, finger-jointed, planed and bonded. However, in order to minimize cracking due to Eigen stresses occurring during the production process, a smaller lamination thickness (in this project: final thickness $t_\ell = 25$ mm) as well as a wood moisture content, which already during production approximately corresponds to the later equilibrium moisture content (in this project: $8 \pm 2\%$), were chosen.

3.1 FINGER JOINTING

Since being of limited length when produced in the sawmills, European beech boards are joined longitudinally by finger joints. The strength of these joints plays a central role regarding the load-bearing capacity of GLT elements, especially in components subjected to tensile stress and laminations located in the tensile zone of beams. The strength of the finger joints was investigated by researchers at the Bern University of Applied Sciences BFH/AHB in Biel. In the following, the conducted tests are briefly summarised and the main results are presented. Further information is available in Clerc et al. (2017) and Lehmann et al. (2018).

The finger-jointed specimens were produced on a production line for softwood GLT with a one-component polyurethane adhesive. The process parameters were adjusted for beech wood according to the experience of the project partner *neue Holzbau AG* (Lungern, Switzerland) in order to achieve satisfying performance of the finger joints. The cross-section dimensions of the laminations after planing were 150×20 mm². In order to get a full representation of the material quality with regard to density and dynamic MOE, the tested specimens were equally chosen from the three strength classes T50, T42 and T33. However, it was made sure that no zones with knots or with fibre deviations were located near the finger joints.

The finger joint strength was assessed by means of 90 bending tests and 130 tension tests performed according to EN 408 (2012). The bending tests were conducted displacement-controlled, the tensile tests were carried out force-controlled. In Tab. 2, the resulting bending strengths ($f_{m,j}$) and tensile strengths ($f_{t,j}$) of the tested finger joints are shown grouped by T-class. For all grades, the finger joint tensile strengths exceed the boards' tensile strengths. Further information on the test setups and the results are available in Clerc et al. (2017) and Lehmann et al. (2018).

3.2 BONDING

During the GLT production, the laminations were bonded using a one-component polyurethane adhesive and a primer, following the findings of investigations of appropriate bonding procedures conducted by the project partners *Henkel Engineered Wood Adhesives* and BFH/AHB Biel (Clerc et al., 2017). The chosen adhesive system exhibited sufficient strength in the tensile shear tests in the dry (A1) and wet state (A4) according to EN 302-1 (2013). The delamination behaviour proved to meet the requirements specified in EN 15425 (2017) when tested according to EN 302-2 (2017). Further information on the investigations of the bond line strength of European beech GLT specimens bonded with different adhesive systems and varying the production parameters can be found in Clerc et al. (2017) and Lehmann et al. (2018).

4 EXPERIMENTAL INVESTIGATIONS ON EUROPEAN BEECH GLT

The experiments on GLT specimens were carried out at Empa Duebendorf and ETH Zürich. The test programme consisted of full-scale testing of European beech GLT specimens subjected to bending, tension parallel to the grain, compression parallel to the grain and shear. In order to be able to quantify the influence of the size of the stressed volume on the mechanical properties (size effect, e.g. Weibull, 1939), the tested specimens differed not only with regard to strength class (GL40, GL48 and GL55) but also in terms of size, i.e., cross-section area and length. Thus, equations for the quantification of the size effect could be deduced from the experiments. Data analysis was conducted assuming lognormal distribution of strength and stiffness, i.e., MOE and shear modulus.

4.1 BENDING STRENGTH AND MOE

4.1.1 MATERIAL AND METHODS

Four-point bending tests according to EN 408 (2012) were performed on European beech GLT beams with heights of 200 mm (width $w = 120$ mm), 400 mm ($w = 160$ mm), 600 mm ($w = 160$ mm) and 800 mm ($w = 180$ mm). Thus, the span varied between ($18 \times 0.20 =$) 3.60 m and 14.40 m. Specimens of the strength classes GL40c (with outer 50% of the cross-sections consisting of T33 grade laminations and inner 50% of the cross-section consisting of T22 grade laminations), GL48c (T42/T22) and GL55c (T50/T33) were investigated (Fig. 2).

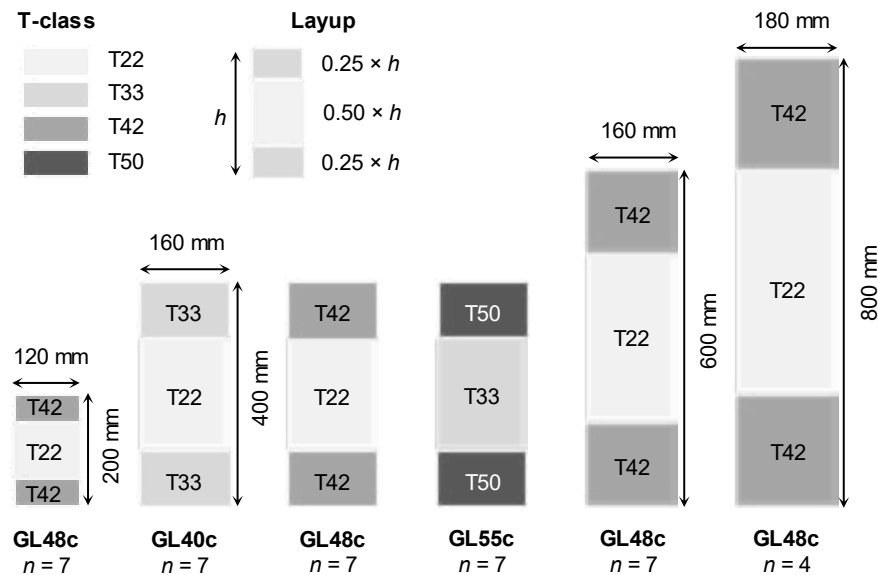


Fig. 2 Cross-section layouts, dimensions and number of the specimens investigated in four-point bending tests.

Seven specimens were tested per series. In each test, the local ($E_{m,loc}$) and global MOE ($E_{m,glob}$), and the bending strength (f_m) were determined according to EN 408 (2012). In the tests on beams with heights of 600 and 800 mm, additionally the shear modulus (G_g) was determined.

4.1.2 RESULTS AND DISCUSSION

The resulting bending strength (f_m) and local MOE ($E_{m,loc}$) determined in the four-point bending tests are summarised in Fig. 3. In the boxplots, the upper and the lower margin of the boxes are defined by the first and third quartiles. The horizontal line within the box represents the median and horizontal lines outside the box represent minima and maxima. Additionally, dots represent outliers that are located more than 1.5 times the interquartile distance above or below the box in Fig. 5.

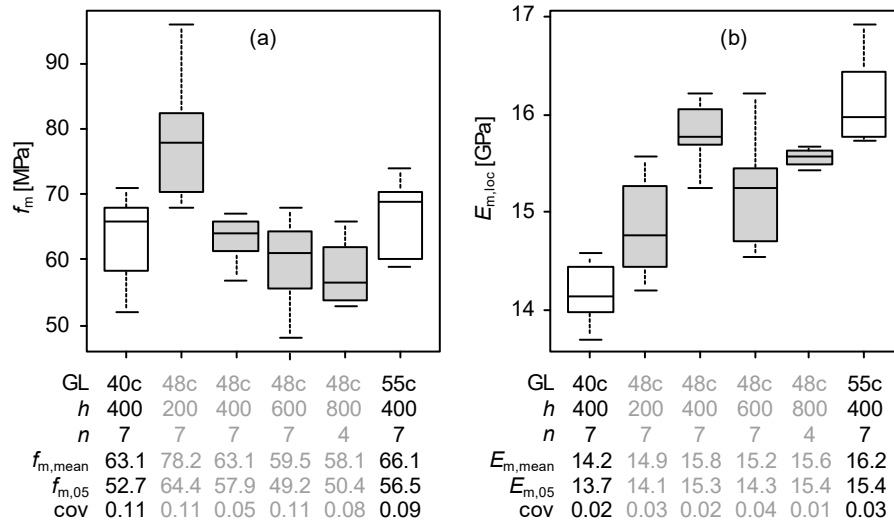


Fig. 3 Bending strength f_m (a) and local bending MOE $E_{m,loc}$ (b) of the tested GLT specimens of strength classes GL40c, GL48c and GL55c. Beam heights of 200, 400, 600 and 800 mm were investigated ($u = 8 \pm 2\%$).

Considering only the beams of strength class GL48c (boxes with grey fill), a significant decrease in strength with increasing beam height is observed (Fig. 3a). For beams with a height of 200 mm, bending strengths of up to 96 MPa were achieved. The pronounced size effect can be explained by the increasing amount of potential weak points, especially of finger joints, in the highly stressed outer zone of the beams.

When analysing the test results of the series with a beam height of 400 mm, the differences in bending strength are very small between the strength classes GL40c, GL48c and GL55c. This finding is attributed to the influence of the finger joints, which were identified as predominant cause of fracture and limiting the strength of the beams independent of the strength class. However, the test results exceeded the targeted characteristic values (5%-fractile values) of bending strength of 40 MPa, 48 MPa and 55 MPa in all strength classes.

The coefficient of variation (cov) is around 0.10 in all series, except in series GL48c / $h = 400$ mm (cov = 0.05). For softwood GLT, Brandner & Schickhofer (2008) report a cov of 0.10 - 0.20. Fink (2014) found cov of 0.14 and 0.13 for softwood GLT beams of strength classes GL24h and GL36h, respectively. In the JCSS Probabilistic Model Code (2006), a cov of 0.15 is listed for $f_{m,g}$ of softwood GLT. The smaller cov of beech GLT found in this project may be due to (i) differences in the strength grading procedures and (ii) the predominant role of the finger joint strength with respect to the bending strength of beech GLT.

Based on the experimental and additional numerical investigations (Ehrhart, 2019), the size effect in bending can be described with Equation 4 with an upper strength limit at a reference height of 400 mm. As hardly any finger joints were present in the outermost laminations of the beams with a height of 200 mm, the results of the respective test series were not accounted for when investigating the size effect.

$$f_{m,g,k} = \min \left\{ f_{m,g,k,ref} \cdot \left(\frac{400}{h} \right)^{0.14} ; f_{m,g,k,ref} \right\} \quad (4)$$

Significant differences between the strength classes can be observed regarding the bending MOE. The calculated mean values of the local bending MOE are $E_{m,loc,mean} = 14.2$ GPa (GL40c), 15.3 GPa (GL48c average over all heights) and 16.2 GPa (GL55c) and can be very well estimated based on the dynamic MOE determined during strength grading of the laminations. According to EN 384 (2019), the (local) bending MOE of softwood GLT may be calculated based on the global bending MOE by means of Equation 5. For tropical hardwoods and chestnut, Ravenshorst & van de Kuilen (2010) reported ratios between the local and global MOE of 1.16 and 1.14, respectively. Based on the results found in our project, Equation 6 was found to describe the relationship between the local and the global MOE best for European beech GLT (coefficient of determination, $r^2 = 0.88$).

$$E_{m,loc,EN384} = 1.30 \cdot E_{m,glob} - 2.60 \quad (5)$$

$$E_{m,loc,Beech} = 1.17 \cdot E_{m,glob} - 1.89 \quad (6)$$

In Fig. 4, the global and local MOE are plotted. For comparison purposes, the relation specified in EN 384 (2019) (Equation 5), the one proposed by Ravenshorst & van de Kuilen (2010) and the relation found in our experiments (Equation 6) are plotted.

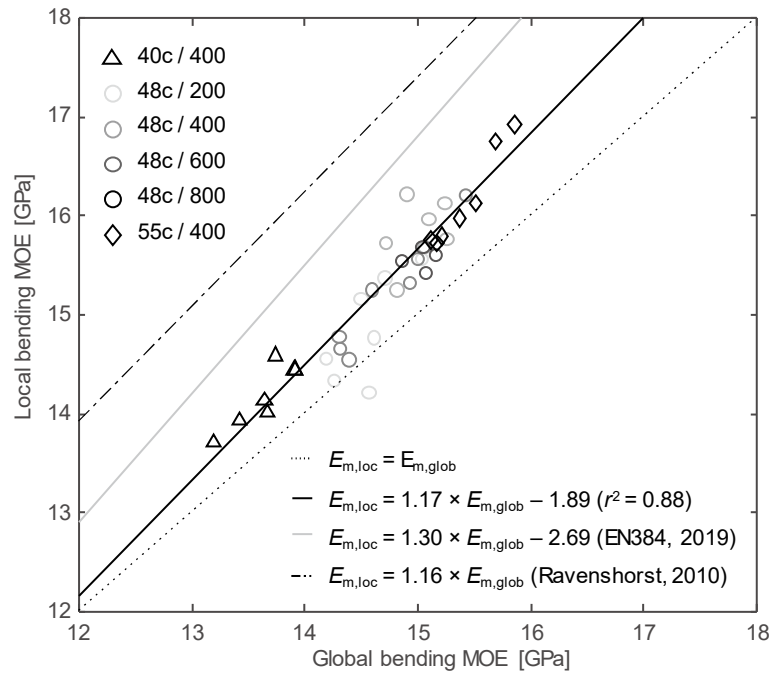


Fig. 4 Local vs. global bending MOE: Experimental data and relationship determined in the project and comparison with the relationship specified in EN 384 (2019) and the one published in Ravenshorst & van de Kuilen (2010).

4.2 TENSILE STRENGTH AND MOE PARALLEL TO THE GRAIN

4.2.1 MATERIAL AND METHODS

In order to evaluate the tensile strength parallel to the grain of European beech GLT, tests were conducted on lamination bundles. Each specimen consisted of three laminations. The cross-section dimensions were $160 \times 75 \text{ mm}^2$ and the free testing length was 3.54 m. All specimens, in each of the three laminations, contained at least one finger joint within the free testing length. For each of the target strength classes GL55h (consisting of T50 laminations), GL48h (T42) and GL40h (T33), seven specimens were tested. The tensile strength ($f_{t,0}$) and the tensile MOE ($E_{t,0}$) parallel to the grain were determined in the tests. Further information on this test series is available in (Ehrhart, 2019).

In addition, it was investigated whether tensile tests on lamination bundles are suitable for supplementing or even replacing the time-consuming and much more expensive four-point bending tests in future. In bending tests, failure predominantly occurs in the outermost, tensile-stressed laminations. By “cutting out” the highly stressed edge area of a beam and conducting a tensile test, material savings of about 95% per test would be possible.

4.2.2 RESULTS AND DISCUSSION

The resulting tensile strength ($f_{t,0}$) and tensile MOE ($E_{t,0}$) parallel to the grain determined in the tension tests on beech GLT lamination bundles are summarised in Tab. 3 grouped by strength class. The mean and 5%-fractile values of strength and MOE are listed. The characteristic values of the tensile strength of the specimens of strength classes T50, T42 and T33 exceed the target fractile values of the respective strength classes with 52.9 MPa ($> 50 \text{ MPa}$), 44.3 MPa ($> 42 \text{ MPa}$) and 36.6 MPa ($> 33 \text{ MPa}$). In EN 14080 (2013), the ratio of the characteristic tensile strength parallel to the grain and the characteristic bending strength is defined as $f_{t,0,g,k} / f_{m,g,k} = 0.8$ for GLT made of softwood and poplar. Compared to the nominal bending strengths of 55 MPa, 48 MPa and 40 MPa, ratios $f_{t,0,g,k} / f_{m,g,k}$ of 0.96 (GL55), 0.92 (GL48) and 0.92 (GL40) were found in this project, exceeding the ratio specified in EN 14080 (2013).

European beech (*Fagus sylvatica* L.) glued laminated timber: Lamination strength grading, production and mechanical properties

With a value of 15.5 GPa, the mean MOE in strength class GL48h (specimens of all beam heights considered) is only slightly higher than that of strength class GL40h (15.2 GPa). Compared to the results of the bending tests (GL48c, all beam heights: 15.3 GPa / GL40c: 14.2 GPa, Fig. 3b), the MOE determined for GL40h is above the average and the MOE determined for GL48h is representative. Amounting to 17.0 GPa, the mean MOE determined for strength class GL55h is significantly higher compared to the mean value found in the bending tests (GL55c: 16.2 GPa, Fig. 3b).

Tab. 3 Mean and 5%-fractile values of tensile strength ($f_{t,0}$, in MPa) and tensile MOE ($E_{t,0}$, in GPa) parallel to the grain determined in tensile tests on beech GLT specimens of strength classes GL55h, GL48h and GL40h with three laminations ($u = 8 \pm 2\%$).

	Symbol	GL55h = T50	GL48h = T42	GL40h = T33
Number of specimens	n	7	7	7
Tensile strength, mean value	$f_{t,0,mean}$	57.7	53.3	43.7
Tensile strength, 5%-fractile value	$f_{t,0,05}$	52.9	44.3	36.6
Coefficient of variation [-]	cov	0.05	0.09	0.10
Tensile MOE, mean value	$E_{t,0,mean}$	17.0	15.5	15.2
Tensile MOE, 5%-fractile value	$E_{t,0,05}$	16.3	14.7	13.9
Coefficient of variation [-]	cov	0.03	0.03	0.06

4.3 COMPRESSIVE STRENGTH AND MOE PARALLEL TO THE GRAIN

4.3.1 MATERIAL AND METHODS

Compression tests parallel to the grain according to EN 408 (2012) were performed on European beech GLT specimens with quadratic cross-sections of the dimensions $150 \times 150 \text{ mm}^2$, $200 \times 200 \text{ mm}^2$ and $280 \times 280 \text{ mm}^2$. The lengths of the specimens were six times the cross-section width and, thus, 900, 1200 and 1680 mm, respectively. The tested specimens belonged to the target strength classes GL55h (assembled with T50 laminations), GL48h (T42) and GL40h (T33). Each sample consisted of seven specimens.

4.3.2 RESULTS AND DISCUSSION

The mean values of compressive strengths ($f_{c,0,mean}$) are very similar in all series and lie between 58.2 MPa (GL48h/280 mm) and 65.8 MPa (GL55h/200 mm) (Fig. 5a). When comparing the strength classes GL40h ($f_{c,0,mean} = 60.4 \text{ MPa}$), GL48h (200 mm: $f_{c,0,mean} = 63.8 \text{ MPa}$), and GL55h ($f_{c,0,mean} = 65.8 \text{ MPa}$), a small (+3 to +6%) increase in compressive strength parallel to the grain for specimens of higher strength classes was determined. The analysis of the test results of the specimens of strength class GL48h with different cross-section size revealed no clear trend regarding size effect. These results correspond well with those reported by Westermayr et al. (2018). Although the majority of the beech laminations tested by Westermayr et al. were of very low quality, the authors report compressive strengths between 49.7 and 70.8 MPa ($f_{c,0,mean} = 57.0 \text{ MPa}$, $u \approx 12\%$) for the 60 specimens tested.

In addition to the high level of compressive strength parallel to the grain and the low variation of the test results, the failure behaviour is particularly noticeable. Local compression of fibres, often in zones with finger joint accumulations, local fibre deviations and knots, lead to a markedly ductile failure behaviour.

The mean value of the compressive MOE ($E_{c,0,mean}$) parallel to the grain determined on the specimens of strength class GL40h is 15.1 GPa, for specimens of grade GL48h 15.7 GPa (all geometries), and for those of grade GL55h 17.0 GPa (Fig. 5b). The marked differences in MOE between the different strength grades most likely results from the strength grading process, in the course of which the dynamic MOE – a very good indicator for the static MOE – is considered.

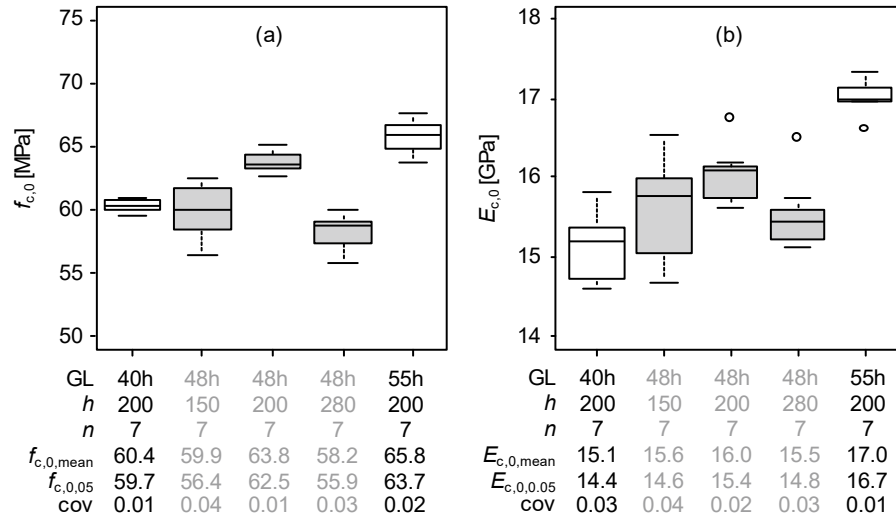


Fig. 5 Compressive strength $f_{c,0}$ (a) and compressive MOE $E_{c,0}$ (b) parallel to the grain of the tested GLT specimens of strength classes GL40h, GL48h and GL55h with cross-section dimensions of 150×150 , 200×200 and 280×280 mm² ($u = 8 \pm 2\%$).

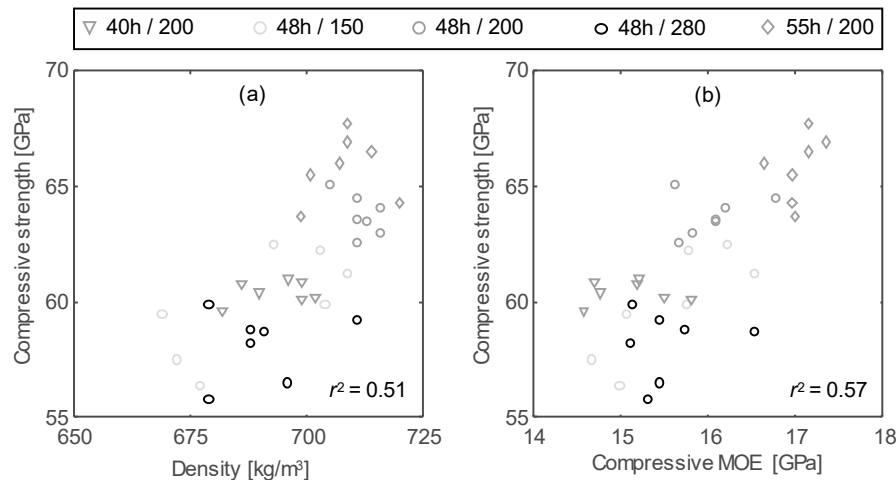


Fig. 6 Relationship between density and compressive strength parallel to the grain (a) and between compressive MOE and compressive strength parallel to the grain (b).

A coefficient of determination of $r^2 = 0.51$ was found for the correlation between density and compressive strength parallel to the grain (Fig. 6a). The correlation between the compressive MOE and the compressive strength parallel to the grain is even higher ($r^2 = 0.57$, Fig. 6b). If both the density (ρ) and the MOE ($E_{c,0}$) have been determined by any non-destructive measurement in advance, the compressive strength parallel to the grain of European beech GLT can be estimated using Equation 7 with a coefficient of determination $r^2 = 0.65$.

$$f_{c,0} = -30.2 + 8.61 \cdot \rho \cdot 10^{-2} + 2.00 \cdot E_{c,0} \cdot 10^{-3} \quad (7)$$

4.5 SHEAR STRENGTH AND MODULUS

4.5.1 MATERIAL AND METHODS

For the determination of shear strength of full-size GLT beams, to date, no harmonized test procedure and set up is available in European standards. Furthermore, according to the current version of the European standard for the design of timber structures Eurocode 5 (2010), size effects in shear are not considered, disregarding numerous

studies that confirmed the influence of the size of the stressed wood volume on the shear strength (e.g. Keenan, 1974, Longworth, 1977, Foschi & Barrett, 1980, Colling, 1986, Rammer, et al., 1996, Gehri, 2010 and Brandner et al., 2012).

In order to (i) investigate the shear strength of European beech GLT, (ii) to assess the influence of the size of the stressed wood volume on the shear strength and (iii) to evaluate the influence of the test configuration on the shear strength, three different test configurations were adopted in this project (Fig. 7). Furthermore, specimens of different sizes in terms of cross-section dimensions and lengths were tested. Specimens belonging to the strength classes GL48c and GL55c were investigated. However, aiming at reducing the probability of premature bending failures, the outermost laminations were always of strength grade T50.

Some 29 of the 42 shear tests were conducted using a short-span three-point bending test configuration with a span of 2.5 times the beam height (type 3P, Fig. 7a). This test configuration is similar to the one used by Büeler (2011) and Steiger & Gehri (2011). Glued-in steel rods were used to transfer the forces at the load application points and at the supports. As described by Steiger & Gehri (2011), accompanying compressive stresses perpendicular to the grain occur in this test configuration, contributing to an apparently higher shear strength. Beam heights of 200, 400 and 600 mm were investigated. In 24 of the above mentioned sample of 29 tests, specimens with an I-shaped cross-section were investigated in order to increase the probability of shear failures and decrease the number of bending failures (web width = $0.75 \times$ girder width, girder height = $0.20 \times$ beam height). Five specimens were tested with rectangular cross-sections ($400 \times 160 \text{ mm}^2$).

For comparative purposes, six specimens were tested with an EN 408-alike compression-shear test configuration (type EN408, Fig. 7b). The cross-section dimensions of these specimens were $200 \times 120 \text{ mm}^2$ and the length was 520 mm. Another seven specimens were tested with a newly developed asymmetric four-point bending test configuration (type 4P, Fig. 7c), which is based on a shear test configuration presented by Basler et al. (1960). Further information on all shear test setups and the measurements is available in Ehrhart et al. (2018b) and Ehrhart (2019).

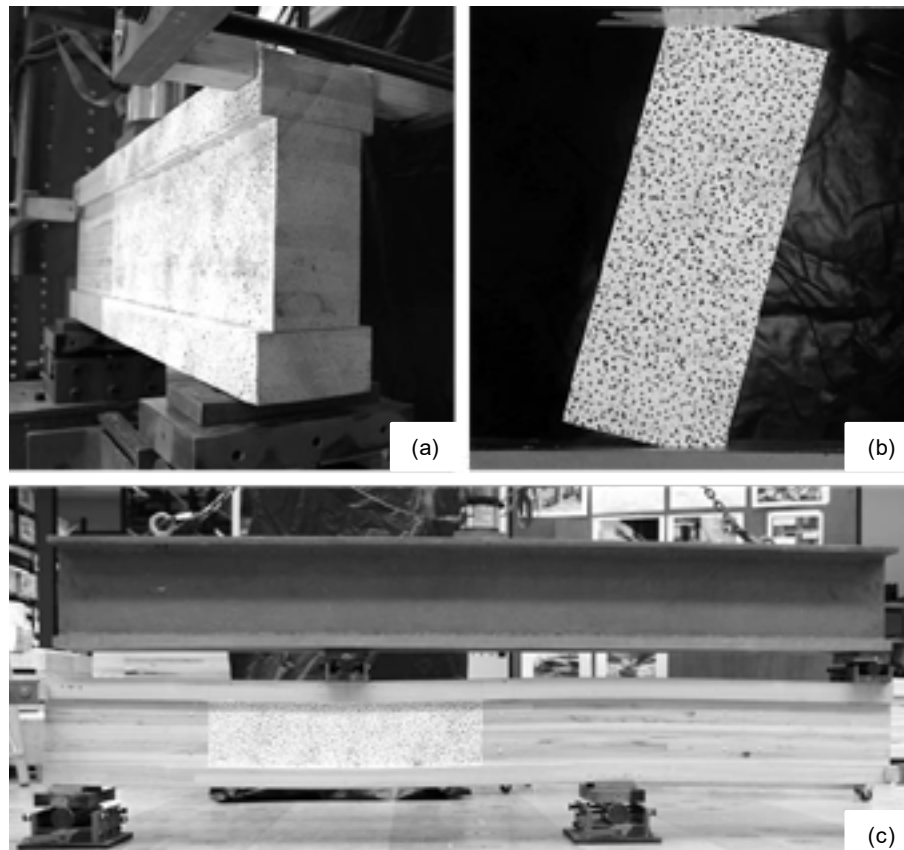


Fig. 7 Short span three-point bending test (type 3P) (a), EN 408-alike compression shear test (type EN408) (b) and asymmetric four-point bending test (type 4P) (c) in the style as presented by Basler et al. (1960).

4.5.2 RESULTS AND DISCUSSION

Not in all tests, shear failures could be achieved. Consequently, censoring of data was considered in the data analysis, following the recommendations by Steiger & Köhler (2005). In 29 of 31 tests on specimens with I-shaped cross-sections, a shear failure could be achieved (percentage of shear failures: $\eta_{\text{shear}} = 94\%$). Compared to tests by Lam et al. (1995) on softwood GLT ($\eta_{\text{shear}} \approx 40\%$) and own tests with rectangular cross-sections ($\eta_{\text{shear}} \approx 20\%$), the proportion of shear failures when using I-shaped cross-sections is much higher and thus this type of cross-section is advisable when investigating specimens with particularly high shear strength, as already recommended by, e.g., Larsen (1987) and Schickhofer (2001). In the EN 408-alike shear tests, mostly compression failures were observed. The resulting shear strengths (f_v) for the different test configurations, cross-section shapes, beam heights and strength classes are shown in Fig. 8.

Depending on the test configuration and the beam size, the shear strengths were found to be in a range of between 8 to 17 MPa. While van de Kuilen et al. (2017) reported shear strengths on a similar level ($f_{v,\text{mean}} = 13.4$ MPa, $\text{cov} = 0.12$), Aicher & Ohnesorg (2011) found much lower shear strengths ($f_{v,\text{mean}} = 6.1$ MPa, $\text{cov} = 0.19$). However, in about 50% of the tests carried out by Aicher & Ohnesorg, a bondline failure occurred, indicating that the shear strength of the used adhesive system was the limiting factor regarding the shear strength of the GLT specimen.

In agreement with the test results published by Schickhofer (2001), no significant difference in shear strength was found for the different strength classes investigated. However, digital image correlation measurements showed that failure had often been initiated in zones with local stress concentrations near knots and bark inclusions.

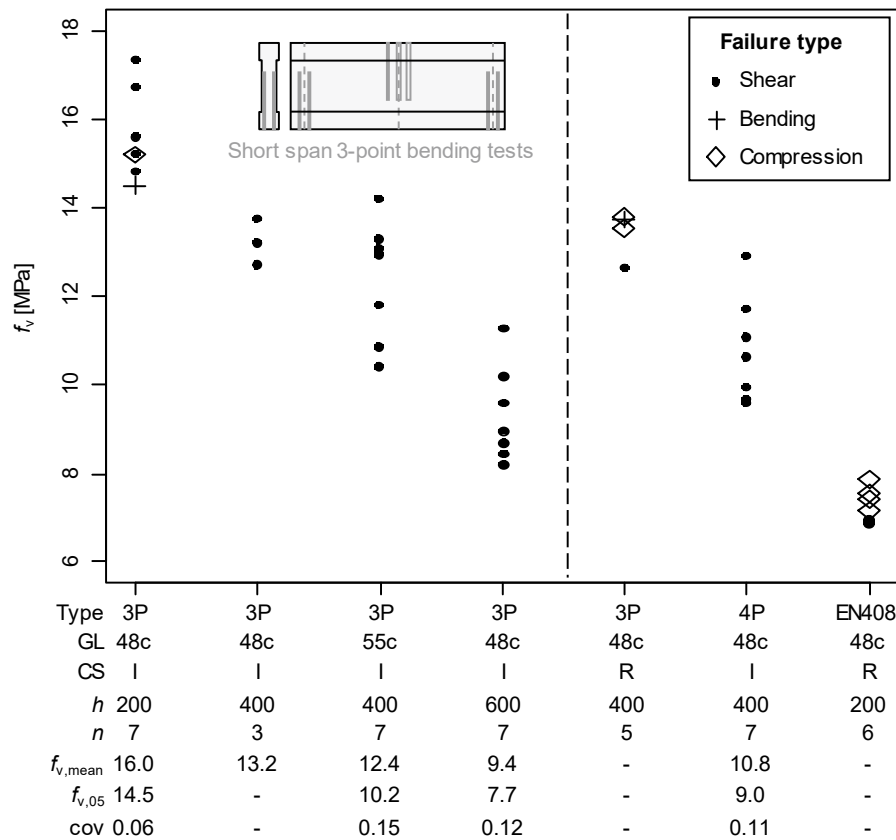


Fig. 8 Shear strength grouped by test configuration type (type), strength class (GL), cross-section type (CS) and beam height (h). Censoring of the data was taken into account when analysing the test results. The markers indicate the type of failure ($u = 8 \pm 2\%$).

A pronounced size effect was observed, i.e., for increasing beam heights, the mean and characteristic values of shear strength decrease significantly. This finding is consistent with previous studies, in which an influence of the beam height (Brandner et al., 2012), the shear area (Keenan, 1974, Gehri, 2010, Rammer, et al., 1996, Soltis & Rammer, 1994) or the beam volume (Longworth, 1977, Colling, 1986, Foschi & Barrett, 1980) on the shear strength

had been reported. Ehrhart (2019) presented a volume-based approach for the consideration of the size effect. Assuming a conservative ratio between bending and shear strength and identifying critical loading conditions, the volume based approach can be simplified to Equation 8 based on the beam height.

$$f_{v,g,k} = \min \left\{ 6.0 \cdot \left(\frac{400}{h} \right)^{0.4} ; 6.0 \right\} \quad (8)$$

In 71 shear field measurements, a mean value of shear modulus $G_{g,mean} = 1.17$ GPa and a 5%-fractile value of $G_{g,05} = 0.97$ GPa were determined (cov = 0.11). These values are 25% higher compared to the values reported by Büeler (2011). However, Büeler used beech laminations of very low quality with a moisture content of $u \approx 12\%$. In the technical approval Z-9.1-679 (2009) for European beech GLT, a mean value of shear modulus of 1.00 GPa and a 5%-fractile value of 0.80 GPa is indicated.

5 MECHANICAL PROPERTIES OF EUROPEAN BEECH GLT

Based on the experimental investigations presented in this paper and additional numerical simulations targeting the bending and tensile strength parallel to the grain (Ehrhart, 2019), the mechanical properties and densities summarised in Tab. 4 have been determined for European beech (*Fagus sylvatica* L.) GLT of the strength classes GL40, GL48 and GL55 with combined and homogeneous layups (Fig. 2). The presented values are valid for a wood moisture content of $u = 8 \pm 2\%$ and refer to a reference height of 400 mm. Size effects on the bending, tension and shear strength shall be considered using Equation 4 ($f_{m,g,k}$ and $f_{t,0,g,k}$) and Equation 8 ($f_{v,g,k}$).

Whilst the MOE in tension and compression parallel to the grain were almost identical for all strength classes GL40h (mean values of 15.2 vs. 15.1 GPa), GL48h (15.5 vs. 15.7 GPa) and GL55h (17.0 vs 17.0 GPa), slightly lower values were found for the local bending MOE (14.2, 15.3 and 16.2 GPa). However, as the range of bending MOE within strength class GL48c was between 14.2 and 16.2 GPa, these differences can rather be attributed to the natural variation of the material properties than to the type of loading. Whereas this finding is of interest in research, the differences are small and hence, the design of beech GLT structural members in practice may be based on only one MOE value which is valid independent of the loading situation. The MOE values listed in Tab. 4 additionally take into account the results of numeric simulations (Ehrhart, 2019).

Tab. 4 Mechanical properties (strength in MPa; MOE and shear moduli in GPa) and density (in kg/m³) of European beech (*Fagus sylvatica* L.) GLT of strength classes GL40, GL48 and GL55 with homogeneous and combined layups according to Fig. 2. The specified values refer to a beam height of 400 mm and a moisture content of $u = 8 \pm 2\%$.

Property	Symbol	GL strength class					
		40c	40h	48c	48h	55c	55h
Bending strength	$f_{m,g,k}$	40.0	40.0	48.0	48.0	55.0	55.0
Tension strength	$f_{t,0,g,k}$	26.0	32.0	30.0	38.4	36.5	44.0
Compression strength	$f_{c,0,g,k}$	40.0	45.0	45.0	50.0	50.0	55.0
Shear strength	$f_{v,g,k}$	6.0					
Modulus of elasticity	$E_{0,g,mean}$	14.0	14.2	15.2	15.4	16.4	16.6
	$E_{0,g,05}$	13.0	13.2	14.2	14.4	15.4	15.6
Shear modulus	$G_{g,mean}$	1.10					
	$G_{g,05}$	0.90					
Density	$\rho_{g,k}$	660					
	$\rho_{g,mean}$	690					

6 CONCLUSIONS AND OUTLOOK

In the presented study, based on extensive experimental and numerical investigations, it was shown that it is possible to produce GLT of strength classes GL40, GL48 and GL55 with homogeneous and combined layups from European beech wood. Rules for a combined visual/machine strength grading approach were developed and presented. The knot size, described by the total knot area ratio, fibre deviations and the dynamic modulus of elasticity were determined to have largest influence on the tensile strength and stiffness parallel to the grain of single

laminations. For further improving the quality of the strength estimation and in order to get a more efficient strength grading process, a non-contact method for the determination of the fibre orientation was developed within this project.

The finger-joint strength and the bondline strength and durability were tested and evaluated according to current European standards. Although these standards were developed for softwood GLT, all requirements were fulfilled using optimised adhesive systems and process parameters. Extensive experimental investigations on European beech GLT have shown that the mechanical properties are considerably higher compared to softwood GLT. Using European beech wood for structural applications allows to extend the range of GLT from currently GL32 (according to EN 14080, 2013) up to GL55 and, thus, to increase the bending, tensile, compressive and shear strength by more than 70%.

Similar to prescriptions in Eurocode 5 (2010), Equation 6 was developed to consider size effects on the bending strength of European beech GLT. However, compared to Eurocode 5 (2010), a slightly higher exponent of 0.14 (instead of 0.10) was found. Furthermore, it is suggested not to increase the bending strength for beams smaller than the reference height, but to decrease the strength of beams larger than the reference height. Additionally, Equation 8 was presented for consideration of the size effect in shear, taking into account results of this project and previous studies confirming the influence of the size of the stressed wood volume on the shear strength.

However, in addition to short-term strength and stiffness, the long-term behaviour and the influence of moisture changes must be taken into account in the design of timber structures. Eurocode 5 (2010) prescribes tabulated values for the modification coefficient k_{mod} and the deformation coefficient k_{def} in order to take into account the duration of load and the service class. Values are prescribed for solid timber according to EN 14081 (2016), softwood GLT according to EN 14080 (2013) and other engineered wood products. No information is available for hardwood GLT and experimental investigations are necessary to provide such values. Furthermore, the buckling curves prescribed in Eurocode 5 (2010) to be used for the equivalent length method were calibrated for softwood GLT. Adaptation for GLT made of European beech and other hardwood species is necessary. In Ehrhart et al. (2019), adapted curves are presented, taking into account the differences in the compression strength-to-stiffness ratios between softwood and beech wood.

ACKNOWLEDGMENTS

The authors gratefully acknowledge the funding received from the *Swiss Federal Office for the Environment FOEN* within the framework of the *Aktionsplan Holz*. Gratitude for the excellent cooperation is expressed to the Swiss sawmillers *Corbat SA*, *Konrad Keller AG*, *Richard Lötscher AG* and *Koller AG*, to the suppliers of the strength grading devices *MiCROTEC* and *Brookhuis* and to the adhesive experts of *Henkel Engineered Wood Adhesives*. Finally, the assistance of the technicians at Empa and ETH Zürich in preparing and carrying out the experiments as well as the input and support by *Holzindustrie Schweiz*, the hardwood GLT specialists of *neue Holzbau AG*, who took care of producing the GLT specimens, and the experts Prof. em. E. Gehri and M. Zimmermann are thankfully acknowledged.

REFERENCES

- Aicher S, Zachary C, Hirsch M (2016) Rolling shear modulus and strength of beech wood laminations. *Holzforschung*, 70(8), pp. 773–781. doi: 10.1515/hf-2015-0229.
- Aicher S, Höfflin L, Behrens W (2001) A study on tension strength of finger joints in beech wood laminations. *Otto-Graf-Journal*, 12, pp. 169–186.
- Aicher S, Ohnesorg D (2011) Shear strength of glued laminated timber made from European beech timber. *European Journal of Wood and Wood Products*, 69, pp. 143–154. doi: DOI 10.1007/s00107-009-0399-9.
- BAFU, BFE, SECO (Publisher) (2017) *Ressourcenpolitik Holz - Strategie, Ziele und Aktionsplan Holz* (in German). Bern, Switzerland.
- BAFU (Publisher) (2018) *Jahrbuch Wald und Holz 2018 - Umwelt-Zustand Nr. 1830* (in German). Bern, Switzerland.
- Blaß HJ, Denzler J, Frese M, Glos P, Linsenmann P (2005) *Biegefestigkeit von Brettschichtholz aus Buche*, in *Karlsruher Berichte zum Ingenieurholzbau - Band 1* (in German). Karlsruhe, Germany: Universitätsverlag Karlsruhe.
- Brandner R, Gattertnig W, Schickhofer G (2012) *Determination of shear strength of structural and glued laminated timber*. CIB - Meeting Forty-Five. Växjö, Sweden. pp. 237–254. Paper 45-12-2.
- Brandner R, Schickhofer G (2008) *Glued laminated timber in bending: New aspects concerning modelling*. *Wood Science and*

European beech (*Fagus sylvatica* L.) glued laminated timber: Lamination strength grading, production and mechanical properties

- Technology*, 42, pp. 401–425. doi: 10.1007/s00226-008-0189-2.
- Basler K, Yen BT, Mueller JA, Thürlimann B (1960) *Web buckling tests on welded plate girders*. Welding Research Council Bulletin Series.
- BS 4978 (1996) - *Specification for Visual strength grading of softwood*. BSI British Standard Institute.
- Büeler M (2011) *Schubverhalten von Brettschichtholzträgern aus Buche und Esche (in German)*. Master's Thesis, ETH Zürich.
- Clerc G, Lehmann M, Volkmer T (2017) *Brettschichtholz aus Laubholz - Technische Grundlagen zur Marktimplementierung als Bauprodukt in der Schweiz - Abschlussbericht Modul 3 (in German)*. Biel, Switzerland.
- Colling F (1986) *Influence of volume and stress distribution on the shear strength and tensile strength perpendicular to grain*. CIB - Meeting Nineteen, Volume 2. Florence, Italy. pp. 254–276. Paper 19-12-3.
- DIN 4074-5 (2008) *Strength grading of wood - Part 5 - Sawn hard wood*. DIN German Institute for Standardization.
- Ehrhart T, Brandner R, Schickhofer G, Frangi A (2015) *Rolling shear properties of some European timber species with focus on Cross Laminated Timber (CLT): Test configuration and parameter Study*. International Network on Timber Engineering Research - Meeting Forty-Eight. Sibenik, Croatia. Paper 48-6-1.
- Ehrhart T, Fink G, Steiger R, Frangi A (2016) *Experimental investigation of tensile strength and stiffness indicators regarding European beech timber*. World Conference on Timber Engineering. Vienna, Austria.
- Ehrhart T, Steiger R, Palma P, Frangi A (2018a) *Estimation of tensile strength of European beech timber boards based on the analysis of density, dynamic MOE and local fibre direction*. World Conference on Timber Engineering. Seoul, Republic of Korea.
- Ehrhart T, Steiger R, Palma P, Frangi A (2018b) *Mechanical properties of European beech (*Fagus sylvatica* L.) glued laminated timber*. International Network on Timber Engineering Research - Meeting Fifty-One. Tallinn, Estonia. pp. 343–360. Paper 51-12-4.
- Ehrhart T, Steiger R, Palma P, Gehri E, Frangi A (2019) *Compression strength and buckling resistance of glued laminated timber columns made of European beech*. International Network on Timber Engineering Research - Meeting Fifty-Two. Tacoma, USA. Paper 52-12-1.
- Ehrhart T (2019) *European beech glued laminated timber*. Doctoral Thesis, ETH Zurich.
- Ehrhart T, Steiger R, Frangi A. (2017) *Impact and detection of grain direction in European beech wood*. International Network on Timber Engineering Research - Meeting Fifty. Kyoto, Japan. pp. 479–482. Technical Note.
- Ehrhart T, Steiger R, Frangi A (2018) *A non-contact method for the determination of fibre direction of European beech wood (*Fagus sylvatica* L.)*. *European Journal of Wood and Wood Products*, 76(3), pp. 925–935. doi: 10.1007/s00107-017-1279-3.
- EN 302-1 (2013) *Adhesives for load-bearing timber structures - Test methods - Part 1 - Determination of longitudinal tensile shear strength*. CEN European Committee for Standardization.
- EN 302-2 (2017) - *Adhesives for load-bearing timber structures - Test methods - Part 2 - Determination of resistance to delamination*. CEN European Committee for Standardization.
- EN 384 (2019) - *Structural Timber - Determination of characteristic values of mechanical properties and density*. CEN European Committee for Standardization.
- EN 408 (2012) *Timber structures - Structural timber and glued laminated timber - Determination of some physical and mechanical properties*. CEN European Committee for Standardization.
- EN 14080 (2013) *Timber structures - Glued laminated timber and glued solid timber - Requirements*. CEN European Committee for Standardization.
- EN 14081-1 (2016) *Timber structures - Strength graded structural timber with rectangular cross section - Part 1 General requirements*. CEN European Committee for Standardization.
- EN 15425 (2017) - *One component polyurethane (PUR) for load-bearing timber structures - Classification and performance requirements*. CEN European Committee for Standardization.
- Eurocode 5 (2010) *Design of timber structures - Part 1-1: General - Common rules and rules for buildings*. CEN European Committee for Standardization.
- Fink G (2014) *Influence of varying material properties on the load-bearing capacity of glued laminated timber*. Doctoral Thesis, ETH Zurich.
- Foschi RO, Barrett JD (1980) *Consideration of size effects and longitudinal shear strength for uncracked beams*. CIB - Meeting Thirteen. Otaniemi, Finland. Paper 13-6-2.
- Frühwald A, Ressel JB, Bernasconi A (2003) *Hochwertiges Brettschichtholz aus Buchenholz (in German)*. Hamburg, Germany.
- Frühwald K, Schickhofer G (2004) *Strength grading of hardwoods*. World Conference on Timber Engineering - Vol. IIIb. Lahti, Finland, pp. 675–679.
- Gehri E (2010) *Shear problems in timber engineering - analysis and solutions*. World Conference on Timber Engineering. Riva

del Garda, Italy.

- Glos P, Lederer B. (2000) *Sortierung von Buchen- und Eichenschnittholz nach der Tragfähigkeit und Bestimmung der zugehörigen Festigkeits- und Steifigkeitskennwerte (in German)*. Munich, Germany.
- Hoffmeyer P (1995) *Wood as a building material, Lecture A4. In: Timber Engineering Step 1: Basis of design, material properties, structural components and joints*. Centrum Hout, Almere, The Netherlands, pp A4/1 – A4/21
- Hübner U (2013) *Mechanische Kenngrößen von Buchen-, Eschen- und Robinienholz für lastabtragende Bauteile (in German)*. Doctoral Thesis, Graz University of Technology.
- JCSS Probabilistic Model Code Part 3: Resistance Models (2006). doi: ISBN 978-3-909386-79-6.
- Keenan FJ (1974) Shear strength of wood beams. *Forest Products Journal*, 24(9), pp. 63–70.
- Van de Kuilen JWG, Gard W, Ravenshorst G, Antonelli V, Kovryga A (2017) Shear strength values for soft- and hardwoods. *International Network on Timber Engineering Research - Meeting Fifty*. Kyoto, Japan. pp. 49–65. Paper 50-6-1.
- Lam F, Yee H, Barrett JD (1995) Shear strength of Canadian softwood structural lumber. *CIB - Meeting Twenty-Eight*. Copenhagen, Denmark. pp. 118–134. Paper 28-6-1.
- Larsen HJ (1987) Determination of shear strength and strength perpendicular to grain. *CIB - Meeting Twenty*. Dublin, Ireland. pp. 155–160. Paper 20-6-3
- Lehmann M, Clerc G, Lehringer C, Strahm T, Volkmer T (2018) Investigation of the bond quality and the finger joint strength of beech glulam. *World Conference on Timber Engineering*. Seoul, Republic of Korea.
- Lindner M, Maroschek M, Netherer S, Kremer A, Barbati A, Carcia-Gonzalo J, Seidl R, Delzon S, Corono P, Kolström M, Lexer MJ, Marchetti M (2010) Climate change impacts, adaptive capacity, and vulnerability of European forest ecosystems. *Forest Ecology and Management*, 259(4), pp. 698–709. doi: 10.1016/j.foreco.2009.09.023.
- Linsenmann P (2016) *European hardwoods for the building sector (EU Hardwoods) – Final report*. Available at: <http://eu-hardwoods.eu>.
- Longworth J (1977) Longitudinal shear strength of timber beams. *Forest Products Journal*, 27(8), pp. 19–23.
- Plos M, Fortuna B, Straze A, Turk G (2018) *Visual Grading of Beech Wood - a Decision Tree Approach*. *World Conference on Timber Engineering*. Seoul, Republic of Korea.
- Rammer D, Soltis L, Lebow P (1996) *Experimental shear strength of unchecked solid-sawn Douglas-fir*. *Forest Service - Research Paper FPL-RP-553*.
- Ravenshorst G, van de Kuilen JWG (2010) Relationships between local, global and dynamic modulus of elasticity for soft- and hardwoods. *CIB - Meeting Forty-Two*. Duebendorf, Switzerland. Paper 42-10-1.
- Schickhofer G (2001) Determination of shear strength values for GLT using visual and machine graded spruce laminations. *CIB - Meeting Thirty-Four*. Venice, Italy. pp. 383–409. Paper 34-12-6.
- Schlottzauer P, Wilhelms F, Lux C, Bollmus S (2018) Comparison of three systems for automatic grain angle determination on European hardwood for construction use. *European Journal of Wood and Wood Products*, 76(3), pp. 911–923. doi: 10.1007/s00107-018-1286-z.
- Soltis L, Rammer D (1994) Shear strength of unchecked glued-laminated timber beams. *Forest Products Journal*, 44(1), pp. 51–77.
- Steiger R, Gehri E (2011) Interaction of Shear Stresses and Stresses Perpendicular to the Grain. *CIB - Meeting Forty-Four*. Alghero, Italy, pp. 135–149. Paper 44-6-2.
- Steiger R, Köhler J (2005) *Analysis of censored data - examples in timber engineering research*. *CIB - Meeting Thirty-Eight*. Karlsruhe, Germany. Paper 38-17-1.
- Weibull W (1939) *A statistical theory of the strength of materials*. Royal Technical University, Stockholm, Sweden.
- Westermayr M, Stapel P, Van de Kuilen JWG (2018) Tensile and Compression Strength of Small Cross Section Beech Glulam Members. *International Network on Timber Engineering Research - Meeting Fifty-One*. Tallinn, Estonia. pp. 307–322. Paper 51-12-2.
- Z-9.1-679 (2009) *Allgemeine bauaufsichtliche Zulassung für BS-Holz aus Buche und BS-Holz Buche-Hybridträger*. Studiengemeinschaft Holzleimbau eV. DIBt Deutsches Institut für Bautechnik.

Yield optimization and surface image-based strength prediction of beech

A. Khaloian Sarnaghi^{1*}, A. Rais^{1,2}, A. Kovryga¹, W. F. Gard³, J.W.G. van de Kuilen^{1,3}

¹Chair of Wood Technology
Technical University of Munich
Munich, 80797, Germany

²Chair of Forest Growth and Yield
Science, Technical University of
Munich, 85354, Germany

³Faculty of Civil Engineering and
Geosciences, Delft University of
Technology, Delft, Netherlands

ABSTRACT

Wood is a strongly anisotropic and heterogeneous material with natural defects that are affecting the uniform scatter of the fiber patterns. European beech (*Fagus sylvatica*) is the species, used for this study. The logs of these species have generally complicated shapes with frequent curvatures, which is in contrast to most of the softwood species with relatively straight log shapes. From structural point of view, these species have fewer knots and natural features, but stronger fiber deviations compared to different softwood species that have complicated knot configurations. This study consists of two parts: 1) log reconstruction and optimization of the cutting pattern, and 2) board reconstruction and strength prediction. Due to the complex structural pattern of hardwoods, the visual grading method is a relatively weak strength predictor for these species. The aim of this study is to develop a numerical method based on the finite element (FE)-analysis to provide a better prediction for the tensile strength of the boards. The analysis covers the scatter of 200 beech boards. By resembling the tensile test setup numerically, the stress concentration factors (SCFs) are calculated, considering the average and maximum stresses around the imperfections. SCFs in combination with the longitudinal stress wave velocity are the numerical parameters, used in the nonlinear regression model for tensile strength prediction. The nonlinear model is checked for different combinations of the numerical parameters to estimate and visualize the potential of the virtual predictions. Performance of the novel criteria is compared to the typical grading criteria (knottiness and the dynamic MoE (MoE_{dyn})), and is shown that the coefficient of determination is higher, when using the virtual methods for tensile strength predictions.

1. INTRODUCTION

Due to easier accessibility and sustainability of beech hardwood in central Europe, as well as its higher strength and durability in engineering applications, the interest of the market for this species, and its usage in different studies and applications are being increased. It needs to be remarked that beech logs have generally strong frequent curvatures that affect their yield. Therefore, the aim of this study is to optimize the yield of the straight boards out of shorter logs initially, and to virtually predict the tensile strength of the beech boards later. Therefore, two separate numerical steps are the focus of this study, giving us the opportunity to 1) reconstruct and analyse the complex beech logs and predict their yield based on point clouds, and 2) to reconstruct beech boards with detailed consideration of the knots on the basis of their surface images and to predict the tensile strength.

In case of the log reconstruction (first step of this study), 3D X-ray and CT-scanning are making it possible to analyze the surface, as well as its internal features. This allows extracting the optimized yield of the logs to categorize timber boards for different applications. Internal features in logs, such as knots and cracks and their effects on yield has been studied previously (Steele et.al. 1993, Bhandakar et.al. 2006, Boukadida et.al. 2012). Additionally, an automatic algorithm has been provided for the geometrical recognition of the knots (Longuetaud et.al. 2004, 2012). Therefore, logs with strong geometrical non-uniformities can be reconstructed in order to predict the possible yield and to reduce the waste of the material for engineering applications. In case of the board reconstruction (second step of this study), consideration of the natural features with their comprehensive geometrical representation including the angle of rotation, shape and the coordinate directions in the bulk material helps for better strength predictions. These natural features (knots) influence the fiber pattern in wood, which correspondingly affect the global stiffness direction along

* Ani Khaloian Sarnaghi: Tel.: +49 89 2180 6716; E-mail: sarnaghi@hfm.tum.de

the boards and finally the strength of the material. As knots are the main strength governing parameters, numerical methods with more accurate geometrical reconstruction of the knots may be an alternative method to improve the strength prediction of the material. Different studies focused on the structural modelling of wood and predicting the strength reduction and failure, resulting from structural non-uniformities (Goodman and Bodig 1980; Phillips et al. 1981; Cramer and Goodman 1986; Foley 2001; Baño et al. 2010; Jenkel and Kaliske 2013; Hackspiel et al. 2014; Lukacevic and Füssl 2014). The basis of most of these models is a 2D flow-grain analogy (Goodman and Bodig 1978; Foley 2001), which is extended for the 3D case here to consider the vector component in the third direction as well (Khaloian et al. 2017).

As higher stresses are developing around the geometrical non-uniformities, stress concentration factors around knots (Khaloian and Van de Kuilen 2019a) as well as the stress wave velocity in the boards (Khaloian and Van de Kuilen 2019b) are multiple parameters that are used in this study for prediction of the strength of beech boards. These are the main parameters that are influenced by the natural features in timber. Small and linear dislocation of the elements due to the small impact of the stress wave, especially over the knot boundaries, is the main reason for reduction of the velocity of the wave, when traveling forth and back through the board.

2. MATERIALS AND METODS

2.1. GENERAL

European beech (*Fagus sylvatica*) is the species, used for this study. The temporal experimental plots are located in the low mountain region Spessart in the north of Bavaria. In total, 16 different stands in two different Bavarian forest enterprises are selected in order to find appropriate beech trees. Altogether, 100 sampled beech trees are equally contributed to one of the five following stand types: pure beech stand and mixed stands of beech with Douglas-fir, Norway spruce, oak and pine. A number of 50 samples are randomly selected for the numerical analysis. The age of the sampled stands and trees ranges from 80 to 140 years.

The site conditions are assumed to be constant as the source rocks are sandstone of similar properties and these rocks developed to brown earths. In the same way, climate with temperature and precipitation is assumed to be comparable for all stands as well.

The logs have been sawn to boards when the top diameter was at least about 230mm without bark. Logs have been sawn using a band saw. It was tried to get as many center-boards as possible with the preferred cross-section of 50mm×150mm (discussed later). From the outer parts of the stems, side-boards of smaller cross-section (40mm×80mm) were cut out (Rais et al. 2018).

The roundwood was scanned with a Riegl LMS-Z420i laser scanning system. Selected and virtually reconstructed 50 logs of 4.1 m in this study cover diameters between 250-660 mm. The shapes of the logs are covering a scatter, including logs with strong frequent curvatures in different coordinate directions (shown in Figure 1), and the logs with relatively straight shapes.

In the second step of this study, for the geometrical reconstruction of the boards and their strength predictions, 200 lower quality beech boards with up to 22 knots are used for the numerical analysis. All beech boards that are numerically reconstructed in this study are tested in tension (EN 408 (2010)), and the strength values (presented as average in Table 1) are used for the validation of the model. Additionally, the visual grading parameters (DEB, DAB) are provided in an average form in Table 1, which represent the knot parameters and are later used for validation of the extracted virtual knot parameters.

Table 1: Material and mechanical properties of the boards used for the simulations

Species	PK	Length (mm)		Thickness (mm)		Width (mm)		Strength (Mpa)		Density (Kg/m ³)		MoE _{static} (MPa)		DEB (-)		DAB (-)		
		avg.	CoV	avg.	CoV	avg.	CoV	avg.	CoV	avg.	CoV	avg.	CoV	avg.	CoV	avg.	CoV	
Beech	Beech1	100	3102	0.003	24	0.01	151	0.003	31	0.43	758	0.05	11100	0.18	0.18	0.55	0.20	0.61
	Beech2	100	3102	0.002	24	0.01	100	0.002	34	0.44	773	0.05	11300	0.24	0.21	0.55	0.24	0.59

2.2. LOG AND BOARD RECONSTRUCTION

For estimation of the yield, the geometrical model of the logs are reconstructed virtually. This process is done based on the observed point clouds from the laser scanning of the logs. An example of a geometrical configuration of a beech log is shown in Figure 1 and is compared to a spruce log. It is qualitatively shown in this figure that the beech log has

strong geometrical non-uniformities with frequent curvatures, whereas the spruce one has a relatively straight shape. Therefore, yield may be strongly influenced by the shape of the logs, especially when the length of the boards is the point of interest.

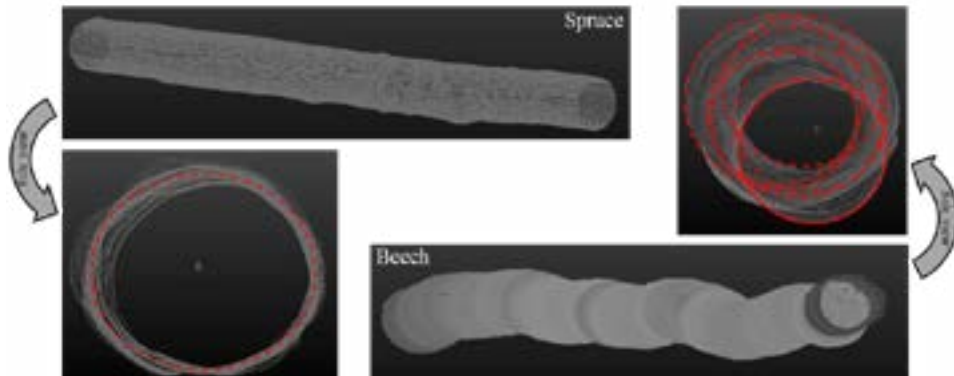


Figure 1: Comparison of log curvature of spruce and beech (the red circles on the side view of the samples help to understand how strong the curvature is)

The side view of the spruce log in Figure 1 has a more uniform geometrical shape, close to a circle that makes it possible to cut longer straight boards. However, in the case of the beech log, multiple circles can be seen in the cross-section of the log, which show the strong curvatures of the structure.

After approximating the surface normals for the reconstruction of the surface of the log and applying the mesh algorithms, the surface is reconstructed with a relatively fine mesh. Dense points are giving the opportunity for the reconstruction of the curved and non-smooth surfaces in this case.

Normals are computed as a weighted product over the nearest neighbors, after finding the tangential planes by computing the centroid of each vertex as the average of all nearest neighbors. Poisson Surface Reconstruction and the Ball Pivoting algorithms are used for the surface reconstruction in this study. Poisson reconstruction is a global solution that considers all the data at once in contrast to many implicit surface fitting methods that segment the data into regions for local fitting. Thus, the data noise is visible in this formulation. However, Poisson reconstruction can create smooth surfaces that robustly approximate noisy data (Kazhdan et.al. 2006).

The second meshing algorithm that is used in this study is the Ball Pivoting algorithm. By combining the points, got from the laser scanning, and after interpolating the given point cloud, this algorithm computes a triangle mesh for the structure. The principle of this method is that a ball of a user specified radius, ρ , pivots between the points and if it touches the three points without containing any other point, these three points form a triangle. Therefore, in this method the edges are being constructed by pivoting the ball from one sample point to the others. This process is continuing until the time when all the points are considered (Bernardini et.al. 1999). When the sampling density of the points are too low, some of the edges are not being created and this causes formation of holes in the structure during the reconstruction process.

The way that the whole log reconstruction process works in this study as well as the required file formats during this process are presented in Figure 2.

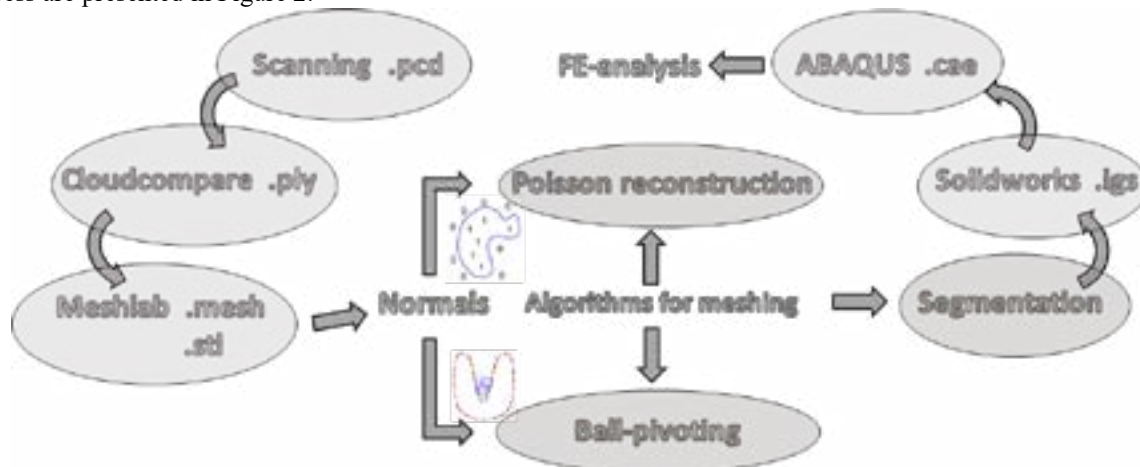


Figure 2: Flowchart, showing the process of the log reconstruction

Cutting process in this study is done solely by considering the curvature of the logs, without considering the effect of the internal features on the quality of the boards (invisible), i.e. the outermost points on the log surface are considered as boundaries that are limiting the cutting pattern. Information about the bark (thickness), the defects, etc. is not extractable from the point clouds. Due to the complex geometrical configuration of the beech logs, different cutting patterns need to be taken into account to optimize yield. This includes especially the length and the width effects. Therefore, initially an unstructured mesh is being created by considering all different cutting configurations and then the unnecessary cuts are being deleted to come to the optimized number of the predictions (Figure 3).

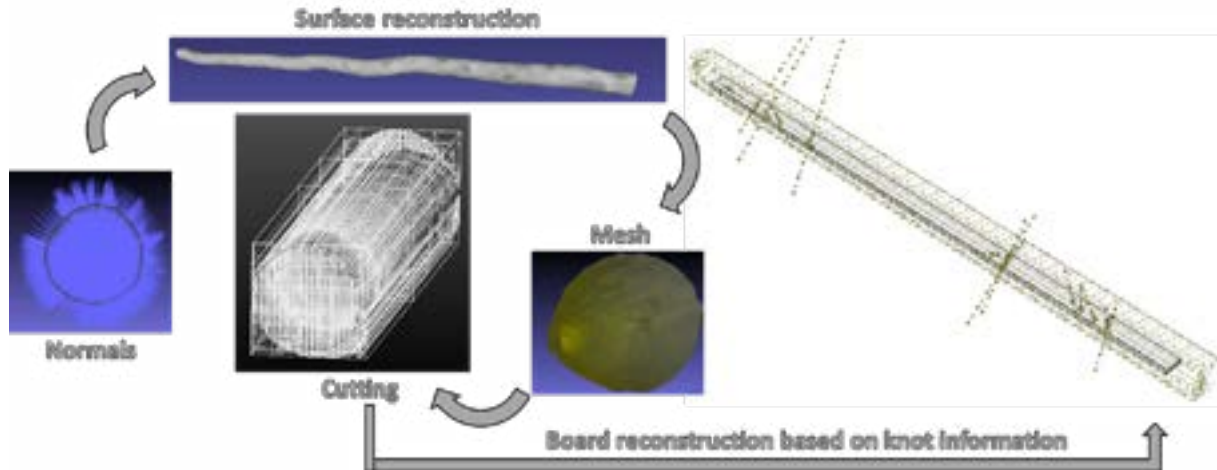


Figure 3: Surface reconstruction, mesh generation, cutting pattern and board reconstruction with knots

In the second step, a comprehensive geometrical model of the boards is reconstructed based on the surface information of the knots from the visual grading. For each knot, separate axis of rotation and plane is defined, to represent the complete geometry of the knots based on the location of the pith. The reconstructed surface of the log, the generated mesh, considering different board configurations with different dimensions and the reconstructed board are presented in Figure 3. It is shown in Figure 3 that if CT-scan is used for the scanning of the logs, the reconstruction from log to boards can be done almost automatically. Laser-scanning in this study provides the surface information of the logs, thus the information about the boards can not be extracted from the logs directly. Therefore, this process is done in two steps here (as explained before).

2.3. CASE ANALYSIS

In total, 30 beech logs are chosen for the validation of the numerical procedure. The beech logs are chosen randomly from the mixture of beech-pine and beech-Douglas fir stands. As mentioned before, the logs have been cut in the sawmills to the boards of $40*80*4000 \text{ mm}^3$ and $50*150*4000 \text{ mm}^3$. To be able to be comparable to the actual conditions, similar procedure is used for the numerical analyses as well. Saw thickness of 5 mm is considered for the analysis, which is implemented numerically by distancing the boards from each other.

In order to do the sensitivity analysis for the model, and as virtual cutting gives the opportunity to analyze different configurations, four different configurations are considered here for the reference samples, and the results are compared to the real values, obtained from the saw mills. The four configurations are as follows:

- Case1: If only boards of small dimensions ($40*80 \text{ mm}^2$ cross-section) are extracted from the logs
- Case2: If only boards of big dimensions ($50*150 \text{ mm}^2$ cross-section) are extracted from the logs
- Case3: If as many boards are extracted from the logs, regardless of the dimensional aspects. Therefore, it is possible to extract more boards of smaller dimensions and fewer boards of bigger dimensions.
- Case4: Similar to the real condition, to extract as many center-boards of bigger dimension first as possible and then to extract smaller boards from the rest of the log volume.

Each of the above mentioned cases are analyzed separately and are compared to the actual condition (similar to Case4 configuration).

2.4. SET-UP OF CUTTING PATTERN FOR CURRENT STUDY

In the current study, 20 extra logs have been selected to analyze the dimensional effects. These logs represent the scatter of the curvatures and diameters of the beech logs. By running totally 540 analyses (to analyze the four Cases, explained before), considering 27 board configurations (shown in Table 2) for each of the 20 logs, the dimensional effects are analyzed on the yield. Similarly, a sawing thickness of 5 mm is implemented for this set of the simulations as well.

Table 2: Dimensions of the boards

	Thickness (mm)	Width (mm)	Length (mm)
Log	20	80	2000
		120	3000
	25	80	2000
		120	3000
	30	80	2000
		120	3000

3. RESULTS AND DISCUSSION

3.1 CASE AND SENSATIVITY ANALYSIS

For all above mentioned cases (1-4), the correlation is found (in Table 3) with the number and the volume of the boards that are extracted from the logs in reality (a case similar to Case4). As the focus of this part is to analyze how sensitive the model is, when considering a different cutting pattern than the one applied in the reality, this correlation analysis is performed. Case1 and Case2 are considered the extreme limit conditions of these analyses, by including boards with only small or big cross-sections.

Table 3: Correlation between the actual and virtual number of the boards and their volume

y=ax+b							
Number of boards (actual-virtual)	a	b	R ²	Volume of boards (actual-virtual)	a	b	R ²
Case1	0.498	-0.29	0.87	Case1	1.071	0.03	0.89
Case2	1.107	0.69	0.83	Case2	1.046	-0.01	0.90
Case3	1.012	-0.89	0.84	Case3	1.013	0.04	0.94
Case4	1.001	-1.38	0.96	Case4	0.955	-0.03	0.94

By knowing the real log volume in each case, the yield (in percent) is calculated (k) using the following equation:

$$k = \left(\frac{V_{boards}}{V_{real_log}} \right) * 100 \quad (1)$$

where V_{board} is the total volume of the extracted boards from the log, and V_{real_log} is the total volume of the log.

3.2. VALIDATION OF THE MODEL FOR THE TEST SAMPLES

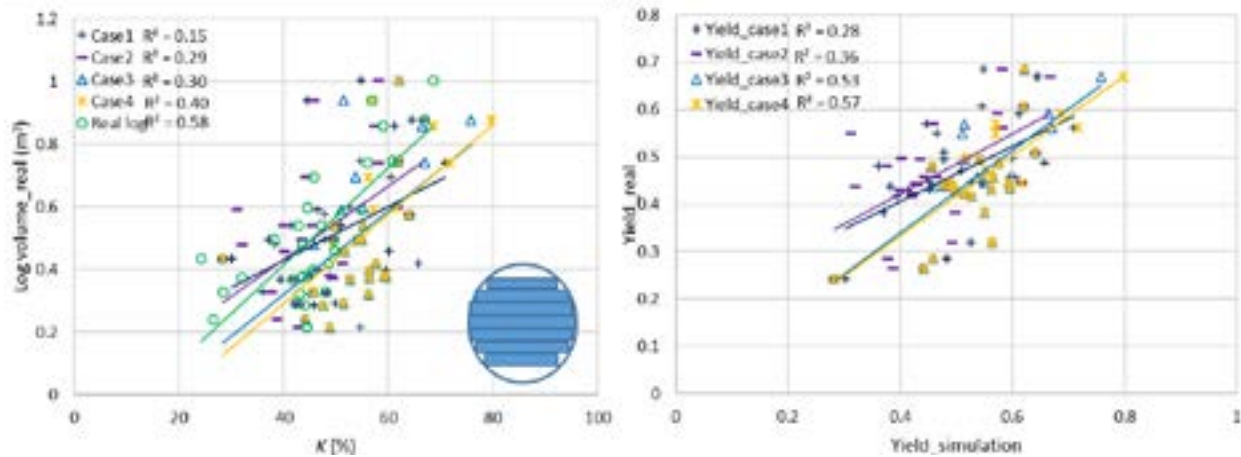
By correlating the total number of the virtual boards with the real boards, a R^2 value of 0.96 is obtained, showing the high accuracy of the virtual procedure (shown in Table 3).

The k value is calculated for the four mentioned cases as well as the real case of the sawn boards. By considering the average percentage of k , case1 model gives 7.6% increase in volume usage compared to the real case, case2= 0.9%, case3= 17% and case4=19.5% increase respectively. This shows that case2 model with only big boards has the lowest yield. However, by optimizing the cutting pattern, in total 19.5% increase in yield can be expected, neglecting the quality of the boards. As mentioned before, this increase may be due to the lack of information about the quality of the log, the location of the bark, the knots and the defects and correspondingly, consideration of the outermost points of the

logs for the analysis. Therefore, as virtual board extraction is done based on the maximum volume of the logs, yield may be slightly overestimated numerically. A comparison between the virtual k value of each case and the real (total) log volume is presented in Figure 4.

The correlation between k and the V_{real_log} in the real case is $R^2=0.58$ (shown in Figure 4). This correlation reduces during the sensitivity analysis from Case4 to Case1, as the volume of the boards that are being extracted from the logs in each case is reducing respectively (based on equation 1 and as shown in Table 3).

By correlating the yield of each of four cases to the real yield of the log ($Y=k/100$), Case4 is found to be the optimized condition, with higher R^2 value (presented in Figure 4).



y=ax+b							
Log volume-k	a	b	R^2	Yield _{real} -Yield _{simulation}	a	b	R^2
Case1	0.009	0.08	0.15	Case1	0.583	0.17	0.28
Case2	0.012	-0.04	0.29	Case2	0.637	0.17	0.34
Case3	0.013	-0.21	0.30	Case3	0.873	-0.01	0.53
Case4	0.014	-0.28	0.40	Case4	0.85	-0.01	0.57
Real log	0.016	-0.21	0.58				

Figure 4: Relation between actual and virtual log volumes and yield. Coefficients of the linear correlation and the resulting R^2 values are shown under each figure.

The correlation is much lower in Case1 and Case2 models. This confirms that an optimum mixture of the small- and big-sized boards needs to be considered to be able to increase the yield.

3.3. VIRTUAL CUTTING AND DIMENSIONAL EFFECTS

As the focus in this part of the study is to analyze the length effects, boards with lengths of 2, 3, and 4 m are cut from logs of 4.1 m length. The number of the boards, in case of cutting directly 4 m long boards and deviding them to half, or cutting directly 2 m long boards from the log, has been analyzed. This case was checked for the boards with 20, 25, 30 mm thickness and 80, 120, and 160 mm width, respectively. The results are shown in Figure 5. To show how the length of the boards may affect the volume and the yield, a schematic presentation of the cutting is provided in Figure 5 as well, for straight and curved logs. Similar analyses are performed to figure out the width effects (for the boards of 80 mm or 160 mm width). It is shown that among the coordinate dimensions of the beech boards, length has the main effect on the yield of the logs. This is due to the strong curvatures and geometrical non-uniformities of beech logs. Therefore, cutting shorter boards (2m) in comparison to the longer ones (4m) results in a 15.5% increase in the yield. The difference between the number of the boards in cases of cutting 3m or 4m boards is negligible, due to the strong curvature of the logs. However, the board thickness and the width do not have considerable effects on the number of the boards, extracted from the log and correspondingly the volume and the yield. By comparing the total number of the boards with width of 80 mm to the ones with width of 160 mm, an increase of 1.5% is obtained, when cutting smaller boards.

As the thickness of 20, 25, and 30mm are considered in this project, it is difficult to make a clear conclusion about the influence of the thickness of the boards on the yield of the material. However, as generally a mixed cutting pattern is used (similar to the logs in this study, where boards with bigger dimensions are cut first from the center and then smaller boards from the rest of the material), an assumption can be made that the thickness of the boards, similar to the width effects, does not have a significant influence on the yield of the material.

Therefore, by considering the economic costs and aspects, the dimensional effects can be neglected in straight logs in contrast to the logs with curvatures.

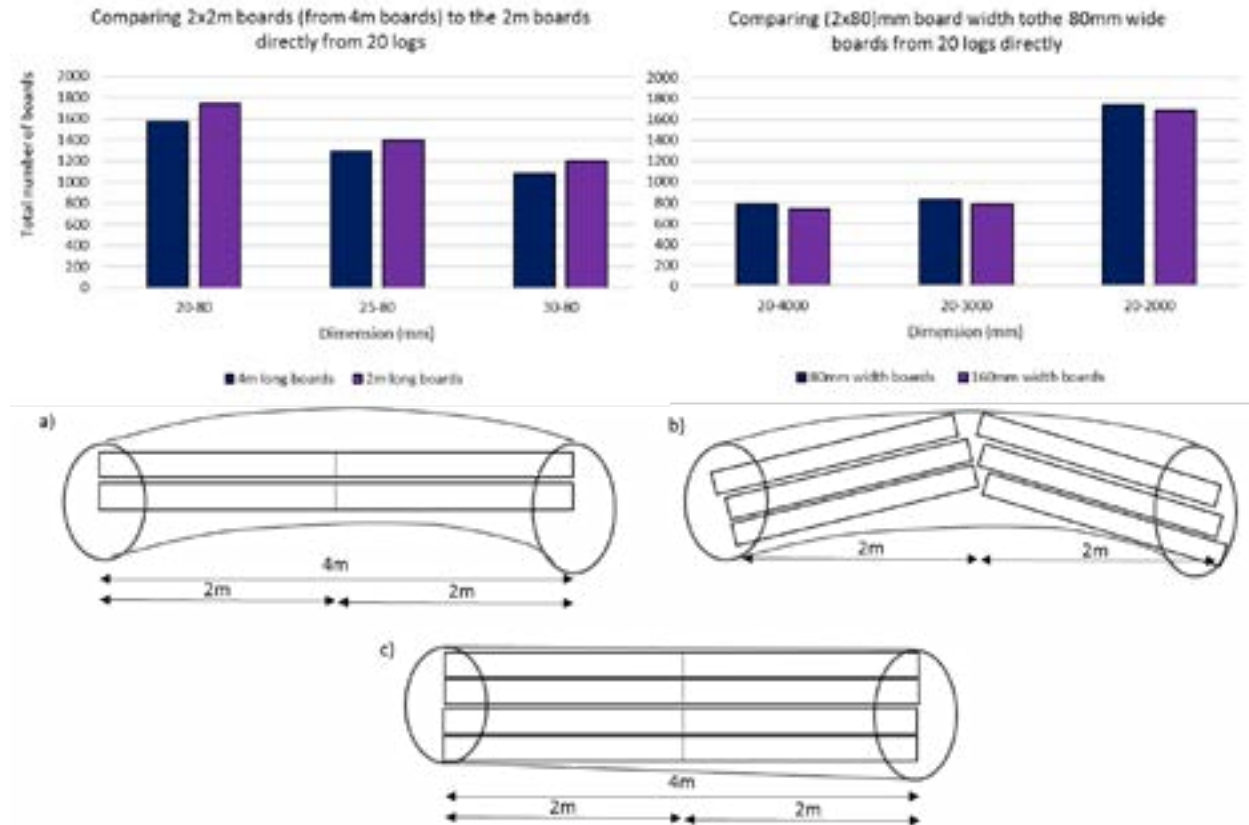


Figure 5: Comparison between 2m and 2x2m boards as well as 80mm and 2x80mm wide boards. a,b) Representation of an exaggerated view of a curved log with the boards, and c) is a schematic view of an example straight log

3.4. VIRTUAL STRENGTH PREDICTION

As knots are the main causes of the geometrical non-uniformities in wood, the stress distribution and the stress wave velocity do not remain constant through the board. By considering the single and multiple effects of the maximum and average stresses that are developing around the knots (SCF_i) as well as the velocity of the stress wave, when passing through the knots, four material parameters are introduced to predict the strength of the material virtually (Khaloian and Van de Kuilen 2019a,b).

In order to reduce the dependency of the numerical simulations on the input parameters, the average density of beech samples ($\rho=760 \text{ kg/m}^3$) is used as an input parameter for the density.

By running the numerical analysis for about 200 lower quality beech boards with strong fiber deviations, it is shown that due to the strong geometrical complexity of beech boards, MoE_{dyn} is not enough as a single parameter for strength predictions ($R^2=0.5$ compared to $R^2=0.4$ for tests and simulations, respectively). Knot factors and their geometrical representations and effects on the development of the stresses are playing an important role as well for the strength prediction of the lower quality boards (Figure 6).

When comparing only the simulated knot parameters based on the stress developments under tensile loading (SCF_1 , SCF_2 and SCF_3) to the measured knot parameters from visual grading (DEB, DAB), significant improvements are seen in the quality of the predictions based on the numerical parameters ($R^2= 0.54$ compared to $R^2= 0.15$).

By performing a nonlinear multiple regression analysis between the numerical and test parameters with the tensile strength, mathematical equation 2 is given.

$$f = \sum_{i=1}^n a_i \cdot e^{b_i \cdot SCF_i} + c \cdot MoE_{dyn} + d \quad (2)$$

Where: n is the number of the SCFs required for the strength predictions, SCF_i are the stress concentration factors, presented above. The parameter f is the tensile strength, MoE_{dyn} is the dynamic modulus of elasticity, and a, b, c, d, e are the constants, provided in Table 4.

Table 4: Coefficients of Equation 2

	a_1	a_2	b_1	b_2	c	d
f	-15.89	-35.35	0.11	0.21	0.0024	73.24

Additionally, a comparison between the numerical and experimental parameters and the tensile strength is presented in Figure 6.

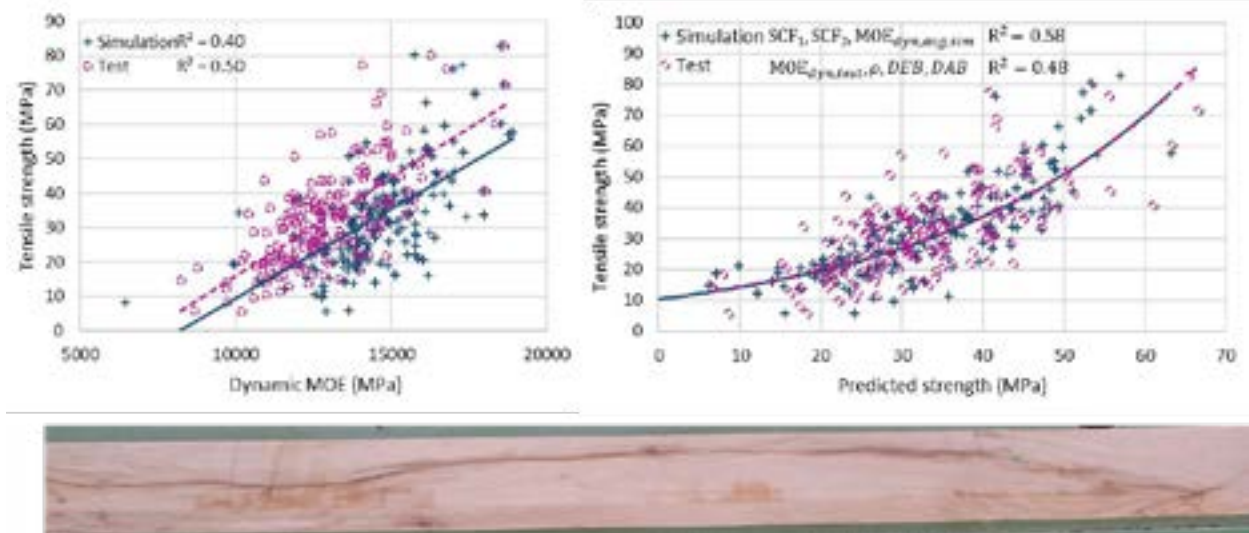


Figure 6: Comparison of the tested and simulated parameters to the measured tensile strength and an example of beech board with extreme fiber deviation

By considering the geometrical effects of the knots on the tensile strength of the boards in the numerical simulations, the predictions are improving considerably. However, for the low quality boards in this study, usage of only two stress concentration factors in combination with the numerical MoE_{dyn} (by application of the average density) in multiple regression analysis are enough for the prediction of the tensile strength ($R^2=0.58$). Addition of the third SCF is not improving the quality of the predictions to more than 10% ($R^2=0.59$ compared to $R^2=0.58$). Therefore, this parameter is not considered as an extra parameter for the tensile strength predictions.

4. CONCLUSION

Due to the strong anisotropy, heterogeneity and geometrical non-uniformity of beech samples, different aspects need to be considered in the numerical simulations to be able to improve the quality of the predictions. First, due to the possible frequent curvatures in beech logs, an optimum configuration needs to be defined to be able to increase the yield. In this study, by considering the outermost points of the beech logs from observed point clouds for the reconstruction of the logs, and without considering the quality of the extracted boards, an increase of about 15.5% in the yield of the logs is expected by cutting shorter boards. It is shown that the width and thickness effects can be neglected, due to their small influence (1.5% increase) on the yield. Additionally, by considering the economic costs, the dimensional effects can be neglected in very straight logs. Therefore, length effects need to be considered in the cases

of logs with curvatures.

In the case of modelling low-quality beech boards with strong fiber deviations, it is shown that consideration of the knot geometries has a considerable influence on the prediction of the tensile strength, beside the numerically simulated MoE_{dyn} , when applying the average density of the specimen. It is shown that usage of two numerically extracted stress concentration factors in combination with the calculated MoE_{dyn} in a multiple regression analysis gives a higher correlation with the tensile strength compared to the measured knot parameters (DEB and DAB) in combination with the actual board density and the measured MoE_{dyn} . The $R^2=0.58$ compared to $R^2=0.48$ respectively for the simulations and the tests show the strength of the developed virtual method for tensile strength predictions.

ACKNOWLEDGEMENT

The authors gratefully acknowledge the support of the Bayerischer Landesanstalt für Wald und Forstwirtschaft for funding the project X042 "Beechconnect" which allowed for the work presented in this paper.

REFERENCES

- Baño, V. Arriaga, F. Soilán, A. Guaita, M. 2010. *F.E.M. analysis of the strength loss in timber due to the presence of knots*. World Conference on Timber Engineering, Riva del Garda, Italy. ISBN: 978-88-901660—3-7.
- Bernardini, F. Mittleman, J. Rushmeier, H. Silva, C. Taubin, G. 1999. *The Ball-Pivoting Algorithm for Surface Reconstruction*. *IEEE Transactions on Visualization and Computer Graphics*. 5(4):349-359. DOI: 10.1109/2945.817351
- Bhandarkar, SM. Luo, X. Daniels, R. Tollner, EW. 2006. *A novel featurebased tracking approach to the detection, localization, and 3-D reconstruction of internal defects in hardwood logs using computer tomography*. *Pattern Anal Appl* 9:155–175. doi:10.1007/s10044-006-0035-9
- Boukadida, H. Longuetaud, F. Colin, F. Freyburger, C. Constant, T. Leban, JM. Mothe, F. 2012. *PithExtract: a robust algorithm for pith detection in computer tomography images of wood—application to 125 logs from 17 tree species*. *Comput Electron Agric* 85:90–98. doi:10.1016/j.compag.2012.03.012
- Cramer, S.M. Goodman, J.R. 1986. *Failure modeling: A basis for strength prediction of lumber*. *Wood Fiber Sci* 18: 446-459.
- EN 408 (2010) *Timber structures—structural timber and glued laminated timber—determination of some physical and mechanical properties*. CEN, Brussels, Belgium.
- Foley, C. 2001. *A three-dimensional paradigm of fibre orientation in timber*. *Wood Sci Technol* 35: 453–65.
- Goodman, J.R. Bodig, J. 1978. *Mathematical model of the tension behavior of wood with knots and cross grain*. *Proc. First Int. Conf. On Wood Fracture, Banff, Alberta*.
- Goodman, J.R. Bodig, J. 1980. *Tension behavior of wood – an anisotropic, inhomogeneous material*. *Structural research report No. 32*. Colorado State University, Fort Collins.
- Hackspiel, C. de Borst, K. Lukacevic, M. 2014. *A numerical simulation tool for wood grading model development*. *Wood Sci. Technol* 48(3):633-649. DOI 10.1007/s00226-014-0629-0.
- Jenkel, C. Kaliske, M. 2013. *Analyse von Holzbauteilen unter Berücksichtigung struktureller Inhomogenitäten (Analysis of timber components taking into account structural inhomogeneities) (In German)*. *Bauingenieur*. 88: 494-507.
- Kazhdan, M. Bolitho, M. Hoppe, H. 2006. *Poisson Surface Reconstruction*. *Eurographics Symposium on Geometry Processing*. 61-70
- Khaloian, A. Gard, W.F. van de Kuilen, J.W.G. 2017. *3D FE-numerical modelling of growth defects in medium dense European hardwoods*. *Proceedings of the sixth international scientific conference on hardwood processing, Lahti, Finland*, 60-67.
- Khaloian Sarnaghi, A. van de Kuilen, J.W.G. 2019a. *Strength prediction of timber boards using 3D FE-analysis*. *Construction and Building Materials* 202: 563-573. doi: 10.1016/j.conbuildmat.2019.01.032.
- Khaloian Sarnaghi, A. van de Kuilen, J.W.G. 2019b. *An advanced virtual grading method for wood based on surface information of knots*. *Wood Sci. Technol*. 0043-7719. DOI: 10.1007/s00226-019-01089-w
- Longuetaud, F. Leban, J.M. Mothe, F. Kerrien, E. Berger, M.O. 2004. *Automatic detection of pith on ct images of spruce logs*. *Computers and Electronics in Agriculture* 44: 107–119
- Longuetaud, F. Mothe, F. Kerautret, B. Krähenbühl, A. Hory, L. Leban, J. Debled-Rennesson, I. 2012. *Automatic knot detection and measurements from x-ray ct images of wood: A review and validation of an improved algorithm on softwood samples*. *Computers and Electronics in Agriculture* 85: 77–89

Lukacevic, M. Füssl, J. 2014. Numerical simulation tool for wooden boards with a physically based approach to identify structural failure. *Eur. J. Wood Prod.* 72:497–508.

Phillips, G.E. Bodig, J. Goodman, J.R. 1981. Flow-grain Analogy. *Wood Science*. 14: 55-65.

Rais, A. Jacobs, M. Khaloian, A. Van de Kuilen, J.-W.G. Pretzsch, H. 2018. Qualitätsorientiertes 3D-Scanning im Mischwald. *Forstwissenschaftliche Tagung 2018 Göttingen, 24. bis 26. September 2018*. Edited by C. Ammer, M. Bredemeier, and G. Von Arnim. p. 446.

Steele, P. Wagner, F. Kumar, L. Araman, P.A. 1993. The value versus volume yield problem for live-sawn hardwood sawlogs. *For Prod J* 43:35–40.

A timber guardrail for highways made with hardwoods

J.W.G. van de Kuilen^{1*}, V. Antonelli², and I. De Pauw³

¹Biobased Structures and Materials
TU Delft
Delft, the Netherlands / Wood
Technology, TU Munich, Germany

²Lightweight Structures
Consultant
Munich, Germany / Delft, the
Netherlands

³IDEAL&CO, Amsterdam, the
Netherlands / Fac. of Industrial
Design, Delft University of
Technology

ABSTRACT

*A timber guardrail made of sustainable tropical hardwoods has been developed in the Netherlands. The guardrail is an environmentally friendly alternative for zinc-coated steel barriers. The guardrail is made of a combination of two durable hardwood species: angelim vermelho (*Dinizia excelsa*) from Brazil and azobé (*Lophira alata*) from Africa. Full-scale tests have shown that the guardrail is able to withstand the impact of a 13000 kg bus driving at a speed of 70 km/h and an impact angle of 20 ° as well as that of a car of 900 kg having an impact speed of 100 km/h and same angle. Steam bent curved boards are used as energy absorbers from the passenger car impact. After the full-scale tests with the bus, no damage was found in the timber elements, and the guardrail had only to be straightened, saving repair costs during the service life of a guardrail. The guardrail fulfils the requirements specified in European standard EN 1317 Road Safety Systems for the H2 level with accident severity index of 1.0.*

1. INTRODUCTION

The In the Netherlands a wooden guardrail for highways has been developed with the shape of a tulip. The development was initiated due to concerns of zinc pollution caused by steel guardrails and the environmental impact in general of steel. The hot-dipped galvanised steel guardrails have a zinc layer to protect them against corrosion. However, this layer slowly leaches into the environment during the working life and an estimated 3000 tons of zinc leaches to the environment each year in Europe because of this. In the development to a more sustainable society, an alternative for the steel and concrete guardrails has been developed. Although timber guardrails already exist in a number of countries, they are either not suitable for highways or made of a combination of steel and timber. Europe has more than 75000 km of motorways based on 2017 data according to Eurostat. With an approximate lifetime of 20 years for a guardrail, the market potential for an environmentally friendly alternative is large. The timber alternative has been developed in a project sponsored by the Dutch Road Authority, the Dutch Timber Information Centre and Delft University of Technology.

2. REQUIREMENTS FOR THE NEW GUARDRAIL

In conjunction with the highway authority, a list of requirements was generated that should be fulfilled. A distinction was made between requirements specifically dealing with guardrails and other, more general requirements. In Europe the safety level of guardrails is regulated in standard: EN 1317-1 - Terminology and general criteria for test methods, and EN 1317-2 – Performance classes, impact test acceptance criteria and test methods. The three main criteria that define the capabilities of a safety barrier are the containment level, the impact severity and the deformation of the restraint system. The containment level represents the capacity of the guardrail to withstand vehicle impacts. The standard specifies the characteristics of the tests, in terms of vehicle impact speed, impact angle and vehicle mass. The requirements for Dutch highways are for a H2 containment level and are given in Table 1.

* Corresponding author: Tel.: +49 (0)89 2180 6462; E-mail: vandekuilen@tum.de

A timber guard rail for highways made of hardwoods

Table 1: Requirements for a guardrail at H2 Level

Test	Speed (km/h)	Angle (°)	Mass (kg)	Vehicle
TB 11	100	20	900	Car
TB 51	70	20	13000	Bus

The standard gives three impact severity levels A, B and C as a function of the Acceleration Severity Index (ASI value). This value, derived from accelerometers mounted inside the test car, should preferably be not more than 1.0, (level A) but definitely not more than 1.4 (level B) or 2.0 (Level C). When the requirements for Level A are fulfilled, the possibility of passengers surviving the crash is good and is the preferred level.

During a collision, no elements may be loosened from the main guardrail, thus endangering other people or traffic, nor may structural parts penetrate into the passenger compartment of the vehicle.

Additional requirements are:

- Animals have to be able to trespass the guardrail without problems.
- The environmental impact has to be less than that of an equivalent steel guardrail.
- 'cladding' of steel elements with timber is not allowed, and at least 60% of the guardrail has to be made of structural timber.
- The life-cycle costs of the timber guardrail shall not exceed those of an equivalent steel guardrail. The cost in mass production may be maximally 20% higher.
- The design has to be recognizable as timber guardrail and be innovative.

The objective regarding the performance of the guardrail was ranked top priority, as the highway authority wanted to demonstrate the feasibility of timber as a modern construction material. The development of the guardrail was divided in a number of stages, starting with information analysis, conceptual design, crash simulations and engineering and finally a number of prototype and full-scale tests.

2.1. INFORMATION ANALYSIS

The requirements were discussed and analysed in close cooperation with the highway authority. A patent search was performed to find existing systems and technologies that could serve as a basis. Some patents came up on a timber guardrail, consisting a combination of roundwood and steel plates, but approved for secondary roads only.

The functional performance of the current types of guardrail were also thoroughly analysed and experiences from the highway authority were discussed in-depth. This cooperation was maintained throughout the project to receive feedback on the design but also to increase the acceptance level of a timber guardrail as a viable product. It was concluded that a new working concept was needed for the timber guardrail to be able to fully utilize the material properties of timber.

2.2. CONCEPTUAL DESIGN

The first step in the development stage consisted in the use of creative technologies to generate concepts for guardrails. Brainstorm sessions and technical discussions with experts resulted in about 200 designs. Together with the highway authority, this was then brought down to 4 viable concepts, each having about 7 alternatives.

In the end, the highway authority decided that the "Tulip" design concept should be developed into a prototype. An artist impression of the tulip and some alternatives are shown in figure 1 and 2. The Tulip was valued as most innovative and was chosen for further development, accepting that the design involved some more 'unknown' parameters with respect to performance and manufacturing, as well as expected final costs.

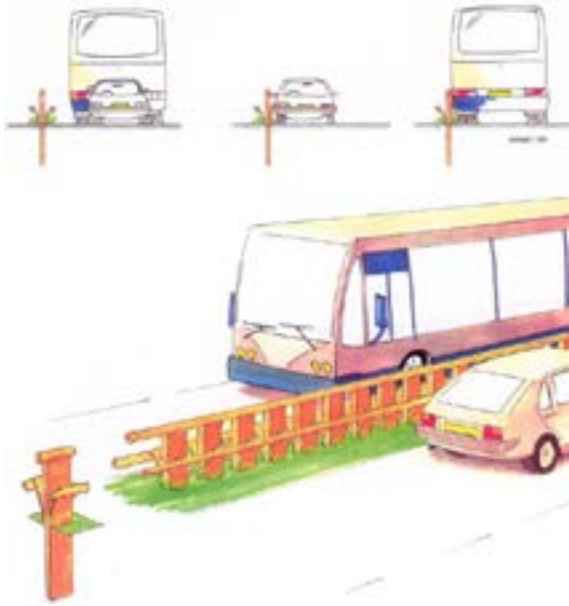


Figure 1: Chosen design for further development.

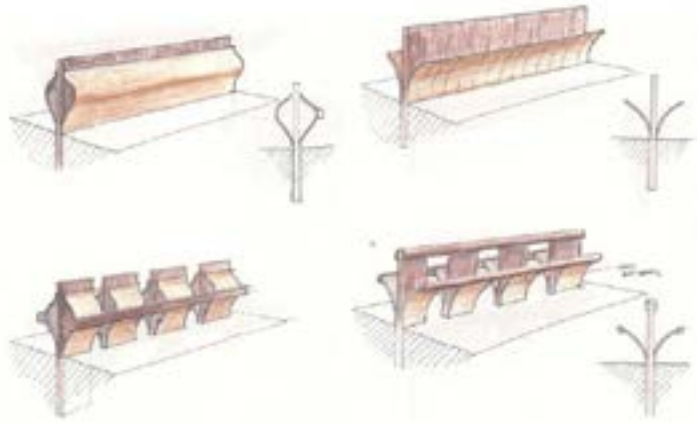


Figure 2: Design alternatives with steam bent timber.

3. STEAM BENT TIMBER

The guardrail has a small steam bent timber 'leaf' allowing small cars with occupants to be decelerated within acceptable levels (ASI-value) and a larger double beam 'flower', supported by posts, to withstand a bus impact. Steam bent timber elements were expected to have good energy dissipating behaviour, but no quantitative data was available. The steam bent leaf is curved into a specific shape that allows for energy dissipation without the timber splintering or loosening from the rail during impact. Consequently, a series of tests were carried out on small clear specimens sawn from new boards, on steam bent boards, as well as boards that were steam bent and then straightened again in a reverse process. Compression tests were carried out on small clear specimens of Angelim Vermelho and French Oak with sizes 20 x 20 x 60 mm and tension tests were carried out on 20 x 20 x 200 mm. The boards were carefully selected at the sawmill and could be considered defect free. The same quality of boards should be used in the actual guardrail, since boards with defects cannot be bent properly without cracking of the convex face or compression (buckling) failures of the concave face [Stevens and Turner, 1970]. The wood fibres that are 'crushed' during the bending process with steam can be straightened again without breakage of the fibres and without cracking the elements. Only when the board is curved in the opposite direction, failure (cracking) will occur.

The typical stress-strain diagram for Angelim Vermelho as calculated by Abaqus on a reference block with a compression strength of about 58 MPa and a tensile strength of around 60 MPa is shown in figure 3. The stiffness difference between compression and tension is noticeable, as well as the large non-linear deformation capacity in compression. Furthermore, in tensile the material behaves brittle with a slight non-linearity.

The prototype of the joint between the post and the steam bent elements was designed with two steel bolts M16. The white nylon spacer between post and board is 20 mm thick and allows for a larger stroke, giving more energy absorption, but also allows water and dirt to run through in the final application, increasing the durability of the system. In order to be able to calculate the stresses in the steam bent timber, a new non-linear material model was developed and implemented in the Finite Element Code Abaqus [Pronk et al. 2002].

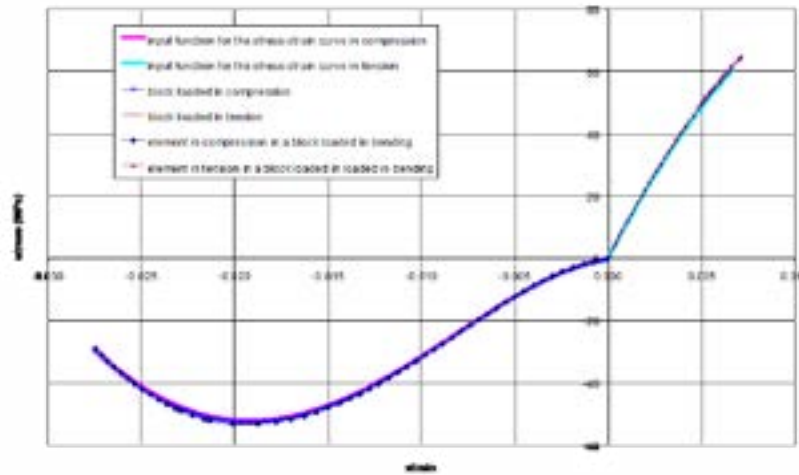


Figure 3. Stress-strain diagram of steam-bent timber for the guardrail simulations

After the preliminary material testing of the steam bent timber, a prototype was built to investigate the behavior of the system 'pile – connection – leaf – car rail'. The system was not tested under impact, but under quasi-static loading. The goal was twofold. On the one hand, the energy dissipation needed to be determined, and secondly, the robustness of the system needed to be verified, as no cracks or failures were supposed to happen in a crash situation. The behavior of the system under loading (rotated under 90° with respect to the application) is shown in figure 4.



Figure 4. Three stages of bending of the steam bent element with car rail, connected to the pile with two bolts and white coloured spacers.

From figure 5, the large energy dissipation capacity of the system can be seen, as the surface under the curve is quite large. In future work, the dynamic impact behavior of the system could be evaluated in more depth, as it remains uncertain if the energy dissipation under impact loading is the same as under quasi-static loading. The quasi-static loading values were used in the subsequent simulations, that showed to be pretty accurate when compared to the actual test results from the full scale tests.

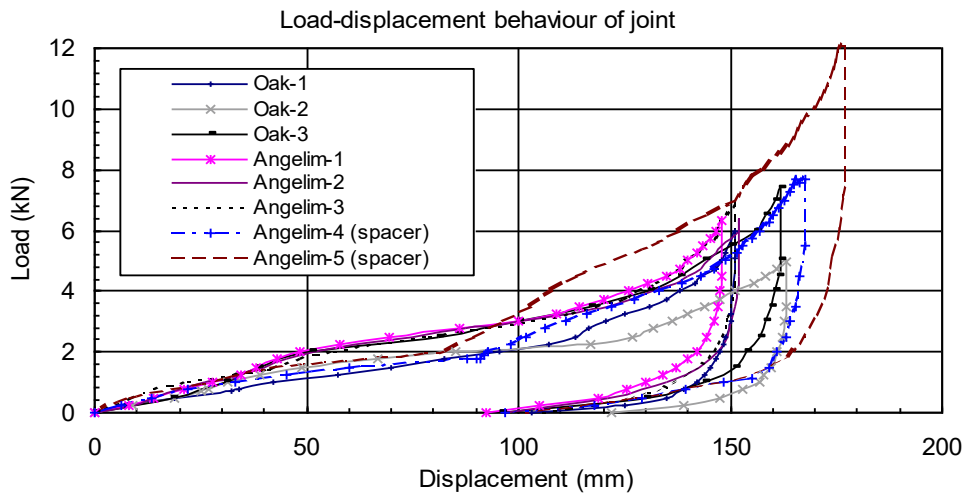


Figure 5. Load-displacement relationship of the car rail connected to the pile.

4. CRASH SIMULATIONS AND ENGINEERING

4.1. INTRODUCTION

After the selection of the “Tulip” design concept, an inventory was made of the design parameters that would determine the sizes and shapes of the prototype components. The Tulip consists of a short pile in the ground (post), a top rail (bus rail), a small 'leaf' of steam bent timber (car board) connected to the post just above ground level and a small rail (car rail) that are connected to the piles through the car boards. These elements were modelled in a Multi-Body analysis program (MADYMO®) and a parameter study was performed. Crash simulations performed with this program give an indication of the necessary strength/size ratios for the different elements with output of system deformations, but also ASI-values. The elements and joints that were analysed in the simulations and are given in Table 2. The choice of wood species was postponed as long as possible to ensure freedom in design and manufacturing. Instead of selecting a wood species, the optimisation of the design was performed with the parameters strength/stiffness and natural durability/structural detailing measures, but also in contact with industry concerning manufacturing and wood availability.

Table 2. Parameters to be analysed in the crash simulations

Parameter:	Mechanical property	Axes	Remark
Depth of post	Soil strength/stiffness	x, y, z	laboratory research required
Size of post	Bending strength/stiffness	x, y, z	includes torsion and spacing
Joint post – bus rail	Strength/stiffness	x, y, z	-
Size of bus rail	Bending strength/stiffness axial strength/stiffness	x, y, z	-
Joint post - car board	Rotational stiffness	x	laboratory research required
Size of car board	Bending strength/stiffness	x, y, z	includes torsion and spacing
Joint car board – car rail	Strength/stiffness	x, y, z	-
Size of car rail	Bending strength stiffness, axial strength /stiffness	x, y, z	includes torsion

Apart from the timber components, the longitudinal joints for the car rail and the bus rail were designed and analysed. The crash simulations predicted the loads on these joints and an increased strength for loading periods lasting not more 30 milliseconds [Bocchio et al., 2001] was taken into account.

During the engineering phase, laboratory tests were performed on two components of the Tulip: the post in the ground and the car board (steam bent timber). A static calculation had shown that the post should be placed at 1-meter depth, but the reaction forces could only roughly be estimated. Therefore, a steel tank was filled with sand usually used in roads. Then a post was placed in the ground and a sway mass was used to determine impact forces and moment-rotation behaviour, both parallel and perpendicular to the traffic direction.

After the laboratory tests, additional Multi-Body analyses were performed that included the test results. The final required dimensions of the elements were determined, and the vehicle behaviour was analysed for stability and re-entry behaviour. For the bus, the strength and integrity of the system is important. The impact of a 13.000 kg bus was a challenge to master but after a number of changes in parameters it was found that a bus rail from Strength Class D60 in accordance with European strength class standard EN 338 should be able to perform well under these conditions. A lower strength class combined with larger dimensions of this element was felt to change the design too much. The post could be made of a lower strength class and alternatives for the post are possible by varying the spacing and/or the thickness. In figure 6 some timesteps from for a car and a bus simulation are given. After these calculations and simulations, the technical drawings were prepared for the prototype.



Figure 6. Simulation images for car (left) and bus (right)

4.2. SIMULATION RESULTS AND PROTOTYPE BUILDING

After the numerical simulations the design was finalised and technical drawings were made for a prototype. An unexpected results from the simulations was that, besides transversal forces also large vertical (upwards) forces needed to be taken into account, especially for the bus crash. These forces cause double bending in the rail, increasing the required sizes considerably. In addition, the vertical forces have to be transferred to the piles, for which considerable diameter bolts are needed (about M20). Considering end and side distances and minimum spacings, this resulted in a bus rail consisting of two half circles with a radius of 150 mm. Since these dimensions were not available in angelim vermelho it was decided to make these rails of azobé (*Lophira alata*), which is a tropical species from Africa with comparable mechanical characteristics. The prototype is shown in Figure 6. The prototype was tested using large bags filled with a sand-filled plywood box. Tests were done on the car rail with an equivalent speed and energy as the transverse component of a car impact. For the bus, the speed of the sandbag was higher, but since the mass of the



Figure 7. 18-meter prototype of guardrail and sandbag test

sandbag was about one-tenth of that of a bus, the total impact energy of this test was about 25% of that of the transverse component of a bus. The main conclusion of these tests was that the prototype seemed to be robust enough. After this test, some slight alterations were made to the connections, mainly for aesthetic reasons. It was decided to replace 20 mm bolts by 20 mm threaded rods, to be mounted from the backside of the rail.

5. FULL SCALE TESTING

For the full-scale tests a guardrail of 80 meters in length was installed at the Test Centre Lelystad of the Dutch Vehicle Technology Information Centre RDW. A total of 4 crash tests were performed, one of which failed as the impact angle during the first bus test did not comply with the requirements. Firstly, a car crash test was performed in accordance with EN 1317. The car used was a Peugeot 205. The impact speed of the car was 100.3 km/h and the impact angle 20°. Although roll behaviour and re-entry angle fulfilled the requirements as specified, the ASI-value was determined at 1.46 or 4% above the limit of 1.4 as specified in the standard. Consequently, the guardrail has not passed the test and modifications are necessary before approval can be obtained. The difference between the simulated ASI value and the actual ASI value is thought to be caused for a great part by the difference in soil behaviour between the laboratory test and the soil behaviour on the test site. On the test site, in fact, a combination of saturated clay and sand is present, while sand was used in the laboratory test. A sensitivity study showed that under these conditions the simulated ASI value could have been 1.3. Another reason for the higher ASI value is the high friction between car and guardrail in the full-scale test. After having examined the damages on the guardrail and the analysis of the test data, it appeared that the friction had caused an increase in the longitudinal acceleration. As a second bus test had to be performed, this gave the opportunity for an improved version of the car rail to be tested. A top view from four stages of this test is shown in Figure 8. The new car rail was optimized for more energy dissipation and an ASI-Value of 1.0 could be achieved, classifying the rail in the best class for small cars.



Figure 8. Top view with a high speed camera of the car impact on the guardrail, Full-scale test with a 900 kg car (Test TB 11 according to EN 1317)

The second bus test was successful, whereas the first bus test did not go according to protocol. After the towing truck released the bus, the vehicle deviated from the intended track, and the impact angle became 26° instead of 20°. As a result, the kinetic impact energy was $\sin^2(26)/\sin^2(20) = 1.64$ times the intended impact energy. The speed of the impact was estimated to be between 65 and 70 km/h. Although the bus did not crash through the barrier, the primary rail broke and this is not allowed according to EN 1317. However, with the results from the first test, the second prototype A sequence of high-speed camera photographs of the backside of the bus is shown in figure 8. After the test, the guardrail is inspected for failures. No cracks or other damage occurred to the posts or the bus rail. The guardrail only has to be straightened, saving repair costs and traffic lane closures.



Figure 8. Back view from a full-scale test with a bus. No damage to the timber, except a need for straightening, saving repair time and costs.

6. SUMMARY

A timber guardrail for highways has been developed and successfully tested. After laboratory test on small elements and a many crash simulations, full-scale tests have shown that the guardrail fulfils all the requirements as specified in EN 1317 for both a car and a bus. The ASI-value was determined at 1.0, which is just within Class A. After impact, only minor repairs are necessary, saving time and money on traffic lane closures. The guardrail is ready for application along European roads for a H2 containment level in accordance with EN 1317.

ACKNOWLEDGEMENTS

The development of this guardrail was made possible through a joint development program with contributions from Rijkswaterstaat, Centrum Hout and TU Delft. A special word of thanks goes to Wim Bak who has been the primary driver of this project within the former Dienst Weg en Waterbouwkunde, a specialist department of Rijkswaterstaat dealing with road and hydraulic structures.

REFERENCES

- ABAQUS User manual, Hibbitt, Karlsson & Sorensen, Inc., 2001*
- Bocchio, N., Van de Kuilen, J.W.G., Ronca, P. Impact loading tests on timber beams, IABSE Conference on Innovative Wooden Structures and Bridges, Lahti, Finland, 2001*
- EN 1317. Roadside Safety Systems*
- MADYMO 5.4, TNO Road-Vehicles Research Institute, The Netherlands.
- Pronk, M., Van de Kuilen, J.W.G., Antonelli, V., An advanced non-linear material model for timber, 7th World Conference on Timber Engineering, WCTE 2002, Shah Alam, Malaysia*
- Stevens, T.C., Turner, N, Wood Bending Handbook, 1970.*
- Writing User Subroutines with ABAQUS, Hibbitt, Karlsson & Sorensen, Inc.*

Portuguese hardwoods: an overview of its potential for construction purposes

C. Martins¹, P. Santos¹, and A. M. P. G. Dias^{1*}

¹ISISE, Department of Civil Engineering
University of Coimbra
Coimbra, 3030-788, Portugal

ABSTRACT

The effects of the climate changes are becoming more evident in Europe and consequently with a clear effect in the Forest areas. A number of examples were reported of hardwood plantations replacing Norway spruce which is considered as not adapted to altering growth conditions (Schmidt and Knorz, 2010). Portuguese Forest also changed in the last decades, this change was boosted as result of the wildfires which affected a significant percentage of softwood area. A major consequence of these effects is the conversion of softwood areas to Blue gum plantations which presents faster economic benefits for land owners. Data from 2010 reported in the 6th National Forestry Inventory (ICNF, 2013) refers that hardwoods occupies 69% of the Portuguese forest area (3154800 ha). The present paper intends to present an overview of the potential of Portuguese hardwoods focusing on construction applications based on recent studies performed at University of Coimbra and SerQ – Forest Innovation and Competences Center. Valuation of hardwood species has been considered through the non-destructive and destructive assessment of their mechanical properties as sawn wood. Its potential was also assessed for more technological engineered wood products such as glulam, CLT and SIP. The results obtained are presented and discussed, these show a significant ability and potential of these species to be used in construction based products.

1. INTRODUCTION

Portuguese forest and the wood products obtained from the forest represents a significant contribution for the Portuguese economy being responsible for 3% of Gross Domestic Product (GDP) in 2015 (ICNF, 2019). Data from the 6th Nacional Forestry Census (ICNF, 2013) indicated that 35.4% of Portuguese land area is occupied by forest, which is close to the average of the European Union countries (37.6%). The same report lists the 22 most common species grouped in softwoods (7) and hardwoods (15). The higher number of hardwood species is in line with the occupied area, representing 69% being the Blue Gum with 26% the dominant species, followed by Cork Oak (23%), Holm Oak (11%), Oak (2%), Chestnut (1%), Acacia (0.2%) and a group of other hardwoods (Poplar, Beech, Ash, and others) with 6%. Portuguese law prohibits the felling of species like Cork Oak and Holm Oak, and due to their characteristics, they do not have a significant potential for construction applications, decreasing the available area of hardwood forest for this type of applications to approximately 35%.

Regarding softwoods, Maritime pine is the most common softwood specie used for construction applications as sawn wood and non-structural products (pallets, panels, pellets and furniture). Nevertheless, a decrease of 27% of Maritime pine was observed between 1995 and 2010, corresponding to approximately 263 000 ha (ICNF, 2013). Recent studies on hardwoods all over the world have demonstrated the potential of several European hardwood species to be used in products with higher added-value than the usual applications that in Portugal are mainly: i) pulp and paper; ii) pellets; plywood; iii) furniture and iv) energy applications.

The present paper intends to provide an overview of the Portuguese hardwoods potential for being used for construction applications, such as: sawn wood, glued laminated timber (glulam), cross-laminated timber (CLT) and structural insulated panel (SIP).

* Corresponding author: A. M. P. G. Dias; E-mail: alfgdias@dec.uc.pt

2. SAWN WOOD

2.1. BLUE GUM

Blue gum is a fast growing hardwood with typically high density values, varying between 750-850 kg/m³, with origin in Australia being widely known as Tasmania blue gum. It was introduced in south-western Europe (Portugal and Spain) and Northern Africa in the mid-19th century for industrial purposes, such as timber and paper pulp production (Cesaroli et al., 2016). Blue gum is an evergreen tree with a straight trunk with up to 2m diameter and 40-55m tall (Franke and Marto, 2014). Data from the 6th National Forest Inventory indicates the area where this specie is dominant in around 26% of the Portuguese forest area, corresponding to approximately 812 000 ha, being observed an increase of 13% of its area between 1995 and 2010. Cesaroli et al. (2016) mentioned that in Europe Blue gum covers 1.3 million ha mainly in Iberian Peninsula (more than 80%), France and Italy.

Despite the availability of Blue gum its use for construction applications is reduced, typically associated with sawing and drying issues (Franke and Marto, 2014). However, several studies have been reported during the last two decades addressing drying schedules to obtain 12% moisture content sawn timber and avoiding the reported problems such as the risk of collapse of the cells. Vásquez and Saavedra (2002) present a drying schedule proposal for 30 mm thick sawn boards to obtain 12% in approximately 30-35 days. A pre-drying period at 27°C and 80% RH during 15-20 days decreases the moisture content from 65% up to 30%. The following period was controlled by drying and conditioning stages in order to have the moisture content in the boards homogenous and recovering the occurred collapse in the wood. The study performed by Franke and Marto (2014) assessed different issues regarding Blue gum including the sawing (Saw-Dry-Rip method – SDR and Tangential Sawing - TS) and drying process (kiln drying - KD and vacuum drying - VD). The authors concluded that SDR method conducted to better performance in terms of internal cracks and distortion compared to TS. The presence of collapse and internal cracks was more evident in the VD process. However, the final moisture content was not comparable as the final moisture content with VD was around 8.8% after 260 hours (approximately 11 days) and the final moisture content with KD was 26% (SDR method) and 37% (TS method) after 14 days of drying.

The number of studies in Europe on which the mechanical properties of sawn wood of *Eucalyptus globulus* is analyzed is limited. In some of these studies, clear wood specimens (LNEC, 1997) are addressed while in other, sawn boards on Eucalyptus from Galicia, Spain (Alvite et al., 2002) are tested. A recent study on Blue gum grown in Portuguese forest focused on the assessment of mechanical properties on sawn wood beams (75 mm x 75 mm) and on the potential of non-destructive methods for prediction of mechanical properties, namely modulus of elasticity and bending strength was published by Martins (2015). Strong correlation coefficients were determined between dynamic and static modulus of elasticity ($r = 0.94$) and significant correlations were found with bending strength ($r = 0.59$ for dynamic modulus of elasticity and $r = 0.61$ for static modulus of elasticity). Average values of 905 kg/m³, 18.2 GPa and 75.3 MPa were obtained respectively for density, modulus of elasticity and bending strength.

2.2. POPLAR

Poplar is a fast growing hardwood with a relatively low density, ranging between 280 kg/m³ and 520 kg/m³ for 12% of moisture content, consequently light and soft for machining processes (FAO, 1979). The International Poplar Commission (IPC) refers the advantages of Poplar at sequestering carbon, contributing to the adaptation and mitigation of the effects of climate change (FAO, 2016). Data reported to IPC from twenty-one member countries and three non-member countries refers a total of 54 million ha of natural and 31.4 million ha of planted Poplar areas. 99% of natural Poplars occur in the Russian Federation, Canada, United States and China while 96% of planted Poplar resources are in Canada and China. According to Chinese State Forest Administration a total 38 Poplar clones were registered.

Poplar has been used in construction applications for many centuries, namely in rural areas of some European countries, such as Italy where numerous buildings were built between the 17th and 19th centuries (Castro, 2007). More recently, it has been used in the production of plywood, carpentry and packaging (Acker et al. 2016). A wide variety of engineered wood products made of Poplar and Willow are listed by Acker et al. (2016), with detailed information regarding the strengths, weaknesses, opportunities and threats for 12 products (sawn wood, glulam, CLT, fibreboards, plywood, veneer and others...).

In Europe the main clones of Poplar are white poplar (*Populus alba* L.) present in riparian steppe and coastal forest of central and southern Europe, black poplar (*Populus nigra* L.) which grows typically in riparian mixed forests and does not tolerate drought or shade and Euroasian aspen (*Populus tremula* L.) which is native to cool temperate and boreal regions of Europe and Asia (FAO, 2016). The dominant clones in Portugal are: white poplar, black poplar and hybrid poplar and are considered within the group of other hardwoods (ICNF, 2013).

In line with the diversity of Poplar clones, the mechanical properties have a wide variation according to the specific clone and also to the growth location. A study performed on *Populus x Canadensis* (PC) by Green et al. (1999) showed values varying between 320 and 400 kg/m³ for density, 7 and 10 GPa for modulus of elasticity and 40 to 70 MPa for bending strength. Similar study was performed by Casado et al. (2010) with 12 years old *Populus x euroamericana* trees. Average values of 383 kg/m³, 7.8 GPa and 38 MPa were obtained for density, modulus of elasticity and bending strength, respectively. Hodousek et al. (2017) considered not only the determination of the mentioned mechanical properties but also the use of longitudinal vibration method as a tool to predict the static modulus of elasticity. An average density of 406 kg/m³ (291-502 Kg/m³) was determined and average modulus of elasticity of 10.1 GPa (7.3 - 14.3 GPa). The correlation coefficient between dynamic and static modulus of elasticity was strong (around 0.90).

Also the mechanical properties of clear wood specimens from Poplar grown in Portuguese forest were assessed by tension and compression tests (Monteiro et al. 2019). Average values of modulus of elasticity of 10.4 GPa and 10.2 GPa for tension and compression were obtained. Regarding the strength properties an average value of 32.7 MPa was obtained and for tension strength the average value was 69.2 MPa.

2.3. BLACKWOOD

Blackwood species (*Acacia melanoxylon* R. Br.) is considered mainly for carpentry and cabinet applications being typically highly valued. According to Knapic et al. (2006), Blackwood has its origin in temperate forests of south-east Australia and Tasmania and is considered a versatile and highly adaptive tree species being spread all over the world due to its ornamental value and the dark color of the wood color of high quality (Figure 1). Despite the quality of wood, in Europe, the species is considered as invasive being the seeds stimulated by fire (Knapic et al., 2006). Knapic et al. (2006) also refers that in Portugal, Blackwood occurs mainly as mixed stands with Maritime pine (*Pinus pinaster* Ait.) or Stone pine (*Pinus pinea* L.) in the West Coast or in pure stands or mixed with pines and other hardwoods in the inner part of Portugal. According to 6th National Forestry Inventory, *Acacia* spp. represents around 5 000 ha (0.2%) of the total Portuguese forest area.



Figure 1: Blackwood visual aspect.

Several scientific studies have been developed on Blackwood being mainly focused on the silviculture of the specie (Zwann, 1982, Nicholas and Brown, 2002, Bradbury et al., 2010), anatomic properties (Knapic et al., 2006 and Santos et al., 2013) and physical properties (Machado et al., 2014). Also the potential for pulp and paper production was evaluated showing great potential (Lourenço et al, 2008 and Anjos et al., 2011), especially for writing and printing paper production (Santos et al., 2006). The variation of physical properties (density) and mechanical properties of Blackwood was evaluated by Machado et al. (2014) on clear wood samples collected from four different stands and within the trees collected. The authors evidenced the potential of Blackwood as an alternative species to supply the industry with valuable hardwood timber. An average density of 654kg/m³ was determined, and average values of 14.1 GPa and 139.0 MPa were obtained for modulus of elasticity and bending strength. It was also mentioned the significant differences found between the trees, which gave an opportunity for an accurate selection of the raw material to increase the wood quality.

At the present moment a research study is undergoing at SerQ – Forest Innovation and Competences Center with participation of University of Coimbra and National Laboratory of Civil Engineering aiming to proceed with mechanic characterization of a large sample of sawn wood with cross sectional dimensions of 50 mm by 120 mm (Martins and Knapic, 2019). The main objective so far was the study of the performance of non-destructive tools for prediction of mechanic properties in bending, namely the correlation between dynamic and static modulus of elasticity.

Longitudinal vibration method was considered as was previously validated for other species, like Maritime pine (Dias et al., 2014), Poplar (Hodousek et al., 2017) and Blue gum (Martins, 2015).

Two samples of 40 boards from different locations (Azores Islands – AI and North of Portugal – NP) were measured in their dimensions (width, thickness and length), moisture content and weight. The cross section dimensions were measured in three different locations (both ends and mid-length), such as the moisture content was recorded by an electrical moisture meter at mid-length and at both 60 cm from each end as required by EN 13183-1 (CEN, 2002) (Figure 1). The referred data was considered as input to the software of Machine Timber Grader (MTG) which considers longitudinal vibration method in its device (Figure 2).

After the non-destructive test the dynamic modulus of elasticity was recorded and static tests were performed following EN 408 (CEN, 2012). The test was performed with a constant rate of displacement (0.36 mm/s) up to 40% of the estimated failure load. The applied load was measured by a load cell of 200 kN of maximum capacity and deflections were measured by LVDT's with 20 and 50 mm of maximum capacity (Figure 3).



Figure 2: Measurement of moisture content and dynamic modulus of elasticity test.

Sample AI had average values of density of 595 kg/m³ while sample NP had average density of 702 kg/m³, with 10.0% and 10.3% of coefficient of variation (COV) being in line with typical values for the most common species used in construction. In terms of dynamic modulus of elasticity average values of 13.5 GPa and 14.8 GPa were measured, respectively for AI and NP samples. In terms of static modulus of elasticity, average values of 13.6 GPa and 14.4 GPa were determined for AI and NP samples, respectively. The present values (density and modulus of elasticity) are in line with previous values obtained for clear wood specimens by Machado et al. (2014).



Figure 3: Static modulus of elasticity test layout.

The statistical analysis of the data collected (density, static and dynamic modulus of elasticity) revealed a good agreement between the density and both modulus of elasticity with correlation coefficients between 0.63 and 0.67. The use of longitudinal vibration method could be considered as an effective and reliable tool for the prediction of static modulus of elasticity as the correlation coefficients values between the two variables were 0.97 and 0.96 for AI and NP samples, respectively (Figure 4).

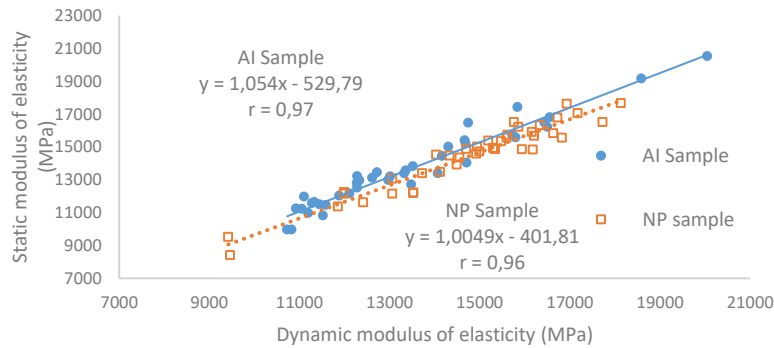


Figure 4: Correlation between dynamic and static modulus of elasticity.

2.4. CHESTNUT

Chestnut wood is obtained from the sweet Chestnut tree (*Castanea sativa* Mill.) which is the only native species of the genus in Europe, as is considered a medium-large deciduous tree that could reach 30-35m. Its distribution in Europe is wide, covering an area of more than 2.5 million ha, being 89% concentrated in a list of few countries (France, Italy, Spain, Portugal and Switzerland) (Conedera et al., 2016). In Portugal, Chestnut timber was one of the timber species commonly used for roof and floor structures (Martins et al., 2013). However, the information of the mechanical properties is scarce with few studies available. Some studies were performed with focus on the evaluation of the compressive and tensile properties on clear wood specimens of old and new chestnut timber (Lourenço et al., 2007 and Feio et al., 2007). The mechanical properties in bending and compression on elements with structural dimensions and the use of non-destructive methods was considered by Martins et al. (2013). An average density of 576 kg/m³ was determined while average values of 10.0 GPa and 48.7 MPa were obtained for modulus of elasticity and bending strength. For compression strength parallel to grain an average value of 39.6 MPa was measured. The study of chestnut properties is of great interest due to its suitability for external use, as it has a high tannin content that acts as a protection against decay (Conedera et al., 2016).

3. ENGINEERED WOOD PRODUCTS

3.1. GLUED LAMINATED TIMBER

Glued Laminated Timber (glulam) has been developed in the early 1890s and is the most common engineered wood product used in construction during last decades (APA, 2008). The use of glulam has several advantages compared with sawn wood, namely: i) higher cross sections and spans; ii) aesthetic and architectural aspect; iii) less variability in terms of properties and iv) higher fire resistance. Since its origin softwoods have been the most common species used on its production, being Douglas fir and Southern pine the most common species used in United States of America, and Spruce and Scots pine the most common species used in Europe (Pontífice de Sousa, 1990). Even though the referred species have the market domain, several studies have been developed in the last decades to assess the feasibility of using either other softwoods, like Maritime pine (Gaspar et al., 2009). More recently, hardwoods have been the focus of research due to their potential in terms of mechanical properties as well as their potential to foresee the threats of climatic changes like Ash (Knorz et al., 2014), Beech (Schmidt et al., 2010) and (Ohnesorge et al., 2010), and Birch (Boruszewski et al., 2011).

Recently some studies have been developed considering the assessment of the potential of some hardwoods available in the Portuguese forest for glulam production (Martins 2018). Poplar has low density being comparable to Spruce, which lead to a deep analysis of its bonding performance with several adhesive references commercially available for structural applications following the requirements of EN 14080 (CEN, 2013) (Martins et al., 2017). In general, a good bonding performance was obtained for phenol-resorcinol-formaldehyde (PRF) and melamine-urea-formaldehyde (MUF) adhesives while emulsion polymer isocyanate (EPI) adhesive did not show adequate performance in terms of delamination tests as it occurs also with one-component polyurethane (PUR) adhesive. However, additional tests were made with PUR adhesive with application of a polyol primer developed for Blue gum

showing a significant improvement of delamination performance. Later Martins et al. (2018) carried a study on 18 glulam beams made of Poplar to assess the efficiency of Longitudinal Vibration Method (LVM) and Transformed Section Method (TSM) to predict both modulus of elasticity and bending strength. The test results evidenced the potential of Poplar for glulam production with average values of 428 kg/m³ for density, 11.0 GPa for modulus of elasticity and 52.5 MPa for bending strength. It should be mentioned that through the average and characteristic values a GL24c strength class could be assigned to Poplar glulam even without considering a restrictive selection of the raw material. Finally, a strong correlation was obtained between dynamic and static modulus of elasticity ($r = 0.80$) and bending strength ($r = 0.81$). TSM proved to be more accurate to predict the mechanical properties as demonstrated by the correlation coefficients of 0.93 (static modulus of elasticity) and 0.87 (bending strength).

The potential of Blue gum for glulam production has been mentioned in a reduced number of studies focusing on the bonding performance (Lopez-Suevos and Richter 2009, Franke and Marto, 2014) or mechanical properties (Alvite et al., 2002). Despite the high mechanical properties of Blue gum comparing to other hardwoods, bonding performance presented by previous studies mentioned some issues that requires additional research. Three different adhesive types (PUR, MUF and PRF) were adopted by (Lopez-Suevos and Richter, 2009), being observed a significant improvement at delamination tests (Method A – EN 14080) in the first series of tests for all adhesives when a primer (HMR or n-HMR) was considered. In the second test series the primer influence was evaluated only for PUR adhesive. Delamination average values were clearly below the limit of 5% (2nd cycle) adopted for softwoods. Franke and Marto (2014) considered two adhesive references of PUR adhesive for production of non-structural and structural elements of Blue gum grown in Portuguese forest. In both scenarios and for both adhesive references the bonding performance was not adequate (Method B – EN 14080).

Martins et al. (2019) presents preliminary results of an undergoing study on the mechanical characterization of glulam made of Blue gum and also the production of mixed glulam made of five lamellas being the two external lamellas of Blue gum and the three central lamellas of Poplar, both grown in Portuguese forest. Interesting results were obtained in terms of mechanical properties of Blue gum glulam (4 beams with 92 x 120 x 2300 mm³) with an average value of 24.2 GPa and 121.4 MPa for modulus of elasticity and bending strength, respectively. Other interesting observation was the high structural efficiency obtained by the mixed glulam beams, with a significant decrease of density (32%) for 659 Kg/m³ keeping high mechanical properties, namely 19.6 GPa for modulus of elasticity and 91.0 MPa for bending strength.

A research study is under development to assess the bonding and mechanical performance of using other hardwoods (Blackwood) as single glulam beams as well as mixed glulam beams made entirely of hardwoods or mixing with softwoods like Sugi (Figure 5).



Figure 5: Blackwood glulam beam (left) and mixed glulam beam made with Blackwood and Sugi (right).

3.2. POTENTIAL FOR CLT/SIP'S APPLICATION

Another potential application of hardwood species on construction products that has been studied are cross-laminated timber or structural insulated panels.

The possibility of use orthogonal glued layers (as in CLT) made of mixed Blackwood/Maritime pine lamellas has been assessed recently (Santos et al., 2019). The bonding of a series of pairs of crossed-layers made using a one-component PUR adhesive with pre-application of a polyol primer with different clamping pressures was tested to assess its efficiency. The results showed that it is possible to fulfill the EN 16351 (CEN, 2015) requirements regarding the bonding quality, either in respect to short-term behavior (shear strength) and long-term (delamination) using a

clamping pressure of 0.1 MPa. From the results, a characteristic value for the shear strength of 4.53 MPa was obtained (EN 16351 requires a minimum of 1.25 MPa). Although a part of the sample (14.3 %) failed the criteria for the delamination visible at the glue line, after splitting the layers as demand by EN 16351 (CEN, 2015), none of the specimens failed in what regard to the wood failure percentage limits, and thus fulfilling the delamination criteria. These results are thus encouraging for the use of this type of hybrid solution made of a hardwood and softwood for CLT panels.

The mechanical behavior of a five-layer hybrid beam made of two external Blackwood lamellas, two crossed Maritime pine layers and an inner layer made of polyurethane rigid foam with a density of 40 kg/m³ (Figure 6) has also been tested in bending following the EN 408 (CEN, 2012). The wood layers had a thickness of 20 mm, the polyurethane foam had 120 mm thickness and the width of the beam was 126 mm. The use of Blackwood in the external lamellas is preferred to Maritime pine because, besides it has quite similar mechanical properties to that softwood, it has a superior natural durability (Carvalho, 1997) and esthetically is more appellant.

From the test, a maximum load of 14.2 kN for a 1.8 m span, was measured and a plastic behavior was observed due to crushing foam nature of the polyurethane layer (Figure 7). The result for this hybrid beam is in line with the results obtained in other tested equivalent beams (but with the wood elements all made of Maritime pine) and thus showing its potential to use on SIP-type elements.



Figure 6: Load – Aspect of the hybrid Blackwood-Maritime pine-Polyurethane foam beam.

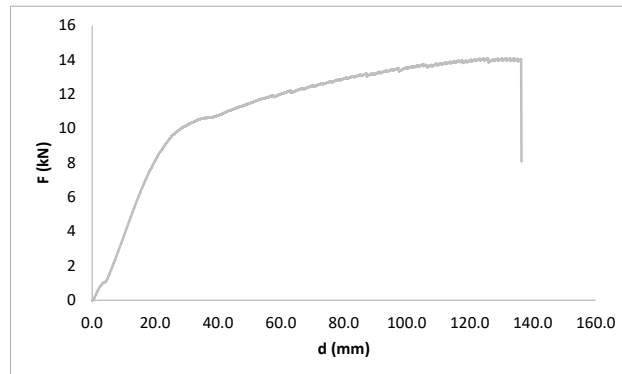


Figure 7: Load – displacement curve of the hybrid Blackwood-Maritime pine-Polyurethane foam beam.

4. FINAL REMARKS

There is a large potential of Portuguese hardwoods for construction applications. However, the use of wood based products has been largely governed by softwood species, most of which imported from Europe. In the present paper, the authors intended to show the diversity of hardwood species available in Portuguese forest, as well as to demonstrate the most recent studies that have been carried out to prove the potential of some hardwoods in high added-value products and of great quality.

SerQ and University of Coimbra have been engaged on the mechanical characterization of hardwood species available at sawmills and that have high aesthetically quality. The subject was not only on the product obtained from the primary transformation sector (sawn wood), but also on engineered wood products with higher added-value on market (Glulam, CLT and SIP).

Despite the wide diversity of Poplar clones available, simple measurements combined with the use of longitudinal vibration method provided a reliable way to characterize the quality of the raw-material available at sawmills. Thus, the prediction of the mechanical properties is less time consuming and avoid the breakage of material. The same could be applied and was validated for other hardwoods like Blue gum and Blackwood, through high correlation coefficients between dynamic and static properties.

Hardwoods could be considered as an alternative to softwoods due to their fast growth rates and their inherent capacity to surpass the climatic changes threats. The use of hardwoods species for engineered wood products is also an alternative to softwoods providing high quality products with superior mechanical properties. However, the

technological information available is still limited to allow a wider use, namely in what regards to grading and bonding.

ACKNOWLEDGEMENTS

This work was partly financed by FEDER funds through the Competitiveness Factors Operational Programme – COMPETE and by national funds through FCT – Foundation for Science and Technology, within the scope of the Project POCI-01-0145-FEDER-007633. The authors acknowledge the financial support of the Operational Program Competitiveness and Internationalization R&D Projects Companies in Co-promotion, Portugal 2020, within the scope of the project OptimizedWood – POCI-01-0247-FEDER-017867. The authors wish to thank Foundation for Science and Technology for the PhD grants with the references: PD/BD/52656/2014 given to Carlos Martins and PD/BD/113786/2015 given to Pedro Santos, to Henkel, Dynea AS and Jowat for providing the adhesives and finally to Pedrosa & Irmãos Lda for the collaboration given concerning the timber.

REFERENCES

- Acker, J. V., N. Defoirdt and J. V. d. Bulcke (2016). *Enhanced potential of poplar and willow for engineered wood products. 2nd Conference on Engineered Wood Products based on Poplar/willow Wood.* J. V. Acker. León, Spain, Ghent University.
- Alvite, J. D. B., M. C. Touza Vásquez and F. S. Infante (2002). *Manual de la madeira de eucalipto blanco.* Ourense, Fundación para o Fomento da Calidade Industrial e Desenvolvemento Tecnológico de Galicia.
- Anjos, O., A. Santos and A. Simões (2011). "Effect of *Acacia melanoxylon* fiber morphology on papermaking potential." *Appita Journal* 64(2): 185-191.
- APA (2008). *Glulam Product Guide.* www.apawood.org, APA - The Engineered Wood Association.
- Boruszewski, P. J., P. Borysiuk, M. L. Maminski and M. Grzeskiewicz (2011). "Gluability of thermally modified beech and birch wood." *Wood Material Science and Engineering* 6(4): 6.
- Bradbury, G. J., C. L. Beadle and B. M. Potts (2010). "Genetic control in the survival, growth and form of *Acacia melanoxylon*." *New Forest* 39(2): 139-156.
- Carvalho, A. (1997). *Madeiras Portuguesas - Estrutura anatómica, Propriedades e Utilizações. Vol. 1 & 2 (in Portuguese).* Direcção Geral das Florestas, Lisboa.
- Casado, M., L. Acuña, D. Vecilla, E. Relea, A. Basterra, G. Ramón and G. López (2010). *The influence of size in predicting the elastic modulus of *Populus x euroamericana* timber using vibration techniques.* 1st International Conference on Structures and Architecture, Guimarães, Portugal, CRC Press, Boca Raton, FL.
- Castro, G. (2007). *Aplicaciones del chopo en la construcción.* Boletín de información técnica de AITIM. N° 248: 24-28.
- CEN (2002). *EN 13183-1 - Moisture content of a piece of sawn timber - Part 1: Determination by oven dry method.* Brussels.
- CEN (2012). *EN 408 - Timber structures - Structural timber and glued laminated timber - Determination of some physical and mechanical properties.* Brussels.
- CEN (2013). *EN 14080 - Timber structures - Glued laminated timber and glued solid timber - Requirements.* Brussels.
- CEN. (2015). *EN 16351 - Timber structures - Cross laminated timber – Requirements.* Brussels..
- Cesaroli, S., M. C. Caldeira, J. S. Pereira, G. Caudullo and D. de Rigo (2016). *Eucalyptus globulus and other eucalyptus in Europe: distribution, habitat, usage and threats.* European Atlas of Forest Tree Species. J. San-Miguel-Ayanz, D. de Rigo, G. Caudullo, T. Houston Durran and A. Mauri, Publication of the European Union, Luxembourg.
- Dias, A. M. P. G., J. S. Machado and P. Santos (2014). *Uso de produtos de madeira de alto desempenho em aplicações estruturais.* 5as Jornadas Portuguesas de Engenharia de Estruturas. Lisbon, Portugal.
- FAO (1979). *Poplars and Willows in Wood Production and Land Use.* Rome, Italy, Food and Agriculture Organization of the United Nations.
- FAO (2016). *Poplars and Other Fast-Growing Trees - Renewable Resources for Future Green Economies: Synthesis of Country Progress Reports - Activities Related to Poplar and Willow Cultivation and Utilization - 2012 through 2016.* Working Paper IPC/15. I. P. Commission. Rome, Italy, Food and Agriculture Organization of the United Nations.
- Franke, S. and J. Marto (2014). *Investigation of Eucalyptus globulus wood for the use as an engineered material.* WCTE 2014 - World Conference on Timber Engineering. Quebec City, Canada.
- Gaspar, F., H. Cruz, A. Gomes and L. Nunes (2009). "Production of glued laminated timber with copper azole treated maritime

- pine." *European Journal of Wood and Wood Products* 68(2): 207-218.
- Green, D. W., J. E. Winandy and D. E. Kretschmann (1999). *Mechanical Properties of Wood. Wood as a engineering material.* Madison, WI, Forest Products Laboratory.
- Hodousek, M., A. M. P. G. Dias, C. Martins, A. F. S. Marques and M. Bohm (2017). "Comparison of Non-Destructive Methods Based on Natural Frequency for Determining the Modulus of Elasticity of *Cupressus lusitanica* and *Populus x canadensis*." *Bioresources* 12(1): 270-282.
- ICNF (2013). *IFN6 - Áreas dos usos do solo e das espécies florestais de Portugal Continental em 1995, 2005 e 2010. I. d. C. d. N. e. d. Florestas.* Lisboa: 34.
- ICNF. (2019). "Economic value of Portuguese forest -<http://www2.icnf.pt/portal/florestas/fileiras/econ>." Retrieved July 6th.
- Knapic, S., F. Tavares and H. Pereira (2006). "Heartwood and sapwood variation in *Acacia melanoxylon* R. Br. trees in Portugal." *Forestry* 79(4).
- Knorz, M., M. Schmidt, S. Torno and J. W. van de Kuilen (2014). "Structural bonding of ash (*Fraxinus excelsior* L.): resistance to delamination and performance in shearing tests." *European Journal of Wood and Wood Products* 72(3): 297-309.
- LNEC (1997). *M6 - Eucalipto comum.* Lisbon, Portugal.
- Lopez-Suevos, F. and K. Richter (2009). "Hydroxymethylated Resorcinol (HMR) and Novolak-Based HMR (n-HMR) Primers to Enhance Bond Durability of *Eucalyptus globulus* Glulams." *Journal of Adhesion Science and Technology* 23(15): 1925-1937.
- Lourenço, A., I. Baptista, J. Gominho and H. Pereira (2008). "The influence of heartwood on the pulping properties of *Acacia melanoxylon* wood." *Journal of Wood Science* 54(6): 464-469.
- Machado, J. S., J. L. Louzada, A. J. A. Santos, L. Nunes, O. Anjos, J. Rodrigues, R. M. S. Simões and H. Pereira (2014). "Variation of wood density and mechanical properties of blackwood (*Acacia melanoxylon* R. Br.)." *Materials and Design* 56: 975-980.
- Martins, C. (2018). *Health Assessment of Glued Laminated Timber Elements (in Portuguese).* PhD, University of Coimbra.
- Martins, C., A. M. P. G. Dias and H. Cruz (2017). *Glulam made by Poplar: delamination and shear strength tests.* ISCHP 2017 - International Scientific Conference on Hardwood Processing, Lahti, Finland.
- Martins, C., A. M. P. G. Dias and H. Cruz (2018). "The use of NDTs for prediction of mechanical properties of Poplar glued laminated timber." (in submission).
- Martins, C., A. M. P. G. Dias and H. Cruz (2019). *Blue gum: Assessment of its potential for load bearing structures.* ISCHP 2019 - International Conference on Hardwood Processing, Delft, The Netherlands.
- Martins, C. and Knapic, S. (2019). *Caracterização mecânica da madeira de Acácia.* Internal Report RP/SERQ/190702. Sertão, Portugal.
- Martins, M. (2015). *Eucalyptus globulus characterization for structural applications (in Portuguese).* MSc, University of Coimbra.
- Monteiro, S. R. S., C. E. J. Martins, A. M. P. G. Dias and H. Cruz (2019). "Mechanical Characterization of Clear Wood from Portuguese Poplar." *Bioresources* (submitted).
- Nicholas, G. J. and I. Brown (2002). "Blackwood a handbook for growers and users." New Zealand Forest Research Institute.
- Ohnesorge, D., K. Richter and G. Becker (2010). "Influence of wood properties and bonding parameters on bond durability of European Beech (*Fagus sylvatica* L.) glulams." *Annals of Forest Science* 67(6).
- Pontífice de Sousa, P. M. (1990). *Structures of Glued Laminated Timber, Feasibility of using Maritime pine (in Portuguese).* Tese para especialista, LNEC.
- Santos, A., R. Simões and M. Tavares (2013). "Variation of some wood macroscopic properties along the stem of *Acacia melanoxylon* R. Br. Adult trees in Portugal." *Forest Syst* 22(3).
- Santos, A. J. A., O. M. S. Anjos and R. M. S. Simões (2006). "Papermaking potential of *Acacia dealbata* and *Acacia melanoxylon*." *Appita Journal* 59(1): 58-64.
- Santos P., R. Correira J., Godinho L., Dias A.M.P.G., Dias A. (2019) "Bonding quality assessment of cross-layered Maritime pine elements glued with one-component polyurethane adhesive". *Construction and Building Materials* 211: 571-582
- Schmidt, M. and M. Knorz (2010). *Gluing of european beech (fagus sylvatica L.) and douglas fir (Pseudotsuga menziessii Mirb.) for load bearing timber structures* WCTE 2010 - 11th World Conference on Timber Engineering, Riva del Garda, Trentino, Italy: 10.
- Schmidt, M., P. Glos and G. Wegener (2010). "Gluing of European beech wood for load bearing timber structures." *European Journal of Wood and Wood Products* 68(1): 43-57.
- Touza Vázquez, M. C. and F. Pedras Saavedra (2002). *Una propuesta industrial de secado de madera de eucalipto blanco (Eucalyptus globulus) de Galicia.* CIS-Madera.
- Zwaan, J. G. (1982). "The silviculture of blackwood (*Acacia melanoxylon*). ." *South African Forest Journal* 121: 39-43.



Poster Presentations

Evaluation of Drying and Anatomical Characteristic of Mongolian Oak Lumber by Kiln Drying due to storage time after sawing

Wood Properties and Drying Characteristics of Korean Sawtooth Oak (*Quercus acutissima* Carruth.) Wood

Vertical Forest Engineering: Applications of Vertical Forests with Self-Growing Connections in High-Rise Buildings

Ageing phenomena of oak wood-animal glue bonded assemblies for preservation of cultural heritage

US Hardwoods and Market Opportunities in Easter Europe

Deep Learning for Lumber Identification

Evaluation of Drying and Anatomical Characteristic of Mongolian Oak Lumber by Kiln Drying due to storage time after sawing

Yoon-Seong Chang*, Min-Ji Kim, Hyun-Kyeong Shin and Yeonjung Han

Dept. of Forest Products
National Institute of Forest Science
Seoul, 02455, Republic of Korea

ABSTRACT

*Based on the 2017 statistics of the Korea Forest Service, the amount of annual production of domestic roundwood was 4.5 million m³. Twenty eight percent of the production was hardwood roundwood. About 80% of the hardwood was *Quercus* species. The hardwood roundwoods were mainly used for wood chips (50%) and medium density fiberboard (MDF)(26%). Only 6% of the hardwood roundwoods were used for sawn timber. Most of oak forests in Korea were not managed well. Therefore, diameter of oak trees was relatively small with lots of flaws, such as inside decay, discoloration etc., since many of them were reproduced by sprout forest. Oak trees produced from unmanaged forests are prone to drying defects. To overcome this proneness, drying and anatomical characteristic of Mongolian Oak (*Quercus mongolica*) lumber (thickness 30 mm x width 100 mm x length 1,900 mm) were investigated in this study. Shrinkage and color difference (E) due to kiln dry was measured. In order to evaluate drying defects, the degree of surface check was investigated. Warp of lumber, such as cup, bow, crook, and twist, were also measured after drying process. Tylosis formation between one month and six months after sawing was observed microscopically. In order to develop value-added products from domestic oaks, the yield rate from standing tree to the flooring board were calculated. It is expected that efficient production plan for the value added products from domestic oak species would be proposed based on the results of this study, which are not being used as commercial sawn timber in Korea currently.*

1. INTRODUCTION

Along with the pine trees, oak trees are widely distributed on the Korean Peninsula, and most of them are natural or secondary forest. Based on the 2017 statistics of the Korea Forest Service, the area of Oak and mixed forest accounted for about 3.7million ha(61%). However, compared to management and utilization of coniferous forests, it is insufficient to research on those of oak and other broadleaved trees. Oak wood was used for various purposes in low-value utilization such as bed log, wood chip, and firewood in Republic of Korea. Therefore, it is urgent to develop utilization technology for enhancing the value-added domestic oak wood product.

Also, Korean oak trees grow slowly in a poorly managed forest condition unlike European and American oak tree. So the diameter of oak trees was small with lots of flaws (discoloration, insect damage etc.) since many of them were reproduced by sprout forest. Therefore, they are prone to drying defects. To use wood as a material, moisture content (MC) must be reduced through drying process. The common method of drying timber to 12% MC is conventional kiln drying (KD). To reduce drying defects and improve drying speed, pre-surfacing and pre-steaming treatment were applied to KD system. Domestic oak timber with pre-surfacing treatment had increased the drying speed by 7.4% and the drying defects were remarkably decreased compared with untreated timber. However, pre-steaming treatment had no significant difference from untreated timber(Han and Jung 1986; Kang 1992). Northern red oak under microscopic investigation found occasional cracks in the cell walls, and a reduced fiber lumen size in the steamed samples. The reduced lumen size was attributed to a disruption in the warty layer by steaming, resulting in increased swelling of the fiber walls(Kubinsky 1971).

Discoloration after logging can occur during the storage of logs and green timber or during drying(Simpson, 1991). Shortly after felling, the logs may be discolored due to physiological and biochemical activities similar to those in the standing tree, when the surfaces are exposed to oxygen (Bauch, 1984). Since time, temperature and humid storage conditions contribute to this development, rapid sawing and drying are recommended (Simpson, 1991). The objective

* Corresponding author: Yoon-Seong Chang ; E-mail: jang646@korea.kr

of this study is to assess drying and anatomical characteristic characteristics of domestic hardwood timber, especially oak species, dried by KD system due to storage time after sawing.

2. MATERIALS AND METHODS

2.1. PREPARATION OF SAMPLES

The Oak (*Quercus mongolica*) wood used for manufacturing flooring was harvested at Pyeongchang-gun, Gangwon-do Province, Republic of Korea. 12 oak logs were harvested and transported to a local sawmill where the logs were divided into two groups. The first group was sawn 23 days after harvesting, while the second group was stored on the log yard for another 168 days prior to sawing. The logs were stored at the low temperatures during winter and early spring, average temperature 5.8°C and RH 58%. The volume of the logs was calculated according to KS F 2163. The below equation was used for calculating the volume of logs.

$$V = D^2 \cdot L \cdot 10^{-6} \quad (1)$$

where, V = volume of log (m³); D = (small) end diameter of log (mm); L = length of log (m)



Figure 1: The mongolian oak log for sawing.

The volume of oak wood which was used in this study was 5.7m³. From twelve logs, 1.4 m³ green boards (30 × 100 × 1,900 mm³) were prepared for Kiln drying. Samples were end-coated with urethane paint in order to minimize the effect of end drying. Average oven-dry density and initial moisture content were 0.79 (± 0.03) g/cm³, 73.9 (± 7.1) %, respectively.

2.2. KILN DRYING AND DRYING PROPERTY

Drying was conducted in a 0.7 m³ capacity experimental-scale conventional kiln drying (After 1 and 6 months). Air flow through the stack was provided by the fan located at one side of the kiln with air velocity of 1.5 m/s. The samples were stacked on 20 mm by 20 mm stickers. The stacks were restrained by placing concrete block on top of the stack to minimize warping. Drying condition was set according to Table 1.

Table 1: Kiln drying schedule(modified T11-B3)

Moisture Step (%)	Temperature(°C)		Relative humidity(%)	Equilibrium Moisture Content(%)
	Dry-bulb	Wet-bulb		
Above 35	65	62	83	14.0
35 to 30	65	57	66	9.5

Evaluation of Drying and Anatomical Characteristic of Mongolian Oak Lumber by Kiln Drying due to storage time after sawing

35 to 30	65	54	57	8.0
35 to 30	71	57	51	6.8
20 to 30	71	54	43	5.8
Below 15	76	57	39	5.1
Conditioning	82	76	78	10.8

Shrinkage of boards in width and thickness was determined by measuring its dimension before and after drying. Two measuring baselines were drawn along R and T directions at cross section to measure the length of the same position by digital calliper(CD-20APX, Mitutoyo).



Figure 2: digital caliper (CD-20APX, Mitutoyo)

Color difference(E) before and after drying was measured. The spectrum of reflected light was measured in the visible region (360–740 nm) with a portable spectrophotometer (JP/CM-600d, Konica Minolta). CIEL*a*b* color scale, where L* stands for lightness, a* stands for redness, and b* stands for yellowness, was used to quantify the color changes. In order to evaluate dry defects, the degree of surface check was investigated. Warp of board such as cup, bow, crook, and twist were also measured after drying. The residual drying stress was evaluated by prong test.



Figure 3: portable spectrophotometer (JP/CM-600d, Konica Minolta)

2.3. ANATOMICAL PROPERTY

In order to find out why drying was performed smoothly with relatively strong drying condition, the anatomical characteristics according to the storage time (from 1 to 6 months) were conducted. To observe the radial section of the test material, a specimen of $1 \times 1 \times 1 \text{ cm}^3$ was prepared. Glycerin and distilled water were added with a solution made from 1:3 to 4 ratio with a heating mantle, and it was sliced 15 to $20 \mu\text{m}$ thick by using microtome. Samples dyed 1% safranin solution and dehydrated with an alcohol (30, 60, 90, 99.7%). The slice was made of permanent preparation, which was observed by using optical microscope (axio imager M2, Carl Zeiss, Germany).

3. RESULTS AND DISCUSSION

3.1. DRYING PROPERTY

Figure 2 shows the drying curve of Kiln drying at one month after harvesting (O) and six months (S) after sawing. The difference in drying speed over time was compared by applying improved drying schedule (T11-B3). After 148 hours of KD at O, average moisture content (AMC) of O was $70\% (\pm 6.8)$, and final moisture content (FMC) reached $9.3\% (\pm 1.2)$. After 103 hours of KD at S, the AMC was 30%, and the FMC reached $9.7\% (\pm 1.2)$. Comparing the drying rate at the same moisture content interval (From 30 to 10%), it was assessed that the drying rate was 0.23%/hr at O and 0.21%/hr at S, which was about 10% slowly.

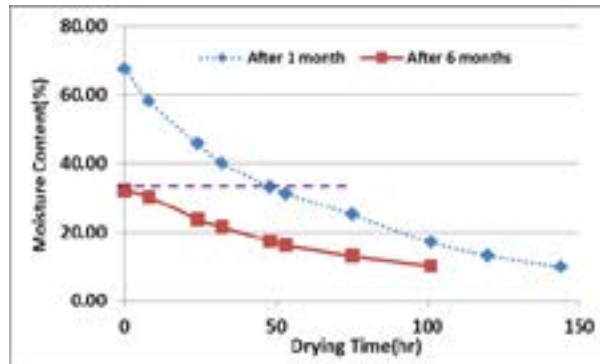


Figure 4: Drying curve of oak board kiln-dried at storage time

The shrinkage rates of dried oak board in width (tangential direction) and thickness (radial direction) by KD was $6.8\% (\pm 1.3)$ and $4.3\% (\pm 0.9)$, respectively. The amount of cupping, bowing and crooking were negligibly low, and no twisting was detected. It might be placing a concrete loading block on top of the board stack during KD. The difference of color between before and after drying of the KD dried oak board was the greatest (Figure 10). The color difference (ΔE) of KD before and after drying was $8.8 (\pm 1.2)$. It was decreased in lightness and increased in redness and yellowness. Discoloration of wood during drying may result in loss of quality and value of the oak board. The discoloration reduces the quality of dried board if the color of the dried wood is not within the range that is considered to be natural for the wood species. In order to produce lighter-colored wood products, the initial drying temperature and the drying schedule should be improved for enhancing quality and value of the oak board.



Figure 5: Drying stresses measured by prong test of KD board by prong test((a): 72hr, (b): after conditioning)

The sawing, drying, finishing yields were 28.8 %, 26.1 % and 7.1 %, respectively. The size of final product(flooring) is 22 mm(thickness) x 85 mm(width) x 1,100 mm(length). The cumulative yield was 7.1 %, which means 92.9 % of volume of log was not used for manufacturing flooring. Therefore, it is expected that the use of high value-added products made of domestic oak species such as flooring and furniture could be commercialized if technology development for high production yield with kiln drying and reducing final product size are applied to enhance economic point of view.



Figure 6: The production processing for oak flooring.

3.2. ATOMINICAL PROPERTY

A number of tylosis were sharply observed in radial sections from three months after sawing. Tylosis of sapwood is almost same level. Tylosis of heartwood and transition(boundary layer between sapwood and heartwood) are increased during storage time.

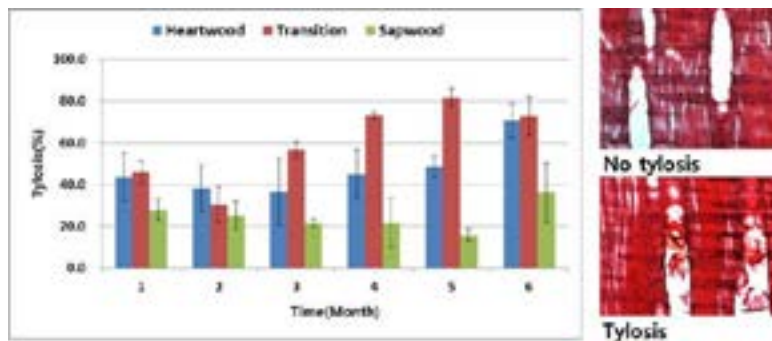


Figure 7: Change of tylosis formation between one month and six months after sawing

Compared to the previous results of drying, it is thought to be due to prompt drying before the formation of tylosis within one month, which did not produce additional tylosis after sawing. Therefore, it is deemed that drying work can be performed within a short period of time after logging to control the associated dryness. It was believed that domestic oak trees in Korea can be used for high value-added purposes with low drying defects if they are properly managed and processed.

4. CONCLUSION

Even though adopting modified drying schedule, there were no observation of obvious wood defects. It is expected that the modified schedule can reduce drying time of hardwoods. In further studies, the improved schedule for hardwood drying by KD will be suggested. The results applied that it is possible to include a domestic species in the traditional range of wood flooring products. It is expected to expand the utilization of domestic oak trees based on the

appropriate final product size for enhancing production yield and development of drying and anatomical research results in the future.

REFERENCES

- Bauch, J. 1984. *Discolouration in the wood of living and cut trees. IAWA Bulletin*, 5, 92-98.
- Chang Y. S., H. K. Shin, S. Kim, Y. Han, M. J. Kim, C.D. Eom, Y.G. Lee and K.B. Shim. 2017. *Evaluation of drying properties and yields of domestic Quercus species for enhancing utilization. Journal of Korean Wood Science Technology* 45(5):622-628.
- Chang Y. S., H. K. Shin, S. Kim and K. B. Shim. 2018. *Drying characteristics of Quercus Mongolica lumber by kiln drying and radio frequency-vacuum drying system. World Conference on Timber Engineering 2018.*
- Han G. S. and H. S.Jung. 1986. *Effect of presurfacing on drying rate and drying defect of Quercus grosseserrata Bl. Journal of Korean Wood Science and Technology* 14(4):29-39.
- Kang H. Y. 1992. *Presteaming effect on properties of native oak lumber. Journal of Korean Wood Science and Technology* 20(2):73-80.
- Kang H. Y. and S. W. Kim. 2004. *Air- and kiln-drying the boards and disks of Quercus variabilis. Journal of Korean Wood Science and Technology* 32(1):52-58.
- Kubinsky, E. 1971. *Influence of steaming on the properties of Quercus rubra L. wood. Holzforschung* 25(3)78-83.
- Murmanis L. 1975. *Formation of tyloses in felled Quercus rubra L. Wood Sci. and Tech.* 9:3-14.
- Rodolfo C., T. Livio, and A. Ottaviano. 2007. *White beech: a tricky problem in the drying process. Proceedings of International scientific conference on hardwood processing.*
- Simpson W. T. 1991. *Dry kiln Operator`s Manual Handbook, USDA Forest Service.*

Wood Properties and Drying Characteristics of Korean Sawtooth Oak (*Quercus acutissima* Carruth.) Wood

Yeonjung Han^{1*} and Yoon-Seong Chang¹

¹Department of Forest Products
National Institute of Forest Science
Seoul, 02455, Republic of Korea

ABSTRACT

The objective of this study was to present the wood properties and drying characteristics of sawtooth oak (Quercus acutissima Carruth.) for the spread of its utilization in South Korea. The annual ring, latewood ratio, dimension of vessels, density, and shrinkage of specimens manufactured from five sawtooth oak trees were measured and compared by age class. And drying rate and drying defects of sawtooth oak boards were measured during kiln-drying. In order to present the processing performance of surface on sawtooth oak wood, the roughness on radial and tangential sections after sawing and planing process was measured by roughness tester and the texture of surface on each section was observed by stereoscopic microscope. It is expected that the fundamental properties of Korean sawtooth oak wood presented in this study will contribute to the extension of utilization of Korean oak species.

1. INTRODUCTION

The forest area (6,383,441 ha) in South Korea occupies is 64% of total land area (10,036,372 ha) and the growing stock is 971,599,553 m³ on the basis of 2017 (Korea Forest Service 2018). The proportion of broad-leaved and mixed forest is 49% and 12%, respectively. Of that, forest area and growing stock of *Quercus* species are 975,181 ha and 133,606,365 m³, respectively.

Quercus species are widespread across Asia, Europe, North America and Africa (Fang et al. 2011). *Quercus* species have been used for different purposes such as timber, charcoal, bed logs for the cultivation of mushrooms, raw material for tannin extract, and bioenergy (Lee et al. 2008, Okamura et al. 2001, Oshima et al. 1997). The sawtooth oak (*Quercus acutissima* Carruth.) broadly inhabits the deciduous broad-leaved forest zone of eastern Asia, as a frontier species of deforest areas (Jung and Tamai 2012). The sawtooth oak is one of the domestic hardwood species (Kim 2002) that manly inhabits at altitudes below 600 m and grows straightly up to 20 – 30 m height.

As mentioned above, *Quercus* species, which can be used for various purposes, is used in low-grade applications such as bed log for mushroom, handle of tools, and charcoal in Korea. *Quercus* species for use as timber and lumber is being imported. As of 2011, oak wood was imported 8,000 m³ and 4,400 m³ in the form of lumber and log, respectively. Because *Quercus* species were no continuous supply of high quality wood required by the lumber industry, it was not treated as wood in Korea. Also, forest policy in Korea was focused on forest greenification, which put emphasis on the cultivation of rapid grown species. From now on, a national policy is needed to raise oak trees which have great potential value as timber resource.

It was commonly accepted that wood from trees grown in certain locations under certain conditions was stronger, more durable, more easily worked with tools, or finer grained than wood from trees in other locations (Wiemann 2010). In the present study, anatomical and physical properties of domestic sawtooth oak wood were measured and presented. The specimens were taken from five sawtooth oak trees. The age class of sawtooth oak trees was IV, V, and VI, respectively. The ring width, proportion of latewood, length and diameter of vessel elements, density, and shrinkage were measured by each age class of sawtooth oak wood. The drying rate and drying defects of sawtooth oak wood during kiln-drying were measured. To analyze the surface processability of sawtooth oak wood, the roughness of radial and tangential section after cutting specimens was measured by roughness tester and the surface texture was observed

* Corresponding author: Yeonjung Han; E-mail: yeonjungh@korea.kr

by stereoscopic microscope. It is expected that the domestic sawtooth oak wood will be utilized in various ways through the results in this study.

2. MATERIALS AND METHODS

2.1. MATERIALS

The domestic sawtooth oak (*Quercus acutissima* Carruth.) were felled in the area of Andong-si, Gyeongsangbuk-do, Korea to measure the wood properties and drying characteristics. The disks with 50-mm thickness were collected from five sawtooth oak wood and the strips (radial direction) with 30-mm width were prepared from each disk. After planing the cross section of each strip, the cross section images were obtained using scanner (Epson, Japan). The width of earlywood and latewood in obtained images was measured using WinDENDRO™ (Régent Instrument Inc. Canada). The IV, V, and VI age class in five sawtooth oak wood were two, two, and one, respectively. The mean, earlywood, latewood, juvenilewood, and maturewood ring width of each age class of sawtooth oak wood were described in Table 1.

Table 1: Annual ring width of sawtooth oak

Age class		IV	V	VI
Ring width (mm)	Mean	5.005 ±2.011	3.930 ±1.998	2.760 ±0.774
	Earlywood	0.873 ±0.342	0.790 ±0.253	0.706 ±0.104
	Latewood	4.182 ±2.007	3.140 ±1.859	2.054 ±0.750
	Juvenile wood	5.880 ±2.213	5.369 ±2.175	2.642 ±1.062
	Mature wood	3.851 ±0.636	2.742 ±0.530	2.826 ±0.563

2.2. METHODS

Two strips of 30-mm and 20-mm thickness were manufactured from the strip (30-mm width × 50-mm thickness) in the sawtooth oak disks. The strips of 30-mm and 20-mm thickness were used for measurement of density and vessel elements size, respectively. The strips were cut with five annual rings intervals from pith to bark in order to measure the length and diameter of vessel elements. The length and diameter of vessel elements were measured using the image analysis program (DeltaFix, Netherlands), after the preparats of vessel elements were made by the Schultz method (Seo et al. 2014).

The specimens with 20-mm (width) × 20-mm (thickness) × 20-mm (length) prepared for measuring the density and shrinkage. The basic density, oven-dry density, and shrinkage from green to oven-dry of sawtooth oak wood were calculated by measuring the weight and dimension of green and oven-dry conditions.

Table 2: Kiln schedule for sawtooth oak wood

Step	Moisture content (%)	Dry-bulb temperature (°C)	Wet-bulb temperature (°C)	Equilibrium moisture content (%)
1	Above 40	43.3	41.1	17.7
2	40 to 35	43.3	40.6	16.6
3	35 to 30	43.3	38.9	13.6
4	30 to 25	48.9	41.1	10.0
5	25 to 20	54.0	37.8	5.7
6	20 to 15	60.0	32.2	2.9
7	15 to final	82.2	54.4	3.5

The eighty eight sawtooth oak boards were dried in a laboratory-scale kiln (Drying Eng., Korea) according to the FPL (Forest Products Laboratory, US Forest Service) kiln-drying schedule (T4-C2; Table 2; Boone et al. 1988). The initial moisture content (MC) of the boards ranged from 34.7 to 64.9%. Drying was continued until a final target MC of 12% in the board was reached. The boards (130-mm width × 25-mm thickness × 2.7-m length) were stacked eight wide and 11 high. The internal dimensions of the kiln were 1.5 × 1.5 × 4.0 m³, and the walls were insulated using 100 mm of urethane foam. The air velocity was 2 m/s, and the airflow was parallel to the longitudinal axis of the boards. Drying defects such as cup, bow, crook, and twist were measured after drying. The cup was measured by selecting the farthest point from the plane after the widthwise edges of the board contacted the plane. The bow and crook were measured by selecting the farthest point from the plane after the longitudinal edges of the board contacted the plane. The twist was measured taking into consideration the height of the remaining vertex away from the plane after the rest of the vertices were in contact with plane.

After circular sawing, band sawing, and planing of sawtooth oak boards, the roughness of radial and tangential sections were measured by roughness tester (Time HighTech, China) and the surface texture was observed by stereoscopic microscope. And the roughness of sawtooth oak was compared with the Japanese larch wood that was widely used in Korea. Although the profiles representing surface roughness were various (International Organization for Standard 1997), in present study, three parameters (R_a , R_t , and R_p) were presented that express the roughness of entire surface. The average of ordinates (R_a), maximum peak to valley roughness height (R_t), and maximum profile peak height (R_p) were shown in Figure. 1 and the average of ordinates can be calculated as shown in equation 1.

$$R_a = \frac{1}{l} \int_0^l |Z(x)| dx \quad (1)$$

where, l = sample length and $Z(x)$ = ordinate values.

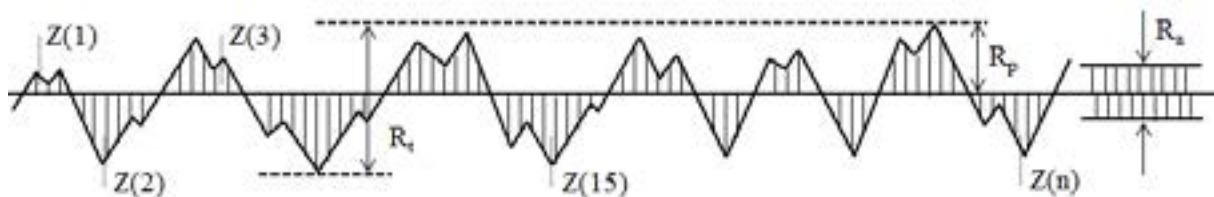


Figure 1: Digitized representation of a 3A Common red oak board.

3. RESULTS AND DISCUSSION

3.1. ANATOMICAL AND PHYSICAL PROPERTIES OF SAWTOOTH OAK

The length and diameter of vessels dissociated from sawtooth oak were measured to 0.01 μm length unit (Figure 2). The length and diameter of vessels was 376.8 μm (60.2 SD) and 280.7 μm (43.1 SD) in IV age class, 379.6 μm (55.6 SD) and 266.4 μm (38.9 SD) in V age class, and 373.6 μm (61.7 SD) and 268.7 μm (39.9 SD) in VI age class, respectively. The dimension of the vessels was measured relatively large, as a result of collecting the vessels mainly distributed in earlywood. A typical ring-porous wood has very large earlywood vessels with diameters from 200 to 350 μm (Siau 1995). It was similar to the result in this study.

Density (or specific gravity) is one of the most important physical properties of wood (Desch and Dinwoodie 1996, Bowyer et al. 2003). Base on the oven-dry weight, the average basic density and oven-dry density was 688.4 kg/m³ (37.1 SD) and 781.8 kg/m³ (37.8 SD), respectively. In hardwood, density is dependent not only fiber wall thickness, but also on the amount of void space occupied by vessels and parenchyma (Wood Handbook Ch.3, Wiedenhoef). The reason for the high density of sawtooth oak wood was that the ring width of latewood was larger than those of earlywood. The shrinkage of sawtooth oak specimens from initial MC (32.5-48.0%) to oven dry condition were 0.269% (0.189 SD) in longitudinal, 3.985% (0.892 SD) in radial, and 7.980% (1.357 SD) in tangential direction. Because of the high density and shrinkage of sawtooth oak wood, it is necessary to analyze the lumbering, planing, and drying process.

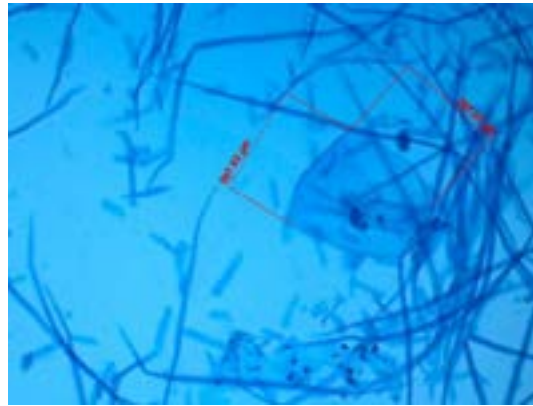


Figure 2: The length and diameter of vessel in sawtooth oak.

3.3. DRYING CHARACTERISTICS OF SAWTOOTH OAK

The average changes in MC for 130 mm (width) × 25 mm (thickness) × 2.7 m (length) sawtooth oak boards in accordance with the drying schedule (T4-C2) is shown in figure 3. Drying was conducted for 262 h, and 10 specimens among the dried sawtooth oak boards among the in kiln were used to measure the average changes in MC. The initial MCs of 10 specimens ranged from 34.7 to 64.9%, and the final MC of the specimens was 5.5% (2.1 SD), the average drying rate was 0.166%/h (0.029 SD) which ranged from 0.115%/h to 0.250%/h due to the wide variation of initial MCs within the specimens.

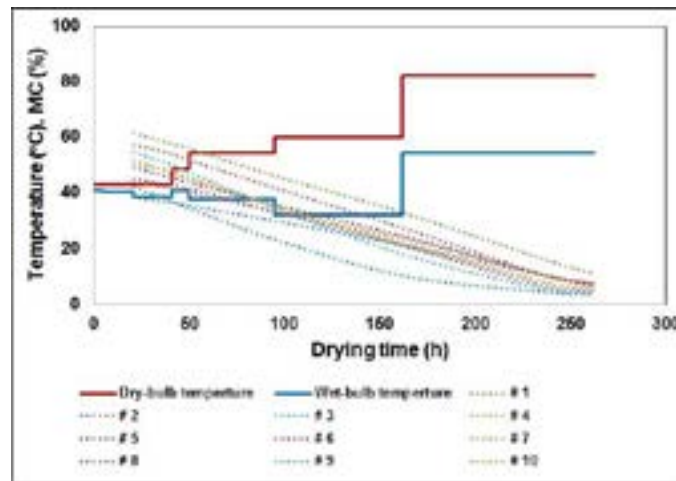


Figure 3: The MC change of sawtooth oak wood during kiln drying.

The cup, bow, crook, and twist of sawtooth oak boards were 1.409 (0-4.59), 3.474 (0-11.19), 7.038 (1.34-10.73), and 5.030 (1.74-7.97) mm, respectively. These values are similar to the results obtained from a previous study of the drying defects of larch wood (Han et al. 2016). In this study, cup and twist were suppressed by applying an upper load to the stacked boards during kiln drying. However, crook was measured relatively large, so other ways are required to solve this problem.

Table 3: Warp of sawtooth oak after drying

Warp ¹ (mm) and its rate (%)			
Cup	Bow	Crook	Twist
1.409	3.474	7.038	5.030
(1.084) ²	(0.174) ³	(0.352) ³	(0.252) ³

¹ Distance between surface of board and surface of plate

² The rate in the case of cup : warp / width × 100

³ The rate in the case of bow, crook, and twist : warp / length × 100

3.3. SURFACE CHARACTERISTICS AFTER SAWING AND PLANING

After circular sawing, band sawing, and planing of sawtooth oak and Japanese larch wood, the roughness of radial and tangential sections were presented in Table 3 as three roughness parameters R_a , R_t , and R_p . The roughness of radial and tangential section found to have no significant difference in both sawtooth oak and Japanese larch wood. Also, it can be seen that the roughness parameters decrease after planing. However, the roughness after band sawing was not measured out of range in roughness tester. The roughness of sawtooth oak wood after wood processing was smaller than coniferous Japanese larch wood. To identify these causes, each surface of sawtooth oak and Japanese larch wood was observed through the stereoscopic microscope.

Table 4: Surface roughness of sawtooth oak wood and Japanese larch wood after wood processing

		Sawtooth oak			Japanese larch		
		Circular sawing	Band sawing	Planing	Circular sawing	Band sawing	Planing
Radial section	R_a	2.580 (0.576 SD)	Out of range ¹	1.767 (0.428 SD)	4.250 (1.086 SD)	Out of range ¹	2.608 (0.824 SD)
	R_t	22.806 (7.788 SD)		15.418 (6.020 SD)	32.978 (6.960 SD)		19.988 (5.914 SD)
	R_p	5.798 (1.106 SD)		4.675 (1.370 SD)	9.817 (2.462 SD)		5.972 (1.739 SD)
Tangential section	R_a	2.444 (0.485 SD)		1.723 (0.688 SD)	3.558 (1.803 SD)		3.042 (0.602 SD)
	R_t	23.238 (4.350 SD)		17.700 (8.956 SD)	26.732 (9.573 SD)		23.064 (4.096 SD)
	R_p	6.065 (1.259 SD)		4.280 (1.974 SD)	8.758 (2.938 SD)		8.178 (1.576 SD)

¹ The range of roughness tester : $\pm 40 \mu\text{m}$

Microscopic photographs of 150 times on radial and tangential section of sawtooth oak wood after circular sawing, band sawing, and planing were shown in figure 4 and 5. Compared to the circular sawing, there were many tissue destruction and saw mark left on the surface after band sawing.

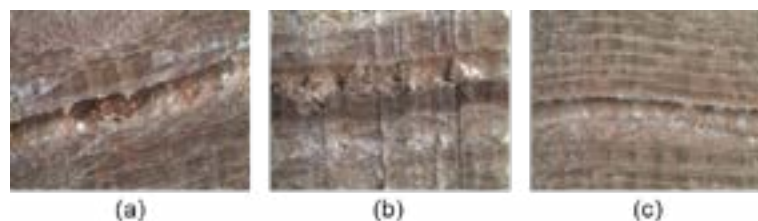


Figure 4: Radial section image of sawtooth oak after wood processing (a: circular sawing, b: band sawing, c: planing).

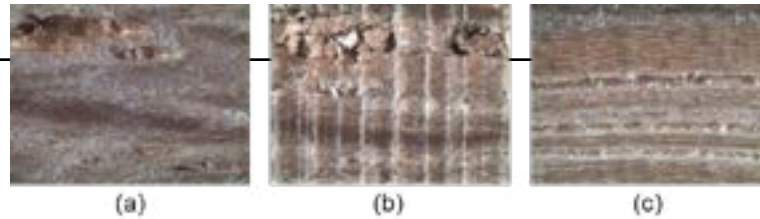


Figure 5: Tangential section image of sawtooth oak after wood processing (a: circular sawing, b: band sawing, c: planing).

In figure 6 and 7, the radial and tangential section of Japanese larch wood after wood processing were presented for comparison of sawtooth oak wood. Many trace of broken fibers after circular and band sawing were observed on the surface of Japanese larch with relative long tracheids. Therefore, it was considered that the surface of Japanese larch wood was measured roughly compared to the sawtooth oak wood.

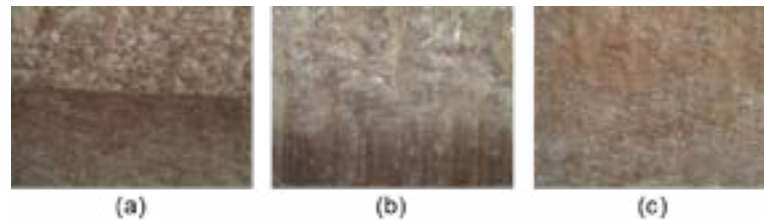


Figure 6: Radial section image of Japanese larch after wood processing (a: circular sawing, b: band sawing, c: planing).

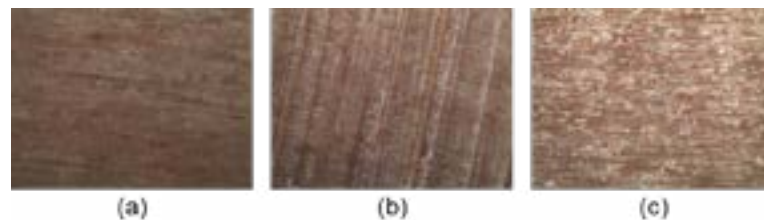


Figure 7: Tangential section image of Japanese larch after wood processing (a: circular sawing, b: band sawing, c: planing).

4. SUMMARY

The objective of this study was to present the wood properties and drying characteristics of sawtooth oak for the spread of its utilization in South Korea. The annual ring width of sawtooth oak showed a tendency to decrease with increasing age class. The dimension of vessels was similar to typical ring-porous species. As a result of kiln-drying experiment on sawtooth oak with high basic density (688.4 kg/m^3) and shrinkage (3.985% in radial and 7.980% in tangential direction), the drying rate was 0.166%/h. Drying defects except for crook, was not significant. The surface on sawtooth oak wood after band sawing was rougher than circular sawing.

REFERENCES

- Boone, R. S., C. J. Kozlik, P. J. Bois, and E. M. Wengert. 1988. *Dry Kiln Schedules for Commercial Woods: Temperate and Tropical*. USDA Forest Products Laboratory GTR-57. DOI: 10.2737/FPL-GTR-57.
- Bowyer, J., R. Shmulsky, and J. G. Haygreen. 2003. *Forest Products and Wood Science: An Introduction*. Iowa State Press, Iowa City. 554 pp.
- Desch, H. E. and J. M. Dinwoodie. 1996. *Timber structure, properties, conversion and use*. Macmillan Press, UK. 306 pp.
- Fang, S., Z. Liu, Y. Cao, D. Liu, M. Yu, and L. Tang. 2011. *Sprout development, biomass accumulation and fuelwood characteristics from coppiced plantations of *Quercus acutissima**. *Biomass Bioenergy* 35(7):3104-3114.
- Han, Y., J. H. Park, Y. S. Chang, Y. Park, J. K. Oh, J. P. Hong, J. J. Lee, and H. Yeo. 2016. *The effect of controlling the drying*

- distortion of laminas on the productions yield of cross-laminated timber (CLT) using Larix kaempferi wood. Eur. J. Wood Prod.* 74(4):519-526.
- International Organization for Standard. 1997. *Geometrical product Specifications (GPS) – Surface texture: Profile method – Terms, definitions and surface texture parameters. ISO-4287.*
- Jung, N. C. and Y. Tamai. 2012. *Anatomical observation of polyphenol changes in epidermal cells during the development of Quercus acutissima-Scleroderma verrucosum ectomycorrhize. Trees* 26(2):301-310.
- Kim, C. 2002. *Mass loss rates and nutrient dynamics of decomposing fine roots in a sawtooth oak and a Korean pine stands. Korean J. Ecol. Sci.* 1(2):101-105.
- Korea Forest Service. 2018. *Statistical Yearbook of Forestry. Korea Forest Service, Daejeon, Korea. 444 pp.*
- Lee, S. H., M. S. Eom, K. S. Yoo, N. C. Kim, J. K. Jeon, Y. K. Park, B. H. Song, and S. H. Lee. 2008. *The yields and composition of bio-oil produced from Quercus acutissima in a bubbling fluidized bed pyrolyzer. J. Analytical Appl. Pyrolysis* 83(1):110-114.
- Okamura, M., T. Taniguchi, and T. Kondo. 2001. *Efficient embryogenic callus induction and plant regeneration from embryonic axis explants in Quercus acutissima. J. Forest Res.* 6(2):63-66.
- Oshima, K., Y. Tang, and L. Washitani. 1997. *Spatial and seasonal patterns of microsite light availability in remnant fragment of deciduous riparian forest and their implication in the conservation of Arisaema heterophyllum, a threatened plant species. J. Plant Res.* 110(3):321-327.
- Seo, J. W., C. D. Eom, S. Y. Park. 2014. *Study on the variation of inter-annual tracheid length for Korean red pine from Sokwang-ri in Uljin. J. Korean Wood Sci. Technol.* 42(6):646-652.
- Wiedenhoeft, A. 2010. "Chapter 3-Structure and Function of Wood", in *Wood Handbook–Wood as an Engineering Material. USDA Forest Products Laboratory GTR-190. DOI: 10.2737/FPL-GTR-190.*
- Wiemann, M. C. 2010. "Chapter 2-Characteristics and Availability of Commercially Important Woods", In *Wood Handbook–Wood as an Engineering Material. USDA Forest Products Laboratory GTR-190. DOI: 10.2737/FPL-GTR-190.*

Vertical Forest Engineering: Applications of Vertical Forests with Self-Growing Connections in High-Rise Buildings

Xiuli Wang¹, Wolfgang Gard¹, and J.W.G van de Kuilen^{1,2}

¹Biobased Structures and Materials
Delft University of Technology
Delft, The Netherlands

²Chair of Wood Technology
Technical University of Munich
Munich, Germany

ABSTRACT

Living architecture is thriving. The integration of buildings with vegetation has become a necessity in many metropolitan areas of the world today, including Singapore, New York City, Shanghai and Milan, to name a few. It expands the potential of vertical and horizontal, exterior and interior, exposed and enclosed spaces in a building that can be used to accommodate plants. Green infrastructures have benefits both on urban and building scales. They can be categorized into green roofs and vertical greenery systems that can be divided further into green façade, green/living wall, green terraces, elevated forests and vertical forests. There are many design and planting considerations for architects, structural engineers and botanists when using living architectures to mimic natural systems, such as climatic and regional considerations, primary functions and design objectives, structural support systems, maintenance, irrigation and so on. Plants used for vertical greenery are more likely to be hardwood species to adjust solar radiation during cooling and heating periods, and also for aesthetic pleasure. Take Bosco Verticale, which is located in Milan, as an example to look into engineering methods when trees grow on balconies of high rise buildings. It could be concluded that planting restraint safety system and regular maintenance are necessary for trees growing in the sky. But the change of growing conditions causes various problems such as stability and growth of trees. Instead of using steel cages and bracings to prevent falling off of trees in the sky, the concept of self-growing connections is proposed to provide the stability of vertical forests. This paper is meant to generate awareness of the possibilities of the integration of greenery vertically with buildings, show application considerations, and inspire future developments in typologies and integration with forests.

Ageing phenomena of oak wood-animal glue bonded assemblies for preservation of cultural heritage

Yasmine Mosleh¹, Hans Poulis¹ Wolfgang Gard², J.W.G Van de Kuilen^{2,3}, Paul Van Duin⁴

¹Aerospace
Engineering Faculty
Delft University of
Technology
Delft, The
Netherlands

¹Biobased Structures
and Materials
Delft University of
Technology
Delft, The
Netherlands

²Chair of Wood
Technology
Technical University
of Munich
Munich, Germany

⁴Rijksmuseum
Amsterdam, The
Netherlands

ABSTRACT

The structural preservation of panel paintings and decorated furniture as significant parts of Dutch cultural heritage, requires comprehensive knowledge on the long term behaviour of their constituent materials namely wood and animal glues. A decorated cabinet crafted by Jan van Mekeren (1684-1744) is chosen as the case study. The environment-induced ageing of wooden artefacts is often due to failure of the glue joints between the wooden parts. This behaviour is largely not understood.

US Hardwoods and Market Opportunities in Easter Europe

Eva Haviarova¹, Henry Quesada²

¹Department of Forestry and Natural Resources
University of Company
West Lafayette, Indiana, 47907, USA

²Department of Sustainable Biomaterials
Virginia Tech
Blacksburg, VA, 47907, USA

ABSTRACT

In the last two decades the US hardwood industry has experienced an important increase in exports to key markets in Southeast Asia, and Western Europe. Exports of log, lumber, and veneer played a major role in forest products overall sales. The increase in exports has allowed the US hardwood industry to remain competitive and continue to support much needed economic development in US hardwood regions such as the Mid-West and the Eastern hardwood region. However, with ongoing changes, new market opportunities need to be explored. There is still little information available on international hardwood markets in Eastern European emerging economies where the solid furniture manufacturing industry consume high quality of hardwood lumber. Favorable labor costs, progressive design, and an increasing environmental orientation in these countries are key factors that sustain not only the furniture industry but also the architectural woodworking industry.

The goal of this project was to identify opportunities, asses the level of interest and feasibility for exporting US hardwood lumber to selected Eastern Europe countries (Slovenia, Slovakia, Poland and Czech Republic). The main activities of the project included the identification of the hardwood lumber characteristics in the selected countries from secondary and primary research sources. Additional sources of information included available industry and government reports, interviews with industry, industry associations, and government representatives in selected countries. This study will present summary of findings.

Deep Learning for Lumer Identification

Fanyou Wu¹, Rado Gazo¹, Bedrich Benes², and Eva Haviarova¹

¹Department of Forestry and Natural Resources
University of Company
West Lafayette, Indiana, 47907, USA

²Department of Sustainable Biomaterials
Virginia Tech
Blacksburg, VA, 47907, USA

ABSTRACT

Current lumber scanners used in industrial wood manufacturing plants such as rough mills and flooring plants are used to measure, evaluate the quality, and optimize processing of solid wood. Because various wood species differ significantly in their color, grain structure, natural characteristics, defects and density, for their optimal performance, the scanner sensors often need to be calibrated for each individual species. When production switches from one species to the next, the scanner settings have to be manually changed to new species. In this study, we attempt to automate species recognition based on image recognition so that the manufacturing equipment can automatically adapt to species being processed, or even be able to process batches of mixed species.

Recently, deep-learning techniques have demonstrated their usefulness in wood identification based on macroscopic cross-section images. Because such images are not easily obtained, this approach is not well suited for an industrial application. In this study, we used 4,736 transversal board face images of 11 hardwood species acquired by Microtec Goldeneye 300 Multi-Sensor Quality Scanner™. Most images were 70 x 500 pixels and were used to train the Convolution Neural Network (CNN)-ResNet. We achieved accuracy of 84% when identifying a single testing image of 224x224 pixels and 94% when applying majority voting without any parameter tuning. The average processing time was 0.07 seconds on GPU and 0.64 seconds on CPU. We expect that on-going work to increase training sample size and parameter fine-tuning will further increase the accuracy.
